frontiers | Research Topics

Stem cell technologies meet stem cell biology to shine new light into tropical infectious diseases

Edited by
Alena Pance and Gabriel Rinaldi

Published in
Frontiers in Cellular and Infection Microbiology

ISSN 1664-8714
ISBN 978-2-8325-4907-0
DOI 10.3389/978-2-8325-4907-0

About Frontiers

Frontiers is more than just an open access publisher of scholarly articles: it is a pioneering approach to the world of academia, radically improving the way scholarly research is managed. The grand vision of Frontiers is a world where all people have an equal opportunity to seek, share and generate knowledge. Frontiers provides immediate and permanent online open access to all its publications, but this alone is not enough to realize our grand goals.

Frontiers journal series

The Frontiers journal series is a multi-tier and interdisciplinary set of open-access, online journals, promising a paradigm shift from the current review, selection and dissemination processes in academic publishing. All Frontiers journals are driven by researchers for researchers; therefore, they constitute a service to the scholarly community. At the same time, the *Frontiers journal series* operates on a revolutionary invention, the tiered publishing system, initially addressing specific communities of scholars, and gradually climbing up to broader public understanding, thus serving the interests of the lay society, too.

Dedication to quality

Each Frontiers article is a landmark of the highest quality, thanks to genuinely collaborative interactions between authors and review editors, who include some of the world's best academicians. Research must be certified by peers before entering a stream of knowledge that may eventually reach the public - and shape society; therefore, Frontiers only applies the most rigorous and unbiased reviews. Frontiers revolutionizes research publishing by freely delivering the most outstanding research, evaluated with no bias from both the academic and social point of view. By applying the most advanced information technologies, Frontiers is catapulting scholarly publishing into a new generation.

What are Frontiers Research Topics?

Frontiers Research Topics are very popular trademarks of the *Frontiers journals series*: they are collections of at least ten articles, all centered on a particular subject. With their unique mix of varied contributions from Original Research to Review Articles, Frontiers Research Topics unify the most influential researchers, the latest key findings and historical advances in a hot research area.

Find out more on how to host your own Frontiers Research Topic or contribute to one as an author by contacting the Frontiers editorial office: frontiersin.org/about/contact

Stem cell technologies meet stem cell biology to shine new light into tropical infectious diseases

Topic editors

Alena Pance — University of Hertfordshire, United Kingdom

Gabriel Rinaldi — Aberystwyth University, United Kingdom

Citation

Pance, A., Rinaldi, G., eds. (2024). *Stem cell technologies meet stem cell biology to shine new light into tropical infectious diseases*. Lausanne: Frontiers Media SA.

doi: 10.3389/978-2-8325-4907-0

Table of contents

frontiers | Frontiers in Cellular and Infection Microbiology

TYPE Editorial
PUBLISHED 07 May 2024
DOI 10.3389/fcimb.2024.1411728

OPEN ACCESS

EDITED AND REVIEWED BY
Tania F. De Koning-Ward,
Deakin University, Australia

*CORRESPONDENCE
Alena Pance
a.pance@herts.ac.uk
Gabriel Rinaldi
gabriel.rinaldi@aber.ac.uk

RECEIVED 03 April 2024
ACCEPTED 09 April 2024
PUBLISHED 07 May 2024

CITATION
Pance A and Rinaldi G (2024) Editorial: Stem cell technologies meet stem cell biology to shine new light into tropical infectious diseases.
Front. Cell. Infect. Microbiol. 14:1411728.
doi: 10.3389/fcimb.2024.1411728

Editorial: Stem cell technologies meet stem cell biology to shine new light into tropical infectious diseases

Alena Pance[1*] and Gabriel Rinaldi[2*]

[1]School of Life and Medical Sciences, University of Hertfordshire, Hatfield, United Kingdom, [2]Department of Life Sciences, Aberystwyth University, Aberystwyth, United Kingdom

KEYWORDS

embryonic stem cells, induced pluripotent stem cells, organoids, parasite stem cells, tropical infectious diseases, protozoan parasites, metazoan parasites, vectors

Editorial on the Research Topic

Stem cell technologies meet stem cell biology to shine new light into tropical infectious diseases

Innovative technologies have revolutionized fundamental and translational biomedical research over the last decade. The increasing use of Embryonic Stem Cells and the reprogramming of Induced Pluripotent Stem Cells (iPSCs), in tandem with the advent of genome editing, have given access to cell types, cellular processes and molecular mechanisms that had previously been out of reach. Particularly in the field of parasitic infectious diseases, culture systems that replicate natural niches where these pathogens dwell are extremely difficult to develop in the laboratory. Continuous access to primary cell samples is challenging; cell types involved in host-parasite interactions are extremely difficult to maintain *in vitro* or *ex vivo* and many other challenges hinder progress in understanding the biology of pathogens, including their development and interaction with hosts. The opportunities offered by these cutting-edge technologies in this field are extraordinary, though not without their own hurdles to overcome. These include reliable differentiation protocols to generate high-quality model systems, and development of novel assays to assess parasite invasion, host interaction, immune evasion, and infection establishment. Moreover, the perception and acceptance of these model systems within the scientific community also represents a challenge. Tackling all these elements will pave the way towards the discovery of novel control strategies for infectious diseases. In this Special Research Topic, we examine recent developments and applications of Stem Cell technologies and further explore new approaches that will enrich and widen the horizon for understanding tropical infectious diseases. Furthermore, the biology of recently described Stem Cell systems in complex metazoan parasites, which are being revealed through cellular, molecular, and 'omics' approaches, is discussed. Insights into toti- and pluri-potent cells of parasites critical for their development and host interaction will unveil targets for novel diagnostic and control strategies.

Over half of the world's population, particularly in the most impoverished regions of the globe, are at risk of infection with two major groups of parasites. These organisms are

the main focus of this Research Topic: protozoa and metazoa parasites, including apicomplexa and helminths, respectively. Here, we have assembled 12 articles that contribute to this exciting and thriving field.

Malaria is one of the first infectious diseases to which this technology has been applied. Two cell types are mainly involved in this disease: hepatocytes, which are inaccessible for experimental studies, and erythrocytes, which are genetically elusive because they are anucleated. The opportunity to manipulate erythrocytes is described by Satchwell in his analysis of how Stem Cell technologies can help unravel the mechanisms underlying the erythrocytic life cycle of malaria parasites. It is also clearly highlighted by Pance et al., who show that erythrocytic cells can be derived from a variety of Stem Cells, including patient-reprogrammed iPSCs. This allows modification using site-specific genome editing as well as preserving specific genomic backgrounds. This approach not only facilitates access to a specific cell type, the natural niche of the parasite, but also facilitates the study of the impact of specific human proteins on the infection and disease progression. In this line, a novel development is introduced by Parres-Mercader et al. which envisions the generation of 2D and 3D culture organoid systems that mimic the mosquito midgut and salivary gland environments to study the intra-vector developmental stages of malaria parasites. Outcomes of these approaches will shine light on to strategies for transmission control.

The pathogenic agent of the American Trypanosomiasis or Chagas Disease, *Trypanosoma cruzi*, is one of the organisms that has long lacked adequate culturing systems, as it preferentially invades cardiac muscle. The use of Stem Cells has facilitated the production of cardiomyocytes *in-vitro*, providing a natural environment, and enabling the use of 'omics' approaches to study the infection, as shown by Venturini et al. A time course experiment of the infection revealed activation of immunity-related genes and demonstrated that the parasite exploits cardiomyocyte stress response and inflammation to establish the infection. Excitingly, the possibility of disease-specific responses has been explored by Oliveira et al. using iPS-derived cardiomyocytes generated from patients with chronic and asymptomatic disease. This study reveals significant transcriptomic differences between the two disease states and starts unraveling molecular mechanisms underlying cell damage in chronic cardiomyopathy. Moreover, the authors hypothesize that the immune response may contribute to a milder pathogenesis. In addition, the poorly explored role of the intestinal tissue infection during the oral transmission of trypanosomes and development of the chronic disease is moving within reach by using murine colon organoids as presented by Daghero et al. Successful invasion and replication was achieved in these 2D and 3D cellular structures, showing marked differences with cultures using intestinal cell lines, reflecting a more natural environment. Finally, while *in-vitro* systems to study intra-vector developmental stages of trypanosomes have not yet taken advantage of Stem Cell technologies, Smircich et al. pointed out the potential contribution of 3D insect-derived culture systems in this neglected field.

The emergence of 2D and 3D culture systems providing specific intestinal models to characterize the life and sexual stages of *Toxoplasma gondii* in the enteric epithelium is comprehensibly explored by Sena et al. This Review of novel experimental platforms being developed highlights important challenges and opportunities to advance this field in the near future. The exciting prospects of these cellular systems to dissect the molecular mechanisms underlying the impact of *T. gondii* infection on pregnancy are also analyzed and discussed by Faral-Tello et al., paving the way to a better understanding of the infection in the maternal-foetal interface and hence revealing targets for novel control strategies.

Metazoan parasites, such as helminths, rely on complex Stem Cell systems to develop throughout their complex life cycles where the parasite metamorphosizes across different body plans. These systems represent a continuous source of differentiated cells that facilitate healing of parasite tissues that are exposed to adverse conditions within the host. Some of these cells underlie the tumor-like growth of the metacestode stage of the tapeworm *Echinococcus multilocularis* within host organs. Using 'omics' approaches, Herz et al. identified >1,100 genes associated with germinative cells, some of which were validated and characterized by *in situ* hybridization and pulse-chase experiments. Furthermore, the authors characterized the transcriptomic profile of primary cell cultures derived from whole parasites, initiating the understanding of molecular mechanisms that would advance the establishment of helminth-derived cell lines for the first time. In a similar fashion, but using the model tapeworm *Hymenolepis microstoma*, Montagne et al. explored cell proliferation and differentiation during the parasite's development, employing a combination of molecular and imaging approaches. This first comprehensive dissection of a model parasite development provides a platform for equivalent studies on helminths that infect humans and animals. The free-living nematode *Caenorhabditis elegans* also represents an extremely useful model for which 'bulk' and single-cell omics-based datasets coupled with functional genomics tools are available. Davies et al. reviewed the latest studies on the molecular mechanisms employed by the bacterium *Pasteuria* spp. for specific host recognition. The development of microbial biocontrol products including *Pasteuria* to specifically infect root-knot nematodes promises novel control avenues. The authors discussed key findings involving worm Stem Cell-like cells, named Seam Cells that appear to play a critical role in the recognition of the parasite by the bacteria.

The broad collection of articles in this Research Topic, >50% of which originated from endemic countries, shows the importance of Stem Cell-based approaches to understand some of the most devastating diseases affecting humans and animals worldwide. The development of culture systems recapitulating definitive host and vector conditions and the opportunities to study patient-specific effects and human polymorphisms as well as the role of parasite Stem Cells offer unlimited potential to unravel biology and discover new avenues for prevention and treatment (Figure 1).

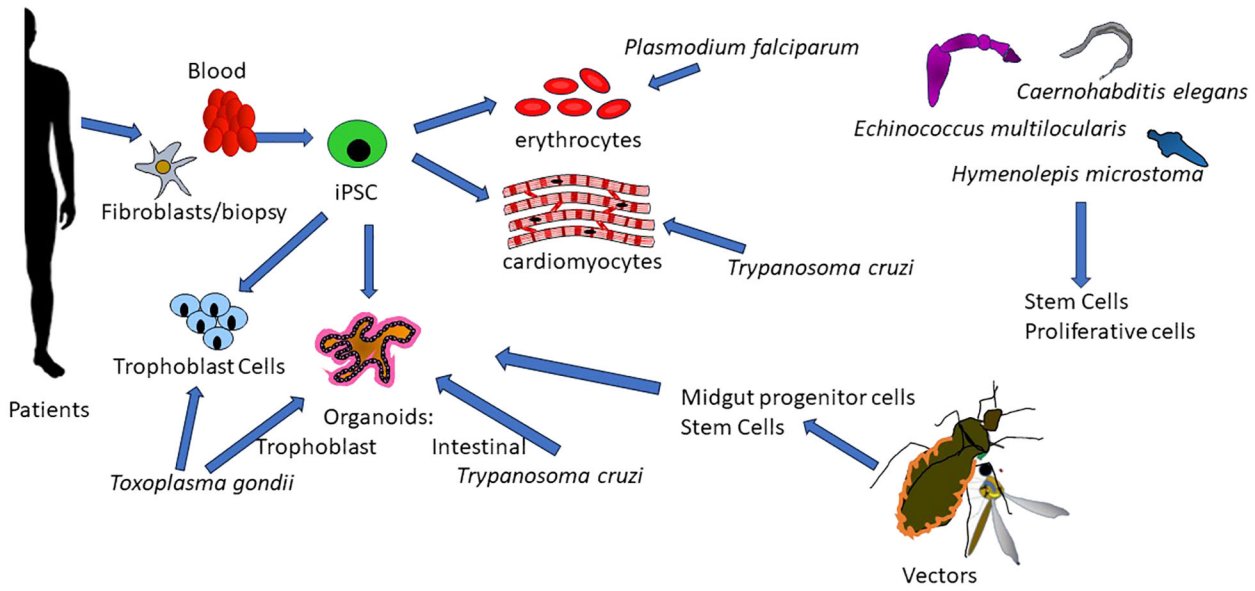

FIGURE 1
Stem Cell-based approaches to study tropical infectious diseases. Induced Pluripotent Stem Cell lines (iPSC) can be derived from blood cells or fibroblasts. These iPSCs can be cultured and stored indefinitely and differentiated into different cell types relevant to the study of parasites: erythrocytes, cardiomyocytes, or trophoblasts. Organoids can also be generated from iPSCs to provide tridimensional niches mimicking the natural environments where these parasites dwell. The potential for replicating these advances in the vectors involved in the transmission of these diseases is also being developed. Understanding of stem and proliferative cells in multicellular metazoan parasites is a new field, leading to better knowledge of the biology of these parasites and hence revealing targets for novel control strategies.

We look forward to future developments of Stem Cell tools and their combination with genome editing and single cell omics studies to drive and advance this fascinating and promising field.

Author contributions

AP: Conceptualization, Writing – original draft, Writing – review & editing. GR: Conceptualization, Writing – original draft, Writing – review & editing.

Conflict of interest

The authors declare that the research was conducted in the absence of any commercial or financial relationships that could be construed as a potential conflict of interest.

The author(s) declared that they were an editorial board member of Frontiers, at the time of submission. This had no impact on the peer review process and the final decision.

Publisher's note

frontiers | Frontiers in Cellular and Infection Microbiology

ORIGINAL RESEARCH
published: 07 July 2022
doi: 10.3389/fcimb.2022.904747

Different Transcriptomic Response to *T. cruzi* Infection in hiPSC-Derived Cardiomyocytes From Chagas Disease Patients With and Without Chronic Cardiomyopathy

Theo G. M. Oliveira[1,2,3], Gabriela Venturini[1,4], Juliana M. Alvim[1], Larissa L. Feijó[3], Carla L. Dinardo[3], Ester C. Sabino[5], Jonathan G. Seidman[4], Christine E. Seidman[4,6,7], Jose E. Krieger[1,2] and Alexandre C. Pereira[1,2,4]*

[1] Laboratório de Genética e Cardiologia Molecular, Instituto do Coração (InCor), Hospital das Clínicas, Faculdade de Medicina, Universidade de São Paulo (HC/FMUSP), São Paulo, Brazil, [2] Instituto do Coração (InCor), Hospital das Clínicas, Faculdade de Medicina, Universidade de São Paulo (HC/FMUSP), São Paulo, Brazil, [3] Fundação Pró-Sangue Hemocentro de São Paulo, Divisão de Pesquisa – São Paulo, SP, Brazil, [4] Genetics Department, Harvard Medical School, MA, United States, [5] Instituto do Medicina Tropical (IMT), Universidade de São Paulo – São Paulo, SP, Brazil, [6] Cardiovascular Division, Brigham and Women's Hospital, & Harvard Medical School, Boston, MA, United States, [7] Howard Hughes Medical Institute, Chevy Chase, MD, United States

OPEN ACCESS

Edited by:
Alena Pance, Wellcome Sanger Institute (WT), United Kingdom

Reviewed by:
Danilo Ciccone Miguel, State University of Campinas, Brazil
Maria Ana Duhagon, Universidad de la República, Uruguay

***Correspondence:**
Theo G. M. Oliveira, gremen.theo@gmail.com

Specialty section:
This article was submitted to Parasite and Host, a section of the journal Frontiers in Cellular and Infection Microbiology

Received: *25 March 2022*
Accepted: *16 June 2022*
Published: *07 July 2022*

Citation:
Oliveira TGM, Venturini G, Alvim JM, Feijó LL, Dinardo CL, Sabino EC, Seidman JG, Seidman CE, Krieger JE and Pereira AC (2022) Different Transcriptomic Response to T. cruzi Infection in hiPSC-Derived Cardiomyocytes From Chagas Disease Patients With and Without Chronic Cardiomyopathy. Front. Cell. Infect. Microbiol. 12:904747. doi: 10.3389/fcimb.2022.904747

Chagas disease is a tropical zoonosis caused by *Trypanosoma cruzi*. After infection, the host present an acute phase, usually asymptomatic, in which an extensive parasite proliferation and intense innate immune activity occurs, followed by a chronic phase, characterized by low parasitemia and development of specific immunity. Most individuals in the chronic phase remain without symptoms or organ damage, a state called indeterminate IND form. However, 20 to 40% of individuals develop cardiac or gastrointestinal complications at any time in life. Cardiomyocytes have an important role in the development of Chronic Chagas Cardiomyopathy (CCC) due to transcriptional and metabolic alterations that are crucial for the parasite survival and replication. However, it still not clear why some infected individuals progress to a cardiomyopathy phase, while others remain asymptomatic. In this work, we used hiPSCs-derived cardiomyocytes (hiPSC-CM) to investigate patterns of infection, proliferation and transcriptional response in IND and CCC patients. Our data show that *T. cruzi* infection and proliferation efficiency do not differ significantly in PBMCs and hiPSC-CM from both groups. However, RNA-seq analysis in hiPSC-CM infected for 24 hours showed a significantly different transcriptional response to the parasite in cells from IND or CCC patients. Cardiomyocytes from IND showed significant differences in the expression of genes related to antigen processing and presentation, as well as, immune co-stimulatory molecules. Furthermore, the downregulation of collagen production genes and extracellular matrix components was

significantly different in these cells. Cardiomyocytes from CCC, in turn, showed increased expression of mTORC1 pathway and unfolded protein response genes, both associated to increased intracellular ROS production. These data point to a differential pattern of response, determined by baseline genetic differences between groups, which may have an impact on the development of a chronic outcome with or without the presentation of cardiac symptoms.

Keywords: chagas disease, chagas cardiomyopathy, iPSC (induced pluripotent stem cell), *Trypanosoma cruzi (T. cruzi*), RNA-Seq, cardiomyocytes (CMs)

INTRODUCTION

Chagas disease (ChD), also referred as American trypanosomiasis, is a tropical anthropozoonosis traditionally endemic in rural areas of South and Central America where the transmission of *Trypanosoma cruzi* (*T. cruzi*) occurs through the contact with contaminated feces of Triatomine insects (also known as "kissing bugs"). Although the number of new cases and deaths has been decreasing since 1980's, in 2010 ChD was still responsible for approximately 12.000 deaths per year in endemic countries (Lidani et al., 2019), where 6 million people live with the disease according to the Pan American Health Organization (PAHO – paho.org). In the United States, it is estimated that at least 300.000 people have ChD, most of them immigrants from endemic countries (Pérez-Molina and Molina, 2017).

Initially, ChD presents an acute phase in which *T. cruzi* proliferates in high amounts and its presence is easily detected in the blood stream. This phase is rarely symptomatic and can be taken as a common seasonal disease where fever and malaise are two common symptoms (Pérez-Molina and Molina, 2017). The acute phase is followed by the chronic phase in which the parasite vanishes from the circulation and IgG antibodies can be detected by serological tests. The most intriguing aspect of the chronic phase is that while 70% of individuals will remain in an asymptomatic indeterminate (IND) state for life, 30% will develop chronic Chagas cardiomyopathy (CCC) which is the most severe consequence of *T. cruzi* infection and affects individuals after a latency period of 10 to 30 years leading to late-stage heart failure, arrhythmias and thromboembolic events (Ribeiro et al., 2012). Curiously, it is still unclear how low intensity immune response, parasite persistence and cardiac tissue injury and remodeling interact to modulate the disease progression (Rassi et al., 2017).

The investigation of the transcriptional response to *T. cruzi* infection in non-phagocytic cells has been successful in describing the main pathways immediately disturbed by the parasite (ranging from 3 to 72 hours post infection or hpi) and the common responses between different cell types (Li et al., 2016). Within the first 24 hours of infection a broad-spectrum host transcriptional remodeling is important for parasite survival and replication. Cellular alterations such as increased mitochondrial oxidative metabolism, increased protein synthesis and cell cycle arrest were detected in human fibroblasts (Houston-Ludlam et al., 2016; Oliveira et al., 2020). Defense responses through type I interferon and chemokines production were repeatedly observed in fibroblasts, endothelial and smooth muscle cells (Costales et al., 2009) as well as in murine and human primary cardiomyocytes (Libisch et al., 2018).

Although transcriptomic studies using cardiac biopsies from chronic patients were important in defining the inflammatory landscape of CCC, these findings depict a long-term scenario in which many of the initial aspects of the response to the parasite infection cannot be determined. Furthermore, the limitation in obtaining cardiac biopsies, and the intrinsic distinction of heart function, from IND patients precludes a true comparative set-up which could reveal group-specific aspects of chronic ChD susceptibility. Similarly, murine or human cardiac cell lineages used in cellular models do not reveal patient-specific features, leaving important questions about the difference in cardiomyocyte transcriptional response between CCC and IND patients still unanswered.

In this study, we aimed to capture the early transcriptional responses to *T. cruzi* infection by generating human induced pluripotent stem-cell (hiPSC)-derived cardiomyocytes (hiPSC-CM) from both groups of ChD patients and re-infect these cells with the highly virulent *T. cruzi* Y strain for 24 hours, 30 days after differentiation. Our results show that in terms of infection capacity, *T. cruzi* can infect and replicate with the same efficiency inside PBMCs and hiPSC-CM of IND and CCC patients. Transcriptional responses in the first 24 hours of infection, however, revealed a different response against the parasite, with IND cardiomyocytes showing a more orchestrated pattern of innate immune activation and antigen presentation. These results bring new information regarding the capacity of patient-specific cardiomyocytes in dealing with the parasite invasion as well as setting a proper response to infection that is crucial to establish an early regulatory scenario which may have important implications in the chronic phase of ChD.

MATERIALS AND METHODS

Ethics Statement and Patient Selection

This work was approved by the local ethics committee (Comissão de Ética para Análise de Projetos de Pesquisa – CAPPesq – CAAE: 89242218.0.0000.0068). Patients were selected from a cohort of the Instituto de Medicina Tropical (IMT – Universidade de São Paulo). We included patients with at least two confirmed serological tests for ChD. Indeterminate (IND) patients should present normal ECG and chest X-ray in at least

two visits and chronic cardiac (CCC) patients should present cardiomegaly with ECG abnormalities in the absence or presence of left ventricle dysfunction (VEF<30%). Patients with previous history of myocardial infarction or any inherited cardiomyopathy were not included. All patients signed an informed consent. **Supplemental Table S1** shows age and sex information of included individuals as well as the main clinical features of CCC patients.

PBMCs Extraction

Peripheral blood mononuclear cells (PBMCs) were extracted using Vacutainer® CPT™ Tubes (BD) from five IND (IND1 to IND5) and six CCC (CCC1 to CCC6) patients. Briefly, 16 ml of blood were collected in two CPT tubes and centrifuged at 1800 x g for 40 minutes. After separation, the buffy coat was washed two times with PBS 1x and incubated for 15 minutes with erythrocyte lysing buffer. Cells were counted in a hemocytometer and 2.5 to $3x10^6$ PBMCs were frozen per vial.

Trypanosoma cruzi Culture

The Y strain of *T.cruzi* modified to express GFP in the amastigote state (Ramirez et al., 2000) was gently provided by Prof. Sergio Schenkman (Universidade Federal de São Paulo – UNIFESP). *T. cruzi* trypomastigotes were co-cultured with LLC-MK2 cells (*Macaca mulatta*) in RPMI 10% FBS 1% PS in T175 flasks. The culture was daily monitored for the proliferation of intracellular parasites and media was changed every 72hs. New LLC-MK2 cells were added to the culture whenever needed. When high amounts of trypomastigotes were present, the supernatant was collected, centrifuged at 500 x g for 15 minutes and filtered in a 40μm cell strainer for *debris* removal. Trypomastigotes were harvested on the same day of infection assays.

PBMCs Infection and Flow Cytometry Analysis

PBMCs were thawed and plated at 2 $x10^4$ cells/well in 24-well plates with RPMI 10% FBS 1% PS and maintained at 37°C 5% CO_2. A time course of infection was conducted with 5 time points (0, 3, 6, 24 and 48 hpi) in duplicate with a trypomastigote/cell ratio of 10:1 in a final volume of 1 mL. Time points 3, 6 and 24 hpi were defined as the infection period while the 48 hpi time point was defined as the proliferation period. Thus, after 24 hours of infection, the cells from the 48hpi time point were harvested and centrifuged for media change and removal of non-infecting parasites. Experiments were always conducted with one cardiac patient, one indeterminate patient and one non-chagasic control (CTRL) in parallel. A total of five experimental rounds were performed. After infection, cells were centrifuged in PBS 1x and labeled with anti-CD3 PE (T lymphocytes), anti-CD19 PECy5 (B lymphocytes) and anti-CD14 APC (monocytes) for 30 minutes at 4°C. Samples were analyzed in a BD Accuri™ C6 with a minimal threshold of 20.000 events inside the "classical" lymphocyte gate. The infection rate was calculated using the amount of GFP+ events and the replication rate was calculated with the mean intensity of GFP+ across time points. The replication rate between 24 and 48hpi was calculated as the 48/24hpi GFP intensity ratio. Results were generated in GraphPad Prism 8. ANOVA was used for three-group comparisons while T-test was used for pairwise comparisons. A p-value < 0.05 was considered as the statistical cutoff for significance.

hiPSC Production

Human induced-pluripotent stem cells (hiPSC) from three CCC (CCC4, CCC5 and CCC6) and two IND (IND4 and IND5) patients were obtained through erythroblast reprogramming as previously reported (Chou et al., 2011; Dowey et al., 2012). The adjusted protocol was gently provided by Prof[a]. Lygia da Veiga Pereira (Instituto de Biociências, IB/USP). Briefly, PBMCs were thawed and maintained in an erythroid enrichment media for 10 to 12 days. Media was composed of StemSpan (STEM CELL Technologies) supplemented with IGF-1 at 40ng/mL; SCF at 100ng/mL; IL-3 at 10ng/mL and EPO at 2U/mL (R&D systems). Dexamethasone was added at 1μM/mL for lymphocyte depletion. From D-12 to D-3 cells were cultivated at a density of $2x10^6$ cells/well in a 24-well plate. Usually on D-3, the culture was highly enriched for erythroblasts, so the density was changed to $1x10^6$ cells/well and cells were kept in a 6-well plate. When the density reached $2x10^6$ cells/well again, erythroblasts were directed to reprogramming (D0). A total of $1x10^6$ erythroblasts were nucleoporated with 1.25μg of EPI5™ Episomal iPSC Reprogramming Kit (Thermo Fisher) in a Nucleofector 2b (T-016 program) using the Human CD34+ Cell Nucleofector™ Kit (Lonza). At D2, media was changed to DMEM-High 10% FBS with GlutaMax® (Thermo Fisher) and cells were transferred to one well of a 12-well plate containing GelTrex™ (Thermo Fisher) and were adhered to the matrix by centrifugation at 200 x g for 30 minutes. On D3, media was changed for E8 media (Thermo Fisher) supplemented with bFGF (20ng/mL) and Sodium Butirate (NaB, 0,25mM). From this point, E8 media was changed every other day. First colonies usually appeared between D8 and D12 after reprogramming. First colonies were picked around D15. At least three different clones with typical iPSC morphology were characterized for pluripotency markers with immunofluorescence and flow cytometry.

Cardiomyocyte Differentiation

hiPSC-CM were obtained using the WNT-C59 protocol as previously reported (Sharma et al., 2018) with minor adjustments. Before starting the differentiation protocol, we prepared hiPSC by doing at least three long passages (1:15-20 split) followed by three short passages (1:2-3 split) with StemFlex media (Thermo Fisher) supplemented with 10 μM of rho kinase inhibitor (ROCKi). Cells were maintained in 6-well plates through the entire process. When confluence was around 80%, media was changed for RPMI B27- (RB-) supplemented with 9μM of CHIR99021 for 24 hours. The starting day was defined as Day 0 (D0). At D1 cells were washed with PBS 1x and fresh RB- was added to the culture (no CHIR99021). Cells were then kept untouched until D3 when RB- supplemented with 2μM of WNT-C59 (1:5000 dilution) was added to the wells. At D5 WNT-C59 was removed, cells were washed with PBS 1x and fresh RB- was added. At D7, RB- was changed for RPMI B27+ (RB+) with 1% PS. Beating hiPSC-CM were usually observed

between D8 and D10. Once beating cells were observed in several spots of the well, RB+ with no glucose was added to the culture for non-cardiomyocyte removal. Glucose starving was maintained for 2 to 6 days (1 to 3 media changes), depending on the rate of cell death and visual inspection of non-beating or fibroblast-like cells. After the starving period, hiPSC-CM were maintained with RB+ 1% PS until D20, when cells were passaged with Trypsin (Thermo Fisher), filtered on a 100μm cell strainer, counted and evaluated for purity by the quantification of cardiac troponin through flow cytometry (**Supplemental Figure S4**). Cells were plated on 96-well plates at a density of $5x10^4$ cells/well and on 24-well plates at a density of $1x10^6$ cells/well for immunofluorescence and RNA-seq experiments, respectively.

Immunofluorescence Analysis

An immunofluorescence assay was conducted in 5 time points (0, 3, 6, 24 and 48 hpi). hiPSC-CM were incubated with parasites in RB+ 1%PS in a parasite/cell ratio of 10:1. After the period of incubation, cells were washed with PBS 1x and fixed with PFA 4% for 20 minutes at room temperature. Nuclei were stained with DAPI and cells were analyzed in an EVOS™ M7000 Imaging System (Thermo Fisher) at the same day of fixation. Eight random fields of each well were captured and GFP+ amastigotes and stained nuclei were counted in a custom MATLAB (Mathworks Inc.) script developed by our group (data not published). The parasite/nuclei ratio was used as input variable for ANOVA in GraphPad Prism 8.

RNA-Seq Experiment

Day 30 hiPSC-CM were infected with *T. cruzi* in a parasite/cell ratio of 10:1. Two infected and two non-infected replicates were generated per differentiated clone. RNA-seq replicates were maintained in contact with trypomastigotes in RB+ 1% PS for 24 hours at 37°C 5% CO_2. Previous studies have shown that 24 hpi is enough for the Y strain to cause significant transcriptional modifications in human cardiomyocytes and other cell types (Houston-Ludlam et al., 2016; Bozzi et al., 2019). In addition, at 24 hpi no significant intracellular replication has taken place. At 24 hpi cells were washed twice with PBS 1x for extracellular parasites removal and lysed with TRIzol™ reagent (Thermo Fisher) for RNA extraction. Non-infected replicates were maintained in the same condition as infected ones. Library preparation was conducted using the Nextera library preparation method. RNA-Seq libraries were pooled and run on four lanes (one flow cell) using the Illumina NextSeq500 platform. Coverage calculation was adjusted to generate 30–50M reads per replicate. The raw reads were aligned by STAR to human genome (hg38).

Differential Gene Expression and Pathway Enrichment Analysis

Differential gene expression (DE) analysis was conducted with DESeq2 (Love et al., 2014) package in RStudio. Genes with a sum of counts lower than 10 reads were considered as low count genes and were removed before analysis. DESeq2 object was designed considering differentiation batch, group (CCC or IND), time (0 or 24 hpi) and an interaction term for time and group. The IND group and 0 hpi were defined as reference levels. In the present analysis we were particularly interested in genes with a differential response between groups upon *T. cruzi* infection. Thus, we have selected genes with a significant interaction term p adjusted value (padj < 0.05).

Gene Set Enrichment Analysis (GSEA) was carried out with a gene list ranked by the formula |signal(log2FoldChange) x -log10 (padj)| using the gene set enrichment (gse) function of ClusterProfiler (Wu et al., 2021) package. Heat maps were created with Morpheus web-tool (https://software.broadinstitute.org/morpheus) and KEGG pathways were plotted with the Pathview (Luo and Brouwer, 2013) package in Rstudio.

RESULTS

T. cruzi Infection and Replication Efficiency in PBMCs and hiPSC-CM

To establish whether *T. cruzi* infection efficiency was different between IND and CCC patients, we conducted time course infection experiments both in PBMCs and hiPSC-CM. The PBMC infection experiments were analyzed based on the following variables: percentage of GFP+ events over time (parasite infection), mean GFP intensity over time (parasite replication) and GFP 48/24 hpi intensity ratio (to measure the increase in GFP intensity between 24 and 48 hpi). To assure that the number of cells did not differ over time or by cell type, we compared the number of cells analyzed between groups and did not observe any statistical difference. It was possible to observe, however, that monocytes and B lymphocytes tend to diminish in number over time, while T lymphocytes remain practically constant (**Supplemental Figure S1**). Monocytes were the cell type with the highest percentage of GFP+ events over time (**Figure 1**, Panel A) reaching at certain points an infection rate above 50%, while T and B lymphocytes maintain a lower and constant rate of infection. When comparing the number of GFP+ events between the groups for each analyzed cell type it was not possible to detect a significant difference in any of the four time-points of infection.

When comparing the mean GFP intensity between groups for each cell type, it was again possible to observe that monocytes are the cell type with the greatest increase over time (**Figure 1B**), with a significant increase in the mean GFP intensity already at 24 hpi. Interestingly, T lymphocytes show an increasing tendency from 48 hpi onwards, which indicates a later increase in parasite replication compared to monocytes. Again, when comparing the GFP intensity between the groups for each analyzed cell type it was not possible to identify a significant difference at any time of infection. As for the 48/24 hpi GFP intensity ratio we did not observe a significant difference between groups, for any of the analyzed cell types (**Supplemental Figure S2**). However, when comparing the difference of this same variable considering only the cell type, we observed that monocytes have a significantly higher GFP intensity ratio of 48/24 hpi compared to T and B lymphocytes, suggesting different intracellular replication dynamics among these cell types (**Figure 1C**).

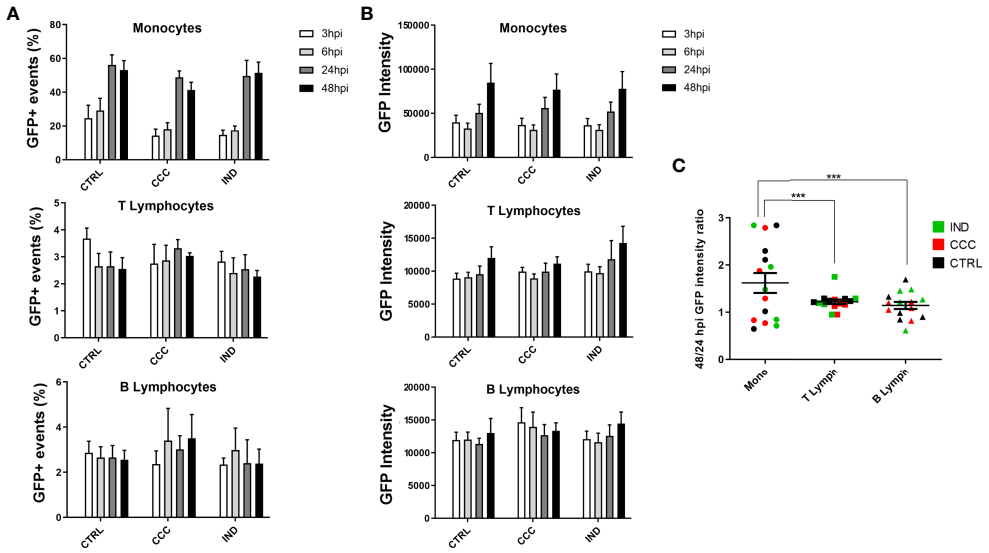

FIGURE 1 | Results from infection assay of PBMCs by flow cytometry with GFP-expressing Y strain. **(A)** The infection rate over time points was analyzed through the percentage of GFP+ events in Monocytes, T and B Lymphocytes. **(B)** The proliferation rate over time points was analyzed through the GFP intensity across times points in Monocytes, T and B Lymphocytes. **(C)** The 48/24 hpi GFP intensity ratio was used to calculate the proliferation between 24 and 48 hpi in Monocytes, T and B Lymphocytes. (n = 5 CCC; 5 IND and 5 Non-infected controls). The symbol *** means $P \leq 0.001$.

The same time-course experiment was performed in hiPSC-CM for both groups, with the readout defined as the number of intracellular amastigotes per cell nuclei. **Figure 2** shows how intracellular amastigotes were detected overtime in immunofluorescence images. Similar to what was used for PBMCs, the interval between 3 to 24 hpi was defined as the *T.cruzi* infection period and the interval between 24 to 48 hpi as the replication period. It was possible to detect GFP+ amastigotes already at 3 hpi and at 48 hpi most of nuclei were surrounded by highly GFP-expressing amastigotes, confirming the increment of GFP intensity overtime. After performing an ANOVA for detecting differences in the increasing parasite/cell ratio, no

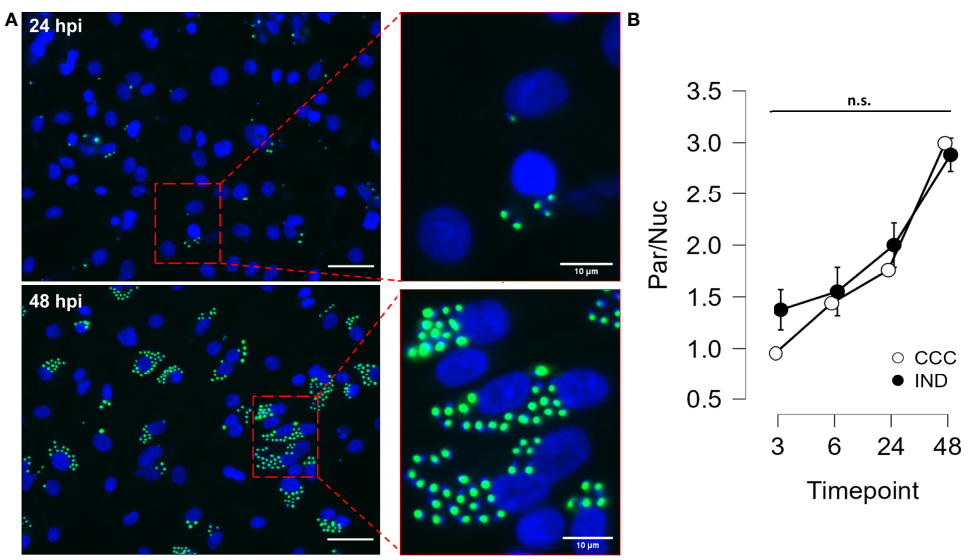

FIGURE 2 | Results from hiPSC-CM infection assay with GFP-expressing Y strain. **(A)** hiPSC-CM were infected with *T. cruzi* Y strain modified to express GFP in the amastigote form. Cell nuclei were stained with DAPI (blue) (Left panel bars = 40µm). **(B)** Time course (3, 6, 24 and 48 hpi) analysis of infection in hiPSC-CM from IND and CCC patients. Nuclei and amastigotes were counted in a custom script and the Parasite/Nucleus ratio was compared along time points. (n = 3 CCC and 2 IND). n.s., not significant.

significant difference was observed between groups at any time point.

RNA-Seq Results

A total of 20 replicates (6 CCC_0hpi, 6 CCC_24hpi, 4 IND_0hpi and 4 IND_24hpi) were sequenced in a single run. In total, 577 million reads were generated with an average of 28.8 million reads per sample. Count distributions per sample are shown in **Supplemental Figure S3**. Reads were checked for quality and adaptor trimming with FASTQC before alignment and count generation. All samples passed QC steps and were used for further analysis. Principal component analysis (PCA) revealed a clone-related pattern of clustering. Interestingly, no differentiation batch effects were observed (**Figure 3A**). PC1 accounted for 50% of the sample's variance, indicating that most of the variability among samples can be explained by phenotype group. Hierarchical clustering show that most clones tend to cluster together paired by time (**Figure 3B**).

GSEA Reveal Group Specific Responses to Infection

In total, 463 DEGs with an adjusted p-value (padj) < 0.05 were selected from the interaction term (time:group) output after DE analysis (from now on we will refer to DEG as those with a significant interaction term). Of these, 395 (215 positive and 180 negative L2FC – **Figure 3C**) had a valid entrez ID and were used for further analysis.

Gene set enrichment analysis (GSEA) was performed to check for group-specific enrichments. At first, we applied the padj <.05 DEGs list to GSEA with Hallmark [MSigDB collections (Liberzon et al., 2015)] gene sets, however no significant associations were found for any condition. Using a cutoff with padj < 0.1 we incremented our DEGs list to 719 genes with a valid entrez ID and ranked the list as mentioned in the methods section. We limited the analysis to a minimum and maximum set size of 5 and 500, respectively, and a maximum of 1000 permutations. Hallmark GSEA revealed three gene sets associated with the CCC group: EM transition (EMT), mTORC1 signaling and unfolded protein response (UPR). Two gene sets were associated with IND: Interferon (IFN) alpha response and gamma response. **Figure 4** shows GSEA plots for significant terms with its FDR values (panels A and C). In total, 28 genes with negative L2FC (IND) and 30 genes with positive L2FC (CCC) were associated to a gene set. **Supplemental Table S2** includes non-significant terms associated with each phenotype.

Figure 5 shows the expression of genes inside the enriched gene sets along the time course of infection. IFN response is a well-known early response to *T. cruzi* infection and, although both groups significantly upregulated IFN response genes the effect of infection resulted in a more acute shifting in the expression of these genes in the IND group. Conversely, all gene sets enriched in CCC suffered a significant downregulation in IND cardiomyocytes after infection. UPR and mTORC1 signaling were upregulated in CCC group as a response to infection while EMT remained stable from 0 to 24 hpi.

The gene list with significant DEGs (padj < 0.05) from the interaction term was submitted to GSEA with Reactome so that we could unravel more specific pathways by which enriched genes were acting. We applied the same parameters for set size and permutation used in the previous analysis. The pattern of association reproduced the Hallmark GSEA results, with immune-related pathways associated with IND and ECM and collagen production associated with CCC. There was an increment of 12 and 9 genes assigned to a pathway for IND and CCC, respectively (**Supplemental Figure S5**). Reactome

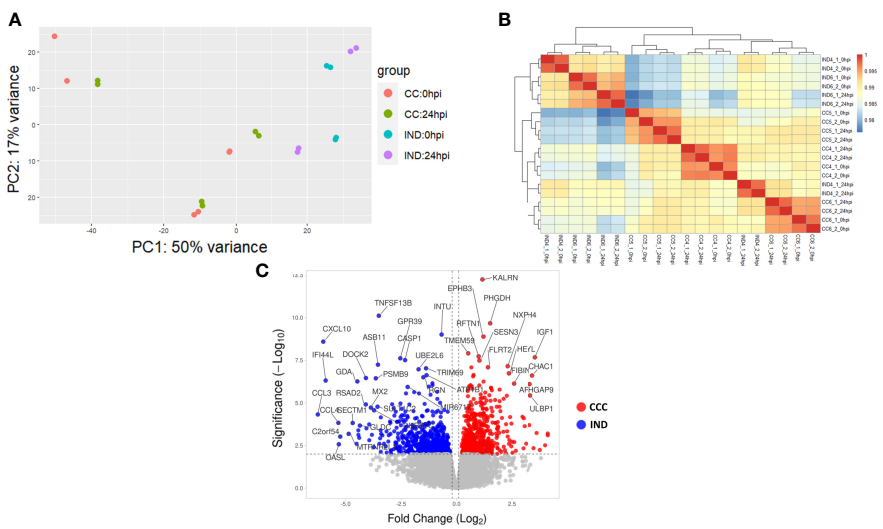

FIGURE 3 | RNA-seq results. **(A)** PCA plot showing the variability among CCC and IND replicates at 0 and 24 hpi (CCC replicates = 6 CCC_0hpi, 6 CCC_24hpi. IND replicates = 4 IND_0hpi and 4 IND_24hpi). **(B)** Hierarchical clustering of replicates. **(C)** Volcano plot showing the L2FC distribution of DEGs in the interaction term output.

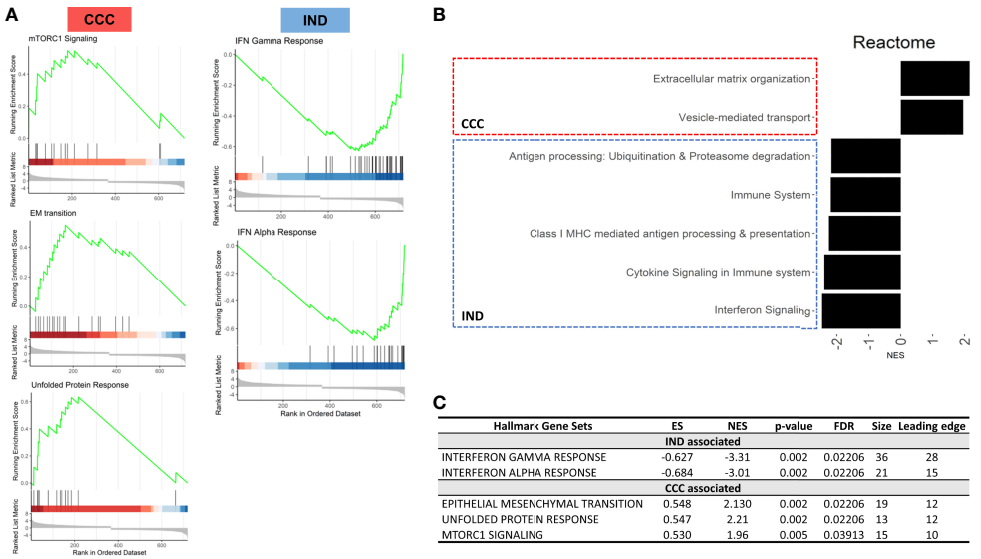

C

Hallmark Gene Sets	ES	NES	p-value	FDR	Size	Leading edge
IND associated						
INTERFERON GAMMA RESPONSE	-0.627	-3.31	0.002	0.02206	36	28
INTERFERON ALPHA RESPONSE	-0.684	-3.01	0.002	0.02206	21	15
CCC associated						
EPITHELIAL MESENCHYMAL TRANSITION	0.548	2.130	0.002	0.02206	19	12
UNFOLDED PROTEIN RESPONSE	0.547	2.21	0.002	0.02206	13	12
MTORC1 SIGNALING	0.530	1.96	0.005	0.03913	15	10

FIGURE 4 | Results from GSEA with Hallmark terms. **(A)** GSEA plots showing the rank distribution of DEGs in Hallmark gene sets and the association with each phenotype (red bars – CCC; blue bars – IND). **(B)** Reactome plot with the NES for the pathways associated to each group. **(C)** Hallmark gene sets associated with each phenotype. ES, Enrichment Score; NES, Normalized enrichment score; FDR, False-discovery rate.

specified not only the association of IFN related pathways with the IND phenotype, but also returned other important processes of immune-cells recruitment and establishment of adaptive immune response such as antigen processing (ubiquitination and proteasome degradation) and class MHC-I presentation. **Figure 4** shows the associated Reactome pathways (Panel B) with normalized enrichment score (NES). The connection plot of leading-edge genes can be found in **Supplemental Figure S6B**.

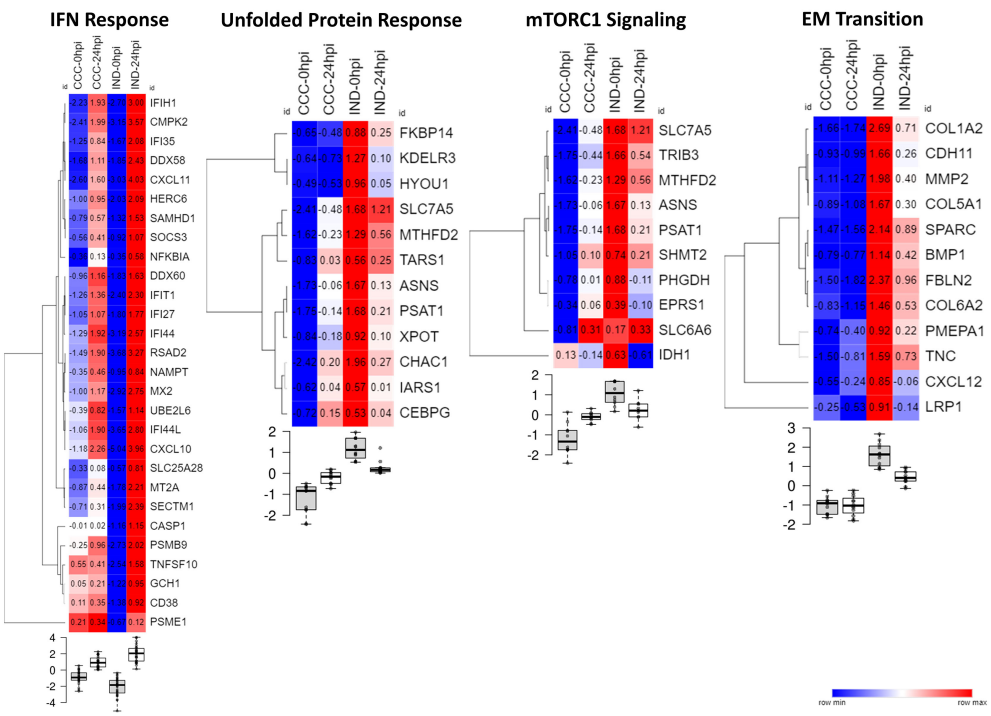

FIGURE 5 | Heat maps showing the normalize expression of significant DEGs across conditions in their respective Hallmark gene set. Samples were normalized by the mean counts. Below each heat map the boxplots show the level of gene expression at every time point (0 or 24 hpi) for each group (CCC or IND).

CCC-Associated DEGs Include Key ER Stress Response and ECM Remodeling Genes

The unfolded protein response is mainly triggered by endoplasmic reticulum (ER) stress. Inside this gene set there were genes related to increase in protein translation (*TARS1*, *IARS1* and *ASNS*) as well as ER stress-mediated apoptosis (*CHAC1* and *CEBPG*). Collagen-production genes (*COL1A2*, *COL6A2, COL5A1* and *COLGALT2)* and other genes related to structural composition of ECM (*TNC*, *FBLN2*, *BMP1* and *MMP2*) are related both to "EM transition" (Hallmark) and "Extracellular-matrix organization" (Reactome). The gene sets "Vesicle-mediated transport" and "extracellular-matrix organization" were connected by *SPARC* and *COL1A2* genes (**Supplemental Figure S6B**), probably indicating vesicle mobilization either in the exporting of ECM components and in the vesicle-mediated entrance of *T. cruzi*. Concordantly, mTORC1 signaling genes up-regulation may contribute to these phenomena once these genes are involved in the formation of the parasitophorous vacuole, a crucial structure in *T.cruzi* internalization and proliferation.

IND-Associated DEGs Include Chemokines, HLA-Coding Genes and Co-Stimulatory Molecules

Among significant DEGs associated to the IND group there were two MHC-coding genes: *HLA-F* (class I) and *HLA-DBQ1* (class II). Furthermore, CD38, a molecule involved in attachment and T cell engagement was also associated. No HLA coding genes were significantly associated with the CCC group. Interestingly, the expression of HLA class II molecules, which is preferentially expressed by professional antigen-presenting cells (pAPCs), was previously reported in PSC-derived cardiomyocytes after IFN-γ induction (Didié et al., 2017). Thus, we decided to check the expression of major HLA I and II coding genes and the main co-stimulatory molecules across conditions (**Figure 6B**). Of all HLA-related genes with positive expression in our dataset, all classical HLA-class I molecules were majorly upregulated in IND cardiomyocytes at 24 hpi while both groups presented upregulation of HLA-class II genes, although no gene was upregulated in both groups. Along with CD38, CD274 (PD-L1) and CD40 also presented a higher expression in the IND group after infection although no significance was observed. The KEGG plot of antigen processing and presentation (**Figure 6A**) shows that both class I and II MHC branches are exclusively associated to IND group DEGs (negative fold change). Two chemokine genes were significantly associated with the IND group: *CXCL10* and *CXCL11*. Both bind to the CXCR3 receptor on the cell surface of activated T lymphocytes and NK cells.

DISCUSSION

The effects of *T. cruzi* infection on host cells have been of major interest and have been studied in several cellular models using HeLa, HUVEC, LLC-MK2, PBMCs, murine and primary human cardiomyocytes, among many others (Duran-Rehbein et al., 2014). One of the main obstacles to understand the transcriptional remodeling of human target tissues, especially in the case of patients with severe organ impairment, is the lack of non-invasive techniques to obtain viable tissues for experimentation. Recently, hiPSC-CM were shown to be a feasible platform to investigate *T. cruzi* infection allowing quick responses regarding the infective behavior of the parasite in human cardiac cells (Bozzi et al., 2019), as well as in the screening of drugs or molecules that can influence its infective and proliferative capacity (da Silva Lara et al., 2018; Sass et al., 2019). Here, we successfully generated hiPSC-CM from chronic ChD patients to study the dynamics of *T. cruzi* invasion and proliferation. Our model was able to replicate the molecular effects of early infection in both asymptomatic and individuals with end-stage cardiomyopathy and, despite the small RNA-seq sample size, we could detect important changes in the transcriptional host response in a patient-specific scenario. Although it is known that the clinical outcomes are also influenced by the parasite strain and that using patient-specific strains would be ideal for establishing a reinfection model, we opted to exclusively use the Y strain of *T. cruzi* due to two main reasons: First, the Y strain was isolated in Brazil and it is a member of the TcII discrete type unit (DTU) which was reported as the most frequent in Brazilian patients (Nielebock et al., 2020). Second, because of its application in other important studies tracing infective/proliferative behavior and the host transcriptional changes during the infection of hiPSC-CM (da Silva Lara et al., 2018; Bozzi et al., 2019).

Using the modified Y strain and specific labeling of PBMCs we could efficiently distinguish the rate of infection and parasite replication in monocytes, T and B lymphocytes from both IND and CCC patients. Although no group differences were found, by comparing the *in vitro* infection rates of T and B lymphocytes in our model with previous works (Velge et al., 1991; Souza et al., 2004), we confirmed the low rate of infection in these cell types, but now showing that this rate is maintained up to 48 hpi without a significant increase (**Figure 1A**), and also confirming the ability of *T. cruzi* to proliferate within these cells (**Figure 1B**).

The rate of monocyte infection reported in the literature is variable, since the protocols vary in the hpi curve and in the cells preparation, hindering the direct comparison of our results (Souza et al., 2004; Souza et al., 2007). Some groups choose to infect only adherent monocytes without the presence of other PBMCs, not exploring the effects of the presence of other cells at the time of infection. Still, data on monocyte infection indicate that *T. cruzi* has a high capacity to infect these cells, and at just 3 hpi the infection rate varies between 29% and 80% (Duran-Rehbein et al., 2014). Our results show that at 3 hpi the preferential infection is also for monocytes, with a significant increase in the infection rate in the subsequent hours, indicating that the presence of other PBMCs in the medium does not seem to alter the initial preference of *T. cruzi*. The professional phagocytic role of monocytes may also be a contributing factor to higher rates of infection at 3 hpi since monocytes are activated

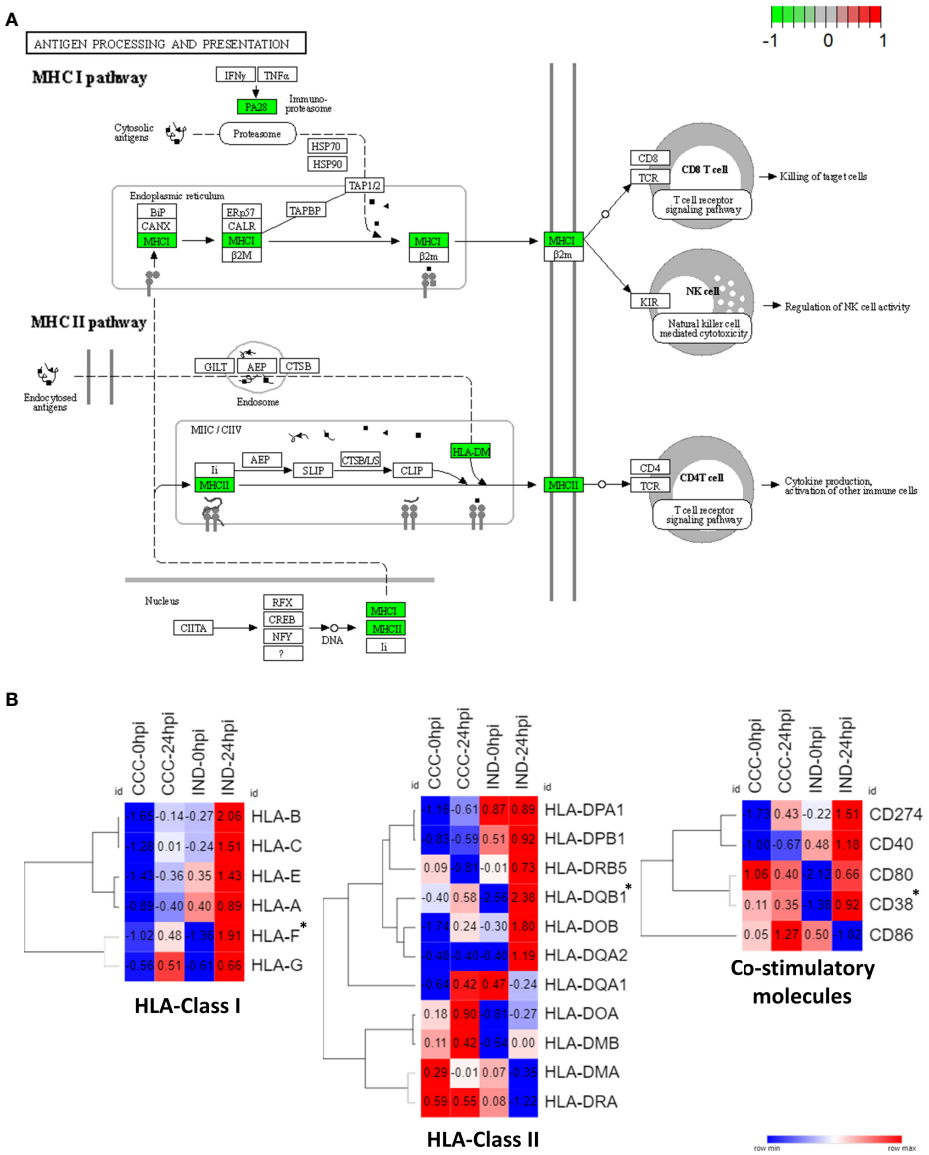

FIGURE 6 | HLA expression pathways in IND and CCC cardiomyocytes. **(A)** DEGs were plotted against KEGG antigen processing and presentation pathway and both MHC I and MHC II pathways had a positive association with IND (green – IND association; red – CCC association). **(B)** Heat maps showing the normalized expression of HLA Class I and Class II genes across all conditions. *DEGs with statistical significance.

through *T. cruzi* molecular patterns, as well as to the sharper drop in the number of cells analyzed over time. In addition, although there is a decrease in the number of monocytes over time, the 48/24 hpi GFP intensity ratio (**Figure 1C**) shows that the replication efficiency of the parasite in monocytes is greater than in T and B lymphocytes, indicating that this type of cell is more conductive to parasitic replication. This last observation is intriguing, taken the known role of these cells in parasite clearance. Further studies aiming at a better understanding of the role of monocytes in early *T. cruzi* infection are warranted.

Interestingly, similar to what was seen in PBMCs, no significant differences were observed between IND and CCC hiPSC-CM when infected with *T. cruzi* (**Figure 2B**). The fact that the efficiency of infection and replication in cardiomyocytes is equal in both groups anticipates that the phenotypic outcomes are unlikely to be a matter of parasitic burden. In view of these results, globally exploring the transcriptional response to infection becomes a feasible option to identify transcriptional responses that could shed light on the molecular strategy adopted to overcome the intracellular disturbances caused by infection and to avoid the parasite segregation in the heart tissue.

Differences in the profile of innate immune response and cardiac function were already described when comparing IND and CCC patients. Results from plasma quantification revealed that IND patients present higher levels of serum IL-10 and IL-17A while CCC patients present higher levels of pro-

inflammatory IL-6, TNF-α and IFN-γ correlated with impaired LV ejection (Sousa et al., 2017). Interestingly, the same pattern of cytokine expression was also seen in blood monocytes from IND and CCC patients when infected *in vitro* with *T. cruzi* (Souza et al., 2004; Sousa et al., 2014). Studies suggest that INF-γ and TNF-α would be the key mediators of a pro-inflammatory scenario that would lead CCC individuals to develop cardiac tissue injury and that a distinct cytokine landscape upon *T. cruzi* infection would be the reason for IND patients to remain asymptomatic (Chevillard et al., 2018). Transcriptomic analysis of cardiac biopsies from end-stage CCC patients revealed INF-γ as the main expressed cytokine, responsible for triggering the expression of several inflammatory genes (Cunha-Neto et al., 2005). This unbalanced scenario could at least in part explain why these patients present more cardiac tissue injury, with the presence of leukocyte infiltration and fibrosis.

Interestingly, the interferon response appeared in our results as a highly sensitive driver in the cellular response to infection with a considerable fraction of genes differently modulated between groups associated to this pathway. Both type I and II IFN cascades are mediated by TLR recognition in the cell and phagosome membranes and were shown to be crucial in the control of *T. cruzi* replication (Koga et al., 2006). In the GSEA the IFN signaling was statistically associated with the IND group which presented a highly homogeneous IFN-related gene expression at 24 hpi (**Figure 5**).

The triggering of IFN-inducible genes in infected cardiomyocytes is crucial to parasite proliferation control, however the shifting from a protective to a deleterious effect is elusive (Ferreira, 2014). Our results point to a protective role of IFN-inducible genes in IND hiPSC-CM in the first 24 hpi, in which a timely and well-orchestrated response to *T. cruzi* infection seemed crucial to establish an efficient crosstalk between innate and adaptive immune response. Accordingly, *HLA-F* (class I) and *HLA-DQB1* (class II) were significantly associated with IND in GSEA results, and all HLA Class I genes were upregulated in this group at 24 hpi (**Figure 6B**). Of note, *HLA-DQB1* gene was previously shown to confer protection against cardiac or digestive disease in Brazilian chagasic patients (Deghaide et al., 1998). Other molecules such as CD38 (significantly upregulated), CD247, CD40 and CD80 were also upregulated in the IND groups at 24 hpi, establishing a proper scenario for leukocyte stimulation and activation. Importantly, CD247 (PD-L1) is known to be a crucial immunological checkpoint involved in the immune regulation of T cells and the treatment with checkpoint inhibitors led to increased leukocyte infiltration and heart damage in *T. cruzi* infected mice (Fonseca et al., 2018).

Interestingly, the expression of ECM-related genes was sensitive to infection in IND cardiomyocytes while remained unchanged in CCC. At early moments of infection, *T. cruzi* is known to interact with components of ECM inducing matrix remodeling and some of the genes associated to "EM transition" (Hallmark) and "ECM organization" (Reactome) are part of the proposed *T. cruzi*-ECM interactome (*MMP2*/*COL1A2*/*COL6A2*/*COL5A1*) regulated by the parasite molecule gp38 (Nde et al., 2012). The regulation of both pro-fibrotic and anti-fibrotic genes was shown in primary human cardiomyocytes at early moments of infection, indicating that cardiac cells are able to respond to the parasite-induced production of ECM components (Udoko et al., 2016). Thus, the downregulation of ECM-related genes by IND cardiomyocytes might indicate a better control in the expression of ECM-remodeling genes, protecting cells from acquiring a pro-fibrotic phenotype.

We could also detect pathways that work in opposite directions after infection. Both mTORC1 signaling and UPR were upregulated in CCC but downregulated in IND at 24 hpi (**Figure 5**). The mTORC1 signaling is crucial in early moments of infection, as shown by Libisch et al. (2018) (Libisch et al., 2018). Briefly, the authors observed that activation of mTORC1 signaling upon infection in human cardiomyocytes induces mitochondrial biogenesis and increased reactive-oxygen species (ROS) production leading to oxidative damage and the development a pathological phenotype. Also, ROS-mediated ER stress is a known phenomenon which causes the misfolding of proteins and activation of UPR (Cao and Kaufman, 2014). Some of the molecules triggered by UPR induce apoptotic signaling, which is the case of CCAAT/enhancer-binding protein (C/EBP) transcription factors. Here, the *CEBPG* gene was upregulated in CCC as result of infection. The knockdown of *CHOP*, a main C/EBP family member highly active under ER stress, in a murine model of cardiac overload resulted in less cardiac dysfunction indicating that C/EBP transcription factors are key regulators of cardiomyocyte apoptosis under pathological stress (Wang et al., 2021).

The production of ROS in infected cells is understood as an active response to parasite elimination, but with the consequence of generating damage to the myocardium as shown in animal models of CCC (Paiva et al., 2018) and also favoring the parasite's survival and causing DNA damage to the host (Florentino et al., 2021). In CCC hiPSC-CM, the activation of the mTORC1 pathways indicates that ROS response is the main strategy for these cells to avoid *T. cruzi* proliferation but with consequences to the correct function to the translational machinery of the cell, leading to the activation of ER-stress response and consequent apoptosis, generating an unfavorable scenario for the functioning and survival of the cell.

CONCLUSION

Although our model does not fully recapitulates the chronic aspects of CCC nor the interplay among the several discrete typing units (DTUs) of *T. cruzi* and innate immune cells and hiPSC-CM, our results point to a differential landscape in which infected IND cardiomyocytes exhibit a favorable immunological profile that promptly upregulates molecules involved in the innate-adaptive crosstalk, leading to a better orchestration of antigen processing and presentation as well as the downregulation of stress-related genes that could lead to oxidative stress and cardiomyocyte damage. On the other hand, an unbalanced homeostatic profile at 24 hpi disfavors the control of infection-induced ROS and ER-

stress in CCC hiPSC-CM that superimposes its ability to develop a specific response to the parasite which in turn results in a long-term dependence of a primary IFN-mediated response. In conclusion, baseline genetic differences modulate group-specific responses to infection which may impact in the presentation of different clinical outcomes.

DATA AVAILABILITY STATEMENT

The datasets presented in this study can be found in online repositories. The name of the repository and accession number can be found below: GEO, NCBI; GSE203525.

ETHICS STATEMENT

The studies involving human participants were reviewed and approved by Comissão de Ética para Análise de Projetos de Pesquisa – CAPPesq - Hospital das Clínicas da Faculdade de Medicina da USP – CAAE: 89242218.0.0000.0068. The patients/participants provided their written informed consent to participate in this study.

AUTHOR CONTRIBUTION

TO and AP conceptualized and designed the study, analyzed data, and wrote the manuscript. CD and ES assisted the conceptualization and design of the study. GV designed experiments and assisted data analysis. JA and LF performed experiments. JS, CS, JK and AP assisted with funding and final manuscript elaboration. All authors contributed to the article and approved the submitted version.

FUNDING

This work was supported by Conselho Nacional de Pesquisa - CNPq (#420168/2016-8) and Fundação de Amparo à Pesquisa do Estado de São Paulo – FAPESP (#17/20593-7, #17/13706-0 and #19/11821-1). AP, CS and JS received funding for this study from NHLBI R01HL133165.

ACKNOWLEDGMENTS

The authors thank Prof. Lygia da Veiga Pereira (IB/USP) for providing the protocols and training for hiPSC production and Prof. Sergio Schenkman (DMIP/UNIFESP) for providing the modified version of *T. cruzi* Y strain. We also thank the Howard Hughes Medical Institute (CE Seidman) and FAPESP (AP, JK, ES).

SUPPLEMENTARY MATERIAL

The Supplementary Material for this article can be found online at: https://www.frontiersin.org/articles/10.3389/fcimb.2022.904747/full#supplementary-material

REFERENCES

Bozzi, A., Sayed, N., Matsa, E., Sass, G., Neofytou, E., Clemons, K. V., et al. (2019). Using Human Induced Pluripotent Stem Cell-Derived Cardiomyocytes as a Model to Study Trypanosoma Cruzi Infection. *Stem Cell Rep.* 12, 1–10. doi: 10.1016/j.stemcr.2019.04.017

Cao, S. S., and Kaufman, R. J. (2014). Endoplasmic Reticulum Stress and Oxidative Stress in Cell Fate Decision and Human Disease. *Antioxid. Redox Signal.* 21, 396–413. doi: 10.1089/ars.2014.5851

Chevillard, C., Paulo, J., Nunes, S., and Frade, A. F. (2018). Disease Tolerance and Pathogen Resistance Genes May Underlie Trypanosoma Cruzi Persistence and Differential Progression to Chagas Disease Cardiomyopathy. *Front. Immunol.* 9, 1–14. doi: 10.3389/fimmu.2018.02791

Chou, B.-K., Mali, P., Huang, X., Ye, Z., Dowey, S. N., Resar, L. M., et al. (2011). Efficient Human iPS Cell Derivation by a Non-Integrating Plasmid From Blood Cells With Unique Epigenetic and Gene Expression Signatures. *Cell Res.* 21, 518–529. doi: 10.1038/cr.2011.12

Costales, J. A., Daily, J. P., and Burleigh, B. A. (2009). Cytokine-Dependent and-Independent Gene Expression Changes and Cell Cycle Block Revealed in Trypanosoma Cruzi-Infected Host Cells by Comparative mRNA Profiling. *BMC Genomics* 10, 1–17. doi: 10.1186/1471-2164-10-252

Cunha-Neto, E., Dzau, V. J., Allen, P. D., Stamatiou, D., Benvenutti, L., Higuchi, M. L., et al. (2005). Cardiac Gene Expression Profiling Provides Evidence for Cytokinopathy as a Molecular Mechanism in Chagas' Disease Cardiomyopathy. *Am. J. Pathol.* 167, 305–313. doi: 10.1016/S0002-9440(10)62976-8

da Silva Lara, L., Andrade-Lima, L., Magalhães Calvet, C., Borsoi, J., Lopes Alberto Duque, T., Henriques-Pons, A., et al. (2018). Trypanosoma Cruzi Infection of Human Induced Pluripotent Stem Cell-Derived Cardiomyocytes: An *In Vitro* Model for Drug Screening for Chagas Disease. *Microbes Infect.* 20, 312–316. doi: 10.1016/j.micinf.2018.03.002

Deghaide, N. H. S., Dantas, R. O., and Donadi, E. A. (1998). HLA Class I and II Profiles of Patients Presenting With Chagas' Disease. *Dig. Dis. Sci.* 43, 246–252. doi: 10.1023/A:1018829600200

Didié, M., Galla, S., Muppala, V., Dressel, R., and Zimmermann, W.-H. (2017). Immunological Properties of Murine Parthenogenetic Stem Cell-Derived Cardiomyocytes and Engineered Heart Muscle. *Front. Immunol.* 8. doi: 10.3389/fimmu.2017.00955

Dowey, S. N., Huang, X., Chou, B.-K., Ye, Z., and Cheng, L. (2012). Generation of Integration-Free Human Induced Pluripotent Stem Cells From Postnatal Blood Mononuclear Cells by Plasmid Vector Expression. *Nat. Protoc.* 7, 2013–2021. doi: 10.1038/nprot.2012.121

Duran-Rehbein, G. A., Vargas-Zambrano, J. C., Cuéllar, A., Puerta, C. J., and Gonzalez, J. M. (2014). Mammalian Cellular Culture Models of Trypanosoma Cruzi Infection: A Review of the Published Literature. *Parasite* 21, 38. doi: 10.1051/parasite/2014040

Ferreira, L. R. P. (2014). Interferon-γ and Other Inflammatory Mediators in Cardiomyocyte Signaling During Chagas Disease Cardiomyopathy. *World J. Cardiol.* 6, 782. doi: 10.4330/wjc.v6.i8.782

Florentino, P. T. V., Mendes, D., Vitorino, F. N. L., Martins, D. J., Cunha, J. P. C., Mortara, R. A., et al. (2021). and Oxidative Stress in Human Cells Infected by Trypanosoma Cruzi. *PloS Pathog.* 17, 1–20. doi: 10.1371/journal.ppat.1009502

Fonseca, R., Salgado, R. M., da Silva, H. B., do Nascimento, R. S., D'Império-Lima, M. R., and Alvarez, J. M. (2018). Programmed Cell Death Protein 1-PDL1 Interaction Prevents Heart Damage in Chronic Trypanosoma Cruzi Infection. *Front. Immunol.* 9. doi: 10.3389/fimmu.2018.00997

Houston-Ludlam, G. A., Belew, A. T., and El-Sayed, N. M. (2016). Comparative Transcriptome Profiling of Human Foreskin Fibroblasts Infected With the

Sylvio and Y Strains of Trypanosoma Cruzi. *PloS One* 11, 1–15. doi: 10.1371/journal.pone.0159197

Koga, R., Hamano, S., Kuwata, H., Atarashi, K., Ogawa, M., Hisaeda, H., et al. (2006). TLR-Dependent Induction of IFN-β Mediates Host Defense Against Trypanosoma Cruzi. *J. Immunol.* 177, 7059–7066. doi: 10.4049/jimmunol.177.10.7059

Liberzon, A., Birger, C., Thorvaldsdóttir, H., Ghandi, M., Mesirov, J. P., and Tamayo, P. (2015). The Molecular Signatures Database Hallmark Gene Set Collection. *Cell Syst.* 1, 417–425. doi: 10.1016/j.cels.2015.12.004

Libisch, M. G., Faral-Tello, P., Garg, N. J., Radi, R., Piacenza, L., and Robello, C. (2018). Early Trypanosoma Cruzi Infection Triggers Mtorc1-Mediated Respiration Increase and Mitochondrial Biogenesis in Human Primary Cardiomyocytes. *Front. Microbiol.* 9. doi: 10.3389/fmicb.2018.01889

Lidani, K. C. F., Andrade, F. A., Bavia, L., Damasceno, F. S., Beltrame, M. H., Messias-Reason, I. J., et al. (2019). Chagas Disease: From Discovery to a Worldwide Health Problem. *J. Phys. Oceanogr.* 49. doi: 10.3389/fpubh.2019.00166

Li, Y., Shah-Simpson, S., Okrah, K., Belew, A. T., Choi, J., Caradonna, K. L., et al. (2016). Transcriptome Remodeling in Trypanosoma Cruzi and Human Cells During Intracellular Infection. *PloS Pathog.* 12, e1005511. doi: 10.1371/journal.ppat.1005511

Love, M. I., Huber, W., and Anders, S. (2014). Moderated Estimation of Fold Change and Dispersion for RNA-Seq Data With Deseq2. *Genome Biol.* 15, 1–21. doi: 10.1186/s13059-014-0550-8

Luo, W., and Brouwer, C. (2013). Pathview: An R/Bioconductor Package for Pathway-Based Data Integration and Visualization. *Bioinformatics* 29, 1830–1831. doi: 10.1093/bioinformatics/btt285

Nde, P. N., Lima, M. F., Johnson, C. A., Pratap, S., and Villalta, F. (2012). Regulation and Use of the Extracellular Matrix by Trypanosoma Cruzi During Early Infection. *Front. Immunol.* 3. doi: 10.3389/fimmu.2012.00337

Nielebock, M. A. P., Moreira, O. C., das Chagas Xavier, S. C., de Freitas Campos Miranda, L., de Lima, A. C. B., de Jesus Sales Pereira, T. O., et al. (2020). Association Between Trypanosoma Cruzi DTU TcII and Chronic Chagas Disease Clinical Presentation and Outcome in an Urban Cohort in Brazil. *PloS One* 15, 1–15. doi: 10.1371/journal.pone.0243008

Oliveira, A. E. R., Grazielle-Silva, V., Ferreira, L. R. P., and Teixeira, S. M. R. (2020). Close Encounters Between Trypanosoma Cruzi and the Host Mammalian Cell: Lessons From Genome-Wide Expression Studies. *Genomics* 112, 990–997. doi: 10.1016/j.ygeno.2019.06.015

Paiva, C. N., Medei, E., and Bozza, M. T. (2018). ROS and Trypanosoma Cruzi: Fuel to Infection, Poison to the Heart. *PloS Pathog.* 14, 1–19. doi: 10.1371/journal.ppat.1006928

Pérez-Molina, J. A., and Molina, I. (2017). Chagas Disease. *Lancet* 6736, 1–13. doi: 10.1016/S0140-6736(17)31612-4

Ramirez, M. I., Yamauchi, L. M., De Freitas, L. H. G., Uemura, H., and Schenkman, S. (2000). The Use of the Green Fluorescent Protein to Monitor and Improve Transfection in Trypanosoma Cruzi. *Mol. Biochem. Parasitol.* 111, 235–240. doi: 10.1016/S0166-6851(00)00309-1

Rassi, A.Jr., Marin Neto, J. A., and Rassi, A. (2017). Chronic Chagas Cardiomyopathy: A Review of the Main Pathogenic Mechanisms and the Efficacy of Aetiological Treatment Following the BENznidazole Evaluation for Interrupting Trypanosomiasis (BENEFIT) Trial. *Mem. Inst. Oswaldo Cruz* 112, 224–235. doi: 10.1590/0074-02760160334

Ribeiro, A. L., Nunes, M. P., Teixeira, M. M., and Rocha, M. O. C. (2012). Diagnosis and Management of Chagas Disease and Cardiomyopathy. *Nat. Rev. Cardiol.* 9, 576–589. doi: 10.1038/nrcardio.2012.109

Sass, G., Tsamo, A. T., Chounda, G. A. M., Nangmo, P. K., Sayed, N., Bozzi, A., et al. (2019). Vismione B Interferes With Trypanosoma Cruzi Infection of Vero Cells and Human Stem Cell-Derived Cardiomyocytes. *Am. J. Trop. Med. Hyg.* 101, 1359–1368. doi: 10.4269/ajtmh.19-0350

Sharma, A., Toepfer, C. N., Schmid, M., Garfinkel, A. C., and Seidman, C. E. (2018). Differentiation and Contractile Analysis of GFP-Sarcomere Reporter hiPSC-Cardiomyocytes. *Curr. Protoc. Hum. Genet.* 96, 21.12.1–21.12.12. doi: 10.1002/cphg.53

Sousa, G. R., Gomes, J. A. S., Damasio, M. P. S., Nunes, M. C. P., Costa, H. S., Medeiros, N. I., et al. (2017). The Role of Interleukin 17-Mediated Immune Response in Chagas Disease: High Level is Correlated With Better Left Ventricular Function. *PloS One* 12, 1–14. doi: 10.1371/journal.pone.0172833

Sousa, G. R., Gomes, J. A. S., Fares, R. C. G., Damásio, M. P. D. S., Chaves, A. T., Ferreira, K. S., et al. (2014). Plasma Cytokine Expression is Associated With Cardiac Morbidity in Chagas Disease. *PloS One* 9, 1–9. doi: 10.1371/journal.pone.0087082

Souza, P. E. A., Rocha, M. O. C., Menezes, C. A. S., Coelho, J. S., Chaves, A. C. L., Gollob, K. J., et al. (2007). Trypanosoma Cruzi Infection Induces Differential Modulation of Costimulatory Molecules and Cytokines by Monocytes and T Cells From Patients With Indeterminate and Cardiac Chagas' Disease. *Infect. Immun.* 75, 1886–1894. doi: 10.1128/IAI.01931-06

Souza, P. E. A., Rocha, M. O. C., Rocha-Vieira, E., Menezes, C. A. S., Chaves, A. C. L., Gollob, K. J., et al. (2004). Monocytes From Patients With Indeterminate and Cardiac Forms of Chagas' Disease Display Distinct Phenotypic and Functional Characteristics Associated With Morbidity. *Infect. Immun.* 72, 5283–5291. doi: 10.1128/IAI.72.9.5283-5291.2004

Udoko, A. N., Johnson, C. A., Dykan, A., Rachakonda, G., Villalta, F., Mandape, S. N., et al. (2016). Early Regulation of Profibrotic Genes in Primary Human Cardiac Myocytes by Trypanosoma Cruzi. *PloS Negl. Trop. Dis.* 10, 1–23. doi: 10.1371/journal.pntd.0003747

Velge, P., Kusnierz, J., Ouaissi, A., Marty, B., Pham, B. N., and Capron, A. (1991). Trypanosoma Cruzi: Infection of T Lymphocytes and Their Destruction by Antibody-Dependent Cell-Mediated Cytotoxicity. *Eur. J. Immunol.* 21, 2145–2152. doi: 10.1002/eji.1830210924

Wang, X., Wei, W., Wu, J., Kang, L., Wu, S., Li, J., et al. (2021). Involvement of Endoplasmic Reticulum Stress-Mediated Activation of C/EBP Homologous Protein in Aortic Regurgitation-Induced Cardiac Remodeling in Mice. *J. Cardiovasc. Transl. Res* 15 340–349. doi: 10.1007/s12265-021-10162-4

Wu, T., Hu, E., Xu, S., Chen, M., Guo, P., Dai, Z., et al. (2021). Clusterprofiler 4.0: A Universal Enrichment Tool for Interpreting Omics Data. *Innovation(China)* 2, 100141. doi: 10.1016/j.xinn.2021.100141

Conflict of Interest: The authors declare that the research was conducted in the absence of any commercial or financial relationships that could be construed as a potential conflict of interest.

Publisher's Note: All claims expressed in this article are solely those of the authors and do not necessarily represent those of their affiliated organizations, or those of the publisher, the editors and the reviewers. Any product that may be evaluated in this article, or claim that may be made by its manufacturer, is not guaranteed or endorsed by the publisher.

frontiers | Frontiers in Cellular and Infection Microbiology

TYPE Mini Review
PUBLISHED 14 November 2022
DOI 10.3389/fcimb.2022.1039520

OPEN ACCESS

EDITED BY
Alena Pance,
University of Hertfordshire,
United Kingdom

REVIEWED BY
Cedric Ghevaert,
University of Cambridge,
United Kingdom
Cecile Crosnier,
University of York, United Kingdom

*CORRESPONDENCE
Timothy J. Satchwell
T.Satchwell@bristol.ac.uk

SPECIALTY SECTION
This article was submitted to Parasite and Host, a section of the journal Frontiers in Cellular and Infection Microbiology

RECEIVED 08 September 2022
ACCEPTED 21 October 2022
PUBLISHED 14 November 2022

CITATION
Satchwell TJ (2022) Generation of red blood cells from stem cells: Achievements, opportunities and perspectives for malaria research. *Front. Cell. Infect. Microbiol.* 12:1039520.
doi: 10.3389/fcimb.2022.1039520

Generation of red blood cells from stem cells: Achievements, opportunities and perspectives for malaria research

Timothy J. Satchwell*

School of Biochemistry, University of Bristol, Bristol, United Kingdom

Parasites of the genus *Plasmodium* that cause malaria survive within humans by invasion of, and proliferation within, the most abundant cell type in the body, the red blood cell. As obligate, intracellular parasites, interactions between parasite and host red blood cell components are crucial to multiple aspects of the blood stage malaria parasite lifecycle. The requirement for, and involvement of, an array of red blood cell proteins in parasite invasion and intracellular development is well established. Nevertheless, detailed mechanistic understanding of host cell protein contributions to these processes are hampered by the genetic intractability of the anucleate red blood cell. The advent of stem cell technology and more specifically development of methods that recapitulate *in vitro* the process of red blood cell development known as erythropoiesis has enabled the generation of erythroid cell stages previously inaccessible in large numbers for malaria studies. What is more, the capacity for genetic manipulation of nucleated erythroid precursors that can be differentiated to generate modified red blood cells has opened new horizons for malaria research. This review summarises current methodologies that harness *in vitro* erythroid differentiation of stem cells for generation of cells that are susceptible to malaria parasite invasion; discusses existing and emerging approaches to generate novel red blood cell phenotypes and explores the exciting potential of *in vitro* derived red blood cells for improved understanding the broad role of host red blood cell proteins in malaria pathogenesis.

KEYWORDS

malaria, red blood cell, reticulocyte, erythropoiesis, stem cell, erythroid, *Plasmodium*

Introduction

Infection of humans by parasites of the genus *Plasmodium* that cause malaria results in approximately 240 million clinical cases and 627,000 deaths per year according to recent statistics (WHO, 2021). Most deaths occur in children under the age of five and more than 90% are concentrated in endemic regions of western and Sub-Saharan Africa. *Plasmodium* parasites possess a complex life cycle that includes stages in both the female Anopholes mosquito and the human liver; however, all of the symptoms that characterise this disease occur as a result of the human blood stage in which successive rounds of invasion, intracellular replication within, egress and reinvasion of circulating red blood cells enables the parasites exponential expansion.

Red blood cells, the body's most abundant cell type and the host for asexual replication of malaria parasites, are highly specialised cells, uniquely adapted for their primary function of delivery of oxygen around the body. They contain no nucleus or intracellular organelles, have a finite lifespan of approximately 120 days, a cytoplasmic protein component dominated by abundant haemoglobin and a unique membrane-cytoskeletal architecture that facilitates deformation and transit through sub-cellular diameter microcapillaries.

In humans red blood cells are generated through a specific process of stem cell differentiation known as erythropoiesis. Proerythroblasts, first derived from multipotent haematopoietic stem cells, undergo a complex process of differentiation that occurs in contact with macrophages in so-called erythroblastic islands within the bone marrow niche. Driven by the actions of the glycoprotein hormone erythropoietin, erythroblasts undergo a series of cell divisions in which the cell dramatically transforms both transcriptionally and morphologically: reducing its volume, haemoglobinising, remodelling its membrane properties, degrading intracellular organelles whilst condensing and ultimately expelling its own nucleus, which is phagocytosed by the erythroblastic island macrophage to leave a nascent anucleate reticulocyte (Figure 1). The reticulocyte exits the bone marrow, entering the circulation where it completes its maturation to generate the characteristically familiar biconcave erythrocyte. In healthy adults, the continuous loss or clearance of the finitely life-spanned red blood cell is maintained in equilibrium through the ongoing production of new red blood cells at a rate of around 2 million cells every second (Palis, 2014).

Efforts to recapitulate the process of erythropoiesis *ex vivo* with the ultimate goal of producing *in vitro* derived red blood cells as a transfusion product have been longstanding and varied. Myriad approaches that address the key obstacles of efficient terminal differentiation and enucleation, sustainability, yield, scalability and cost have been and continue to be developed to this end (Lim et al., 2021; Pellegrin et al., 2021). For the malaria research community, enabled access *ex vivo* to invasion susceptible erythroid cells of increasing interest such as reticulocytes and erythroblasts in quantities amenable to study offers new opportunities for insight. Perhaps most excitingly however the capacity for derivation of red blood cells from their nucleated precursors *ex vivo* has opened the door to genetic manipulation of red blood cells and the opportunity for targeted exploration of the role of host red blood cell proteins in multiple aspects of malaria pathogenesis.

This review will highlight applications of erythroid stem cell biology to the study of malaria conducted to date, discuss alternative approaches for the generation of *in vitro* derived erythroid and red blood cells, their respective advantages and disadvantages and highlight challenges and opportunities in the application and use of such cells for malaria studies.

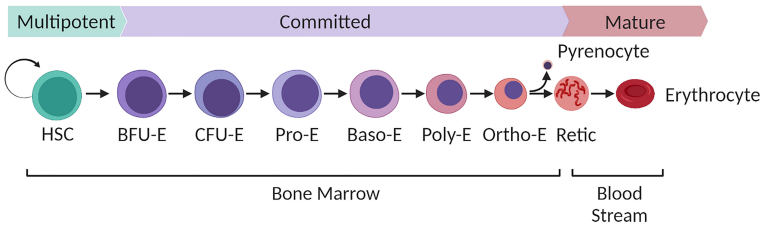

FIGURE 1
Overview of human bone marrow adult definitive erythropoiesis. Multipotent haematopoietic stem cells with long term self-renewal capacity differentiate along a continuum of cell stages defined by their expansive capacity, degree of commitment to the erythroid lineage and morphological characteristics as illustrated. Burst forming units (BFU-E), the earliest committed erythroid cells expand predominantly in response to stem cell factor with the combined synergistic influence of erythropoietin driving continued proliferation of Colony forming units (CFU-E). Terminal differentiation of resultant proerythroblasts to enucleated reticulocytes takes place within the bone marrow niche within erythroblastic islands that consist of multiple differentiating erythroblasts docked to a central macrophage. Terminal differentiation is characterised by progression through a series of morphologically defined stages (proerythroblast, basophilic erythoblast, polychromatic erythroblasts, orthochromatic erythroblast and reticulocyte). The process is characterised by loss of cellular volume, haemoglobinisation, expression of erythroid specific genes, nuclear condensation, organelle degradation and extrusion of the condensed nucleus (pyrenocyte) to generate a nascent reticulocyte. The pyrenocyte is phagocytosed by the macrophage and the reticulocyte enters the bloodstream, completing its maturation to definitive biconcave erythrocyte in the circulation over the subsequent 24-48 hours. Figure created with BioRender.com.

In vitro erythropoiesis – Primary cell models

Although multiple sources of erythroid precursors have since been demonstrated, with different degrees of efficiency and success, to undergo terminal differentiation, the most widely applied approach thus far utilises primary haematopoietic stem cells isolated from bone marrow, umbilical cord or peripheral blood. Expansion of a subset of stem cells, enriched initially through CD34+ cell isolation (Giarratana et al., 2005; Giarratana et al., 2011; Griffiths et al., 2012) or expanded directly from peripheral blood mononuclear cells (Van Den Akker et al., 2010) using a cocktail of growth factors that include erythropoietin, interleukin 3 and stem cell factor allows for the expansion of large numbers of proerythroblasts that can be differentiated to generate enucleated reticulocytes (young red blood cells). Reticulocytes generated using this approach exhibit similar characteristics to *in vivo* derived reticulocytes (Giarratana et al., 2011; Griffiths et al., 2012; Moura et al., 2018; Heshusius et al., 2019), undergo maturation to biconcave erythrocytes upon transfusion (Giarratana et al., 2011; Kupzig et al., 2017) and showed favourable circulatory half-life in a proof of principle human clinical trial (Giarratana et al., 2011).

Crucially, in the context of malaria, reticulocytes derived through *in vitro* culture of primary HSCs have been demonstrated in multiple studies to support invasion by malaria parasites *Plasmodium falciparum* (Tamez et al., 2009; Bei et al., 2010; Fernandez-Becerra et al., 2013; Egan et al., 2015) and plasmodium vivax (Panichakul et al., 2007; Noulin et al., 2012; Roobsoong et al., 2015; Kanjee et al., 2021) with several of these studies also reporting successful invasion of late stage nucleated orthochromatic erythroblasts.

Sustainable sources of erythroid cells

Whilst there are many advantages to the use of primary HSCs, the finite proliferative capacity of this cell source, challenges of efficient genetic manipulation and need for repeated transductions between experimental cultures each from a new donor source have encouraged the search for more sustainable sources of erythroblasts.

Induced pluripotent stem cells

The development of methodology allowing for the reprogramming of somatic cells by expression of four transcription factors (Oct4, Sox2, c-Myc and Klf4) to pluripotency was a landmark in stem cell biology (Takahashi et al., 2007; Yu et al., 2007). The initial promise that accompanied the development of induced pluripotent stem cells (iPSC) that could be directed into the erythroid lineage as a limitless robust source of *in vitro* derived red blood cells however has yet to be fulfilled. Conceptually iPSC cell lines offer a level of sustainability, versatility and genetic tractability that makes them a valuable alternative to primary HSCs. However, difficulties associated with variation between lines, persistence of embryonic and/or fetal haemoglobin, low rates of expansion, incomplete differentiation and poor enucleation as well as the complexity of protocols required to differentiate such cells have plagued the quest for iPSC generated red blood cells (Dias et al., 2011; Trakarnsanga et al., 2014; Focosi and Pistello, 2016). Efforts to improve methodologies for the derivation of such lines and their subsequent differentiation remain a highly active area of research (Bernecker et al., 2019; Hansen et al., 2019; Lim et al., 2021), however application of such lines for generation of cells suitable for malaria studies so far is extremely limited (Pance et al., 2021).

Immortalised erythroid cell lines

Generation of immortalised erythroblast cell lines, capable of infinite proliferation whilst retaining the capacity to undergo terminal erythroid differentiation and enucleation has presented a holy grail within the erythroid biology research community. Such lines could provide a sustainable source of isogenic erythroid precursors, be readily genetically manipulated, selected or clonally screened for the derivation of modified sublines and cryopreserved for long term and repeated experimentation. Immortalisation at a committed stage of erythropoiesis also reduces the culture time required to obtain reticulocytes, which for culture from HSCs takes approximately 18-21 days.

Retention of capacity for complete terminal differentiation whilst maintaining a state of continuous proliferation is a significant biological and technological difficulty. Long established erythroleukemic cell lines such as K562 (Lozzio and Lozzio, 1975) and HEL cells do not faithfully recapitulate aspects of normal erythropoiesis including the key step of enucleation (Kanjee et al., 2017) and thus are not capable of generating cells suitable for malaria studies. Some such lines are receptive of chemical induction to haemoglobinise and/or undertake stunted differentiation. The JK-1 cell line for example can be induced to generate nucleated erythroblasts with a polychromatic erythroblast-like morphology that notably support invasion by *P. falciparum* (Kanjee et al., 2017). Readily genetically manipulatable, these cells provide a means of insight into requirement of host receptors for successful attachment and invasion and were employed to investigate a functional association between host receptors basigin and CD44 during *P. falciparum* invasion. Nevertheless, in interpreting effects or excluding contribution of proteins

using this nucleated cell model it is important to appreciate that cytoplasmic and membrane composition as well as context and presentation of proteins differs between cells pre and post enucleation and care must be taken in extrapolating mechanisms to circulating red blood cells. JK-1 cells do not support further parasite development beyond initial invasion excluding their use to study other aspects of parasite development and pathology.

In 2017, Trakarnsanga et al. reported the first adult human immortalised erythroblast cell line capable of undergoing terminal erythroid differentiation and enucleation to generate functional adult reticulocytes that express beta globin (Trakarnsanga et al., 2017). Unlike erythroleukemic cell lines, BEL-A cells were immortalised by expression of a doxycycline inducible HPV16 E6/E7 construct in healthy adult bone marrow CD34+ HSCs using an approach first employed by Kurita et al. for the generation of HIDEP (iPSC-derived) and HUDEP (cord blood derived) erythroid progenitor cell lines (Kurita et al., 2013).

BEL-A cells can be maintained in continuous expansive culture through supplementation with erythropoietin, stem cell factor, dexamethasone and doxycycline and can be induced to undergo differentiation by transition to a differentiation media that includes erythropoietin, human serum and holotransferrin and through the removal of doxycycline yielding a mixed culture comprising apoptosed cells, orthochromatic erythroblasts and enucleated reticulocytes (Trakarnsanga et al., 2017; Hawksworth et al., 2018). Reticulocytes derived through BEL-A cell differentiation can be purified by leukofiltration and are proteomically equivalent to reticulocytes derived from primary HSCs (Trakarnsanga et al., 2017).

Whilst an obsession with 'enucleation percentages' that do not incorporate variations in cell expansion during differentiation, viability and lineage purity between different systems and cell lines is often unhelpful (Daniels et al., 2020), current literature suggests this adult bone marrow derived erythroblast line to give the greatest reticulocyte yield amongst similar equivalents (Kurita et al., 2013; Kurita et al., 2019; Scully et al., 2019; Daniels et al., 2020).

Unquestionably rates of conversion of orthochromatic erythroblasts derived from cell lines to reticulocytes at present fail to match those observed in primary HSC derived cells. This is perhaps unsurprising given the tight regulation of cell cycle involved in both cell replication and enucleation (Daniels et al., 2021; Wang et al., 2022) and the requirement for its dysregulation in order to facilitate erythroblast immortalisation (Daniels et al., 2021). However, despite this, the sustainable nature of this erythroblast source and the opportunity for sophisticated genetic manipulation that it enables allows several advantages as an alternative for generation of novel host cell models as discussed below.

A route to the inaccessible

New insight into the role of erythroblast infection

The capacity for malaria parasites to infect cells within the erythroid lineage that are not definitive circulating erythrocytes has long been recognised (Marchiafava and Bigmani, 1894; Craik, 1920; Shushan and Adams, 1937). Increased tropism for (in the case of *P. falciparum* (Wilson et al., 1977; Pasvol et al., 1980)) and restricted infection of (in the case of *P. vivax* (Craik, 1920; Hegner, 1938)) reticulocytes has been accepted for decades. Observations of parasitised erythroblasts in bone marrow was reported as early as 1894 (Marchiafava and Bigmani, 1894; Feldman and Egan, 2022). Only more recently however have questions been raised as to the possible reasons for and implications behind infection of more immature erythroid cells. One reason for this is the difficulties associated with obtaining immature erythroid cells in quantities amenable to controlled invasion studies *ex vivo*.

In vitro culture of erythroid cells has allowed for the generation of proerythroblasts and subsequent intermediately differentiated erythroblasts that can be exposed to malaria parasites for tracking of both host and parasite cellular development. In 2009 Tamez and colleagues used *in vitro* derived erythroid cells to assess stage specific susceptibility of human erythroblasts to *P. falciparum* infection, reporting efficient invasion and intracellular development of parasites within orthochromatic erythroblasts (Tamez et al., 2009).

More recently, Neveu et al. employed the same approach to investigate the reported presence of sexual stage gametocytes in bone marrow and the prospective role of erythroblast infection as an enabler of gametocytogenesis (Neveu et al., 2020). In their study, Neveu and colleagues demonstrate that nucleated polychromatic erythroblasts support immature (sexual stage) gametocyte development from stage I to IV for 8 days leading to the production of mature gametocytes within reticulocytes as both parasite and host cell continue to differentiate. Gametocyte development was observed to slow the differentiation of the host erythroid cell, increasing the period in which the cell remains nucleated to complete its development prior to enucleation and the release of mature gametocyte containing reticulocytes into the circulation for subsequent transmission.

Gametocytogenesis is known to involve extensive remodelling of host cell properties and co-option of host protein components (Tiburcio et al., 2012; Tiburcio et al., 2015; Neveu and Lavazec, 2019). The nucleated erythroid cells in which this newly identified aspect of gametocytogenesis takes place however exist only within the experimentally inaccessible bone marrow in humans. The demonstration that *in vitro* derived erythroblasts recapitulate this intriguing process thus

provides a window to study this complex aspect of malaria pathogenesis by application of stem cell biology to malaria as well as a potential *ex vivo* model for putative drug screening approaches. Exploitation of new tools that allow for genetic manipulation of these host cells in addition to cellular resources and lines generated in other areas offers much potential for future insight in this area (Figure 2).

The much-sought reticulocyte

The widely accepted endpoint of most successful *in vitro* erythroid culture systems is the youngest class of circulating red blood cells, otherwise known as reticulocytes (Giarratana et al., 2011; Griffiths et al., 2012; Shah et al., 2014; Heshusius et al., 2019; Pellegrin et al., 2021; Bernecker et al., 2022). The immediate precursor to the mature biconcave erythrocyte, the term reticulocyte describes enucleated cells (of evolving maturity) that are generated following extrusion of the erythroblast condensed nucleus (pyrenocyte) and *in vivo* exit the bone marrow to enter the bloodstream and circulate the body, remodelling their membrane to achieve biconcavity as they do so. Although able to effectively function in the same way as the slightly more mature definitive erythrocyte, reticulocytes are larger in size, contain residual RNA (classically detectable with nucleic acid binding dyes such as thiazole orange) and retain expression of the transferrin receptor CD71 (at varying levels) that is lost progressively during maturation (Malleret et al., 2013; Ovchynnikova et al., 2018; Stevens-Hernandez and Bruce, 2022).

Reticulocytes can be successfully invaded by a broad range of malaria parasites including *P. falciparum*, *knowlesi*, *ovale* and *vivax* (Mcqueen and Mckenzie, 2004). *P. falciparum*, which is responsible for the most severe form of malaria exhibits a variably reported preference for reticulocytes (Wilson et al., 1977; Pasvol et al., 1980; Lim et al., 2013), this may reflect the increased surface area for attachment, differences in membrane tension or energetic state of these newly generated cells. *P. vivax* invasion in contrast is restricted to these more immature red blood cells, which account for just 0.5-1% of circulating red blood cells. Since reticulocytes can be invaded by multiple species of *Plasmodium* (even where essential host surface receptors required differs), they provide an extremely valuable model to generate insight into surface receptor independent, or downstream aspects of malaria parasite invasion and host protein co-option that may be conserved across species.

For the study of *P. vivax* invasion, access to reticulocytes in sufficient quantity and of sufficient levels of purity to be useful for invasion studies has proved a major obstacle for many years. The capacity for *in vitro* stem cell differentiation to derive relatively large, pure populations of these cells from a single donor without the need to pool samples (e.g. from multiple cord blood units) has already recently yielded insight into variation in receptor reliance that exists between strains (Kanjee et al., 2021).

Famously, the study of *P. vivax* has been hampered by the absence of the kind of *in vitro* system for continuous maintenance of parasites in culture with which Trager and Jensen revolutionised *P. falciparum* research (Trager and Jensen, 1976). The recent demonstration of sustained *P. vivax* blood stage infection and transmission in a humanised mouse model with human HSPC transplantation is an exciting development (Luiza-Batista et al., 2022b). The observation that much of the parasite biomass (comprising asexual and in particular sexual parasite stages) occurred in the bone and thus the prospective importance of nucleated erythroblast infection adds further intrigue and potential for *in vivo* insights. Similarities between *P. knowlesi* and *vivax* have also been exploited as a means for screening *P. vivax* blood stage malaria candidates (Ndegwa et al., 2021). Despite these advances, the drive for a continuous culture system to propagate *P. vivax* remains. The complexities and obstacles to establishment of such a system are manifold, likely extending beyond solely the requirement for large numbers of permissive reticulocytes (elegantly reviewed elsewhere (Bermudez et al., 2018; Gunalan et al., 2020; Thomson-Luque and Bautista, 2021)). Success in continuous propagation of *P. vivax ex vivo* in reticulocytes of any source has been minimal. Clearly however, in the ability to generate reticulocytes (and earlier erythroid cells) that are susceptible, at least to invasion, by *P. vivax*, stem cell biology has an important role to play whether directly or indirectly in any future development of such a system (Figure 2).

Manipulating host protein expression

Historically, studies of malaria parasite invasion of the red blood cell have focused predominantly upon identification of the proteins on the surface of the host red blood cell (Salinas and Tolia, 2016; Satchwell, 2016) and more fervently, the merozoite itself, that mediate attachment, potentially providing targets for vaccine design (Beeson et al., 2016). Elegant use of proteases, blocking antibodies and the identification and study of rare naturally occurring red blood cell phenotypes with receptor mutations or null phenotypes have provided valuable information regarding the requirements for and functional redundancy of individual receptors and recent years have seen the reporting of a new swathe of receptors with implied or demonstrated roles in merozoite attachment and invasion (Tham et al., 2010; Crosnier et al., 2011; Bhalla et al., 2015; Egan et al., 2015; Egan et al., 2018; Olivieri et al., 2021). However, there remains much that we do not understand regarding the contribution of host proteins both at and beneath the surface of the red blood cell to this process.

Perhaps the biggest obstacle to elucidation of the function and contribution of red blood cell proteins in malaria infection is

the inability to manipulate protein expression in the genetically intractable anucleate erythrocyte. Previous reliance upon the identification of often vanishingly rare naturally occurring phenotypes to provide insight is inefficient and precludes hypothesis driven investigation of host protein involvement in invasion. The capacity to derive reticulocytes (young red blood cells) that are susceptible to invasion by malaria parasites through *in vitro* culture and differentiation of haematopoietic stem cells (Tamez et al., 2009; Bei et al., 2010; Fernandez-Becerra et al., 2013; Noulin et al., 2014; Egan et al., 2015) unlocks new possibilities previously inaccessible to red blood cell biologists.

Ex vivo access to nucleated erythroid progenitor cells (from various sources as outlined in this review) allows for the genetic manipulation of cells, inducing alterations to protein expression that can be retained during subsequent terminal erythroid differentiation to produce enucleated red blood cells with novel phenotypes. As improvements in erythroid culture methodology and advances in genetic manipulation and gene editing approaches have boomed over the last decade, so the level of sophistication of this approach has, and continues to increase.

Primary cell successes so far

In 2010 Bei et al. exploited lentiviral transduction of primary CD34+ HSCs to express shRNA for specific depletion of the host EBA175 binding receptor Glycophorin A (Bei et al., 2010). By differentiating these transduced cells, the authors were able to derive reticulocytes with an 80% reduction in expression of GPA that exhibited substantially reduced invasion compared to control by *P. falciparum*, confirming the important role played by this protein and validating the approach for host focused studies of invasion receptor requirements. The same approach was used as part of the seminal identification of basigin as the

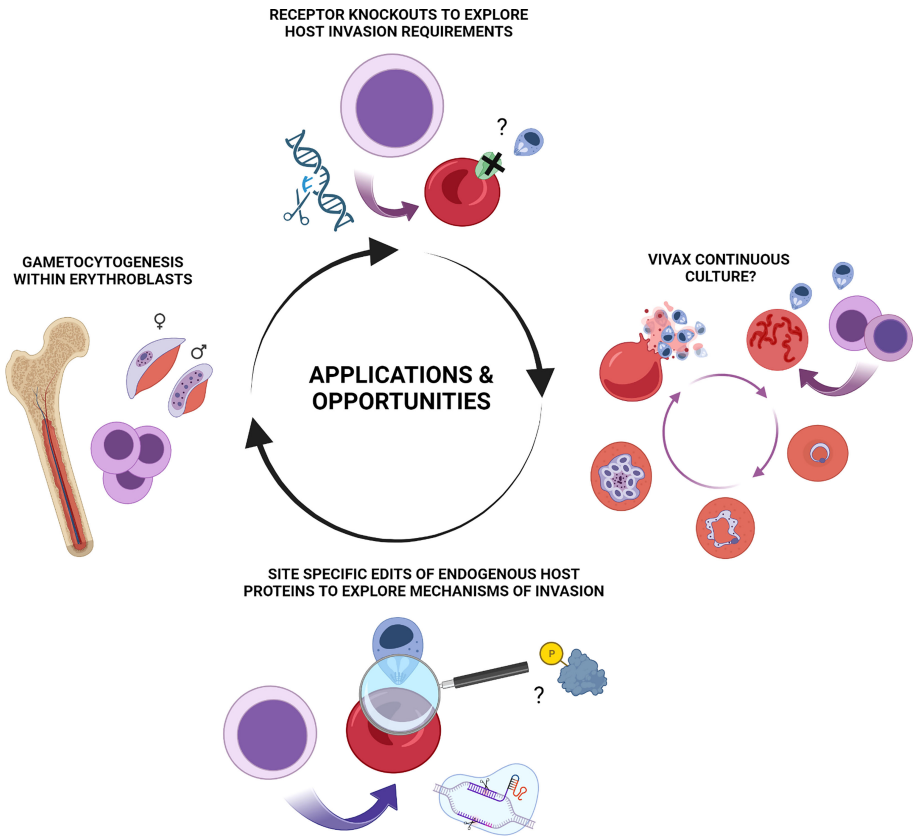

FIGURE 2
Summary of applications and potential opportunities for erythroid stem cell biology to study of malaria pathogenesis. Illustrative summary of applications and opportunities which include generation of novel *in vitro* derived red blood cell phenotypes for exploration of host protein contribution to invasion, host cell remodelling and other aspects of pathogenesis of blood stage *Plasmodium falciparum* and Plasmodium vivax infection. CRISPR-mediated NHEJ mediated knock outs, lentiviral rescue experiments and HDR mediated site-specific editing of endogenous loci are each applicable to *in vitro* erythroid cultures. Emerging and future opportunities include exploration of nucleated erythroblasts as a preferential host environment for gametocytogenesis and the long-standing enigma and quest for a means of continuous *ex vivo* propagation of *Plasmodium vivax*. Figure created with BioRender.com.

essential PfRh5 binding receptor necessary for successful *P. falciparum* invasion (Crosnier et al., 2011), by Niang and colleagues to explore GPC-STEVOR binding and rosetting (Niang et al., 2014) and was further expanded by Egan et al. who employed an shRNA library screen to identify roles for CD55 and CD44 in invasion (Egan et al., 2015).

Derivation of *in vitro* cultured reticulocytes from $CD34^+$ cells in combination with shRNA provides a powerful system for the identification of candidate receptors important in invasion (Egan et al., 2015). However, the finite proliferative capacity of primary haematopoietic stem cells, necessitating repeat transduction between experiments and limiting selection time, together with the incomplete depletion of receptor expression by shRNA, imposes limitations to the complexity of experiments that can be performed using this approach. Development of sustainable enucleation competent immortalised sources of erythroid cells accompanied by the explosion in CRISPR-Cas9 mediated gene editing advancements have gone a long way toward overcoming some of these issues, though challenges do remain.

Modified cell lines

One of the major benefits of cell lines over primary cells is the relative ease with which such cells can be manipulated at the genetic level. Expanding BEL-A cells can be lentivirally transduced with high efficiency (Trakarnsanga et al., 2017), are amenable to CRISPR-Cas9 mediated gene editing for the generation of stable clonal cell lines [evidenced through the generation of reticulocytes with knock out of individual and multiple blood groups (Hawksworth et al., 2018; Satchwell et al., 2019)]. Whilst the karyotypic abnormalities and possibility of genetic drift intrinsic to immortalised cell lines is a consideration in gene editing of such cells, the fact that both edited and unedited sublines derive from the same donor eliminating the impact of donor variability and polymorphisms between experiments is an additional advantage. Leukofiltered purified BEL-A derived reticulocytes were demonstrated to support both invasion by and complete intracellular development and egress of *P. falciparum* at rates equivalent to that of primary CD34+ HSC derived reticulocytes (Satchwell et al., 2019). CRISPR mediated knockout of basigin and lentiviral complementation studies were further employed by Satchwell et al. (Satchwell et al., 2019), validating this cell system as a means for interrogation of host protein requirements for successful *P. falciparum* invasion and excluding a requirement for the basigin cytoplasmic domain in invasion. Orthochromatic erythroblasts derived from a similarly immortalised line (EJ) were found to support invasion by both *P. falciparum* and *P. vivax*, albeit less permissively than primary erythrocytes and reticulocytes respectively (likely a reflection of differences in host membrane-cytoskeletal protein context and membrane properties of these more immature cells). DARC (Duffy) knockout and re-expression abrogated and rescued invasion by *P. vivax* respectively (Scully et al., 2019).

Future opportunities

To date, most insight derived through genetic manipulation of *in vitro* derived red blood cells has come through depletion of expression of host cell surface receptors, first by shRNA (Bei et al., 2010; Egan et al., 2015) and more recently through CRISPR-Cas9 non homologous end joining (NHEJ) mediated gene knockout (Kanjee et al., 2017; Satchwell et al., 2019; Scully et al., 2019; Shakya et al., 2021). In facilitating the knock-down or knockout of receptors for which naturally occurring null phenotypes do not exist or are extremely rare this approach has tremendous value. For studies of *P. vivax*, the ability to generate invasion susceptible reticulocytes (and erythroblasts) and to knock out candidate receptors should increase our understanding of the repertoire of host cell proteins that may be involved in invasion by this species.

As technology and methodologies advance however, so too do the possibilities for further insight using stem cell derived red blood cells. By complementing a BSG knockout (KO) line with a wild type and truncated BSG open reading frame Satchwell and colleagues were able to expand upon the use of KOs alone to interrogate the requirement for a specific intracellular receptor domain for the first time (Satchwell et al., 2019). Expansion of this knock out and mutant rescue approach for dissection of the requirements of different host protein components required for successful invasion will be of future interest. Further, active development of successful protocols for homology directed repair based 'knock ins', enabled by the ability to screen immortalised erythroblast clones for site specific edits is an exciting new frontier that paves the way for a more refined dissection of the role played by red blood cell proteins in *Plasmodium* invasion and development.

Site specific requirements of host cell proteins in malaria parasite invasion, development and host remodelling have been widely documented and postulated, with many as yet unidentified contributions undoubtedly still to be uncovered. These range from single nucleotide polymorphisms, sites of glycosylation (Goerdeler et al., 2021) and palmitoylation (Kumari et al., 2022) of receptors to phosphorylation sites within membrane and cytoskeletal adaptor proteins. By enabling their alteration (deletion, disruption or replacement with phospho-modification incompetent residues for example),

immortalised erythroid cell lines allow for the role of such sites to be dissected within a true cellular context, providing a powerful tool for new mechanistic insight. Interrogation of the role of specific domains, regulatory sites and residues on endogenously expressed host membrane and cytoskeletal proteins (including exploration of the role of the swathe of reported post-translational modifications associated with invasion (Bouyer et al., 2016; Zuccala et al., 2016; Aniweh et al., 2017; Sisquella et al., 2017) and their relevance to the induction of transient host cytoskeletal clearance (Zuccala and Baum, 2011)) can inform our understanding of malaria pathogenesis and contribute to the increased acceptance of and search for potential host directed therapeutic opportunities (Adderley et al., 2020; Chien et al., 2021; Wei et al., 2021) (Figure 2).

Challenges

For all the exciting opportunities for novel insight use of *in vitro* derived red blood cells present for malaria research, their application to such studies is not without its practical challenges. Manipulating erythroblasts with a view to generation of enucleated red blood cells must consider the need to ensure that the programme of differentiation and enucleation is not compromised, and pleiotropic effects of alterations carefully assessed and considered.

Where donor red blood cells are plentiful and easily accessible, derivation of *in vitro* derived red blood cells, particularly those that have undergone genetic manipulation represents a considerable investment of labour and resource. It is not always possible (or rather, feasible) to replicate assays that may be considered routine using donor red blood cells. Where flow cytometry assays of parasitemia using nucleic acid staining dyes is routine for donor erythrocytes, the confounding nuclear signal where orthochromatic erythroblasts are studied prohibits this means of assessment and in the ideal situation where purified reticulocytes are studied residual RNA in reticulocytes necessitates careful controls (Satchwell et al., 2019). Miniaturisation of assays and manual inspection of cytospin preparations (Bei et al., 2010; Egan et al., 2015; Satchwell et al., 2019; Kanjee et al., 2021) have been powerful enablers of *in vitro* red blood cell use however efforts to adapt and improve flow cytometry based assessment through robust, nucleic acid labelling, use of fluorescent parasite lines (Neveu et al., 2020), label free assessment of parasitemia (Frita et al., 2011; Pance et al., 2021) or *via* advanced technologies such as Imaging Flow Cytometry (Luiza-Batista et al., 2022a) represent important endeavours. Ongoing efforts within the community of researchers seeking to improve and optimise *in vitro* erythroid culture enucleation rates, scalability and purification methods are of continued importance to improve accessibility (Lim et al., 2021; Pellegrin et al., 2021; Gallego-Murillo et al., 2022).

Conclusions

Malaria is a complex and multi-faceted disease, caused as it is, by a parasite that transitions between multiple forms, residing in multiple host cells throughout its lifecycle, each presenting their own unique difficulties for study. In the case of the red blood cell host, genetic intractability of the mature cell and inaccessibility of its increasingly interesting precursors have presented major historical obstacles to detailed understanding of the ways in which host proteins resist, contribute or are co-opted during malaria invasion and pathogenesis. Stem cell biology and the more recent use of immortalised erythroid cells has already demonstrated its value to malaria research, identifying new and overlooked host protein requirements for invasion and opening up new areas for investigation. We look forward to the exciting new avenues, insights and opportunities for interventions that it may uncover in the coming years.

Data availability statement

This study did not involve any underlying data.

Author contributions

TJS conceptualised and wrote the review. The author confirms being the sole contributor of this work and has approved it for publication.

Funding

TJS was supported by the UK Medical Research Council Grant ID. MR/V010506/1.

Conflict of interest

The author declares that the research was conducted in the absence of any commercial or financial relationships that could be construed as a potential conflict of interest.

Publisher's note

References

Adderley, J. D., John Von Freyend, S., Jackson, S. A., Bird, M. J., Burns, A. L., Anar, B., et al. (2020). Analysis of erythrocyte signalling pathways during Plasmodium falciparum infection identifies targets for host-directed antimalarial intervention. *Nat. Commun.* 11, 4015. doi: 10.1038/s41467-020-17829-7

Aniweh, Y., Gao, X., Hao, P., Meng, W., Lai, S. K., Gunalan, K., et al. (2017). P. falciparum RH5-basigin interaction induces changes in the cytoskeleton of the host RBC. *Cell Microbiol.* 19 (9), e12747. doi: 10.1111/cmi.12747

Beeson, J. G., Drew, D. R., Boyle, M. J., Feng, G., Fowkes, F. J., and Richards, J. S. (2016). Merozoite surface proteins in red blood cell invasion, immunity and vaccines against malaria. *FEMS Microbiol. Rev.* 40, 343–372. doi: 10.1093/femsre/fuw001

Bei, A. K., Brugnara, C., and Duraisingh, M. T. (2010). *In vitro* genetic analysis of an erythrocyte determinant of malaria infection. *J. Infect. Dis.* 202, 1722–1727. doi: 10.1086/657157

Bermudez, M., Moreno-Perez, D. A., Arevalo-Pinzon, G., Curtidor, H., and Patarroyo, M. A. (2018). *plasmodium vivax in vitro* continuous culture: the spoke in the wheel. *Malar J.* 17, 301. doi: 10.1186/s12936-018-2456-5

Bernecker, C., Ackermann, M., Lachmann, N., Rohrhofer, L., Zaehres, H., Arauzo-Bravo, M. J., et al. (2019). Enhanced ex vivo generation of erythroid cells from human induced pluripotent stem cells in a simplified cell culture system with low cytokine support. *Stem Cells Dev.* 28, 1540–1551. doi: 10.1089/scd.2019.0132

Bernecker, C., Matzhold, E. M., Kolb, D., Avdili, A., Rohrhofer, L., Lampl, A., et al. (2022). Membrane properties of human induced pluripotent stem cell-derived cultured red blood cells. *Cells* 11, 2473. doi: 10.3390/cells11162473

Bhalla, K., Chugh, M., Mehrotra, S., Rathore, S., Tousif, S., Prakash Dwivedi, V., et al. (2015). Host ICAMs play a role in cell invasion by mycobacterium tuberculosis and Plasmodium falciparum. *Nat. Commun.* 6, 6049. doi: 10.1038/ncomms7049

Bouyer, G., Reininger, L., Ramdani, G., Phillips, L. ,. D., Sharma, V., Egee, S., et al. (2016). Plasmodiumfalciparum infection induces dynamic changes in the erythrocyte phospho-proteome. *Blood Cells Mol. Dis.* 58, 35–44. doi: 10.1016/j.bcmd.2016.02.001

Chien, H. D., Pantaleo, A., Kesely, K. R., Noomuna, P., Putt, K. S., Tuan, T. A., et al. (2021). Imatinib augments standard malaria combination therapy without added toxicity. *J. Exp. Med.* 218 (10), e20210724. doi: 10.1084/jem.20210724

Craik, R. (1920). A note on the erythrocytes in malaria. *Lancet* 195 (5047), 1110. doi: 10.1016/S0140-6736(00)92210-4

Crosnier, C., Bustamante, L. Y., Bartholdson, S. J., Bei, A. K., Theron, M., Uchikawa, M., et al. (2011). Basigin is a receptor essential for erythrocyte invasion by Plasmodium falciparum. *Nature* 480, 534–537. doi: 10.1038/nature10606

Daniels, D. E., Downes, D. J., Ferrer-Vicens, I., Ferguson, D. C. J., Singleton, B. K., Wilson, M. C., et al. (2020). Comparing the two leading erythroid lines BEL-a and HUDEP-2. *Haematologica* 105, e389–e394. doi: 10.3324/haematol.2019.229211

Daniels, D. E., Ferguson, D. C. J., Griffiths, R. E., Trakarnsanga, K., Cogan, N., Macinnes, K. A., et al. (2021). Reproducible immortalization of erythroblasts from multiple stem cell sources provides approach for sustainable RBC therapeutics. *Mol. Ther. Methods Clin. Dev.* 22, 26–39. doi: 10.1016/j.omtm.2021.06.002

Dias, J., Gumenyuk, M., Kang, H., Vodyanik, M., Yu, J., and Thomson, J. A. (2011). Generation of red blood cells from human induced pluripotent stem cells. *Stem Cells Dev.* 20, 1639–1647. doi: 10.1089/scd.2011.0078

Egan, E. S., Jiang, R. H., Moechtar, M. A., Barteneva, N. S., Weekes, M. P., Nobre, L. V., et al. (2015). Malaria. a forward genetic screen identifies erythrocyte CD55 as essential for Plasmodium falciparum invasion. *Science* 348, 711–714. doi: 10.1126/science.aaa3526

Egan, E. S., Weekes, M. P., Kanjee, U., Manzo, J., Srinivasan, A., Lomas-Francis, C., et al. (2018). Erythrocytes lacking the langereis blood group protein ABCB6 are resistant to the malaria parasite Plasmodium falciparum. *Commun. Biol.* 1, 45. doi: 10.1038/s42003-018-0046-2

Feldman, T. P., and Egan, E. S. (2022). Uncovering a cryptic site of malaria pathogenesis: Models to study interactions between plasmodium and the bone marrow. *Front. Cell Infect. Microbiol.* 12, 917267. doi: 10.3389/fcimb.2022.917267

Fernandez-Becerra, C., Lelievre, J., Ferrer, M., Anton, N., Thomson, R., Peligero, C., et al. (2013). Red blood cells derived from peripheral blood and bone marrow CD34(+) human haematopoietic stem cells are permissive to plasmodium parasites infection. *Mem Inst Oswaldo Cruz* 108, 801–803. doi: 10.1590/0074-0276108062013019

Focosi, D., and Pistello, M. (2016). Effect of induced pluripotent stem cell technology in blood banking. *Stem Cells Transl. Med.* 5, 269–274. doi: 10.5966/sctm.2015-0257

Frita, R., Rebelo, M., Pamplona, A., Vigario, A. M., Mota, M. M., Grobusch, M. P., et al. (2011). Simple flow cytometric detection of haemozoin containing leukocytes and erythrocytes for research on diagnosis, immunology and drug sensitivity testing. *Malar J.* 10, 74. doi: 10.1186/1475-2875-10-74

Gallego-Murillo, J. S., Iacono, G., van der Wielen, L. A. M., Van Den Akker, E., Von Lindern, M., and Wahl, S. A. (2022). Expansion and differentiation of ex vivo cultured erythroblasts in scalable stirred bioreactors. *Biotechnol. Bioeng.* 119 (11), 3096–3116. doi: 10.1002/bit.28193

Giarratana, M. C., Kobari, L., Lapillonne, H., Chalmers, D., Kiger, L., Cynober, T., et al. (2005). Ex vivo generation of fully mature human red blood cells from hematopoietic stem cells. *Nat. Biotechnol.* 23, 69–74. doi: 10.1038/nbt1047

Giarratana, M. C., Rouard, H., Dumont, A., Kiger, L., Safeukui, I., Le Pennec, P. Y., et al. (2011). Proof of principle for transfusion of *in vitro*-generated red blood cells. *Blood* 118, 5071–5079. doi: 10.1182/blood-2011-06-362038

Goerdeler, F., Seeberger, P. H., and Moscovitz, O. (2021). Unveiling the sugary secrets of plasmodium parasites. *Front. Microbiol.* 12, 712538. doi: 10.3389/fmicb.2021.712538

Griffiths, R. E., Kupzig, S., Cogan, N., Mankelow, T. J., Betin, V. M., Trakarnsanga, K., et al. (2012). Maturing reticulocytes internalize plasma membrane in glycophorin a-containing vesicles that fuse with autophagosomes before exocytosis. *Blood* 119, 6296–6306. doi: 10.1182/blood-2011-09-376475

Gunalan, K., Rowley, E. H., and Miller, L. H. (2020). A way forward for culturing *plasmodium vivax*. *Trends Parasitol.* 36, 512–519. doi: 10.1016/j.pt.2020.04.002

Hansen, M., Von Lindern, M., Van Den Akker, E., and Varga, E. (2019). Human-induced pluripotent stem cell-derived blood products: state of the art and future directions. *FEBS Lett.* 593, 3288–3303. doi: 10.1002/1873-3468.13599

Hawksworth, J., Satchwell, T. J., Meinders, M., Daniels, D. E., Regan, F., Thornton, N. M., et al. (2018). Enhancement of red blood cell transfusion compatibility using CRISPR-mediated erythroblast gene editing. *EMBO Mol. Med.* 10 (6), e8454. doi: 10.15252/emmm.201708454

Hegner, R. (1938). Relative frequency of ring-stage plasmodia in reticulocytes and mature erythrocytes in man an monkey. *Am. J. Trop. Med. Hyg.* 27, 690–718. doi: 10.1093/oxfordjournals.aje.a118422

Heshusius, S., Heideveld, E., Burger, P., Thiel-Valkhof, M., Sellink, E., Varga, E., et al. (2019). Large-Scale *in vitro* production of red blood cells from human peripheral blood mononuclear cells. *Blood Adv.* 3, 3337–3350. doi: 10.1182/bloodadvances.2019000689

Kanjee, U., Gruring, C., Babar, P., Meyers, A., Dash, R., Pereira, L., et al. (2021). *plasmodium vivax* strains use alternative pathways for invasion. *J. Infect. Dis.* 223, 1817–1821. doi: 10.1093/infdis/jiaa592

Kanjee, U., Gruring, C., Chaand, M., Lin, K. M., Egan, E., Manzo, J., et al. (2017). CRISPR/Cas9 knockouts reveal genetic interaction between strain-transcendent erythrocyte determinants of Plasmodium falciparum invasion. *Proc. Natl. Acad. Sci. U.S.A.* 114, E9356–E9365. doi: 10.1073/pnas.1711310114

Kumari, G., Rex, D. A. B., Goswami, S., Mukherjee, S., Biswas, S., Maurya, P., et al. (2022). Dynamic palmitoylation of red cell membrane proteins governs susceptibility to invasion by the malaria parasite, Plasmodium falciparum. *ACS Infect. Dis.* 8 (10), 2106–2118. doi: 10.1021/acsinfecdis.2c00199

Kupzig, S., Parsons, S. F., Curnow, E., Anstee, D. J., and Blair, A. (2017). Superior survival of ex vivo cultured human reticulocytes following transfusion into mice. *Haematologica* 102, 476–483. doi: 10.3324/haematol.2016.154443

Kurita, R., Funato, K., Abe, T., Watanabe, Y., Shiba, M., Tadokoro, K., et al. (2019). Establishment and characterization of immortalized erythroid progenitor cell lines derived from a common cell source. *Exp. Hematol.* 69, 11–16. doi: 10.1016/j.exphem.2018.10.005

Kurita, R., Suda, N., Sudo, K., Miharada, K., Hiroyama, T., Miyoshi, H., et al. (2013). Establishment of immortalized human erythroid progenitor cell lines able to produce enucleated red blood cells. *PloS One* 8, e59890. doi: 10.1371/journal.pone.0059890

Lim, C., Hansen, E., Desimone, T. M., Moreno, Y., Junker, K., Bei, A., et al. (2013). Expansion of host cellular niche can drive adaptation of a zoonotic malaria parasite to humans. *Nat. Commun.* 4, 1638. doi: 10.1038/ncomms2612

Lim, Z. R., Vassilev, S., Leong, Y. W., Hang, J. W., Renia, L., Malleret, B., et al. (2021). Industrially compatible transfusable iPSC-derived RBCs: Progress, challenges and prospective solutions. *Int. J. Mol. Sci.* 22. doi: 10.3390/ijms22189808

Lozzio, C. B., and Lozzio, B. B. (1975). Human chronic myelogenous leukemia cell-line with positive Philadelphia chromosome. *Blood* 45, 321–334. doi: 10.1182/blood.V45.3.321.321

Luiza-Batista, C., Nardella, F., Thiberge, S., Serra-Hassoun, M., Ferreira, M. U., Scherf, A., et al. (2022a). Flowcytometric and ImageStream rna-fish gene expression, quantification and phenotypic characterization of blood sporozoites and sporozoites from human malaria species. *J. Infect. Dis.* 225, 1621–1625. doi: 10.1093/infdis/jiab431

Luiza-Batista, C., Thiberge, S., Serra-Hassoun, M., Nardella, F., Claes, A., Nicolete, V. C., et al. (2022b). Humanized mice for investigating sustained *plasmodium vivax* blood-stage infections and transmission. *Nat. Commun.* 13, 4123. doi: 10.1038/s41467-022-31864-6

Malleret, B., Xu, F., Mohandas, N., Suwanarusk, R., Chu, C., Leite, J. A., et al. (2013). Significant biochemical, biophysical and metabolic diversity in circulating human cord blood reticulocytes. *PloS One* 8, e76062. doi: 10.1371/journal.pone.0076062

Marchiafava, E., and Bigmani, A. (1894). "On summer-autumn malarial fevers," in *Two monographs on malaira and the parasites of malairal fevers*. Ed. E. Marchiafava (London: New Syndenham Society), 1–232.

Mcqueen, P. G., and Mckenzie, F. E. (2004). Age-structured red blood cell susceptibility and the dynamics of malaria infections. *Proc. Natl. Acad. Sci. U.S.A.* 101, 9161–9166. doi: 10.1073/pnas.0308256101

Moura, P. L., Hawley, B. R., Mankelow, T. J., Griffiths, R. E., Dobbe, J. G. G., Streekstra, G. J., et al. (2018). Non-muscle myosin II drives vesicle loss during human reticulocyte maturation. *Haematologica* 103, 1997–2007. doi: 10.3324/haematol.2018.199083

Ndegwa, D. N., Kundu, P., Hostetler, J. B., Marin-Menendez, A., Sanderson, T., Mwikali, K., et al. (2021). Using plasmodium knowlesi as a model for screening *plasmodium vivax* blood-stage malaria vaccine targets reveals new candidates. *PloS Pathog.* 17, e1008864. doi: 10.1371/journal.ppat.1008864

Neveu, G., and Lavazec, C. (2019). Erythrocyte membrane makeover by Plasmodium falciparum gametocytes. *Front. Microbiol.* 10, 2652. doi: 10.3389/fmicb.2019.02652

Neveu, G., Richard, C., Dupuy, F., Behera, P., Volpe, F., Subramani, P. A., et al. (2020). Plasmodium falciparum sexual parasites develop in human erythroblasts and affect erythropoiesis. *Blood* 136, 1381–1393. doi: 10.1182/blood.2019004746

Niang, M., Bei, A. K., Madnani, K. G., Pelly, S., Dankwa, S., Kanjee, U., et al. (2014). STEVOR is a Plasmodium falciparum erythrocyte binding protein that mediates merozoite invasion and rosetting. *Cell Host Microbe* 16, 81–93. doi: 10.1016/j.chom.2014.06.004

Noulin, F., Borlon, C., Van Den Eede, P., Boel, L., Verfaillie, C. M., D'alessandro, U., et al. (2012). Cryopreserved reticulocytes derived from hematopoietic stem cells can be invaded by cryopreserved *plasmodium vivax* isolates. *PloS One* 7, e40798. doi: 10.1371/journal.pone.0040798

Noulin, F., Manesia, J. K., Rosanas-Urgell, A., Erhart, A., Borlon, C., Van Den Abbeele, J., et al. (2014). Hematopoietic stem/progenitor cell sources to generate reticulocytes for *plasmodium vivax* culture. *PloS One* 9, e112496. doi: 10.1371/journal.pone.0112496

Olivieri, A., Lee, R. S., Fratini, F., Keutcha, C., Chaand, M., Mangano, V., et al. (2021). Structural organization of erythrocyte membrane microdomains and their relation with malaria susceptibility. *Commun. Biol.* 4, 1375. doi: 10.1038/s42003-021-02900-w

Ovchynnikova, E., Aglialoro, F., Von Lindern, M., and Van Den Akker, E. (2018). The shape shifting story of reticulocyte maturation. *Front. Physiol.* 9, 829. doi: 10.3389/fphys.2018.00829

Palis, J. (2014). Primitive and definitive erythropoiesis in mammals. *Front. Physiol.* 5, 3. doi: 10.3389/fphys.2014.00003

Pance, A. L. B., Ling, B., Mwikali, K., Koutsourakis, M., Agu, C., Rouhani, F., et al. (2021). Stem cell technology provides novel tools to understand human variation in *Plasmodium falciparum* malaria. *BioRxiv* 2021.06.30.450498. doi: 10.1101/2021.06.30.450498

Panichakul, T., Sattabongkot, J., Chotivanich, K., Sirichaisinthop, J., Cui, L., and Udomsangpetch, R. (2007). Production of erythropoietic cells *in vitro* for continuous culture of *plasmodium vivax*. *Int. J. Parasitol.* 37, 1551–1557. doi: 10.1016/j.ijpara.2007.05.009

Pasvol, G., Weatherall, D. J., and Wilson, R. J. (1980). The increased susceptibility of young red cells to invasion by the malarial parasite Plasmodium falciparum. *Br. J. Haematol* 45, 285–295. doi: 10.1111/j.1365-2141.1980.tb07148.x

Pellegrin, S., Severn, C. E., and Toye, A. M. (2021). Towards manufactured red blood cells for the treatment of inherited anemia. *Haematologica* 106, 2304–2311. doi: 10.3324/haematol.2020.268847

Roobsoong, W., Tharinjaroen, C. S., Rachaphaew, N., Chobson, P., Schofield, L., Cui, L., et al. (2015). Improvement of culture conditions for long-term *in vitro* culture of *plasmodium vivax*. *Malar J.* 14, 297. doi: 10.1186/s12936-015-0815-z

Salinas, N. D., and Tolia, N. H. (2016). Red cell receptors as access points for malaria infection. *Curr. Opin. Hematol.* 23, 215–223. doi: 10.1097/MOH.0000000000000219

Satchwell, T. J. (2016). Erythrocyte invasion receptors for Plasmodium falciparum: new and old. *Transfus Med.* 26, 77–88. doi: 10.1111/tme.12280

Satchwell, T. J., Wright, K. E., Haydn-Smith, K. L., Sanchez-Roman Teran, F., Moura, P. L., Hawksworth, J., et al. (2019). Genetic manipulation of cell line derived reticulocytes enables dissection of host malaria invasion requirements. *Nat. Commun.* 10, 3806. doi: 10.1038/s41467-019-11790-w

Scully, E. J., Shabani, E., Rangel, G. W., Gruring, C., Kanjee, U., Clark, M. A., et al. (2019). Generation of an immortalized erythroid progenitor cell line from peripheral blood: A model system for the functional analysis of plasmodium spp. invasion. *Am. J. Hematol.* 94, 963–974. doi: 10.1002/ajh.25543

Shah, S., Huang, X., and Cheng, L. (2014). Concise review: stem cell-based approaches to red blood cell production for transfusion. *Stem Cells Transl. Med.* 3, 346–355. doi: 10.5966/sctm.2013-0054

Shakya, B., Patel, S. D., Tani, Y., and Egan, E. S. (2021). Erythrocyte CD55 mediates the internalization of Plasmodium falciparum parasites. *Elife* 10, 61516. doi: 10.7554/eLife.61516.sa2

Shushan, M., Blitz, O., and Adams, C. G. (1937). The role of reticulocytes in malaria. *J. Lab. Clin. Med.* 22, 364–370.

Sisquella, X., Nebl, T., Thompson, J. K., Whitehead, L., Malpede, B. M., Salinas, N. D., et al. (2017). Plasmodium falciparum ligand binding to erythrocytes induce alterations in deformability essential for invasion. *Elife* 6, e21083. doi: 10.7554/eLife.21083.015

Stevens-Hernandez, C. J., and Bruce, L. J. (2022). Reticulocyte maturation. *Membranes (Basel)* 12 (3), 311. doi: 10.3390/membranes12030311

Takahashi, K., Tanabe, K., Ohnuki, M., Narita, M., Ichisaka, T., Tomoda, K., et al. (2007). Induction of pluripotent stem cells from adult human fibroblasts by defined factors. *Cell* 131, 861–872. doi: 10.1016/j.cell.2007.11.019

Tamez, P. A., Liu, H., Fernandez-Pol, S., Haldar, K., and Wickrema, A. (2009). Stage-specific susceptibility of human erythroblasts to Plasmodium falciparum malaria infection. *Blood* 114, 3652–3655. doi: 10.1182/blood-2009-07-231894

Tham, W. H., Wilson, D. W., Lopaticki, S., Schmidt, C. Q., Tetteh-Quarcoo, P. B., Barlow, P. N., et al. (2010). Complement receptor 1 is the host erythrocyte receptor for Plasmodium falciparum PfRh4 invasion ligand. *Proc. Natl. Acad. Sci. U.S.A.* 107, 17327–17332. doi: 10.1073/pnas.1008151107

Thomson-Luque, R., and Bautista, J. M. (2021). Home sweet home: *plasmodium vivax*-infected reticulocytes-the younger the better? *Front. Cell Infect. Microbiol.* 11, 675156. doi: 10.3389/fcimb.2021.675156

Tiburcio, M., Niang, M., Deplaine, G., Perrot, S., Bischoff, E., Ndour, P. A., et al. (2012). A switch in infected erythrocyte deformability at the maturation and blood circulation of Plasmodium falciparum transmission stages. *Blood* 119, e172–e180. doi: 10.1182/blood-2012-03-414557

Tiburcio, M., Sauerwein, R., Lavazec, C., and Alano, P. (2015). Erythrocyte remodeling by Plasmodium falciparum gametocytes in the human host interplay. *Trends Parasitol.* 31, 270–278. doi: 10.1016/j.pt.2015.02.006

Trager, W., and Jensen, J. B. (1976). Human malaria parasites in continuous culture. *Science* 193, 673–675. doi: 10.1126/science.781840

Trakarnsanga, K., Griffiths, R. E., Wilson, M. C., Blair, A., Satchwell, T. J., Meinders, M., et al. (2017). An immortalized adult human erythroid line facilitates sustainable and scalable generation of functional red cells. *Nat. Commun.* 8, 14750. doi: 10.1038/ncomms14750

Trakarnsanga, K., Wilson, M. C., Griffiths, R. E., Toye, A. M., Carpenter, L., Heesom, K. J., et al. (2014). Qualitative and quantitative comparison of the proteome of erythroid cells differentiated from human iPSCs and adult erythroid cells by multiplex TMT labelling and nanoLC-MS/MS. *PloS One* 9, e100874. doi: 10.1371/journal.pone.0100874

Van Den Akker, E., Satchwell, T. J., Pellegrin, S., Daniels, G., and Toye, A. M. (2010). The majority of the *in vitro* erythroid expansion potential resides in CD34 (-) cells, outweighing the contribution of CD34(+) cells and significantly increasing the erythroblast yield from peripheral blood samples. *Haematologica* 95, 1594–1598. doi: 10.3324/haematol.2009.019828

Wang, S., Zhao, H., Zhang, H., Gao, C., Guo, X., Chen, L., et al. (2022). Analyses of erythropoiesis from embryonic stem cell-CD34(+) and cord blood-CD34(+) cells reveal mechanisms for defective expansion and enucleation of embryomic stem cell-erythroid cells. *J. Cell Mol. Med.* 26, 2404–2416. doi: 10.1111/jcmm.17263

Wei, L., Adderley, J., Leroy, D., Drewry, D. H., Wilson, D. W., Kaushansky, A., et al. (2021). Host-directed therapy, an untapped opportunity for antimalarial intervention. *Cell Rep. Med.* 2, 100423. doi: 10.1016/j.xcrm.2021.100423

WHO (2021). *World malaria report 2021* (Geneva: World Health Organization).

Wilson, R. J., Pasvol, G., and Weatherall, D. J. (1977). Invasion and growth of Plasmodium falciparum in different types of human erythrocyte. *Bull. World Health Organ* 55, 179–186.

Yu, J., Vodyanik, M. A., Smuga-Otto, K., Antosiewicz-Bourget, J., Frane, J. L., Tian, S., et al. (2007). Induced pluripotent stem cell lines derived from human somatic cells. *Science* 318, 1917–1920. doi: 10.1126/science.1151526

Zuccala, E. S., and Baum, J. (2011). Cytoskeletal and membrane remodelling during malaria parasite invasion of the human erythrocyte. *Br. J. Haematol* 154, 680–689. doi: 10.1111/j.1365-2141.2011.08766.x

Zuccala, E. S., Satchwell, T. J., Angrisano, F., Tan, Y. H., Wilson, M. C., Heesom, K. J., et al. (2016). Quantitative phospho-proteomics reveals the plasmodium merozoite triggers pre-invasion host kinase modification of the red cell cytoskeleton. *Sci. Rep.* 6, 19766. doi: 10.1038/srep19766

frontiers | Frontiers in Cellular and Infection Microbiology

TYPE Original Research
PUBLISHED 06 February 2023
DOI 10.3389/fcimb.2023.1098457

OPEN ACCESS

EDITED BY
Gabriel Rinaldi,
Aberystwyth University, United Kingdom

REVIEWED BY
María Lucía Piacenza Bengochea,
Universidad de la República, Uruguay
Rafael Tiburcio,
Gonçalo Moniz Institute (IGM), Brazil

*CORRESPONDENCE
Christine E. Seidman
cseidman@genetics.med.harvard.edu

SPECIALTY SECTION
This article was submitted to Parasite and Host, a section of the journal Frontiers in Cellular and Infection Microbiology

RECEIVED 14 November 2022
ACCEPTED 16 January 2023
PUBLISHED 06 February 2023

CITATION
Venturini G, Alvim JM, Padilha K, Toepfer CN, Gorham JM, Wasson LK, Biagi D, Schenkman S, Carvalho VM, Salgueiro JS, Cardozo KHM, Krieger JE, Pereira AC, Seidman JG and Seidman CE (2023) Cardiomyocyte infection by *Trypanosoma cruzi* promotes innate immune response and glycolysis activation. *Front. Cell. Infect. Microbiol.* 13:1098457. doi: 10.3389/fcimb.2023.1098457

Cardiomyocyte infection by *Trypanosoma cruzi* promotes innate immune response and glycolysis activation

Gabriela Venturini[1,2], Juliana M. Alvim[2], Kallyandra Padilha[2], Christopher N. Toepfer[1,3,4], Joshua M. Gorham[1], Lauren K. Wasson[1], Diogo Biagi[5], Sergio Schenkman[6], Valdemir M. Carvalho[7], Jessica S. Salgueiro[7], Karina H. M. Cardozo[7], Jose E. Krieger[2], Alexandre C. Pereira[1,2], Jonathan G. Seidman[1] and Christine E. Seidman[1,8,9]*

[1]Department of Genetics, Harvard Medical School, Boston, MA, United States, [2]Laboratory of Genetics and Molecular Cardiology, University of São Paulo Medical School, São Paulo, Brazil, [3]Division of Cardiovascular Medicine, Radcliffe Department of Medicine, University of Oxford, Oxford, United Kingdom, [4]Wellcome Centre for Human Genetics, University of Oxford, Oxford, United Kingdom, [5]LizarBio Therapeutics, Sao Paulo, Brazil, [6]Department of Microbiology, Immunology and Parasitology, Escola Paulista de Medicina, São Paulo, Brazil, [7]Division of Research and Development, Fleury Group, São Paulo, SP, Brazil, [8]Division of Cardiovascular Medicine, Department of Medicine, Brigham and Women's Hospital, Boston, MA, United States, [9]Howard Hughes Medical Institute, Chevy Chase, MD, United States

Introduction: Chagas cardiomyopathy, a disease caused by *Trypanosoma cruzi* (*T. cruzi*) infection, is a major contributor to heart failure in Latin America. There are significant gaps in our understanding of the mechanism for infection of human cardiomyocytes, the pathways activated during the acute phase of the disease, and the molecular changes that lead to the progression of cardiomyopathy.

Methods: To investigate the effects of *T. cruzi* on human cardiomyocytes during infection, we infected induced pluripotent stem cell-derived cardiomyocytes (iPSC-CM) with the parasite and analyzed cellular, molecular, and metabolic responses at 3 hours, 24 hours, and 48 hours post infection (hpi) using transcriptomics (RNAseq), proteomics (LC-MS), and metabolomics (GC-MS and Seahorse) analyses.

Results: Analyses of multiomic data revealed that cardiomyocyte infection caused a rapid increase in genes and proteins related to activation innate and adaptive immune systems and pathways, including alpha and gamma interferons, HIF-1α signaling, and glycolysis. These responses resemble prototypic responses observed in pathogen-activated immune cells. Infection also caused an activation of glycolysis that was dependent on HIF-1α signaling. Using gene editing and pharmacological inhibitors, we found that *T. cruzi* uptake was mediated in part by the glucose-facilitated transporter GLUT4 and that the attenuation of glycolysis, HIF-1α activation, or GLUT4 expression decreased *T. cruzi* infection. In contrast, pre-activation of pro-inflammatory immune responses with LPS resulted in increased infection rates.

Conclusion: These findings suggest that *T. cruzi* exploits a HIF-1α-dependent, cardiomyocyte-intrinsic stress-response activation of glycolysis to promote intracellular infection and replication. These chronic immuno-metabolic responses by cardiomyocytes promote dysfunction, cell death, and the emergence of cardiomyopathy.

KEYWORDS

Chagas cardiomyopathy, *Trypanosoma cruzi*, metabolism, inflammation, glycolysis

1 Introduction

Heart failure is a global epidemic that affects 38 million patients worldwide and is the result of multiple underlying cardiovascular and systemic disorders (Heidenreich et al., 2013; Roger, 2013; Braunwald, 2015; Benjamin et al., 2018). Infectious diseases and their associated inflammatory responses are substantial causes of heart failure in low and low-middle income countries where the majority of the world lives. In Latin America, *Trypanosoma cruzi* (*T. cruzi*), an endemic parasite that causes Chagas cardiomyopathy, is the most common infectious cause of heart failure. The World Health Organization (WHO) estimates that across the Americas, Chagas disease has a global disease burden (disability-adjusted life-years) that is 7.5-fold greater than malaria (Mathers et al., 2018). Chagas disease is not restricted to Latin America, and in 2016, analyses estimated that 240,000 U.S. citizens and an additional 100,000 undocumented residents had *T. cruzi* infection, accounting for 30,000-45,000 Chagas cardiomyopathy cases and 60-300 congenital infections that annually occur in this country (Manne-Goehler et al., 2016; Bocchi et al., 2017). California, Florida, New York, and Texas each had over 10,000 cases/year (Manne-Goehler et al., 2016).

Acute *T. cruzi* infection causes nonspecific and mild symptoms that often escape clinical attention and promotes unrecognized life-long chronic infection (Maguire, 2006). Approximately 20-30% of asymptomatic, but chronically infected individuals, develop cardiomyopathy, which emerges years or decades after the initial or repeated infections (Costa et al., 2017). Chagas cardiomyopathy has no tailored treatment options and management mainly addresses symptom relief (Martinez et al., 2020).

There are considerable gaps in understanding Chagas cardiomyopathy pathogenesis (Bonney et al., 2019). *T. cruzi* infects and elicits a rapid immune response in most tissues that clears the parasite. However, case reports demonstrate myocardial reactivation of viable parasites with immunosuppression, implying that the heart, similar to the gastrointestinal system, can provide a cellular reservoir for the parasite (Burgos et al., 2010; Nagajyothi et al., 2012; Lewis and Kelly, 2016; Ward et al., 2020). The mechanisms by which *T. cruzi* lays dormant in the heart and evades the immune response is unknown. However, the consequences are readily identified, as chronic host-pathogen interactions evoke cardiac remodeling and the emergence of heart failure decades after acute infection (Higuchi et al., 2003; Machado et al., 2012; Pérez-Mazliah et al., 2021).

Human iPSC-derived cardiomyocytes (iPSC-CMs) infected with *T. cruzi* have provided some insights into host-pathogen interactions. Previous analyses of these cellular models demonstrate increased reactive oxidant species (ROS), mammalian target of rapamycin (mTOR)-activation of oxidative phosphorylation, and production of inflammatory cytokines that are predicted to promote immune cell migration (Dias et al., 2017; Libisch et al., 2018; Bozzi et al., 2019). However, the processes that trigger and integrate these diverse and fundamental changes in cardiomyocyte biology are unknown. Moreover, whether these changes in cardiomyocytes are adaptative and protective or detrimental to parasite or cardiomyocyte survival is unknown.

We exploited the iPSC-CMs model of *T. cruzi* infection to discern genome-wide transcriptional responses to *T. cruzi* infection and validated these with proteomic and metabolic analyses. Our studies uncover highly integrated immuno-metabolic responses that are intrinsic to *T. cruzi*-infected cardiomyocytes and closely resemble prototypic responses in pathogen-activated immune cells. Using pharmacological and genetic perturbations of key signaling molecules we demonstrate that the parasite capitalizes on these responses to augment infection and increase intracellular replication. Together these data demonstrate that a highly conserved innate immune response and metabolic rewiring occurs in cardiomyocytes that is used by the parasite to promote intracellular infection and replication and evokes profound changes in cardiomyocyte physiology and function.

2 Materials and methods

2.1 Isolation and maintenance of *T. cruzi* Y-strain trypomastigotes

T. cruzi trypomastigotes (Y strain) and GFP-Y strain (Ramirez et al., 2000) (kindly provided by Dr. Sergio Schenkman lab) were derived from the supernatants of infected LLC-MK2 culture cells grown. Briefly, sub-confluent cultures of LLC-MK2 cells were infected with $5x10^6$ trypomastigotes. Free parasites were removed after 24 hours, and the cell cultures were maintained in 2% FBS-RPMI 1640. Five days following infection, free trypomastigote forms were found in the cell supernatants. Parasite containing supernatant were collected, centrifuged at 2000xg for 20min, resuspended in RPMI plus B27 supplement, counted in a Neubauer Chamber and added to the cells in the desired MOI.

2.2 Human induced pluripotent stem cells derived cardiomyocyte (iPSC-CM) infection protocol

iPSC-CMs were differentiated as previously described (Sharma et al., 2018a). All experiments were carried out between day 30-35 of differentiation. iPSC-CMs were infected with purified trypomastigotes in RPMI media plus B27 in a MOI of 1 (number parasite/number cardiomyocyte) for omics experiments; and MOI 5 for image experiments. Media was changed after 24 hours to remove free parasites. All experiments were performed with 3 independent iPSC-CM differentiation and infection.

2.3 RNA-sequencing analysis

RNA-sequencing analysis were performed as described (Sharma et al., 2020) with few modifications. Briefly, after Trizol RNA extraction, libraries were prepared using the Nextera library preparation method. RNA-Seq library samples were pooled and ran on the Illumina NextSeq500 platform. Sequenced reads were aligned with STAR (Engström et al., 2013). Read counts per gene were normalized using DEseq2 and used for group comparison (Love et al., 2014). Gene pathway enrichment analysis were conducted using clusterProfiler (Yu et al., 2012) using the Hallmark Database Gene Set as reference (Liberzon et al., 2015).

2.4 Proteomics analysis

After 48 hours, non-infected and infected cells ($1x10^6$ cells) were scrapped with 300 µL of protein extraction buffer (8M urea and 50 mM of ammonium bicarbonate). Digestion and mass spectrometry methods were performed as described (Malagrino et al., 2017) with few modifications. Briefly, total protein (100 µg) extracts were treated with 2.5 µL of 100 mM DTT at 60°C for 30 minutes and alkylated with 2.5 µL of 300 mM iodoacetamide for 30 minutes at room temperature in the dark. Proteins were then enzymatically digested with 10 µL of trypsin 0.05 µg/µL for 16 hours at 37°C. To stop the digestion, we added 10 µL of 5% trifluoroacetic acid (TFA). Tryptic peptide solution was centrifuged at 16,000xg for 30 minutes at 6°C and peptides were desalted with zip-tip C18.

2.5 Metabolomics analysis

Metabolomic analyses were performed as described (Venturini et al., 2019), with few modifications. After 3, 24 and 48 hours of infection, $1x10^6$ cells were washed with cold PBS and scrapped with 1 mL of cold Acetonitrile:Isopropanol:MilliQ water (3:3:2 v/v/v) for metabolite extraction. Metabolites were centrifuged at 15800xg at 0°C for 5 minutes. An aliquot of supernatant (900 µL) was transferred to a new tube and both, protein pellet and supernatant, were dried during 18 hours in speed-vac. The metabolites were resuspended in 1 mL of cold Acetonitrile:MilliQ water (1:1 vol/vol), centrifuged at 15800xg at 0°C for 5 minutes and 900 µL of supernatant were transferred to a new tube. 5 µL of myristic acid D27 (3 mg/mL) was added as internal standard and retention time index and the solution was dried for 18 hours. Metabolites were derivatized with 20 µL of methoxylamine diluted in pyridine (40 mg/mL) for 16 hours at room temperature, following addition of 90 µL of MSTFA with 1% of TMCS and one hour of incubation at room temperature. Metabolites were centrifuged at 15800xg at 0°C for 5 minutes and 100 µL of supernatant were transferred to a glass insert. After derivatization, 1 µL of this derivative was used for Gas Chromatography Mass Spectrometry (GC/MS) analysis.

2.6 Extracellular metabolic flux analysis

Glucose and lactate in media were measured using an electrolyte counter (FLEX ABL800 Radiometer Medical, Bronsho, Denmark). SeaHorse XF Mito Stress Assay and SeaHorse XF Glycolytic Rate Assay (Agilent Technologies) were performed according to manufacturer's instruction in a 96 wells Seahorse XF. Briefly, iPSC-CM were plated in 96 well seahorse plates coated with matrigel 5 days before the experiment. Seahorse XF Base Medium (XBMS) was supplemented with 1 mM sodium pyruvate, 2 mM glutamine, and 10 mM glucose and set up to pH 7.6 at 37°C. iPSC-CM were rinsed with XBMS and incubated with 180 µL at 37°C without CO_2 for one hour. Mitochondrial chain or glycolytic pathway inhibitors from the Seahorse XF Cell Mito Stress Test (Agilent Technologies) were resuspended in XMBS following manufacturer protocol, then diluted to 10x final concentrations and loaded into the sensor cartridge ports for injection. Final concentrations were 1 µM oligomycin (ATP synthase inhibitor), 2.5 µM FCCP (which uncouples ETC activity from ATP synthesis), 1 µM each of rotenone and antimycin A (R/A) (ETC complex I and III inhibitors) and 50 mM of 2DG (Hexokinase inhibitor). The Seahorse XF96 was programed to mix for 3 minutes, wait 2 minutes then obtain measurements for 3 minutes. This cycle was repeated 3 times after each drug injection. Basal respiration was calculated as the difference between OCR at baseline and that after R/A injection. Spare respiratory capacity (SRC) was calculated as the difference between OCR after FCCP injection and that at baseline. Data were normalized by total protein measured using BCA assay.

2.7 Drug treatments

All drug treatment experiments were carried out with a MOI of 5. iPSC-CMs were pre-treated 16 hours before the infection with drugs and maintained over 48 hours of infection (unless a different condition is explicated in the Results section). Twenty-four hours after infection, media was changed by fresh media containing the drug to remove free parasites. Controls were performed using media or the vehicle. Drugs used in this are described in Supplementary Material Table 1.

2.8 HIF-1α mutagenesis using CRISPR technology

CRISPR clones were developed as previously described (Sharma et al., 2018b; Sharma et al., 2020). Briefly, gRNA sequences were designed

using CRISPR design tool (https://portals.broadinstitute.org/gpp/public/analysis-tools/sgrna-design). gRNAs were cloned in a plasmid using Zero Blunt TOPO PCR Cloning Kit (Thermo Scientific), and isolated colonies were purified using MiniPrep (Quiagen). PGP1 cells (Lee et al., 2009) were transfected with 40 µM of Cas-9 plasmid (pSpCas9(BB)-2A-Puro V2.0 (PX459). (Addgene plasmid # 62988) and 25 µM of sgRNA using AMAXA Nucleofactor (Lonza). At 48 hours post transfection, cells were selected with puromycin (1 µg/mL). Selected cells replated in low confluence to allow single cell colony growth. Isolated colonies were picked and sequenced by Sanger and MiSeq methods to confirm editing. Subcloning was carried out, as necessary to ensure that a clone contained one genotype. Two clones HIF-1$\alpha^{\Delta 301/-}$ and HIF-1$\alpha^{\Delta 301\text{-}305/+}$ (Supplemental Figure 9D) were selected for cardiomyocytes differentiation and subsequent studies.

HIF-1α gRNA sequence:

TGTACAAAAAAGCAGGCTTTAAAGGAACCAATTCAGTC GACTGGATCCGGTACCAAGGTCGGGCAGGAAGAGGGC CTATTTCCCATGATTCCTTCATATTTGCATATACGATAC AAGGCTGTTAGAGAGATAATTAGAATTAATTTGACTGTAA ACACAAAGATATTAGTACAAAATACGTGACGTAGAA AGTAATAATTTCTTGGGTAGTTTGCAGTTTTAAAATTATGT TTTAAAATGGACTATCATATGCTTACCGTAACTTGAA AGTATTTCGATTTCTTGGCTTTATATATCTTGT GGAAAGGACGAAACACCGCTAAAGGACAAGTCACCACG TTTTAGAGCTAGAAATAGCAAGTTAAAATAAGGCTA GTCCGTTATCAACTTGAAAAAGTGGCACCGAGTCGGTGCTT TTTTTCTAGACCCAGCTTTCTTGTACAAAGTTGGCATTA

Primer's sequence:

Forward – GTTTTCCAAAACAATGATGAACA

Reverse – TGAGAAATAAACATTTTTGGGGA

2.9 Lentivirus

Lentivirus particles for GLUT4 silencing were produced using SLC2A4 – GLUT4 Human shRNA Plasmid Kit (Sigma) according to manufacturer instructions. iPSC-CM were transduced with GLUT4 or scramble particles over 48 hours prior to *T. cruzi* infection. Cell contractility after GLUT4 silencing was measured using SarcTrack (Toepfer et al., 2019).

2.10 High content screening analysis

4x10^4 iPSC-CM cells were plated in a 96 wells plate for microscopy analysis. After drug treatment and infection, cells were washed with PBS and fixed with 4% PFA diluted in PBS for 30 minutes. Cells were blocked for one hour with 2% casein and incubated for 3 hours with phalloidin conjugated with Alexa 555 for actin staining and DAPI for nuclei and parasite staining. Cells were washed and kept in PBS until analysis. Images were acquired in a high content screening microscope IN Cell Analyzer 2200 (GE Life Science) and Arrayscan xTi (Thermo Scientific) with 12 photos per well in 400x magnification, 5 wells per group. The number of cells and parasites were counted using a MATLAB script specifically developed for this procedure.

3 Results

3.1 Transcriptomic and proteomic profiles of *T. cruzi* infected iPSC-CMs

We characterized the infection cycle of *T. cruzi* trypomastigotes in 30-day old iPSC-CMs. Parasites were inoculated (MOI = 5) resulting in infection of approximately 20% of exposed iPSC-CMs at 6 hours post infection (hpi). Intracellular parasite replication occurred between 24 and 48 hpi and infected iPSC-CMs burst after 72 hpi (Figures 1A, B, and Figures S1A, S1B). A similar infection cycle was observed in rat neonatal cardiomyocytes (Figure S1C).

We performed and compared RNA-seq of control iPSC-CMs (unexposed to parasite) and infected iPSC-CM cultures at 24 hpi and 48 hpi (Figure 1C and Tables S1–S3).

The infection of iPSC-CM *T. cruzi* resulted in many transcriptional changes, as represented in the PCA plot (Figure 1C), and detailed described in Supplementary Tables (Tables S4–S7). We identified an abrupt decrease in expression of genes participants of contractile apparatus, such as sarcomere and cytoskeleton proteins (Figure S2, Tables S6, S7). In comparison to controls, infected iPSC-CMs had decreased transcripts levels of key contractile proteins including actin and actinin isoforms *(ACTA1, ACTN2)*, myosin (*MYH7, MYH11, MYH9*), myosin associated light chains *(MYL7, MYL2)*, and troponins *(TNNT2, TNNC2)*.

By contrast, infection caused a marked enrichment of molecular pathways associated with immune/inflammatory activation. Infected cells had increased expression of several C-type lectin receptors and toll-like receptor (TLRs) genes that recognize pathogen-associated molecular patterns, including *CLEC17A, TLR3, TLR5* and the *TLR* adaptor protein *MYD88* (Tables S2, S5). TRIM genes that encode tripartite motif proteins, and TRIM-target genes (*DDX58*; retinoic acid inducible gene-1) that evoke downstream TLRs signals, were also increased. Notably, infected iPSC-CMs had increased expression of *HELZ2* and *PHF11*, which encode molecules that enable persistent expression of TLR-induced immune activation. In addition, and in agreement with previous data in literature, infected iPSC-CMs also had signatures associated with markedly increased mTOR activation, being the top enriched canonical pathway identified in our data (Figure 1D).

RNA-seq data also showed enhanced interferon-mediated signaling (Figures 1D, 1E), including interferon induced genes *(IFI27, IFI30, IFI35, IFI44, IFIT1, IFIT2, IFIT3, IFITM1, IFITM2, IFITM3, IFIH1, IFR1, IFR7, IFR8, IFR9, ISG15, ISG20)*, chemoattractant molecules and chemokine receptors *(CCL2, CCL5, CCL21, IL6R, IL1R, CXCL10, CXCL11)*, and cytokines *(IL1B, IL6, IL16, IL15)*.

Glycolysis was identified as another canonical pathway that was upregulated in transcriptomic data at 24 hpi and 48 hpi (Figures 1D, 1F, 2A, and Tables S4, S5). We observed upregulation of key enzyme genes in this metabolic pathway, including *HK2* and *HK1, LDHA, PFK*, and *PGM*.

Hypoxia was also a highly enriched gene pathway identified by RNA-seq analyses (Figure 1D, 1G and Tables S4, S5). Activation of HIF-1α signaling is a common phenomenon to many human

10.3389/fcimb.2023.1098457

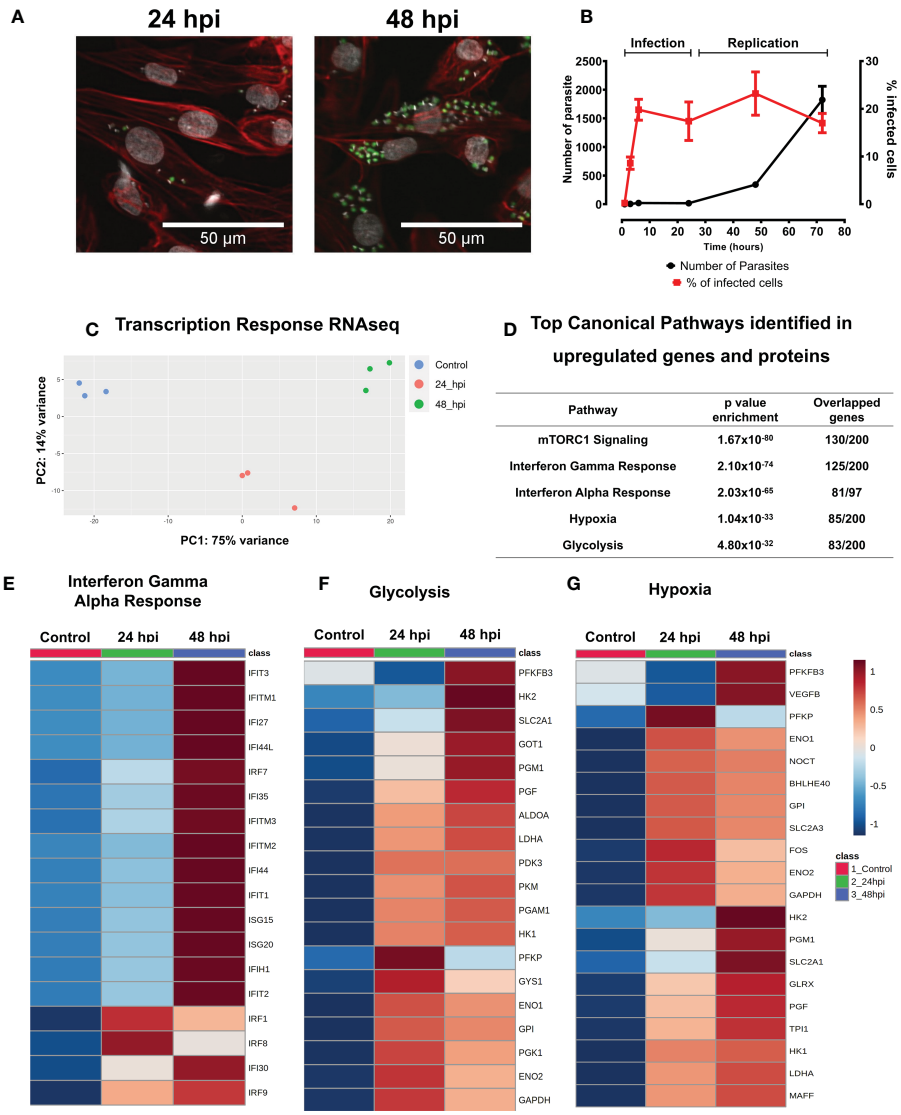

FIGURE 1
T. cruzi infected IPSC-CMs activate immune responses. **(A)** With a multiplicity of infection (MOI) 5:1 (parasite:cell), 20% of iPSC-CMs contain parasites at 24 hours that multiply 4-fold by 48 hpi, and lyse cells by 72 hpi. Fluorescent images are at 24 hpi and 48 hpi detect GFP-tagged *T. cruzi* (green), phalloidin-strained actin (red) and DAPI-stained nuclei (grey). **(B)** Percentage of infected iPSC-CMs and parasite numbers during infection and replication phases. **(C)** Transcriptomic profiles of iPSC-CMs displayed by principal component analyses. Control, uninfected (blue), 24 hpi (red) and 48 hpi (green) showing overall difference among groups in a PCA plot. **(D)** Top Canonical Pathways enriched by both, genes and proteins, upregulated after 24 hpi and 48 hpi. **(E–G)**. Heatmaps of differentially expressed genes involved in glucose metabolism, HIF-1α signaling, and interferon signaling.

infections including bacterial, viral and intracellular parasites such as *Leishmania amazonensis* and *Toxoplasma gondii*. HIF-1α levels were increased in iPSC-CMs at 24 hpi (Figure 2F), possibly due to increased phosphorylation of ERK (Figure S4B) or AKT-mTOR signaling that can augment HIF-1α translation (Semenza, 2003). Levels of transcripts encoding prolyl hydroxylases *(EGLN2)* and von Hippel Lindau protein *(VHL)* that promote HIF-1α degradation were unchanged in infected compared to control iPSC-CMs. Moreover, RNA-seq data showed increased expression of multiple direct gene targets of HIF-1α activation. At 48 hpi, transcripts encoding proteins that regulate glucose metabolism *(HK1, HK2, GPI, ENO1, ENO2, GAPDH, LDHA, PFKBP3, PFKP, PGM1, PGK1, TPI* and *GLUT1 (SLC2A1))* and *VEGFB* were significantly increased (Figure 1F and Tables S2, S5).

The expression of Interferon alpha/gamma (IFN) pathway-related genes was significantly and positively correlated with hypoxia and glycolysis pathway-related genes (as described in Tables S15, S16, with R values greater than 0.7 and FDR-corrected p-values less than 0.005). Specifically, 93 IFN pathway genes positively correlated with 27 hypoxia pathway genes and 20 glycolysis pathway genes and increased over the course of infection (0 hpi < 24 hpi < 48 hpi). Seventy-two (72) IFN pathway genes, 4 hypoxia pathway genes, and 8 glycolysis genes increased only at 48 hpi and were positively correlated (0 hpi = 24 hpi < 48 hpi); and 7 IFN pathway genes, 6 hypoxia pathway genes, and 3 glycolysis pathway genes increased only at 24 hpi and were positively correlated (0 hpi = 48 hpi < 24 hpi).

10.3389/fcimb.2023.1098457

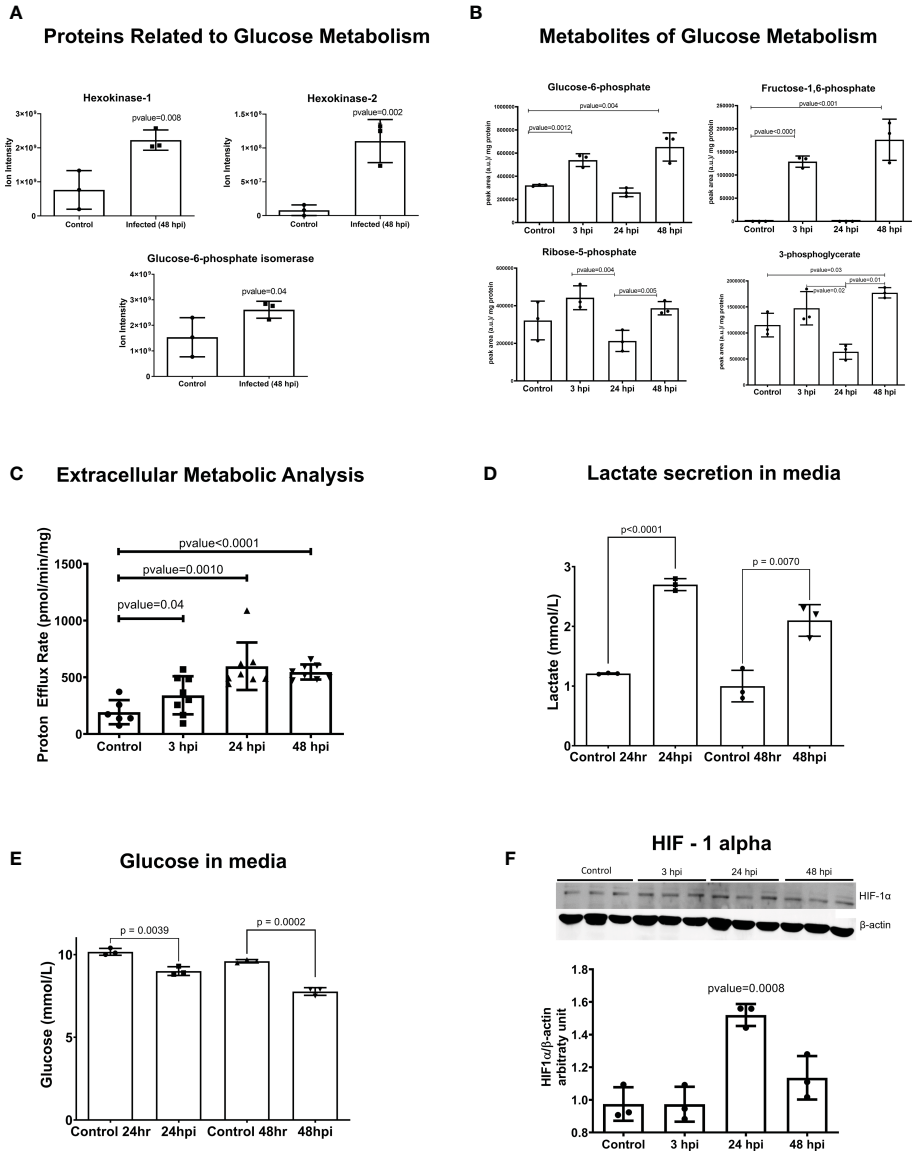

FIGURE 2
Glycolysis is activated in iPSC-CMs after *T. cruzi* infection. **(A)** Mass spectrometry (Ion Intensity) demonstrate increased levels of key metabolic regulatory enzymes (hexokinase 1 (HK1), hexokinase 2 (HK2) and glucose-6-phosphate isomerase (GPI). **(B)** Intermediate metabolites of glycolysis are increases at 3 hpi, demonstrating an early glycolytic switch after infection. **(C)** Extracellular metabolic flux analysis shows proton efflux rate in infected IPSC-CMs. **(D)** Lactate secreted in the media after parasite infection. **(E)** Glucose concentration in media showing the consumption after parasite infection. **(F)** HIF-1α protein is increased in iPSC-CMs at 24 hpi, consistent with transcriptomic data. Data reflect three independent replicates for each experiment. Statistical analyses used ANOVA test with Bonferroni correction or t-test when appropriate and p-value<0.05 was considered significant.

Oxidative phosphorylation was a pathway slightly enriched at 24 hpi, but highly increased at 48 hpi, concomitant to glycolysis (Tables S4, S5).

We confirmed our findings from transcriptional data using shotgun proteomics (Figure S3, Tables S10, S11). At 48 hpi, we observed high enrichment in the interferon-gamma-mediated signaling pathway, as well as the expression of transcriptional regulators for interferons *(IRF1, DTX3L)* and molecules activated by interferons *(HERC5, ISG15, MX1)*. We also identified a similar profile in glycolytic enzymes and TCA-related genes.

Our comprehensive analysis of transcriptomic and proteomic data reveals that *T. cruzi* infection in iPSC-CMs stimulates a robust immune response, characterized by the activation of the mTOR-HIF-1α signaling pathway and glycolytic metabolism. Notably, these same pathogen-induced signals are also observed in monocytes and macrophages, where they stimulate the activation of glycolysis. This suggests that *T. cruzi* infection may exploit common immune and metabolic pathways to facilitate its own replication and spread within host cells.

3.2 Metabolic rewiring during *T. cruzi* infection

The glycolytic activation occurs in pathogen-activated macrophages, perturbing the mitochondrial tricarboxylic acid (TCA) cycle so as to increase succinate, a proinflammatory metabolite that enhances HIF-1α activity (Tannahill et al., 2013;

Mills and O'Neill, 2016; Mills et al., 2016). Given evidence for both increased HIF-1α activity and a glycolytic activation in *T. cruzi*-infected iPSC-CMs, we performed metabolomic and extracellular metabolic flux analyses to profile the glycolytic metabolism (Figures 2B, C) and TCA cycle (Figures S6, S7).

Metabolomic data, consistent with RNA-seq and proteomic data, showed upregulation of glycolysis intermediates after infection. These metabolites increased from the beginning of infection at 3 hpi and remained upregulated at 48 hpi. However, it is worth noting that the dynamic nature of metabolism means that the production-to-consumption ratio of a metabolite may not always be accurately captured using an unlabeled metabolomic approach. This could explain why we observed decreased glycolytic intermediates at 24 hpi.

Our extracellular metabolic analysis (Figure 2C) demonstrated an increase in proton efflux rate starting at 3 hpi, which was sustained until 48 hpi, consistent with the findings from our metabolomics data. Additionally, we observed significant differences in glucose consumption and lactate secretion in the media after infection (Figures 2D, E). Analyses throughout the infection cycle showed transiently increased levels of citrate at 3 hpi and sustained increased levels of succinate through 48 hpi. Progression through the TCA cycle should normally increase fumarate and malate as a downstream consequence of increased succinate levels. However, this was not observed (Figure S6) and instead our data suggest an unbalance in the TCA cycle that sustains increased succinate levels. Additionally, RNA-seq data indicated increased expression of succinate dehydrogenases (SDHB; Table S2) which increases mitochondrial oxidation of succinate and ROS production. We also observed increased catabolism of several amino acids (glutamine, isoleucine, threonine, and valine) in iPSC-CMs after 24 hpi, indicating that intense anaplerosis likely contributes to TCA production of succinate, as was previously observed in macrophages (Corcoran and O'Neill, 2016).

Infected iPSC-CMs had increased oxygen consumption rate (OCR), and maximally increased mitochondrial respiration was observed at 48 hpi (Figure S6B). Extracellular flux experiments showed incomplete coupling of ATP production with oxygen consumption, which is indicative of mitochondrial proton leak (Figure S5A). In addition, increased secretion of nitric oxide was identified in the culture media after 24 hpi (Figure S5B). These abnormalities would increase ROS levels, which is known to improve *T. cruzi* replication in macrophages. In concordance with increased OCR, we identified genes and proteins from oxidative phosphorylation upregulated at 48 hpi (Tables S5, S11) and 498 upregulated genes (Table S2) related to mitochondria metabolism, structure, transporters/channels, and dynamics based on the MitoCarta Inventory (Rath et al., 2020).

Altogether, metabolomics analysis showed activation of glycolysis since the first hours of infection remaining up to 48 hpi; an unbalance of TCA, with upregulation of succinate that was not followed by fumarate and malate, amino acid anaplerosis and increased OCR after infection.

3.3 Manipulation of immuno-metabolic signals in *T. cruzi* infected-iPSC-CMs

We considered whether attenuating components of immuno-metabolic signals identified in *T. cruzi*-infected iPSC-CMs would influence susceptibility to parasite infection and/or parasite replication. We assessed parasite infectivity by quantifying the numbers of intracellular *T. cruzi* per total number of iPSC-CMs at 24 hpi. The same assessment at 48 hpi was used to index parasite replication rates.

First, we tested a multi-faceted polyphenolic compound, resveratrol. Pre-treatment (16 hours prior to parasite inoculation) and chronic supplementation with resveratrol to iPSC-CMs and neonatal rat cardiomyocytes (Figures S5C, S5D) did not alter parasite infection but significantly depressed amastigote proliferation rates (Figures S5C–S5E).

To further probe the effects of these agents on metabolism, we considered whether perturbations in cellular glucose and glycolysis influenced susceptibility to *T. cruzi* infection (Figure 3A). Pre-treatment of *T. cruzi* cultures with 2DG for 16 hours did not alter the parasite's infectivity or replication rates (Figure S8A). However, iPSC-CMs treated with 2DG had 60% lower infection rates and no amastigote replication (Figure 3B and Figures S8A, S8G). Timed delivery of 2DG throughout the parasites' life cycle (Figures S8B, C) demonstrated that administration within the first 4 hours after inoculation resulted in greatest attenuation of intracellular *T. cruzi* at 24 and 48 hpi. Parallel experiments in rat neonate cardiomyocytes confirmed these findings (Figure S8D).

As 2DG reduces intracellular glucose, we considered if 2DG-attenuated infectivity might result from de-glycosylation of membrane proteins that participate in parasite entry. To address this, we provided supplementary mannose to reduce the incorporation of 2DG in N-linked glycosylation reactions (Kurtoglu et al., 2007). Mannose did not alter the 2DG effects on parasite infection or intracellular replication (Figure S8E).

Pre-treatment of iPSC-CMs with 3PO, phosphofructokinase inhibitor, had no effect on parasite infection or replication (Figure 3C).

Because a glycolysis activation by cardiomyocytes increases glucose uptake through glucose-facilitated transporters GLUT1 and GLUT4 (Kraegen et al., 1993), we considered whether these membrane proteins might facilitate *T. cruzi* entry. As the levels of GLUT1 were indetectable in iPSC-CMs (Figure S9B), we only modulated GLUT4 levels. We initially tested compounds that inhibit several glucose-facilitated transporters. In comparison to vehicle-treated cells, phloretin, broadly GLUT inhibitor, significantly reduced infection and parasite replication (Figure 3D). Quercetin, another broadly GLUT inhibitor, silenced parasite infection and replication (Figure S8F), and WZB117, specific *GLUT1* and *GLUT4* inhibitor, (Figure 3E) reduced infection by approximately 50%.

We then employed genetic approaches to modulate *GLUT4* expression. Cells transfected with shRNAs attenuated human *GLUT4* transcripts to approximately 25% normal levels (Figure S9A), without causing morphologic or contractile deficits (Figure S9C). *GLUT4* shRNA-treated iPSCs-CM had approximately 50% lower infectivity at 24 and 48 hpi (Figure 3G). As these data inferred the possible involvement of *GLUT4* in *T. cruzi* infectivity, we capitalized on iPSC-CMs with an endogenous activating missense variant in *PRKAG2* that causes a 2-fold increase in *GLUT4* expression (Hinson et al., 2016). *PRKAG2*-mutant iPSC-CMs exposed to *T. cruzi* showed significantly increased infection and replication rates (Figure 3H).

With pharmacological and genetic data that implicated the GLUT4 transporter in parasite infection and replication, we

10.3389/fcimb.2023.1098457

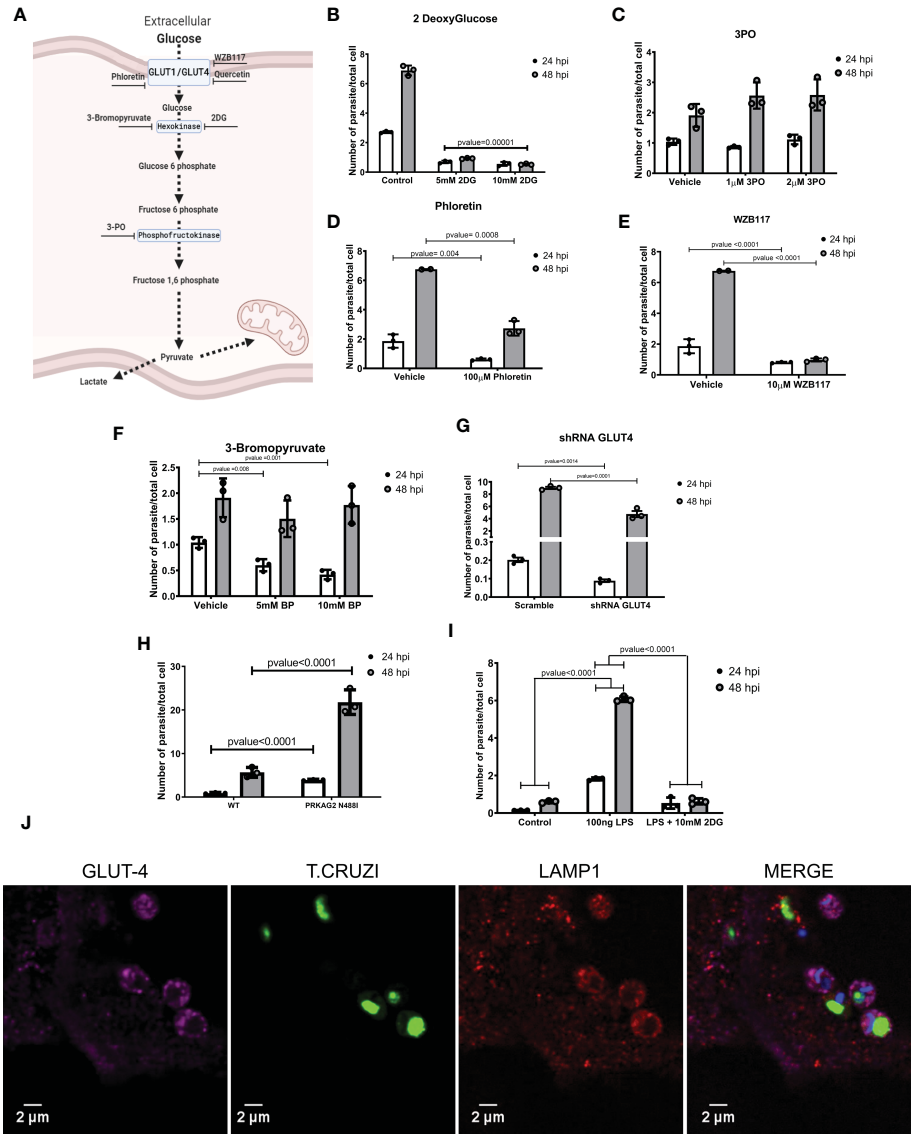

FIGURE 3
Inhibiting glycolysis impaired *T. cruzi* proliferation. **(A)** A schematic of glycolytic enzymes and inhibitors studied. **(B)** 2DG-treatment of iPSC-CMs concurrent with *T. cruzi* exposure decreased infection and cell division. **(C)** Inhibition of phosphofructokinase did not alter infection or parasite division. Inhibition of glucose transporters with **(D)** phloretin (nonspecific inhibitor) and **(E)** WZ117 (specific for GLUT1 and GLUT4) decreased infection and cell division. **(F)** Inhibition of hexokinase II by 3-bromopyruvate decreased intracellular parasites at 24 hpi but not at 48 hpi. **(G)** iPSC-CMs transduced with shRNAs targeting GLUT4 had significantly fewer intracellular parasites at 48 hpi. **(H)** PRKAG2-mutant iPSC-CMs with 2-fold higher GLUT4 levels show increased infection and parasite replication rates. **(I)** LPS-primed iPSC-CMs increased intracellular parasites at 24 hpi, while inhibition of glycolysis normalized infection rate. **(J)** Confocal images of fluorescently labeled, *T. cruzi* -infected iPSC-CMs (3 hpi) demonstrate co-localization of GLUT4 (magenta), lysosomal membrane protein 1 (red), and *T. cruzi* (green). Nuclei are DAPI stained. Data reflect three independent replicates for each experiment. Statistical analyses used ANOVA test with Bonferroni correction and p-value<0.05 was considered significant.

considered if *T. cruzi* hijacked this membrane protein for cell entry. Using immunofluorescence and confocal imaging we found colocalized GLUT4, parasite, and lysosome-membrane associated protein-1 (LAMP1) in iPSC-CMs at 3 hpi (Figure 3J). Together these data and pharmacological studies suggest that diversion of host metabolism promoted parasite entry concurrent with activation of glycolytic metabolism.

Prior studies suggest central roles of HIF-1α signaling in both glycolytic metabolism and innate signaling in immune cells (Corcoran and O'Neill, 2016). To consider if HIF-1α similarly serves as linchpin in infected iPSC-CMs, we analyzed two independent HIF-1α mutant lines (Figures S9D–G). HIF-1α$^{\Delta 301\text{-}305/+}$ iPSC-CMs express a heterozygous inframe deletion of five amino acids 301-305; HIF-1α$^{\Delta 301/-}$ iPSC-CMs express an inframe deletion of residue 301 opposite to a null allele. In comparison to WT iPSC-CMs, HIF-1α mutant lines had 60% lowered *T. cruzi* infection rates (Figure 4A). Using proton efflux rates as an index of glycolysis, we found substantially reduced rewiring of metabolism in infected HIF-1α$^{\Delta 301/-}$ iPSC-CMs. While proton efflux was comparable in uninfected mutant and WT iPSC-CMs (Figure 4B), infected HIF-1α$^{\Delta 301/-}$ iPSC-CMs did not augment proton efflux nor increase oxygen consumption rates, which occurred in WT iPSC-CMs (Figure 4C). We interpret these data to indicate that HIF-1α activation is necessary for glycolytic activation after *T. cruzi* infection of iPSC-CMs and promotes intracellular entry and parasite replication.

10.3389/fcimb.2023.1098457

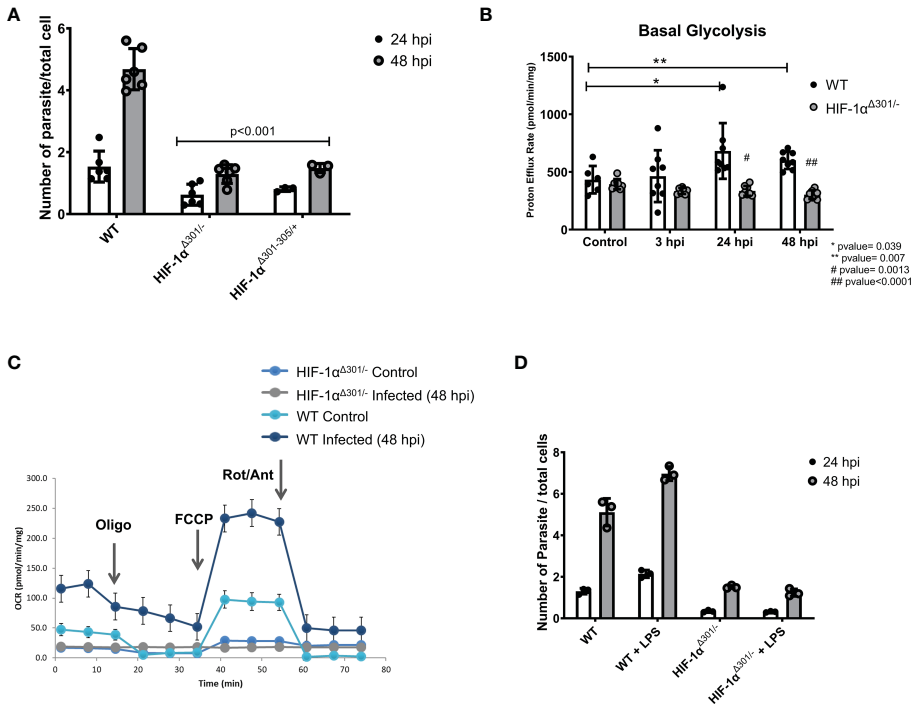

FIGURE 4
HIF-1α is required for glycolytic switch after *T. cruzi* infection. **(A)** Two iPSC-CMs lines carrying HIF-1α$^{\Delta 301/-}$(compound inframe deletion of amino acid 301 and a null allele) or HIF-1α$^{\Delta 301\text{-}305/+}$ (a heterozygous inframe deletion of amino acids 301- 305) have lower infection and replicate rates compared to WT cells. **(B)** HIF-1α$^{\Delta 301/-}$ iPSC-CMs did not activate proton efflux, an indicator of glycolytic activation. **(C)** Extracellular metabolic flux analyses demonstrated lower mitochondrial respiratory activity (oxygen consumption rate; OCR) in HIF-1α$^{\Delta 301/-}$ iPSC-CMs at 48 hpi compared to WT. **(D)** HIF-1α$^{\Delta 301/-}$ iPSC-CMs were unresponsive to LPS-priming. Data reflects six **(A, B)** and three **(C, D)** independent replicates for each experiment. Statistical analyses used ANOVA test with Bonferroni correction and p-value<0.05 was considered significant.

3.4 Modulation of adaptive human cellular response suggests co-evolution of *T. cruzi* to exploit defense mechanisms

Innate immune activation with concurrent metabolic remodeling is a highly conserved response that is carried out by immune cells in response to many pathogens to benefit the host. Immune cells that are primed to activate immuno-metabolic responses are able to reduce infection rates and improve survival when subsequently inoculated with a pathogen (Cheng et al., 2014). To discern whether immuno-metabolic changes observed in infected iPSC-CMs benefited the host or parasite we used two approaches.

Our study protocol infected approximately 20% of exposed iPSC-CMs. This allowed us to consider if uninfected bystander iPSC-CMs were influenced by *T. cruzi*-mediated responses in infected cells, such as increased expression of secreted cytokines like IL-1β and IL-6. Capitalizing on the GFP-tagged parasites, we FACS-sorted infected and bystander iPSC-CMs at 48 hpi and compared RNA-seq data (Tables S8, S9). Remarkably, despite the considerable transcriptional changes in infected cells, RNA-seq showed no evidence for innate/immune responses or the mTOR-HIF-1α pathway activation in bystander iPSC-CMs. Additionally, bystander cells showed minimal changes in other transcripts that might suggest activation of a protective pathway.

Next, we asked whether pretreatment of iPSC-CMs with lipopolysaccharides (LPS), an endotoxin that increases innate immune-metabolic signaling and ROS production would influence *T. cruzi* infection. iPSC-CMs treated with LPS for 16 hours were viable and exhibited cell structures comparable to untreated iPSC-CMs, suggesting little or no toxicity from this treatment. In comparison to naive iPSC-CMs, pre-treatment with LPS increased *T. cruzi* infection and replication (Figure 3J). LPS appeared to activate the glycolysis pathway, as co-administration of 2DG with *T. cruzi* to LPS-treated iPSC-CMs normalized infection rates to that observed in naive iPSC-CMs (Figure 3I). Moreover, HIF-1α mutant iPSC-CMs were unresponsive to LPS pre-activation infectivity (Figure 4D). Comparison of RNA-seq data from LPS-treated WT and HIF-1α$^{\Delta 301/-}$ iPSC-CMs showed that mutant iPSC-CMs failed to upregulate pathways involved in mTORC1 signaling, oxidative phosphorylation, and glycolysis (Tables S12–14).

Together our data support the conclusion that *T. cruzi* infection activates intrinsic inflammatory and immune-metabolic responses in cardiomyocytes that trigger HIF-1α-mediated metabolic rewiring. The resultant activates glycolysis, increasing levels of glucose transporters that facilitate parasite infectivity.

4 Discussion

We found that human iPSC-CMs infected with *T. cruzi* exhibit a genetic program that is typically found in inflammatory cells. Through transcriptomic, proteomic, and metabolomic analysis of *T. cruzi*-infected iPSC-CMs, we observed the activation of innate immune responses, including TLRs, interferons, and cytokines, which triggered the upregulation of glycolysis in iPSC-CMs through

the activation of a pathway involving AKT, mTOR, and HIF-1α. This increase in glycolysis, mediated by HIF-1α, led to an increase in GLUT4 in the plasma membrane, which may facilitate *T. cruzi* entry into host cells.

Our data considerably expand prior studies that demonstrate cytokine expression in *T. cruzi* -infected iPSC-CMs (Bozzi et al., 2019), and indicate robust interferon signaling, similar to observations in other infected cell lineages, and infected patients and animal models (Kierszenbaum et al., 1995; Laucella et al., 2004; Bruno et al., 2020).

Although healthy cardiomyocytes preferentially metabolize fatty acids, infected iPSC-CMs adopted glycolysis with increased glucose consumption and lactate secretion. The same glycolysis activation was identified in CD4 T-cells during both the acute and chronic phases of *T. cruzi* infected mice (Ana et al., 2021). Additionally, upregulation of glycolysis genes such as *PFKB, PDK3* and *PGAM1* have been described in the hearts of *T. cruzi* infected mice (Bruno et al., 2020).

Oxidative phosphorylation and increased OCR described here were also identified in other studies cells (Koo et al., 2018; Libisch et al., 2018; Katherine et al., 2019; Choudhuri et al., 2021). Like activated immune cells, infected iPSC-CMs showed accumulation of succinate and increased succinate dehydrogenase expression that likely contributed to HIF-1α stabilization and activation, oxidative stress, and increased the expression of pro-inflammatory molecules IL-1β and IL-6 (Tannahill et al., 2013; Mills and O'Neill, 2014; Corcoran and O'Neill, 2016; Mills and O'Neill, 2016).

Finding that cardiomyocytes, monocytes, macrophages, and dendritic cells share a cell autonomous immune-metabolic pathway underscores its importance for pathogen control. The evolution of these responses enhances defensive roles to combat a wide range of intracellular pathogens. Indeed, biochemical activation of this pathway with LPS causes trained immunity in monocytes that elicits strong protective responses when restimulated by different pathogens including viruses, bacteria, fungi (Fecher et al., 2019), mycobacterium (Gleeson et al., 2016; Ogryzko et al., 2019) and parasites (McGettrick et al., 2016). Moreover, microbes have evolved strategies to evade this pathway, including the production of indole pyruvate by the extracellular parasite *T. brucei* that promotes HIF-1α degradation and reduces IL-1β production (McGettrick et al., 2016).

However, our data suggest that *T. cruzi* has highjacked this defensive pathway to advance parasite infection and proliferation in cardiomyocytes. By pharmacological and genetic targeting to alter different arms of the immuno-metabolic response we show that the glycolysis activation in cardiomyocytes after infection benefits the parasite, not the host. Silencing the expression of glucose transporters or 2DG-inactivation of glycolysis attenuated infection. Conversely, cardiomyocytes expressing a constitutively active *PRKAG2* variant that increases glucose transporters (Hinson et al., 2016) or LPS-treatment, increased infection, and amastigote proliferation.

These studies and immunofluorescence data that colocalize glucose transporters and *T. cruzi* within lysosomes implicate key membrane proteins in parasite entry into cardiomyocytes. HIF-1α may indirectly facilitate this process as infection (and replication) was decreased in HIF-1α-mutant iPSC-CMs. Previous studies indicating that GLUT4 translocation to the membrane is dependent on HIF-1α signaling (Sakagami et al., 2014) further supports our conclusion that HIF-1α signaling facilitates infection. Moreover, the attenuated increase in parasite infection that we observed in LPS-primed HIF-1α mutant iPSC-CMs, and in iPSC-CMs treated with both LPS and 2DG suggests that LPS effects are largely mediated by HIF-1α and glycolysis effects on cardiomyocyte metabolism.

We recognize that cell-based studies cannot fully recapitulate *in vivo* responses. iPSC-CM cultures are devoid of non-cardiomyocyte cells that reside within the myocardium as well as migratory inflammatory cells that can influence cardiomyocyte responses, cardiac architecture, and function. In addition, while this model recapitulates mechanisms related to the acute infection these may differ with chronic infection. Despite these limitations, our studies of iPSC-CMs provide new insights in the pathobiology of *T. cruzi* infected hearts. That bystander cardiomyocytes showed no pro-inflammatory or cytokine responses, despite proximity to infected iPSC-CMs, suggests that the proportion of infected cardiomyocytes may influence recruitment and activation of cytotoxic immune cells to kill *T. cruzi*. Low infection levels that escape immune detection and eradication might promote a cardiac reservoir for parasites (Burgos et al., 2010; Nagajyothi et al., 2012). Yet even low parasite burden evoked profound changes in cardiomyocyte cell biology, as was evident at 24 hpi, when 20% of cells contained only one or two intracellular parasites. Concurrent intermittent, low level cardiomyocyte lysis and reinfection of nearby cells could cause progressive cardiac deterioration as well as immunosuppression-induced reactivation of infection (Burgos et al., 2010; Nagajyothi et al., 2012). Another limitation that should be pointed is that by measuring infection at 24 hpi, it is not possible to distinguish between the initial process of infection and the subsequent survival of the parasite within the host. Both of these processes are occurring at the same time, and the measurements taken at this time point will reflect the combined effects of both infection and parasite persistence.

Other mechanisms besides active parasite replication and cardiomyocyte lysis may contribute to the emergence of chronic cardiomyopathy in 30% of *T. cruzi* infected individuals (Costa et al., 2017; Bonney et al., 2019). Innate immune responses that are trained by exposure to a pathogen or molecular mimicry can be reactivated by a distinct exposure, in part through epigenetic reprogramming (Kleinnijenhuis et al., 2012; Quintin et al., 2012; Cheng et al., 2014). Reactivation of an immuno-metabolic program established in response to other triggers, might also facilitate *T. cruzi* infection. Future epigenetic studies may help to illuminate this possibility.

Additionally, we note that two key components of this program - reduced expression of contractile genes and activation of glycolysis - would impair contractility and limit ATP production. Prior studies in animal models demonstrate that *T. cruzi* infection disrupts sarcomere and cytoskeleton proteins and elicits aberrant Ca2+ transients during both the parasite replication (Adesse et al., 2010; Manque et al., 2011; Caradonna et al., 2013; Bozzi et al., 2019) and cellular burst phases (Bilate et al., 2008). Recent findings connect inflammatory signaling with the loss of sarcomere proteins by showing that iPSC-CMs exposed to interferon gamma reduce contractile force, induce myofibrillar disarray and decrease the expression of contractile

apparatus proteins (Zhan et al., 2021). Downregulation of cardiomyocyte structural proteins, induced by interferon, occurs through JAK/STAT signaling, and inhibition of this pathway abrogates sarcomere disruption (Chen et al., 2021; Zhan et al., 2021). In our study, we found JAK/STAT signaling is upregulated at both 24 hpi and 48 hpi (Tables S4, S5), including STAT1, STAT2, STAT3, STAT5 and JAK3 upregulation (Tables S1, S2).

We suggest that strategies to restore normal cardiomyocyte metabolism may attenuate *T. cruzi* infectivity, improve cardiac energetics, and reduce the emergence of cardiomyopathy and heart failure from Chagas disease.

Data availability statement

The data presented in the study are deposited in the NCBI's Gene Expression Omnibus repository and are accessible through GEO Series accession number GSE223600 (https://www.ncbi.nlm.nih.gov/geo/query/acc.cgi?acc=GSE223600). These records are scheduled to be publicly available on Jan 28, 2023.

Author contributions

GV designed research studies, conducted experiments, acquired, and analyzed data and wrote the manuscript. JA conducted experiments, acquired, and analyzed data. KP conducted experiments and acquired data. CT designed experiments, conducted experiments, and acquired data. JG conducted experiments and acquired data. LW designed experiments, conducted experiments, and acquired data. DB conducted experiments and provided reagents. SS provided reagents. VC, JSS, and KC conducted experiments and acquired data. JK designed research studies and provided reagents. AP designed research studies, analyzed data, and wrote manuscript. JGS designed research studies, analyzed data, and review the manuscript. CS designed research studies, analyzed data, and wrote manuscript. All authors contributed to the article and approved the submitted version.

Funding

These studies were supported in part by National Institutes of Health (NIH) 5R01HL133165 and HL080494 (CES and JGS), the Howard Hughes Medical Institute (CES), fellowship support from the Sao Paulo Research Foundation fellowship 2017/13706-0 and 2019/11821-1 (GV), and the Sir Henry Wellcome fellowship 206466/Z/17/Z, and University of Oxford BHF CRE Intermediate Transition Fellowship RE/18/3/34214 (CT).

Acknowledgments

We thank the Human Neuron Core at Boston Children's Hospital; BCH IDDRC, U54HD090255 for assistance in high content screening images analyses, the MicRoN (Microscopy Resources On the North Quad) core for confocal imaging, and Dr. Ramendra Pandey, Dr. Marilda Savoia and Dr. Edecio Cunha-Neto from the Heart Institute, University of Sao Paulo for kindly providing Y-*T. cruzi* strain.

Conflict of interest

DB is co-founder of LizarBio Therapeutics. CT works as consultant for Myokardia Inc. JS and CS are founders of Myokardia (a Bristol Myers Squibb Subsidiary) and consultants for Maze and BridgeBio. CS serves on the Board of Directors for Merck Pharmaceuticals and the Burroughs Wellcome Fund.

The remaining authors declare that the research was conducted in the absence of any commercial or financial relationships that could be construed as a potential conflict of interest.

Publisher's note

Supplementary material

The Supplementary Material for this article can be found online at: https://www.frontiersin.org/articles/10.3389/fcimb.2023.1098457/full#supplementary-material

References

Adesse, D., Garzoni, L. R., Meirelles, M. D. N., Iacobas, D. A., Iacobas, S., Spray, D. C., et al. (2010). Transcriptomic signatures of alterations in a myoblast cell line infected with four distinct strains of trypanosoma cruzi. *Am. J. Trop. Med. Hygiene.* 82 (5), 846–854. doi: 10.4269/ajtmh.2010.09-0399

Ana, Y., Rojas Marquez, J. D., Fozzatti, L., Baigorrí, R. E., Marin, C., Maletto, B. A., et al. (2021). An exacerbated metabolism and mitochondrial reactive oxygen species contribute to mitochondrial alterations and apoptosis in CD4 T cells during the acute phase of trypanosoma cruzi infection. *Free Radic. Biol. Med.* 163, 268–280. doi: 10.1016/J.FREERADBIOMED.2020.12.009

Benjamin, E. J., Virani, S. S., Callaway, C. W., Chamberlain, A. M., Chang, A. R., Cheng, S., et al. (2018). Heart disease and stroke statistics - 2018 update: A report from the American heart association. *Circulation.* 137, e67–e492. doi: 10.1161/CIR.0000000000000558

Bilate, A. M., Teixeira, P. C., Ribeiro, S. P., Brito, T., Silva, A. M., Russo, M., et al. (2008). Distinct outcomes of trypanosoma cruzi infection in hamsters are related to myocardial parasitism, Cytokine/Chemokine gene expression, and protein expression profile. *J. Infect. Dis.* 198 (4), 614–623. doi: 10.1086/590347

Bocchi, E. A., Bestetti, R. B., Scanavacca, M. I., Cunha Neto, E., and Issa, V. S. (2017). Chronic chagas heart disease management: From etiology to cardiomyopathy treatment. *J. Am. Coll. Cardiol.* 70, 1510–1524. doi: 10.1016/J.JACC.2017.08.004

Bonney, K. M., Luthringer, D. J., Kim, S. A., Garg, N. J., and Engman, D. M. (2019). Pathology and pathogenesis of chagas heart disease. *Annu. Rev. Pathol.* 14, 421. doi: 10.1146/ANNUREV-PATHOL-020117-043711

Bozzi, A., Sayed, N., Matsa, E., Sass, G., Neofytou, E., Clemons, K. V., et al. (2019). Using human induced pluripotent stem cell-derived cardiomyocytes as a model to study

trypanosoma cruzi infection. *Stem Cell Rep*. 12 (6), 1232–1241. doi: 10.1016/J.STEMCR.2019.04.017

Braunwald, E. (2015). The war against heart failure: The lancet lecture. *Lancet*. 385 (9970), 812–824. doi: 10.1016/S0140-6736(14)61889-4

Burgos, J. M., Diez, M., Vigliano, C., Bisio, M., Risso, M., Duffy, T., et al. (2010). Molecular identification of trypanosoma cruzi discrete typing units in end-stage chronic chagas heart disease and reactivation after heart transplantation. *Clin. Infect. Dis*. 51 (5), 485–495. doi: 10.1086/655680

Castro, T. B. R., Canesso, M. C. C., Boroni, M., Chame, D. F., Souza, D. L., Toledo, N. E., et al. (2020). Differential modulation of mouse heart gene expression by infection with two trypanosoma cruzi strains: A transcriptome analysis. *Front. Genet*. 11, 1031. doi: 10.3389/fgene.2020.01031

Cao, X., Fang, L., Gibbs, S., Huang, Y., Dai, Z., Wen, P., et al. (2007). Glucose uptake inhibitor sensitizes cancer cells to daunorubicin and overcomes drug resistance in hypoxia. *Cancer Chemother. Pharmacol*. 59, 495–505. doi: 10.1007/s00280-006-0291-9

Caradonna, K. L., Engel, J. C., Jacobi, D., Lee, C. H., and Burleigh, B. A. (2013). Host metabolism regulates intracellular growth of trypanosoma cruzi. *Cell Host Microbe*. 13 (1), 108–117. doi: 10.1016/j.chom.2012.11.011

Cheng, S. C., Quintin, J., Cramer, R. A., Shepardson, K. M., Saeed, S., Kumar, V., et al. (2014). MTOR- and HIF-1α-mediated aerobic glycolysis as metabolic basis for trained immunity. *Sci. (1979)* 345 (6204):1250684. doi: 10.1126/science.1250684

Chen, Z., Li, B., Zhan, R. Z., Rao, L., and Bursac, N. (2021). Exercise mimetics and JAK inhibition attenuate IFN-γ-induced wasting in engineered human skeletal muscle. *Sci. Adv*. 7, eabd9502. doi: 10.1126/sciadv.abd9502

Chen, Q. M., and Maltagliati, A. J. (2018). Nrf2 at the heart of oxidative stress and cardiac protection. *Physiol. Genomics* 50, 77–97. doi: 10.1152/physiolgenomics.00041.2017

Choudhuri, S., Chowdhury, I. H., and Garg, N. J. (2021). Mitochondrial regulation of macrophage response against pathogens. *Front. Immunol*. 0. doi: 10.3389/FIMMU.2020.622602

Clem, B., Telang, S., Clem, A., Yalcin, A., Meier, J., Simmons, A., et al. (2008). Small-molecule inhibition of 6-phosphofructo-2-kinase activity suppresses glycolytic flux and tumor growth. *Mol. Cancer Ther*. 7, 110–120. doi: 10.1158/1535-7163.MCT-07-0482

Corcoran, S. E., and O'Neill, L. A. J. (2016). HIF1α and metabolic reprogramming in inflammation. *J. Clin. Invest*. 126 (10), 3699–3707. doi: 10.1172/JCI84431

Costa, S., Rassi, S., Freitas, E.M.d M., Gutierrez, N., Boaventura, F. M., de Costa, L.P.d C. S., et al. (2017). Prognostic factors in severe chagasic heart failure. *Arq. Bras. Cardiol*. 108, 246–254. doi: 10.5935/abc.20170027

Dias, P. P., Capila, R. F., do Couto, N. F., Estrada, D., Gadelha, F. R., Radi, R., et al. (2017). Cardiomyocyte oxidants production may signal to *T. cruzi* intracellular development. *PLos Negl. Trop. Dis*. 11, e0005852. doi: 10.1371/journal.pntd.0005852

Engström, P. G., Steijger, T., Sipos, B., Grant, G. R., Kahles, A., Rätsch, G., et al. (2013). Systematic evaluation of spliced alignment programs for RNA-seq data. *Nat. Methods* 10, 1185–1191. doi: 10.1038/nmeth.2722

Fecher, R. A., Horwath, M. C., Friedrich, D., Rupp, J., and Deepe, G. S. (2019). Inverse Correlation between IL-10 and HIF-1α in Macrophages Infected with Histoplasma capsulatum. *J Immunol*. 197 (2), 565–579 doi: 10.4049/jimmunol.1600342

Gleeson, L. E., Sheedy, F. J., Palsson-McDermott, E. M., Triglia, D., O'Leary, S. M., O'Sullivan, M. P., et al. (2016). Mycobacterium tuberculosis induces aerobic glycolysis in human alveolar macrophages that is required for control of intracellular bacillary replication. *J. Immunol*. 196 (6), 2444–2449. doi: 10.4049/jimmunol.1501612

Granchi, C., Fortunato, S., and Minutolo, F. (2016). Anticancer agents interacting with membrane glucose transporters. *Medchemcomm* 7, 1716–1729. doi: 10.1039/c6md00287k

Hamilton, K. E., Rekman, J. F., Gunnink, L. K., Busscher, B. M., Scott, J. L., Tidball, A. M., et al. (2018). Quercetin inhibits glucose transport by binding to an exofacial site on GLUT1. *Biochimie* 151, 107–114. doi: 10.1016/j.biochi.2018.05.012

Heidenreich, P. A., Albert, N. M., Allen, L. A., Bluemke, D. A., Butler, J., Fonarow, G. C., et al. (2013). Forecasting the impact of heart failure in the united states. *Circ. Heart Fail* 6, 606–619. doi: 10.1161/HHF.0b013e318291329a

Higuchi, M. D. L., Benvenuti, L. A., Reis, M. M., and Metzger, M. (2003). Pathophysiology of the heart in chagas' disease: Current status and new developments. *Cardiovasc. Res*. 60 (1), 96–107. doi: 10.1016/S0008-6363(03)00361-4

Hinson, J. T., Chopra, A., Lowe, A., Sheng, C. C., Gupta, R. M., Kuppusamy, R., et al. (2016). Integrative analysis of PRKAG2 cardiomyopathy iPS and microtissue models identifies AMPK as a regulator of metabolism, survival, and fibrosis. *Cell Rep*. 17, 3292–3304. doi: 10.1016/j.celrep.2016.11.066

Ihrlund, L. S., Hernlund, E., Khan, O., and Shoshan, M. C. (2008). 3-bromopyruvate as inhibitor of tumour cell energy metabolism and chemopotentiator of platinum drugs. *Mol. Oncol*. 2, 94–101. doi: 10.1016/j.molonc.2008.01.003

Katherine, P., Nino, B., Maria González-Ortiz, L., Patricia Sánchez-Villamil, J., Celis-Rodríguez, M. A., Lineros, G., et al. (2019). Methodological guide measuring mitochondrial respiration in adherent cells infected with trypanosoma cruzi chagas 1909 using seahorse extracellular flux analyser. *Folia Parasitol*. 66, 16. doi: 10.14411/fp.2019.016

Kierszenbaum, F., Lopes, H. M., Tanner, M. K., and Sztein, M. B. (1995). Trypanosoma cruzi-induced decrease in the level of interferon-gamma receptor expression by resting and activated human blood lymphocytes. *Parasite Immunol*. 17, 207–214. doi: 10.1111/J.1365-3024.1995.TB00890.X

Kleinnijenhuis, J., Quintin, J., Preijers, F., Joosten, L. A. B., Ifrim, D. C., Saeed, S., et al. (2012). Bacille calmette-guérin induces NOD2-dependent nonspecific protection from reinfection *via* epigenetic reprogramming of monocytes. *Proc. Natl. Acad. Sci. U.S.A*. 109, 17537–17542. doi: 10.1073/pnas.1202870109

Konagaya, Y., Terai, K., Hirao, Y., Takakura, K., Imajo, M., Kamioka, Y., et al. (2017). A highly sensitive FRET biosensor for AMPK exhibits heterogeneous AMPK responses among cells and organs. *Cell Rep*. 21, 2628–2638. doi: 10.1016/j.celrep.2017.10.113

Koo, S. J., Chowdhury, I. H., Szczesny, B., Wan, X., and Garg, N. J. (2016). Macrophages promote oxidative metabolism to drive nitric oxide generation in response to trypanosoma cruzi. *Infect. Immun*. 84, 3527–3541. doi: 10.1128/IAI.00809-16

Koo, S. j, Szczesny, B., Wan, X., Putluri, N., and Garg, N. J. (2018). Pentose phosphate shunt modulates reactive oxygen species and nitric oxide production controlling trypanosoma cruzi in macrophages. *Front. Immunol*. 9. doi: 10.3389/fimmu.2018.00202

Kraegen, E. W., Sowden, J. A., Halstead, M. B., Clark, P. W., Rodnick, K. J., Chisholm, D. J., et al. (1993). Glucose transporters and *in vivo* glucose uptake in skeletal and cardiac muscle: Fasting, insulin stimulation and immunoisolation studies of GLUT1 and GLUT4. *Biochem. J*. 295 (1), 287–293. doi: 10.1042/bj2950287

Kurtoglu, M., Gao, N., Shang, J., Maher, J. C., Lehrman, M. A., Wangpaichitr, M., et al. (2007). Under normoxia, 2-deoxy-D-glucose elicits cell death in select tumor types not by inhibition of glycolysis but by interfering with n-linked glycosylation. *Mol. Cancer Ther*. 6 (11), 3049–3058. doi: 10.1158/1535-7163.MCT-07-0310

Kwon, O., Eck, P., Chen, S., Corpe, C. P., Lee, J.-H., Kruhlak, M., et al. Inhibition of the intestinal glucose transporter GLUT2 by flavonoids. *FASEB J. • Res. Communication*. doi. doi: 10.1096/fj.06-6620com

Laucella, S. A., Postan, M., Martin, D., Hubby Fralish, B., Albareda, M. C., Alvarez, M. G., et al. (2004). Frequency of interferon-γ–producing T cells specific for trypanosoma cruzi inversely correlates with disease severity in chronic human chagas disease. *J. Infect. Dis*. 189, 909–918. doi: 10.1086/381682

Lee, J.-H., Park, I.-H., Gao, Y., Li, J. B., Li, Z., Daley, G. Q., et al. (2009). A robust approach to identifying tissue-specific gene expression regulatory variants using personalized human induced pluripotent stem cells. *PLos Genet*. 5 (11), e1000718. doi: 10.1371/journal.pgen.1000718

Lewis, M. D., and Kelly, J. M. (2016). Putting infection dynamics at the heart of chagas disease. *Trends Parasitol*. 32, 899–911. doi: 10.1016/J.PT.2016.08.009

Liberzon, A., Birger, C., Thorvaldsdóttir, H., Ghandi, M., Mesirov, J. P., and Tamayo, P. (2015). The molecular signatures database hallmark gene set collection. *Cell Syst*. 1 (6), 417–425. doi: 10.1016/j.cels.2015.12.004

Libisch, M. G., Faral-Tello, P., Garg, N. J., Radi, R., Piacenza, L., and Robello, C. (2018). Early trypanosoma cruzi infection triggers mTORC1-mediated respiration increase and mitochondrial biogenesis in human primary cardiomyocytes. *Front. Microbiol*. 9. doi: 10.3389/fmicb.2018.01889

Love, M. I., Huber, W., and Anders, S. (2014). Moderated estimation of fold change and dispersion for RNA-seq data with DESeq2. *Genome Biol*. 15, 550. doi: 10.1186/s13059-014-0550-8

Machado, F. S., Jelicks, L. A., Kirchhoff, L., Shirani, J., Nagajyothi, F., Mukherjee, S., et al. (2012). Chagas heart disease: Report on recent developments. *Cardiol. Rev*. 20, 53. doi: 10.1097/CRD.0B013E31823EFDE2

Maguire, J. H. (2006). Chagas' disease — can we stop the deaths? *New Engl. J. Med*. 355, 760–761. doi: 10.1056/nejmp068130

Malagrino, P. A., Venturini, G., Yogi, P. S., Dariolli, R., Padilha, K., Kiers, B., et al. (2017). Proteome analysis of acute kidney injury – discovery of new predominantly renal candidates for biomarker of kidney disease. *J. Proteomics* 151, 66–73. doi: 10.1016/j.jprot.2016.07.019

Manne-Goehler, J., Umeh, C. A., Montgomery, S. P., and Wirtz, V. J. (2016). Estimating the burden of chagas disease in the united states. *PLos Negl. Trop. Dis*. 10 (11), e0005033. doi: 10.1371/journal.pntd.0005033

Manque, P. A., Probst, C. M., Probst, C., Pereira, M. C. S., Rampazzo, R. C. P., Ozaki, L. S., et al. (2011). Trypanosoma cruzi infection induces a global host cell response in cardiomyocytes. *Infect. Immun*. 79, 1855–1862. doi: 10.1128/IAI.00643-10

Martinez, S. J., Romano, P. S., and Engman, D. M. (2020). Precision health for chagas disease: Integrating parasite and host factors to predict outcome of infection and response to therapy. *Front. Cell Infect. Microbiol*. 0. doi: 10.3389/FCIMB.2020.00210

Mathers, C., Stevens, G. A., Mahanani, W. R., Fat, D. M., and Hogan, D. (2018). WHO methods and data sources for country-level causes of death 2000-2016. *Global Health Estimates Technical Paper WHO/HIS/IER/GHE/2018.3, Department of Information, Evidence and Research*. (Geneva: WHO).

McGettrick, A. F., Corcoran, S. E., Barry, P. J. G., McFarland, J., Crès, C., Curtis, A. M., et al. (2016). Trypanosoma brucei metabolite indolepyruvate decreases HIF-1α and glycolysis in macrophages as a mechanism of innate immune evasion. *Proc. Natl. Acad. Sci*. 113, E7778–E7787. doi: 10.1073/PNAS.1608221113

Mills, E. L., Kelly, B., Logan, A., Costa, A. S. H., Varma, M., Bryant, C. E., et al. (2016). Succinate dehydrogenase supports metabolic repurposing of mitochondria to drive inflammatory macrophages. *Cell*. 167 (2), 457–470.E13. doi: 10.1016/j.cell.2016.08.064

Mills, E., and O'Neill, L. J. (2014). Succinate: a metabolic signal in inflammation. *Trends Cell Biol*. 24, 313–320. doi: 10.1016/j.tcb.2013.11.008

Mills, E. L., and O'Neill, L. A. (2016). Reprogramming mitochondrial metabolism in macrophages as an anti-inflammatory signal. *Eur. J. Immunol*. 46 (1), 13–21. doi: 10.1002/eji.201445427

Nagajyothi, F., Machado, F. S., Burleigh, B. A., Jelicks, L. A., Scherer, P. E., Mukherjee, S., et al. (2012). Mechanisms of trypanosoma cruzi persistence in chagas disease. *Cell Microbiol.* 14 (5), 634–643. doi: 10.1111/j.1462-5822.2012.01764.x

Nizet, V., and Johnson, R. S. (2009). Interdependence of hypoxic and innate immune responses. *Nat. Rev. Immunol.* 9, 609–617. doi: 10.1038/nri2607

Ogryzko, N. V., Lewis, A., Wilson, H. L., Meijer, A. H., Renshaw, S. A., and Elks, P. M. (2019). Hif-1α-Induced expression of il-1β protects against mycobacterial infection in zebrafish. *J. Immunol.* 202, 494–502. doi: 10.4049/jimmunol.1801139

Ojelabi, O. A., Lloyd, K. P., Simon, A. H., De Zutter, J. K., and Carruthers, A. (2016). WZB117 (2-fluoro-6-(m-hydroxybenzoyloxy) phenyl m-hydroxybenzoate) inhibits GLUT1-mediated sugar transport by binding reversibly at the exofacial sugar binding site. *J. Biol. Chem.* 291, 26762–26772. doi: 10.1074/jbc.M116.759175

Park, J. B., and Levine, M. (2000). Intracellular accumulation of ascorbic acid is inhibited by flavonoids *via* blocking of dehydroascorbic acid and ascorbic acid uptakes in HL-60, U937 and jurkat cells. *J. Nutr.* 130, 1297–1302. doi: 10.1093/jn/130.5.1297

Pérez-Mazliah, D., Ward, A. I., and Lewis, M. D. (2021). Host-parasite dynamics in chagas disease from systemic to hyper-local scales. *Parasite Immunol.* 43 (2):e12786. doi: 10.1111/pim.12786

Quintin, J., Saeed, S., Martens, J. H. A., Giamarellos-Bourboulis, E. J., Ifrim, D. C., Logie, C., et al. (2012). Candida albicans infection affords protection against reinfection *via* functional reprogramming of monocytes. *Cell Host Microbe* 12, 223–232. doi: 10.1016/j.chom.2012.06.006

Ramirez, M. I., Yamauchi, L. M., de Freitas, L. H. G., Uemura, H., and Schenkman, S. (2000). The use of the green fluorescent protein to monitor and improve transfection in trypanosoma cruzi. *Mol. Biochem. Parasitol.* 111, 235–240. doi: 10.1016/S0166-6851(00)00309-1

Rath, S., Sharma, R., Gupta, R., Ast, T., Chan, C., Durham, T. J., et al. (2020). MitoCarta3.0: an updated mitochondrial proteome now with sub-organelle localization and pathway annotations. *Nucleic Acids Res.* 49, 1541–1547. doi: 10.1093/nar/gkaa1011

Roger, V. L. (2013). Epidemiology of heart failure. *Circ. Res.* 113, 646–659. doi: 10.1161/CIRCRESAHA.113.300268

Rossetti, L., Smith, D., Shulman, G. I., Papachristou, D., and DeFronzo, R. A. (1987). Correction of hyperglycemia with phlorizin normalizes tissues sensitivity to insulin in diabetic rats. *J. Clin. Invest.* 79, 1510–1515. doi: 10.1172/JCI112981

Sakagami, H., Makino, Y., Mizumoto, K., Isoe, T., Takeda, Y., Watanabe, J., et al. (2014). Loss of HIF-1α impairs GLUT4 translocation and glucose uptake by the skeletal muscle cells. *Am. J. Physiology-Endocrinol. Metab.* 306, E1065–E1076. doi: 10.1152/ajpendo.00597.2012

Semenza, G. L. (2003). Targeting HIF-1 for cancer therapy. *Nat. Rev. Cancer* 3, 721–732. doi: 10.1038/nrc1187

Sharma, A., Toepfer, C. N., Schmid, M., Garfinkel, A. C., Seidman, C. E., Sharma, A., et al. (2018a). "Differentiation and contractile analysis of GFP-sarcomere reporter hiPSC-cardiomyocytes," in *Current protocols in human genetics* (Hoboken, NJ, USA: John Wiley & Sons, Inc), 21.12.1–21.12.12. doi: 10.1002/cphg.53

Sharma, A., Toepfer, C. N., Ward, T., Wasson, L., Agarwal, R., Conner, D. A., et al. (2018b). "CRISPR/Cas9-mediated fluorescent tagging of endogenous proteins in human pluripotent stem cells," in *Current protocols in human genetics* (Hoboken, NJ, USA: John Wiley & Sons, Inc), 21.11.1–21.11.20. doi: 10.1002/cphg.52

Sharma, A., Wasson, L. K., Willcox, J. A. L., Morton, S. U., Gorham, J. M., Delaughter, D. M., et al. (2020). GATA6 mutations in hiPSCs inform mechanisms for maldevelopment of the heart, pancreas, and diaphragm. *Elife* 9, 1–28. doi: 10.7554/eLife.53278

Strobel, P., Allard, C., Perez-Acle, T., Calderon, R., Aldunate, R., and Leighton, F. (2005). Myricetin, quercetin and catechin-gallate inhibit glucose uptake in isolated rat adipocytes. *Biochem. J.* 386, 471–478. doi: 10.1042/BJ20040703

Tannahill, G. M., Curtis, A. M., Adamik, J., Palsson-McDermott, E. M., McGettrick, A. F., Goel, G., et al. (2013). Succinate is an inflammatory signal that induces IL-1β through HIF-1α. *Nature* 496, 238–242. doi: 10.1038/nature11986

Toepfer, C. N., Sharma, A., Cicconet, M., Garfinkel, A. C., Mücke, M., Neyazi, M., et al. (2019). SarcTrack. *Circ. Res.* 124, 1172–1183. doi: 10.1161/CIRCRESAHA.118.314505

Tone, K., Stappers, M. H. T., Willment, J. A., and Brown, G. D. (2019). C-type lectin receptors of the dectin-1 cluster: Physiological roles and involvement in disease. *Eur. J. Immunol.* 49, 2127–2133. doi: 10.1002/eji.201847536

Valera Vera, E. A., Sayé, M., Reigada, C., Damasceno, F. S., Silber, A. M., Miranda, M. R., et al. (2016). Resveratrol inhibits trypanosoma cruzi arginine kinase and exerts a trypanocidal activity. *Int. J. Biol. Macromol.* 87, 498–503. doi: 10.1016/j.ijbiomac.2016.03.014

Venturini, G., Malagrino, P. A., Padilha, K., Tanaka, L. Y., Laurindo, F. R., Dariolli, R., et al. (2019). Integrated proteomics and metabolomics analysis reveals differential lipid metabolism in human umbilical vein endothelial cells under high and low shear stress. *Am. J. Physiol. Cell Physiol.* 317, C326–C338. doi: 10.1152/ajpcell.00128.2018

Vilar-Pereira, G., Carneiro, V. C., Mata-Santos, H., Vicentino, A. R. R., Ramos, I. P., Giarola, N. L. L., et al. (2016). Resveratrol reverses functional chagas heart disease in mice. *PLos Pathog.* 12, e1005947. doi: 10.1371/journal.ppat.1005947

Wan, X., and Garg, N. J. (2021). Sirtuin control of mitochondrial dysfunction, oxidative stress, and inflammation in chagas disease models. *Front. Cell Infect. Microbiol.* 0. doi: 10.3389/FCIMB.2021.693051

Ward, A. I., Olmo, F., Altherton, R. L., Taylor, M. C., and Kelly, J. M. (2020). Trypanosoma cruzi amastigotes that persist in the colon during chronic stage murine infections have a reduced replication rate. *Open Biol.* 10, 200261. doi: 10.1098/RSOB.200261

Werth, N., Beerlage, C., Rosenberger, C., Yazdi, A. S., Edelmann, M., Amr, A., et al. (2010). Activation of hypoxia inducible factor 1 is a general phenomenon in infections with human pathogens. *PLos One* 5, 1–12. doi: 10.1371/JOURNAL.PONE.0011576

Wood, T. E., Dalili, S., Simpson, C. D., Hurren, R., Mao, X., Saiz, F. S., et al. (2008). A novel inhibitor of glucose uptake sensitizes cells to FAS-induced cell death. *Mol. Cancer Ther.* 7, 3546–3555. doi: 10.1158/1535-7163.MCT-08-0569

Xintaropoulou, C., Ward, C., Wise, A., Marston, H., Turnbull, A., and Langdon, S. P. (2015). A comparative analysis of inhibitors of the glycolysis pathway in breast and ovarian cancer cell line models. *Oncotarget* 6, 25677–25695. doi: 10.18632/oncotarget.4499

Yu, G., Wang, L. G., Han, Y., and He, Q. Y. (2012). ClusterProfiler: An r package for comparing biological themes among gene clusters. *OMICS.* 16 (5), 284–287. doi: 10.1089/omi.2011.0118

Zhang, S., Kim, C. C., Batra, S., McKerrow, J. H., and Loke, P. (2010). Delineation of diverse macrophage activation programs in response to intracellular parasites and cytokines. *PLos Negl. Trop. Dis.* 4, e648. doi: 10.1371/JOURNAL.PNTD.0000648

Zhan, R. Z., Rao, L., Chen, Z., Strash, N., and Bursac, N. (2021). Loss of sarcomeric proteins *via* upregulation of JAK/STAT signaling underlies interferon-γ-induced contractile deficit in engineered human myocardium. *Acta Biomater.* 126, 144–153. doi: 10.1016/j.actbio.2021.03.007

Zinkernagel, A. S., Johnson, R. S., and Nizet, V. (2007). Hypoxia inducible factor (HIF) function in innate immunity and infection. *J. Mol. Med.* 85, 1339–1346. doi: 10.1007/S00109-007-0282-2

frontiers | Frontiers in Cellular and Infection Microbiology

TYPE Review
PUBLISHED 09 March 2023
DOI 10.3389/fcimb.2023.1130901

OPEN ACCESS

EDITED BY
Alena Pance,
University of Hertfordshire, United Kingdom

REVIEWED BY
Dolores Correa,
Anahuac University of North Mexico, Mexico
Bellisa Freitas Barbosa,
Federal University of Uberlandia, Brazil

*CORRESPONDENCE
Maria E. Francia
mfrancia@pasteur.edu.uy

SPECIALTY SECTION
This article was submitted to Parasite and Host, a section of the journal Frontiers in Cellular and Infection Microbiology

RECEIVED 23 December 2022
ACCEPTED 23 February 2023
PUBLISHED 09 March 2023

CITATION
Faral-Tello P, Pagotto R, Bollati-Fogolín M and Francia ME (2023) Modeling the human placental barrier to understand *Toxoplasma gondii*´s vertical transmission. *Front. Cell. Infect. Microbiol.* 13:1130901. doi: 10.3389/fcimb.2023.1130901

Modeling the human placental barrier to understand *Toxoplasma gondii*´s vertical transmission

Paula Faral-Tello[1], Romina Pagotto[2], Mariela Bollati-Fogolín[2] and Maria E. Francia[1,3]*

[1]Laboratory of Apicomplexan Biology, Institut Pasteur de Montevideo, Montevideo, Uruguay, [2]Cell Biology Unit, Institut Pasteur de Montevideo, Montevideo, Uruguay, [3]Departamento de Parasitología y Micología, Facultad de Medicina, Universidad de la República, Montevideo, Uruguay

Toxoplasma gondii is a ubiquitous apicomplexan parasite that can infect virtually any warm-blooded animal. Acquired infection during pregnancy and the placental breach, is at the core of the most devastating consequences of toxoplasmosis. *T. gondii* can severely impact the pregnancy's outcome causing miscarriages, stillbirths, premature births, babies with hydrocephalus, microcephaly or intellectual disability, and other later onset neurological, ophthalmological or auditory diseases. To tackle *T. gondii's* vertical transmission, it is important to understand the mechanisms underlying host-parasite interactions at the maternal-fetal interface. Nonetheless, the complexity of the human placenta and the ethical concerns associated with its study, have narrowed the modeling of parasite vertical transmission to animal models, encompassing several unavoidable experimental limitations. Some of these difficulties have been overcome by the development of different human cell lines and a variety of primary cultures obtained from human placentas. These cellular models, though extremely valuable, have limited ability to recreate what happens *in vivo*. During the last decades, the development of new biomaterials and the increase in stem cell knowledge have led to the generation of more physiologically relevant *in vitro* models. These cell cultures incorporate new dimensions and cellular diversity, emerging as promising tools for unraveling the poorly understood *T. gondii*´s infection mechanisms during pregnancy. Herein, we review the state of the art of 2D and 3D cultures to approach the biology of *T. gondii* pertaining to vertical transmission, highlighting the challenges and experimental opportunities of these up-and-coming experimental platforms.

KEYWORDS

Toxoplasma gondii, human placenta, trophoblast, maternal-fetal interface, vertical transmission, *in vitro* models

1 Introduction

Toxoplasma gondii is an ubiquitous apicomplexan parasite that can infect virtually any warm-blooded animal, and has the ability to access and infect immune-privileged sites such as the brain, the eye and the placenta. The parasite is transmitted among animals by ingestion of persistent cysts lodged in the brain or skeletal muscle. When a felid consumes chronically infected tissues with bradyzoite, the parasite can initiate its sexual differentiation cycle within its intestinal epithelium. Gametes can sexually recombine which will eventually lead to shedding of unsporulated oocysts. Upon contact with oxygen, oocysts will sporulate and lead to infective environmentally resistant oocysts (Ferguson, 2002) that can be consumed by intermediate hosts, including pregnant women. Altogether, these characteristics make *T. gondii* one of the most successful zoonotic parasites worldwide (Flegr et al., 2014).

Acquired infection during pregnancy and placental breach is at the core of the most devastating consequences of toxoplasmosis. *T. gondii* can severely impact the pregnancy's outcome causing miscarriages, stillbirths, premature birth, babies born with conditions such as hydrocephalus, microcephaly or intellectual disability, and other later onset neurological, ophthalmological or auditory diseases (Torgerson and Mastroiacovo, 2013). Clinical manifestations may vary depending on gestation period, fetal size, inoculum, and genetic background of the triad: mother, fetus and parasite (Dubey et al., 2021). In humans, it is well established that the outcome is dependent on the trimester of gestation. Infections in early pregnancy are often associated with pregnancy loss (Dubey et al., 2021), while mid gestation and third trimester infections are more frequent and often result in fetal malformation (Desmonts and Couvreur, 1974a; Desmonts and Couvreur, 1974b).

It has been observed that congenital toxoplasmosis is more frequent when acute infection occurs during the second half of pregnancy, particularly the third trimester where placental layers separating maternal blood from fetal blood are thinner (Błaszkowska and Góralska, 2014) and blood flow increases substantially. However, these observations must be analyzed considering the generalized worldwide sub-diagnosis of toxoplasmosis (Nayeri et al., 2020), and that the etiology behind most spontaneous abortions (first trimester) remain undetermined, among which *T. gondii* should not be ruled out (Nayeri et al., 2020). Moreover, latent infection is highly prevalent (Rostami et al., 2020) and is responsible for many neuropathological effects, pre-eclampsia, thyroid diseases and infertility, among others (Rostami et al., 2016). Although the associations between latent infection and different gestational outcomes are still under active debate (Mocanu et al., 2022), there is evidence of association with slower fetal development and slower acquisition of postnatal motor skills (Kaňková and Flegr, 2007; Kaňková et al., 2012). On the other hand, in those countries that include screening tests in routine prenatal care schemes, opportune treatment can impact differently vertical transmission rates between first and third-trimester congenital infections.

It has long been accepted that chronic infections prevent reinfections and protect the fetus from vertical transmission. However, this paradigm has recently been challenged, as growing evidence suggests that reinfection is possible when a genetically distinct strain reinfects a seemingly "immunized" individual (Elbez-Rubinstein et al., 2009; Jensen et al., 2015). This is important since different strains circulate worldwide, particularly in South America where there is a predominance of atypical strains (Galal et al., 2019).

The host's proper modulation of her immunity during the course of gestation is paramount to its maintenance and to a healthy outcome. Thus, interfering with parasite-specific factors would be the safest intervention strategy in the context of pregnancy. However, their involvement in vertical transmission still remains unclear. In fact, except for a handful of exceptions, the parasite factors licensing vertical transmission remain virtually unidentified (Arranz-Solís et al., 2021).The role of the immune system in protecting the fetus against *T. gondii* has been exhaustively studied, and specific alleles in immune response-related genes that might favor or prevent vertical transmission have been described (Reviewed in (Ortiz-Alegría et al., 2010). However, the host's immune system has also been shown to be the target of parasite-specific factors which by way of modulating cellular mobility, use them as trojan horses for dissemination (Ortiz-Alegría et al., 2010). Three secreted parasite factors, TgWIP, Tg14-3-3 and ROP17, have been shown to generate hypermobility of dendritic cells, monocytes and natural killer cells which the parasite uses to reach immune-privileged sites (Arranz-Solís et al., 2021). CCL22 is a chemokine which plays critical roles in immune-tolerance. GRA28 is a dense-granule secreted protein that modulates the secretion of CCL22 in the host infected cells, including placental cells. Parasites lacking GRA28 are not able to disseminate (Rudzki et al., 2021). GRA28 was also recently shown to impact infected macrophage mobility by inducing a dendritic cell like behavior, caused by the transcriptional rewiring of the infected cell (Hoeve et al., 2022).

In vitro modeling of the life stages of *T. gondii* has been traditionally limited to 2D cultures whereby the fast growing tachyzoite form of the parasite expands quickly and efficiently, allowing for the generation of large amounts of material for different analyses. Albeit *in vitro* bradyzoites do not bear an absolute biological resemblance to their *in vivo* counterparts, the partial access to their biology offered by *in vitro* models has greatly contributed to our understanding of the chronic forms of parasite persistence (Mayoral et al., 2020).

In stark contrast, the interplay among tachyzoites, bradyzoites and host factors, in the context of transplacental transmission cannot thus far be mimicked in traditional 2D cultures. The study of these aspects of parasite biology has thus far relied on animal models, encompassing several unavoidable experimental limitations. Nonetheless, recent technological breakthroughs in 3D and 2D culture systems provide promising routes for exploring aspects of parasitic life traditionally inaccessible. Herein, we review the state of the art of 3D and 2D cultures to approach one of the most poorly understood aspects of the biology of *T. gondii*, highlighting the challenges and experimental opportunities of these up-and-coming experimental platforms.

2 Placental architecture

The placenta is a temporary fetal-maternal organ responsible for most communications between mother and fetus. It is formed during embryo implantation at the place where fetal membranes contact the surface of the epithelium of the uterine mucosa (Moore et al., 2019). The placenta is a very divergent organ that varies among different species regarding its exterior form, the number of membranes, vascular arrangement and the number of tissues separating fetal blood from maternal blood (Furukawa et al., 2014). The human placenta is hemochorial, meaning that vascularized chorionic villi (fetal portion) float freely fully bathed in maternal blood. This close proximity is the result of an active and deep invasion process led by a specific type of embryonic tissue called trophoblast (TB). TB forms early after fertilization in the morula stage (12-32 cells zygote) and will differentiate into cell subtypes according to location and function. Cytotrophoblast cells (CTB) consist of flattened cells surrounding the blastocyst and will form the fetal part of the placenta (Moore et al., 2019). CTB forms a layer of mononucleated cells that are mitotically active and give rise to the syncytiotrophoblast (STB), a rapidly expanding increasing mass of fused cells where no cell boundaries are observable (Moore et al., 2019). Until week 20, fetal villi are covered through all their extension with CTB and STB and after the 20th week, CTB disappears over large areas leaving only STB to stand between maternal blood and fetal endothelium (Figures 1A, B). CTB subtypes are extravillous TB (EVT) that abandon the fetal villi margins to migrate towards the decidua and forms a column that anchors to the decidua, and endovascular CTB, which migrates and colonizes spiral arteries regulating the vascular remodeling that is needed to secure blood flow (Pollheimer et al., 2014). The mentioned cell types are highlighted in Figure 1C.

How *T. gondii* crosses the placental barrier, infects the trophoblast, reaches fetal vascularity and disseminates, remains virtually unknown. This is partially owed to the difficulties and complexity of accurate placental human models and the ethical concerns associated with using human-derived samples. Nevertheless, from infections on model animals and different cell types, including human placenta-derived models, a number of mechanisms have been proposed. These include: 1) Infection of the maternal decidua and immune decidual cells which includes the trojan horse strategy; 2) Infection of EVT, fetal cells that deeply invade maternal endometrium; 3) Direct molecular adhesion of parasites to STB; 4) Active degradation of extracellular matrix (ECM) and 5) Infection as a consequence of inflammation-induced tissue damage. These alternatives are exhaustively reviewed in (Megli and Coyne, 2021; Rojas-Pirela et al., 2021).

In terms of temporal development and placental architecture, two scenarios can be identified that represent moments of particular vulnerability for vertical transmission. As mentioned, fetal trophoblast invades maternal decidua as deep as to encounter spiral arteries during the first trimester. This creates a scenario in which parasites present in maternal blood and/or surrounding tissues may directly contact fetal cells (Figure 1A). On the other hand, by mid second trimester and through term, barriers between fetal and maternal blood are reduced to fetal endothelium, STB and a discontinuous CTB (Moalli et al., 2011). Here, fetal villous trees are fully bathed in maternal blood. This critical difference in placental architecture is represented in Figures 1B, C.

3 Cell derived models to study *T. gondii* in the human placenta

3.1 Immortalized cell lines

Cancer-derived and *in vitro* immortalized trophoblastic cells have been traditionally used to model placenta. These cell lines are easily obtained and manipulated, but they have abnormal karyotypes and altered gene expression, which may not faithfully represent trophoblast *in vivo* behavior (Apps et al., 2009; Novakovic et al., 2011; Kallol et al., 2018). By far, the most widely used trophoblast cell line is BeWo. BeWo cells are choriocarcinoma derived and originally developed as a cancer research model and for the *in vitro* production of human chorionic gonadotropin (hCG) (Hart et al., 1968; Pattillo et al., 1971). BeWo have been extensively used in *T. gondii* research to study infection in the context of the maternal fetal interface. In this cell line, *T. gondii* concentrates around intercellular junctions and regulates host´s ICAM-1 (Intercellular Adhesion Molecule 1), suggesting that the parasite exploits the paracellular route for invasion (Barragan et al., 2005; Pfaff et al., 2005a). Infections in BeWo showed that these cells are more susceptible to *T. gondii* than HeLa cells (uterine cervical tumor derived). Consistently, both cell lines produce different immune effectors in response to infection (Pfaff et al., 2005b; Oliveira et al., 2006).Additionally, ICAM-1 expression in both cell lines is differentially induced by TGF-β1 and IFN-γ, suggesting a different modulation of susceptibility to infection(Teixeira et al., 2021). Another interesting finding is the parasite's ability to modulate apoptosis as an evasion strategy to survive. This has been observed in a broad range of trophoblast models, including BeWo (Angeloni et al., 2009), JEG-3 (Wei et al., 2018), HTR8/SVneo (Guirelli et al., 2015), isolated primary trophoblasts (Liu et al., 2013), and additionally, a human monocyte cell line, THP-1 (da Silva Castro et al., 2021).

As mentioned, one particularly susceptible moment for *T. gondii* to meet fetal trophoblast is during EVT invasion of placental formation. Experiments in immortalized EVT (HTR8/SVneo) (Graham et al., 1993) indicate that this type of trophoblast is highly susceptible to *T. gondii's* infection (Milian et al., 2019; Ye et al., 2020).

Classical immune response to *T. gondii* infection entails a pro-inflammatory response, with the production of multiple cytokines and immune effectors, including IL-6, IL-12, IL-10, (TNF)-α, interleukin (IL)-1β and IFN-γ, among many others. Macrophage migration inhibitory factor (MIF) is a pro-inflammatory factor needed to control *T. gondii* infection (Flores et al., 2008), playing a pivotal role in the control of the infection particularly during gestation. MIF's differential expression among first and third trimester placental explants (De Oliveira Gomes et al., 2011) has

10.3389/fcimb.2023.1130901

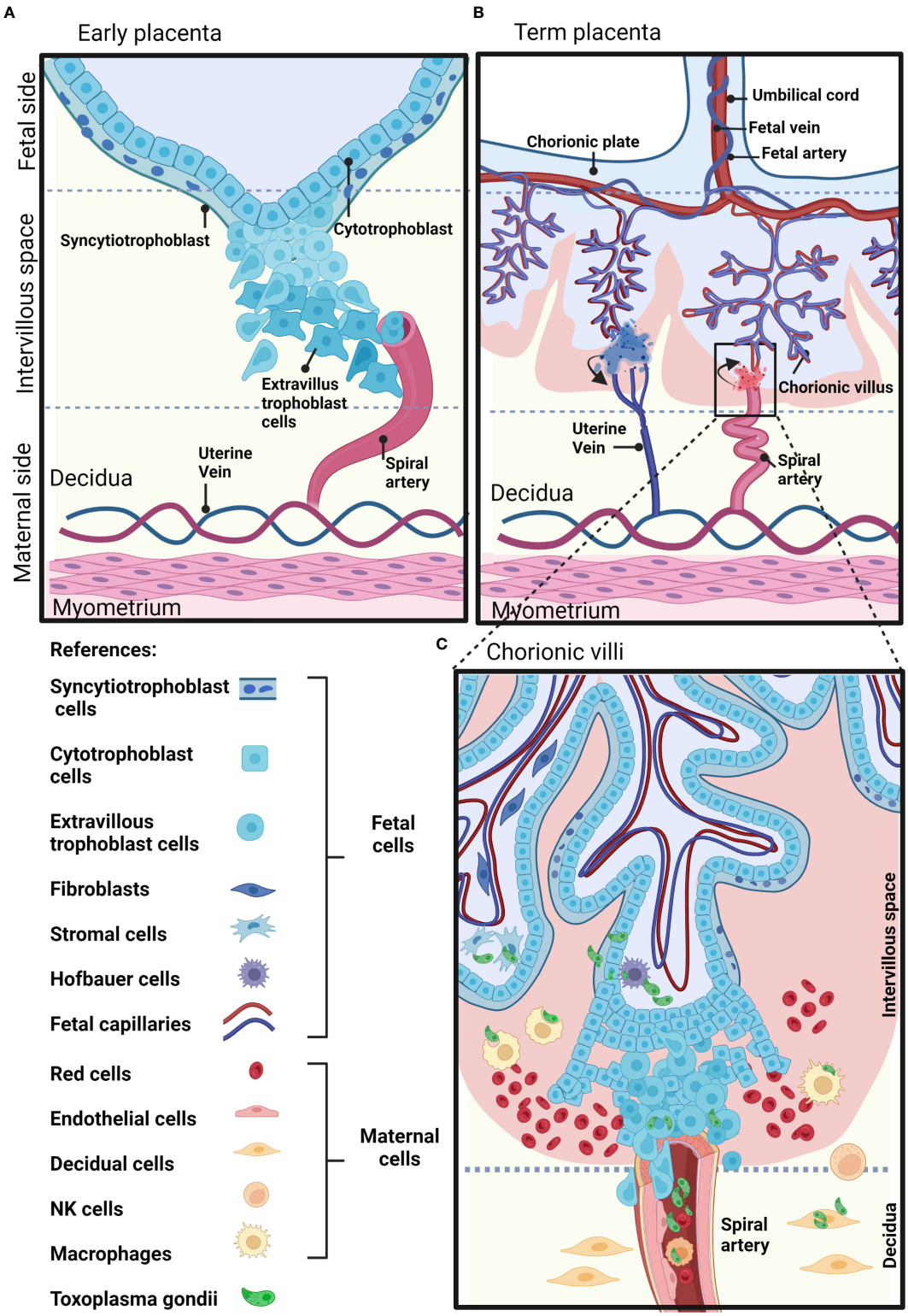

FIGURE 1
Schematic representation of a human placenta at two developmental time points. **(A)** Early placenta. The cytotrophoblasts fuse together and form the polynucleated syncytiotrophoblast layer, or differentiate into invasive extravillous trophoblasts. Extravillous trophoblasts invade the maternal decidua, and remodel the maternal arteries. **(B)** Term placenta. The fetal part of the fetal-maternal interface consists of chorionic villi that extend from the chorionic plate into the intervillous space and bathe in maternal blood. On the maternal side, the decidua is in direct contact with fetal membranes and the invading fetal extravillous trophoblasts. The maternal blood enters the intervillous space through spiral arteries and leaves this compartment through uterine veins. **(C)** The inset shows representative maternal and fetal cell types on a longitudinal section of a human-term placenta. Parasite structures indicating sites susceptible to *T. gondii* infection are shown in green. Created with BioRender.com.

been linked to the higher susceptibility to congenital infection of the third trimester. Trophoblast models have been instrumental in deciphering cell-type specific routes of immune modulation elicited by *T. gondii* infection. EVTs display higher levels of MIF, its receptor, CD74, and co-receptor, CD44, than CTB. *T. gondii* infection further induces MIF production in EVTs. Surprisingly, MIF pharmacological inhibition in EVT leads to a significant decrease in *T. gondii´*s proliferation. In contrast, addition of recombinant MIF (rMIF) to infected EVTs, leads to increased CD44 co-receptor expression, ERK1/2 phosphorylation, COX-2 expression, and IL-8 production, all of which seem to favor *T. gondii´*s proliferation (Milian et al., 2019). On the other hand, BeWo cells naturally exhibit reduced expression of MIF, and this has been associated with higher susceptibility to infection by *T. gondii* (De Oliveira Gomes et al., 2011; Milian et al., 2019).

Trophoblast models have also served in demonstrating that *T. gondii* down-modulates the production of IL-6 and MIF by ways of inducing cyclooxygenase (COX-2) and prostaglandin E2 (PGE2) production. Lipid droplets are known sites of production and accumulation of COX-2. Consistently, it was observed that *T. gondii* induces an increase in lipid droplets in both BeWo and HTR-8/SVneo cells (de Souza et al., 2021).

Heme Oxygenase 1 (HO-1) activity controls parasite replication, and the expression is particularly diminished in EVT, which is also more susceptible to infection than CTB. This observation is supported by the differential expression of this enzyme in the immortalized models HTR8/SVneo compared to BeWo (Almeida et al., 2021) and their primary culture equivalents (Bilban et al., 2009).

3.2 Placental models derived from primary cells

Primary cells are cells that have been isolated from a tissue of a multicellular organism. This type of culture is often restricted in terms of the number of viable passages, and more demanding of particular growth conditions and supplements. At the same time, primary cells provide a more representative platform to work as they are genetically stable and retain the functional and morphological characteristics of their tissue of origin. In the following sections, we will review primary cell models used to study host-*T. gondii* interactions, following the logic of placental architecture from the maternal myometrium to the fetal capillaries, recapitulating the subsequent tissue layers that parasites must cross in order to reach the new individual.

3.2.1 Decidual cells

The decidua refers to the gravid endometrium. The decidua basalis (db) is the particular endometrial portion that eventually forms the placenta. The db becomes separated from the uterus after parturition. The decidua controls trophoblast invasion through hormonal production (Moore et al., 2020). In addition, during the process of decidualization, endometrial resident cells acquire specific characteristics to serve as a rich source of nutrition for the embryo. Another important function of decidual resident cells is to set up the regulatory tolerogenic, yet immune active, state needed for the fetus to thrive (Van Der Zwan et al., 2017). These special features may not be present in counterpart cells residing in other tissues. Primary decidual cells can be obtained from full term placenta db tissue, and diverse cell types can be recognized based on expression patterns of specific marker.

Decidual fibroblasts (Ander et al., 2018) and dNKs (Zhang et al., 2015) are highly permissive to infection by *T. gondii*, and their response to infection is related to TB apoptosis and subsequent damage to the placental barrier. In *T. gondii*-infected primary decidual macrophages, different molecular pathways are activated biasing their differentiation towards an M1 phenotype, thus weakening their M2 tolerance function (Li et al., 2017; Zhang et al., 2019), which is paramount to a healthy pregnancy. Decidual dendritic cells, key players in the maintenance of the tolerogenic state of the placenta, are also induced to a dysfunctional phenotype during *T. gondii* infection (Sun et al., 2022). On the other hand, different immune cells acquire a highly migratory phenotype after they get infected (Ueno et al., 2015; Ólafsson and Barragan, 2020), and they do so without stimulating immune responses (Courret et al., 2006; Lambert et al., 2006; Hoeve et al., 2022), all of which is beneficial for *T. gondii's* dissemination. Evidence regarding this trojan horse phenomenon has been obtained from measures of the migration patterns of *in vitro* infected bone-marrow derived DCs in a BeWo-coated transwell system, from infections in pregnant mice and in human PBMCs derived from peripheral blood (Lambert et al., 2006; Lambert et al., 2009; Collantes-Fernandez et al., 2012; Hoeve et al., 2022). To our knowledge, the migratory phenotype and trojan horse strategy has not been observed yet in human decidual cells.

3.2.2 Trophoblast cells

Primary human trophoblasts (PHT) can be obtained from fresh placental tissue through enzymatic dispersion and immunomagnetic purification (Salomon et al., 2015). Purified CTBs have proliferative capacity and, with the addition of epidermal growth factor (EGF), the cells can undergo robust differentiation forming STB-like cells. It has been shown that CTB and STB obtained from primary cultures can be readily infected with *T. gondii*, protecting them from apoptosis, except when co-cultured with Interferon gamma producing dNKs (Abbasi et al., 2003; Zhang et al., 2015). On the other hand, STBs are less susceptible to *T. gondii* attachment and replication compared with primary CTBs and trophoblast cell lines (BeWo, JEG-3) (Ander et al., 2018). Please note that *T. gondii's* infection has been assayed for an array of intermediate host-derived trophoblasts. These include, but are not limited to, mice (Wang et al, 2018) and sheep (Fernández-Escobar et al, 2021). Varying results regarding infectivity have been obtained, likely reflecting host-specie and parasite-strain specific dynamics.

3.2.3 Fetal endothelial cells

As transplacental passage of *T. gondii* may occur by migration across epithelial/endothelial barriers, endothelial

cells are relevant models to take into consideration when studying vertical transmission.

There are two types of endothelial cells that form the placenta vasculature. The human placental microvascular endothelial cells (HPMECs), present in the fetal capillaries of chorionic villi, and the macrovascular human umbilical vein endothelial cells (HUVECs). The first ones are obtained from the distal side of the human placenta, and purified by magnetic isolation of CD31 marker (Huang et al., 2018). As for the HUVEC cells, they are obtained from the umbilical cord vein by collagenase digestion (Siow, 2012). These endothelial cells differ in morphology and function (Lang et al., 2003). Particularly, HPMECs have higher responses to FGF2, VEGF and EG-VEGF, factors that promote angiogenesis (Huang et al., 2018). Regarding *T. gondii*, it has been reported that HUVECs and HMEC-1 (a stable cell line from dermal human microvasculature) present different infection susceptibility to two *T. gondii* strains (ME49 and RH) in a cell type/parasite combination dependent fashion (Cañedo-Solares et al., 2013). HUVECs cells have also been used to demonstrate that *T. gondii* induces the remodeling of the endothelial cytoskeleton and alteration of the cell barrier function (Franklin-Murray et al., 2020).In addition, infection of bovine derived vein endothelial cells (BUVECs) displays altered progression through the cell cycle (Velásquez et al., 2019), with increased host cell proliferation and an enhanced number of multinucleated cells. HUVEC are also frequently applied in the development of more complex placental models, resembling the fetal compartment, from 2D co cultures (Wong et al., 2020), to organ-on-a-chip systems (Lee et al., 2016).

3.2.4 Fetal macrophages

Other immune cells that are highly abundant in the human placenta are the fetal-origin macrophages called Hofbauer cells (HBCs). These cells are thought to play an important role in protecting the fetus from vertical infections and to influence trophoblast and placental vascular development (Thomas et al., 2020; Fakonti et al., 2022). To our knowledge, there are no reports of HBC responses to *T. gondii* infections. Nonetheless, observational studies of another apicomplexan parasite, *Plasmodium falciparum* determined a subtle decrease in anti-inflammatory M2 percentage of HBCs in infected placentas from primigravidas. Most importantly, this study determined this phenotype to be highly predictive of decreased fetal body weight, suggesting a protective effect of M2-type HBCs on fetal growth (Gaw et al., 2019). As a similar shift towards M1 phenotype has been reported for decidual macrophages when infected with *T. gondii* (Zhang et al., 2019), it would be interesting to evaluate HBCs' phenotypes in this condition.

3.3 Stem cell derived models

Primary cultures display several advantages over immortalized cell lines. Because they are derived directly from tissue and not genetically modified, they usually retain many of the differentiated characteristics of the cell *in vivo*, providing excellent models for studying normal physiology and cellular metabolism. However, they can be arduous to obtain, have a finite lifespan and a limited expansion capacity, making it difficult to sustainably work with them. An alternative to primary culture is the use of stem cells, which are a reproducible, natural and renewable source of cells. Stem cells can be differentiated into diverse cell types under defined culture conditions (Snykers et al., 2009; Mummery et al., 2012; Kim et al., 2016).

3.3.1 Mesenchymal stem cell-derived models

One source of fetal cell models used to study congenital transmissions are the mesenchymal stem cells isolated from human umbilical cord. During infection with *T. gondii* these cells are induced towards autophagic cell death by a mechanism that involves downregulation of mitochondrial stress factor Mcl-1 (Chu et al., 2017).

3.3.2 Trophoblast stem cells

Okae and collaborators have reported the derivation of human trophoblast stem cells (hTSC) from CTB and blastocysts. These cell lines were further able to differentiate in CTB, STB and EVT, and showed transcriptomes similar to primary trophoblast cells meeting the criteria for human trophoblast cells proposed by Lee and collaborators (Lee et al., 2016; Okae et al., 2018). Another putative hTSC line is the USFB6, obtained from an eight-cells human morula. These cells have a more mesenchymal-like morphology than the TSC population isolated by Okae. However, trophoblast criteria have not been completely determined (Zdravkovic et al., 2015). Some differentiation protocols manage to accurately recapitulate hallmarks of TB including syncytialization and migration (Gerami-Naini et al., 2004; Castel et al., 2020). Trophoblast-like cells can also be obtained by differentiation of human embryonic stem cells (hESC) and induced pluripotent stem cells (iPSC). The most common approach to experimentally induce hESC differentiation towards trophoblast-like cells is BMP4 treatment. However, differentiation in this model system is difficult to control, as other cell types (mesodermal and endothelial cells) also appear in the culture, protocols are highly variable, and it is not clear to what extent they accurately mimic real TSCs (Gamage et al., 2016).

3.3.3 Trophoblast organoids

Trophoblast organoids are an additional promising cellular model derived from stem cells. These long-term expanding cellular structures, can be developed from first trimester placental villi (Haider et al., 2018; Turco et al., 2018) or TSC derived from hIPSC (Karvas et al., 2022). These cultures organize into villous-like structures, and recapitulate differentiated subtypes of TB (CTB, EVT and STB), adding 3D orientation. Though, to our knowledge, trophoblast organoids have not been used to study *T. gondii*´s infection, recently, TSC-derived organoids have shown to recapitulate placental viral infectivity to Zika and SARS-CoV-2 virus (Karvas et al., 2022). These findings reinforce the relevance of trophoblast organoid models for studying other pathogens implicated in adverse pregnancy outcomes.

3.4 Human placental explants

Higher levels of model complexity have been achieved through the use of material from embryos and placentas from spontaneous or voluntary abortions. As mentioned before, TSCs derived from blastocysts have the ability to differentiate into different types of functional CTB, STB and EVT (Okae et al., 2018). Placental explants are an alternative source of all of these cell types. Robbins and collaborators isolated chorionic villi trees from placentas of 4-8 weeks of gestational age and reproduced the villous region and the EVT which invades uterine decidua. Their results indicate that it is the EVTs that are more susceptible to *T. gondii* infection (Robbins et al., 2012). In all cases, access to this material is limited and dependent on local legislation.

However, given the material is available, isolation of HPE is a simple procedure. If the appropriate culture conditions are provided, placental cells can be cultured for up to 5 days, maintaining tissue architecture and viability. Additionally, HPE represents a platform to study STBs which cannot be isolated because of their syncytial nature. STB resistance to attachment of *T. gondii* was also observed in second-trimester chorionic villous explants. Interestingly, transcriptional analysis showed that only 22 out of 172 genes are similarly induced between infected explants and infected isolated primary TBs (Ander et al., 2018), highlighting the importance of tissue architectural context in cellular responses. MIF is upregulated with *T. gondii* infection in first trimester HPE and results in increased monocyte adhesion (THP-1 cells) to fetal villi, possibly facilitating pathogen transfer across the placental barrier (Ferro et al., 2008). Differences in the induction of MIF are found to be gestational age dependent as it is upregulated in first-trimester HPE but not in third-trimester HPE(De Oliveira Gomes et al., 2011). These findings, together with differences in frequencies of congenital toxoplasmosis according to gestational age, may point towards the use of distinct mechanisms of transplacental passage by *T gondii*. While migration in infected macrophages may be exploited during the first trimester, extracellular passage could be happening in full term placenta whereby cellular barriers are weakened.

Kremmerling and collaborators compared the infectivity of *T. gondii* and *T. cruzi* in explants derived from human, canine and ovine full-term placentas. Their findings indicate that in all scenarios *T. gondii* invades more efficiently and induces more tissue damage than *T. cruzi* (Liempi et al., 2020). On the contrary, when zooming in on the molecular alterations of placenta upon infection, the same group showed that in HPE a stronger pro-inflammatory response occurs during *T. cruzi* infection when compared to *T. gondii*. Additionally, parasites stimulate distinct repertoires of immune response mediators, TLRs, cytokines, and signaling pathways (Castillo et al., 2017; Liempi et al., 2019). Authors correlate these findings to the fact that vertical transmission of Chagas disease is less frequent than vertical transmission of toxoplasmosis(Castillo et al., 2017; Liempi et al., 2019). The association of immunological silence and a more successful transplacental passage has been described for *T. cruzi* isolates with a history of transgenerational congenital transmission, in a murine vertical transmission model (Faral-Tello et al., 2022). Immune response silencing of the placenta could also underlie in part *T. gondii*'s success in vertical transmission, though this hasn't been experimentally addressed.

3.5 Other placental 3D models

Placental models have been improved with the advent of technologies that allow the generation of three-dimensional (3D) cultures. As mentioned, in the 3D context, the biological environment is better recreated allowing more relevant results at the anatomical and physiological level (Antoni et al., 2015). Among three dimensional systems, spheroids (Fennema et al., 2013) are the simpler ones. They can be technically constructed in two ways: taking advantage of the natural abilities of some cell types to aggregate and self-assemble into spherical structures, or by giving the culture a biocompatible spheroidal support such as hydrogel or collagen (Ryu et al., 2019). In this way, these multicellular structures can recreate the original cell-cell and cell-matrix junctions, key structures to study host-pathogen interactions.

Spheroids have contributed to recreating crucial stages of the life cycle of some parasites that were not being fully modeled in conventional cultures. For example, the reconstruction of the complete cycle, including the *in vitro* reactivation, of the *Plasmodium falciparum* in hepatocytes was achieved using this model (Chua et al., 2019). Novel mechanisms of *T. cruzi* migration through the paracellular route were observed using spheroids (Jones et al., 2017). Fundamental results for more complete understanding of the phenomena of mobility, migration, replication, egress and development of the sexual stages of *T. gondii* were only achievable *in vitro* by applying three-dimensionality (Ramírez-Flores et al., 2022). Moreover, spheroids have been used to recreate a complex placental process like trophoblast invasion (Wong et al., 2019), contributing substantially to understanding processes at the maternal-fetal interface. Spontaneous syncytialization (STB formation) of TB was only accomplished by 3D culture of JEG-3 cell line. This model allowed mimicking STB resistance to *T. gondii* when co cultured with human microvascular endothelial cells in a bioreactor 3D system (McConkey et al., 2016). This resistance phenotype was previously observed only in *ex vivo* infections of first trimester HPE (Robbins et al., 2012).

Advantages regarding the culture of immortalized cell lines enable the development of more complex 3D systems. Recently, BeWo cells were used for the construction of a placenta-inspired 3D bioprinted barrier model. Through the co-culture of TB (BeWo), placental fibroblasts (simulating placental stroma) and endothelial cells, authors were able to mimic the barrier that separates maternal blood from fetal blood in the full term human placental villous, achieving two weeks stability of the culture, without the use of an artificial membrane filter (Kreuder et al., 2020).

Organs-on-a-chip, which are 3D microfluidic devices that involve different cells to simulate activities, mechanics and physiological responses of an entire organ, have already been constructed to

mimic the placenta (Blundell et al., 2016; Lee et al., 2016; Arumugasaamy et al., 2018; Nishiguchi et al., 2019; Yin et al., 2019). Most of these placenta-on-a-chip systems have been constructed using immortalized trophoblastic cell lines, BeWo and others. An exception is the work by Nishiguchi and collaborators, who used primary CTBs isolated from first and third trimester chorionic villi to this end (Nishiguchi et al., 2019). To our knowledge, microfluidic systems have neither been used to study *T. gondii*'s infection process nor host-pathogen interactions. However, work by Arumugasaamy and collaborators achieved productive experimental infections using Zika virus (Arumugasaamy et al., 2018) and Zhu and collaborators evaluated the inflammatory response of fetal (endothelial) and maternal cells (BeWo) to *E. coli*, incorporating THP-1 cells in the fluidic system (Qin et al., 2018). These models bear a great potential to study the biology underlying transplacental passage of pathogens, while also enabling the search for potential therapeutics directed to treat women`s chronic conditions during gestation, instead of the currently used strategy of suppressing medication, an area that has long been neglected in medical research (Couzin-Frankel, 2022).

4 Discussion: Challenges and opportunities for modeling *T. gondii*´s vertical transmission

The first difficulty in studying congenital transmission of *T. gondii in vitro* is faithfully modeling placental tissue complexity. Although hypotheses of transplacental passage have been formulated based on other models, mechanisms of parasitism occurring at the maternal-fetal interface have traditionally been out of reach to researchers because of the lack of accurate models.

The placenta has a complex cellular structure which varies greatly along gestation, and among species (Furukawa et al., 2014). Therefore, results obtained in animal models do not necessarily reproduce what happens in humans. In this sense, the development of different human cell lines and a variety of primary cultures obtained from human placentas have allowed us to approach specific biological phenomena. Significant steps forward have been possible, impacting our understanding of infection susceptibility of different cell types, signaling mechanisms triggered during invasion, immune responses and manipulation.

TABLE 1 *In vitro* models of human placenta for studying the biology of *Toxoplasma gondii*.

Cell model	Name and reference	Source	Representative cell type	*T. gondii* associated studies and references
Cancer cell line 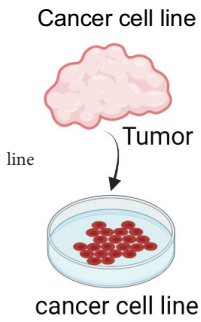	BeWo (Pattillo et al., 1968)	Choriocarcinoma explant	CTB/STB	Membrane adhesion(Teixeira et al., 2021); Infectionsusceptibility; (Almeida et al., 2019); Apoptosis modulation (da Silva Castro et al., 2021); Antiparasitic drugs (Ietta et al., 2017; Costa et al., 2021); Immune response (Castro et al., 2013).
	JEG-3 (Kohler and Bridson, 1971)	Choriocarcinoma explant	STB	2D and 3D infections (McConkey et al., 2016); Host apoptosis and RE stress (Wei et al., 2018).
	JAR (Pattillo et al., 1971)	Gestational choriocarcinoma	CTB	Infection and replication (Ander et al., 2018).
Immortalized cell line 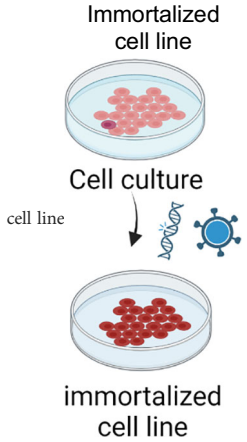	TCL-1 (Lewis et al., 1996)	Chorionic membrane	EVT	N/D
	ACH3P (Hiden et al., 2007)	Choriocarcinoma and first trimester trophoblast	CTB and EVT	N/D
	HPT-8 (Zhang et al., 2011)	First trimester placenta	EVT	N/D
	Swan 71 (Straszewski-Chavez et al., 2009)	First trimester placenta	CTB	N/D
	HTR-8/ SVneo	First trimester villous explant	EVT/CTB	Susceptibility to infection (Almeida et al., 2019); Modulation of cell death (da Silva Castro et al., 2021); Intracellular proliferation

(Continued)

TABLE 1 Continued

Cell model	Name and reference	Source	Representative cell type	*T. gondii* associated studies and references
	(Graham et al., 1993)			signaling (Milian et al., 2019); Antiparasitic treatment (Costa et al., 2021).
Primary 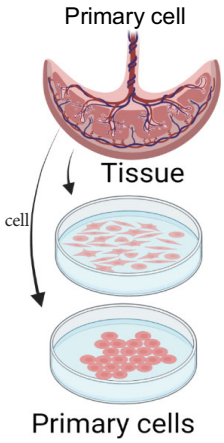	PHT (Human trophoblast cells)	Placenta	CYT and STB	Invasion, attachmentand replication (Abbasi et al., 2003; Ander et al., 2018)
	Decidual-derived cells	Decidua basalis	NK, fibroblast, macrophages, dDC	Invasion and susceptibility (Zhang et al., 2015; Ander et al., 2018); M1 and M2 phenotype switch (Li et al., 2017); Dysfunction of dDC (Sun et al., 2022).
	HUVEC (Jaffe et al., 1973)	Umbilical cord vein	Venous endothelial cells	Barrier function dysregulation (Franklin-Murray et al., 2020); Endothelial invasion (Cañedo-Solares et al., 2013).
Stem 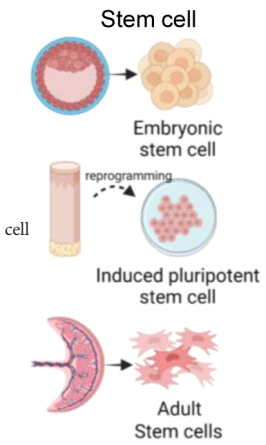	hTSC (Okae et al., 2018)	Blastocist/first trimester placenta	Trophoblast stem cells	N/D
	iTP (Chen et al., 2013)	Human fetal fibroblast	Trophoblast progenitor cells	N/D
	hUC-MSC (Chu et al., 2017)	Umbilical cord mesenchymal stem cells	mesenchymal stem cells	Host cell autophagy and apoptosis (Chu et al., 2017)
	hPSC-TS (Mischler et al., 2021)	Differentiated hESC or hiPSC	Trophoblast stem cells	N/D
	Organoids (Haider et al., 2018; Turco et al., 2018)	Stem cell/Villous tissue from first trimester placenta	trophoblast stem cells, CTB STB and EVT	N/D

*N/D, non-determined.

Models have also provided platforms for testing antiparasitic drugs (for more details, see Table 1). Nonetheless, these cellular models, though immensely instrumental to a number of biological questions, pose limitations to our ability to fully recreate the *in vivo* biology.

Importantly, cellular models usually rely on one or two different cell types, which cannot recreate the complex multicellular architecture of the original tissue. These limitations are solved, at least partly, by HPE, in which the structure, cellular diversity and interactions of the original tissue are better maintained, allowing placenta modeling closer to reality. Nevertheless, as a human primary culture, HPEs (obtained from term placenta or abortions) also harbor some challenges, especially regarding accessibility, reproducibility and maintenance, making it difficult to sustainably work with them.

Additionally, explants plated on culture dishes likely poorly mimic the characteristics of *in vivo* contact with parasites. In particular, parasitic load, and the way parasites access the villi are likely altered. For example, parasites firstly contacting the fetal part of the villous explants, something that would not occur *in situ* given the anatomy of the placenta, cannot be avoided.

Material from first trimester placentas has shown great potential in modeling different types of cells and placental processes. Access to these samples could be possible in countries where voluntary interruption of pregnancy is legal. However, the use of this material for research purposes has ethical constraints including specific medical procedures and coordinated efforts of the scientific and medical community. In the last years, the advances on stem cell technology have allowed scientists to surpass some of these limitations, enabling the establishment of more physiologically relevant *in vitro* cellular models, namely developing trophoblast organoids, in which genetically stable stem cells give rise to 3D cellular structures, resembling various aspects of the original tissue. Even when new challenges such as reproducibility, cellular differentiation degree, long-term culture maintenance, and 3D analytical tools development must still be overcome, the achievements made up to now indicate that we are on the right track.

It is fair to envision that these cellular models, coupled with bioprinted or organ-on-a-chip technology, will enable the development of more complex systems, integrating other cellular components (immune, stromal, endothelial cells) and fluidic forces. These improvements will allow scientists to delve deeper into how *T. gondii* invades fetal cells from maternal tissue, if there is a cell-type tropism for the parasite at the placenta or if there is a particular stage in the invasion process that could be used as a target for new drug development, contributing to shed light on the -so far- hidden mechanisms of *T. gondii* vertical transmission.

Author contributions

PF-T and MF conceived this manuscript. RP and PF-T created the Figure and Table. MF and MB-F contributed to funding acquisition. All authors contributed to the article and approved the submitted version.

Funding

This project was funded by a G4 grant to MF by the Institut Pasteur International Network and FOCEM (MERCOSUR Structural Convergence Fund), COF 03/11.MEF, MB-F, RP and PF-T are members of the SNI (National Research System, Uruguay) and researchers of PEDECIBA.

Acknowledgments

All figures were created with BioRender.com. Licenses: GQ24ZW9LXW and BE250KMXEZ.

Conflict of interest

The authors declare that the research was conducted in the absence of any commercial or financial relationships that could be construed as a potential conflict of interest.

Publisher's note

References

Abbasi, M., Kowalewska-Grochowska, K., Bahar, M. A., Kilani, R. T., Winkler-Lowen, B., and Guilbert, L. J. (2003). Infection of placental trophoblasts by toxoplasma gondii. *J. Infect. Dis.* 188, 608–616. doi: 10.1086/377132

Almeida, M. P. O., Ferro, E. A. V., Briceño, M. P. P., Oliveira, M. C., Barbosa, B. F., and Silva, N. M. (2019). Susceptibility of human villous (BeWo) and extravillous (HTR-8/SVneo) trophoblast cells to toxoplasma gondii infection is modulated by intracellular iron availability. *Parasitol. Res.* 118, 1559–1572. doi: 10.1007/s00436-019-06257-2

Almeida, M. P. O., Mota, C. M., Mineo, T. W. P., Ferro, E. A. V., Barbosa, B. F., and Silva, N. M. (2021). Heme oxygenase-1 induction in human BeWo trophoblast cells decreases toxoplasma gondii proliferation in association with the upregulation of p38 MAPK phosphorylation and IL-6 production. *Front. Microbiol.* 12. doi: 10.3389/fmicb.2021.659028

Ander, S. E., Rudzki, E. N., Arora, N., Sadovsky, Y., Coyne, C. B., and Boyle, J. P. (2018). Human placental syncytiotrophoblasts restrict toxoplasma gondii attachment and replication and respond to infection by producing immunomodulatory chemokines. *MBio* 9. doi: 10.1128/mBio.01678-17

Angeloni, M. B., Silva, N. M., Castro, A. S., Gomes, A. O., Silva, D. A. O., Mineo, J. R., et al. (2009). Apoptosis and s phase of the cell cycle in BeWo trophoblastic and HeLa cells are differentially modulated by toxoplasma gondii strain types. *Placenta* 30, 785–791. doi: 10.1016/j.placenta.2009.07.002

Antoni, D., Burckel, H., Josset, E., and Noel, G. (2015). Three-dimensional cell culture: A breakthrough in vivo. *Int. J. Mol. Sci.* 16, 5517–5527. doi: 10.3390/ijms16035517

Apps, R., Murphy, S. P., Fernando, R., Gardner, L., Ahad, T., and Moffett, A. (2009). Human leucocyte antigen (HLA) expression of primary trophoblast cells and placental cell lines, determined using single antigen beads to characterize allotype specificities of anti-HLA antibodies. *Immunology* 127, 26–39. doi: 10.1111/j.1365-2567.2008.03019.x

Arranz-Solís, D., Mukhopadhyay, D., and Saeij, J. J. P. (2021). Toxoplasma effectors that affect pregnancy outcome. *Trends Parasitol.* 37, 283–295. doi: 10.1016/j.pt.2020.10.013

Arumugasaamy, N., Ettehadieh, L. E., Kuo, C. Y., Paquin-Proulx, D., Kitchen, S. M., Santoro, M., et al. (2018). Biomimetic placenta-fetus model demonstrating maternal–fetal transmission and fetal neural toxicity of zika virus. *Ann. Biomed. Eng.* 46, 1963–1974. doi: 10.1007/s10439-018-2090-y

Barragan, A., Brossier, F., and Sibley, L. D. (2005). Transepithelial migration of toxoplasma gondii involves an interaction of intercellular adhesion molecule 1 (ICAM-1) with the parasite adhesin MIC2. *Cell. Microbiol.* 7, 561–568. doi: 10.1111/j.1462-5822.2005.00486.x

Bilban, M., Haslinger, P., Prast, J., Klinglmüller, F., Woelfel, T., Haider, S., et al. (2009). Identification of novel trophoblast invasion-related genes: Heme oxygenase-1 controls motility *via* peroxisome proliferator-activated receptor γ. *Endocrinology* 150, 1000–1013. doi: 10.1210/en.2008-0456

Błaszkowska, J., and Góralska, K. (2014). Parasites and fungi as a threat for prenatal and postnatal human development. *Ann. Parasitol* 60 (4), 225–234.

Blundell, C., Tess, E. R., Schanzer, A. S. R., Coutifaris, C., Su, E. J., Parry, S., et al. (2016). A microphysiological model of the human placental barrier. *Lab. Chip* 16, 3065–3073. doi: 10.1039/c6lc00259e

Cañedo-Solares, I., Calzada-Ruiz, M., Ortiz-Alegría, L. B., Ortiz-Muñiz, A. R., and Correa, D. (2013). Endothelial cell invasion by toxoplasma gondii: Differences between cell types and parasite strains. *Parasitol. Res.* 112, 3029–3033. doi: 10.1007/s00436-013-3476-2

Castel, G., Meistermann, D., Bretin, B., Firmin, J., Blin, J., Loubersac, S., et al. (2020). Generation of human induced trophoblast stem cells. *bioRxiv* 2020, 9.15.298257. doi: 10.1101/2020.09.15.298257

Castillo, C., Muñoz, L., Carrillo, I., Liempi, A., Gallardo, C., Galanti, N., et al. (2017). Ex vivo infection of human placental chorionic villi explants with trypanosoma cruzi and toxoplasma gondii induces different toll-like receptor expression and cytokine/chemokine profiles. *Am. J. Reprod. Immunol.* 78, 1–8. doi: 10.1111/aji.12660

Castro, A. S., Alves, C. M. O. S., Angeloni, M. B., Gomes, A. O., Barbosa, B. F., Franco, P. S., et al. (2013). Trophoblast cells are able to regulate monocyte activity to control toxoplasma gondii infection. *Placenta* 34, 240–247. doi: 10.1016/j.placenta.2012.12.006

Chen, Y., Wang, K., Gong, Y. G., Khoo, S. K., and Leach, R. (2013). Roles of CDX2 and EOMES in human induced trophoblast progenitor cells. *Biochem. Biophys. Res. Commun.* 431, 197–202. doi: 10.1016/j.bbrc.2012.12.135

Chu, J-Q., Jing, K-P., Gao, X., Li, P., Huang, R., Niu, Y-R., et al. (2017). Cell cycle toxoplasma gondii induces autophagy and apoptosis in human umbilical cord mesenchymal stem cells via downregulation of mcl–1 toxoplasma gondii induces autophagy and apoptosis in human umbilical cord mesenchymal stem cells via downregulation of. *Cell Cycle* 16, 477–486. doi: 10.1080/15384101.2017.1281484

Chua, A. C. Y., Ananthanarayanan, A., Ong, J. J. Y., Wong, J. Y., Yip, A., Singh, N. H., et al. (2019). Hepatic spheroids used as an *in vitro* model to study malaria relapse. *Biomaterials* 216. doi: 10.1016/J.BIOMATERIALS.2019.05.032

Collantes-Fernandez, E., Arrighi, R. B. G., Álvarez-García, G., Weidner, J. M., Regidor-Cerrillo, J., Boothroyd, J. C., et al. (2012). Infected dendritic cells facilitate

systemic dissemination and transplacental passage of the obligate intracellular parasite neospora caninum in mice. *PloS One* 7, e32123. doi: 10.1371/journal.pone.0032123

Costa, I. N., Ribeiro, M., Silva Franco, P., da Silva, R. J., de Araújo, T. E., Milián, I. C. B., et al. (2021). Biogenic silver nanoparticles can control toxoplasma gondii infection in both human trophoblast cells and villous explants. *Front. Microbiol.* 11. doi: 10.3389/fmicb.2020.623947

Courret, N., Darche, S., Sonigo, P., Milon, G., Buzoni-Gâtel, D., and Tardieux, I. (2006). CD11c- and CD11b-expressing mouse leukocytes transport single toxoplasma gondii tachyzoites to the brain. *Blood* 107, 309–316. doi: 10.1182/blood-2005-02-0666

Couzin-Frankel, J. (2022). The pregnancy gap. *Science* 375, 1216–1220. doi: 10.1126/science.adb2029

da Silva Castro, A., Angeloni, M. B., de Freitas Barbosa, B., de Miranda, R. L., Teixeira, S. C., Guirelli, P. M., et al. (2021). BEWO trophoblast cells and toxoplasma gondii infection modulate cell death mechanisms in THP-1 monocyte cells by interference in the expression of death receptor and intracellular proteins. *Tissue Cell* 73, 101658. doi: 10.1016/j.tice.2021.101658

De Oliveira Gomes, A., De Oliveira Silva, D. A., Silva, N. M., De Freitas Barbosa, B., Silva Franco, P., Angeloni, M. B., et al. (2011). Effect of macrophage migration inhibitory factor (MIF) in human placental explants infected with toxoplasma gondii depends on gestational age. *Am. J. Pathol.* 178, 2792–2801. doi: 10.1016/j.ajpath.2011.02.005

Desmonts, G., and Couvreur, J. (1974a). Congenital toxoplasmosis. a prospective study of 378 pregnancies. *N. Engl. J. Med.* 290, 1110–1116. doi: 10.1056/NEJM197405162902003

Desmonts, G., and Couvreur, J. (1974b). Toxoplasmosis in pregnancy and its transmission to the fetus. *Bull. N. Y. Acad. Med.* 50, 146.

de Souza, G., Silva, R. J., Milián, I. C. B., Rosini, A. M., de Araújo, T. E., Teixeira, S. C., et al. (2021). Cyclooxygenase (COX)-2 modulates toxoplasma gondii infection, immune response and lipid droplets formation in human trophoblast cells and villous explants. *Sci. Rep.* 11, 12709. doi: 10.1038/S41598-021-92120-3

Dubey, J. P., Murata, F. H. A., Cerqueira-Cézar, C. K., Kwok, O. C. H., and Villena, I. (2021). Congenital toxoplasmosis in humans: An update of worldwide rate of congenital infections. *Parasitology*, 1406–1416. doi: 10.1017/S0031182021001013

Elbez-Rubinstein, A., Ajzenberg, D., Dardé, M. L., Cohen, R., Dumètre, A., Yera, H., et al. (2009). Congenital toxoplasmosis and reinfection during pregnancy: Case report, strain characterization, experimental model of reinfection, and review. *J. Infect. Dis.* 199, 280–285. doi: 10.1086/595793

Fakonti, G., Pantazi, P., Bokun, V., and Holder, B. (2022). Placental macrophage (Hofbauer cell) responses to infection during pregnancy: A systematic scoping review. *Front. Immunol.* 12. doi: 10.3389/fimmu.2021.756035

Faral-Tello, P., Greif, G., Romero, S., Cabrera, A., Oviedo, C., González, T., et al. (2022). Trypanosoma cruzi isolates naturally adapted to congenital transmission display a unique strategy of transplacental passage. *bioRxiv* 1, 769–792. doi: 10.1101/2022.06.30.498325

Fennema, E., Rivron, N., Rouwkema, J., van Blitterswijk, C., and De Boer, J. (2013). Spheroid culture as a tool for creating 3D complex tissues. *Trends Biotechnol.* 31, 108–115. doi: 10.1016/J.TIBTECH.2012.12.003

Ferguson, D. J. P. (2002). Toxoplasma gondii and sex: Essential or optional extra? *Trends Parasitol.* 18, 351–355. doi: 10.1016/s1471-4922(02)02330-9

Fernández-Escobar, M., Calero-Bernal, R., Regidor-Cerrillo, J., Vallejo, R., Benavides, J., Collantes-Fernández, E., et al. (2021). *In vivo* and *in vitro* models show unexpected degrees of virulence among toxoplasma gondii type II and III isolates from sheep. *Vet. Res.* 52, 82. doi: 10.1186/s13567-021-00953-7

Ferro, E. A. V., Mineo, J. R., Ietta, F., Bechi, N., Romagnoli, R., Silva, D. A. O., et al. (2008). Macrophage migration inhibitory factor is up-regulated in human first-trimester placenta stimulated by soluble antigen of toxoplasma gondii, resulting in increased monocyte adhesion on villous explants. *Am. J. Pathol.* 172, 50–58. doi: 10.2353/ajpath.2008.070432

Flegr, J., Prandota, J., Sovičková, M., and Israili, Z. H. (2014). Toxoplasmosis - a global threat. correlation of latent toxoplasmosis with specific disease burden in a set of 88 countries. *PloS One* 9 (3), e90203. doi: 10.1371/journal.pone.0090203

Flores, M., Saavedra, R., Bautista, R., Viedma, R., Tenorio, E. P., Leng, L., et al. (2008). Macrophage migration inhibitory factor (MIF) is critical for the host resistance against toxoplasma gondii. *FASEB J.* 22, 3661–3671. doi: 10.1096/FJ.08-111666

Franklin-Murray, A. L., Mallya, S., Jankeel, A., Sureshchandra, S., Messaoudi, I., and Lodoen, M. B. (2020). Toxoplasma gondii dysregulates barrier function and mechanotransduction signaling in human endothelial cells. *mSphere* 5. doi: 10.1128/msphere.00550-19

Furukawa, S., Kuroda, Y., and Sugiyama, A. (2014). A comparison of the histological structure of the placenta in experimental animals. *J. Toxicol. Pathol.* 27, 11–18. doi: 10.1293/tox.2013-0060

Galal, L., Hamidović, A., Dardé, M. L., and Mercier, M. (2019). Diversity of toxoplasma gondii strains at the global level and its determinants. *Food Waterborne Parasitol.* 15, e00052. doi: 10.1016/j.fawpar.2019.e00052

Gamage, T. K. J. B., Chamley, L. W., and James, J. L. (2016). Stem cell insights into human trophoblast lineage differentiation. *Hum. Reprod. Update* 23, 77–103. doi: 10.1093/humupd/dmw026

Gaw, S. L., Hromatka, B. S., Ngeleza, S., Buarpung, S., Ozarslan, N., Tshefu, A., et al. (2019). Differential activation of fetal hofbauer cells in primigravidas is associated with decreased birth weight in symptomatic placental malaria. *Malar. Res. Treat.* 2019. doi: 10.1155/2019/1378174

Gerami-Naini, B., Dovzhenko, O. V., Durning, M., Wegner, F. H., Thomson, J. A., and Golos, T. G. (2004). Trophoblast differentiation in embryoid bodies derived from human embryonic stem cells. *Endocrinology* 145, 1517–1524. doi: 10.1210/en.2003-1241

Graham, C. H., Hawley, T. S., Hawley, R. G., MacDougall, J. R., Kerbel, R. S., Khoo, N., et al. (1993). Establishment and characterization of first trimester human trophoblast cells with extended lifespan. *Exp. Cell Res.* 206, 204–211. doi: 10.1006/excr.1993.1139

Guirelli, P. M., Angeloni, M. B., Barbosa, B. F., Gomes, A. O., Castro, A. S., Franco, P. S., et al. (2015). Trophoblast-macrophage crosstalk on human extravillous under toxoplasma gondii infection. *Placenta* 36, 1106–1114. doi: 10.1016/j.placenta.2015.08.009

Haider, S., Meinhardt, G., Saleh, L., Kunihs, V., Gamperl, M., Kaindl, U., et al. (2018). Self-renewing trophoblast organoids recapitulate the developmental program of the early human placenta. *Stem Cell Rep.* 11, 537–551. doi: 10.1016/j.stemcr.2018.07.004

Hart, R. G., Pattillo, R. A., Gey, G. O., Delfs, E., and Mattingly, R. F. (1968). Human hormone production *in vitro*. *Sci. (80-.).* 159, 1467–1469. doi: 10.1126/science.159.3822.1467

Hiden, U., Prutsch, N., Gauster, M., Weiss, U., Frank, H. G., Schmitz, U., et al. (2007). The first trimester human trophoblast cell line ACH-3P: A novel tool to study autocrine/paracrine regulatory loops of human trophoblast subpopulations - TNF-α stimulates MMP15 expression. *BMC Dev. Biol.* 7, 1–13. doi: 10.1186/1471-213X-7-137

Hoeve, A. L., Braun, L., Rodriguez, M. E., Saeij, J. P. J., Hakimi, M., Barragan, A., et al. (2022). Article the toxoplasma effector GRA28 promotes parasite dissemination by inducing dendritic cell-like migratory properties in infected macrophages the toxoplasma effector GRA28 promotes parasite dissemination by inducing dendritic cell-like migratory prop. *Cell Host Microbe* 30 (11), 1570–1588.e7. doi: 10.1016/j.chom.2022.10.001

Huang, X., Jia, L., Qian, Z., Jia, Y., Chen, X., Xu, X., et al. (2018). Diversity in human placental microvascular endothelial cells and macrovascular endothelial cells. *Cytokine* 111, 287–294. doi: 10.1016/j.cyto.2018.09.009

Ietta, F., Maioli, E., Daveri, E., Gonzaga Oliveira, J., Da Silva, R. J., Romagnoli, R., et al. (2017). Rottlerin-mediated inhibition of toxoplasma gondii growth in BeWo trophoblast-like cells. *Sci. Rep.* 7, 1–9. doi: 10.1038/s41598-017-01525-6

Jaffe, E. A., Nachman, R. L., Becker, C. G., and Minick, C. R. (1973). Culture of human endothelial cells derived from umbilical veins. identification by morphologic and immunologic criteria. *J. Clin. Invest.* 52, 2745–2756. doi: 10.1172/JCI107470

Jensen, K. D. C., Camejo, A., Melo, M. B., Cordeiro, C., Julien, L., Grotenbreg, G. M., et al. (2015). Toxoplasma gondii superinfection and virulence during secondary infection correlate with the exact ROP5/ROP18 allelic combination. *MBio* 2015. doi: 10.1128/mBio.02280-14

Jones, E. J., Korcsmaros, T., Carding, S. R., and Francis©, T. (2017). Mechanisms and pathways of toxoplasma gondii transepithelial migration. *Tissue Barriers* 5, 1–11. doi: 10.1080/21688370.2016.1273865

Kallol, S., Moser-Haessig, R., Ontsouka, C. E., and Albrecht, C. (2018). Comparative expression patterns of selected membrane transporters in differentiated BeWo and human primary trophoblast cells. *Placenta* 72-73, 48–52. doi: 10.1016/j.placenta.2018.10.008

Kaňková, Š., and Flegr, J. (2007). Longer pregnancy and slower fetal development in women with latent "asymptomatic" toxoplasmosis. *BMC Infect. Dis.* 7, 1–7. doi: 10.1186/1471-2334-7-114

Kaňková, Š., Šulc, J., Křivohlavá, R., Kuběna, A., and Flegr, J. (2012). Slower postnatal motor development in infants of mothers with latent toxoplasmosis during the first 18months of life. *Early Hum. Dev.* 88, 879–884. doi: 10.1016/j.earlhumdev.2012.07.001

Karvas, R. M., Khan, S. A., Verma, S., Yin, Y., Kulkarni, D., Dong, C., et al. (2022). Stem-cell-derived trophoblast organoids model human placental development and susceptibility to emerging pathogens. *Cell Stem Cell* 29 (5), 810–825. doi: 10.1016/j.stem.2022.04.004

Kim, H. D., Lee, E. A., Choi, Y. H., An, Y. H., Koh, R. H., Kim, S. L., et al. (2016). High throughput approaches for controlled stem cell differentiation. *Acta Biomater.* 34, 21–29. doi: 10.1016/j.actbio.2016.02.022

Kohler, P. O., and Bridson, W. E. (1971). Isolation of hormone-producing clonal lines of human choriocarcinoma. *J. Clin. Endocrinol. Metab.* 32, 683–687. doi: 10.1210/jcem-32-5-683

Kreuder, A. E., Bolaños-Rosales, A., Palmer, C., Thomas, A., Geiger, M. A., Lam, T., et al. (2020). Inspired by the human placenta: A novel 3D bioprinted membrane system to create barrier models. *Sci. Rep.* 10. doi: 10.1038/s41598-020-72559-6

Lambert, H., Hitziger, N., Dellacasa, I., Svensson, M., and Barragan, A. (2006). Induction of dendritic cell migration upon toxoplasma gondii infection potentiates parasite dissemination. *Cell. Microbiol.* 8, 1611–1623. doi: 10.1111/j.1462-5822.2006.00735.x

Lambert, H., Vutova, P. P., Adams, W. C., Loré, K., and Barragan, A. (2009). The toxoplasma gondii-shuttling function of dendritic cells is linked to the parasite genotype. *Infect. Immun.* 77, 1679–1688. doi: 10.1128/IAI.01289-08

Lang, I., Pabst, M. A., Hiden, U., Blaschitz, A., Dohr, G., Hahn, T., et al. (2003). Heterogeneity of microvascular endothelial cells isolated from human term placenta and macrovascular umbilical vein endothelial cells. *Urban Fischer* 2003, 163–173. doi: 10.1078/0171-9335-00306

Lee, J. S., Romero, R., Han, Y. M., Kim, H. C., Kim, C. J., Hong, J. S., et al. (2016). Placenta-on-A-chip: A novel platform to study the biology of the human placenta. *J. Matern. Neonatal Med.* 29, 1046–1054. doi: 10.3109/14767058.2015.1038518

Lewis, M. P., Clements, M., Takeda, S., Kirby, P. L., Seki, H., Lonsdale, L. B., et al. (1996). Partial characterization of an immortalized human trophoblast cell-line, TCL-1, which possesses a CSF-1 autocrine loop. *Placenta* 17, 137–146. doi: 10.1016/S0143-4004(96)80006-3

Li, Z., Zhao, M., Li, T., Zheng, J., Liu, X., Jiang, Y., et al. (2017). Decidual macrophage functional polarization during abnormal pregnancy due to toxoplasma gondii: Role for LILRB4. *Front. Immunol.* 8. doi: 10.3389/fimmu.2017.01013

Liempi, A., Castillo, C., Medina, L., Galanti, N., Maya, J. D., Parraguez, V. H., et al. (2020). Comparative ex vivo infection with trypanosoma cruzi and toxoplasma gondii of human, canine and ovine placenta: Analysis of tissue damage and infection efficiency. *Parasitol. Int.* 76, 102065. doi: 10.1016/j.parint.2020.102065

Liempi, A., Castillo, C., Medina, L., Rojas, M., Maya, J. D., Parraguez, V. H., et al. (2019). Ex vivo infection of human placental explants with trypanosoma cruzi and toxoplasma gondii: Differential activation of NF kappa b signaling pathways. *Acta Trop.* 199, 105153. doi: 10.1016/j.actatropica.2019.105153

Liu, T., Zhang, Q., Liu, L., Xu, X., Chen, H., Wang, H., et al. (2013). Trophoblast apoptosis through polarization of macrophages induced by Chinese toxoplasma gondii isolates with different virulence in pregnant mice. *Parasitol. Res.* 112, 3019–3027. doi: 10.1007/s00436-013-3475-3

Mayoral, J., Di Cristina, M., Carruthers, V. B., and Weiss, L. M. (2020). Toxoplasma gondii: Bradyzoite differentiation *in vitro* and *in vivo*. *Methods Mol. Biol.* 2071, 269–282. doi: 10.1007/978-1-4939-9857-9_15

McConkey, C. A., Delorme-Axford, E., Nickerson, C. A., Kim, K. S., Sadovsky, Y., Boyle, J. P., et al. (2016). A three-dimensional culture system recapitulates placental syncytiotrophoblast development and microbial resistance. *Sci. Adv.* 2, e1501462. doi: 10.1126/sciadv.1501462

Megli, C. J., and Coyne, C. B. (2021). Infections at the maternal-fetal interface: An overview of pathogenesis and defence. *Nat. Rev. Microbiol* 2021, 67–82. doi: 10.1038/s41579-021-00610-y

Milian, I. C. B., Silva, R. J., Manzan-Martins, C., Barbosa, B. F., Guirelli, P. M., Ribeiro, M., et al. (2019). Increased toxoplasma gondii intracellular proliferation in human extravillous trophoblast cells (HTR8/SVneo line) is sequentially triggered by MIF, ERK1/2, and COX-2. *Front. Microbiol.* 10. doi: 10.3389/fmicb.2019.00852

Mischler, A., Karakis, V., Mahinthakumar, J., Carberry, C. K., Miguel, A. S., Rager, J. E., et al. (2021). Two distinct trophectoderm lineage stem cells from human pluripotent stem cells. *J. Biol. Chem.* 296. doi: 10.1016/j.jbc.2021.100386

Moalli, F., Jaillon, S., Inforzato, A., Sironi, M., Bottazzi, B., Mantovani, A., et al. (2011). Pathogen recognition by the long pentraxin PTX3. *J. BioMed. Biotechnol.* 2011, 830421. doi: 10.1155/2011/830421

Mocanu, A. G., Stoian, D. L., Craciunescu, E. L., Ciohat, I. M., Motofelea, A. C., Navolan, D. B., et al. (2022). The impact of latent toxoplasma gondii infection on spontaneous abortion history and pregnancy Outcomes: A Large-scale study. *Microorganisms* 10, 1–12. doi: 10.3390/MICROORGANISMS10101944

Moore, K., Persaud, T., and Torchia, M. (2019). *The devolping human: Clinically oriented embriology 11th edition* (Philadelphia, PA, USA: Elsevier).

Moore, K. L., Persaud, T. V. N., and Torchia, M. G. (2020). *Before we are borne. 10th ed* (China: Elsevier).

Mummery, C. L., Zhang, J., Ng, E. S., Elliott, D. A., Elefanty, A. G., and Kamp, T. J. (2012). Differentiation of human embryonic stem cells and induced pluripotent stem cells to cardiomyocytes: A methods overview. *Circ. Res.* 111, 344–358. doi: 10.1161/CIRCRESAHA.110.227512

Nayeri, T., Sarvi, S., Moosazadeh, M., Amouei, A., Hosseininejad, Z., and Daryani, A. (2020). The global seroprevalence of anti-toxoplasma gondii antibodies in women who had spontaneous abortion: A systematic review and meta-analysis. *PloS Negl. Trop. Dis.* 14 (3), e0008103. doi: 10.1371/JOURNAL.PNTD.0008103

Nishiguchi, A., Gilmore, C., Sood, A., Matsusaki, M., Collett, G., Tannetta, D., et al. (2019). *In vitro* placenta barrier model using primary human trophoblasts, underlying connective tissue and vascular endothelium. *Biomaterials* 192, 140–148. doi: 10.1016/j.biomaterials.2018.08.025

Novakovic, B., Gordon, L., Wong, N. C., Moffett, A., Manuelpillai, U., Craig, J. M., et al. (2011). Wide-ranging DNA methylation differences of primary trophoblast cell populations and derived cell lines: Implications and opportunities for understanding trophoblast function. *Mol. Hum. Reprod.* 17, 344–353. doi: 10.1093/molehr/gar005

Okae, H., Toh, H., Sato, T., Hiura, H., Takahashi, S., Shirane, K., et al. (2018). Derivation of human trophoblast stem cells. *Cell Stem Cell* 22, 50–63.e6. doi: 10.1016/j.stem.2017.11.004

Ólafsson, E. B., and Barragan, A. (2020). The unicellular eukaryotic parasite toxoplasma gondii hijacks the migration machinery of mononuclear phagocytes to promote its dissemination. *Biol. Cell* 112, 239–250. doi: 10.1111/boc.202000005

Oliveira, J. G., Silva, N. M., Santos, A. A. D., Souza, M. A., Ferreira, G. L. S., Mineo, J. R., et al. (2006). BeWo trophoblasts are unable to control replication of toxoplasma gondii, even in the presence of exogenous IFN-γ. *Placenta* 27, 691–698. doi: 10.1016/j.placenta.2005.06.006

Ortiz-Alegría, L. B., Caballero-Ortega, H., Cãedo-Solares, I., Rico-Torres, C. P., Sahagún-Ruiz, A., Medina-Escutia, M. E., et al. (2010). Congenital toxoplasmosis: Candidate host immune genes relevant for vertical transmission and pathogenesis. *Genes Immun* 2010, 363–373. doi: 10.1038/gene.2010.21

Pattillo, R. A., Gey, G. O., Delfs, E., and Mattingly, R. F. (1968). *In vitro* identification of the trophoblastic stem cell of the human villous placenta. *Am. J. Obs. Gynecol* 100, 582–588. doi: 10.1016/s0002-9378(15)33497-9

Pattillo, R., Ruckert, A., Hussa, R., Bernstein, R., and Delfs, E. (1971). The jar cell line - continous human multihormone production and controls. *In Vitro* 6, 398–399.

Pfaff, A. W., Georges, S., Abou-Bacar, A., Letscher-Bru, V., Klein, J. P., Mousli, M., et al. (2005a). Toxoplasma gondii regulates ICAM-1 mediated monocyte adhesion to trophoblasts. *Immunol. Cell Biol.* 83, 483–489. doi: 10.1111/j.1440-1711.2005.01356.x

Pfaff, A. W., Villard, O., Klein, J. P., Mousli, M., and Candolfi, E. (2005b). Regulation of toxoplasma gondii multiplication in BeWo trophoblast cells: Cross-regulation of nitric oxide production and polyamine biosynthesis. *Int. J. Parasitol.* 35, 1569–1576. doi: 10.1016/j.ijpara.2005.08.003

Pollheimer, J., Fock, V., and Knöfler, M. (2014). Review: The ADAM metalloproteinases - novel regulators of trophoblast invasion? *Placenta* 35, S57–S63. doi: 10.1016/j.placenta.2013.10.012

Qin, J., Zhu, Y., Yin, F., Wang, H., Wang, L., and Yuan, J. (2018). Placental barrier-on-a-Chip: Modeling placental inflammatory responses to bacterial infection. *ACS Biomater. Sci. Eng.* 4, 3356–3363. doi: 10.1021/acsbiomaterials.8b00653

Ramírez-Flores, C. J., Perdomo, A. M. T., Gallego-López, G. M., and Knoll, L. J. (2022). Transcending dimensions in apicomplexan research: From two-dimensional to three-dimensional *In vitro* cultures. *Microbiol. Mol. Biol. Rev.* 86, 1–26. doi: 10.1128/MMBR.00025-22

Robbins, J. R., Zeldovich, V. B., Poukchanski, A., Boothroyd, J. C., and Bakardjiev, A. I. (2012). Tissue barriers of the human placenta to infection with toxoplasma gondii. *Infect. Immun.* 80, 418–428. doi: 10.1128/IAI.05899-11

Rojas-Pirela, M., Medina, L., Rojas, M. V., Liempi, A. I., Castillo, C., Pérez-Pérez, E., et al. (2021). Congenital transmission of apicomplexan parasites: A review. *Front. Microbiol.* 12. doi: 10.3389/fmicb.2021.751648

Rostami, A., Riahi, S. M., Gamble, H. R., Fakhri, Y., Nourollahpour Shiadeh, M., Danesh, M., et al. (2020). Global prevalence of latent toxoplasmosis in pregnant women: A systematic review and meta-analysis. *Clin. Microbiol. Infect.* 26, 673–683. doi: 10.1016/j.cmi.2020.01.008

Rostami, A., Seyyedtabaei, S. J., Aghamolaie, S., Behniafar, H., Lasjerdi, Z., Abdolrasouli, A., et al. (2016). Seroprevalence and risk factors associated with toxoplasma gondii infection among rural communities in northern Iran. *Rev. Inst. Med. Trop. Sao Paulo* 58. doi: 10.1590/S1678-9946201658070

Rudzki, E. N., Ander, S. E., Coombs, R. S., Alrubaye, H. S., Cabo, L. F., Blank, M. L., et al. (2021). Toxoplasma gondii GRA28 is required for placenta-specific induction of the regulatory chemokine CCL22 in human and mouse. *MBio* 12, e01591–21. doi: 10.1128/mBio.01591-21

Ryu, N. E., Lee, S. H., and Park, H. (2019). Spheroid culture system methods and applications for mesenchymal stem cells. *Cells* 8 (12), 1620. doi: 10.3390/cells8121620

Salomon, O. D., Feliciangeli, M. D., Quintana, M. G., Afonso, M. M., and Rangel, E. F. (2015). Lutzomyia longipalpis urbanisation and control. *Mem Inst Oswaldo Cruz* 110, 831–846. doi: 10.1590/0074-02760150207

Siow, R. C. M. (2012). Culture of human endothelial cells from umbilical veins. *Methods Mol. Biol.* 806, 265–274. doi: 10.1007/978-1-61779-367-7_18

Snykers, S., De Kock, J., Rogiers, V., and Vanhaecke, T. (2009). *In vitro* differentiation of embryonic and adult stem cells into hepatocytes: State of the art. *Stem Cells* 27, 577–605. doi: 10.1634/stemcells.2008-0963

Straszewski-Chavez, S. L., Abrahams, V. M., Alvero, A. B., Aldo, P. B., Ma, Y., Guller, S., et al. (2009). The isolation and characterization of a novel telomerase immortalized first trimester trophoblast cell line, swan 71. *Placenta* 30, 939–948. doi: 10.1016/j.placenta.2009.08.007

Sun, X., Xie, H., Zhang, H., Li, Z., Qi, H., Yang, C., et al. (2022). B7-H4 reduction induced by toxoplasma gondii infection results in dysfunction of decidual dendritic cells by regulating the JAK2/STAT3 pathway. *Parasites Vectors* 15, 1–17. doi: 10.1186/s13071-022-05263-1

Teixeira, S. C., Silva, R. J., Lopes-Maria, J. B., Gomes, A. O., Angeloni, M. B., Fermino, M. L., et al. (2021). Transforming growth factor (TGF)-β1 and interferon (IFN)-γ differentially regulate ICAM-1 expression and adhesion of toxoplasma gondii to human trophoblast (BeWo) and uterine cervical (HeLa) cells. *Acta Trop.* 224. doi: 10.1016/j.actatropica.2021.106111

Thomas, J. R., Appios, A., Zhao, X., Dutkiewicz, R., Donde, M., Lee, C. Y. C. C., et al. (2020). Phenotypic and functional characterization of first-trimester human placental macrophages, hofbauer cells. *J. Exp. Med.* 218, e20192386. doi: 10.1084/JEM.20192386

Torgerson, P. R., and Mastroiacovo, P. (2013). La charge mondiale de la toxoplasmose: une étude systématique. *Bull. World Health Organ.* 91, 501–508. doi: 10.2471/BLT.12.111732

Turco, M. Y., Gardner, L., Kay, R. G., Hamilton, R. S., Prater, M., Hollinshead, M. S., et al. (2018). Trophoblast organoids as a model for maternal–fetal interactions during human placentation. *Nature* 564, 263–267. doi: 10.1038/s41586-018-0753-3

Ueno, N., Lodoen, M. B., Hickey, G. L., Robey, E. A., and Coombes, J. L. (2015). Toxoplasma gondii-infected natural killer cells display a hypermotility phenotype *in vivo*. *Immunol. Cell Biol.* 93, 508–513. doi: 10.1038/icb.2014.106

Van Der Zwan, A., Bi, K., Norwitz, E. R., Crespo, Â.C., Claas, F. H. J., Strominger, J. L., et al. (2017). Mixed signature of activation and dysfunction allows human decidual CD8+ T cells to provide both tolerance and immunity. *Proc. Natl. Acad. Sci. U. S. A.* 115, 385–390. doi: 10.1073/PNAS.1713957115/-/DCSUPPLEMENTAL

Velásquez, Z. D., Conejeros, I., Larrazabal, C., Kerner, K., Hermosilla, C., and Taubert, A. (2019). Toxoplasma gondii-induced host cellular cell cycle dysregulation is linked to chromosome missegregation and cytokinesis failure in primary endothelial host cells. *Sci. Rep.* 9, 1–16. doi: 10.1038/s41598-019-48961-0

Wang, C., Cheng, W., Yu, Q., Xing, T., Chen, S., Liu, L., et al. (2018). Toxoplasma Chinese 1 strain of WH3Δrop16I/III /gra15II genetic background contributes to abnormal pregnant outcomes in murine model. *Front. Immunol.* 9. doi: 10.3389/fimmu.2018.01222

Wei, W., Zhang, F., Chen, H., Tang, Y., Xing, T., Luo, Q., et al. (2018). Toxoplasma gondii dense granule protein 15 induces apoptosis in choriocarcinoma JEG-3 cells through endoplasmic reticulum stress. *Parasites Vectors* 11. doi: 10.1186/s13071-018-2835-3

Wong, M. K., Li, E. W., Adam, M., Selvaganapathy, P. R., and Raha, S. (2020). Establishment of an *in vitro* placental barrier model cultured under physiologically relevant oxygen levels. *Mol. Hum. Reprod.* 26, 353–365. doi: 10.1093/molehr/gaaa018

Wong, M. K., Wahed, M., Shawky, S. A., Dvorkin-Gheva, A., and Raha, S. (2019). Transcriptomic and functional analyses of 3D placental extravillous trophoblast spheroids. *Sci. Rep. 2019 91* 9, 1–13. doi: 10.1038/s41598-019-48816-8

Ye, W., Sun, J., Li, C., Fan, X., Gong, F., Huang, X., et al. (2020). Adenosine A_3 receptor mediates ERK1/2- and JNK-Dependent TNF-α production in toxoplasma gondii-Infected HTR8/SVneo human extravillous trophoblast cells. *Korean J. Parasitol.* 58, 393–402. doi: 10.3347/kjp.2020.58.4.393

Yin, F., Zhu, Y., Zhang, M., Yu, H., Chen, W., and Qin, J. (2019). A 3D human placenta-on-a-chip model to probe nanoparticle exposure at the placental barrier. *Toxicol. Vitr.* 54, 105–113. doi: 10.1016/j.tiv.2018.08.014

Zdravkovic, T., Nazor, K. L., Larocque, N., Gormley, M., Donne, M., Hunkapillar, N., et al. (2015). Human stem cells from single blastomeres reveal pathways of embryonic or trophoblast fate specification. *Dev.* 142, 4010–4025. doi: 10.1242/dev.122846

Zhang, D., Ren, L., Zhao, M., Yang, C., Liu, X., Zhang, H., et al. (2019). Role of Tim-3 in decidual macrophage functional polarization during abnormal pregnancy with toxoplasma gondii infection. *Front. Immunol.* 10. doi: 10.3389/fimmu.2019.01550

Zhang, L., Zhang, W., Shao, C., Zhang, J., Men, K., Shao, Z., et al. (2011). Establishment and characterization of a spontaneously immortalized trophoblast cell line (HPT-8) and its hepatitis b virus-expressing clone. *Hum. Reprod.* 26, 2146–2156. doi: 10.1093/humrep/der153

Zhang, L., Zhao, M., Jiao, F., Xu, X., Liu, X., Jiang, Y., et al. (2015). Interferon gamma is involved in apoptosis of trophoblast cells at the maternal-fetal interface following toxoplasma gondii infection. *Int. J. Infect. Dis.* 30, e10–e16. doi: 10.1016/J.IJID.2014.10.027

frontiers | Frontiers in Cellular and Infection Microbiology

TYPE Brief Research Report
PUBLISHED 09 March 2023
DOI 10.3389/fcimb.2023.1082524

OPEN ACCESS

EDITED BY
Gabriel Rinaldi,
Aberystwyth University, United Kingdom

REVIEWED BY
Maria Duque-Correa,
University of Cambridge, United Kingdom
David Smith,
Moredun Research Institute,
United Kingdom

*CORRESPONDENCE
Marcelo A. Comini
mcomini@pasteur.edu.uy
Mariela Bollati-Fogolín
mbollati@pasteur.edu.uy

SPECIALTY SECTION
This article was submitted to Parasite and Host, a section of the journal Frontiers in Cellular and Infection Microbiology

RECEIVED 28 October 2022
ACCEPTED 20 February 2023
PUBLISHED 09 March 2023

CITATION
Daghero H, Pagotto R, Quiroga C, Medeiros A, Comini MA and Bollati-Fogolín M (2023) Murine colon organoids as a novel model to study *Trypanosoma cruzi* infection and interactions with the intestinal epithelium. *Front. Cell. Infect. Microbiol.* 13:1082524. doi: 10.3389/fcimb.2023.1082524

Murine colon organoids as a novel model to study *Trypanosoma cruzi* infection and interactions with the intestinal epithelium

Hellen Daghero[1], Romina Pagotto[1], Cristina Quiroga[2], Andrea Medeiros[2,3], Marcelo A. Comini[2]* and Mariela Bollati-Fogolín[1]*

[1]Cell Biology Unit, Institut Pasteur Montevideo, Montevideo, Uruguay, [2]Redox Biology of Trypanosomes Lab, Institut Pasteur de Montevideo, Montevideo, Uruguay, [3]Department of Biochemistry, Faculty of Medicine, University of the Republic, Montevideo, Uruguay

Chagas disease (CD) is a life-threatening illness caused by the parasite *Trypanosoma cruzi* (*T. cruzi*). With around seven million people infected worldwide and over 50,000 deaths per year, CD is a major public health issue in Latin America. The main route of transmission to humans is through a triatomine bug (vector-borne), but congenital and oral transmission have also been reported. The acute phase of CD presents mild symptoms but may develop into a long-lasting chronic illness, characterized by severely impaired cardiac, digestive, and neurological functions. The intestinal tissue appears to have a key role during oral transmission and chronic infection of CD. In this immune-privileged reservoir, dormant/quiescent parasites have been suggested to contribute to disease persistence, infection relapse, and treatment failure. However, the interaction between the intestinal epithelium and *T. cruzi* has not been examined in depth, in part, due to the lack of *in vitro* models that approximate to the biological and structural complexity of this tissue. Therefore, to understand the role played by the intestinal tissue during transmission and chronic infection, physiological models resembling the organ complexity are needed. Here we addressed this issue by establishing and characterizing adult stem cell-derived colonoid infection models that are clinically relevant for CD. 3D and 2D systems of murine intestinal organoids infected with *T. cruzi* Dm28c (a highly virulent strain associated with oral outbreaks) were analyzed at different time points by confocal microscopy. *T. cruzi* was able to invade and replicate in intestinal epithelial primary cells grown as intact organoids (3D) and monolayers (2D). The permissiveness to pathogen infection differed markedly between organoids and cell lines (primate and intestinal human cell lines). So far, this represents the first evidence of the potential that these cellular systems offer for the study of host-pathogen interactions and the discovery of effective anti-chagasic drugs.

KEYWORDS

Chagas disease, HT-29 cells, intestinal organoids, murine colon organoids, *Trypanosoma cruzi*

1 Introduction

Chagas disease (CD) is a zoonotic disease, endemic in Latin America, caused by the protozoan parasite *Trypanosoma cruzi* (*T. cruzi*) (Rassi et al., 2010). The parasite is mainly transmitted to humans and other animals by hematophagous insects from the Triatominae subfamily. However, congenital, oral, and blood-borne transmission has also been reported for CD (Pereira et al., 2009; Requena-Méndez et al., 2015).

T. cruzi presents a complex life cycle that involves a transition from replicative to non-replicative but highly infective stages. In the insect's gut, epimastigote forms multiply and differentiate into infective and non-replicative metacyclic trypomastigotes (MTs). The trypomastigotes are able to infect a wide range of mammalian cell types. In the cytosol of the host cell, the trypomastigotes differentiate into amastigotes, which upon several cycles of binary division, transform into motile trypomastigotes that lyse the cell mechanically. In most cases, the acute phase of CD presents mild and non-specific symptoms and is characterized by high levels of extracellular parasites. In about 30 - 40% of infected people, the disease develops to a chronic stage characterized by parasite colonization of several tissues such as the heart, colon, and gut mesenteric ganglia and muscle (Lidani et al., 2019). Disease morbidity and mortality are associated with cardiac and/or digestive damage and dysfunction. However, tissue tropism and clinical manifestations depend on many factors, especially the parasite genetics and the immune response of the host, making it difficult to predict the clinical development of the disease (Andersson et al., 2003). To date, only two drugs are available for CD treatment: benznidazole and nifurtimox. Both have been demonstrated to be effective in the acute phase, but they present considerable side effects and are not useful for treating the chronic CD stage.

The host's gastrointestinal tract is a key site for *T. cruzi* persistence since dormant/quiescent parasites residing in this immune-privileged location have been suggested to contribute to disease persistence, infection relapse and treatment failure (Ward et al., 2020). Parasite nests have been frequently detected in the muscle layer surrounding the colon of chronically infected mice. However, little is known about the capability of *T. cruzi* to establish infections and/or damage the intestinal epithelium. Moreover, murine models of CD are not only disputed because of ethical concerns but also because they have many limitations to model chronic CD (Fonseca-Berzal et al., 2018). Some of these limitations can be overcome by *in vitro* cell culture methods (Martello et al., 2013; Rodríguez et al., 2020).

Recent advances in stem cell biology and 3D culture systems have led to the development of valuable tools for exploring host-parasite interaction *in vitro*. Intestinal organoids, consisting of a differentiated, polarized epithelium with a central lumen, can be obtained by culturing intestinal stem cells (ISCs) (Sato et al., 2009). The ISCs reside at the crypt base within specialized niches where they self-renew to maintain a functional epithelium throughout life (Barker, 2014). When cultured under appropriate conditions, the ISCs can divide and rearrange themselves recapitulating the architecture and function of the tissue. The different epithelial cell types are present in these cultures, both absorptive and secretory lineages, hence representing a valuable system for performing functional studies of the intestinal epithelium. These advances in intestinal stem cell-derived organoid culture have broadened the *in vitro* repertoire of studies for host-parasite interactions for a wide range of enteric parasites (Wilke et al., 2019; Holthaus et al., 2021; Holthaus et al., 2022; Lamisere et al., 2022).

Here we addressed the establishment of 2D and 3D murine colon organoids (colonoids) to investigate *T. cruzi* tissue infection. Our data show that *T. cruzi* is able to invade the epithelium from both sides of the organoids (apical and basolateral surface) and that invasion and replication appear to be cell-type specific.

2 Materials and methods

2.1 Mammalian cell culture

HT-29 (ATCC HTB-38) and Vero (ATCC CCL-81) cells were cultured in Dulbecco's Modified Eagle Medium (DMEM) supplemented with 10% (v/v) Fetal Bovine Serum (FBS) in 25 or 75 cm^2 tissue culture flasks. Cells were routinely incubated at 37°C, 5% CO_2 in a humidified incubator and subcultured when reaching a 70-80% confluence for HT-29 or 40-60% for Vero cells.

2.2 Murine colon-derived organoid culture

Colon tissues of C57BL/6J mice (6-8 weeks-old male and female) were collected by dissection. Three cm long tissue sections were flushed with sterile PBS supplemented with 1% (w/v) penicillin/streptomycin. Samples were sliced longitudinally, cut into 0.5 cm fragments and then washed in cold PBS until the supernatant was clear. Following a 20 min incubation in ethylenediamine tetraacetic acid (EDTA) 10 mM in PBS with gentle agitation, fragments were resuspended in shaking buffer (0.1% (w/v) BSA in PBS) and pipetted up and down 5 times with a 10 mL pipette to facilitate crypt release. Upon examination by microscopy, crypt-containing fractions were pooled and filtered using a 70 µm cell strainer. After a centrifugation step at 200 g for 5 min at 4°C, the isolated crypts were counted and resuspended in Reduced Growth Factor Cultrex® Basement Membrane Extract (R&D Systems) at 250 crypts/20 µL matrix. The crypt/matrix droplets were incubated for 10 min at 37°C to allow matrix polymerization and organoid medium was added (Advanced DMEM/F12, Gibco), 1% (w/v) L-glutamine, 1% (w/v) penicillin/streptomycin, 50% (v/v) L-WRN conditioned medium, 10 nM gastrin (PeproTech), and 10 µM Y-27632 (PeproTech). Organoids were incubated at 37°C in a 5% CO_2 humidified atmosphere. For maintenance, the medium was renewed every 3 days with an organoid medium without Y-27632. Organoids were subcultured every 4-7 days in a ratio of 1:2 or 1:3 and used at day 3 for 3D infection assays.

2.3 Murine organoid-derived monolayer

For growing intestinal organoids in a monolayer format, a black clear-bottom 96-multiwell plate (Corning) was pre-coated with 50 µL per well of a 1:10 Cultrex-BME®-PBS solution. The plate was incubated for 2 h at room temperature and then at 37°C until use. Full-grown 3D organoids were detached from matrix domes using ice-cold PBS and then centrifuged at 300 g for 5 min at 4°C. The cell pellet was resuspended in TrypLE Express 1X (Gibco) supplemented with 10 µM Y-27632 and incubated at 37 °C for 5-7 min. For facilitating cell disaggregation, the suspension was vortexed every 2 min. After TrypLE inactivation with complete culture medium, the cells were counted and seeded in the pre-coated plate ($5x10^4$ cells/well). The culture medium was supplemented with 2.5 µM CHIR99021 (PeproTech), 10 µM SB202190 (Sigma-Aldrich), 1 mM N-acetyl cysteine (Sigma-Aldrich) and 10 mM Nicotinamide (Sigma-Aldrich), and replaced every 2-3 days.

2.4 Generation of infective *Trypanosoma cruzi*

Epimastigotes of *T. cruzi* strain DM28c (clone TcI) were cultivated in batch for 12-15 days in liver infusion tryptose (LIT) medium supplemented with 10% (v/v) FBS, 100 U/mL of penicillin, 100 µg/mL streptomycin and 40 µM of Hemin at 28°C. Next, Vero cells (2.5×10^5 cells/mL in T-25 flasks containing DMEM + 10% (v/v) FBS) were infected at a 10:1 (parasite:Vero cell) ratio with MTs present in the supernatant of the aged epimastigote´s culture. The culture was monitored for the proliferation of intracellular parasites and the medium (DMEM + 2% (v/v) FBS) was replaced every 48 h. When high amounts of extracellular trypomastigotes were detected (6-7 days post-infection), the supernatant was collected, centrifuged at 1250 g for 10 min and the parasite pellet resuspended in fresh DMEM + 10% (v/v) FBS. After 4-24 h incubation at 37°C and 5% CO_2, swimming parasites were recovered from the supernatant by centrifugation at 1250 g for 10 min, resuspended in complete organoid culture medium and counted under the light microscope. The parasite density was adjusted by dilution in the complete organoid culture medium. The procedure was performed immediately before the organoid´s infection assay.

2.5 Infection assays

For the 3D infection assays, each independent experiment was performed with organoids obtained from different mice (4 different organoid lines), and from both sexes. Organoids were removed from the BME matrix domes, washed with PBS and centrifuged at 300 g for 5 min at 4°C. To adjust the number of parasites to the corresponding MOI to be tested, organoids contained in a single well of a 6-well plate were dissociated into a single-cell suspension by incubating them with TrypLE for 5 min at 37°C and used as a proxy to determine the number of viable cells per well (counted under a light microscope). Once the number of cells was determined, the number of parasites needed was calculated considering the desired MOI. Then, intact organoids were removed from the BME matrix domes, washed with PBS and centrifuged at 300 g for 5 min at 4°C. Upon removal of the supernatant, the organoid pellet was incubated for 2 h at 37°C with the appropriate number of infective *T. cruzi* trypomastigotes in 100 µL of complete organoid medium supplemented with Y-27632. Thereafter, the infected organoids were centrifuged at 300 g for 5 min, resuspended in BME matrix, plated in a black clear-bottom 96 multiwell plate in 7 µL drops and cultured for 72 h in complete organoid medium supplemented with Y-27632.

For the infection of organoids in 2D, each independent experiment was performed with organoids obtained from different mice (2 different organoid lines) and from both sexes. The wells for the organoid monolayer were pre-coated with a BME matrix 1:10 dilution in PBS for 2 h at 37° C. The single-cell suspension from organoids was obtained by incubating the suspended organoids with TrypLE for 5 min at 37°C and the MOI was adjusted using the number of cells seeded per well. For Vero and HT-29 cells was $1.5x10^4$ cells/well and for organoid single-cell suspension was $5x10^4$ cells/well. Once the monolayers were established, the infective trypomastigotes were added directly to the cell culture and incubated for 2 or 24 h. Then, the medium was removed and the monolayer was washed thrice with PBS (pre-warmed at 37°C). Complete organoid medium supplemented with Y-27632 was added and the culture plate was further incubated for 48 h to 72 h.

2.6 Immunofluorescence staining

Infected organoids were washed with PBS three times and fixed with 4% (w/v) paraformaldehyde (PFA) in PBS for 1 h at room temperature (RT). Permeabilization was performed by treating the samples with 0.5% (v/v) Triton X-100 in PBS for 15 min at RT. After blocking with 2% (w/v) BSA in PBS for 2 h at RT, the samples were incubated with parasite-specific primary antibodies (polyclonal rabbit serum anti-*T. cruzi* trypanothione reductase or polyclonal mouse anti-*T. cruzi* mitochondrial peroxiredoxin), or anti-Ki67 antibody (ab 15580 from Abcam), Wheat Germ Agglutinin (WGA) Alexa Fluor 555 (Invitrogen 1:1000 dilution) and methyl green (4 µg/mL) or Hoechst 33342 (1:1000 dilution) in 2% (w/v) BSA, 0.1% (v/v) Triton X-100 in PBS overnight at 4°C. Next, the samples were washed three times with PBS and incubated with the secondary antibody anti-rabbit IgG Alexa Fluor 488 (Invitrogen) (1:500 dilution), or anti-rabbit IgG Cy5 (Invitrogen) (1:500 dilution), anti-mouse IgG Alexa Fluor 488 (1:300 dilution) and Phalloidin Texas Red (ThermoFisher) (1:100 dilution) or Phalloidin-Alexa Fluor 647 (ThermoFisher) (1:200 dilution) for 1 h in the dark at RT.

2.7 Image acquisition and analysis

Confocal images were acquired using Zen Black software (Zeiss; Darmstadt, Germany) on a laser confocal microscope Zeiss LSM 880 equipped with 25X (Gly immersion) and/or 40X (oil

immersion) objectives and 488 nm, 561 nm and 631 nm lasers. Images were processed using Fiji software (Schindelin et al., 2012). For the detection of parasites in infected 3D-organoids, Z-stack images were obtained from 5 random fields per condition and quantification was performed with the 3D Object counter plugin from Fiji, using nuclei staining for counting all cells and trypanothione reductase or mitochondrial peroxiredoxin signal for counting *T. cruzi* amastigotes.

2.8 Statistical analysis

Data were expressed as the median and interquartile range of replicates from one representative experiment, out of three independent experiments executed, unless otherwise indicated. The statistical analysis was performed using GraphPad Prism. For comparing two groups, an unpaired Mann-Whitney Test was applied. A p-value of less than 0.05 was considered significantly different.

3 Results

3.1 *Trypanosoma cruzi* is able to invade colon-derived organoids from the basolateral side

During the chronic stage of the infection, the colonization of the intestinal tissue by *T. cruzi* is expected to occur *via* extravasation of blood circulating trypomastigotes to the interstitial space, followed by the invasion of cells from the basal layer of the organ. Smooth muscle and nervous system cells surrounding the colon have been shown to be a target of parasite infection (Vazquez et al., 2015; Ward et al., 2020; Khan et al., 2021). However, the interaction of *T. cruzi* with the intestine has been explored only by traditional cell culture techniques (Figure 1), and still there are no reports on the capacity of the parasite to colonize colon epithelial cells, despite this organ being a major target of infection, damage, and persistence of this pathogen. Thus, to address this question, intact colon-derived organoids were co-incubated for 2 h with *T. cruzi* trypomastigotes isolated from infected Vero cells, and cell invasion was monitored by confocal microscopy (Figure 2A). The representative image of Figure 2B shows that under this condition, only a minor fraction of colonoid cells are infected by the parasite. Suspecting that this may be caused by a physical impediment of the parasites to move freely through the matrix, next, the organoids were exposed to trypomastigotes before embedding them into the matrix. Thus, organoids were removed from the Cultrex BME matrix without disrupting them and were incubated with trypomastigotes for 2 h in suspension (MOI 1:15, epithelial cells:trypomastigotes) before replating them in BME matrix (Figure 2A). As shown in Figure 2C, this procedure led to a significant increase in the number of colonoids' infection foci that, nonetheless, were restricted to some cells of the organoids. To further test whether this pattern of parasite colonization is specific, the intact colonoids were infected in suspension with a higher MOI (1:100; Figure 2D). Although this condition resulted in an overall (but not statistically significant) increase in the number of parasites per infected cell (Figure 2E), the infection was yet localized in specific cells/areas of the organoids (Figure 2D). To study parasite kinetics in infected colonoids, parasite load was quantified by confocal microscopy at 24, 48 and 72 h post infection (Figure 3). At time point 24 h, only one or two parasites were detected *per* infected cell (Figure 3A). This number increased by 6- to 19-folds after 48 h and 72 h, indicating that the pathogen was able to replicate inside the infected cells (Figure 3B). An important observation is that irrespective of the

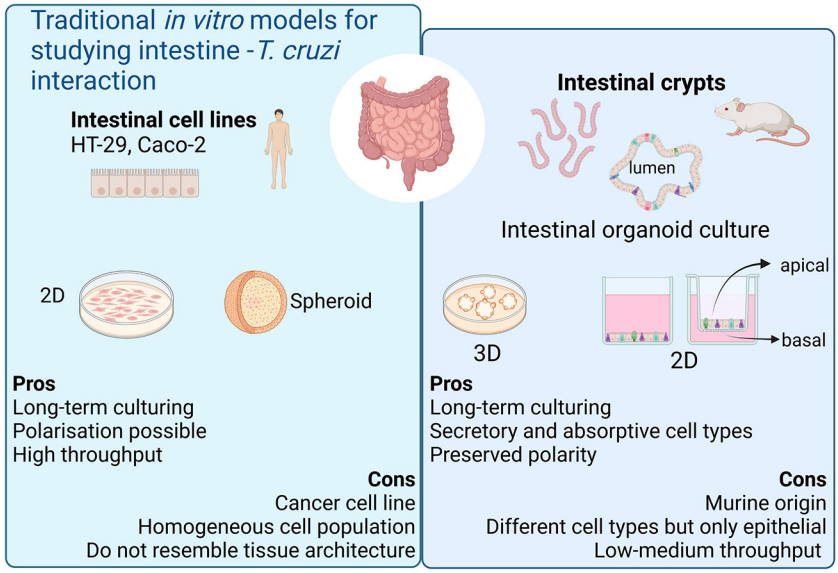

FIGURE 1
Current *in vitro* models for modeling chronic Chagas Disease. Created with BioRender.com (agreement number BV2506JOHI).

10.3389/fcimb.2023.1082524

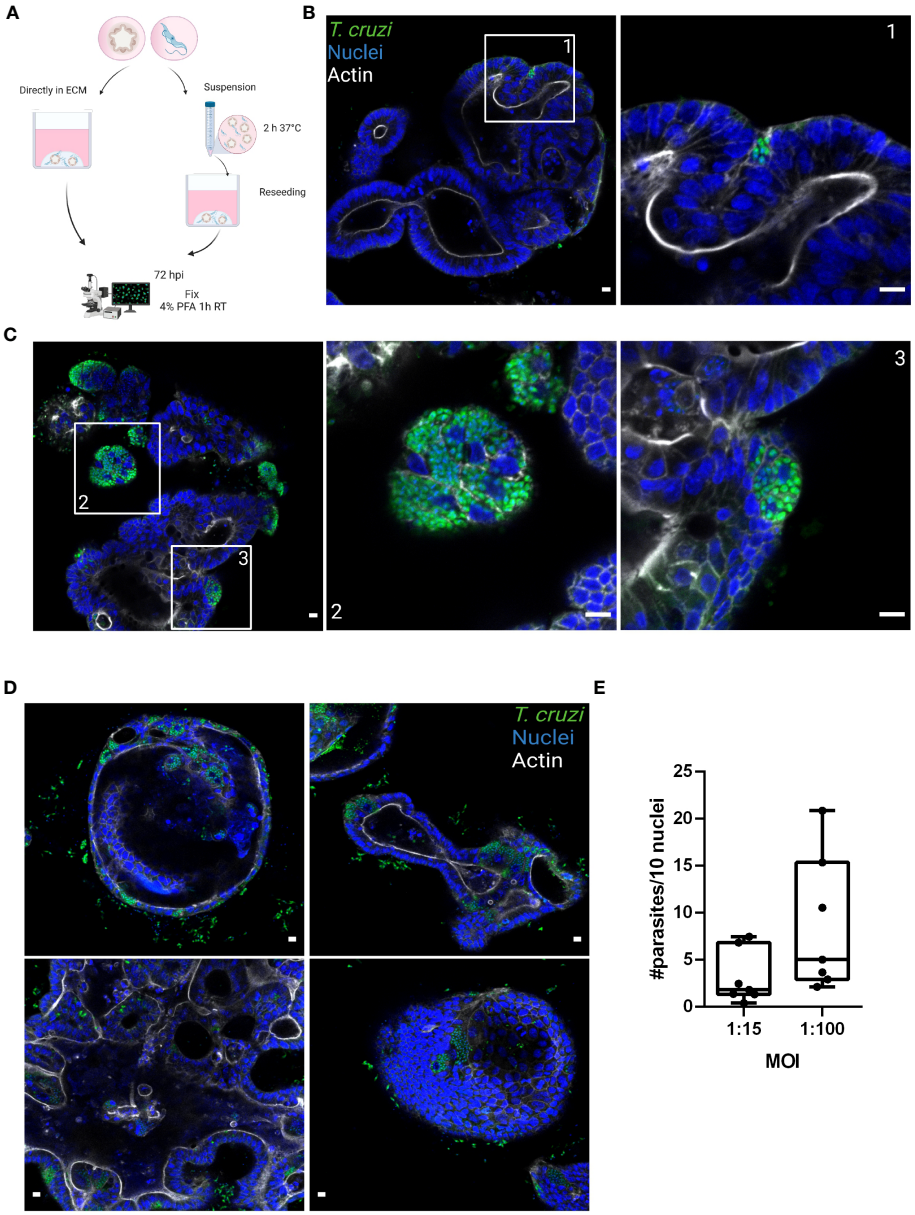

FIGURE 2
Basolateral infection of organoids by *T. cruzi*. **(A)** Schematic representation of the infection protocol. Murine colon-organoids were removed from the matrix and either directly re-plated with the parasites or incubated for 2 h in suspension at 37°C before being re-plated. At 72 h post-infection parasite load was assessed by confocal microscopy. Created with BioRender.com (agreement number RW2506JDYE) **(B)** Representative image of organoids infected with parasites (MOI 1:15) included directly in the matrix. **(C)** Representative image of organoids infected with parasites in the absence of matrix. **(D)** Organoids infected with a MOI of 1:100 show discrete parasite nests. **(E)** Number of intracellular parasites every 10 cells over a 72 h period of infection. Data from one representative experiment out of 2 independent experiments (different organoid lines per experiment). Data are expressed as median and interquartile range and compared using Mann-Whitney test (n = 7). Scale bar: 10 µm. Nuclei (blue): methyl green staining, *T. cruzi* (green): anti-trypanothione reductase immune-staining, and Actin (white): phalloidin Texas Red staining.

infection conditions, the internalized trypomastigotes were able to differentiate into replicative amastigotes, visualized as small rounded cells, which actively divided inside the colonoid cells.

3.2 *Trypanosoma cruzi* is able to infect proliferative and non-proliferative cells

Since the infection sites were restricted to some cells of the organoids regardless of the MOI used, we were interested in determining if the parasites had a preference for infecting proliferative or non-proliferative cell types. Thus, parasites and organoids were incubated for 2 h in suspension with a 1:15 MOI and then further cultured for 72 h. The organoid-derived proliferating cells (stem cells and progenitor cells) were detected using anti-Ki67 staining (Figure 4). Both proliferative (Ki67 positive; Figure 4A) and non-proliferative cells (Ki67 negative; Figure 4B) were infected by parasites. On the other hand, specialized secretory cells such as goblet cells were identified by WGA staining of the organoids but, interestingly, no parasites were infecting them (Figure 4C).

10.3389/fcimb.2023.1082524

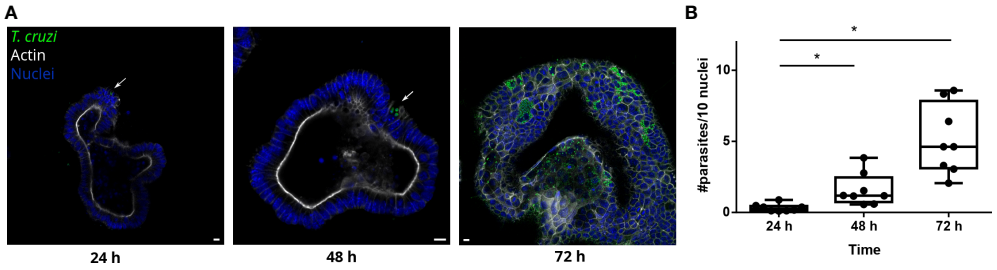

FIGURE 3
T. cruzi is able to invade and replicate inside organoids. **(A)** Representative images of organoids infected with parasites (MOI 1:15) and incubated for 24, 48 or 72 h. Arrows indicate infected cells. **(B)** Number of intracellular parasites every 10 cells at different time points. Data from one representative experiment out of 2 independent experiments (different organoid lines per experiment). Data are expressed as median and interquartile range and compared using Mann-Whitney test (n = 8) $p<0.05$. Scale bar: 10 µm. Nuclei (blue): Hoechst 33342 staining, *T. cruzi* (green): anti-trypanothione reductase immune-staining, and Actin (white): phalloidin Texas Red staining. *$p<0.05$.

3.3 *Trypanosoma cruzi* invades colon-derived cells from their apical side in a discrete fashion

In order to facilitate the apical access of the parasite to the full repertoire of epithelial cells present in the colon-derived organoids, organoid monolayers were prepared and used for infection. To generate a simplified monolayer culture system similar to the conventional 2D culture, the organoids were removed from the BME matrix, dissociated both mechanically and enzymatically, and the cell suspension was seeded in a pre-coated multi-well plate (Figure 5A). Once the monolayer reached confluence,

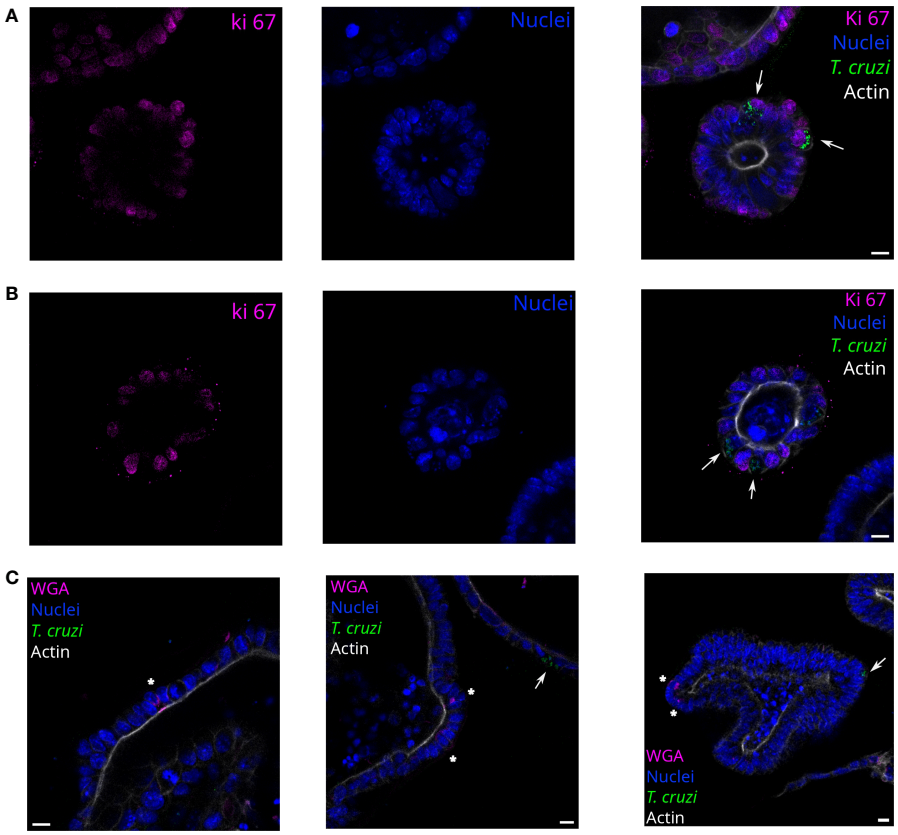

FIGURE 4
T. cruzi infects proliferating or non-proliferating cells but not goblet cells. Representative images of organoids infected with parasites (MOI 1:15) and incubated for 72 h. Arrows indicate infected cells. Parasites are able to infect Ki67 positive **(A)** and negative **(B)** cells. Nuclei (blue): Hoechst 33342 staining, *T. cruzi* (green): anti-mitochondrial peroxiredoxin immune-staining, and Actin (white): phalloidin Texas Red staining. **(C)** Labeled goblet cells (indicated with *) were uninfected, while some infected cells were detected in the same field. Nuclei (blue): Hoechst 33342 staining, *T. cruzi* (green): anti-mitochondrial peroxiredoxin immune-staining, Actin (magenta): phalloidin-Alexa Fluor 647 staining, and goblet cells (white): WGA-Alexa Fluor 555 staining. Scale bar: 10 µm.

10.3389/fcimb.2023.1082524

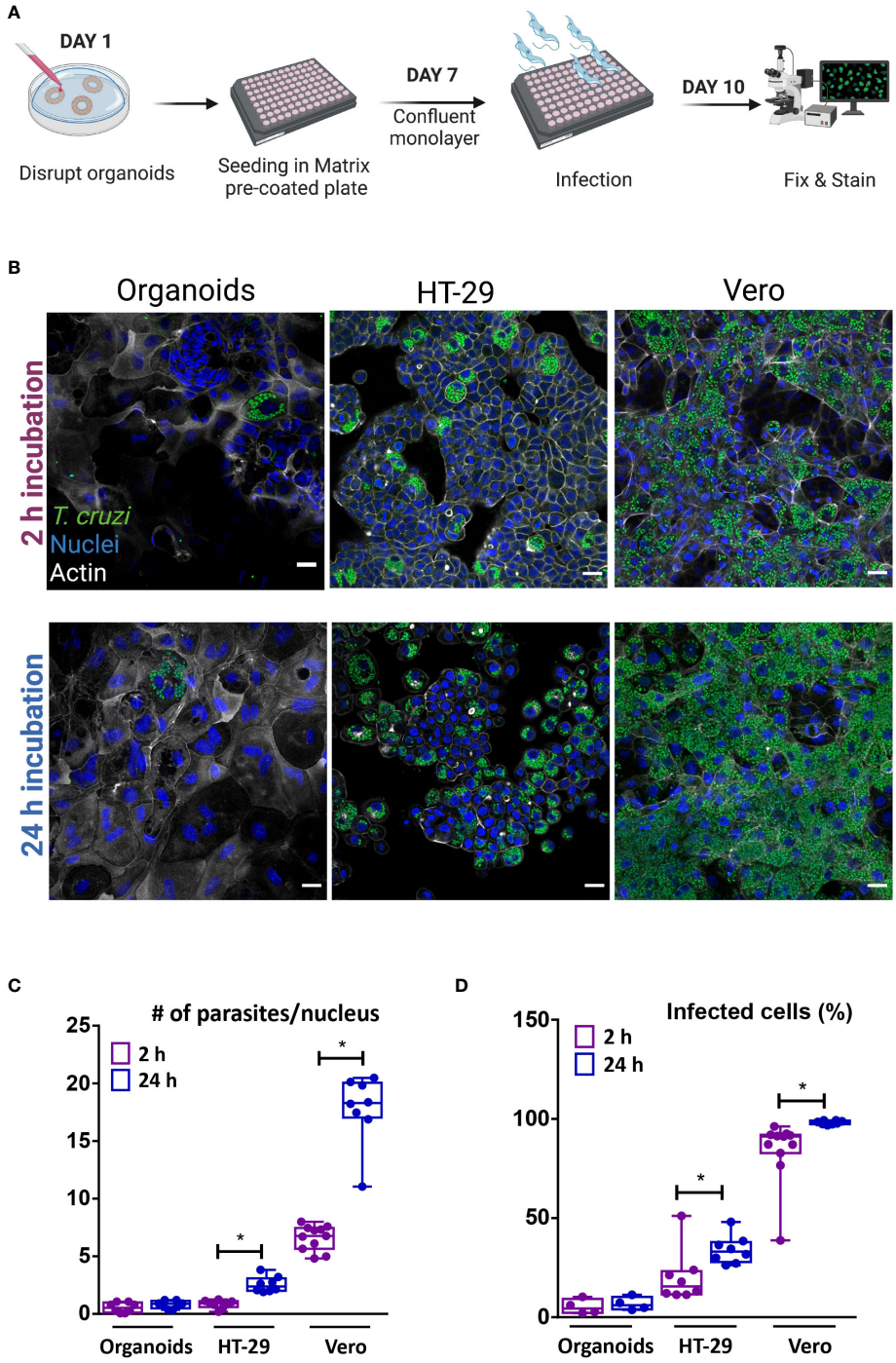

FIGURE 5
Apical organoid and cell-line infection by *T cruzi*. **(A)** Schematic representation of the infection protocol. Vero, HT-29 cells and murine colon-organoid derived cells were seeded as monolayers. After reaching confluence, cells were incubated with the parasites for 2 h or 24 h at 37°C and further incubated at 37°C for 72 h. Created with BioRender (agreement number WV2506JDUP) **(B)** Representative images of 2D infected cells (MOI 1:15). **(C)** Number of intracellular parasites per host-cell nucleus over a 72 h period of infection. **(D)** Quantification of the percentage of cells infected with at least one parasite. Infection rate was improved with longer incubation time for HT-29 and Vero cells, while organoid-derived monolayers showed similar parasite load, regardless of time exposure. Data from one representative experiment out of 2 independent experiments (different organoid lines per experiment). Data are expressed as median and interquartile range and compared using Mann-Whitney test (n = 8), *p<0.05. Scale bar: 25 µm. Nuclei (blue): methyl green staining, *T. cruzi* (green): anti-trypanothione reductase immune-staining, and Actin (white): phalloidin Texas Red staining.

trypomastigotes were added at a 1:15 MOI (epithelial cells: trypomastigotes) and incubated for 2 or 24 h. Upon removal of non-internalized parasites, the incubation was extended for a total of 72 h (Figure 5B). For comparison purposes, tumoral cell lines from human colon (HT-29 cell line) and green monkey kidney (Vero cell line) were infected with *T. cruzi* under the same conditions used for organoid cells. Similar to the results obtained in the basolateral infections of intact organoids, *T. cruzi* infected

only a discrete number of epithelial cells despite the large area of cells available in the 2D culture (Figure 5B). Extending the time the monolayer was exposed to extracellular trypomastigotes (i.e. from 2 to 24 h) did not result in significant changes in the number of infected cells or parasite burden per cell (Figure 5C, D). Notably, a short infection time (2 h) also led to a selective infection of human intestinal epithelial cells HT-29, though the number of parasites/cells and of infected cells was slightly higher than that observed in organoid-derived cells. Contrary to the results obtained for the organoid monolayer, extending the exposure of the HT-29 intestinal cell line to trypomastigotes (24 h incubation) resulted in a significant 3- to 4-folds increase in the level of infected cells and parasites/cell (Figure 5C, D). Nonetheless, the level of infection achieved on this cell line was not as massive as that obtained in Vero cells (Figure 5B). In fact, a 2 h incubation of this cell type with trypomastigotes resulted in 75% infection of the cell monolayer, a value that reached a maximum of 98% when the incubation was extended to 24 h (Figures 5B, D). The number of amastigotes per Vero cell doubled when the incubation time was extended from 2 to 24 h, which can likely be ascribed to a higher number of trypomastigotes invading a single cell (Figures 5C). For all conditions tested, the parasite was able to complete its differentiation and multiplication cycle inside the different host cells. Overall, this data indicates that certain organoid- and tumor-derived cells from the colon are susceptible to infection by *T. cruzi* Dm28c, while stable cell lines from primate-derived kidney are highly permissive to parasite invasion.

4 Discussion

Intestinal organoids have been used in the study of the biology and development of the intestinal epithelium (Clevers, 2016; Puschhof et al., 2021), as well as in understanding the interaction with different pathogens and the gut microbiota (Han et al., 2021). However, these models had yet not been applied to model CD (Breyner et al., 2020). The intestinal-related infection, particularly in the colon segment, during the chronic stage of CD, plays an important role as a parasite reservoir that is refractory to drug treatment and immunological recognition. The lack of appropriate models to study this parasite-organ interaction in depth has prompted us to undertake the development and preliminary characterization of infection protocols of colon-derived organoids, which are closer to resembling physiological conditions.

The conditions for infecting murine colon-derived organoids in 3D and 2D formats with *T. cruzi* trypomastigotes are described here, to our knowledge, for the first time. The method for the infection of mouse colon-derived organoid epithelial sheets here reported is simple and economic. It is adapted to a 96-well plate format, where no transwell is needed and media and staining solutions volume are significantly reduced when compared to other chamber or plate formats. Performing the infection of intact organoids embedded in an extracellular matrix, or devoid of the supportive matrix with culture-derived (highly infective) trypomastigotes proved successful. Mimicking tissue colonization in the chronic stage of CD (i.e. basolateral infection), the parasites were capable of invading and replicating in epithelial cells. Infection experiments at extended time points may reveal if the parasites are also able to reach the organoid lumen by paracellular or intracellular migration. Notably, the invasion appears to be cell-type specific because even exposing the host cells to a 100-fold excess of parasite cells, yet resulted in a discrete number of colonoid cells being permissive to infection. A similar outcome was obtained when the infection was performed from the apical side of a 2D monolayer of organoid cells. Although the primary site of body penetration during oral transmission of CD is yet unknown, our result indicates that the parasite is able to establish infections in colon epithelial cells when accessing them from the lumen. Therefore, the 2D culture system may be of interest to studying the oral transmission route of *T. cruzi* since it avoids the use of microinjection techniques to access the organoid from the luminal surface.

An intriguing finding was that discrete foci of infected cells were observed in both spatial arrangements of the murine organoids, 3D and 2D, as well as in human-derived colon cell lines. This differed markedly from the massive infection achieved in a kidney-derived epithelial cell line of primate origin. Our results suggest that the reason for the susceptibility of certain colon-derived cells to be infected by *T. cruzi* cannot be ascribed to species-specific origin of the host cells nor to cell polarization because, as mentioned above, the phenomenon was observed in murine- and human-derived cells, the former infected from both the apical and basolateral side. It is therefore tempting to speculate that a combination of host (e.g., receptors, different cell types) and pathogen-specific factors and signals determine this selectivity. In fact, *T. cruzi* entry to the host cells is a multifactorial process that may follow actin-dependent or lysosome-dependent and -independent mechanisms (de Souza et al., 2010). Although not yet fully understood, the current evidence supports that for invading non-phagocytic cells, *T. cruzi* exploits a highly conserved cellular pathway for the repair of plasma membrane lesions (Fernandes and Andrews, 2012). This process is largely determined by parasite-induced signaling pathways that involve primary membrane injury, followed by lysosome recruitment and content release at the site of entry, which favor an active internalization of the pathogen inside ceramide/lysosome enriched vacuoles. Such a peculiar mechanism of pathogen entry along with the fact that the membrane of muscle cells is frequently exposed to mechanical stress, and, therefore, has an exacerbated turnover for membrane repair, has been a major argument to explain the tropism of the parasite for muscle cells. On the other hand, non-professional phagocytic cells metabolically- (starvation) or pharmacologically-induced to undergo autophagy proved highly susceptible to *T. cruzi* infection (Romano et al., 2009). Also, the composition of the membrane (microdomains) has been demonstrated to be an additional factor contributing to *T. cruzi* invasion of phagocytic and non-phagocytic cells (Barrias et al., 2007; Fernandes et al., 2007). Which of these or, perhaps, novel factors contribute to the observed tropism of *T. cruzi* for certain colon-derived cells needs to be further investigated. In our experiments, proliferative and non-proliferative cells were infected by parasites, but specific cell types were not yet identified to be responsible for the discrete zones of infection within the organoid. However, we did not observe mucin-secreting cells (goblet cells)

infected by *T. cruzi*. In the intestine (and also other tissues), goblet cells are specialized in creating a protective mucus layer that mechanically prevents the contact of epithelial cells with external factors (from microorganisms to macromolecules; Birchenough et al., 2015). Thus, it is tempting to speculate that this dense barrier of heavily glycosylated proteins is responsible for blocking the access of the parasite to the goblet and surrounding cells. At this point is worth recalling that our experimental conditions for growing organoids promote stem cell proliferation rather than cell differentiation. Therefore, further experiments using differentiated organoids should be performed to better model the interactions of *T. cruzi* with the intestinal epithelia.

Generally compared to the *in vivo* methods, intestinal organoids can provide a less expensive and more rapid model to study intestinal cell-*T. cruzi* interaction. Since the availability of tissue from patients with digestive forms of CD is scarce, the murine intestinal organoids are an alternative to bypass this limitation (Breyner et al., 2020). However, future studies in human organoids derived from healthy donors may help improve the infection model to better mimic human disease. Moreover, while murine intestinal organoids, such as those used in this study, present only the epithelial compartment, organoid co-culture systems with other cell types such as nervous, stromal (Pastuła et al., 2015), and immune cells (Noel et al., 2017) have been developed and may be very useful to increase the complexity of the system for dissecting host-pathogen interaction in CD.

5 Conclusion

A simple and economic method that allows to model the infection of 2D and 3D intestinal organoids from murine colon by *T. cruzi* has been established. The study delivered interesting preliminary information about parasite invasion and proliferation in the host tissue. The organoid model represents a valuable tool to understand several aspects of the host-pathogen interaction that may translate into more effective treatments of CD.

Data availability statement

The raw data supporting the conclusions of this article will be made available by the authors, without undue reservation.

Ethics statement

The animal study was reviewed and approved by Comisión de Ética en el Uso de Animales (CEUA) - Institut Pasteur de Montevideo (Protocol #002-21).

Author contributions

HD contributed to experimental design, the data acquisition, analysis and writing of the manuscript. RP contributed to the experimental design, data acquisition and analysis. CQ contributed to data acquisition. AM contributed to data acquisition and to experimental design. MB-F contributed to funding acquisition and experimental design. MAC contributed to experimental design. All authors contributed to the article and approved the submitted version.

Funding

This project was funded by ANII (PhD fellowship, FMV_1_2019_1_156213 and EQL_2013_X_1_2), ACIP grant (ACIP 532-22) from Institut Pasteur Paris, and FOCEM (MERCOSUR Structural Convergence Fund), COF 03/11. HD and CQ received a fellowship from Sistema Nacional de Becas, ANII. AM, MAC, MB-F and RP are members of the SNI (National Research System, Uruguay) and PEDECIBA.

Acknowledgments

The authors gratefully acknowledge the Advanced Bioimaging Unit and the Laboratory Animal Biotechnology Unit at the Institut Pasteur de Montevideo for their support and assistance in the present work. Dr. R. Luise Krauth-Siegel (Heidelberg University, Germany) and Dr. Carlos Robello (Unidad de Biología Molecular, Institut Pasteur de Montevideo, Uruguay) are gratefully acknowledged for providing antibodies against *T. cruzi*-trypanothione reductase and -mitochondrial peroxiredoxin, respectively. Figures 1, 2A, 5A were created with BioRender.com.

Conflict of interest

The authors declare that the research was conducted in the absence of any commercial or financial relationships that could be construed as a potential conflict of interest.

Publisher's note

References

Andersson, J., Örn, A., and Sunnemark, D. (2003). Chronic murine chagas' disease: The impact of host and parasite genotypes. *Immunol. Lett.* 86, 207–212. doi: 10.1016/S0165-2478(03)00019-1

Barker, N. (2014). Adult intestinal stem cells: critical drivers of epithelial homeostasis and regeneration. *Nat. Rev. Mol. Cell Biol.* 15, 19–33. doi: 10.1038/nrm3721

Barrias, E. S., Dutra, J. M. F., De Souza, W., and Carvalho, T. M. U. (2007). Participation of macrophage membrane rafts in trypanosoma cruzi invasion process. *Biochem. Biophys. Res. Commun.* 363, 828–834. doi: 10.1016/j.bbrc.2007.09.068

Birchenough, G. M. H., Johansson, M. E. V., Gustafsson, J. K., Bergström, J. H., and Hansson, G. C. (2015). New developments in goblet cell mucus secretion and function. *Mucosal Immunol.* 8, 712–719. doi: 10.1038/mi.2015.32

Breyner, N. M., Hecht, M., Nitz, N., Rose, E., and Carvalho, J. L. (2020). *In vitro* models for investigation of the host-parasite interface - possible applications in acute chagas disease. *Acta Tropica* 202, 105262. doi: 10.1016/j.actatropica.2019.105262

Clevers, H. (2016). Modeling development and disease with organoids. *Cell* 165, 1586–1597. doi: 10.1016/j.cell.2016.05.082

de Souza, W., de Carvalho, T. M. U., and Barrias, E. S. (2010). Review on trypanosoma cruzi: Host cell interaction. *Int. J. Cell Biol.* 2010, 295394. doi: 10.1155/2010/295394

Fernandes, M. C., and Andrews, N. W. (2012). Host cell invasion by trypanosoma cruzi: a unique strategy that promotes persistence. *FEMS Microbiol. Rev.* 36, 734–747. doi: 10.1111/j.1574-6976.2012.00333.x

Fernandes, M. C., Cortez, M., Geraldo Yoneyama, K. A., Straus, A. H., Yoshida, N., and Mortara, R. A. (2007). Novel strategy in trypanosoma cruzi cell invasion: Implication of cholesterol and host cell microdomains. *Int. J. Parasitol.* 37, 1431–1441. doi: 10.1016/j.ijpara.2007.04.025

Fonseca-Berzal, C., Arán, V. J., Escario, J. A., and Gómez-Barrio, A. (2018). Experimental models in chagas disease: a review of the methodologies applied for screening compounds against trypanosoma cruzi. *Parasitol. Res.* 117, 3367–3380. doi: 10.1007/s00436-018-6084-3

Han, X., Mslati, M. A., Davies, E., Chen, Y., Allaire, J. M., and Vallance, B. A. (2021). Creating a more perfect union: Modeling intestinal bacteria-epithelial interactions using organoids. *Cell. Mol. Gastroenterol. Hepatol.* 12, 769–782. doi: 10.1016/j.jcmgh.2021.04.010

Holthaus, D., Delgado-Betancourt, E., Aebischer, T., Seeber, F., and Klotz, C. (2021). Harmonization of protocols for multi-species organoid platforms to study the intestinal biology of toxoplasma gondii and other protozoan infections. *Front. Cell. Infect. Microbiol.* 10. doi: 10.3389/fcimb.2020.610368

Holthaus, D., Kraft, M. R., Krug, S. M., Wolf, S., Müller, A., Betancourt, E. D., et al. (2022). Dissection of barrier dysfunction in organoid-derived human intestinal epithelia induced by giardia duodenalis. *Gastroenterology* 162, 844–858. doi: 10.1053/j.gastro.2021.11.022

Khan, A. A., Langston, H. C., Costa, F. C., Olmo, F., Taylor, M. C., McCann, C. J., et al. (2021). Local association of trypanosoma cruzi chronic infection foci and enteric neuropathic lesions at the tissue micro-domain scale. *PloS Pathog.* 17, e1009864. doi: 10.1371/journal.ppat.1009864

Lamisere, H., Bhalchandra, S., Kane, A. V., Zeng, X.-L., Mo, D., Adams, W., et al. (2022). Differential response to the course of cryptosporidium parvum infection and its impact on epithelial integrity in differentiated versus undifferentiated human intestinal enteroids. *Infect. Immun.* 90, e0039722. doi: 10.1128/iai.00397-22

Lidani, K. C. F., Andrade, F. A., Bavia, L., Damasceno, F. S., Beltrame, M. H., Messias-Reason, I. J., et al. (2019). Chagas disease: From discovery to a worldwide health problem. *Front. Public Health* 7. doi: 10.3389/fpubh.2019.00166

Martello, L. A., Wadgaonkar, R., Gupta, R., Machado, F. S., Walsh, M. G., Mascareno, E., et al. (2013). Characterization of trypanosoma cruzi infectivity, proliferation, and cytokine patterns in gut and pancreatic epithelial cells maintained *in vitro*. *Parasitol. Res.* 112, 4177–4183. doi: 10.1007/s00436-013-3609-7

Noel, G., Baetz, N. W., Staab, J. F., Donowitz, M., Kovbasnjuk, O., Pasetti, M. F., et al. (2017). A primary human macrophage-enteroid co-culture model to investigate mucosal gut physiology and host-pathogen interactions. *Sci. Rep.* 7, 45270. doi: 10.1038/srep45270

Pastuła, A., Middelhoff, M., Brandtner, A., Tobiasch, M., Höhl, B., Nuber, A. H., et al. (2015). Three-dimensional gastrointestinal organoid culture in combination with nerves or fibroblasts: A method to characterize the gastrointestinal stem cell niche. *Stem Cells Int.* 2016, e3710836. doi: 10.1155/2016/3710836

Pereira, K. S., Schmidt, F. L., Guaraldo, A. M. A., Franco, R. M. B., Dias, V. L., and Passos, L. A. C. (2009). Chagas' disease as a foodborne illness. *J. Food Prot.* 72, 441–446. doi: 10.4315/0362-028X-72.2.441

Puschhof, J., Pleguezuelos-Manzano, C., Martinez-Silgado, A., Akkerman, N., Saftien, A., Boot, C., et al. (2021). Intestinal organoid cocultures with microbes. *Nat. Protoc.* 16, 4633–4649. doi: 10.1038/s41596-021-00589-z

Rassi, A., Rassi, A., and Marin-Neto, J. A. (2010). Chagas disease. *Lancet* 375, 1388–1402. doi: 10.1016/S0140-6736(10)60061-X

Requena-Méndez, A., Aldasoro, E., de Lazzari, E., Sicuri, E., Brown, M., Moore, D. A. J., et al. (2015). Prevalence of chagas disease in Latin-American migrants living in Europe: A systematic review and meta-analysis. *PloS Negl. Trop. Dis.* 9, e0003540. doi: 10.1371/journal.pntd.0003540

Rodríguez, M. E., Rizzi, M., Caeiro, L. D., Masip, Y. E., Perrone, A., Sánchez, D. O., et al. (2020). Transmigration of trypanosoma cruzi trypomastigotes through 3D cultures resembling a physiological environment. *Cell. Microbiol.* 22, e13207. doi: 10.1111/cmi.13207

Romano, P. S., Arboit, M. A., Vázquez, C. L., and Colombo, M. I. (2009). The autophagic pathway is a key component in the lysosomal dependent entry of trypanosoma cruzi into the host cell. *Autophagy* 5, 6–18. doi: 10.4161/auto.5.1.7160

Sato, T., Vries, R. G., Snippert, H. J., van de Wetering, M., Barker, N., Stange, D. E., et al. (2009). Single Lgr5 stem cells build crypt-villus structures *in vitro* without a mesenchymal niche. *Nature* 459, 262–265. doi: 10.1038/nature07935

Schindelin, J., Arganda-Carreras, I., Frise, E., Kaynig, V., Longair, M., Pietzsch, T., et al. (2012). Fiji: an open-source platform for biological-image analysis. *Nat. Methods* 9, 676–682. doi: 10.1038/nmeth.2019

Vazquez, B. P., Vazquez, T. P., Miguel, C. B., Rodrigues, W. F., Mendes, M. T., de Oliveira, C. J. F., et al. (2015). Inflammatory responses and intestinal injury development during acute trypanosoma cruzi infection are associated with the parasite load. *Parasites Vectors* 8, 206. doi: 10.1186/s13071-015-0811-8

Ward, A. I., Lewis, M. D., Khan, A. A., McCann, C. J., Francisco, A. F., Jayawardhana, S., et al. (2020). *In vivo* analysis of trypanosoma cruzi persistence foci at single-cell resolution. *mBio* 11, e01242–e01220. doi: 10.1128/mBio.01242-20

Wilke, G., Funkhouser-Jones, L. J., Wang, Y., Ravindran, S., Wang, Q., Beatty, W. L., et al. (2019). A stem-Cell-Derived platform enables complete cryptosporidium development *In vitro* and genetic tractability. *Cell Host Microbe* 26, 123–134.e8. doi: 10.1016/j.chom.2019.05.007

frontiers | Frontiers in Cellular and Infection Microbiology

TYPE Original Research
PUBLISHED 06 April 2023
DOI 10.3389/fcimb.2023.1138456

OPEN ACCESS

EDITED BY
Alena Pance,
University of Hertfordshire, United Kingdom

REVIEWED BY
Veronica Jimenez,
California State University, Fullerton, United States
Robert P Hirt,
Newcastle University, United Kingdom

*CORRESPONDENCE
Beatriz Garat
bgarat@fcien.edu.uy
Pablo Smircich
psmircich@fcien.edu.uy

SPECIALTY SECTION
This article was submitted to Parasite and Host, a section of the journal Frontiers in Cellular and Infection Microbiology

RECEIVED 05 January 2023
ACCEPTED 20 March 2023
PUBLISHED 06 April 2023

CITATION
Smircich P, Pérez-Díaz L, Hernández F, Duhagon MA and Garat B (2023) Transcriptomic analysis of the adaptation to prolonged starvation of the insect-dwelling *Trypanosoma cruzi* epimastigotes. *Front. Cell. Infect. Microbiol.* 13:1138456. doi: 10.3389/fcimb.2023.1138456

Transcriptomic analysis of the adaptation to prolonged starvation of the insect-dwelling *Trypanosoma cruzi* epimastigotes

Pablo Smircich[1,2]*, Leticia Pérez-Díaz[1], Fabricio Hernández[1], María Ana Duhagon[1,3] and Beatriz Garat[1]*

[1]Sección Genómica Funcional, Facultad de Ciencias, Universidad de la República, Montevideo, Uruguay, [2]Laboratorio de Bioinformática, Departamento de Genómica, Instituto de Investigaciones Biológicas Clemente Estable, Montevideo, Uruguay, [3]Departamento de Genética, Facultad de Medicina Universidad de la República, Montevideo, Uruguay

Trypanosoma cruzi is a digenetic unicellular parasite that alternates between a blood-sucking insect and a mammalian, host causing Chagas disease or American trypanosomiasis. In the insect gut, the parasite differentiates from the non-replicative trypomastigote forms that arrive upon blood ingestion to the non-infective replicative epimastigote forms. Epimastigotes develop into infective non-replicative metacyclic trypomastigotes in the rectum and are delivered *via* the feces. In addition to these parasite stages, transitional forms have been reported. The insect-feeding behavior, characterized by few meals of large blood amounts followed by long periods of starvation, impacts the parasite population density and differentiation, increasing the transitional forms while diminishing both epimastigotes and metacyclic trypomastigotes. To understand the molecular changes caused by nutritional restrictions in the insect host, mid-exponentially growing axenic epimastigotes were cultured for more than 30 days without nutrient supplementation (prolonged starvation). We found that the parasite population in the stationary phase maintains a long period characterized by a total RNA content three times smaller than that of exponentially growing epimastigotes and a distinctive transcriptomic profile. Among the transcriptomic changes induced by nutrient restriction, we found differentially expressed genes related to managing protein quality or content, the reported switch from glucose to amino acid consumption, redox challenge, and surface proteins. The contractile vacuole and reservosomes appeared as cellular components enriched when ontology term overrepresentation analysis was carried out, highlighting the roles of these organelles in starving conditions possibly related to their functions in regulating cell volume and osmoregulation as well as metabolic homeostasis. Consistent with the quiescent status derived from nutrient restriction, genes related to DNA metabolism are regulated during the stationary phase. In addition, we observed differentially expressed genes related to the unique

parasite mitochondria. Finally, our study identifies gene expression changes that characterize transitional parasite forms enriched by nutrient restriction. The analysis of the here-disclosed regulated genes and metabolic pathways aims to contribute to the understanding of the molecular changes that this unicellular parasite undergoes in the insect vector.

KEYWORDS

Trypanosoma cruzi, life cycle, transcriptomics, starvation, differentiation

Introduction

Trypanosoma cruzi is a digenetic parasitic kinetoplastid that alternates between an invertebrate host—Triatominae vector—and a mammalian host and causes Chagas disease or American trypanosomiasis (Chagas, 1909), a life-threatening problem currently affecting 6-7 million people mainly in endemic areas of Latin America (https://www.who.int/news-room/fact-sheets/detail/chagas-disease-(american-trypanosomiasis). *T. cruzi* has been classified in several Discrete Typing Units (DTUs, TcI to TcVI and TcBat). This genetic diversity is associated with differences in virulence heterogeneity, geographical distribution, insect host and is differentially sampled in domestic and/or sylvatic cycles (Noireau et al., 2009; Brenière et al., 2016). Since the parasite can infect a wide range of mammalian hosts that can be considered urban reservoirs, zoonotic transmission has been recognized as a public health issue (Urdaneta-Morales, 2014). In humans, though the infection can be achieved through blood transfusions or organ transplant, congenitally from mother to child, or by accidental ingestion of contaminated food, *T. cruzi* is mainly transmitted to mammals by blood-sucking insects of the subfamily Triatominae widely distributed in Latin America and currently expanding from rural to urban areas (Alarcón de Noya et al., 2022).

In the vector, the non-replicative *T. cruzi* trypomastigotes that arrive with blood ingestion differentiate from the non-infective epimastigote forms, which actively replicate in the vector's midgut and progress through the rectum developing the infective non-replicative metacyclic trypomastigotes. In addition, other parasite forms have been recognized in the digestive tract of the insect and in the *in vitro* metacyclogenesis process, which was later confirmed (Kollien and Schaub, 2000; Tyler and Engman, 2001; Nepomuceno-Mejía et al., 2010; Shaw et al., 2016; Gonçalves et al., 2018; De Souza and Barrias, 2020), and recently designated as transitional epimastigotes (De Souza and Barrias, 2020).

A role for these forms as a stage in the life cycle of *T. cruzi* developed in response to nutrient availability in the insect intestinal environment was early proposed (Kollien and Schaub, 1998). Indeed, the long starvation periods that follow the abundant blood ingestion of triatomine sharply affect not only parasite population density but also the proportion of developmental stages, increasing the proportion of transitional forms while decreasing metacyclic trypomastigotes and epimastigotes in insects starved for more extended periods (Kollien and Schaub, 1998). It is considered that the triatomine nutritional behavior derives from the fact that having few meals but of large blood amounts minimizes the danger that the vertebrate may cause to blood-sucking insects (Sterkel et al., 2017). Considering not only morphological changes but also transcriptional and post-transcriptional events, mature stationary phase epimastigotes have been proposed as a distinctive pre-adaptive stage with the ability to differentiate into the metacyclic form or to return to the replicative epimastigote stage depending on the availability of nutrients (Hernández et al., 2012). More recently, the transitional epimastigote has also been claimed as a distinctive developmental stage (De Souza and Barrias, 2020). Understanding developmental processes in the insect host has proven to be a challenging task. Several factors that influence this process *in vivo* cannot be readily reproduced on *in-vitro* models. Emerging technologies of tissue and 3D cell culture may overcome some of these issues. Indeed, pharmacological analysis for the prevention and treatment of diseases caused by unicellular parasites is being improved using these methods to model host-parasite interactions (Pance, 2021). In *T. cruzi* ony a few reports using these methodologies have been described in the literature and are limited to mammalian stages mostly in cardiac tissues (da Silva Lara et al., 2018; Bozzi et al., 2019; Sass et al., 2019a; Sass et al., 2019b). The relevance of studying host-parasite interactions also in mammalian gastrointestinal tissue has been recognized (Breyner et al., 2020). It would be interesting to develop such approaches by using insect-derived cells. While these emerging strategies will necessarily improve the current understanding of parasite-insect-host interactions, reductionist *in vitro* approaches are still valuable tools to gain insight into the molecular mechanisms involved.

Despite its pervasive constitutive transcription, *T. cruzi* exhibits exceptional metabolic flexibility to respond to environmental stress. Proteomic and transcriptome studies have shown that the parasites display gene expression changes when entering the stationary growth phase. Differential expression of genes related to the cell cycle, pathogenesis, and metabolic processes (Santos et al., 2018) or proteins related to replication status and autophagy (Avila et al., 2018) have been found. Using metabolomics targeted at energy metabolism and oxidative imbalance, a finely tuned metabolic switch from glucose to amino acid consumption has been revealed at the beginning of the stationary growth phase (Barisón

et al., 2017). However, the effects of prolonged nutrient restriction on insect-dwelling parasite forms have only been partially accounted for. Using an approach of sudden nutrient restriction to the epimastigotes reaching the stationary growth phase, the study of the impact on the unique mitochondria of *T. cruzi* epimastigotes revealed structural changes, organelle swelling and impaired oxidative phosphorylation with increased ROS levels and overexpressed antioxidant enzymes, as well as an exacerbated expression of different autophagy-related genes (Pedra-Rezende et al., 2021). In addition, the alkalinization of acidocalcisomes through histidine ammonia-lyase has recently been demonstrated to be essential for survival under starvation conditions (Mantilla et al., 2021). Besides, prolonged nutrient starvation of *T. cruzi* epimastigotes increased mitochondrial rRNAs and some mRNAs (Shaw et al., 2016)in different strains (Gerasimov et al., 2022). Interestingly, while mitochondrial-encoded respiratory complex subunit mRNA abundances also increase, a similar pattern was not found for the nuclear-encoded subunit mRNAs (Shaw et al., 2016).

To understand the molecular changes derived from the nutritional restrictions that *T. cruzi* slowly undergoes in the insect vector, we here present and analyze the transcriptomes obtained from axenic epimastigotes cultured *in vitro* for a prolonged period without further nutrient supplementation. Although the parasite population in the prolonged stationary phase cannot be considered homogenous, we found that it remains molecularly uniform and differs from exponentially growing epimastigotes. This parasite population is characterized by a total RNA per cell content of approximately one-third of that of exponentially growing parasites and a distinctive transcriptomic profile. Besides the expected expression changes of genes related to surface proteins (Santos et al., 2018), the persistent differentially expressed genes (DEGs) could be categorized in three GO terms: vacuoles, including reservosome and contractile vacuole, chromosome, and the kinetoplast. The analysis of the DEGs suggests a role for intracellular organelles in the adaptation to starving conditions and derived changes in the culture through a quiescent status preserving metabolic homeostasis and osmoregulation. Finally, we identified genes whose expression profiles cannot be attributed to the differentiation to infective metacyclic trypomastigotes (metacyclogenesis), thus could be delineating the molecular markers of the transitional parasite forms induced by nutrient restriction.

Materials and methods

Parasite culture

Epimastigotes of the *T. cruzi* Dm28c strain (TcI DTU) (Contreras et al., 1988) were cultured at 28°C in fresh BHI medium (Oxoid) supplemented with heat-inactivated 10% Fetal Bovine Serum (Capricorn) and penicillin (100 units/mL) and streptomycin (100 µg/mL). The parasite culture was initiated by $1x10^6$ cells/mL previously maintained in the mid-exponential growth phase through continuous dilutions. Three biological replicates were assessed. For each independent experiment, parasites were counted directly by light microscopy using a Neubauer chamber in triplicate. Metacyclic trypomastigotes were distinguished based on morphological features and relative nucleus to kinetoplast location using DAPI- and HE-stained PFA-fixed parasites. Several images were acquired, and at least 100 cells were counted for each independent triplicate experiment.

RNA extraction and evaluation

Total RNA was extracted from $2x10^7$ parasites using Trizol reagent (Life Technologies) as described by the manufacturer. RNA cleanup was performed using DNA-free kit (Life Technologies) according to the manufacturer's instructions. Purified RNA was quantified using Nanodrop by evaluating the absorbance at 260 and 280 nm, and the quality and integrity were assessed using an Agilent RNA 6000 Nano Chip on a Bioanalyzer 2100 (Agilent Technologies).

Transcriptomic assays and data analysis

Three independent replicates of each condition were sequenced at Macrogen using Illumina TruSeq™ RNA Sample Preparation Kit v2 and HiSeq 2500 (http://www.macrogen.com). Trimmomatic (Bolger et al., 2014) was used to obtain high-quality reads that were mapped to the Esmeraldo-like *T. cruzi* genome (version 29, http://tritrypdb.org) using bowtie2 in –very sensitive mode (Langmead and Salzberg, 2012). The number of reads per gene was determined using htseq-count (Anders et al., 2015). For further analysis, only genes with at least 0.5 counts per million in at least one sample were kept. Between 5.8 and 8.9 million reads were mapped per sample. Nine thousand seven hundred seventy-six genes met our exclusion criteria and were used for further analysis. For all pairwise comparisons, differentially expressed genes were assessed using the DEseq2 package available in R (Love et al., 2014). To determine differentially expressed genes (DEGs), a log2 fold change (FC) of |1| and a false discovery rate (FDR) less than 0.05 was considered. Overrepresentation of GO terms among DEGs lists was established using Cluster Profiler in R (Wu et al., 2021), setting a Bonferroni adjusted p-value of less than 0.1 as a cutoff for significance. Statistical analyses and plots were performed in R unless otherwise specified.

Results and discussion

Prolonged *in vitro* culture of *T. cruzi* epimastigotes without nutrient renewal leads to a decay of total RNA per cell content

Parasite life cycle depends on complex interactions with biological, chemical and physical factors in the natural host. The host microbiome, temperature and nutritional environment including the contribution of parasite autophagy have been

recognized as relevant variables that affect differentiation (Jimenez et al., 2008; Li et al., 2011; Díaz-Albiter et al., 2016; Teotônio et al., 2019; Cruz-Saavedra et al., 2020; Paes et al., 2020).

In order to study the transcriptomic changes provoked by the nutrient restriction that *T. cruzi* encounters in the bug´s digestive tract, we initiated *in vitro* cultures with mid-log phase epimastigotes in complete cell culture media and allowed them to grow without medium replenishment. Under these conditions, parasites actively replicate and grow exponentially at day 7 (E), reaching stationary growth on day 14 (early stationary phase, Se). Although the cultures were maintained until day 35, a decline of the growth plateau was evident after day 30. Considering the observed growth curve, in addition to the parasite populations mentioned above (E and Se), we analyzed parasites on day 21 (intermediate stationary phase, Si) and day 28 (final stationary phase, Sf) to evaluate the effects of prolonged culture without medium replenishment.

Parasite morphology was used as a phenotypic marker of the developmental stage. Either metacyclic trypomastigotes, whose presence at low proportion in epimastigote cultures is widely recognized, and transitional forms also previously reported were observed. The percentage of metacyclic trypomastigotes that was detected since the very beginning at low percentages (below 10%), at least untill the intermediate stationary phase plateau (3.8 ± 1.7%, 5.4 ± 0.4% and 7.9 ± 0.6% for E, Se and Si respectively), sharply surpassed 30% at the end of the stationary phase (32.1 ± 5.4% for Sf). Given the characteristics of the transitional forms (displaying a positioning of the kinetoplast, flagellum, and nucleus corresponding to the epimastigote stage but with non-classical epimastigote morphology of the cell body and flagellum) they cannot be precisely quantified by visual inspection (Tyler and Engman, 2001; Nepomuceno-Mejía et al., 2010; Shaw et al., 2016; Gonçalves et al., 2018; De Souza and Barrias, 2020). Nevertheless, enrichment of transitional forms was observed in the stationary phase (Se, Si, and Sf). It has been proposed that flagellar elongation may provide an extended surface for nutrient uptake in unfavorable nutrient conditions (Tyler and Engman, 2001). Meanwhile, repositioning of the kinetoplast has only been observed in the later stages of the metacyclogenesis process (Gonçalves et al., 2018).

As a first step in transcriptomic analysis, the total RNA content per cell during the culture period was determined (Figure 1). The exponentially growing epimastigotes exhibit a total RNA content per cell (1.02 ± 0.53 pg) similar to previous reports in a different culture medium (0.6 ± 0.1 pg (Pastro et al., 2017)). As expected, the exponentially growing epimastigotes contain more total RNA per cell than the parasites in the stationary phase (0.36 ± 0.10 pg for Se). This value remains constant for the parasite population in the middle of the growth plateau (0.33 ± 0.09 pg for Si). Still, it diminishes even more at the beginning of the growth decline (0.17 ± 0.12 pg for Sf). Concordantly, transcription activity in exponentially growing epimastigotes has been estimated to be about six to ten times more active than in stationary cells (Nepomuceno-Mejía et al., 2010). In addition, under nutritional stress, an increase in the number of cytoplasmic granules (Santos et al., 2018), which are associated with mRNA degradation (Cassola et al., 2007; Holetz et al., 2007) has been described.

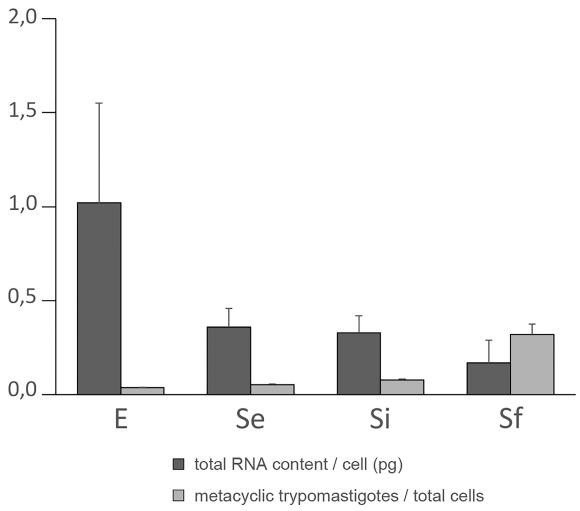

FIGURE 1
Total RNA content/cell and percentage of metacyclic trypomastigote during prolonged cultures of *T. cruzi* epimastigotes. Total RNA content/cell (pg) and % of metacyclic trypomastigotes of the parasite population of three independent biological replicates for each of the selected points of the epimastigote long-lasting growth curve: exponentially phase (E) and early, intermediate, and final stationary phase (Se, Si, and Sf respectively). Standard errors are indicated.

The increase in metacyclic trypomastigotes in the parasite populations may contribute to some extent to the observed changes in total RNA content per cell particularly for the final stationary phase (Sf). Meanwhile, a constant value expanding from the early to the intermediate stationary phase (Se to Si), clearly different from the exponentially growing parasite populations (E), was observed along the *T. cruzi* culture in nutrient-restricted conditions.

Persistent expression changes are found in starving conditions of *in vitro* cultured *T. cruzi* epimastigotes

RNA-seq analysis of three biological replicates for the parasite populations either in the exponential (E) or stationary phase at the three selected points (Se, Si, and Sf) was performed. Principal component analysis (PCA) of the transcriptomic data groups together the three independent biological replicates of each parasite population (Figure 2A). In addition, the first component, which explains more than 80% of the variation, clearly joins Se and Si and separates them from the exponentially growing epimastigotes (E) and the parasite population at critical nutrient restriction (Sf). This is further supported by the hierarchical cluster analysis of the differentially expressed genes (DEGs, 797 genes Supplementary Table 1), which joins Se and Si despite the gradual profile changes (Figure 2B). Indeed, neither up nor downregulated genes could be detected between Se and Si (log2FC, FDR < 0.05) (Table 1). Nonetheless, the number of differentially expressed transcripts gradually increases when comparing E to the successive stationary phase points analyzed (169, 311, and 691 DEGs for Se, Si, and Sf vs.

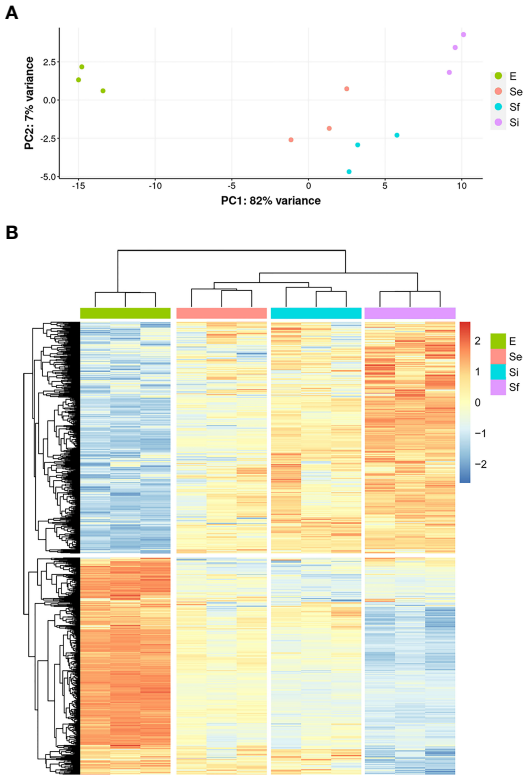

FIGURE 2
Transcriptomic data during prolonged cultures of *T. cruzi* epimastigotes. Analysis of transcriptomic data derived from polyA +RNA of three independent biological replicates of selected parasite population of the epimastigote long-lasting growth curve: exponentially phase (E) and early, intermediate, and final stationary phase (Se, Si, and Sf, respectively). **(A)** Principal Component Analysis of individual replicates. **(B)** Hierarchical clustering of differentially expressed genes.

E, respectively). Besides, a lower number of DEGs is observed when comparing Se or Si to Sf (88 and 77, respectively). A similar number of up and downregulated transcripts were observed within DEGs for the different comparisons.

Since the persistence of a homogeneous transcriptomic core (at least from Se to Si), clearly different from the exponentially growing parasite population (E), may reflect the molecular distinctiveness of *T. cruzi* parasites in prolonged culture conditions, we focused on the analysis of the shared DEGs of Se and Si vs. E (Se⋂Si DEGs). When E was used as reference, a high percentage (approx. 80%) of the Se DEGs were shared with Si (135 out of 169); instead, for Si, the percentage of DEGs shared with Se was lower (43,4%, 135 out of 311) (Figure 3A). Fewer DEGs were found when comparing the common DEGs between Se and Si vs. Sf (Supplementary Table 1). Interestingly, of the 4 possible intersections of the common up or downregulated genes of Se and Si vs E and Sf, only one (intersection of upregulated Se and Si vs E with downregulated Se and Si vs Sf) was not void. Two transcripts, coding for an NLI interacting factor-like phosphatase and a hypothetical protein with homology to cyclin10 (TcCLB.506525.120, TcCLB.503885.100) showed a significant increase in expression from E to Sf. The expression of both proteins is highly upregulated in metacyclic trypomastigotes (13 and 27 times, respectively) (Smircich et al., 2015).

The Se⋂Si DEGs include genes coding for hypothetical proteins whose proportion is similar to that of the whole genome (28%, 38 out of 135 being 19 genes upregulated, 10 conserved and 1 conserved pseudogene, and 19 genes downregulated, 17 conserved). Gene ontology analysis identified a single enriched category in the upregulated Se⋂Si DEGs: trans-sialidase activity 12/32, molecular function ontology, and three enriched categories in the downregulated Se⋂Si DEGs (Figure 3B): vacuole/vesicle 10/60, chromosome 13/60 and kinetoplast (6/60), cellular component ontology, which may be persistently acting under nutritional stress.

In accordance with omics approaches of epimastigotes in the early stationary phase (Santos et al., 2018), surface proteins are well represented among the upregulated Se⋂Si DEGs in our study (33%, 21 out of 63), accompanying the transition to metacyclic trypomastigotes. In addition to the 12 genes and 4 pseudogenes coding for proteins of the trans-sialidase superfamily of genes (TcTSs) identified in the gene ontology analysis (4 in Group II, 2 in Group IV, 3 in Group V, 1 in Group VII and 2 unclassified), 3 genes putatively coding for GP63, one for a mucin associated MASP, and a pseudogene for a type II mucin are also upregulated (Supplementary Table 1). Conversely, only two mucin genes are found among the downregulated Se⋂Si DEGs (TcCLB.506533.142, TcCLB.509147.50, belonging to the subfamily of mucins that are present at the surface of the epimastigote stage (TcSMUGL) [Urban et al., 2011)]. Surface proteins play different roles in the parasite's life cycle progression, host-cell interplay, immune system evasion, and persistence of the parasite (Pech-Canul et al., 2017). To shed light on the development of the infectivity ability, we carried out a deeper analysis of the dynamics of these multi-gene families (TcTS, Mucins and DGFs) together with the analysis of other genes involved in the pathogenesis (to be published elsewhere). In view of the diversity of GO terms downregulated under our conditions, we further analyzed these genes to get insights into the molecular processes modulated.

The Se⋂Si DEGs code for enzymes that are themselves and/or their products involved in various cellular regulatory pathways. Cell organization is based on a complex metabolic network composed of numerous, sometimes redundant, but coordinated routes that grant homeostatic equilibrium. While the subcellular location and roles displayed by the Se⋂Si DEGs in response to nutrient restriction conditions must be investigated, we further analyzed the DEGs included in the major downregulated cellular components revealing potential biological roles.

DEGs related to vacuole/vesicle functionality are found in starving conditions of *in vitro* cultured *T. cruzi* epimastigotes

The Se⋂Si DEGs downregulated in the enriched categories including vacuole and vesicle terms (see Figure 3) code for ten proteins that have been identified as associated with one or more different organelles (Table 2), including 4 (out of 71) associated with reservosome fractions (Sant'Anna et al., 2009) as well as 7 (out of 107) associated to the contractile vacuole fraction (Ulrich et al., 2011).

TABLE 1 Number of significant up/downregulated genes at each analyzed time point.

	E	Se	Si	Sf
E		79	170	363
Se	90		0	53
Si	141	0		18
Sf	328	35	59	

The number of significantly up (above diagonal) or down (below diagonal) regulated genes at each of the stationary phase selected points: early (Se), intermediate (Si) and final stationary phase (Sf) is shown. The IDs of these differentially expressed genes are presented in Supplementary Table S1.

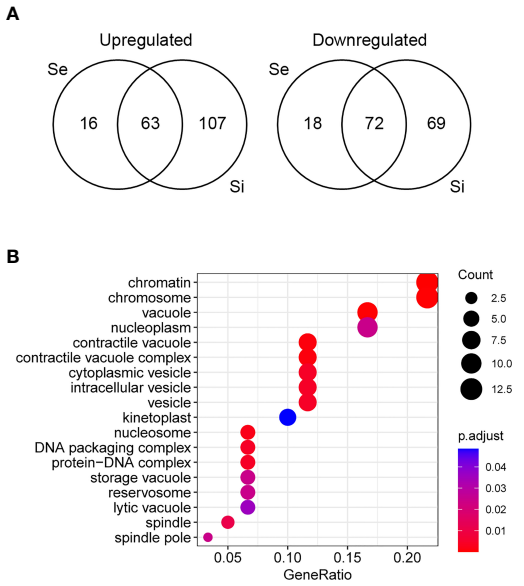

FIGURE 3
Analysis of differentially expressed genes of *T. cruzi* epimastigotes during prolonged cultures. The identified DEGs of early and intermediate stationary phase (Se and Si, respectively) in comparison to exponentially growing epimastigotes (E) were analyzed. **(A)** Venn diagrams. **(B)** Gene ontology analysis of downregulated Se⋂Si vs E DEGs.

Reservosomes are organelles dedicated to storing macromolecules ingested by endocytosis in *T. cruzi* epimastigotes (Soares and De Souza, 1988) that fuel the requirements of energy and amino acid dependence of metacyclogenesis and are not present as such in further developmental stages (Soares and de Souza, 1991; Sant'Anna et al., 2008; Vidal et al., 2017). During metacyclogenesis, increased cruzipain relocation to reservosomes and increased proteolytic activity induced by autophagy have been described (Soares et al., 1989; Alvarez et al., 2008; Vanrell et al., 2017; Losinno et al., 2021). It is worth noting that for the cysteine peptidase (Table 2), in addition to the proteolytic molecular function associated to the reservosomes, a role in the cell cycle and postranscriptional regulation of gene expression has been proposed for the *T. brucei* ortholog (Tb927.6.560) (Archer et al., 2011; Erben et al., 2014). In addition, both cyclophilin A and vacuolar proton pyrophosphatase 1 have been detected associated not only with reservosomes (Table 2) but also with chromatin (Leandro de Jesus et al., 2017). Finally, as its name reveals, this later protein has also been identified in an enriched contractile vacuolar fraction (Ulrich et al., 2011).

Contractile Vacuole Complexes (CVC) are organelles dedicated to regulating cell volume, present in several protists devoid of a cell wall, and are linked to acidocalcisomes, initially described in trypanosomatids but later found in many species (Docampo et al., 2005; Docampo et al., 2013; Jimenez et al., 2022). This compartmentalization constitutes a means to regulate osmotic pressure through cAMP signaling and microtubule-dependent fusion and the intracellular pH through alkalization/acidification, features that have also been implicated in parasite persistence, infection, and survival under starvation conditions (Galizzi et al., 2013; Mantilla et al., 2021). Nonetheless, the CVC is being recognized as a plastic organelle with pleiotropic functions in *T. cruzi*, including not only calcium homeostasis, cell volume and osmo regulation but also the trafficking functions in secretory and endocytic pathways involving the flagellar pocket, acidocalcisomes, mitochondria and the endoplasmic reticulum (Jimenez et al., 2022). Pyruvate phosphate dikinase is well known for its location and role in the ATP/ADP balance in glycosomes (Bringaud et al., 1998). The vacuolar proton pyrophosphatase 1 is one of the main pumps responsible for the acidocalcisomes acidification and may play a similar role in reservosomes. In *T. brucei*, acidification of acidocalcisomes is essential for initiating autophagy (Li and He, 2014), a critical process in metacyclogenesis (Vanrell et al., 2017). Globally these activities, which are preferentially located in these organelles, may modulate the rapid increase in short and long-chain polyPs levels detected during the lag phase of epimastigote growth (Ruiz et al., 2001). Related to cAMP signaling, the upregulated Se⋂Si DEGs of the *T. cruzi* parasites in starving conditions include four putative receptor-type adenylate cyclase (TcCLB.507465.10, TcCLB.507467.10, TcCLB.509267.3, TcCLB.509449.10). The increase in intracellular cAMP concomitantly with the upregulation of adenylyl cyclases expression (both mRNA and protein) together with their relocalization to the flagellum in response to nutritional stress has been reported (Hamedi et al., 2015). In addition, a serine-threonine protein kinase (TcCLB.510741.70) is also upregulated. Serine-threonine kinases are a group of enzymes that play crucial roles in cellular proliferation and differentiation (Orr et al., 2000) and are considered the major effectors of cAMP in eukaryotic cells (Lander et al., 2021). Conversely, the expression of a putative protein kinase (TcCLB.507837.20) is downregulated. Protein phosphorylation plays a significant role in cell signaling, gene expression, differentiation, and global control of DNA/RNA-mediated processes.

It is worth mentioning the presence of inositol-3-phosphate (IP3) synthase (TcCLB.503639.10) among the downregulated DEGs, despite not being detected in the enriched contractile vacuole fraction (Ulrich et al., 2011). Its product, IP3, plays a role in calcium homeostasis and osmoregulation of acidocalcisomes

TABLE 2 Downregulated Se∩Si DEGs in the enriched categories including vacuole and vesicle terms.

GeneID	Gene product	Product location
TcCLB.503893.30	hypothetical protein, conserved	CVC*
TcCLB.506893.100	UMP-CMP kinase, mitochondrial, putative	CVC*
TcCLB.506925.300	cyclophilin a, putative	Reservosomes*
TcCLB.508209.100	10 kDa heat shock protein, putative	CVC*
TcCLB.508719.30	hypothetical protein, conserved	CVC*
TcCLB.509445.10	tryparedoxin peroxidase, putative	Reservosomes*
TcCLB.509551.30	mitochondrial phosphate transporter, putative	CVC*
TcCLB.510101.140	pyruvate phosphate dikinase, putative	CVC*
TcCLB.510535.100	cysteine peptidase C (CPC), putative	Reservosomes*
TcCLB.510773.20	Vacuolar proton pyrophosphatase 1, putative	Reservosomes*, CVC*

The protein products have been identified as associated with one or more different organelles including reservosome fractions (Reservosomes*) (Sant'Anna et al., 2009) and contractile vacuole fraction (CVC*) (Ulrich et al., 2011).

(Docampo and Huang, 2015). In addition, IP3 is involved either in surface protein synthesis and also regulation in *T. brucei*(Cestari, 2020; Cestari and Stuart, 2020) and carbon metabolism, which, together with the downregulated phosphomannose isomerase (TcCLB.503677.10), lies at the beginning of the major pathway, either modulating the contribution of the glucose 6-phosphate to all the inositol containing compounds, or the fructose 6-phosphate to all the mannose containing compounds. Similarly, the gene coding for the mevalonate-diphosphate decarboxylase (TcCLB.507993.330) is also downregulated. The mevalonate pathway is highly conserved and mediates the production of metabolites vital for cellular metabolism, growth, and differentiation, such as isoprenoids, which feed into biosynthetic pathways for sterols, dolichol, ubiquinone, heme, isopentenyl adenine, and prenylated proteins (Goldstein and Brown, 1990).

Acidocalcisomes also contain large amounts of amino acids, four times more concentrated than the whole cell, with 90% arginine and lysine likely as free amino acids and are not involved in the amino acid mechanism of volume regulation (Rohloff et al., 2003). Two genes putatively encoding enzymes involved in arginine metabolism: an amidinotransferase (TcCLB.505989.110) and an S-adenosylhomocysteine hydrolase, SAHH, (TcCLB.511589.200) are downregulated Se⋂Si DEGs. They may be acting to preserve arginine levels, which are similar in epimastigotes in exponential and stationary phases (Barisón et al., 2017). Another gene related to tyrosine metabolism: 2,4-dihydroxyhept-2-ene-1,7-dioic acid aldolase (TcCLB.503991.39), is also a downregulated Se⋂Si DEG. These DEGs plus the downregulated gene putatively coding for cytosolic malate dehydrogenase (TcCLB.506937.10) and the upregulation of several genes coding for amino acid permeases and transporters (5 putative permeases and one transporter (TcCLB.508923.10, TcCLB.511325.40, TcCLB.507811.100, TcCLB.511325.50, TcCLB.507101.10, TcCLB.511325.25) describe a global profile coinciding with the starvation-induced metabolic switch from glucose to amino acid consumption previously reported (Barisón et al., 2017). A wide range of biological functions has been proposed for cell or intracellular membrane transport proteins of kinetoplastids, establishing physiological properties such as membrane potential and responses to osmolarity, and in sensing and responding to changes in the environment (Landfear, 2019).

Related to autophagy, which has been involved in parasite survival during starvation and differentiation (Alvarez et al., 2008), the upregulation of a putative microtubule-associated protein 1A/1B light chain 3 (TcCLB.510533.180), a ubiquitin-like modifier involved in formation of vacuoles for autophagy was found. Nonetheless, we found the downregulation of a gene coding for a tubulin chaperone (tubulin binding cofactor A-like protein putative, TcCLB.509069.30) specific for the tight association of the alpha- and beta-tubulin subunits, as well as two genes for proteasome activator protein pa26, putative (TcCLB.503841.10, TcCLB.511001.240), with functional similarities to the eukaryotic PA28, a family of proteasome regulators whose members have controversial effects in promoting cellular growth and progression through the cell cycle. Their levels correlate with increased susceptibility to apoptosis, nuclear structure, and organization and effective DNA damage response, but specific functions in the context of adaptive cellular responses require further investigation (Cascio, 2021).

Interestingly, the gene coding for a protein 12 of the flagellum attachment zone (FAZ) (TcCLB.504153.260) is upregulated. FAZ is a morphogenetic structure with crucial regulatory roles in cell length and organelle positioning (Sunter and Gull, 2016) and its modulation has been involved in a variety of intermediate morphologies found under starvation conditions (Gonçalves et al., 2018).

In summary, long-term culture of *T. cruzi* epimastigotes without nutrient addition triggers the regulation of transcripts involved in specific vacuole/vesicle functionality, describing a complex metabolic network enabling the adaptation to the starving conditions while modulating the metacyclogenesis process.

Starving conditions provoke expression changes of genes coding for proteins involved in the DNA/RNA functionality of *in vitro* cultured *T. cruzi* epimastigotes

The downregulated Se⋂Si DEGs in the chromatin/chromosome category (see Figure 3B) code for thirteen proteins that have been identified in a chromatin proteomic approach (Leandro de Jesus et al., 2017) (13 out of 60).

Four of these 13 genes are included in the category nucleosome/DNA packaging/protein-DNA complex. In addition, we find other 8 genes putatively coding for proteins related to this category, that were not identified using the above-mentioned chromatin approach. They include genes coding for a histone modification enzyme (Histone-lysine N-methyltransferase TcCLB.511417.70), a fragment of the retrotransposon hot spot protein (RHS) (TcCLB.511415.11) whose orthologue has been proposed to participate in control of chromatin structure and gene expression (Bernardo et al., 2020), two kinetoplast associated proteins (TcCLB.511039.10 and TcCLB.511529.80) which are involved in kDNA condensation and have been implied in cell proliferation and differentiation (de Souza et al., 2010), a chromosomal passenger complex 2 (TcCLB.506221.110) related to the regulate chromosome segregation and cytokinesis, a PIF1 helicase-like protein (TcCLB.506775.90) crucial for mitochondrial genome maintenance (Bochman et al., 2010; Liu et al., 2010), a DNA ligase (TcCLB.506287.209) and a mitochondrial DNA primase (TcCLB.503831.40).

The *T. brucei* ortholog of the product gene involved in RNA modification (Table 3) has been proposed to be a cytochrome oxidase subunit participating as an accessory factor in specific RNA editing (Sprehe et al., 2010). The other 8 genes (Table 3) code for proteins present in the chromatin proteomic approach and putatively code for proteins either of unknown function or that have been identified for DNA/RNA unrelated functions.

In addition to these 21 genes (13 identified by ontology analysis plus 8 through annotation characteristics), the downregulated Se⋂Si DEGs also include 6 genes related to DNA/RNA functionality: coding for ribosomal proteins (60S ribosomal protein L28, TcCLB.510101.40 and ribosomal protein S29 TcCLB.509201.15) and elongation factor (Elongation factor Tu, mitochondrial, TcCLB.506357.40); a mitochondrial RNA binding protein (TcCLB.510509.50), a poly(A) polymerase (TcCLB.510317.30) and an RNA binding protein (PSP1 C-terminal conserved region, TcCLB.506223.40).

Conversely only 6 of the upregulated Se⋂Si DEGs were found to be related to DNA/RNA functionality, including genes that putatively code for: an RNA binding protein (TcCLB.503683.30), whose ortholog in *T. brucei* has been proposed as an RNA expression modulator participating in the cell cycle (Erben et al., 2014; Lueong et al., 2016; Crozier et al., 2018), mismatch repair protein MSH4 (either a gene TcCLB.509967.20 and a pseudogene TcCLB.511911.30), that has been proposed to be involved in meiotic recombination based on its lack of an N-terminal mismatch interaction indicating the absence of function in the mismatch repair (Passos-Silva et al., 2010) as well as two small nuclear RNAs (snRNA U3, TcCLB.504427.244 and U6, TcCLB.503865.12) components of the spliceosome, which are transcribed by pol III, similarly as vault RNAs and other non-polyadenylated RNAs such as tRNAs, 5S rRNA, 7SL RNA (Kolev et al., 2019) with potential additional roles in regulation of various aspects of RNA biogenesis, from transcription to polyadenylation and RNA stability. Finally, we include in this subgroup the upregulated DEG (TcCLB.506203.10) coding for a nucleoside transporter which provides metabolic precursors for the synthesis of nucleic acids and energy metabolites as ATP and GTP, which are required for parasite viability in all life cycle stages because of the strict dependence on preformed purine salvage (Landfear et al., 2004; Boswell-Casteel and Hays, 2017).

Concordantly with the quiescent status, 20 out of the 135 Se⋂Si DEGs (fisher test p-value < 1e-13) were identified as peaking genes during different phases of the epimastigote cell cycle (Chávez et al., 2017) (Supplementary Figure 1). Only 2 are upregulated: one putatively coding for an amino acid permease (TcCLB.507811.100) and the other for a hypothetical protein (TcCLB.509203.14). The downregulated cell cycle peaking genes include two of the DEGs identified by ontology analysis (TcCLB.507105.50 and TcCLB.508321.21), the 8 DEGs identified by annotation terms, 4 DEGs coding for hypothetical proteins (TcCLB.506567.110, TcCLB.507809.39, TcCLB.506239.10 and TcCLB.507709.120) and 4 PAD (Protein Associated with Differentiation) DEGs putatively coding for proteins involved in different cellular functions: a cytosolic malate dehydrogenase (TcCLB.506937.10), a kinesin (TcCLB.506503.80), a nucleoporin NUP92 (TcCLB.504769.80) and an ESAG8-associated protein (TcCLB.511753.60). ESAG8-associated protein has been suggested to be involved in antigenic variation and development in *T. brucei*, and its ablation is related to the induction of the cell surface transporter PAD1 (Batram et al., 2014). PADs are surface protein markers that discriminate between the transmission stages in *T. brucei* (Dean et al., 2009). Interestingly, among the upregulated Se⋂Si DEGs, we identified PAD8 (TcCLB.509707.10). Most of the downregulated peaking genes (11 out of 18) are from the S phase, which corresponds to the DNA and organelle replication period.

In summary, nutrient depletion of *T. cruzi* epimastigotes triggers the downregulation of transcripts involved in cell proliferation and the control of chromatin structure. Nonetheless, complex regulatory networks that may affect not only the cell replication process but also different steps, such as mRNA maturation and translation, have been described. Interestingly, the up and downregulation of splicing ribonucleic factors may point to specific transcript processing control as previously described for mitochondrial RNA of nutrient-restricted *T. cruzi* epimastigotes (Shaw et al., 2016). The revealed up and downregulation of RNA binding proteins in response to nutrient depletion may account for the existence of active post-transcriptional regulons.

TABLE 3 Downregulated SeᑎSi DEGs in the chromatin/chromosome category.

GeneID	Gene product	Product function
TcCLB.506735.10	mitochondrial processing peptidase alpha subunit, putative	DNA/RNA unrelated functions
TcCLB.506925.300	cyclophilin a, putative	DNA/RNA unrelated functions*
TcCLB.507105.50	hypothetical protein	unknown
TcCLB.507817.18	histone H3, putative	nucleosome/DNA packaging/protein-DNA complex
TcCLB.508321.21	histone H2A, putative	nucleosome/DNA packaging/protein-DNA complex
TcCLB.508675.29	calpain-like cysteine peptidase, putative	DNA/RNA unrelated functions
TcCLB.508719.30	hypothetical protein, conserved	unknown **
TcCLB.509551.30	mitochondrial phosphate transporter, putative	DNA/RNA unrelated functions*
TcCLB.509965.290	p22 protein precursor, putative	RNA modification
TcCLB.510101.140	pyruvate phosphate dikinase, putative	DNA/RNA unrelated functions**
TcCLB.510525.80	histone H2A, putative	nucleosome/DNA packaging/protein-DNA complex
TcCLB.510525.90	histone H2A, putative	nucleosome/DNA packaging/protein-DNA complex
TcCLB.510773.20	Vacuolar proton pyrophosphatase 1, putative	DNA/RNA unrelated functions *,**

The protein products have been identified in chromatin proteomic approaches (Leandro de Jesus et al., 2017). Those also associated with other subcellular locations are indicated: *, reservosome fractions (Sant'Anna et al., 2009) and **, contractile vacuole fraction (Ulrich et al., 2011).

A set of nuclear-encoded mitochondrial transcripts is downregulated in starving conditions of *in vitro* cultured *T. cruzi* epimastigotes

A high percentage of mitochondrial-related genes among the downregulated Se⋂Si DEGs was immediately noted. Thus, it was not surprising that kinetoplast appeared as an enriched term in the ontological analysis (see Figure 3).

In order to obtain a thorough inventory of the mitochondrial-related genes in the Se⋂Si DEGs, we extracted the genes with the term "mitochondria" in the TriTrypDB, mainly expanded by the database of nuclear genes encoding predicted mitochondrial proteins, MiNT, we have previously reported (Becco et al., 2019). We found 28 out of 135 Se⋂Si DEGs upon nutrient restriction code for mitochondrial products (Figure 4A). Most of them (24 out of 28) are downregulated, whereas only four are upregulated. Among the Se⋂Si DEGs, in addition to these 28 DEGs, we noted the presence of a gene coding for a putative NADH-cytochrome b5 reductase (TcCLB.511047.40) which is also downregulated. Interestingly, overexpression of a cytochrome b5 reductase-like protein causes the loss of kinetoplast DNA in *T. brucei* (Motyka et al., 2006).

The downregulation of several nucleus-encoded components of the electron transport chain has been previously reported (Shaw et al., 2016) and is here confirmed (Figure 4B).

The four upregulated Se⋂Si DEGs coding for mitochondrial products include an ascorbate peroxidase (TcCLB.503745.30) that participates in oxidative damage prevention and is associated with the microsomal fraction in *T. cruzi* and is therapeutically exploitable because of its absence in the human host (Wilkinson et al., 2002), a putative DNAJ (TcCLB.508989.60) and two receptor-type adenylate cyclase (TcCLB.509267.3, TcCLB.509449.10).

Meanwhile, among the downregulated Se⋂Si DEGs coding for mitochondrial products, four were identified in the ontology analysis with the cellular component term: vesicle/vacuolar, including the genes coding for the hypothetical protein (TcCLB.503893.30), the mitochondrial UMP-CMP kinase (TcCLB.506893.100), the co-chaperone Hsp 10 (GroES) (TcCLB.508209.100) and the mitochondrial phosphate transporter (TcCLB.509551.30). Summing to this latter function, we identified another DEG coding for a putative mitochondrial cation transporter (TcCLB.509197.39). Besides, five additional genes coding for conserved hypothetical proteins (TcCLB.458015.4, TcCLB.504051.49, TcCLB.506289.30, TcCLB.507083.40 and TcCLB.507105.50) appeared among the downregulated Se⋂Si DEGs coding for mitochondrial products, supporting their involvement in the mitochondrial response to nutrient restriction. With the chaperone function, in addition to the co-chaperone Hsp 10 (GroES), we also found the downregulation of a gene putatively coding for a rotamase (TcCLB.510259.50) (Perrone et al., 2018) and a mitochondrial GrpE (TcCLB.507929.20) which is classically known to help fold proteins newly imported into mitochondria in conjunction with Hsp10 and Hsp60 (Fernandes et al., 2005) and may act in concurrence with DNAJ (Tibbetts et al., 1998). Although the expansion of the DNAJ family in kinetoplastids may support a diversification of roles in cellular homeostasis (Folgueira and Requena, 2007; Urményi et al., 2014), the presence of various components of the DNAJ/GRPE may support their suggested role in mitochondrial DNA maintenance and replication (Týč et al., 2015). As mentioned above, several Se⋂Si downregulated DEGs code for mitochondrial proteins involved in these processes and/or in DNA/RNA functionality (TcCLB.503831.40, TcCLB.506287.209, TcCLB.506357.40, TcCLB.506735.10, TcCLB.506775.90, TcCLB.509965.290, TcCLB.510509.50, TcCLB.511039.10 and TcCLB.511529.80) and in part support the reported effects of

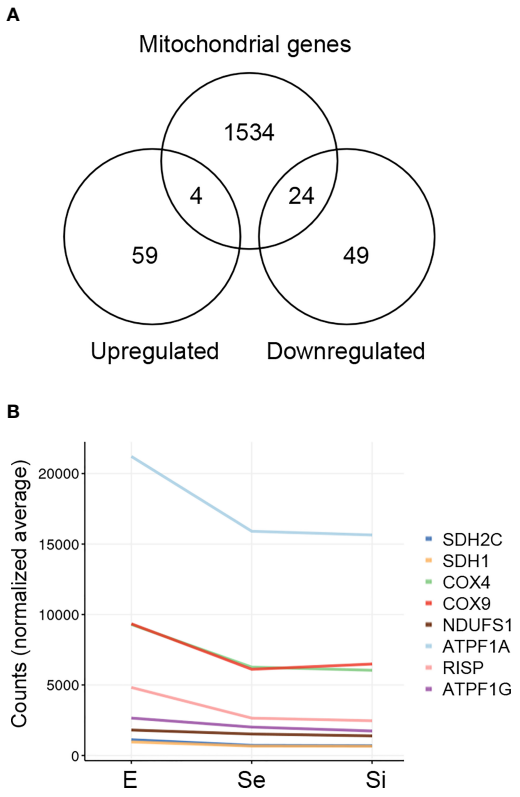

FIGURE 4
Mitochondrion-related DEGs of *T. cruzi* epimastigotes during prolonged cultures. The identified DEGs of early and intermediate stationary phase (Se and Si, respectively) in comparison to exponentially growing epimastigotes (E) were analyzed. **(A)** Venn diagrams comparing the Se⋂Si vs E DEGs with the genes with mitochondria term in TriTrypDB. **(B)** Spaghetti plot of nuclear genes encoding predicted mitochondrial proteins whose expression changes in starving conditions were previously reported (Shaw et al., 2016).

nutrient restriction on the mitochondrion of *T. cruzi* epimastigotes (Shaw et al., 2016; Pedra-Rezende et al., 2021).

Finally, a group of Se⋂Si putatively code for mitochondrial products involved in redox metabolism, including the upregulated ascorbate peroxidase and the downregulated NADH-cytochrome b5 reductase (TcCLB.511047.40) already mentioned, a prostaglandin F synthase reductase (pseudogene, TcCLB.506213.50) and a glutathione-S-transferase/glutaredoxin (TcCLB.508265.10) (Figure 5A). Outside the mitochondrial compartment, the gene putatively coding for the cytosolic malate dehydrogenase mentioned above, and at least three more genes coding for proteins involved in alternative pathways where the reduced form of trypanothione is consumed, are downregulated: a lactoylglutathione lyase-like protein glyoxalase (TcCLB.510743.70) (Sousa Silva et al., 2012), a ribonucleoside-diphosphate reductase small chain (TcCLB.511555.80), and the tryparedoxin peroxidase already presented with the vacuolar term. Globally these findings may indicate an increased role of the ascorbate peroxidase in maintaining the oxidized status of trypanothione while the pathways involved in the detoxification of oxoaldehydes, metals, and drugs in the synthesis of deoxyribonucleotides and decomposition of peroxides are decreased (Figure 5B). Interestingly, we did not find an increase in transcripts for ascorbate peroxidase in metacyclic trypomastigotes (Smircich et al., 2015), suggesting that the upregulation of this enzyme may be a characteristic of the transitional parasites in the early and intermediate stationary phase.

Distinctive gene expression of *T. cruzi* epimastigotes in starving conditions

To identify genes that characterize the transitional forms we searched upregulated Se⋂Si DEGs whose transcriptome values in metacyclic trypomastigote were lower than that of the exponentially growing epimastigotes from our previous data (Smircich et al., 2015); thus, the upregulation cannot be attributable to the metacyclogenesis process. This is the case for the expression profile exhibited by the ascorbate peroxidase (see above). In addition, we looked for the complementary profile, v.g. downregulated Se⋂Si DEGs whose transcriptome values in metacyclic trypomastigote were higher than that of the exponentially growing epimastigotes from our previous data (Smircich et al., 2015); thus, the downregulation cannot be attributable to the metacyclogenesis process.

We found that at least 10 genes can be distinctively attributed to transitional parasite forms enriched by nutrient restriction (Figure 6 and Supplementary Figure 2). In addition to the gene coding for the ascorbate peroxidase, two genes encoding conserved hypothetical proteins are upregulated exclusively during the starvation period (TcCLB.507677.160 and TcCLB.510103.24). Both orthologs have been described as nodulin-like and/or as members of the major facilitator superfamily of transporters (MFS). Nodulins were first described in legumes and are specifically expressed during the development of symbiotic root nodules (Legocki and Verma, 1980). Nonetheless, their importance for the transport of nutrients, solutes, amino acids or hormones, and plant development, even in non-nodulating plants, has been widely recognized (Denancé et al., 2014). Meanwhile, MFS is the largest known superfamily of secondary active transporters, responsible for carrying a broad spectrum of substrates (for a review, see (Drew et al., 2021)). While TcCLB.507677.160 orthologs in *T. brucei* are related to pyruvate transport, an essential pathway in parasite differentiation (Sanchez, 2013), TcCLB.510103.24 is related to proteins associated with PADs which, as previously mentioned, are markers of parasite differentiation in *T. brucei* (Dean et al., 2009). Besides, genes putatively coding for three amino acid permeases (TcCLB.507101.10, TcCLB.508923.10, and TcCLB.511325.40), a protein associated with differentiation PAD8 (TcCLB.509707.10) and a mismatch repair protein MSH4 (TcCLB.509967.20) showed distinctive upregulated expression during the starvation period. On the other hand, two genes encoding a conserved hypothetical protein TcCLB.503697.140, and a poly(A) polymerase, TcCLB.510317.30, are downregulated during the starvation period while upregulated during metacyclogenesis.

Only four of these 10 genes (TcCLB.509967.20, TcCLB.510317.30, TcCLB.507677.160, TcCLB.509707.10) have homologs in the *T. brucei* genome. Members of the families of homologs of two of them (pyruvate transporter TcCLB.507677.160

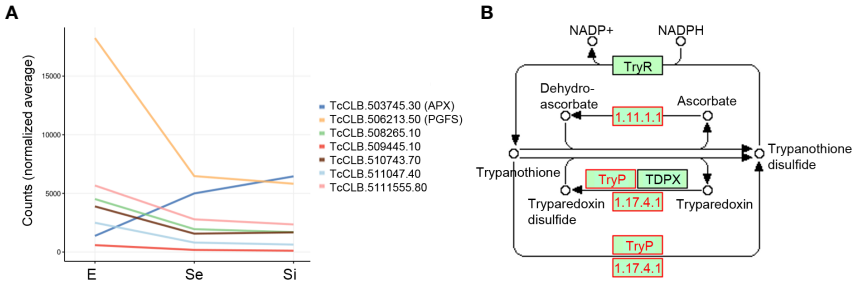

FIGURE 5
Trypanothione metabolism related DEGs of *T. cruzi* epimastigotes during prolonged cultures. Selected DEGs related to trypanothione metabolism of early and intermediate stationary phase (Se and Si respectively) in comparison to exponentially growing epimastigotes (E) were analyzed. **(A)** Gene expression of selected DEGs is presented as a spaghetti plot from Se and Si. TcCLB.503745.30: ascorbate peroxidase, TcCLB.506213.50: prostaglandin F synthase reductase, TcCLB.508265.10: glutathione-S-transferase/glutaredoxin, TcCLB.509445.10: tryparedoxin peroxidase, TcCLB.510743.70: lactoylglutathione lyase-like protein glioxilase, TcCLB.511047.40: NADH-cytochrome b5 reductase, TcCLB.511555.80: ribonucleoside-diphosphate reductase small chain. **(B)** Metabolic chart of the trypanothione reduction pathways indicating the enzymes involved. In red enzymes Ribonucleoside-diphosphate reductase large chain (EC: 1.17.41): TcCLB.506933.20, TcCLB.511555.80, TcCLB.506933.20, TcCLB.511555.80; Tryparedoxin peroxidase (EC:1.11.1.-): TcCLB.509445.10; TcCLB.509445.10; Ascorbate-dependent peroxidase (EC:1.11.1.11): TcCLB.503745.30.

and PAD gene families TcCLB.509707.10) have been proposed as markers of differentiation clusters obtained by single-cell RNA-seq (Briggs et al., 2021; Hutchinson et al., 2021; Howick et al., 2022). The fact that in Leishmania all 10 genes have homologs may suggest more similar differentiation processes in these parasites with intracellular stages. Even though the number of the here-disclosed DEGs is low, they contrast the presumptive progressive transcriptomic changes from epimastigotes to metacyclic trypomastigotes. The set of genes revealed here may be considered as a molecular signature of the transitional parasite form that *T. cruzi* epimastigotes adopt under starvation conditions.

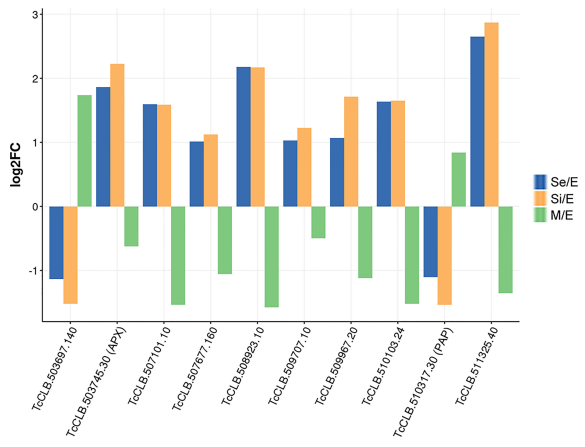

FIGURE 6
DEGs of *T. cruzi* epimastigotes during prolonged cultures with a distinctive expression profile either from exponentially growing epimastigotes or metacyclic trypomastigotes. The expression profile of DEGs of early and intermediate stationary phase (Se and Si, respectively) in comparison to exponentially growing epimastigotes and of DEGs of metacyclic trypomastigotes (M) in comparison to exponentially growing epimastigotes from our previous data (Smircich et al., 2015) were analyzed to identify distinctive expression profile of starving parasites either from epimastigotes or metacyclic trypomastigotes.

Conclusions

Different *in vitro* approaches, resembling the progressively nutrient-restricted environment *T. cruzi* deals with inside the digestive tract of the vector, have contributed to understanding several aspects of the insect-dwelling differentiation process.

Understanding the molecular mechanisms underlying the differentiation process in this unicellular organism that is able to rapidly adapt to several host-changing environments may contribute to shedding light on the complex biological processes that individual cells may display in response to different host stimuli.

Aiming to reveal genes distinctly expressed by *T. cruzi* in the starving periods that the insect host undergoes, we analyzed the transcriptomic changes of epimastigotes maintained in culture for extended periods without media refreshment leading to nutrient restriction. Genes related to surface proteins, the management of protein quality or content, the reported switch from glucose to amino acid consumption and the redox challenge were found to be differentially expressed. Control of the adaptation to nutrients restriction relies on regulated metabolic and molecular processes, including DNA, RNA, and histone modification pathways, which in turn depend on the enzymes that catalyze these modifications as well as in the transport and production of metabolites generated in specific compartments of the cell. Contractile vacuole, and reservosomes appeared as cellular components in the enriched vacuole/vesicle ontology terms, highlighting the relevant roles of these organelles in cell volume, osmoregulation and metabolic homeostasis in starving conditions. Whether these changes are part of a pre-established differentiation program triggered in our conditions or a response to specific stimuli in our culture remains to be studied. Although ontology analysis is biased by the available data, the detailed revision of DEGs further supports the obtained results. Concordantly with the quiescent status derived from nutrient restriction, cell cycle peaking genes were enriched among the Se⋂Si DEGs). In addition, we observed a remarkable number of differentially expressed genes related to the unique parasite mitochondrion, that

may be coordinately acting with intramitochondrial regulation of expression to alleviate the nutritional restriction stress.

Remarkably, some of the differentially expressed genes remain stable in the stationary phase versus exponentially growing epimastigotes and do not follow the expected metacyclogenesis profile. This finding could be considered consistent with the proposed existence of an intermediate stage between epimastigotes and metacyclic trypomastigotes. Particularly, the distinctive expression profiles of genes related to transport and differentiation were revealed. Interestingly, homologous genes in *T. brucei* have been identified as important markers of differentiation in recent scRNA-seq experiments. Similar work on *T. cruzi* facilitated by single-cell approaches may enrich the data presented here.

Comparative transcriptomic approaches performed in parasites obtained from insect hosts during the starvation period may provide further insights. Besides, novel technologies that enable 3D cell cultures to simulate the environment of specific organs, just emerging in the field of trypanosomatids (Sutrave and Richter, 2021), may facilitate the host interaction analysis. Nevertheless, the gene expression changes here presented, triggered and persistently maintained in epimastigotes culture by starvation and associated physicochemical changes may support the existence of a transitional parasite form in *T. cruzi* life cycle between epimastigotes and metacyclic trypomastigotes in the insect host.

Data availability statement

The datasets presented in this study can be found in online repositories. The names of the repository/repositories and accession number(s) can be found below: NCBI, BioProject ID PRJNA915394.

Author contributions

PS and BG conceived aims and strategies. PS, LP-D, MD, and BG designed the experiments. LP-D and FH performed parasite culture and quantification, RNA extraction, and quantification. PS performed the bioinformatic analysis. PS and BG analyzed the data. PS and BG wrote the first draft of the manuscript. All authors contributed to manuscript revision, read, and approved the submitted version.

Funding

This work was supported by CSIC I+D Grupo 108725, UdelaR, and PEDECIBA, Uruguay.

Acknowledgments

We acknowledge all members of the Sección Genómica Funcional at Facultad de Ciencias, UDELAR, and the Departmento de Genómica at IIBCE for constant discussion and technical support. We also thank the colleagues that have provided critical insight into this study.

Conflict of interest

The authors declare that the research was conducted in the absence of any commercial or financial relationships that could be construed as a potential conflict of interest.

Publisher's note

All claims expressed in this article are solely those of the authors and do not necessarily represent those of their affiliated organizations, or those of the publisher, the editors and the reviewers. Any product that may be evaluated in this article, or claim that may be made by its manufacturer, is not guaranteed or endorsed by the publisher.

Supplementary material

The Supplementary Material for this article can be found online at: https://www.frontiersin.org/articles/10.3389/fcimb.2023.1138456/full#supplementary-material

References

Alarcón de Noya, B., Díaz-Bello, Z., Ruiz-Guevara, R., and Noya, O. (2022). 'Chagas disease expands its epidemiological frontiers from rural to urban areas'. *Front. Trop. Dis.* 3. doi: 10.3389/fitd.2022.799009

Alvarez, V. E., Kosec, G., Sant'Anna, C., Turk, V., Cazzulo, J. J., and Turk, B. (2008). 'Autophagy is involved in nutritional stress response and differentiation in *Trypanosoma cruzi*'. *J. Biol. Chem.* 283 (6), 3454–3464. doi: 10.1074/jbc.M708474200

Anders, S., Pyl, P. T., and Huber, W. (2015). 'HTSeq–a Python framework to work with high-throughput sequencing data'. *Bioinformatics* 31 (2), 166–169. doi: 10.1093/bioinformatics/btu638

Archer, S. K., Inchaustegui, D., Queiroz, R., and Clayton, C. (2011). 'The cell cycle regulated transcriptome of *Trypanosoma brucei*'. *PLoS One* 6 (3), e18425. doi: 10.1371/journal.pone.0018425

Avila, C. C., Mule, S. N., Rosa-Fernandes, L., Viner, R., Barisón, M. J., Costa-Martins, A. G., et al. (2018). 'Proteome-wide analysis of *Trypanosoma cruzi* exponential and stationary growth phases reveals a subcellular compartment-specific regulation'. *Genes* 9 (8). doi: 10.3390/genes9080413

Barisón, M. J., Rapado, L. N., Merino, E. F., Furusho Pral, E. M., Mantilla, B. S., Marchese, L., et al. (2017). 'Metabolomic profiling reveals a finely tuned, starvation-induced metabolic switch in *Trypanosoma cruzi* epimastigotes'. *J. Biol. Chem.* 292 (21), 8964–8977. doi: 10.1074/jbc.M117.778522

Batram, C., Jones, N. G., Janzen, C. J., Markert, S. M., and Engstler, M. (2014). 'Expression site attenuation mechanistically links antigenic variation and development in *Trypanosoma brucei*'. *eLife* 3, e02324. doi: 10.7554/eLife.02324.018

Becco, L., Smircich, P., and Garat, B. (2019). 'Conserved motifs in nuclear genes encoding predicted mitochondrial proteins in *Trypanosoma cruzi*'. *PLoS One* 14 (4), e0215160. doi: 10.1371/journal.pone.0215160

Bernardo, W. P., Souza, R. T., Costa-Martins, A. G., Ferreira, E. R., Mortara, R. A., Teixeira, M. M.G., et al. (2020). 'Genomic organization and generation of genetic

variability in the RHS (Retrotransposon hot spot) protein multigene family in'. *Genes* 11 (9). doi: 10.3390/genes11091085

Bochman, M. L., Sabouri, N., and Zakian, V. A. (2010). 'Unwinding the functions of the Pif1 family helicases'. *DNA Repair* 9 (3), 237–249. doi: 10.1016/j.dnarep.2010.01.008

Bolger, A. M., Lohse, M., and Usadel, B. (2014). 'Trimmomatic: a flexible trimmer for illumina sequence data'. *Bioinformatics* 30 (15), 2114–2120. doi: 10.1093/bioinformatics/btu170

Boswell-Casteel, R. C., and Hays, F. A. (2017). 'Equilibrative nucleoside transporters-a review'. *Nucleosides nucleotides Nucleic Acids* 36 (1), 7–30. doi: 10.1080/15257770.2016.1210805

Bozzi, A., Sayed, N., Matsa, E., Sass, G., Neofytou, E., Clemons, K. V., et al. (2019). 'Using human induced pluripotent stem cell-derived cardiomyocytes as a model to study trypanosoma cruzi infection'. *Stem Cell Rep.* 12 (6), 1232–1241. doi: 10.1016/j.stemcr.2019.04.017

Brenière, S. F., Waleckx, E., and Barnabé, C. (2016). 'Over six thousand trypanosoma cruzi strains classified into discrete typing units (DTUs): Attempt at an inventory'. *PLoS Negl. Trop. Dis.* 10 (8), e0004792. doi: 10.1371/journal.pntd.0004792

Breyner, N. M., Hecht, M., Nitz, N., Rose, E., and Carvalho, J. L. (2020). '*In vitro* models for investigation of the host-parasite interface - possible applications in acute chagas disease'. *Acta tropica* 202, 105262. doi: 10.1016/j.actatropica.2019.105262

Briggs, E. M., Rojas, F., McCulloch, R., Matthews, K. R., and Otto, T. D. (2021). 'Single-cell transcriptomic analysis of bloodstream trypanosoma brucei reconstructs cell cycle progression and developmental quorum sensing'. *Nat. Commun.* 12 (1), 5268. doi: 10.1038/s41467-021-25607-2

Bringaud, F., Baltz, D., and Baltz, T. (1998). 'Functional and molecular characterization of a glycosomal PPi-dependent enzyme in trypanosomatids: pyruvate, phosphate dikinase'. *Proc. Natl. Acad. Sci. United States America* 95 (14), 7963–7968. doi: 10.1073/pnas.95.14.7963

Cascio, P. (2021). 'PA28γ: New insights on an ancient proteasome activator'. *Biomolecules* 11 (2). doi: 10.3390/biom11020228

Cassola, A., De Gaudenzi, J. G., and Frasch, A. C. (2007). 'Recruitment of mRNAs to cytoplasmic ribonucleoprotein granules in trypanosomes'. *Mol. Microbiol.* 65 (3), 655–670. doi: 10.1111/j.1365-2958.2007.05833.x

Cestari, I. (2020). 'Phosphoinositide signaling and regulation in *Trypanosoma brucei*: Specialized functions in a protozoan pathogen'. *PLoS Pathog.* 16 (1), e1008167. doi: 10.1371/journal.ppat.1008167

Cestari, I., and Stuart, K. (2020). 'The phosphoinositide regulatory network in *Trypanosoma brucei*: Implications for cell-wide regulation in eukaryotes'. *PLoS Negl. Trop. Dis.* 14 (10), e0008689. doi: 10.1371/journal.pntd.0008689

Chagas, C. (1909). 'Nova tripanozomiaze humana: estudos sobre a morfolojia e o ciclo evolutivo do schizotrypanum cruzi n. gen., n. sp., ajente etiolojico de nova entidade morbida do homem'. *Memórias do Instituto Oswaldo Cruz* 1, 159–218. doi: 10.1590/S0074-02761909000200008

Chávez, S., Eastman, G., Smircich, P., Becco, L. L., Oliveira-Rizzo, C., Fort, R, et al. (2017). 'Transcriptome-wide analysis of the *Trypanosoma cruzi* proliferative cycle identifies the periodically expressed mRNAs and their multiple levels of control'. *PLoS One* 12 (11), e0188441. doi: 10.1371/journal.pone.0188441

Contreras, V. T., Araujo-Jorge, T. C., Bonaldo, M. C., Thomaz, N., Barbosa, H. S., Meirelles de, M. N., et al. (1988). 'Biological aspects of the dm 28c clone of trypanosoma cruzi after metacyclogenesis in chemically defined media'. *Memorias do Instituto Oswaldo Cruz* 83 (1), 123–133. doi: 10.1590/S0074-02761988000100016

Crozier, T. W. M., Tinti, M., Wheeler, R. J., Ly, T., Ferguson, M. A. J., Lamond, A. I., et al. (2018). 'Proteomic analysis of the cell cycle of procylic form *Trypanosoma brucei*'. *Mol. Cell. Proteomics* 17, 1184–1195. doi: 10.1074/mcp.RA118.000650

Cruz-Saavedra, L., Muñoz, M., Patiño, L. H., Vallejo, G. A., Guhl, F., Ramírez, J. D., et al. (2020). 'Slight temperature changes cause rapid transcriptomic responses in trypanosoma cruzi metacyclic trypomastigotes'. *Parasites Vectors* 13 (1), 255. doi: 10.1186/s13071-020-04125-y

da Silva Lara, L., Andrade-Lima, L., Magalhães Calvet, C., Borsoi, J., Lopes Alberto Duque, T., Henriques-Pons, A., et al. (2018). 'Trypanosoma cruzi infection of human induced pluripotent stem cell-derived cardiomyocytes: an *in vitro* model for drug screening for chagas disease'. *Microbes infection / Institut Pasteur* 20 (5), 312–316. doi: 10.1016/j.micinf.2018.03.002

Dean, S., Marchetti, R., Kirk, K., and Matthews, K. R. (2009). 'A surface transporter family conveys the trypanosome differentiation signal'. *Nature* 459 (7244), 213–217. doi: 10.1038/nature07997

Denancé, N., Szurek, B., and Noël, L. D. (2014). 'Emerging functions of nodulin-like proteins in non-nodulating plant species'. *Plant Cell Physiol.* 55 (3), 469–474. doi: 10.1093/pcp/pct198

De Souza, W., and Barrias, E. S. (2020). 'May the epimastigote form of *Trypanosoma cruzi* be infective?'. *Acta tropica* 212, 105688. doi: 10.1016/j.actatropica.2020.105688

de Souza, F. S. P., Rampazzo de, R. C. P., Manhaes, L., Soares, M. J., Cavalcanti, D. P., Krieger, M. A., et al. (2010). 'Knockout of the gene encoding the kinetoplast-associated protein 3 (KAP3) in *Trypanosoma cruzi*: effect on kinetoplast organization, cell proliferation and differentiation'. *Mol. Biochem. Parasitol.* 172 (2), 90–98. doi: 10.1016/j.molbiopara.2010.03.014

Díaz-Albiter, H. M., Ferreira, T. N., Costa, S. G., Rivas, G. B., Gumiel, M., Cavalcante, D. R., et al. (2016). 'Everybody loves sugar: first report of plant feeding in triatomines'. *Parasites Vectors* 9, 114. doi: 10.1186/s13071-016-1401-0

Docampo, R., de Souza, W., Miranda, K., Rohloff, P., and Moreno, S. N.J. (2005). 'Acidocalcisomes - conserved from bacteria to man', nature reviews. *Microbiology* 3 (3), 251–261. doi: 10.1038/nrmicro1097

Docampo, R., Jimenez, V., Lander, N., Li, Z.-H., and Niyogi, S. (2013). 'New insights into roles of acidocalcisomes and contractile vacuole complex in osmoregulation in protists'. *Int. Rev. Cell Mol. Biol.* 305, 69–113. doi: 10.1016/B978-0-12-407695-2.00002-0

Docampo, R., and Huang, G. (2015). 'Calcium signaling in trypanosomatid parasites'. *Cell calcium* 57 (3), 194–202. doi: 10.1016/j.ceca.2014.10.015

Drew, D., North, R. A., Nagarathinam, K., and Tanabe, M. (2021). 'Structures and general transport mechanisms by the major facilitator superfamily (MFS)'. *Chem. Rev.* 121 (9), 5289–5335. doi: 10.1021/acs.chemrev.0c00983

Erben, E. D., Fadda, A., Lueong, S., Hoheisel, J. D., and Clayton, C. (2014). 'A genome-wide tethering screen reveals novel potential post-transcriptional regulators in *Trypanosoma brucei*'. *PLoS Pathog.* 10 (6), e1004178. doi: 10.1371/journal.ppat.1004178

Fernandes, M., Silva, R., Rössle, S. C., Bisch, P. M., Rondinelli, E., and Urményi, T. P. (2005). 'Gene characterization and predicted protein structure of the mitochondrial chaperonin HSP10 of *Trypanosoma cruzi*'. *Gene* 349, 135–142. doi: 10.1016/j.gene.2004.11.047

Folgueira, C., and Requena, J. M. (2007). 'A postgenomic view of the heat shock proteins in kinetoplastids'. *FEMS Microbiol. Rev.* 31 (4), 359–377. doi: 10.1111/j.1574-6976.2007.00069.x

Galizzi, M., Bustamante, J. M., Fang, J., Miranda, K., Soares Medeiros, L. C., Tarleton, R. L., et al. (2013). 'Evidence for the role of vacuolar soluble pyrophosphatase and inorganic polyphosphate in *Trypanosoma cruzi* persistence'. *Mol. Microbiol.* 90 (4), 699–715. doi: 10.1111/mmi.12392

Gerasimov, E. S., Ramirez-Barrios, R., Yurchenko, V., and Zimmer, S. L. (2022). 'strain and starvation-driven mitochondrial RNA editing and transcriptome variability'. *RNA* 28 (7), 993–1012. doi: 10.1261/rna.079088.121

Goldstein, J. L., and Brown, M. S. (1990). 'Regulation of the mevalonate pathway'. *Nature* 343 (6257), 425–430. doi: 10.1038/343425a0

Gonçalves, C. S., Ávila, A. R., de Souza, W., Motta, M. C.M., and Cavalcanti, D. P. (2018). 'Revisiting the *Trypanosoma cruzi* metacyclogenesis: morphological and ultrastructural analyses during cell differentiation'. *Parasites Vectors* 11 (1), 83. doi: 10.1186/s13071-018-2664-4

Hamedi, A., Botelho, L., Britto, C., Fragoso, S. P., Umaki, A. C.S., and Goldenberg, S. (2015). '*In vitro* metacyclogenesis of *Trypanosoma cruzi* induced by starvation correlates with a transient adenylyl cyclase stimulation as well as with a constitutive upregulation of adenylyl cyclase expression'. *Mol. Biochem. Parasitol.* 200 (1-2), 9–18. doi: 10.1016/j.molbiopara.2015.04.002

Hernández, R., Cevallos, A. M., Nepomuceno-Mejía, T., and López-Villaseñor, I. (2012). 'Stationary phase in *Trypanosoma cruzi* epimastigotes as a preadaptive stage for metacyclogenesis'. *Parasitol. Res.* 111 (2), 509–514. doi: 10.1007/s00436-012-2974-y

Holetz, F. B., Correa, A., Avila, A. R., Nakamura, C. V., Krieger, M. A., Goldenberg, S., et al. (2007). 'Evidence of p-body-like structures in *Trypanosoma cruzi*'. *Biochem. Biophys. Res. Commun.* 356 (4), 1062–1067. doi: 10.1016/j.bbrc.2007.03.104

Howick, V. M., Peacock, L., Kay, C., Collett, C., Gibson, W., and Lawniczak, M. K.N. (2022). 'Single-cell transcriptomics reveals expression profiles of *Trypanosoma brucei* sexual stages'. *PLoS Pathog.* 18 (3), e1010346. doi: 10.1371/journal.ppat.1010346

Hutchinson, S., Foulon, S., Crouzols, A., Menafra, R., Rotureau, B., Griffiths, A. D., et al. (2021). 'The establishment of variant surface glycoprotein monoallelic expression revealed by single-cell RNA-seq of *Trypanosoma brucei* in the tsetse fly salivary glands'. *PLoS Pathog.* 17 (9), e1009904. doi: 10.1371/journal.ppat.1009904

Jimenez, V., Paredes, R., Sosa, M. A., and Galanti, N. (2008). 'Natural programmed cell death in t. cruzi epimastigotes maintained in axenic cultures'. *J. Cell. Biochem.* 105 (3), 688–698. doi: 10.1002/jcb.21864

Jimenez, V., Miranda, K., and Augusto, I. (2022). 'The old and the new about the contractile vacuole of *Trypanosoma cruzi*'. *J. eukaryotic Microbiol.* 69, e12939. doi: 10.1111/jeu.12939

Kolev, N. G., Rajan, K. S., Tycowski, K. T., Toh, J. Y., Shi, H., Lei, Y., et al. (2019). 'The vault RNA of plays a role in the production of -spliced mRNA'. *J. Biol. Chem.* 294 (43), 15559–15574. doi: 10.1074/jbc.RA119.008580

Kollien, A. H., and Schaub, G. A. (1998). 'The development of *Trypanosoma cruzi* (Trypanosomatidae) in the reduviid bug triatoma infestans (Insecta): influence of starvation'. *J. eukaryotic Microbiol.* 45 (1), 59–63. doi: 10.1111/j.1550-7408.1998.tb05070.x

Kollien, A. H., and Schaub, G. A. (2000). 'The development of *Trypanosoma cruzi* in triatominae'. *Parasitol. Today* 16 (9), 381–387. doi: 10.1016/S0169-4758(00)01724-5

Lander, N., Chiurillo, M. A., and Docampo, R. (2021). 'Signaling pathways involved in environmental sensing in *Trypanosoma cruzi*'. *Mol. Microbiol.* 115 (5), 819–828. doi: 10.1111/mmi.14621

Landfear, S. M. (2019). 'Protean permeases: Diverse roles for membrane transport proteins in kinetoplastid protozoa'. *Mol. Biochem. Parasitol.* 227, 39–46. doi: 10.1016/j.molbiopara.2018.12.006

Landfear, S. M., Chiurillo, M. A., and Docampo, R. (2004). 'Nucleoside and nucleobase transporters in parasitic protozoa'. *Eukaryotic Cell* 3 (2), 245–254. doi: 10.1128/EC.3.2.245-254.2004

Langmead, B., and Salzberg, S. L. (2012). 'Fast gapped-read alignment with bowtie 2'. *Nat. Methods* 9 (4), 357–359. doi: 10.1038/nmeth.1923

Leandro de Jesus, T. C., Calderano, S. G., Vitorino de, F. N.L., Llanos, R. P., Lopes de, M. C., de Araújo, C. B., et al. (2017). 'Quantitative proteomic analysis of replicative and nonreplicative forms reveals important insights into chromatin biology of *Trypanosoma cruzi*'. *Mol. Cell. proteomics: MCP* 16 (1), 23–38. doi: 10.1074/mcp.M116.061200

Legocki, R. P., and Verma, D. P. (1980). 'Identification of "nodule-specific" host proteins (nodoulins) involved in the development of rhizobium-legume symbiosis'. *Cell* 20 (1), 153–163. doi: 10.1016/0092-8674(80)90243-3

Li, Z.-H., Alvarez, V. E., De Gaudenzi, J. G., Sant'Anna, C., Frasch, A. C.C., Cazzulo, J. J., et al. (2011). 'Hyperosmotic stress induces aquaporin-dependent cell shrinkage, polyphosphate synthesis, amino acid accumulation, and global gene expression changes in trypanosoma cruzi'. *J. Biol. Chem.* 286 (51), 43959–43971. doi: 10.1074/jbc.M111.311530

Li, F.-J., and He, C. Y. (2014). 'Acidocalcisome is required for autophagy in *Trypanosoma brucei*'. *Autophagy* 10 (11), 1978–1988. doi: 10.4161/auto.36183

Liu, B., Yildirir, G., Wang, J., Tolun, G., Griffith, J. D., Englund, P. T., et al. (2010). 'TbPIF1, a *Trypanosoma brucei* mitochondrial DNA helicase, is essential for kinetoplast minicircle replication'. *J. Biol. Chem.* 285 (10), 7056–7066. doi: 10.1074/jbc.M109.084038

Losinno, A. D., Martínez, S. J., Labriola, C. A., Carrillo, C., and Romano, P. S. (2021). 'Induction of autophagy increases the proteolytic activity of reservosomes during metacyclogenesis'. *Autophagy* 17 (2), 439–456. doi: 10.1080/15548627.2020.1720428

Love, M. I., Huber, W., and Anders, S. (2014). 'Moderated estimation of fold change and dispersion for RNA-seq data with DESeq2'. *Genome Biol.* 15 (12), 550. doi: 10.1186/s13059-014-0550-8

Lueong, S., Merce, C., Fischer, B., Hoheisel, J. D., and Erben, E. D. (2016). 'Gene expression regulatory networks in *Trypanosoma brucei*: insights into the role of the mRNA-binding proteome'. *Mol. Microbiol.* 100 (3), 457–471. doi: 10.1111/mmi.13328

Mantilla, B. S., Azevedo, C., Denny, P. W., Saiardi, A., and Docampo, R. (2021). 'The histidine ammonia lyase of *Trypanosoma cruzi* is involved in acidocalcisome alkalinization and is essential for survival under starvation conditions'. *mBio* 12 (6), e0198121. doi: 10.1128/mBio.01981-21

Motyka, S. A., Drew, M. E., Yildirir, G., and Englund, P. T. (2006). 'Overexpression of a cytochrome b5 reductase-like protein causes kinetoplast DNA loss in *Trypanosoma brucei*'. *J. Biol. Chem.* 281 (27), 18499–18506. doi: 10.1074/jbc.M602880200

Nepomuceno-Mejía, T., Lara-Martínez, R., Cevallos, A. M., López-Villaseñor, I., Jiménez-García, L. F., Hernández, R., et al. (2010). 'The *Trypanosoma cruzi* nucleolus: a morphometrical analysis of cultured epimastigotes in the exponential and stationary phases'. *FEMS Microbiol. Lett.* 313 (1), 41–46. doi: 10.1111/j.1574-6968.2010.02117.x

Noireau, F., Diosque, P., and Jansen, A. M. (2009). 'Trypanosoma cruzi: adaptation to its vectors and its hosts'. *Veterinary Res.* 40 (2), 26. doi: 10.1051/vetres/2009009

Orr, G. A., Werner, C., Xu, J., Bennett, M., Weiss, L. M., Takvorkan, P., et al. (2000). 'Identification of novel serine/threonine protein phosphatases in *Trypanosoma cruzi*: a potential role in control of cytokinesis and morphology'. *Infection Immun.* 68 (3), 1350–1358. doi: 10.1128/IAI.68.3.1350-1358.2000

Paes, M. C., Saraiva, F. M.S., Nogueira, N. P., Vieira, C. S.D., Dias, F. A., Rossini, A., et al. (2020). 'Gene expression profiling of trypanosoma cruzi in the presence of heme points to glycosomal metabolic adaptation of epimastigotes inside the vector'. *PLoS Negl. Trop. Dis.* 14 (1), e0007945. doi: 10.1371/journal.pntd.0007945

Pance, A. (2021). The stem cell revolution revealing protozoan parasites' secrets and paving the way towards vaccine development. *Vaccines* 9 (2). doi: 10.3390/vaccines9020105

Passos-Silva, D. G., Rajão, M. A., Nascimento de Aguiar, P. H., Vieira-da-Rocha, J. P., Machado, C. R., Furtado, C., et al. (2010). 'Overview of DNA repair in *Trypanosoma cruzi*, *Trypanosoma brucei*, and leishmania major'. *J. Nucleic Acids* 2010, 840768. doi: 10.4061/2010/840768

Pastro, L., Smircich, P., Di Paolo, A., Becco, L., Duhagon, M. A., Sotelo-Silveira, J., et al. (2017). 'Nuclear compartmentalization contributes to stage-specific gene expression control in'. *Front. Cell Dev. Biol.* 5, 8. doi: 10.3389/fcell.2017.00008

Pech-Canul, Á., de la, C., Monteón, V., and Solis-Oviedo, R.-L. (2017). 'A brief view of the surface membrane proteins from'. *J. Parasitol. Res.* 2017, 3751403. doi: 10.1155/2017/3751403

Pedra-Rezende, Y., Fernandes, M. C., Mesquita-Rodrigues, C., Stiebler, R., Bombaça, A. C.S., Pinho, N., et al. (2021). 'Starvation and pH stress conditions induced mitochondrial dysfunction, ROS production and autophagy in *Trypanosoma cruzi* epimastigotes'. *Biochim. Biophys. Acta Mol. Basis Dis.* 1867 (2), 166028. doi: 10.1016/j.bbadis.2020.166028

Perrone, A. E., Milduberger, N., Fuchs, A. G., Bustos, P. L., and Bua, J. (2018). A functional analysis of the cyclophilin repertoire in the protozoan parasite. *Biomolecules* 8 (4). doi: 10.3390/biom8040132

Rohloff, P., Rodrigues, C. O., and Docampo, R. (2003). 'Regulatory volume decrease in *Trypanosoma cruzi* involves amino acid efflux and changes in intracellular calcium'. *Mol. Biochem. Parasitol.* 126 (2), 219–230. doi: 10.1016/S0166-6851(02)00277-3

Ruiz, F. A., Rodrigues, C. O., and Docampo, R. (2001). 'Rapid changes in polyphosphate content within acidocalcisomes in response to cell growth, differentiation, and environmental stress in *Trypanosoma cruzi*'. *J. Biol. Chem.* 276 (28), 26114–26121. doi: 10.1074/jbc.M102402200

Sanchez, M. A. (2013). 'Molecular identification and characterization of an essential pyruvate transporter from *Trypanosoma brucei*'. *J. Biol. Chem.* 288 (20), 14428–14437. doi: 10.1074/jbc.M113.473157

Sant'Anna, C., Parussini, F., Lourenço, D., de Souza, W., Cazzulo, J. J., Cunha-e-Silva, N. L, et al. (2008). 'All *Trypanosoma cruzi* developmental forms present lysosome-related organelles'. *Histochem. Cell Biol.* 130 (6), 1187–1198. doi: 10.1007/s00418-008-0486-8

Sant'Anna, C., Nakayasu, E. S., Pereira, M. G., Lourenço, D., de Souza, W., Almeida, I. C., et al. (2009). 'Subcellular proteomics of *Trypanosoma cruzi* reservosomes'. *Proteomics* 9 (7), 1782–1794. doi: 10.1002/pmic.200800730

Santos, C. M. B. D., Ludwig, A., Kessler, R. L., Rampazzo de, R. C.P., Inoue, A. H., Krieger, M. A., et al. (2018). '*Trypanosoma cruzi* transcriptome during axenic epimastigote growth curve'. *Memorias do Instituto Oswaldo Cruz* 113 (5), e170404. doi: 10.1590/0074-02760170404

Sass, G., Madigan, R. T., Joubert, L.-M., Bozzi, A., Sayed, N., Wu, J. C., et al. (2019a). 'A combination of itraconazole and amiodarone is highly effective against infection of human stem cell-derived cardiomyocytes'. *Am. J. Trop. Med. hygiene* 101 (2), 383–391. doi: 10.4269/ajtmh.19-0023

Sass, G., Tsamo, A. T., Chounda, G. A.M., Nangmo, P. K., Sayed, N., Bozzi, A., et al. (2019b). 'Vismione b interferes with infection of vero cells and human stem cell-derived cardiomyocytes'. *Am. J. Trop. Med. hygiene* 101 (6), 1359–1368. doi: 10.4269/ajtmh.19-0350

Shaw, A. K., Kalem, M. C., and Zimmer, S. L. (2016). Mitochondrial gene expression is responsive to starvation stress and developmental transition in *Trypanosoma cruzi*. *mSphere* 1 (2). doi: 10.1128/mSphere.00051-16

Smircich, P., Eastman, G., Bispo, S., Duhagon, M. A., Guerra-Slompo, E. P., Garat, B., et al. (2015). 'Ribosome profiling reveals translation control as a key mechanism generating differential gene expression in *Trypanosoma cruzi*'. *BMC Genomics* 16, 443. doi: 10.1186/s12864-015-1563-8

Soares, M. J., and De Souza, W. (1988). 'Cytoplasmic organelles of trypanosomatids: a cytochemical and stereological study'. *J. submicroscopic cytology Pathol.* 20 (2), 349–361.

Soares, M. J., and de Souza, W. (1991). 'Endocytosis of gold-labeled proteins and LDL by *Trypanosoma cruzi*'. *Parasitol. Res.* 77 (6), 461–468. doi: 10.1007/BF00928410

Soares, M. J., Souto-Padrón, T., Bonaldo, M. C., Goldenberg, S., and de Souza, W. (1989). 'A stereological study of the differentiation process in*Trypanosoma cruzi*'. *Parasitol. Res.* 75, 522–527. doi: 10.1007/bf00931160

Sousa Silva, M., Ferreira, A. E.N., Gomes, R., Tomás, A. M., Ponces Freire, A., Cordeiro, C., et al. (2012). 'The glyoxalase pathway in protozoan parasites'. *Int. J. Med. microbiology: IJMM* 302 (4-5), 225–229. doi: 10.1016/j.ijmm.2012.07.005

Sprehe, M., Fisk, J. C., McEvoy, S. M., Read, L. K., and Schumacher, M. A. (2010). 'Structure of the *Trypanosoma brucei* p22 protein, a cytochrome oxidase subunit II-specific RNA-editing accessory factor'. *J. Biol. Chem.* 285 (24), 18899–18908. doi: 10.1074/jbc.M109.066597

Sterkel, M., Oliveira, J. H.M., Bottino-Rojas, V., Paiva-Silva, G. O., and Oliveira, P. L. (2017). 'The dose makes the poison: Nutritional overload determines the life traits of blood-feeding arthropods'. *Trends Parasitol.* 33 (8), 633–644. doi: 10.1016/j.pt.2017.04.008

Sunter, J. D., and Gull, K. (2016). 'The flagellum attachment zone: "The cellular ruler" of trypanosome morphology'. *Trends Parasitol.* 32 (4), 309–324. doi: 10.1016/j.pt.2015.12.010

Sutrave, S., and Richter, M. H. (2021). 'The Truman show for protozoan parasites: A review of *in vitro* cultivation platforms'. *PLoS NTD* 15 (8), e0009668. doi: 10.1371/journal.pntd.0009668

Teotônio, I. M. S. N., Dias, N., Hagström-Bex, L., Nitz, N., Francisco, A. F., Hecht, M., et al. (2019). 'Intestinal microbiota - a modulator of the trypanosoma cruzi-vector-host triad'. *Microbial pathogenesis* 137, 103711. doi: 10.1016/j.micpath.2019.103711

Tibbetts, R. S., Jensen, J. L., Olson, C. L., Wang, F. D., and Engman, D. M. (1998). 'The DnaJ family of protein chaperones in *Trypanosoma cruzi*'. *Mol. Biochem. Parasitol.* 91 (2), 319–326. doi: 10.1016/S0166-6851(97)00214-4

Týč, J., Klingbeil, M. M., and Lukeš, J. (2015). Mitochondrial heat shock protein machinery hsp70/hsp40 is indispensable for proper mitochondrial DNA maintenance and replication. *mBio* 6 (1). doi: 10.1128/mBio.02425-14

Tyler, K. M., and Engman, D. M. (2001). 'The life cycle of *Trypanosoma cruzi* revisited'. *Int. J. Parasitol.* 31 (5-6), 472–481. doi: 10.1016/S0020-7519(01)00153-9

Ulrich, P. N., Jimenez, V., Park, M., Martins, V. P., Atwood, J. 3rd, Moles, K., et al. (2011). 'Identification of contractile vacuole proteins in *Trypanosoma cruzi*'. *PLoS One* 6 (3), e18013. doi: 10.1371/journal.pone.0018013

Urban, I., Santurio, L. B., Chidichimo, A., Yu, H., Chen, X., Mucci, J., et al. (2011). 'Molecular diversity of the *Trypanosoma cruzi* TcSMUG family of mucin genes and proteins'. *Biochem. J.* 438 (2), 303–313. doi: 10.1042/BJ20110683

Urdaneta-Morales, S. (2014). 'Chagas' disease: an emergent urban zoonosis. the caracas valley (Venezuela) as an epidemiological model'. *Front. Public Health* 2, 265. doi: 10.3389/fpubh.2014.00265

Urményi, T. P., Silva, R., and Rondinelli, E. (2014). 'The heat shock proteins of *Trypanosoma cruzi*'. *Sub-cellular Biochem.* 74, 119–135. doi: 10.1007/978-94-007-7305-9_5

Vanrell, M. C., Losinno, A. D., Cueto, J. A., Balcazar, D., Fraccaroli, L. V., Carrillo, C., et al. (2017). 'The regulation of autophagy differentially affects *Trypanosoma cruzi* metacyclogenesis'. *PLoS Negl. Trop. Dis.* 11 (11), e0006049. doi: 10.1371/journal.pntd.0006049

Vidal, J. C., Alcantara, C. D. E. L., Souza, DE W., and Cunha-E-Silva, N. L. (2017). 'Lysosome-like compartments of *Trypanosoma cruzi* trypomastigotes may originate directly from epimastigote reservosomes'. *Parasitology* 144 (6), 841–850. doi: 10.1017/S0031182016002602

Wilkinson, S. R., Obado, S. O., Mauricio, I. L., and Kelly, J. M. (2002). '*Trypanosoma cruzi* expresses a plant-like ascorbate-dependent hemoperoxidase localized to the endoplasmic reticulum'. *Proc. Natl. Acad. Sci. United States America* 99 (21), 13453–13458. doi: 10.1073/pnas.202422899

Wu, T., Hu, E., Xu, S., Chen, M., Guo, P., Dai, Z., et al. (2021). 'clusterProfiler 4.0: A universal enrichment tool for interpreting omics data'. *Innovation (Cambridge (Mass.))* 2 (3), 100141. doi: 10.1016/j.xinn.2021.100141

frontiers | Frontiers in Cellular and Infection Microbiology

TYPE Review
PUBLISHED 26 May 2023
DOI 10.3389/fcimb.2023.1146030

OPEN ACCESS

EDITED BY
Gabriel Rinaldi,
Aberystwyth University, United Kingdom

REVIEWED BY
Alessandra Orfanó,
Yale University, United States
Raquel Godoy,
Fundação Oswaldo Cruz (Fiocruz), Brazil

*CORRESPONDENCE
Elena Gómez-Díaz
elena.gomez@csic.es

SPECIALTY SECTION
This article was submitted to Parasite and Host, a section of the journal Frontiers in Cellular and Infection Microbiology

RECEIVED 16 January 2023
ACCEPTED 04 April 2023
PUBLISHED 26 May 2023

CITATION
Parres-Mercader M, Pance A and Gómez-Díaz E (2023) Novel systems to study vector-pathogen interactions in malaria. *Front. Cell. Infect. Microbiol.* 13:1146030. doi: 10.3389/fcimb.2023.1146030

Novel systems to study vector-pathogen interactions in malaria

Marina Parres-Mercader[1], Alena Pance[2] and Elena Gómez-Díaz[1]*

[1]Instituto de Parasitología y Biomedicina López-Neyra, Consejo Superior de Investigaciones Científicas (IPBLN, CSIC), Granada, Spain, [2]School of Life and Medical Sciences, University of Hertfordshire, Hatfield, United Kingdom

Some parasitic diseases, such as malaria, require two hosts to complete their lifecycle: a human and an insect vector. Although most malaria research has focused on parasite development in the human host, the life cycle within the vector is critical for the propagation of the disease. The mosquito stage of the *Plasmodium* lifecycle represents a major demographic bottleneck, crucial for transmission blocking strategies. Furthermore, it is in the vector, where sexual recombination occurs generating "*de novo*" genetic diversity, which can favor the spread of drug resistance and hinder effective vaccine development. However, understanding of vector-parasite interactions is hampered by the lack of experimental systems that mimic the natural environment while allowing to control and standardize the complexity of the interactions. The breakthrough in stem cell technologies has provided new insights into human-pathogen interactions, but these advances have not been translated into insect models. Here, we review *in vivo* and *in vitro* systems that have been used so far to study malaria in the mosquito. We also highlight the relevance of single-cell technologies to progress understanding of these interactions with higher resolution and depth. Finally, we emphasize the necessity to develop robust and accessible *ex vivo* systems (tissues and organs) to enable investigation of the molecular mechanisms of parasite-vector interactions providing new targets for malaria control.

KEYWORDS

mosquito, Plasmodium, organoids, tissue explant, membrane feeding assay (MFA), *Anopheles*

1 Introduction

Mosquitoes are responsible for the transmission of many life-threatening diseases, causing millions of deaths every year. Malaria is one of the deadliest infectious diseases affecting half of the world's population and causing over half a million deaths per year (WHO, 2022). It is caused by apicomplexan parasites of the *Plasmodium* genus and is transmitted by the bite of a female *Anopheles* mosquito. The parasite survival in the mosquito is necessary for the spread of malaria and is therefore a target for the development of transmission blocking strategies (Yu et al., 2022).

The life cycle of the parasite in the vector begins when a mosquito bites an infected human host and ingests the sexual parasite stages, or gametocytes, along with the blood meal (Figure 1). Gametocytes exposed to the midgut environment are activated, egress from the erythrocytes and differentiate into gametes (Dash et al., 2022). Each male gametocyte divides and generates eight flagellated microgametes in a process called exflagellation. Meanwhile female gametocytes mature and form a single rounded immotile macrogamete. Fertilizations occurs when two gametes fuse resulting in a diploid zygote that initiates meiosis until differentiate into an ookinete (Guttery et al., 2022). This transformation involves several morphological changes that confer the mature ookinete the ability to glide and cross two physical barriers: the peritrophic matrix, secreted by midgut cells after ingestion of a blood meal, and the midgut epithelium. At this point, peritrophic matrix disruption and midgut cell damage triggers the mosquito's immune responses, that results in an important reduction of the parasite population(Simões et al., 2018). Selective forces are very strong, and to survive to this major bottleneck, malaria parasites have developed immune evasion strategies (Inklaar et al., 2022). When the ookinete reaches the basal side of the midgut, it undergoes another morphological change rounding up to form an oocyst. Inside the oocyst, hundreds of sporozoites are produced by mitosis and then released into the mosquito hemocoel. The sporozoites invade the salivary glands(Kojin and Adelman, 2019), waiting to be injected into a new host by the next mosquito bite.

Despite important advances in the identification of the molecular interactions between the parasite and the mosquito (Bennink et al., 2016), we are still far from a complete understanding of the factors and mechanisms that are critical for the development and the survival of the parasite during the sporogonic cycle: gamete mating, zygote formation and recombination, ookinete invasion of the mosquito midgut and immune protection, oocyst multiplication and growth and sporozoite differentiation and activation in the salivary glands (Guttery et al., 2022). Furthermore, the mosquito environment is highly heterogenous from one infection to another, in terms of immune responses, physiology and behavior; depending on the vector species, the mosquito genotype, the type and number of blood meals and the external environment. This variation imposes strong selective constraints favoring phenotypic variation and rapid adaptation in the parasite population (Ruiz and Gómez-Díaz, 2019). How this variation is generated and what are the underlying mechanisms is still unknown.

Contrary to the malaria blood cycle that has been largely studied *in vitro*, the study of the cycle in the vector has been traditionally limited to the experimental infection of the mosquitoes in the laboratory (Blagborough et al., 2013). Although this *in vivo* system recapitulates the natural interactions, it is very heterogenous and complex to scrutinize the regulatory mechanisms and understand the fine detail of key parasite developmental processes like meiosis. Furthermore, since more than half of *Plasmodium* genes are essential for asexual blood-

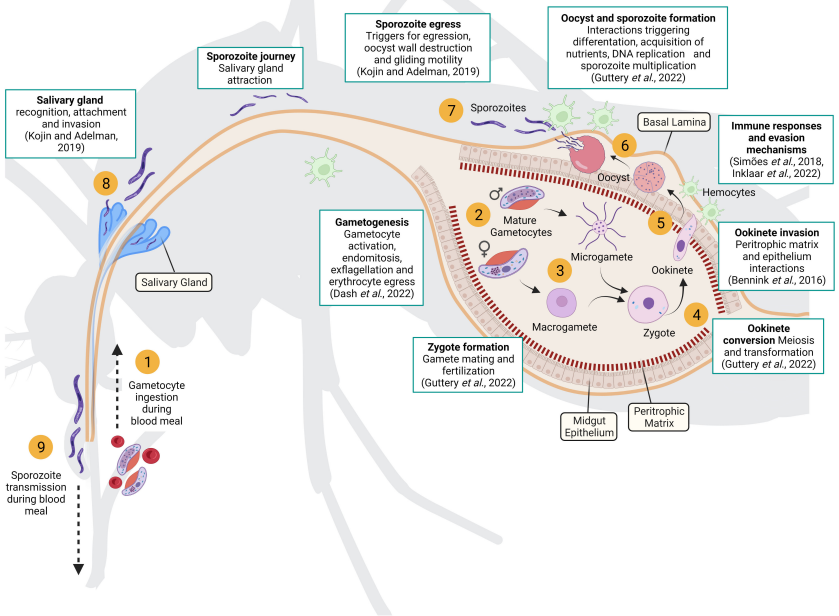

FIGURE 1
Parasite life cycle in the mosquito vector. Gametocytes ingested during a blood meal (1) are activated in the mosquito midgut and differentiated into female and male gametes (2). Fertilization occurs when two gametes fuse (3) resulting in a diploid zygote that initiates meiosis until it differentiates into an ookinete (4). Mature ookinetes can penetrate the peritrophic matrix and midgut epithelium to reach the basal lamina (5), where they develop into oocysts (6). Inside the oocyst, hundreds of sporozoites are produced and then released into the mosquito hemocoel (7). Sporozoites migrate to the salivary glands (8) and are injected by the mosquito into a new host (9). The white boxes highlight key processes underpinning parasite development in the mosquito that require further investigation (recent reviews of each key processes are included). Created with Biorender.com.

stage development or transmission, these cannot be targeted using knockout methods (Bushell et al., 2017; Zhang et al., 2018). Functional genetics studies in *Plasmodium* targeting essential genes rely on generating conditional gene knockdowns. Amongst these, ligand-activated systems are commonly used in erythrocytic stages, but pose the challenge of a precise and controlled delivery of the effector molecule into the mosquito compartment, as well as the potential toxic effects in both organisms (Kudyba et al., 2021). Therefore, a robust, flexible and effective conditional knockdown systems for sporogonic stages is still a major hurdle in the field.

Altogether, there are many unknowns about *Plasmodium* development and adaptation in the mosquito, as well as of the responses of the mosquito to an infection. However, no suitable *in vitro* or *ex vivo* models capable of mimicking the complexity and dynamics of a malaria infection have been developed yet. More generally, this lack of suitable insect study models is generalizable to other pathogens and severely limits our ability to fight vector-borne diseases.

In this contribution we review the different systems (*in vivo*, *in vitro*) that are available to study the parasite life-cycle in the mosquito, highlight the strengths, limitations and recent advances. We contend that the development of novel *ex vivo* mosquito systems, has the potential to advance in our knowledge of pathogen-vector interactions providing novel targets to control the propagation of the disease.

2 The mosquito *in vivo* model

Experimental mosquito infection is widely used in malaria research as it recapitulates the natural infection, allowing the study of parasite development, mosquito responses to the infection as well as their interaction. Despite the many advantages, the heterogeneity and complexity of the organisms involved impose important limitations in terms of scalability, reproducibility and the potential to manipulate the system, which can result in variable performance of the assays, less robust data and a knowledge gap in many research areas (Figure 1). Besides, the infrastructure, material and health and safety considerations for experimental mosquito infections are difficult to establish in many laboratories, and the methodologies are highly time-consuming and laborious.

There are different approaches to infect mosquitoes with disease agents (Table 1), by directly biting an infected host, known as skin feeding assay (SFA), or artificially through a membrane feeding device which contains an infective blood meal, called membrane feeding assay (MFA) (Figures 2A, B). Although the SFA recapitulates better a natural mosquito infection, it has some limitations compared with MFA (Bousema et al., 2013). Apart from ethical restrictions (especially regarding human patients), the number of mosquitoes that can be fed on each infected vertebrate is limited, as is the rearing capacity of animal facilities.

TABLE 1 Systems and strategies used to study mosquito-*Plasmodium* interactions.

Study system	Type	Purpose	Species			References
Experimental mosquito infections	*In vivo*	Transmission blocking assays Parasite life cycle Parasite and mosquito interactions Gene and protein functions related to the infection	Skin Feeding Assay	Any *Plasmodium* species. Mosquitoes feed on an infected host (mainly infected mice with *P.berghei* or *P.yoelii* laboratory strains)	*A.gambaie*, *A.stephensi*, *A.arabiensis*, among others, (laboratory or field-derived)	Blagborough et al., 2013; Bousema et al., 2013; Churcher et al., 2012; Miura et al., 2020
			Direct Membrane Feeding Assay	Any *Plasmodium* species. Gametocytes obtained from an infected host. Mosquitoes feed through a membrane device (*P. falciparum, P. vivax*, among others)		
			Standard Membrane Feeding Assay	Cultivable *Plasmodium* species able to produce gametocytes. Mosquitoes feed through a membrane device (mainly *P. falciparum* laboratory strains and field isolates)		
In vitro culture of Plasmodium mosquito stages	*In vitro*	Culture of *Plasmodium* stages in mosquito	*P. gallinaceum* *P. berghei* *P. yoelii* *P. vivax* *P. falicparum*			Warburg and Miller, 1992; Al-Olayan et al., 2002; Porter-Kelly et al., 2006; McClean et al., 2010; Eappen et al., 2022
Mosquito cell lines culture	*In vitro*	Haemocyte response to *Plasmodium* molecules	None			Akman-Anderson et al.; 2007; Pietri et al., 2015
Polyacrylamide gels	*In vitro*	Ookinete and sporozoite motility	*P. berghei*			Ripp et al., 2021

(Continued)

TABLE 1 Continued

Study system	Type	Purpose	Species	References
Baculovirus expression system in insect cells	*In vitro*	Mosquito-*Plasmodium* protein interactions	*P. falciparum – Anopheles gambiae*	Cui et al., 2020; Niu et al.,2021
Single cell RNA-seq in *Plasmodium*	*In vivo*	Profile the transcriptomics during plasmodium lifecycle in the mosquito	*P. berghei* *P. falciparum*	Howik et al., 2019; Witmer et al., 2021; Real et al., 2021; Mohammed et al., 2023
Single cell RNA-seq in mosquito	*In vivo*	Mosquito immune system in response to blood feeding or infection with *Plasmodium*. Mosquito midguts before and after a blood meal	*Anopheles gambiae – P berghei* *Anopheles gambiae* *Aedes aegypti*	Raddi et al., 2020; Kwon et al., 2021; Cui and Franz, 2020
Explanted midgut	*Ex vivo*	Ookinete locomotion and invasion through the midgut epithelium	*P. gallinaceum – Aedes aegypti* *P. berghei – A. gambiae and A. stephensi*	Zieler and Dvorak 2000; Vlachou et al., 2004

More importantly, there is no control of the gametocyte density in the blood meal or the presence of host serum factors that may interfere with the infection process. A better control of mosquito infection is achieved with MFA, which also allows the use either parasites from infected-hosts (direct membrane feeding assays, DMFA) or *in vitro* cultured parasites (standard membrane feeding assay, SMFA). DMFA better represents the diversity of field parasites but, the heterogeneity of the parasite population can introduce substantial experimental variability. In addition, the accessibility to field samples as well as their handling and transport, can hamper the quality of the assays. Conditions in SMFA are more controlled but gametocyte production capacity could be compromised over time when parasite strains are maintained in continuous *in vitro* culture (Ponnudurai et al., 1982; Brown and Guler, 2020). Moreover, *Plasmodium* species that cannot be cultured *in vitro*, such as *Plasmodium vivax*, *Plasmodium malariae* and *Plasmodium ovale*, are not suitable for this type of assay. These species present culture specificities which we are not able to reproduce yet, such as the particularity of the *P. vivax* to infect reticulocytes instead of mature red blood cells (Thomson-Luque and Bautista, 2021). The mosquito *in vivo* system is the only way to study these species, and DMFA is the strategy used (Miura et al., 2020). Nevertheless, the SMFA is considered the gold standard for evaluating transmission-reducing factors and together with the direct skin feeding assays in mice, is widely and routinely used to study the parasite cycle in the mosquito (Blagborough et al., 2013).

Apart from the methodology used to infect the mosquitoes, multiple parasite and mosquito traits can lead to variable rates of prevalence (percentage of infected mosquitoes) and intensity (number of parasites per mosquito) (Lefèvre et al., 2013; Vallejo et al., 2016; Simões et al., 2017). Parasite factors such as total gametocyte density, maturation stage, and sex ratio have been shown to impact mosquito infection (Churcher et al., 2013; Da et al., 2015; Bradley et al., 2018). There are also important differences between laboratory and field parasite isolates, and most laboratory reference strains have lost their ability to produce gametocytes (Omorou et al., 2022). Additionally, individual mosquito characteristics such as genotype, age, vector competence and susceptibility to infection, feeding and digestion behavior, and physiological state can result in a variable infection success which makes it difficult to reach a standardized and reproducible protocol (Miura et al., 2016). It has even been shown that the intensity of infection could be affected by the mosquito's circadian clock (Habtewold et al., 2022). In the case of *Plasmodium falciparum* and its natural mosquito vectors, there are difficulties in establishing consistent, high-intensity infections in the laboratory. Various factors, like the vector competence of laboratory reared *vs.* field-caught mosquitoes, or the use of human *vs.* artificial serum, are critical parameters that may be difficult to overcome (Aguilar et al., 2005; Bousema et al., 2013). To reach high parasite numbers in SMFA and DMFA assays, a common approach is to use a non-natural interaction commonly between a rodent malaria parasite *Plasmodium berghei* and an *Anopheles* human-biting species. These combinations however are not representative of the natural mosquito environment to which a particular *Plasmodium* species is adapted, and therefore, the output of the interaction must be considered with caution (Boëte, 2005; Cohuet et al., 2006; Dong et al., 2006; Simões et al., 2017). Indeed, the intensity of infection, i.e. oocyst number per mosquito midgut, can differ between *P.*

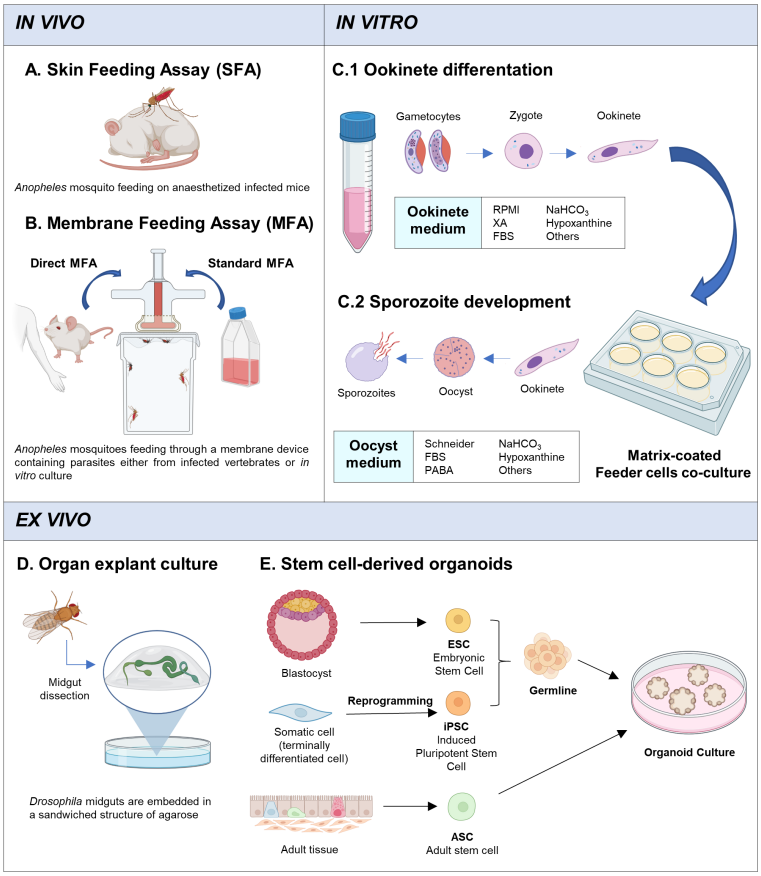

FIGURE 2
In vivo, *in vitro* and *ex vivo* systems. **(A)** Skin Feeding Assay: mosquito bites directly on infected host. **(B)** Membrane Feeding Assay: mosquito feeds through a membrane feeding device which contains infected blood with parasites (gametocytes) from infected-hosts (DMFA) or *in vitro* cultured gametocytes (SMFA). **(C)** Main strategy for *in vitro* culture of Plasmodium mosquito stages. **(C1)** Stage V gametocytes are cultured with ookinete medium for 24h, at 19-26°C (depending on the plasmodium specie). **(C2)** Ookinetes are recovered and pipetted into matrix-coated wells and co-cultured with feeder cells (*Drosophila* S2 cells or others). Oocyst medium is changed periodically until sporozoite development (14-21 days). **(D)** *Ex vivo* culture system developed by Marcchetti et al., (Marchetti et al, 2022). Adult *Drosophila* midguts are dissected and embedded in an agarose sandwich structure with a custom-made culture medium and cultured using an air-media interface. Midguts are maintained alive for up to 3 days. **(E)** Organoids can originate from ESCs, iPSCs, or ASCs. ESCs are derived from the inner cell mass of a blastocyst, iPSCs originate from terminally differentiated cells that have been reprogrammed to become pluripotent stem cell, and, ASCs are isolated from the tissue of interest. ESCs and iPSCs have an additional differentiation step towards the required germline (endoderm, mesoderm, ectoderm). The stem cells are cultured in a defined medium with an extracellular matrix that promotes cell differentiation and 3D structure formation, simulating organ development. Created with Biorender.com.

falciparum and *P. berghei* from tens to hundreds, respectively (Sinden et al. 2004; Aguilar et al., 2005). Mosquito immune responses to *P. falciparum* and *P. berghei* are also slightly different at the transcriptional level (Dong et al., 2006) and depending on the intensity of the infection different immune responses have been reported (Mendes et al., 2011; Simões et al., 2017). These differences can be explained by the fact that the non-natural combination is not constrained by the long-term co-evolution between naturally interacting species, where both organisms have adapted to each other, reducing virulence/resistance, in order to assure parasite survival while reducing mosquito fitness costs linked to the infection process (Shaw et al., 2022). Parameters that differ in natural and non-natural interactions, such as mosquito survival, fecundity and fertility, and parasite developmental rates and transmission efficiency have been reviewed elsewhere (Shaw et al. 2022).

Another challenge in the use of *in vivo* systems is the genetic manipulation of the parasite during the mosquito stages. Gene editing is essential to decipher gene and protein function, and widely used for parasite imaging and for drug/vaccine discovery assays (Okombo et al., 2021). To modify the genome of *Plasmodium*, transgenic parasite strains are better produced during the asexual blood stages because this is when parasites are replicative and haploid, which facilitates their selection and manipulation. Gene disruption strategies, have been essential to decipher parasite protein function playing an important role during mosquito infection. Examples include SOAP (Dessens et al., 2003) and CeLTOS (Kariu et al., 2006) proteins, both expressed in ookinete stages, and involved in parasite survival and dissemination; or transmission-blocking vaccine candidate antigens, like Pfs25, Pfs28, Pfs230 or Pfs48/45 among others (reviewed in Keleta et al., 2021). However, a major drawback for

systematically assigning function is when the gene of interest (GOI) is essential for erythrocytic development or transmission, and therefore complete deletion (knockout) is not possible. At least half of the parasite genome has been described as essential for the completion of the asexual blood cycle for *P. berghei* (Bushell et al., 2017) and *P. falciparum* (Zhang et al., 2018). In order to modulate gene expression of essential genes, several conditional gene knockout and knockdown systems have been developed to study asexual blood-stage parasites. Detailed procedures of conditional expression systems, advantages and disadvantages, their applications at different parasite stages, and future perspectives have been recently reviewed (Kudyba et al., 2021; Briquet et al. 2022).

A few conditional approaches have been applied to mosquito stages. Promoter-swap strategies have been used in *P. berghei* gametocytes (Laurentino et al., 2011; Wall et al., 2018), ookinetes (Siden-Kiamos et al., 2011) and sporozoites (Ishino et al., 2019; Nozaki et al., 2020), which consists in a promoter-exchange of the GOI that maintains the expression in blood-stage parasites but become inactive in mosquito-stage parasites. This strategy, for instance, has allowed to study the role of rhoptry proteins in *P. berghei* sporozoites and salivary gland invasion, which are crucial for erythrocytes infection (Ishino et al., 2019; Nozaki et al., 2020). Another approach is the site-specific recombinase, Cre and Flippase, able to knockout the expression of a target DNA previously flanked with specific sequences LoxP and FRT, respectively. Depending on the orientation of these two-flanking locus, the recombinase enzyme will excise (same directions) or invert (opposite orientation) the targeted DNA. The activation of Flp/FRT recombinase system, which have been successfully implemented in *P. berghei*, is controlled through a stage-specific promoter, restricting the gene editing event to a particular parasite life-stage of interest (Carvalho et al., 2004; Combe et al., 2009; Lacroix et al., 2011). The DiCre system, which is expressed in two enzymatically inactive subunits, require the administration of rapamycin to induce heterodimerization and recombinase activation. Although this strategy makes the recombinase system more flexible, a correct delivery dose in the mosquito as well as the potential toxic effects of the compounds for the insect vector may be an important limitation. Recently, this system has been successfully used to delete essential genes in *P. berghei* prior to transmission to *A. stephensi* mosquitoes (Fernandes et al., 2022). The study demonstrates that silencing the Apical Membrane Antigen 1 (AMA1) and Rhoptry Neck Proteins (RONs) affects sporozoite invasion of salivary glands and invasion of mammalian hepatocytes. In other studies, although the conditional expression of the GOI was successfully achieved, a reduction in parasite number was observed, whether rapamycin was administrated to *A. stephensi* infected with *P. berghei* (Fernandes et al., 2020) or to blood stage *P. falciparum* parasites prior to infection (Tibúrcio et al., 2019). Indeed, it has been demonstrated that rapamycin, an inhibitor of the TOR pathway, boosts the mosquito *A. stephensi* immune response, hindering *P. berghei* development (Feng et al., 2021). Therefore, further investigation is needed to implement a conditional expression system in mosquitoes without affecting its physiology and allowing a tight control of gene expression at any stage of the developmental cycle.

Apart from the pros and cons of different strategies used to study gene function in *Plasmodium* parasites, *in vivo* RNA interference (RNAi) and CRISPR/Cas9 gene silencing approaches in mosquitoes have proven to be very useful in advancing knowledge of the function of mosquito proteins and their potential interactions with malaria parasites. The main strategy used to knock down the expression of a given mosquito gene is using RNAi (Catteruccia and Levashina, 2009). This can be achieved by injecting gene-specific double-stranded RNA (dsRNA) into the adult mosquito or by expressing dsRNA *in situ* from transgenes integrated into the mosquito genome. The exogenous RNA then binds to the homologous mRNA of the candidate gene and causes its degradation. The impact of mosquito gene silencing on parasite survival using the RNAi strategy has uncovered the important function of many proteins involved in parasite midgut invasion, such as AnAPN1 (Dinglasan et al., 2007), FREP1 (Zhang et al., 2015), and P47Rec (Molina-Cruz et al., 2020), and also genes related to mosquito immunity, like LRIM (Osta et al 2004; Billingsley et al., 2021), TEP1 (Blandin et al., 2004), FBN9 and FBN30 (Dong and Dimopoulos, 2009; Li et al., 2013). The RNA delivery injection method is more widely used because it allows gene function to be assessed in a relatively short time, but it requires large numbers of mosquitoes and their physical manipulation can cause damage and stress (Taracena et al., 2022). Furthermore, this type of gene silencing is transient and time-limited. The generation of transgenic lines expressing RNAi, on the other hand, provides stable expression, a supply of mutant mosquitoes and a major control of knockdown using tissue-specific promoters, however it is labor intensive and requires longer periods of time (Catteruccia and Levashina, 2009). In both cases efficiency depends on the endogenous levels of the transcripts and whether expression is restricted to the target tissue or is more widespread. CRISPR/Cas9 gene editing allows a complete gene silencing at the DNA level and has been used to knock out genes in mosquitoes like *A. gambiae* FREP1 (Dong et al., 2018) and *A. stephensi* LRIM (Inbar et al., 2021), however, in both studies this strategy resulted in fitness costs, affecting mosquito's development, fecundity and survival.

3 *In vitro* systems

In vitro culture systems represent a simplification of the biological complexity of an organism but are very useful and necessary to study how this complexity is generated and organized and how it functions. That is, they provide a controlled and isolated environment that permits more detailed analysis and easier manipulation. In the context of human infectious diseases research, *in vitro* systems allow to study the infection process and host-parasite interactions avoiding human experimentation.

In the malaria field, *in vitro* culture is the gold standard for the study of the parasite intraerythrocytic cycle in humans that has led to the identification of host and parasite factors that contribute to

infection (Venugopal et al., 2020). This system has also been widely used for the high throughput screening of novel chemotherapeutics. The *in vitro* culture of the mosquito stages on the other hand, has been far more complicated and this area is still under development.

The major hurdle for *in vitro* culture of mosquito-stages, is that parasite development in the mosquito does not occur intracellularly and therefore the variety of environments, tissues and cellular types involved in the interactions are much more difficult to reproduce *in vitro*.

Although in reality there is no *in vitro* system that recapitulates faithfully the mosquito environment, the temporary culture of the parasite outside the vector is now possible for many *Plasmodium* species (Table 1). Important developments have been achieved in the two rodent malaria parasites: *P. berghei* (Al-Olayan et al., 2002) and *P. yoelii* (Porter-Kelley et al., 2006), while the human malaria parasite *P. falciparum* remains more challenging, at least until recently (Eappen et al., 2022). Advancements in the culture of mosquito stages have opened the door to functional and structural investigations of the sporogonic cycle (Zeeshan et al., 2021) as well as drug screening against mosquito stages (Azevedo et al., 2017), and represent the first step for the development of more complex *in vitro* systems. In the following sub-sections, the most important advances in this area are presented.

3.1 *In vitro* development of *Plasmodium* mosquito stages

The *in vitro* development of *Plasmodium* mosquito stages has been in the spotlight of research for a long time. The entire sporogonic cycle, from gametocytes to sporozoite, achieved *in vitro* was first reported in 1992 for *P. gallinaceum* (Warburg and Miller, 1992) followed by other *Plasmodium* species of both human(Warburg and Schneider, 1993) and non-human (Al-Olayan et al., 2002; Porter-Kelley et al., 2006). The full sporogonic development of *P. falciparum* was first described in 1993 (Warburg and Schneider, 1993), but the method was not reproducible, and the low recovery of parasites after each transformation step, has limited its application. Since then, there have been several attempts to improve the system. Different conditions have been tested and upgraded with more or less success and efficiency such as the culture medium composition, co-cultivation with insect cells and the presence of Matrigel substrate or other components simulating the basal lamina (Ghosh et al., 2010; Itsara et al., 2018; Siciliano et al., 2020).

Some conclusions can be drawn from these studies. The sporogonic development *in vitro* is achieved in two differentiated steps: (1) the gametes activation until ookinete development, followed by (2) oocyst differentiation and sporozoite production (Figure 2C). For the *in vitro* exflagellation and ookinete development, despite some variations, stage V gametocytes are cultured with RPMI medium (supplemented with fetal bovine serum, sodium bicarbonate and hypoxanthine among others) together with factors or conditions that are known to trigger gametocyte differentiation such as the presence of xanthurenic acid or a temperature drop (Billker et al., 1998; Garcia et al., 1998). This method has been widely used in *P. berghei* and has allowed to study many biological processes during sexual development like ookinete formation and invasion, which has been translated to a better understanding of transmission biology of this parasite compared to other species (Guttery et al., 2022). On the other hand, *in vitro* conversion of ookinete to oocyst and sporozoite production are more challenging as the *in vivo* setting in which these processes take place is more complex and the triggering factors as well as the regulatory mechanisms of cell division and differentiation remain mostly unknown (Figure 1). Oocyst differentiation begins when the ookinete reaches the basal lamina, but oocyst maturation until sporozoite release requires a long period of time (around 20 days) and involves multiple mitotic divisions and interactions with the surrounding midgut epithelial cells. To mimic these steps *in vitro*, once ookinetes are obtained, they are recovered and cultured in different conditions. Generally, a supplemented Schneider's medium is used with the presence of insect cells, such *Drosophila melanogaster* S2 cells, and Matrigel or similar substrates. It has been shown that the use of collagen-based matrices and feeder cells improve the conversion rates and the sporozoite production (Al-Olayan et al., 2002; Porter-Kelley et al., 2006; Azevedo et al., 2017). Probably, the role of collagen-based matrices, similar to the midgut basement membrane, is to allow ookinete attachment and enhance oocyst differentiation. More unclear is the role played by insect cells, which might be related to factors secreted that may act as trigger factors for oocyst developmental progression. Despite these advances, mainly in *P. berghei* and *P. yoelii*, oocyst maintenance and differentiation *in vitro* remain challenging, parasite recovery rate is very low and it decreases further over time.

Recently, an improved approach for the complete *P. falciparum* sporogonic development has been described (Eappen et al., 2022). The authors increased considerably the yield of sporozoites obtained, which in addition, were able to infect and transit to blood stages. In that study, sporogonic development was achieved in three steps with specific conditions: exflagellation, ookinete development, and oocyst transformation. Thanks to the presence of S2 feeder cells and Matrigel a high transformation rate from gametocyte to oocyst was obtained. Although the conversion efficiency from oocyst to sporozoite was lower *in vitro* than in the mosquito, the final conversion rate (from gametocytes to sporozoites) was 7.4-fold higher *in vitro*. However, as a caveat, due to the lower conversion rate of oocyst to sporozoites *in vitro*, sporozoite release was forced by mechanical dissociation of mature oocyst, suggesting that still unknown factors are required for a normal development. Furthermore, the sporozoites obtained *in vitro* showed attenuation of their infectivity at the late liver stage, probably indicating that as observed *in vivo*, sporozoite infectivity may be slightly compromised if they do not pass through the salivary glands (Touray et al., 1992; Sato et al. 2014). Although overall gene expression by RNA-seq was similar between sporozoites produced *in vitro* and *in vivo*, many reads were not parasite-specific due to the presence of S2 cells. Altogether, further investigation is needed to decipher observed differences in infectivity.

Another recent development in this area is the use of *in vitro* platforms to study the motility of ookinetes and sporozoites, which

is essential for malaria transmission (Ramírez-Flores et al., 2022). The use of polyacrylamide gels that can be adjusted in elasticity and pore size, allows a more accurate simulation of different mosquito tissues and microenvironments. Accordingly, it has been observed that both ookinete and sporozoite motility and migration paths show differences depending on substrate characteristics (Ripp et al., 2021; Vaughan, 2021).

Altogether, for a successful *in vitro* culture of *Plasmodium* mosquito stages, a major improvement would be the development of new two-dimensional (2D) or three-dimensional (3D) culture systems that enable the sporogonic cycle in a continuous manner and that recapitulate the structural and physiological conditions of the mosquito environment more faithfully.

3.2 Other *in vitro* systems in malaria

Although several mosquito cell lines exist (Walker et al., 2014) none of them is suitable to study the *Plasmodium*-mosquito interactions. Several of the cell lines that have been developed have hemocyte-like properties and have been used to study mosquito immunity (Mishra et al., 2022). Some studies have used *Plasmodium*-derived molecules to study the mosquito cells' immune response, but none has co-cultured the mosquito cell lines with the parasite to study their interactions (Akman-Anderson et al. 2007; Pietri et al., 2015).

Another *in vitro* strategy that has recently been used to uncover *P. falciparum* and *A. gambiae* protein interactions is the baculovirus expression system in insect cells. This system allows the production of recombinant proteins and has been used to discover both parasite (Niu et al., 2021) and mosquito proteins (Cui et al., 2020) involved in mosquito infection. For such purpose, they chose proteins that may directly interact in the midgut lumen: proteins with signal peptides, whose genes are up-regulated after the blood meal in mosquitoes, or are abundantly expressed at sexual stages in parasites. Once the candidate genes were cloned and expressed in the baculovirus system, the recombinant proteins were used in an ELISA assay with mosquito midgut lysates or specific *P. falciparum* stages to detect potential protein interactions. The effects of the protein interactions during the infection process need then to be confirmed *in vivo*. By knocking down the expression of mosquito candidate proteins using RNAi, and analyzing the oocyst number developed after *in vivo* infection, it was possible to uncover both mosquito proteins that protect against infection and proteins that facilitate parasite invasion (Cui et al., 2020). On the other hand, the function of a parasite protein candidate, Pfs16, was assessed using an antibody anti-Pfs16 which significantly reduced the number of oocysts (Niu et al., 2021). Altogether, this strategy allows the detection of potential targets to block malaria transmission.

4 Single cell technologies

Infection is a dynamic process in which parasite and mosquito gene expression patterns and their regulation change spatially and temporally, allowing the parasite to transit between life-stages and adapt to within-host conditions, and the mosquito to respond to an infection by a particular parasite genotype/phenotype. These interactions and their consequences are best represented in an *in vivo* system, but profiling "in bulk" the genome, the epigenome or the transcriptome of the parasite or the mosquito using infected tissues, where many cell types are present, may distort and bias the results. Recent advances in single cell technologies have led to a breakthrough in the analysis of heterogenous samples and environments, allowing a deep understanding of host-parasite interactions at the single cell level (Afriat et al., 2022). With this approach the genetic diversity of an infection can be captured, mapping out gene expression throughout the developmental timeline, detecting key expression and regulatory processes and predicting gene function by association with other co-expressed and functionally annotated genes (Real et al., 2021).

Single cell RNA-seq approaches have been applied widely in different *Plasmodium* species and developmental stages (reviewed in Real and Mancio-Silva, 2022). The data obtained from some of these studies are part of the Malaria Cell Atlas project, which aims to build up a reference map of the parasite transcriptome during its entire development (Howick et al., 2019; Nötzel and Kafsack, 2021).Single-cell transcriptomic data is available for *P. berghei* (Howick et al., 2019; Witmer et al., 2021) and *P. falciparum* (Real et al., 2021; Mohammed et al., 2023) during the life cycle inside the mosquito.

However, regarding mosquitoes, single cell approaches have only been used to study the mosquito immune system in *A. gambiae* and *Aedes aegypti* (Raddi et al., 2020; Kwon et al., 2021). In *A. aegypti* another pioneer study applied single cell RNA-seq to mosquito midguts, before and after a blood meal, revealing changes in cellular composition and transcriptional profile due to infection (Cui and Franz, 2020). This demonstrates that if applied to midguts and salivary glands of *Anopheles* before and after infection, this technology could shed new light on mosquito responses at the single cell level, and reveal the changes induced by the parasite in the expression of different mosquito cell types, as well as the strategies and mechanisms used by the parasite to migrate through the mosquito's body.

A promising approach offered by single cell approaches is to study parasite and mosquito transcriptomic and epigenomics changes simultaneously. The dual scRNA-seq strategy of infected cells has been used to study parasite-host interactions during the erythrocytic cycle and in the liver (Hentzschel et al., 2022; Mancio-Silva et al., 2022). However, the spatial context is lost with the single cell approaches and, in order to study interactions, additional techniques are required to link tissue distribution and transcriptional profiles. Different spatial transcriptomics strategies exist nowadays providing a coordinate map of the distribution of cells in a tissue based on specific gene sets (Williams et al., 2022). If this data is integrated with scRNA-seq it is possible to associate transcriptomic information with specific spatial localization in the native tissue (Longo et al., 2021). In a recent study, scRNA-seq and single-molecule fluorescence *in situ* hybridization (smFISH) data have been combined to study *P. berghei* development in the mouse liver (Afriat et al., 2022). A spatial profile of the interactions between parasite and host cells was achieved, identifying

differences in parasite growth and survival in distinct zones. Nevertheless, the application of this technology in the field is still in its infancy.

5 *Ex vivo* culture systems

Ex vivo systems aim to represent the cellular complexity of organs or tissues found *in vivo* using *in vitro* conditions (outside the organism). These 3D culture systems allow standardized and controlled experimentation, while providing a closer representation of the *in vivo* situation.

One could divide these systems into: tissue explants and engineered tissues and organs (organoids). Tissue explant refers to the culture of small pieces of a tissue extracted from an animal or organ. Organoids are tiny, self-organized three-dimensional tissue cultures that are derived from stem cells. Such cultures can be crafted to replicate much of the complexity of an organ, or to exhibit selected aspects of it.

Mammalian organoids and explant tissues have been widely used to study interactions of many infectious diseases, including apicomplexan parasites like *Plasmodium*, *Toxoplasma*, *Cryptosporidium* and *Eimeria* (Dutta and Clevers, 2017; Ramírez-Flores et al., 2022). These systems allow us to study pathogen biology and host interactions in a more accessible way, overcoming other limitations of the systems mentioned above. It opens up the possibility of performing live-imaging experiments, facilitates gene editing strategies and even allows the culture of organisms that are difficult to grow *in vitro* in traditional 2D culture systems, which lack cellular architecture, extracellular microenvironment and poorly represent the natural niche. Unfortunately, these advances have not been translated to insect models. This is in spite of providing new opportunities to study unknown aspects of parasite-vector interactions but also discover and test new molecules that block pathogen transmission.

5.1 Explanted tissues

In the malaria field, explanted midgut tissues (Zieler and Dvorak, 2000) and entire intact midguts (Vlachou et al., 2004) have been used to study ookinete locomotion and invasion through the epithelium (Table 1). A culture system was developed to maintain the tissue alive while observing the invasion process of ookinetes by microscopy. The tissue viability and cell apoptosis were assessed with dyes and morphological observation, estimating a lifespan of 2-3 hours. While this strategy might be useful for short time processes, i.e. gametocyte activation or zygote formation, mantaining mosquito tissues alive over a longer period of time still represents a hurdle. This limitation does not affect many mammalian tissues, in which the *ex vivo* culture strategy has been widely used to study diverse physiological and pathological processes during longer periods of time (Randall et al. 2011; Russo et al., 2016). For example, it has been applied to study infection by the apicomplexan parasite *Cryptosporidium parvum*. In this case, the murine intestine explant remained alive in culture for 35 days (Baydoun et al., 2017). This reflects a much better understanding of the conditions required for *in vitro* culture of mammalian cells and tissues compared to insects.

An approach that permits to assess the viability of an explanted tissue or organ would be very valuable in the context of malaria. Antonello et al. developed a method to analyse the dynamics of the intestinal epithelium in *Drosophila*, named ReDDM system (Repressible Dual Differential-stability Markers) (Antonello et al., 2015). This method uses the Gal4/UAS system to control the expression of two different fluorescently labelled proteins, with short and long half-lives. When this system is controlled by the expression of a gene only active in progenitor cells, due to the different half-lives of the tagged proteins, it is possible to track cell turnover and distinguish the newly differentiated cells. Interestingly, an improved explant culture of Drosophila midgut has been recently reported (Figure 2D) (Marchetti et al. 2022). The *ex vivo* system sustains the organ alive for up to 3 days and allows live-imaging during that time, enabling monitoring of the tissue epithelial dynamics. We envision that, if leveraged to mosquitoes, these approaches might be a promising tool to monitor the midgut viability and homeostatic activity during an infection process.

5.2 Stem cell technologies and organoids

The advent of stem cells has opened up exciting new applications and opportunities to understand disease mechanisms, recapitulate cellular systems and genetic characteristics (Pance, 2021). Stem cell research boomed in mammalian studies with the capacity to generate induced pluripotent stem (iPS) cell lines and differentiate into specific cell types, making it possible to generate traditional *in vitro* cell culture of a single cell type or more complex multicellular structures that recapitulate the characteristics of an organ, also called organoids (Figure 2E). Another important contribution of these systems is the storage of cell lines, facilitating experimental procedures and also providing greater homogeneity and tractability to the studies performed (Hanna and Hubel, 2009). Such advances have been scarce in insects, including main disease vectors.

As a first step, however, the identification of stem cell types in a variety of insects has been reported (Corley and Lavine, 2006). In the case of mosquitoes, midgut stem cells from the house mosquito *Culex pipiens* have been isolated and cultured, though for a limited period of time (Wassim et al., 2014). This pioneer work demonstrates that it is possible to obtain, culture and store insect stem cells, raising exciting possibilities for the generation of longer-term stem cells cultures capable of supporting a pathogen infection. Nevertheless, similar stem cell types from malaria mosquito vectors are still lacking.

Recently stem cells technologies have been applied to derive different types of human red blood cells to culture the parasites, erythroid precursors and genetically modified mature erythrocytes. This approach has enabled a better understanding of parasite invasion and pathogenesis and offered the possibility of studying patient-derived cell lines that can be preserved and manipulated to understand the impact of genetic variation on the disease (Pance et al., 2021). In the mosquito, however, one great hurdle of this novel technology is that the mosquito stages of *Plasmodium* parasites are extracellular. In this case, stem cell-derived organoids would be much better suited to create an easy manipulable environment simulating the complexity and variety of tissues. Mammalian gut organoids have been recently engineered aiming to harbor and culture unicellular as well as multicellular pathogens (Pance, 2021; Ramírez-Flores et al., 2022) and an application to insects has been suggested (Swevers et al., 2021).

Organoids can be generated from iPS cells, embryonic stem cells or adult stem cells from specific tissues (Figure 2E). The formation of organoids is based on the culture of stem cells with an extracellular matrix, which allows tridimensional structure formation, and niche factors that stimulate self-renewal and induce cellular differentiation. Multiple mammalian organoids such intestines (Almeqdadi et al., 2019; Nikolaev et al., 2020) and salivary glands (Pringle et al., 2016; Tanaka et al., 2018) have been created among others.

The insect midgut epithelium is of particular interest because of its role in nutrition, digestion and immunity as well as a niche for microbiota and an interphase of parasite interactions. The dynamics of the gut epithelium and identification of some of its constituting cell types have been described in *Drosophila* as a model organism, including progenitor cells (Bonfini et al. 2016). Although the *Drosophila* midgut epithelium shares similarities with human intestine, such as cell types and functions, as well as molecular signaling pathways which drive intestinal stem cell (ISC) proliferation and differentiation (Kaur et al., 2018; Capo et al. 2019), the use of stem cell technologies in flies has not been reported to date. Compared to *Drosophila*, the midgut epithelial dynamics of mosquitoes have received much less attention. However, some studies have started filling this gap, highlighting the potential of this system (Hixson et al. 2021).

The mosquito midgut comprises four main cell types: differentiated enterocytes (ECs) and enteroendocrine cells (EEs), and undifferentiated progenitor cells (ISC and enteroblasts, EBs). The common features in the midgut cell composition and cell type markers between *Aedes aegypti* and *Drosophila* was recently reported using scRNA-seq (Cui and Franz, 2020). It was also demonstrated that the mosquito midgut epithelium is a dynamic tissue which changes its cell composition after a blood meal, indicating a proliferative and differentiation response. Furthermore, proliferative cells from the mosquito gut that are responsive to damage and able to repair the epithelium have also been studied (Janeh et al. 2017), although not all mosquito species respond to damage in the same way (Janeh et al. 2019). The signals involved in the regulation of the ISC are poorly understood. It has been speculated that the hormone 20 hydroxyecdysone (20E), which increases after a blood meal, could stimulate the ISC proliferation as has been described in *Drosophila* (Hixson et al. 2021). Similarly, induced pathways after mosquito gut damage such as Jak/Stat, EGFR and Delta-Notch signaling (Janeh et al. 2017; Taracena et al., 2018) may be involved in the epithelium regeneration response. However, much research is required to decipher their role in midgut homeostasis, as well as identify the ISC niche factors that triggers proliferation and differentiation into a specific cell type. Developing these systems and understanding these processes will represent an invaluable contribution to the study of vector-parasite interactions and unravelling of malaria transmission.

6 Concluding remarks

A major complication of any *in vitro* system to study *Plasmodium*-mosquito interactions is that the parasite in the mosquito is extracellular. Indeed, nowadays there is no single, well-established protocol for the complete *in vitro* sporogonic development of any *Plasmodium* species. This is probably because current systems fail to reproduce faithfully all the different environments in the mosquito and also because several key triggering factors enabling the progression of the parasite life cycle in the mosquito still need to be unraveled.

The development of *ex vivo* systems that recapitulate the complexity of the mosquito environment and can be easily handled *in vitro*, may help to overcome some of the limitations of the current *in vitro* and *in vivo* systems, facilitating genome editing of the parasite and assuring high performance and reproducibility of the experiments. Explanted tissues represent a powerful alternative; however, its use is still limited by the amount of time the organ preserves its functionality and integrity, which in the case of mosquitoes is currently unknown.

The availability of proliferative and stem cells from mosquitoes will enable the design of novel 2D and 3D culture systems, such as organoids, simulating mosquito midgut and salivary glands, to support development and transmission of the vector stages of many human parasites, including *Plasmodium*. Renewed efforts in transdisciplinary research and stem cell technologies are needed to identify, isolate, culture and differentiate these cells, and develop three-dimensional structures to facilitate the study of interactions between parasites such as *Plasmodium* and their vectors. Such developments will be fundamental in the quest for novel tools to control infectious diseases.

Author contributions

Conceptualization: MP-M and EG-D. Original draft preparation: MP-M, EG-D, and AP revised it critically and added important intellectual content. All authors contributed to the article and approved the submitted version.

Funding

This review was supported by the Spanish Ministry of Science and Innovation (grant no. PID2019-111109RB-I00), and by La

Caixa Foundation—Health Research Program (grant no. HR20-00635).

Conflict of interest

The authors declare that the research was conducted in the absence of any commercial or financial relationships that could be construed as a potential conflict of interest.

Publisher's note

All claims expressed in this article are solely those of the authors and do not necessarily represent those of their affiliated organizations, or those of the publisher, the editors and the reviewers. Any product that may be evaluated in this article, or claim that may be made by its manufacturer, is not guaranteed or endorsed by the publisher.

References

Afriat, A., Zuzarte-Luís, V., Bahar Halpern, K., Buchauer, L., Marques, S., Chora, Â. F., et al. (2022). A spatiotemporally resolved single-cell atlas of the plasmodium liver stage. *Nature* 611 (7936), 563–569. doi: 10.1038/s41586-022-05406-5

Aguilar, R., Dong, Y., Warr, E., and Dimopoulos, G. (2005). Anopheles infection responses; laboratory models versus field malaria transmission systems. *Acta Trop.* 95, 285–291. doi: 10.1016/j.actatropica.2005.06.005

Akman-Anderson, L., Olivier, M., and Luckhart, S. (2007). Induction of nitric oxide synthase and activation of signaling proteins in anopheles mosquitoes by the malaria pigment, hemozoin. *Infect. Immun.* 75, 4012. doi: 10.1128/IAI.00645-07

Almeqdadi, M., Mana, M. D., Roper, J., and Yilmaz, Ö.H. (2019). Making cell culture more physiological: Gut organoids: mini-tissues in culture to study intestinal physiology and disease. *Am. J. Physiol. Cell Physiol.* 317, C405. doi: 10.1152/AJPCELL.00300.2017

Al-Olayan, E. M., Beetsma, A. L., Butcher, G. A., Sinden, R. E., and Hurd, H. (2002). Complete development of mosquito phases of the malaria parasite *in vitro*. *Sci. (1979)* 295, 677–679. doi: 10.1126/science.1067159

Antonello, Z. A., Reiff, T., Ballesta-Illan, E., and Dominguez, M. (2015). Robust intestinal homeostasis relies on cellular plasticity in enteroblasts mediated by miR-8–escargot switch. *EMBO J.* 34, 2025–2041. doi: 10.15252/EMBJ.201591517

Azevedo, R., Markovic, M., Machado, M., Franke-Fayard, B., Mendes, A. M., and Prudêncio, M. (2017). Bioluminescence method for *In vitro* screening of plasmodium transmission-blocking compounds. *Antimicrob. Agents Chemother.* 61 (6). doi: 10.1128/AAC.02699-16

Baydoun, M., Vanneste, S. B., Creusy, C., Guyot, K., Gantois, N., Chabe, M., et al. (2017). Three-dimensional (3D) culture of adult murine colon as an *in vitro* model of cryptosporidiosis: Proof of concept. *Sci. Rep.* 7, 1–12. doi: 10.1038/s41598-017-17304-2

Bennink, S., Kiesow, M. J., and Pradel, G. (2016). The development of malaria parasites in the mosquito midgut. *Cell Microbiol.* 18, 905–918. doi: 10.1111/CMI.12604

Billingsley, P. F., George, K. I., Eappen, A. G., Harrell, R. A., Alford, R., Li, T., et al. (2021). Transient knockdown of anopheles stephensi LRIM1 using RNAi increases plasmodium falciparum sporozoite salivary gland infections. *Malar J.* 20 (1), 284. doi: 10.1186/S12936-021-03818-8

Billker, O., Lindo, V., Panico, M., Etienne, A. E., Paxton, T., Dell, A., et al. (1998). Identification of xanthurenic acid as the putative inducer of malaria development in the mosquito. *Nature* 392, 289–292. doi: 10.1038/32667

Blagborough, A. M., Delves, M. J., Ramakrishnan, C., Lal, K., Butcher, G., and Sinden, R. E. (2013). Assessing transmission blockade in plasmodium spp. *Methods Mol. Biol.* 923, 577–600. doi: 10.1007/978-1-62703-026-7_40

Blandin, S., Shiao, S. H., Moita, L. F., Janse, C. J., Waters, A. P., Kafatos, F. C., et al. (2004). Complement-like protein TEP1 is a determinant of vectorial capacity in the malaria vector anopheles gambiae. *Cell* 116, 661–670. doi: 10.1016/S0092-8674(04)00173-4

Boëte, C. (2005). Malaria parasites in mosquitoes: Laboratory models, evolutionary temptation and the real world. *Trends Parasitol.* 21, 445–447. doi: 10.1016/j.pt.2005.08.012

Bonfini, A., Liu, X., and Buchon, N. (2016). From pathogens to microbiota: How drosophila intestinal stem cells react to gut microbes. *Dev. Comp. Immunol.* 64, 22–38. doi: 10.1016/J.DCI.2016.02.008

Bousema, T., Churcher, T. S., Morlais, I., and Dinglasan, R. R. (2013). Can field-based mosquito feeding assays be used for evaluating transmission-blocking interventions? *Trends Parasitol.* 29, 53–59. doi: 10.1016/J.PT.2012.11.004

Bradley, J., Stone, W., Da, D. F., Morlais, I., Dicko, A., Cohuet, A., et al. (2018). Predicting the likelihood and intensity of mosquito infection from sex specific plasmodium falciparum gametocyte density. *Elife* 7, e34463. doi: 10.7554/eLife.34463.001

Briquet, S., Gissot, M., and Silvie, O. (2022). A toolbox for conditional control of gene expression in apicomplexan parasites. *Mol. Microbiol.* 117, 618. doi: 10.1111/MMI.14821

Brown, A. C., and Guler, J. L. (2020). From circulation to cultivation: Plasmodium *In vivo* versus *In vitro*. *Trends Parasitol.* 36, 914–926. doi: 10.1016/j.pt.2020.08.008

Bushell, E., Gomes, A. R., Sanderson, T., Anar, B., Girling, G., Herd, C., et al. (2017). Functional profiling of a plasmodium genome reveals an abundance of essential genes. *Cell* 170, 260–272.e8. doi: 10.1016/J.CELL.2017.06.030

Capo, F., Wilson, A., and di Cara, F. (2019). The intestine of drosophila melanogaster: An emerging versatile model system to study intestinal epithelial homeostasis and host-microbial interactions in humans. *Microorganisms* 7 (9), 336. doi: 10.3390/MICROORGANISMS7090336

Carvalho, T. G., Thiberge, S., Sakamoto, H., and Ménard, R. (2004). Conditional mutagenesis using site-specific recombination in plasmodium berghei. *Proc. Natl. Acad. Sci. U.S.A.* 101, 14931. doi: 10.1073/PNAS.0404416101

Catteruccia, F., and Levashina, E. A. (2009). RNAi in the malaria vector, anopheles gambiae. *Methods Mol. Biol.* 555, 63–75. doi: 10.1007/978-1-60327-295-7_5

Churcher, T. S., Blagborough, A. M., Delves, M., Ramakrishnan, C., Kapulu, M. C., Williams, A. R., et al. (2012). Measuring the blockade of malaria transmission – an analysis of the standard membrane feeding assay. *Int. J. Parasitol.* 42, 1037–1044. doi: 10.1016/J.IJPARA.2012.09.002

Churcher, T. S., Bousema, T., Walker, M., Drakeley, C., Schneider, P., Ouédraogo, A. L., et al. (2013). Predicting mosquito infection from plasmodium falciparum gametocyte density and estimating the reservoir of infection. *Elife* 21 (2), e00626. doi: 10.7554/ELIFE.00626

Cohuet, A., Osta, M. A., Morlais, I., Awono-Ambene, P. H., Michel, K., Simard, F., et al. (2006). Anopheles and plasmodium: from laboratory models to natural systems in the field. *EMBO Rep.* 7. doi: 10.1038/SJ.EMBOR.7400831

Combe, A., Giovannini, D., Carvalho, T. G., Spath, S., Boisson, B., Loussert, C., et al. (2009). Clonal conditional mutagenesis in malaria parasites. *Cell Host Microbe* 5, 386–396. doi: 10.1016/J.CHOM.2009.03.008

Corley, L. S., and Lavine, M. D. (2006). A review of insect stem cell types. *Semin. Cell Dev. Biol.* 17, 510–517. doi: 10.1016/J.SEMCDB.2006.07.002

Cui, Y., and Franz, A. W. E. (2020). Heterogeneity of midgut cells and their differential responses to blood meal ingestion by the mosquito, aedes aegypti. *Insect Biochem. Mol. Biol.* 127, 103496. doi: 10.1016/J.IBMB.2020.103496

Cui, Y., Niu, G., Li, V. L., Wang, X., and Li, J. (2020). Analysis of blood-induced anopheles gambiae midgut proteins and sexual stage plasmodium falciparum interaction reveals mosquito genes important for malaria transmission. *Sci. Rep.* 10, 1–12. doi: 10.1038/s41598-020-71186-5

Da, D. F., Churcher, T. S., Yerbanga, R. S., Yaméogo, B., Sangaré, I., Ouedraogo, J. B., et al. (2015). Experimental study of the relationship between plasmodium gametocyte density and infection success in mosquitoes; implications for the evaluation of malaria transmission-reducing interventions. *Exp. Parasitol.* 149, 74–83. doi: 10.1016/J.EXPPARA.2014.12.010

Dash, M., Sachdeva, S., Bansal, A., and Sinha, A. (2022). Gametogenesis in plasmodium: Delving deeper to connect the dots. *Front. Cell Infect. Microbiol.* 12. doi: 10.3389/FCIMB.2022.877907

Dessens, J. T., Sidén-Kiamos, I., Mendoza, J., Mahairaki, V., Khater, E., Vlachou, D., et al. (2003). SOAP, a novel malaria ookinete protein involved in mosquito midgut invasion and oocyst development. *Mol. Microbiol.* 49, 319–329. doi: 10.1046/J.1365-2958.2003.03566.X

Dinglasan, R. R., Kalume, D. E., Kanzok, S. M., Ghosh, A. K., Muratova, O., Pandey, A., et al. (2007). Disruption of plasmodium falciparum development by antibodies against a conserved mosquito midgut antigen. *Proc. Natl. Acad. Sci. U.S.A.* 104, 13461–13466. doi: 10.1073/PNAS.0702239104

Dong, Y., Aguilar, R., Xi, Z., Warr, E., Mongin, E., and Dimopoulos, G. (2006). Anopheles gambiae immune responses to human and rodent plasmodium parasite species. *PloS Pathog.* 2, 0513–0525. doi: 10.1371/JOURNAL.PPAT.0020052

Dong, Y., and Dimopoulos, G. (2009). Anopheles fibrinogen-related proteins provide expanded pattern recognition capacity against bacteria and malaria parasites. *J. Biol. Chem.* 284, 9835–9844. doi: 10.1074/JBC.M807084200

Dong, Y., Simões, M. L., Marois, E., and Dimopoulos, G. (2018). CRISPR/Cas9 -mediated gene knockout of anopheles gambiae FREP1 suppresses malaria parasite infection. *PloS Pathog.* 14 (3), e1006898. doi: 10.1371/JOURNAL.PPAT.1006898

Dutta, D., and Clevers, H. (2017). Organoid culture systems to study host-pathogen interactions. *Curr. Opin. Immunol.* 48, 15–22. doi: 10.1016/J.COI.2017.07.012

Eappen, A. G., Li, T., Marquette, M., Chakravarty, S., Kc, N., Zanghi, G., et al. (2022). *In vitro* production of infectious plasmodium falciparum sporozoites. *Nature* 2022, 1–6. doi: 10.1038/s41586-022-05466-7

Feng, Y., Chen, L., Gao, L., Dong, L., Wen, H., Song, X., et al. (2021). Rapamycin inhibits pathogen transmission in mosquitoes by promoting immune activation. *PloS Pathog.* 17 (2), e1009353. doi: 10.1371/JOURNAL.PPAT.1009353

Fernandes, P., Briquet, S., Patarot, D., Loubens, M., Hoareau-Coudert, B., and Silvie, O. (2020). The dimerisable cre recombinase allows conditional genome editing in the mosquito stages of plasmodium berghei. *PloS One* 15 (10), e0236616. doi: 10.1371/JOURNAL.PONE.0236616

Fernandes, P., Loubens, M., Le Borgne, R., Marinach, C., Ardin, B., Briquet, S., et al. (2022). The AMA1-RON complex drives plasmodium sporozoite invasion in the mosquito and mammalian hosts. *PloS Pathog.* 18. doi: 10.1371/JOURNAL.PPAT.1010643

Garcia, G. E., Wirtz, R. A., Barr, J. R., Woolfitt, A., and Rosenbergt, R. (1998). Xanthurenic acid induces gametogenesis in plasmodium, the malaria parasite. *J. Biol. Chem.* 273, 12003–12005. doi: 10.1074/JBC.273.20.12003

Ghosh, A. K., Dinglasan, R. R., Ikadai, H., and Jacobs-Lorena, M. (2010). An improved method for the *in vitro* differentiation of plasmodium falciparum gametocytes into ookinetes. *Malar J.* 9, 1–7. doi: 10.1186/1475-2875-9-194

Guttery, D. S., Zeeshan, M., Ferguson, D. J. P., Holder, A. A., and Tewari, R. (2022). Division and transmission: Malaria parasite development in the mosquito. *Annu. Rev. Microbiol.* 76, 113–134. doi: 10.1146/annurev-micro-041320-010046

Habtewold, T., Tapanelli, S., Masters, E. K. G., Windbichler, N., and Christophides, G. K. (2022). The circadian clock modulates anopheles gambiae infection with plasmodium falciparum. *PloS One* 17, e0278484. doi: 10.1371/JOURNAL.PONE.0278484

Hanna, J., and Hubel, A. (2009). Preservation of stem cells. *Organogenesis* 5, 134. doi: 10.4161/ORG.5.3.9585

Hentzschel, F., Gibbins, M. P., Attipa, C., Beraldi, D., Moxon, C. A., Otto, T. D., et al. (2022). Host cell maturation modulates parasite invasion and sexual differentiation in plasmodium berghei. *Sci. Adv.* 8 (17), eabm7348. doi: 10.1126/SCIADV.ABM7348

Hixson, B., Taracena, M. L., and Buchon, N. (2021). Midgut epithelial dynamics are central to mosquitoes' physiology and fitness, and to the transmission of vector-borne disease. *Front. Cell Infect. Microbiol.* 11. doi: 10.3389/fcimb.2021.653156

Howick, V. M., Russell, A. J. C., Andrews, T., Heaton, H., Reid, A. J., Natarajan, K., et al. (2019). The malaria cell atlas: Single parasite transcriptomes across the complete plasmodium life cycle. *Science* 365 (6455), eaaw2619. doi: 10.1126/SCIENCE.AAW2619

Inbar, E., Eappen, A. G., Alford, R. T., Reid, W., Harrell, R. A., Hosseini, M., et al. (2021). Knockout of anopheles stephensi immune gene LRIM1 by CRISPR-Cas9 reveals its unexpected role in reproduction and vector competence. *PloS Pathog.* 17 (11), e1009770. doi: 10.1371/JOURNAL.PPAT.1009770

Inklaar, M. R., Barillas-Mury, C., and Jore, M. M. (2022). Deceiving and escaping complement – the evasive journey of the malaria parasite. *Trends Parasitol.* 38, 962–974. doi: 10.1016/J.PT.2022.08.013

Ishino, T., Murata, E., Tokunaga, N., Baba, M., Tachibana, M., Thongkukiatkul, A., et al. (2019). Rhoptry neck protein 2 expressed in plasmodium sporozoites plays a crucial role during invasion of mosquito salivary glands. *Cell Microbiol.* 21 (1), e12964. doi: 10.1111/CMI.12964

Itsara, L. S., Zhou, Y., Do, J., Dungel, S., Fishbaugher, M. E., Betz, W. W., et al. (2018). PfCap380 as a marker for plasmodium falciparum oocyst development *in vivo* and *in vitro*. *Malar J.* 17, 1–13. doi: 10.1186/s12936-018-2277-6

Janeh, M., Osman, D., and Kambris, Z. (2017). Damage-induced cell regeneration in the midgut of aedes albopictus mosquitoes. *Sci. Rep.* 7 (1), 1–10. doi: 10.1038/SREP44594

Janeh, M., Osman, D., and Kambris, Z. (2019). Comparative analysis of midgut regeneration capacity and resistance to oral infection in three disease-vector mosquitoes. *Sci. Rep.* 9 (1), 14556. doi: 10.1038/S41598-019-50994-4

Kariu, T., Ishino, T., Yano, K., Chinzei, Y., and Yuda, M. (2006). CelTOS, a novel malarial protein that mediates transmission to mosquito and vertebrate hosts. *Mol. Microbiol.* 59, 1369–1379. doi: 10.1111/J.1365-2958.2005.05024.X

Kaur, P., Jin, H. J., Lusk, J. B., and Tolwinski, N. S. (2018). Modeling the role of wnt signaling in human and drosophila stem cells. *Genes (Basel)* 9 (2), 101. doi: 10.3390/GENES9020101

Keleta, Y., Ramelow, J., Cui, L., and Li, J. (2021). Molecular interactions between parasite and mosquito during midgut invasion as targets to block malaria transmission. *NPJ Vaccines* 6, 1–9. doi: 10.1038/s41541-021-00401-9

Kojin, B. B., and Adelman, Z. N. (2019). The sporozoite's journey through the mosquito: A critical examination of host and parasite factors required for salivary gland invasion. *Front. Ecol. Evol.* 7. doi: 10.3389/fevo.2019.00284

Kudyba, H. M., Cobb, D. W., Vega-Rodriguez, J., and Muralidharan, V. (2021). Some conditions apply: Systems for studying plasmodium falciparum protein function. *PloS Pathog.* 17 (4), e1009442. doi: 10.1371/JOURNAL.PPAT.1009442

Kwon, H., Mohammed, M., Franzén, O., Ankarklev, J., and Smith, R. C. (2021). Single-cell analysis of mosquito hemocytes identifies signatures of immune cell subtypes and cell differentiation. *Elife* 10, e66192. doi: 10.7554/ELIFE.66192

Lacroix, C., Giovannini, D., Combe, A., Bargieri, D. Y., Späth, S., Panchal, D., et al. (2011). FLP/FRT-mediated conditional mutagenesis in pre-erythrocytic stages of plasmodium berghei. *Nat. Protoc.* 6, 1412–1428. doi: 10.1038/NPROT.2011.363

Laurentino, E. C., Taylor, S., Mair, G. R., Lasonder, E., Bartfai, R., Stunnenberg, H. G., et al. (2011). Experimentally controlled downregulation of the histone chaperone FACT in plasmodium berghei reveals that it is critical to male gamete fertility. *Cell Microbiol.* 13, 1956–1974. doi: 10.1111/J.1462-5822.2011.01683.X

Lefèvre, T., Vantaux, A., Dabiré, K. R., Mouline, K., and Cohuet, A. (2013). Non-genetic determinants of mosquito competence for malaria parasites. *PloS Pathog.* 9, e1003365. doi: 10.1371/JOURNAL.PPAT.1003365

Li, J., Wang, X., Zhang, G., Githure, J. I., Yan, G., and James, A. A. (2013). Genome-block expression-assisted association studies discover malaria resistance genes in anopheles gambiae. *Proc. Natl. Acad. Sci. U.S.A.* 110, 20675–20680. doi: 10.1073/pnas.1321024110

Longo, S. K., Guo, M. G., Ji, A. L., and Khavari, P. A. (2021). Integrating single-cell and spatial transcriptomics to elucidate intercellular tissue dynamics. *Nat. Rev. Genet.* 22, 627–644. doi: 10.1038/s41576-021-00370-8

Mancio-Silva, L., Gural, N., Real, E., Sattabongkot, J., Shalek, A. K., Bhatia Correspondence, S. N., et al. (2022). Ll resource a single-cell liver atlas of plasmodium vivax infection. *Cell Host Microbe* 30, 1–13. doi: 10.1016/j.chom.2022.03.034

Marchetti, M., Zhang, C., and Edgar, B. A. (2022). An improved organ explant culture method reveals stem cell lineage dynamics in the adult drosophila intestine. *Elife* 11, 1–63. doi: 10.7554/ELIFE.76010

McClean, C. M., Alvarado, H. G., Neyra, V., Llanos-Cuentas, A., and Vinetz, J. M. (2010). Optimized *in vitro* production of plasmodium vivax ookinetes. *Am. J. Trop. Med. Hyg* 83, 1183–1186. doi: 10.4269/AJTMH.2010.10-0195

Mendes, A. M., Awono-Ambene, P. H., Nsango, S. E., Cohuet, A., Fontenille, D., Kafatos, F. C., et al. (2011). Infection intensity-dependent responses of anopheles gambiae to the african malaria parasite plasmodium falciparum. *Infect. Immun.* 79, 4708–4715. doi: 10.1128/iai.05647-11

Mishra, R., Hua, G., Bagal, U. R., Champagne, D. E., and Adang, M. J. (2022). Anopheles gambiae strain (Ag55) cultured cells originated from anopheles coluzzii and are phagocytic with hemocyte-like gene expression. *Insect Sci.* 29 (5), 1346–1360. doi: 10.1111/1744-7917.13036

Miura, K., Stone, W. J. R., Koolen, K. M., Deng, B., Zhou, L., Van Gemert, G. J., et al. (2016). An inter-laboratory comparison of standard membrane-feeding assays for evaluation of malaria transmission-blocking vaccines. *Malar J.* 15, 1–9. doi: 10.1186/s12936-016-1515-z

Miura, K., Swihart, B. J., Fay, M. P., Kumpitak, C., Kiattibutr, K., Sattabongkot, J., et al. (2020). Evaluation and modeling of direct membrane-feeding assay with plasmodium vivax to support development of transmission blocking vaccines. *Sci. Rep.* 10, 12569. doi: 10.1038/s41598-020-69513-x

Mohammed, M., Dziedziech, A., Sekar, V., Ernest, M., Alves E Silva, T. L., Balan, B., et al. (2023). Single-cell transcriptomics to define plasmodium falciparum stage transition in the mosquito midgut. *Microbiol. Spectr.* 27, e0367122. doi: 10.1128/SPECTRUM.03671-22

Molina-Cruz, A., Canepa, G. E., Alves E Silva, T. L., Williams, A. E., Nagyal, S., Yenkoidiok-Douti, L., et al. (2020). Plasmodium falciparum evades immunity of anopheline mosquitoes by interacting with a Pfs47 midgut receptor. *Proc. Natl. Acad. Sci. U.S.A.* 117, 2597–2605. doi: 10.1073/PNAS.1917042117

Nikolaev, M., Mitrofanova, O., Broguiere, N., Geraldo, S., Dutta, D., Tabata, Y., et al. (2020). Homeostatic mini-intestines through scaffold-guided organoid morphogenesis. *Nature* 585, 574–578. doi: 10.1038/s41586-020-2724-8

Niu, G., Cui, Y., Wang, X., Keleta, Y., and Li, J. (2021). Studies of the parasite-midgut interaction reveal plasmodium proteins important for malaria transmission to mosquitoes. *Front. Cell Infect. Microbiol.* 11. doi: 10.3389/fcimb.2021.654216

Nötzel, C., and Kafsack, B. F. C. (2021). There and back again: malaria parasite single-cell transcriptomics comes full circle. *Trends Parasitol.* 37, 850–852. doi: 10.1016/j.pt.2021.07.011

Nozaki, M., Baba, M., Tachibana, M., Tokunaga, N., Torii, M., and Ishino, T. (2020). Detection of the rhoptry neck protein complex in plasmodium sporozoites and its contribution to sporozoite invasion of salivary glands. *mSphere* 5 (4), :e00325–20. doi: 10.1128/MSPHERE.00325-20

Okombo, J., Kanai, M., Deni, I., and Fidock, D. A. (2021). Genomic and genetic approaches to studying antimalarial drug resistance and plasmodium biology. *Trends Parasitol.* 37, 476. doi: 10.1016/J.PT.2021.02.007

Omorou, R., Bin Sa'id, I., Delves, M., Severini, C., Kouakou, Y. I., Bienvenu, A.-L., et al. (2022). Protocols for plasmodium gametocyte production *in vitro*: an integrative review and analysis. *Parasites Vectors* 15, 1–12. doi: 10.1186/S13071-022-05566-3

Osta, M. A., Christophides, G. K., and Kafatos, F. C. (2004). Effects of mosquito genes on plasmodium development. *Science* 303, 2030–2032. doi: 10.1126/SCIENCE.1091789

Pance, A. (2021). The stem cell revolution revealing protozoan parasites' secrets and paving the way towards vaccine development citation: Pance, a. the stem cell revolution revealing protozoan parasites' secrets and paving the way towards vaccine development. *Vaccines (Basel)* 9 (2), 105. doi: 10.3390/vaccines9020105

Pance, A., Ling, B., Mwikali, K., Koutsourakis, M., Agu, C., Rouhani, F., et al. (2021). Stem cell technology provides novel tools to understand human variation in plasmodium falciparum malaria. *bioRxiv*, 2021.06.30.450498. doi: 10.1101/2021.06.30.450498

Pietri, J. E., Pietri, E. J., Potts, R., Riehle, M. A., and Luckhart, S. (2015). Plasmodium falciparum suppresses the host immune response by inducing the synthesis of insulin-like peptides (ILPs) in the mosquito anopheles stephensi. *Dev. Comp. Immunol.* 53, 134. doi: 10.1016/J.DCI.2015.06.012

Ponnudurai, T., Meuwissen, J. H. E. T. H., Leeuwenberg, A. D. E. M., Verhave, J. P., and Lensen, A. H. W. (1982). The production of mature gametocytes of plasmodium falciparum in continuous cultures of different isolates infective to mosquitoes. *Trans. R Soc. Trop. Med. Hyg* 76, 242–250. doi: 10.1016/0035-9203(82)90289-9

Porter-Kelley, J. M., Dinglasan, R. R., Alam, U., Ndeta, G. A., Sacci, J. B., and Azad, A. F. (2006). Plasmodium yoelii: Axenic development of the parasite mosquito stages. *Exp. Parasitol.* 112, 99–108. doi: 10.1016/J.EXPPARA.2005.09.011

Pringle, S., Maimets, M., van der Zwaag, M., Stokman, M. A., van Gosliga, D., Zwart, E., et al. (2016). Human salivary gland stem cells functionally restore radiation damaged salivary glands. *Stem Cells* 34, 640–652. doi: 10.1002/STEM.2278

Raddi, G., Barletta, A. B. F., Efremova, M., Ramirez, J. L., Cantera, R., Teichmann, S. A., et al. (2020). Mosquito cellular immunity at single-cell resolution. *Science* 369, 1128–1132. doi: 10.1126/SCIENCE.ABC0322

Ramírez-Flores, C. J., Tibabuzo Perdomo, A. M., Gallego-López, G. M., and Knoll, L. J. (2022). Transcending dimensions in apicomplexan research: from two-dimensional to three-dimensional *In vitro* cultures. *Microbiol. Mol. Biol. Rev.* 86 (2), e0002522. doi: 10.1128/MMBR.00025-22

Randall, K. J., Turton, J., and Foster, J. R. (2011). Explant culture of gastrointestinal tissue: A review of methods and applications. *Cell Biol. Toxicol.* 27, 267–284. doi: 10.1007/s10565-011-9187-5

Real, E., Howick, V. M., Dahalan, F. A., Witmer, K., Cudini, J., Andradi-Brown, C., et al. (2021). A single-cell atlas of plasmodium falciparum transmission through the mosquito. *Nat. Commun.* 12 (1), 3196. doi: 10.1038/S41467-021-23434-Z

Real, E., and Mancio-Silva, L. (2022). Single-cell views of the plasmodium life cycle. *Trends Parasitol.* 38 (9), 748–757. doi: 10.1016/J.PT.2022.05.009

Ripp, J., Kehrer, J., Smyrnakou, X., Tisch, N., Tavares, J., Amino, R., et al. (2021). Malaria parasites differentially sense environmental elasticity during transmission. *EMBO Mol. Med.* 13, e13933. doi: 10.15252/EMMM.202113933

Ruiz, J. L., and Gómez-Díaz, E. (2019). The second life of plasmodium in the mosquito host: gene regulation on the move. *Brief Funct. Genomics* 18, 313–357. doi: 10.1093/BFGP/ELZ007

Russo, I., Zeppa, P., Iovino, P., del Giorno, C., Zingone, F., Bucci, C., et al. (2016). The culture of gut explants: A model to study the mucosal response. *J. Immunol. Methods* 438, 1–10. doi: 10.1016/J.JIM.2016.07.004

Sato, Y., Montagna, G. N., and Matuschewski, K. (2014). Plasmodium berghei sporozoites acquire virulence and immunogenicity during mosquito hemocoel transit. *Infect. Immun.* 82, 1164. doi: 10.1128/IAI.00758-13

Shaw, W. R., Marcenac, P., and Catteruccia, F. (2022). Plasmodium development in anopheles: a tale of shared resources. *Trends Parasitol.* 38, 124–135. doi: 10.1016/J.PT.2021.08.009

Siciliano, G., Costa, G., Suárez-Cortés, P., Valleriani, A., Alano, P., and Levashina, E. A. (2020). Critical steps of plasmodium falciparum ookinete maturation. *Front. Microbiol.* 11. doi: 10.3389/fmicb.2020.00269

Siden-Kiamos, I., Ganter, M., Kunze, A., Hliscs, M., Steinbüchel, M., Mendoza, J., et al. (2011). Stage-specific depletion of myosin a supports an essential role in motility of malarial ookinetes. *Cell Microbiol.* 13, 1996–2006. doi: 10.1111/J.1462-5822.2011.01686.X

Simões, M. L., Caragata, E. P., and Dimopoulos, G. (2018). Diverse host and restriction factors regulate mosquito–pathogen interactions. *Trends Parasitol.* 34, 603–616. doi: 10.1016/J.PT.2018.04.011

Simões, M. L., Mlambo, G., Tripathi, A., Dong, Y., and Dimopoulos, G. (2017). Immune regulation of plasmodium is anopheles species specific and infection intensity dependent. *mBio* 8 (5), e01631–17. doi: 10.1128/MBIO.01631-17

Sinden, R. E., Alavi, Y., and Raine, J. D. (2004). Mosquito–malaria interactions: a reappraisal of the concepts of susceptibility and refractoriness. *Insect Biochem. Mol. Biol.* 34, 625–629. doi: 10.1016/J.IBMB.2004.03.015

Swevers, L., Denecke, S., Vogelsang, K., Geibel, S., and Vontas, J. (2021). Can the mammalian organoid technology be applied to the insect gut? *Pest Manag Sci.* 77, 55–63. doi: 10.1002/PS.6067

Tanaka, J., Ogawa, M., Hojo, H., Kawashima, Y., Mabuchi, Y., Hata, K., et al. (2018). Generation of orthotopically functional salivary gland from embryonic stem cells. *Nat. Commun.* 9, 1–13. doi: 10.1038/s41467-018-06469-7

Taracena, M. L., Bottino-Rojas, V., Talyuli, O. A. C., Walter-Nuno, A. B., Oliveira, J. H. M., Angleró-Rodriguez, Y. I., et al. (2018). Regulation of midgut cell proliferation impacts aedes aegypti susceptibility to dengue virus. *PloS Negl. Trop. Dis.* 12 (5), e0006498. doi: 10.1371/JOURNAL.PNTD.0006498

Taracena, M., Hunt, C., Pennington, P., Andrew, D., Jacobs-Lorena, M., Dotson, E., et al. (2022). Effective oral RNA interference (RNAi) administration to adult anopheles gambiae mosquitoes. *J. Vis. Exp.* 2022 (181), 10.3791/63266. doi: 10.3791/63266

Thomson-Luque, R., and Bautista, J. M. (2021). Home sweet home: Plasmodium vivax-infected reticulocytes–the younger the better? *Front. Cell Infect. Microbiol.* 11. doi: 10.3389/fcimb.2021.675156

Tibúrcio, M., Yang, A. S. P., Yahata, K., Suárez-Cortés, P., Belda, H., Baumgarten, S., et al. (2019). A novel tool for the generation of conditional knockouts to study gene function across the plasmodium falciparum life cycle. *mBio* 10 (5), e01170–e01119. doi: 10.1128/MBIO.01170-19

Touray, M. G., Warburg, A., Laughinghouse, A., Krettli, A. U., and Miller, L. H. (1992). Developmentally regulated infectivity of malaria sporozoites for mosquito salivary glands and the vertebrate host. *J. Exp. Med.* 175, 1607–1612. doi: 10.1084/JEM.175.6.1607

Vallejo, A. F., Rubiano, K., Amado, A., Krystosik, A. R., Herrera, S., and Arévalo-Herrera, M. (2016). Optimization of a membrane feeding assay for plasmodium vivax infection in anopheles albimanus. *PloS Negl. Trop. Dis.* 10, e0004807. doi: 10.1371/JOURNAL.PNTD.0004807

Vaughan, A. (2021). Motile mosquito stage malaria parasites: ready for their close-up. *EMBO Mol. Med.* 13, e13975. doi: 10.15252/EMMM.202113975

Venugopal, K., Hentzschel, F., Valkiūnas, G., and Marti, M. (2020). Plasmodium asexual growth and sexual development in the haematopoietic niche of the host. *Nat. Rev. Microbiol.* 18, 177–189. doi: 10.1038/S41579-019-0306-2

Vlachou, D., Zimmermann, T., Cantera, R., Janse, C. J., Waters, A. P., and Kafatos, F. C. (2004). Real-time, *in vivo* analysis of malaria ookinete locomotion and mosquito midgut invasion. *Cell Microbiol.* 6, 671–685. doi: 10.1111/J.1462-5822.2004.00394.X

Walker, T., Jeffries, C. L., Mansfield, K. L., and Johnson, N. (2014). Mosquito cell lines: History, isolation, availability and application to assess the threat of arboviral transmission in the united kingdom. *Parasit Vectors* 7, 1–9. doi: 10.1186/1756-3305-7-382

Wall, R. J., Ferguson, D. J. P., Freville, A., Franke-Fayard, B., Brady, D., Zeeshan, M., et al. (2018). Plasmodium APC3 mediates chromosome condensation and cytokinesis during atypical mitosis in male gametogenesis. *Sci. Rep.* 8, 1–10. doi: 10.1038/s41598-018-23871-9

Warburg, A., and Miller, L. H. (1992). Sporogonic development of a malaria parasite in vitro. *Sci. (1979)* 255, 448–450. doi: 10.1126/SCIENCE.1734521

Warburg, A., and Schneider, I. (1993). *In vitro* culture of the mosquito stages of plasmodium falciparum. *Exp. Parasitol.* 76, 121–126. doi: 10.1006/EXPR.1993.1014

Wassim, N. M., Soliman, B. A., Hussein, M. I., and Metwaly, H. G. (2014). Isolation of stem cells from the mid gut epithelium of culex pipiens mosquitoes (Diptera: Culicidae). *J. Egypt Soc. Parasitol.* 44, 13–20. doi: 10.12816/0006440

WHO (2022) *World malaria report 2022* (Geneva, Switzerland: World Health Organization). Available at: https://www.who.int/teams/global-malaria-programme/reports/world-malaria-report-2022 (Accessed January 16, 2023).

Williams, C. G., Lee, H. J., Asatsuma, T., Vento-Tormo, R., and Haque, A. (2022). An introduction to spatial transcriptomics for biomedical research. *Genome Med.* 14, 1–18. doi: 10.1186/s13073-022-01075-1

Witmer, K., Dahalan, F. A., Metcalf, T., Talman, A. M., Howick, V. M., and Lawniczak, M. K. N. (2021). Using scRNA-seq to identify transcriptional variation in the malaria parasite ookinete stage. *Front. Cell Infect. Microbiol.* 11. doi: 10.3389/fcimb.2021.604129

Yu, S., Wang, J., Luo, X., Zheng, H., Wang, L., Yang, X., et al. (2022). Transmission-blocking strategies against malaria parasites during their mosquito stages. *Front. Cell Infect. Microbiol.* 12. doi: 10.3389/fcimb.2022.820650

Zeeshan, M., Pandey, R., Ferguson, D. J. P., Tromer, E. C., Markus, R., Abel, S., et al. (2021). Real-time dynamics of plasmodium NDC80 reveals unusual modes of chromosome segregation during parasite proliferation. *J. Cell Sci.* 134 (5), jcs245753. doi: 10.1242/JCS.245753

Zhang, G., Niu, G., Franca, C. M., Dong, Y., Wang, X., Butler, N. S., et al. (2015). Anopheles midgut FREP1 mediates plasmodium invasion *. *J. Biol. Chem.* 290, 16490–16501. doi: 10.1074/JBC.M114.623165

Zhang, M., Wang, C., Otto, T. D., Oberstaller, J., Liao, X., Adapa, S. R., et al. (2018). Uncovering the essential genes of the human malaria parasite plasmodium falciparum by saturation mutagenesis. *Sci. (1979)* 360 (6388), eaap7847. doi: 10.1126/science.aap7847

Zieler, H., and Dvorak, J. A. (2000). Invasion *in vitro* of mosquito midgut cells by the malaria parasite proceeds by a conserved mechanism and results in death of the invaded midgut cells. *Proc. Natl. Acad. Sci. U.S.A.* 97, 11516–11521. doi: 10.1073/pnas.97.21.11516

frontiers | Frontiers in Cellular and Infection Microbiology

TYPE Review
PUBLISHED 29 May 2023
DOI 10.3389/fcimb.2023.1134471

OPEN ACCESS

EDITED BY
Gabriel Rinaldi,
Aberystwyth University, United Kingdom

REVIEWED BY
Mattie Christine Pawlowic,
University of Dundee, United Kingdom
Daniel R. G. Price,
Moredun Research Institute,
United Kingdom

*CORRESPONDENCE
Romina Pagotto
pagotto@pasteur.edu.uy
María E. Francia
mfrancia@pasteur.edu.uy

RECEIVED 30 December 2022
ACCEPTED 25 April 2023
PUBLISHED 29 May 2023

CITATION
Sena F, Cancela S, Bollati-Fogolín M, Pagotto R and Francia ME (2023) Exploring *Toxoplasma gondii*´s Biology within the Intestinal Epithelium: intestinal-derived models to unravel sexual differentiation. *Front. Cell. Infect. Microbiol.* 13:1134471. doi: 10.3389/fcimb.2023.1134471

Exploring *Toxoplasma gondii*´s Biology within the Intestinal Epithelium: intestinal-derived models to unravel sexual differentiation

Florencia Sena[1,2], Saira Cancela[3,4], Mariela Bollati-Fogolín[3,4], Romina Pagotto[3]* and María E. Francia[1,5]*

[1]Laboratory of Apicomplexan Biology, Institut Pasteur Montevideo, Montevideo, Uruguay, [2]Laboratorio de Bioquímica, Departamento de Biología Vegetal, Universidad de la República, Montevideo, Uruguay, [3]Cell Biology Unit, Institut Pasteur Montevideo, Montevideo, Uruguay, [4]Molecular, Cellular, and Animal Technology Program (ProTeMCA), Institut Pasteur Montevideo, Montevideo, Uruguay, [5]Departamento de Parasitología y Micología, Facultad de Medicina, Universidad de la República, Montevideo, Uruguay

A variety of intestinal-derived culture systems have been developed to mimic *in vivo* cell behavior and organization, incorporating different tissue and microenvironmental elements. Great insight into the biology of the causative agent of toxoplasmosis, Toxoplasma gondii, has been attained by using diverse *in vitro* cellular models. Nonetheless, there are still processes key to its transmission and persistence which remain to be elucidated, such as the mechanisms underlying its systemic dissemination and sexual differentiation both of which occur at the intestinal level. Because this event occurs in a complex and specific cellular environment (the intestine upon ingestion of infective forms, and the feline intestine, respectively), traditional reductionist *in vitro* cellular models fail to recreate conditions resembling *in vivo* physiology. The development of new biomaterials and the advances in cell culture knowledge have opened the door to a next generation of more physiologically relevant cellular models. Among them, organoids have become a valuable tool for unmasking the underlying mechanism involved in *T. gondii* sexual differentiation. Murine-derived intestinal organoids mimicking the biochemistry of the feline intestine have allowed the generation of pre-sexual and sexual stages of *T. gondii* for the first time *in vitro*, opening a window of opportunity to tackling these stages by "felinizing" a wide variety of animal cell cultures. Here, we reviewed intestinal *in vitro* and ex vivo models and discussed their strengths and limitations in the context of a quest for faithful models to *in vitro* emulate the biology of the enteric stages of *T. gondii*.

KEYWORDS

Toxoplasma gondii*, sexual differentiation, felinization, intestine, *in vitro* models, *ex vivo models

1 Introduction

Apicomplexans make up a large phylum of parasites characterized by the presence of an apical complex of secretory organelles which allows them to interact with, and invade, their host cell of preference. Beyond the conservation of these organelles, apicomplexan parasites differ greatly in their biology, including the range of host species, and even the cell type they invade within a host (Dubey, 2009). *Toxoplasma gondii*, the causative agent of toxoplasmosis, is arguably one of the most promiscuous parasites within the phylum in terms of host range and cell type preferences. Its multiple routes of infection, ample host cell range (virtually any warm-blooded species), host cell invasion capacity (virtually any nucleated cell), and capacity to chronically persist, render it one of the most successful zoonotic parasites of humans and animals worldwide (Flegr et al., 2014).

T. gondii can be transmitted among animals through the carnivory of persistent cysts lodged in skeletal muscle or brain tissue. Likewise, the parasite is able to cross the placenta and infect the developing fetus if acquired during pregnancy. Finally, it can be ingested from the environment in the form of environmentally resistant oocysts, shed by felids in their feces (Dubey, 2006; Arranz-Solís et al., 2021). The best-studied life stage of the parasite is called the tachyzoite. This fast-replicating form of the parasite is responsible for acute toxoplasmosis. Tachyzoites can be readily grown and maintained *in vitro*, and a plethora of tools for their genetic manipulation have been developed. Though acute infection is the most clinically relevant, the vast majority of acute toxoplasmosis goes unnoticed in immunocompetent individuals quickly turning into latent chronic infections (Pittman and Knoll, 2015). Chronic stages arise by a switch in parasite metabolism to the slow replicating, latent, bradyzoite form. Bradyzoites persist in immune-privileged anatomical sites, such as the brain and the eye, and within skeletal muscle. However, bradyzoites can reactivate if the immune pressure decays. Multiple iterations of reactivation of latent bradyzoites in the eye cause progressive eye loss, even in immunocompetent patients (Sullivan and Jeffers, 2012). Carnivorism of bradyzoites infected tissue leads to their reactivation in the host's intestine, and the systemic dissemination of tachyzoites, thereby closing the cycle of transmission among intermediate hosts (Cerutti et al., 2020). On the other hand, when a wild or domestic felid consumes bradyzoite-infected tissue or an oocyst from the environment, the parasite initiates its sexual differentiation cycle within the cat's intestinal epithelium. Pre-sexual stages of the parasite include merozoites and gamonts, which eventually lead to the formation of fully differentiated gametes. Gametes can sexually recombine, forming oocyst precursor stages, which eventually lead to the shedding of environmentally resistant unsporulated oocyst. Environmental exposure to oxygen induces sporulation, leading to infective oocysts loaded with sporozoites which can persist in the environment for years (Ferguson, 2002) (Figure 1A).

In vitro modeling of the life stages of *T. gondii* has been traditionally limited to 2D cultures whereby the tachyzoite form expands quickly and efficiently, allowing for the generation of large amounts of material for different analyses. This has served to study genome modifications, gene expression control, the parasite's kinome, secretome, proteome, phospho-proteome and genome-wide gene essentiality, among others, using tachyzoites. Despite the importance of persistence of the chronic forms and the role played by cats in the dissemination of *T. gondii*, our understanding of these aspects of parasitic life is limited. Their anatomical sequestration to inaccessible sites such as the brain and eye, and the lack of *in vitro* models to recreate some life stages *ex vivo* challenge our access to their biology. In particular, the interplay among tachyzoites, bradyzoites, and host factors, in the context of stage transitions within the intestinal epithelium cannot thus far be mimicked in traditional 2D cultures. The study of these aspects of parasite biology has traditionally relied on animal models, encompassing a number of unavoidable experimental limitations. However, recent technological breakthroughs in 2D and 3D culture systems provide promising routes for exploring aspects of parasitic life traditionally inaccessible. Herein, we review the state of the art in *in vitro* intestinal models and highlight their potential applications for characterizing different life forms of *T. gondii* within the enteric epithelium. We focus on the challenges and experimental opportunities offered by these up-and-coming experimental platforms for studying the sexual stages of *T. gondii*.

2 Intestine structure

The small intestine, part of the gastrointestinal system, is divided into three sections: duodenum, jejunum, and ileum (Carr and Toner, 1984). The intestinal mucosa comprises the epithelium, the underlying lamina propria, and a thin muscle layer called muscularis mucosa. Together, the lamina propria and the intestinal epithelium are organized into finger-like protrusions known as villi, interspaced by pocket-like invaginations called crypts. The crypt contains intestinal stem cells (ISCs) and Paneth cells characterized by the presence of dense granules containing antimicrobial peptides (AMPs). Paneth cells are interspersed with the ISCs contributing together to the intestinal stem cell niche (Antfolk and Jensen, 2020). The villi contain differentiated cell types collectively known as intestinal epithelial cells (IECs). IECs are frequently replaced by intestinal epithelial stem cells originating at the bottom of crypts, which differentiate along the villus in the so-called crypt-villus axis. Goblet cells provide a protective barrier and help lubricate the inner wall of the intestine layer by producing mucus over the intestinal epithelium. Finally, enteroendocrine cells carry out endocrine functions (Hewes et al., 2020). Additionally, the intestinal epithelium permanently interplays with the immune system; approximately 70% of immune cells are in the gut (Wiertsema et al., 2021).

3 *Toxoplasma gondii* within the intestine

Upon oral infection *via* carnivory or interaction with environmental sporulated oocysts (Figure 1A), parasites enter the

10.3389/fcimb.2023.1134471

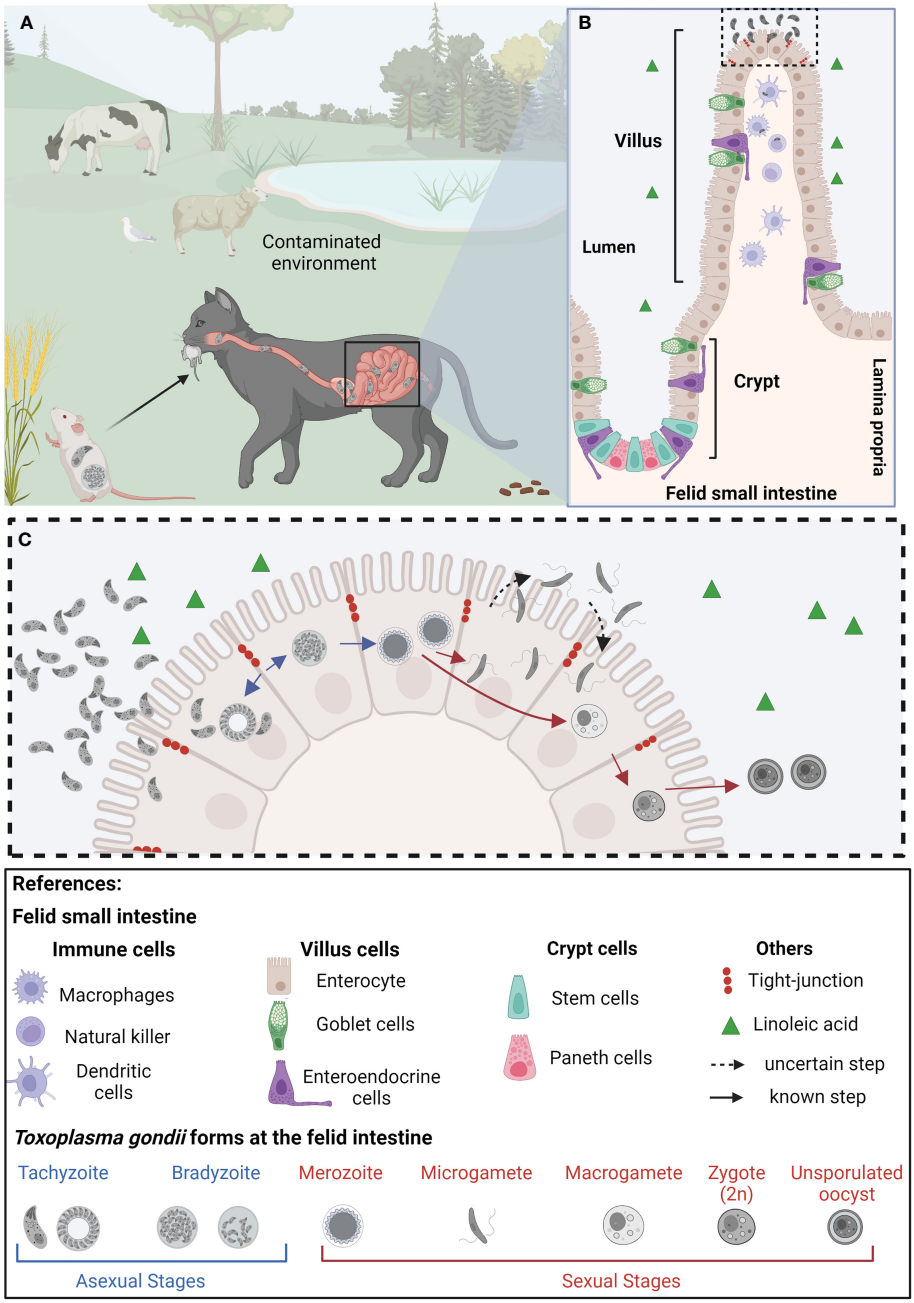

FIGURE 1
Representation of the life cycle of *Toxoplasma gondii* in epithelial cells of the small intestine of felids. **(A)** Felids acquire *Toxoplasma gondii* through consumption of contaminated food and/or water. Once in the small intestine's epithelium, tachyzoites replicate and differentiate into bradyzoites. **(B)** The felid small intestinal epithelium is composed of diverse specialized cell types, all of them originating from intestinal stem cells, located at the base of the crypts. The feline intestinal environment, characterized by the absence of the delta-6-desaturase enzyme, and a consequent increased level of linoleic acid, is the only anatomical site and biochemical environment supporting *T. gondii's* sexual differentiation **(C)** In the epithelial cells, *T. gondii* bradyzoites (haploid cell; 1n) differentiate into merozoites (1n), which further give rise to microgametes (1n) and macrogametes (1n). Through mechanisms not yet completely understood, the microgamete fertilizes the macrogamete generating the zygote (immature oocyst, 2n). These diploid cells are then shed as unsporulated oocysts in the felid's feces, contaminating plants and water sources in the environment, becoming potentially infective to other animals, leading to the beginning of a new infective cycle. Created with BioRender.com.

gastrointestinal system of both intermediate and definitive hosts within days. The cyst wall protects them from the acidic gastric pH and ensures the passage to the small intestine where they excyst upon contact with bile salts and trypsin (Dubey et al., 1998). Parasite invasion and replication takes place at the intestinal villi and subsequently tachyzoites are released into the intestinal lumen, able to invade neighboring villi cells and to disseminate within the host *via* the lamina propria (Dubey, 1997). *T. gondii* dissemination across the different biologic barriers of the gastrointestinal tract requires the activation of specific invasion, attachment, and

transmigration mechanisms which fast-tracks their dissemination to different tissues, such as lymph nodes, heart, eye and brain (Jones et al., 2017).

The initial steps of *T. gondii* infection within the gut rely on its ability to rapidly cross the epithelial barrier of the small intestine (Figure 1B). Astonishingly, this process takes place in a matter of seconds (Jones et al., 2017). Strategies used by *T. gondii* to cross the intestinal epithelium and reach the lamina propria include invasion of the intestinal epithelial cells, transepithelial migration, or by means of a "Trojan horse" mechanism, whereby *T. gondii* hijacks diverse immune cells to go undercover (Dobrowolski and Sibley, 1996; Barragan et al., 2005; Gregg et al., 2013). Parasites actively invade a wide range of cells including intestinal as well as immune cells and undergo an intracellular asexual lytic cycle of intracellular growth and multiplication before rupturing the host cells (Black and Boothroyd, 2000).

Release of newly formed tachyzoites into both the intestinal lumen and underlying tissues of the lamina propria, activate an acute immune response by secretion of a host of inflammatory factors by intestinal tissue-resident cells (Pittman and Knoll, 2015). The recognition of *T. gondii* by cellular innate sensors is the first line of host defense triggering the production of proinflammatory cytokines such as IL-1β and TNF-α by macrophages, neutrophils, and dendritic cells (Coombes et al., 2013; Sasai and Yamamoto, 2019). Altogether, these play a crucial role in the activation of the host immune responses which might ultimately trigger the switch from tachyzoite to bradyzoite (Cerutti et al., 2020).

3.1 Sexual differentiation of *Toxoplasma gondii*

Members of the *Felidae* family act as the only definitive hosts of *T. gondii* being responsible for its horizontal transmission through the distribution of infective oocysts released in their feces (Dubey, 2006). *Via* carnivorism, bradyzoites access the feline intestinal epithelium where they differentiate into merozoites, initiating the parasite's sexual differentiation track (Weiss, 2000; Dubey, 2006). Sexual differentiation encompasses gametogenesis which implies the formation of macro (♀) and microgametes (♂). Their fusion generates diploid zygotes that eventually encyst and are shed in cat's feces as immature oocysts sporulating and becoming infective in the environment (Sibley et al., 2009).

Within the feline intestine bradyzoites turn into merozoites, initiating sexual differentiation. For fertilization to take place, microgametes generated within the feline small intestine swim through the intestinal lumen to find a host cell containing a macrogamete (Ferguson, 2002) (Figure 1C). Ultimately, oocyst formation depends on microgamete motility; in turn, their ability to move lies in their ultrastructure. The ultrastructure of the sexual stages was well documented by electron microscopy studies over 50 years ago, studying small intestine of cats orally infected with *T. gondii* cysts (Pelster and Piekarski, 1971; Dubey and Frenkeñ, 1972; Scholtyseck et al., 1972; Ferguson et al., 1975). The stages of *T. gondii* giving rise to sexual forms differ from each other regarding the number of apical organelles, the shape and electron density of the rhoptries, the location of the nucleus, and the presence or absence of polysaccharide granules (Ferguson and Dubremetz, 2020). The merozoite becomes more spherical and loses the majority of its apical organelles, such as the rhoptries and dense granules, and appears to increase the size of its mitochondrion, which locates at the cell periphery. Sexual-specific organelles are unique signatures of sexual forms of *T. gondii*. Microgametes have an ellipsoid-shaped morphology with two motile flagella per cell assembled at the microgamete´s apex. During differentiation to microgametes, the parasite undergoes schizogony, a cell division mechanism that generates a syncytium-like cell bearing multiple nuclei. Nuclei move to the periphery of the cell with two centrioles, which presumably become basal bodies of the developing flagella. Flagella grow by protruding out into the parasitophorous vacuole. The flagellar axonemes are canonical in ultrastructure, being composed of nine microtubule duplets and a central pair (9 + 2), similar to what is observed in other apicomplexans (Ferguson, 2002; Morrissette and Sibley, 2002; Francia et al., 2016; Tomasina and Francia, 2020). On the other hand, macrogametes have an oval shape and contain numerous electron dense structures within the cytosol named "wall forming bodies." During the development of the macrogamete there exists an increment in the size of the peripherally mitochondrion and the centrally located apicoplast. These changes are accompanied by the surge of an enlarged nucleus showcasing dispersed chromatin and a large nucleolus, with no accompanying nuclear mitosis (Ferguson and Dubremetz, 2020). The wall forming bodies contain polysaccharide granules, lipid droplets, and protein-rich wall forming bodies type W1 and W2 that will contribute to formation of the macrogamete (Freppel et al., 2019). Later on, these will play a crucial role in the formation of the oocyst wall (Ferguson et al., 1975; Ferguson and Dubremetz, 2020).

The study and identification of sexual differentiation components of coccidia parasites could powerfully impact our ability to design transmission-blocking strategies. For example, vaccines incorporating antigens from sexual stages could reduce oocyst formation (Cruz-Bustos et al., 2022). Genetic admixing can occur only if two genetically different strains coexist in the epithelium of the same feline. Therefore, fertilization is key to the generation of natural genetic diversity as this is the only phase in which the parasite exists in a transient state of diploidy. A recent study of 156 distinct parasite genomes present worldwide, concluded that the evolution of unique haplotypes of *T. gondii* generated by sexual admixing in cats, accompanied the evolution of felids from wild to domestic, and the family's expansion in the last five centuries to the Americas (Galal et al., 2022), illustrating the importance of this process. Moreover, understanding the molecular underpinnings of gametogenesis and gamete fusion, could open up the possibility of *in vitro* controlling sexual admixing, opening new avenues for the generation of hybrid strains with biotechnological potential.

The lack of convenient experimental models has long stymied molecular studies of sexual stages of coccidian parasites. The detailed cellular mechanisms governing differentiation, gamete fusion and fertilization have only recently begun to be clarified. Gene transcription analyses of the enteric stages of *T. gondii* could allow the identification of genes expressed in sexual stages providing the potential of being *in vitro* engineered stage conversion by modulating gene expression (Reviewed in

Ramakrishnan and Smith, 2021). Thus far, transcriptomic analyses have relied on *in vivo* generated sexual stages in orally infected felids. While the temporal resolution of these studies is hindered by the natural kinetics of differentiation whereby multiple stages are present at the gut at once, numerous important factors have been put forward as putative controllers of the differentiation process and as essential for fertilization. For example, the expression of the male gamete fusion factor HAP2 has been described as a key factor for *T. gondii* fertilization to take place (Ramakrishnan et al., 2019). This had been previously established for the ortholog in the malaria parasites whereby HAP2 was shown to be essential for fusion of gametes (Liu et al., 2008; Angrisano et al., 2017). *T. gondii* parasites lacking the microgamete-specific gamete fusion protein HAP2 fail at completing fertilization, undergo meiosis and consequently produce aberrant oocysts *in vivo* (Ramakrishnan et al., 2019).

The identification of the key transcription factors controlling gene expression components related to sexual commitment provides an overarching view of the regulatory networks underlying differentiation. A single validated class of apicomplexan transcription factors, the *apetalla* family of DNA binding proteins (ApiAP2s), has been extensively investigated as potential regulators and mediators of parasite differentiation (Sharma et al., 2020). In addition, microorchidia (MORC) was shown to complex with multiple AP2 transcription factors and the lysine deacetylase HDAC3 whose transcriptional control mediates transitions between asexual forms and also the onset of sexual differentiation. Remarkably, conditional silencing of MORC triggers the differentiation of *T. gondii* tachyzoites, in a 2D culture, into bradyzoites, merozoites, and gametocytes (Farhat et al., 2020). Recently, transcription factors from the AP2 family have been described to be implicated in silencing genes necessary for merozoites conversion and development of stages critical for sexual commitment (Antunes et al., 2023; Srivastava et al., 2023). A family member of AP2 transcription factors (AP2XII-2) has been identified to coordinate the recruitment of HDAC3/MORC complex to repress developmentally-controlled genes, such as the AP2X-10 (an oocyst specific AP2) and AAH1 (involved in oocyst maturation) (Srivastava et al., 2023). In addition, AP2XI-2 and AP2XII-1 heterodimers restrict the accessibility of chromatin to the transcriptional machinery by the recruitment of MORC and HDAC3 at merozoite promoter genes (Antunes et al., 2023). Finally, the post-translational N-glycosylation of multiple *T. gondii* proteins at the small intestine of cats orally infected with cysts has been documented (Zhai et al., 2022). However, how these modifications contribute to the sexual stages of *T. gondii* at the small intestine of felids remains unclear.

4 Intestinal *in vitro* and *ex vivo* models to study *T. gondii* biology

Despite its inherent importance and its potential for contributing to prophylactic strategies and biotechnology, little is known about the basic aspects of the mechanisms and biology of sexual differentiation in *T. gondii*. Traditionally, the study of this stage was ethically and technically hampered by the imperative need to use felid animal models. However, enteric cells of cats have arisen as a unique system to study the processes of sexual differentiation of *T. gondii*. In addition, a recent methodological breakthrough identified the biochemical fingerprint that triggers the differentiation of *T. gondii* to its sexual forms in the feline intestine. The study deciphered that a lack of delta-6-desaturase activity, exclusively lacking in the small intestines of cats, and the subsequent accumulation of linoleic acid, are sufficient to trigger the differentiation of *T. gondii* into its sexual stages (Di Genova et al., 2019). Remarkably, the use of a specific inhibitor of the delta-6-desaturase enzyme in mouse intestinal organoid derived monolayers infected with *T. gondii* enhanced the progression through the sexual stages (Di Genova et al., 2019). Furthermore, infected mice treated with a delta-6-desaturase inhibitor and fed a diet rich in linoleic acid resulted in meronts and gametes differentiation leading to infective oocyst shedding in their faces. These findings now allow the potential of "felinizing" 2D cultures of diverse, non-felid derived, origins. However, oocyst production is the ultimate indicator of efficient parasite sex; despite the fact that the feline enteric environment can be chemically mimicked *in vitro*, generating *T. gondii* sexual stages, fertilization does not take place. It is likely that additional factors are required for successful fertilization and oocyst production.

Below we contextualize the use of model systems in increasing order of model complexity (in terms of number of cellular types present, architecture and integration of physiological features) to study *T. gondii´*s biology within the intestine, particularly focusing on sexual differentiation.

4.1 Cell cultures from *Felidae* origin

Two dimensions (2D) cell culture is extremely useful in cell biology and has been widely implemented for the growth and propagation of different apicomplexan parasites (Ramírez-Flores et al., 2022). Traditionally, 2D cultures have served as powerful *in vitro* tools to study invasion, replication, and egress processes, profoundly impacting our understanding of these critical aspects of intracellular parasite life.

The establishment of an optimized system to grow primary Feline Epithelial Intestinal Cells (FEIC) and propagate them *in vitro* was successfully described (Zhao et al., 2018). Prior to this, primary cultures of FEIC obtained from the jejunum-ileum region had been explored as a tool to investigate the sexual differentiation of *T. gondii*, by infecting them with bradyzoites. The development of the syncytial-like forms of *T. gondii* were observed after 6 hours of infection, suggesting the presence of sexual stages of the parasite by light microscopy (Moura et al., 2009). Despite this, the use of FEICs monolayers has not been extensively adopted in the culturing of *T. gondii* most likely because of the complexity to obtain, propagate and preserve these cells (de Muno et al., 2014). In addition, there are ethical concerns with respect to the use of felids as experimental models.

Our understanding of the signals triggering sexual differentiation has exponentially increased. This is providing

researchers with the opportunity to genetically manipulate the parasite factors that repress expression of sexual differentiation specific genes. In addition, mimicking the biochemical environment of the felid's intestine, in any intestinal-derived *in vitro* model system is now also possible. This remarkable breakthrough provides an unprecedented opportunity to address biological questions of *T. gondii* gametogenesis that were inaccessible before without resorting to FEIC, expanding the breadth of cell lines that could be used to mimic these conditions in 2D cultures. In the next section we highlight the models based on cell lines not derived from felids, and their potential contribution to investigating both the mechanisms of intestinal pathogenesis and dissemination, and the complete sexual cycle of *T. gondii* by means of exogenous "felinization" (Table 1).

4.2 Human intestine-derived cell lines from immortalized, primary culture, and stem cells

Immortalized cell lines have been manipulated to proliferate indefinitely and can be cultured for long periods of time. A large number of such human intestinal cell lines have been established, such as, the well-known human colorectal adenocarcinoma-derived cell lines HT-29 and Caco-2. Human colon carcinoma-derived cell lines vary extensively in their degree of differentiation, proliferation, and metabolic properties (Rousset, 1986). Some of these cell lines are able to express differentiation features characteristic of mature intestinal cells, under certain conditions. Thus, Caco-2 cells, originally non polarized cells, can spontaneously differentiate into mature enterocytes with a basal and apical compartment clearly defined when seeded on filter inserts and culture for two to three weeks (Ferruzza et al., 2012). Under these culture conditions Caco-2 cells better recreate enterocyte morphology, with well-developed microvilli on the apical side, tight junctions between cells, and expression of specific hydrolase enzymes at the apical membrane (Sambuy et al., 2005; Verhoeckx, 2015).

T. gondii has successfully infected diverse intestinal cell lines, albeit only replicating asexually. Nevertheless, a bulk of studies have contributed to not only deciphering the mechanisms of *T. gondii* infection of enteroepithelial cells, but have also provided insight into the genetic, cellular, and biochemical mechanisms used by the parasite for dissemination. Caco-2 has been the most widely immortalized cell line used to model the infection of *T. gondii* in the enteric environment. Studies of *T. gondii* infection in Caco-2 cells have determined that infection leads to the loss of integrity of intestinal mucosa by increased paracellular permeability, reduction of transepithelial electrical resistance, loss of cytoskeleton organization, and redistribution of tight junction proteins as strategies to improve invasion (Barragan et al., 2005; Briceño et al., 2016; Ross et al., 2019).

Tight junctions (TJ) are selective gates that control paracellular diffusion of ions and solutes between cells (Zihni et al., 2016). Several enteric pathogens disrupt the TJ of intestinal epithelial cells as an infection strategy, and they have different ways to disrupt them. Tight junction proteins, such as occludin, claudins, zonula occludens (ZOs), and Ig-domain adhesion proteins (IgCAMs) are frequent targets of intestinal pathogens in the process of invasion and infection (Barragan et al., 2005; Briceño et al., 2016). In addition, another strategy to affect the TJ is the alteration of the cytoskeleton which serves to stabilize the TJ structure (Berkes et al., 2003). Overall, *T. gondii* infection transiently alters de TJ stability in Caco-2 cells to facilitate transmigration. The mechanism(s) used by *T. gondii* to interfere with the TJ in the host cell remains to be determined in detail. However, the increase of the permeability of intestinal TJ barrier by *T. gondii* in another immortalized culture cell called T84 (from transplantable human carcinoma cell line of colon) and in Caco-2 have been described to be modulated by proinflammatory cytokines such as IFN-γ or IL-1β from the host cell (Al-Sadi and Ma, 2007; Boivin et al., 2009).

Additionally, SW-480 cells established from colon-derived primary adenocarcinomas and Caco-2 have been used as a model to study parasite multiplication within the host cell. Parasites modulate different host cell pathways to promote their replication. The function of the β-catenin pathway, an intracellular signal transducer in the Wnt signaling pathway, regulates innate immunity for the benefit of parasite multiplication (Majumdar et al., 2019) as well as the early expression of beta-defensin 2 used as a mechanism from the parasite to modulate immune evasion in infected IECs (Morampudi et al., 2011). These studies have highlighted the cross-talk between the host immune system and the mechanisms of invasion and multiplication of *T. gondii*. In this context, defense mechanisms from the host cell using these cell models has been addressed. *T. gondii* tachyzoites successfully invade human colon-derived carcinoma HT29/B6 cells. The infection of HT-29 cells results in high expression of host 14-3-3 proteins as a possible strategy to increase cell survival and may prevent parasite replication (Monroy, 2008).

The lamina propria, underlying the intestinal epithelium, contains dendritic cells, macrophages, and natural killer cells, and they work to modulate the immune response when invading pathogens encounter the intestinal epithelium (Daneman and Rescigno, 2009). Macrophages are present at higher densities along the villi and are located closer to the epithelial cells than dendritic cells (Schulz et al., 2009). The infection of *T. gondii* at the mucous membranes of the lamina propria in the small intestine results in parasite invasion of different cell types, including dendritic cells, macrophages, and intestinal epithelial cells (Lambert and Barragan, 2010). Recently, the parasite effector GRA28 (dense granule protein) led to the upregulation of the macrophage receptor CCR7 generating the acquisition of dendritic cells-like migratory properties on macrophages impacting parasite dissemination in mice (ten Hoeve et al., 2022).

The impact of *T. gondii* infection and dissemination on the mucosa immune response has been well established by the study of intestinal non-immortalized cell line models (Snyder and Denkers, 2021). Nevertheless, those responses are hardly mimicked by the use of cell cultures because the immune components are not naturally integrated into the models, so the appeal of co-culture with immune cells is clear.

Among non-immortalized intestinal cells, primary cells (fully differentiated cells that can be isolated directly from the gut) and

TABLE 1 Epithelial intestinal cells used for studying *T. gondii* and related coccidian parasite biology.

Cell culture model		Origin	Model Complexity Features		Applications	Reference
			Spatial organization	Fluidics		
immortalized cell line	Caco-2	human colorectal adenocarcinoma-derived	2D/3D	no	invasion mechanisms	(Briceño et al., 2016; DeCicco RePass et al., 2017).
	T84	transplantable human carcinoma cell line derived from a lung metastasis of a colon carcinoma	2D	no	electrophysiology/ion transport	(Di Genova and Tonelli, 2016)
	HT-29	human colorectal adenocarcinoma cells	2D/3D	no	ion transport/parasite multiplication	(Kowalik et al., 2004; Monroy, 2008; Cardenas et al., 2020)
	SW-480	large intestine human colorectal cancer	2D	no	parasite multiplication	(Majumdar et al., 2019)
primary cells	mICc12	mouse intestinal epithelium	2D	no	innate intestinal responses	(Mennechet et al., 2002; Gopal et al., 2011)
	IEC-6	rat small intestine- derived epithelium	2D	no	parasite invasion and multiplication	(Dimier and Bout, 1993; Weight et al., 2015)
	FHs 74 Int	human small intestine	2D	no	parasite proliferation	(Quan et al., 2018)
	FEIC	feline epithelial intestinal cells	2D	no	sexual differentiation	(Moura et al., 2009; Zhao et al., 2018)
	MODE-K	murine intestinal epithelial cells	2D	no	epithelial cell responses	(Johnson et al., 2014)
stem-cell derived	HOPX+	pig intestinal stem cells from crypts and treated with adenovirus	2D	no	intestine mucosa responses	(Stewart et al., 2021)
	air-liquid interface (ALI)	mouse intestinal epithelial stem cells and fibroblast	2D	no	life cycle development	(Wilke et al., 2019)
	collagen-supported epithelial sheet	mouse jejunal and ileal tissues	2D/3D	no	parasite-intestinal epithelium interaction	(Luu et al., 2019)
	organoids	livestock proximal jejunum	2D/3D	no	long-term renewable system for infection	(Derricott et al., 2019; Hares et al., 2020)
		duodenal sections from human, chicken, mouse, and porcine	2D	no	parasite-host interactions and parasite co-infections	(Holthaus et al., 2021)
		mouse proximal small intestine	2D/3D	no	immune responses	(Araujo et al., 2021)
		mouse small intestine	2D/3D	no	infection mechanisms	(Betancourt-Delgado et al., 2019)
		human small intestine	2D/3D	no	immune host responses	(Humayun et al., 2022)
		felid fetal small intestine (jejunum)	2D/3D	no	sexual differentiation	(Di Genova et al., 2019)
intestine on-a-chip	human intestinal microphysiological system	human jejunal tissue	3D	yes	innate immune cell responses	(Humayun et al., 2022)
explants	colonic explants	adult murine colon	3D	yes	long-term parasite infection	(Baydoun et al., 2017)

stem cells (fully or partially undifferentiated cells with the ability to differentiate into different specialized cells) can be distinguished. Primary cells can be cultured on different scaffolds including porous membranes and hydrogels to generate fully differentiated monolayers without stem cells, self-renewing monolayers with or without segregation of the stem and differentiated cell types, or proliferative monolayers over a layer of supportive feeder cells. The use of these cell types has relative advantages in the conservation of different cell properties in comparison to immortalized cells (Balimane and Chong, 2005). For example, functional,

morphological, and structural properties like cell permeability changes (Takenaka et al., 2016), expression of proteins defining epithelial character (Anderle et al., 2004), and diversity on different epithelial cells. On the other hand, an important disadvantage of primary cells is the finite *in vitro* lifespan and decreased proliferation capacity, making these models inconvenient for addressing experimental questions that require long-term culturing. Specific media composition and scaffolding properties required to maintain stem cells *in vitro* are critically limiting factors.

Primary small intestinal epithelial cells have been used to study *T. gondii* infection with a focus primarily on the immune responses more than in the host-cell entry machinery. For example, the murine MODE-K and m-ICcl2 intestinal epithelial cells display altered chemokines production and proinflammatory responses after *T. gondii* infection (Mennechet et al., 2002; Gopal et al., 2011; Johnson et al., 2014). In addition, the use of a human fetal small intestinal epithelial cell line (FHs 74 Int) suggested that the activation of the inflammasome upon *T. gondii* infection induces the IL-1β secretion and parasite proliferation in the human small intestinal epithelial cells (Quan et al., 2018). These studies suggest that the modulation of gut inflammatory responses may serve as a mechanism to decrease epithelial cell responses and facilitate parasite dissemination and multiplication.

As described above, the intestinal epithelium is organized into proliferating crypts and differentiated villus. The crypts are the niche for intestinal stem cells (ISC), which are characterized by the expression of the specific marker Lgr5+. Paneth cells, also present at the crypt, help in regulating stem cell self-renewal to maintain intestinal homeostasis. The establishment of a 2D culture system to support ISC monolayer was successfully developed for mice (Liu et al., 2018), and those cells are the best documented ISCs in the study of intestinal infections (Mileto et al., 2020). The isolation of a subpopulation of ISCs from a less proliferative type called HOPX+ may serve a functional role in ISC-mediated regeneration after intestine damage and could control ISC proliferation (Stewart et al., 2021). *T. gondii* infection impairs the HOPX+ stem cell proliferation in the colonic mucosa in *in vivo* experiments (Saraav et al., 2021).

Although 2D cultures are simple, low-cost, scalable, and reproducible, the absence of a third dimension limits their ability to properly mimic the architecture of the tissue nor the cell-cell and cell-extracellular environment interactions. The following section discusses the development of 3D cell culture systems that closely mimics the *in vivo* conditions of the cellular microenvironment, opening new opportunities for achieving the complete *T. gondii* life cycle *in vitro*.

4.3 Intestinal organoids

The use of 2D-cultured cells has been extremely useful for understanding the mechanisms of infection of *T. gondii*. However, our understanding of the particular dynamics of infection happening at the intestinal epithelium has been hindered by the lack of appropriate models that recapitulate its complexity. The generation of three-dimensional (3D) cell cultures have opened new avenues for assessing direct pathogen-epithelium interaction in a more physiological context.

Organoids are tiny multicellular (3D) structures containing multiple-organ specific cells, derived from the self-renewal and self-organization potential of stem cells. They can be generated from adult stem cells (ASCs), embryonic stem cells (ESCs) or induced pluripotent stem cells (iPSCs) (Azar et al., 2021) provided the required growth and differentiation factors are present, in the presence of extracellular matrix components. Physiological resemblance of organoids to their originating organs is conserved at the levels of gene and protein expression, metabolic function, morphology, and the cell interactions occurring within the tissue (Weeber et al., 2015; Zhao et al., 2022). These features make organoids a promising opportunity to tackle the "physiological resemblance" gap between traditional cell cultures and *in vivo* animal experiments.

The first establishment of intestinal organoid culture was described by Sato and colleagues whereby the authors generated a mouse intestinal organoid from isolated crypts and single Lgr5 marker-positive stem cells using a basement membrane matrix and serum-free medium supplemented with Wnt agonist R-spondin 1, BMP signaling antagonist Noggin and epidermal growth factor (Sato et al., 2009; Sato et al., 2011b). This resulted in an *in vitro* model system called "mini-gut". The generated crypt-villus structures consisted of stem cells and specialized epithelial cells i.e. enterocytes, paneth cells, goblet cells and enteroendocrine cells, lacking mesenchymal or hematopoietic lineages. Afterward, human intestinal organoids were established from human ESCs, human iPSCs, and primary human tissue (McCracken et al., 2011; Sato et al., 2011a; Spence et al., 2011). Later on, organoids from other species, including livestock animals (cattle, sheep, pig, horse, chicken) were developed (Powell and Behnke, 2017; Hamilton et al., 2018; Derricott et al., 2019; Mussard et al., 2020). Noteworthy, while intestinal cell models from mouse and human tissue are widely available, little is known about the differentiated cell types present in some farm animal intestinal epithelium (Derricott et al., 2019). Therefore, no cell lines are available to model their intestinal biology, rendering organoids as the only option to gain insight into their particular host-pathogen interaction dynamics.

Organoids have been widely used to study host-pathogen interactions within the intestinal environment, including bacteria, viruses, and parasites, where the presence of multiple cell types closely resembles the *in vivo* situation (Foulke-Abel et al., 2016; Dutta et al., 2017; Barrila et al., 2018; Duque-Correa et al., 2020; Smith et al., 2021). Over the past years, the field of cell culture bioengineering was revolutionized by the generation of organoids from different organisms and organs, many of which have been employed as exceptional *in vitro* systems to support the growth of several apicomplexan parasites (Ramírez-Flores et al., 2022). A caveat of intestinal organoids recreating *in vivo* biology is their inverted topology, where the basal side faces the surrounding culture media and the apical side faces the lumen, lying within the structure. This has required exploring methodologies to

incorporate viable parasites directly into the luminal space, through organoid fragmentation, apical-out organoids or microinjection (Co et al., 2019; Smith et al., 2021).

The continuous division of intestinal epithelial stem cells in 2D and 3D cultures results in a fully differentiated and polarized epithelium that can be generated from different regions of the intestine, including duodenum jejunum, ileum, and colon. Specie-specific models provide opportunities for studying *T. gondii* infection, providing a specific window into its poorly understood sexual differentiation using feline-derived models. Additionally, the generation of intestinal organoids from non-felid organisms provides a potentially attractive tool to study *T. gondii* sexual differentiation, so long as the system allows *in vitro* "felinization" by means of chemically recreating the feline enteric environment. Next, we review some examples of the exciting uses of intestinal organoids to approach the biology of *T. gondii* within this tissue and discuss their applicability for developing new alternatives for studying sexual stages.

4.4 Intestinal organoids to study *T. gondii*

A robust protocol was described to establish and maintain stem-cell enriched organoid cultures and organoid-derived monolayers of human and mouse, but also from pig and chicken. These have proven suitable for *T. gondii* infection (Hares et al., 2020; Holthaus et al., 2021). For some species, particularly livestock, organoids are the only *in vitro* approach available to study *T. gondii*´s biology within their intestine as relevant cell lines are not at all available.

By microinjecting tachyzoites into the lumen of the closed organoid from bovine and porcine origin, researchers observed successful replication of the parasite 24 hours after infection (Derricott et al., 2019). Furthermore, Luu and colleagues developed an organoid derived from murine isolated crypts by the generation of a collagen-supported epithelial sheet with an exposed apical surface (Luu et al., 2019). The organoid was susceptible to the infection and supported replication and motility of *T. gondii* where parasites were observed in Paneth and goblet cells. Finally, after invasion and several cycles of replication within the cells, *T. gondii* egressed and invaded nearby cells. In addition to successful parasite's lytic cycles in 3D intestinal cultures, changes in both the parasite and host cell transcriptomics have been mapped.

Transcriptome and proteome analyses from the small intestine epithelium of cats infected with *T. gondii* showed an increase of oocyst-wall genes and proteins (Ramakrishnan et al., 2019). In line with this, the transcriptome analysis of host epithelial cells from differentiated small intestinal organoids (from duodenal biopsy) after the infection (72 h) with the related coccidia *Cryptosporidium parvum* showed an increase in gene expression of multiple parasite oocyst-wall genes (Heo et al., 2018), highlighting the potential of this system for studying this phenomena *in vitro* using "felinized" intestinal organoids in the case of *T. gondii*. In fact, organoid-derived monolayers from human duodenal biopsy have been used to study the biology of *T. gondii* within the intestine. *T. gondii* infections of this model revealed a novel sequence of molecular events leading to epithelial barrier breakdown in this human primary tissue. These experiments uncovered that adenosine 3´,5´-cyclic monophosphate (cAMP)/protein kinase A (PKA) signaling affects the barrier breakdown by means of inducing TJ disruption in human intestinal epithelial cells (Holthaus et al., 2021).

Finally, co-culture of 3D cell models with immune cells such as dendritic cells was carried out in a stem cell-derived enteroids from mice intestinal epithelium infected with *T. gondii*, opening up the possibility of studying how the crosstalk with the epithelium influences dendritic cells' function, and how the parasite alters these interactions (Hares et al., 2020). The co-culture of organoids directly with components of the immune response is also possible. Intestinal organoids generated from mice small intestine were co-cultured with recombinant murine cytokine IFN-γ, which mediates the death of Paneth cells after the infection with *T. gondii* by the control of the kinase complex mechanistic target of rapamycin (mTORC1) (Araujo et al., 2021).

Different methods using 3D intestinal systems are being developed to recreate more complex and physiological conditions, allowing the incorporation of microvasculature, microbiota, immune cells and microfluidics leading to a next step in 3D modeling with the organ-on-a-chip technology (Palikuqi et al., 2020; Bozzetti and Senger, 2022; Pimenta et al., 2022). The possibility of expansion of the organoid micro-architecture by addition of these factors may aid in understanding the impact of mechanical forces and biological elements on *T gondii´s* intestinal infection.

4.5 Intestine-on-a-chip

Organ-on-a-chip (OOAC) and multiorgan on a chip (MOC) represent the latest advancements in 3D culture technology. They are microscale devices that mimic the complex structure and function of organs by incorporating multiple cell types (OOAC) or multiple organ-specific chips (MOC). In addition, these devices incorporate extracellular matrix and physiological conditions such as fluid flow and mechanical forces allowing control of the cellular microenvironment and the mechanical dynamic of organs. Fluid concentration gradients (i.e. blood vessels), maintenance of geometry of the vasculature and epithelium, nutrient supplementation, metabolite emissions, mechanical stress, contractile properties, cell patterning and other external conditions can be controlled (Rajan et al., 2020; Baddal and Marrazzo, 2021). Overall, OOAC and MOC technologies are particularly useful when the biological question requires an increase in biological complexity of the system. It offers several advantages over traditional 2D and 3D cultures, including improved cell-to-cell matrix interaction, more physiologically relevant models, and real-time monitoring of cellular response. Over the past 10 years, intestinal-on-chip platforms have evolved from simple 2D cultures to include more comprehensive functionality, such as villi structures, intestinal peristalsis, oxygen gradients, and even immune systems and microbiome elements (May et al., 2017; Xiang et al., 2020). They have been used in the search of new clues in host-pathogen interactions including

bacteria, virus, fungi, and parasites (Blutt et al., 2018; Grassart et al., 2019; Sunuwar et al., 2020; Tang et al., 2020). The use of OOAC in apicomplexan parasite research is only initiating. We briefly analyze here the early steps and possibilities that this new technology presents for the study of Apicomplexa focusing specifically on *T. gondii.*

Intestinal or gut OOACs have been designed, and revised protocols for their generation are currently available (Leung et al., 2022; Ramírez-Flores et al., 2022). Duodenum OOAC has been developed from human adult-derived intestinal organoids co-cultured with microvascular endothelial cells separated by a PDMS membrane (polydimethylsiloxane) (Kasendra et al., 2020). This system showed cytoarchitecture, cell-cell interactions, permeability parameters, and gene expression which more closely resemble those of human intestines than organoids do. This technology allows for more biologically faithful drug delivery and pharmacokinetic studies. These microfluidic systems can be used and adapted for research of enteric microorganisms, like *T. gondii*.

Remarkably, a long-lived and tube-shaped intestinal epithelial culture system has been reported by using crypt-like microcavities under flow, induced topography-guided self-organization of a functional epithelium with crypt- and villus-like domains similar to that observed *in vivo*. The culture system showed self-regeneration capacity and response to bacterial infection. Moreover, long-term parasite infection by infecting the mini-gut tubes with *C. parvum* was modeled. Live-cell microscopy showed that the tubular organoids support the entire life cycle and long-term growth of *C. parvum* without affecting tissue integrity, and immunofluorescence assays identified each asexual and sexual stage of *C. parvum* (Nikolaev et al., 2020).

Human intestinal crypts containing functional stem cells, derived from the jejunum region of the small intestine were integrated in an organ-on-chip devices including micro-physiological systems (MPSs) and co-cultured with immune cells (including neutrophils and NK cells) by the integration of an adjacent vascular lumen. The human intestinal tissue MPS supported the invasion, replication, and translocation of *T. gondii* beyond the epithelium (Humayun et al., 2022). *T. gondii* infection of MPSs stimulated a broad range of effector functions in neutrophils and natural killer cells–mediated cytokine production, which may play immunomodulatory roles in the host.

The microbiome presence in a human colon chip model was generated by co-incubation with human microbiome metabolites collected from PolyFermS continuous intestinal fermentation bioreactors. The authors of this study found that microbiome metabolites recapitulate species-specific tolerance in colon chips (Tovaglieri et al., 2019). Regarding oxygen levels, the manipulation of oxygen present in a MPSs from a mouse colon chip was incorporated by culturing under a hypoxia gradient created by flowing oxygenated medium through the basal channel (extracellular matrix-coated chips) while maintaining the entire chip in an anaerobic chamber filled with carbon dioxide and nitrogen gas (Gazzaniga et al., 2021). Finally, the intestinal epithelium is surrounded by smooth muscle layers, with the enteric neural system embedded to control intestinal peristalsis movements that control the motion within the intestinal cavity in a constant forward direction (Sinagoga and Wells, 2015). Artificial peristalsis was introduced into human colonic MPSs made from elastomeric polymer PDMS. The application of cyclic vacuum within the system induces strain and stretching of the porous membrane that recreates peristaltic-like motions, and the dependency of those mechanical forces strongly impacts pathogen invasion within the epithelium (Grassart et al., 2019). Future studies could incorporate biological factors such as specific microbiome, tissue oxygen levels, and peristaltic movements to better recapitulate the *in vivo* microenvironment of the intestine and to examine their influence on the biology of *T. gondii* both in intermediate hosts and in felids by exogenous "*felinization*" of the system.

4.6 Intestinal explants

In the late 60´, Browning and Trier described a successful method to culture human duodenojejunal junction sections that maintained normal morphology, proliferation, and absorption properties of the intestinal epithelium after 24 h (Browning and Trier, 1969). Explants are generated from fragments of native tissue, so they mimic closer than other systems the architecture and cellular composition (including other resident cells i.e immune cells and stromal cells) present in the intestine (reviewed in Randall et al., 2011). The explant culture of the gastrointestinal tract offers an *ex vivo* alternative to studying a wide range of intestinal infections. Noteworthy, however, the application of this technology has thus far been limited as its systematization is hampered by its inherent variability. In addition, explants have a limited lifespan undergoing rapid degeneration in a few days. Recently, however, approaches have been described that allow the maintenance of explant cultures for a prolonged time (Baydoun et al., 2017; Baydoun et al., 2020).

Despite its limitations, valuable data has been attained using these models pertaining to *T. gondii´*s biology. In particular, time-lapse imaging of murine intestinal explants infected with *T. gondii* has revealed parasite spreads through the lumen of the intestine while neutrophils are recruited to foci of infection and preferentially harbor parasites when compared to other leukocytes (Coombes et al., 2013). Mouse colon explants obtained from a severe combined immunodeficiency strain were able to survive and preserve the tissue morphology for 35 days, in the presence of microvilli, villi-like, and crypt-like structures, connective tissue with collagen, fibroblasts, and smooth muscle cells. This 3D model was able to support the growth of *C. parvum* for 27 days, resulting in the identification of previously unknown markers of lesions happening in the long-term infection process (Baydoun et al., 2017). The use of this model for the study of *T. gondii* remains to be explored.

A novel microphysiological system called intestinal explant barrier chip was reported using human and porcine colon explants. This system is based on a dynamic microfluidic microenvironment that extends tissue viability (Amirabadi et al., 2022). This *ex vivo* model revealed regional and interspecies differences in intestine properties since it has a more complex architecture that better preserves the qualities of the originating

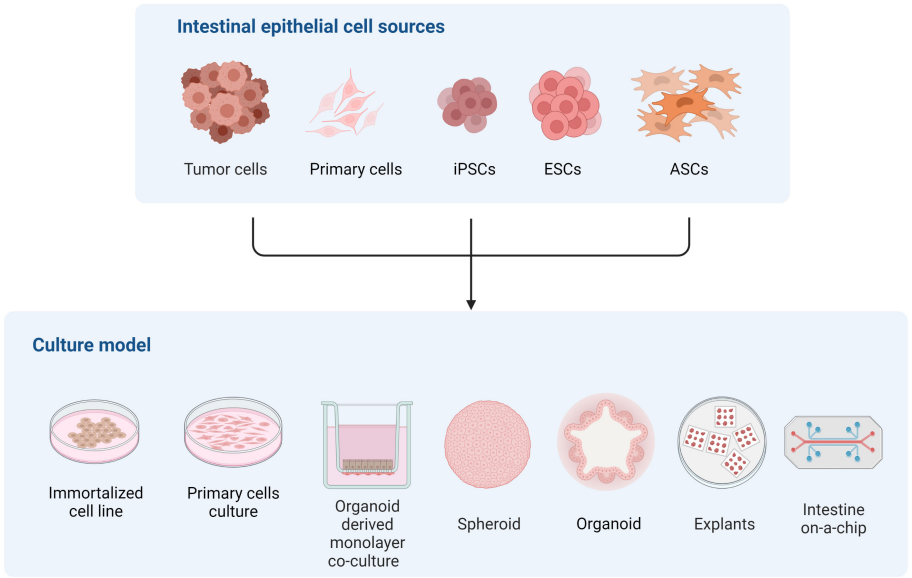

FIGURE 2
Representation of different *in vitro* models of the intestinal epithelium to study multiple aspects of *T. gondii* and related coccidian parasite biology.

tissue. In the future, it would be possible to incorporate microbes like parasites to gain valuable insight into their biology in a species-specific manner.

5 Discussion

5.1 Challenges and opportunities for models to promote *T. gondii* sexual stages

Historically, *T. gondii* research has relied on 2D cell cultures and *in vivo* animal models. Animal models are expensive, time-consuming, and provide no or limited access to analyzing *in vivo* host-parasite interaction at the subcellular level. In addition, there are inherent ethical constraints and animal welfare concerns in working with animal models. In contrast, two-dimensional cultures of mammalian cells represent a cost-effective and convenient system for performing controlled, reproducible, infection studies integrating only a handful of variables. However, growing cells on flat surfaces pose structural constraints which lead to artificial morphology and altered behaviors, distinct from the physiological cell behavior within a tissue.

The intestinal epithelium is an exceptional and unique model to study differentiation to sexual stages of many coccidia parasites, including *T. gondii*. However, recreating the complexity of the intestinal epithelium in an *in vitro* system is challenging, as evidenced by the different cell sources and culture approaches developed to tackle this task (Figure 2). Immortalized cell line such as Caco-2, which have been commonly used for studying *T. gondii* infection of the intestine (Barragan et al., 2005; Monroy, 2008; Briceño et al., 2016; Jones et al., 2017; Ross et al., 2019), can form polarized monolayers of enterocyte-like cells but lack the diversity of intestinal cell types. As a consequence, this model poorly recapitulates the physiology of the normal tissue. On the other hand, intestinal explants provide cellular diversity and natural tissue architecture, but rely heavily on animal-derived sample availability and display limited viability and ample variability, making it suitable for studying early infection and acutely occurring processes only.

Reconstructing host microenvironments including 3D tissue architecture, multicellular complexity, microbiota composition/localization, oxygen tension, transport processes, and biomechanical forces, are key to recreating *in vivo* pathogens' biology *in vitro*. Many efforts have been pursued to develop a new generation of 3D *in vitro* models that more faithfully recapitulate these features, improving their predictive capabilities. In this context, organoids have arisen as alternatives to many of the traditional cell cultures since they are conformed by different intestinal cell types and recapitulate the 3D architecture and polarization of the cells in the intestine. Also, as organoids derive from stem cells, they can be expanded and maintained in culture for long periods of time, and cryopreserved. As an advantage to traditional cell lines, they can be cultured as 2D and 3D systems maintaining organ specificity and genome stability. Together, these particular properties turn the organoid culture model into a promising tool for unraveling *T. gondii* intestinal infection mechanisms both in intermediate and definitive hosts. Moreover, the possibility of recreating the feline intestinal environment in a human or murine organoid system is emerging as a valuable alternative to decipher *T. gondii* sexual differentiation (Di Genova et al., 2019).

Since *T. gondii* enters the intestine through the apical surface, and intact organoids have its apical side lying within the structure, using organoids to study *T. gondii* infection poses some difficulties. Nonetheless, several methodological approaches/strategies can be pursued for achieving *T. gondii* apical epithelial surface infection.

Organoids can be fragmented to expose the apical surface and co-culture with pathogens (Luu et al., 2019; Holthaus et al., 2021). However, it is important to consider parasite invasion requirements and the effect on epithelial architecture since organoid structures are disturbed when this approach is selected. Another possibility is to microinject the pathogen directly into the organoid lumen, without altering organoid structure (Zhang et al., 2014; Wilson et al., 2015; Heo et al., 2018). Although this attractive strategy has been widely successful for bacteria and viruses, it is particularly challenging for parasites in general due to their comparatively larger size, though plausible for protozoa. The lumen condition (levels of oxygen and cell death accumulation) could also interfere with parasite survival and invasion. In this case, organoid-derived monolayers can be an excellent alternative method for culturing organoids in co-culture with parasites in a controlled and reproducible manner allowing direct access to the apical epithelium, maintaining the intestine's cellular diversity. The use of a collagen-supported epithelial sheet model (Luu et al., 2019) or air-liquid interface cultures (Wilke et al., 2019), where cells are differentiated and polarized, have been explored as alternatives to study other complex parasite life cycles, like that of the *Cryptosporidium* species. There exists ample potential for applying these models in the future to the study of *T. gondii*´s biology within the intestine. Last but not least, organoids can also be culture with reverse polarity, where the basal layer is turned inward exposing the apical layer to the external media environment (Kakni et al., 2022). These inside-out organoids could provide important insights into *T. gondii* life cycle and its sexual reproduction.

Regardless of the success of *in vitro* models for shedding light onto *T. gondii*'s infection mechanisms (invasion, multiplication, and egress) (Table 1), data on the underlying events driving stage conversion remains limited largely due to the lack of adequate *in vitro* models that support the completion of the parasite life cycle. The *in vitro* systems used to study host-parasite interaction include organoids from pluripotent stem cells, organoid-derived monolayers, cell lines cultured in 3D silk-protein scaffolds (DeCicco RePass et al., 2017; Cardenas et al., 2020), hollow fiber technology (Morada et al., 2015) and colonic explants (Baydoun et al., 2017). DeCicco RePass et al., 2017 reported a novel bioengineered 3D human intestinal tissue model as a long-term infection system with the advantage of recreating oxygen gradient along the gastrointestinal tract. Altogether these innovative experimental platforms provide exciting alternatives on the quest for models that allow the full life cycle of *T. gondii* to be recreated *in vitro*. Improving these models using microfluidic approaches, incorporating peristaltic and flow conditions as well as co-culture with immune/stromal cells and gut microbiota are the next steps for a better *in vivo*-like environment *in vitro* recreation. Developing chemically "felinized" intestinal organoids, infected with bradyzoites and sporozoites as the sexual stage starting point will be crucial to gaining insight into the molecular underpinnings of *T. gondii*'s sexual cycle.

Author contributions

FS and MF conceived the original idea and scheme of this revision. FS, SC, and RP created the figures and table. MF and MB-F contributed to funding acquisition. All authors contributed to reviewing the literature, wrote and approved the submitted version.

Funding

This project was funded by a G4 grant to MF by the Pasteur Network and FOCEM (MERCOSUR Structural Convergence Fund), COF 03/11. SC received a fellowship from Sistema Nacional de Becas, ANII. MF, MB-F, and RP are members of the SNI (National Research System, Uruguay) and researchers of PEDECIBA, Uruguay.

Conflict of interest

The authors declare that the research was conducted in the absence of any commercial or financial relationships that could be construed as a potential conflict of interest.

Publisher's note

References

Al-Sadi, R. M., and Ma, T. Y. (2007). IL-1β causes an increase in intestinal epithelial tight junction permeability. *J. Immunol.* 178, 4641–4649. doi: 10.4049/jimmunol.178.7.4641

Amirabadi, H. E., Donkers, J. M., Wierenga, E., Ingenhut, B., Pieters, L., Stevens, L., et al. (2022). Intestinal explant barrier chip: long-term intestinal absorption screening in a novel microphysiological system using tissue explants. *Lab. Chip* 22, 326–342. doi: 10.1039/d1lc00669j

Anderle, P., Huang, Y., and Sadée, W. (2004). Intestinal membrane transport of drugs and nutrients: genomics of membrane transporters using expression microarrays. *Eur. J. Pharm. Sci.* 21, 17–24. doi: 10.1016/S0928-0987(03)00169-6

Angrisano, F., Sala, K. A., Da, D. F., Liu, Y., Pei, J., Grishin, N. V., et al. (2017). Targeting the conserved fusion loop of HAP2 inhibits the transmission of plasmodium berghei and falciparum. *Cell Rep.* 21, 2868–2878. doi: 10.1016/j.celrep.2017.11.024

Antfolk, M., and Jensen, K. B. (2020). A bioengineering perspective on modelling the intestinal epithelial physiology *in vitro*. *Nat. Commun.* 11 (1), 6244. doi: 10.1038/s41467-020-20052-z

Antunes, A. V., Shahinas, M., Swale, C., Farhat, D. C., Ramakrishnan, C., Bruley, C., et al. (2023). *In vitro* production of cat-restricted toxoplasma pre-sexual stages by epigenetic reprogramming. *bioRxiv*. doi: 10.1101/2023.01.16.524187

Araujo, A., Safronova, A., Burger, E., López-Yglesias, A., Giri, S., Camanzo, E. T., et al. (2021). IFN-g mediates paneth cell death *via* suppression of mTOR. *Elife* 10, 1–19. doi: 10.7554/eLife.60478

Arranz-Solís, D., Mukhopadhyay, D., and Saeij, J. J. P. (2021). Toxoplasma effectors that affect pregnancy outcome. *Trends Parasitol.* 37, 283–295. doi: 10.1016/j.pt.2020.10.013

Azar, J., Bahmad, H. F., Daher, D., Moubarak, M. M., Hadadeh, O., Monzer, A., et al. (2021). The use of stem cell-derived organoids in disease modeling: an update. *Int. J. Mol. Sci.* 22, 1–39. doi: 10.3390/ijms22147667

Baddal, B., and Marrazzo, P. (2021). Refining host-pathogen interactions: organ-on-chip side of the coin. *Pathogens* 10, 1–13. doi: 10.3390/pathogens10020203

Balimane, P. V., and Chong, S. (2005). Cell culture-based models for intestinal permeability: a critique. *Drug Discovery Today* 10, 335–343. doi: 10.1016/S1359-6446(04)03354-9

Barragan, A., Brossier, F., and Sibley, L. D. (2005). Transepithelial migration of toxoplasma gondii involves an interaction of intercellular adhesion molecule 1 (ICAM-1) with the parasite adhesin MIC2. *Cell. Microbiol.* 7, 561–568. doi: 10.1111/j.1462-5822.2005.00486.x

Barrila, J., Crabbé, A., Yang, J., Franco, K., Nydam, S. D., Forsyth, R. J., et al. (2018). Modeling host-pathogen interactions in the context of the microenvironment: three-dimensional cell culture comes of age. *Infect. Immun.* 86 (11), e00282-18. doi: 10.1128/IAI.00282-18

Baydoun, M., Treizeibré, A., Follet, J., Vanneste, S. B., Creusy, C., Dercourt, L., et al. (2020). An interphase microfluidic culture system for the study of ex vivo intestinal tissue. *Micromachines* 11 (2), 150. doi: 10.3390/mi11020150

Baydoun, M., Vanneste, S. B., Creusy, C., Guyot, K., Gantois, N., Chabe, M., et al. (2017). Three-dimensional (3D) culture of adult murine colon as an *in vitro* model of cryptosporidiosis: proof of concept. *Sci. Rep.* 7, 1–12. doi: 10.1038/s41598-017-17304-2

Berkes, J., Viswanathan, V. K., Savkovic, S. D., and Hecht, G. (2003). Intestinal epithelial responses to enteric pathogens: effects on the tight junction barrier, ion transport, and inflammation. *Gut* 52, 439–451. doi: 10.1136/gut.52.3.439

Betancourt-Delgado, E., Hamid, B., Fabian, B. T., Klotz, C., Hartmann, S., and Seeber, F. (2019). From entry to early dissemination-toxoplasma gondii's initial encounter with its host. *Front. Cell. Infect. Microbiol.* 9. doi: 10.3389/fcimb.2019.00046

Black, M. W., and Boothroyd, J. C. (2000). Lytic cycle of toxoplasma gondii. *Microbiol. Mol. Biol. Rev.* 64, 607–623. doi: 10.1128/mmbr.64.3.607-623.2000

Blutt, S. E., Crawford, S. E., Ramani, S., Zou, W. Y., and Estes, M. K (2018). Engineered human gastrointestinal cultures to study the microbiome and infectious diseases. *Cmgh* 5, 241–251. doi: 10.1016/j.jcmgh.2017.12.001

Boivin, M. A., Roy, P. K., Bradley, A., Kennedy, J. C., Rihani, T., and Ma, T. Y. (2009). Mechanism of interferon-γ-induced increase in T84 intestinal epithelial tight junction. *J. Interf. Cytokine Res.* 29, 45–54. doi: 10.1089/jir.2008.0128

Bozzetti, V., and Senger, S. (2022). Organoid technologies for the study of intestinal microbiota–host interactions. *Trends Mol. Med.* 28, 290–303. doi: 10.1016/j.molmed.2022.02.001

Briceño, M. P., Nascimento, L. A. C., Nogueira, N. P., Barenco, P. V. C., Ferro, E. A. V., Rezende-Oliveira, K., et al. (2016). Toxoplasma gondii infection promotes epithelial barrier dysfunction of caco-2 cells. *J. Histochem. Cytochem.* 64, 459–469. doi: 10.1369/0022155416656349

Browning, T. H., and Trier, J. S. (1969). Organ culture of mucosal biopsies of human small intestine. *J. Clin. Invest.* 48, 1423–1432. doi: 10.1172/JCI106108

Cardenas, D., Bhalchandra, S., Lamisere, H., Chen, Y., Zeng, X.-L., Ramani, S., et al. (2020). Two- and three-dimensional bioengineered human intestinal tissue models for cryptosporidium. *Methods Mol. Biol.* 2052, 373–402. doi: 10.1007/978-1-4939-9748-0

Carr, K. E., and Toner, P. G. (1984). ""Morphology of the intestinal mucosa,"," in *Pharmacology of intestinal permeation i. handbook of experimental pharmacology* (Berlin, Heidelberg: Springer), 1–50. doi: 10.1007/978-3-642-69505-6_1

Cerutti, A., Blanchard, N., and Besteiro, S. (2020). The bradyzoite: a key developmental stage for the persistence and pathogenesis of toxoplasmosis. *Pathogens* 9, 1–21. doi: 10.3390/pathogens9030234

Co, J. Y., Margalef-Català, M., Li, X., Mah, A. T., Kuo, C. J., Monack, D. M., et al. (2019). Controlling epithelial polarity: a human enteroid model for host-pathogen interactions. *Cell Rep.* 26, 2509–2520.e4. doi: 10.1016/j.celrep.2019.01.108

Coombes, J. L., Charsar, B. A., Han, S. J., Halkias, J., Chan, S. W., Koshy, A. A., et al. (2013). Motile invaded neutrophils in the small intestine of toxoplasma gondii-infected mice reveal a potential mechanism for parasite spread. *Proc. Natl. Acad. Sci. USA.* 110 (21), E1913–22. doi: 10.1073/pnas.1220272110

Cruz-Bustos, T., Feix, A. S., Lyrakis, M., Dolezal, M., Ruttkowski, B., and Joachim, A. (2022). The transcriptome from asexual to sexual *in vitro* development of cystoisospora suis (Apicomplexa: coccidia). *Sci. Rep.* 12, 1–17. doi: 10.1038/s41598-022-09714-8

Daneman, R., and Rescigno, M. (2009). The gut immune barrier and the blood-brain barrier: are they so different? *Immunity* 31, 722–735. doi: 10.1016/j.immuni.2009.09.012

DeCicco RePass, M. A., Chen, Y., Lin, Y., Zhou, W., Kaplan, D. L., and Ward, H. D. (2017). Novel bioengineered three-dimensional human intestinal model for long-term infection of cryptosporidium parvum. *Fungal Parasitol. Infect.* 85, 1–11. doi: 10.1128/IAI.00731-16

de Muno, R. M., Moura, M. A., de Carvalho, L. C., Seabra, S. H., and Barbosa, H. S. (2014). Spontaneous cystogenesis of toxoplasma gondii in feline epithelial cells *in vitro*. *Folia Parasitol. (Praha).* 61, 113–119. doi: 10.14411/fp.2014.017

Derricott, H., Luu, L., Fong, W. Y., Hartley, C. S., Johnston, L. J., Armstrong, S., et al. (2019). Developing a 3D intestinal epithelium model for livestock species. *Cell Tissue Res.* 375, 409–424. doi: 10.1007/s00441-018-2924-9

Di Genova, B. M., and Tonelli, R. R. (2016). Infection strategies of intestinal parasite pathogens and host cell responses. *Front. Microbiol.* 7. doi: 10.3389/fmicb.2016.00256

Di Genova, B. M., Wilson, S. K., Dubey, J. P., and Knoll, L. J. (2019). Intestinal delta-6-desaturase activity determines host range for toxoplasma sexual reproduction. *PloS Biol.* 17, 1–19. doi: 10.1371/journal.pbio.3000364

Dimier, I. H., and Bout, D. T. (1993). Rat intestinal epithelial cell line IEC-6 is activated by recombinant inferferon-γ to inhibit replication of the coccidian toxoplasma gondii. *Eur. J. Immunol.* 23, 981–983. doi: 10.1002/eji.1830230435

Dobrowolski, J. M., and Sibley, L. D. (1996). Toxoplasma invasion of mammalian cells is powered by the actin cytoskeleton of the parasite. *Cell* 84, 933–939. doi: 10.1016/S0092-8674(00)81071-5

Dubey, J. P. (1997). Bradyzoite-induced murine toxoplasmosis: stage conversion, pathogenesis, and tissue cyst formation in mice fed bradyzoites of different strains of toxoplasma gondii. *J. Eukaryot. Microbiol.* 44, 592–602. doi: 10.1111/j.1550-7408.1997.tb05965.x

Dubey, J. P. (2006). Comparative infectivity of oocysts and bradyzoites of toxoplasma gondii for intermediate (mice) and definitive (cats) hosts. *Vet. Parasitol.* 140, 69–75. doi: 10.1016/j.vetpar.2006.03.018

Dubey, J. P. (2009). History of the discovery of the life cycle of toxoplasma gondii. *Int. J. Parasitol.* 39, 877–882. doi: 10.1016/j.ijpara.2009.01.005

Dubey, J. P., and Frenkeñ, J. K. (1972). Cyst-induced toxoplasmosis in cats. *J. Protozool.* 19, 155–177. doi: 10.1111/j.1550-7408.1972.tb03431.x

Dubey, J. P., Lindsay, D. S., and Speer, C. A. (1998). Structures of toxoplasma gondii tachyzoites, bradyzoites, and sporozoites and biology and development of tissue cysts. *Clin. Microbiol. Rev.* 11, 267–299. doi: 10.1128/cmr.11.2.267

Duque-Correa, M. A., Maizels, R. M., Grencis, R. K., and Berriman, M. (2020). Organoids – new models for host–helminth interactions. *Trends Parasitol.* 36, 170–181. doi: 10.1016/j.pt.2019.10.013

Dutta, D., Heo, I., and Clevers, H. (2017). Disease modeling in stem cell-derived 3D organoid systems. *Trends Mol. Med.* 23, 393–410. doi: 10.1016/j.molmed.2017.02.007

Farhat, D. C., Swale, C., Dard, C., Cannella, D., Ortet, P., Barakat, M., et al. (2020). A MORC-driven transcriptional switch controls toxoplasma developmental trajectories and sexual commitment. *Nat. Microbiol.* 5, 1–33. doi: 10.1038/s41564-020-0674-4

Ferguson, D. J. P. (2002). Toxoplasma gondii and sex: essential or optional extra? *Trends Parasitol.* 18, 351–355. doi: 10.1016/s1471-4922(02)02330-9

Ferguson, D. J. P., and Dubremetz, J. F. (2020). "The ultrastructure of toxoplasma gondii," in *Toxoplasma gondii: the model apicomplexan-perspectives and methods* (Elsevier), 21–61.

Ferguson, D. J. P., Hutchison, W. M., and Siim, J. C. (1975). The ultrastructural development of the macrogamete and formation of the oocyst wall of toxoplasma gondii. *Acta Pathol. Microbiol. Scand. Sect. B Microbiol.* 83, 491–505. doi: 10.1111/j.1699-0463.1975.tb00130.x

Ferruzza, S., Rossi, C., Scarino, M. L., and Sambuy, Y. (2012). A protocol for differentiation of human intestinal caco-2 cells in asymmetric serum-containing medium. *Toxicol. Vitr.* 26, 1252–1255. doi: 10.1016/j.tiv.2012.01.008

Flegr, J., Prandota, J., Sovičková, M., and Israili, Z. H. (2014). Toxoplasmosis - a global threat. correlation of latent toxoplasmosis with specific disease burden in a set of 88 countries. *PloS One* 9 (3), e90203. doi: 10.1371/journal.pone.0090203

Foulke-Abel, J., In, J., Yin, J., Zachos, N. C., Kovbasnjuk, O., Estes, M. K., et al. (2016). Human enteroids as a model of upper small intestinal ion transport physiology and pathophysiology. *Gastroenterology* 150, 638–649.e8. doi: 10.1053/j.gastro.2015.11.047

Francia, M. E., Dubremetz, J. F., and Morrissette, N. S. (2016). Basal body structure and composition in the apicomplexans toxoplasma and plasmodium. *Cilia* 5, 3–9. doi: 10.1186/s13630-016-0025-5

Freppel, W., Ferguson, D. J. P., Shapiro, K., Dubey, J. P., Puech, P. H., and Dumètre, A. (2019). Structure, composition, and roles of the toxoplasma gondii oocyst and sporocyst walls. *Cell Surf.* 5, 100016. doi: 10.1016/j.tcsw.2018.100016

Galal, L., Ariey, F., Gouilh, M. A., Dardé, M. L., Hamidović, A., Letourneur, F., et al. (2022). A unique toxoplasma gondii haplotype accompanied the global expansion of cats. *Nat. Commun.* 13 (1), 5778. doi: 10.1038/s41467-022-33556-7

Gazzaniga, F. S., Camacho, D. M., Wu, M., Silva Palazzo, M. F., Dinis, A. L. M., Grafton, F. N., et al. (2021). Harnessing colon chip technology to identify commensal bacteria that promote host tolerance to infection. *Front. Cell. Infect. Microbiol.* 11. doi: 10.3389/fcimb.2021.638014

Gopal, R., Birdsell, D., and Monroy, F. P. (2011). Regulation of chemokine responses in intestinal epithelial cells by stress and toxoplasma gondii infection. *Parasite Immunol.* 33, 12–24. doi: 10.1111/j.1365-3024.2010.01248.x

Grassart, A., Malardé, V., Gobba, S., Sartori-Rupp, A., Kerns, J., Karalis, K., et al. (2019). Bioengineered human organ-on-chip reveals intestinal microenvironment and mechanical forces impacting shigella infection. *Cell Host Microbe* 26, 435–444.e4. doi: 10.1016/j.chom.2019.08.007

Gregg, B., Taylor, B. C., John, B., Tait-Wojno, E. D., Girgis, N. M., Miller, N., et al. (2013). Replication and distribution of toxoplasma gondii in the small intestine after oral infection with tissue cysts. *Infect. Immun.* 81, 1635–1643. doi: 10.1128/IAI.01126-12

Hamilton, C. A., Young, R., Jayaraman, S., Sehgal, A., Paxton, E., Thomson, S., et al. (2018). Development of *in vitro* enteroids derived from bovine small intestinal crypts. *Vet. Res.* 49, 1–15. doi: 10.1186/s13567-018-0547-5

Hares, M. F., Tiffney, E. A., Johnston, L. J., Luu, L., Stewart, C. J., Flynn, R. J., et al. (2020). Stem cell-derived enteroid cultures as a tool for dissecting host-parasite interactions in the small intestinal epithelium. 43 (2), e12765. doi: 10.1111/pim.12765

Heo, I., Dutta, D., Schaefer, D. A., Iakobachvili, N., Artegiani, B., Sachs, N., et al. (2018). Modelling cryptosporidium infection in human small intestinal and lung organoids. *Nat. Microbiol.* 3, 814–823. doi: 10.1038/s41564-018-0177-8

Hewes, S. A., Wilson, R. L., Estes, M. K., Shroyer, N. F., Blutt, S. E., and Grande-Allen, K. J. (2020). *In vitro* models of the small intestine: engineering challenges and engineering solutions. *Tissue Eng. - Part B Rev.* 26, 313–326. doi: 10.1089/ten.teb.2019.0334

Holthaus, D., Delgado-Betancourt, E., Aebischer, T., Seeber, F., and Klotz, C. (2021). Harmonization of protocols for multi-species organoid platforms to study the intestinal biology of toxoplasma gondii and other protozoan infections. *Front. Cell. Infect. Microbiol.* 10. doi: 10.3389/fcimb.2020.610368

Humayun, M., Ayuso, J. M., Park, K. Y., Martorelli Di Genova, B., Skala, M., Kerr, S. C., et al. (2022). Innate immune cell response to host-parasite interaction in a human intestinal tissue microphysiological system. *Sci. Adv.* 8, 1–18. doi: 10.1126/sciadv.abm8012

Johnson, S. L., Gopal, R., Enriquez, A., and Monroy, F. P. (2014). Role of glucocorticoids and toxoplasma gondii infection on murine intestinal epithelial cells. *Parasitol. Int.* 63, 687–694. doi: 10.1016/j.parint.2014.05.005

Jones, E. J., Korcsmaros, T., and Carding, S. R. (2017). Mechanisms and pathways of toxoplasma gondii transepithelial migration. *Tissue Barriers* 5, 1–11. doi: 10.1080/21688370.2016.1273865

Kakni, P., López-Iglesias, C., Truckenmüller, R., Habibović, P., and Giselbrecht, S. (2022). Reversing epithelial polarity in pluripotent stem cell-derived intestinal organoids. *Front. Bioeng. Biotechnol.* 10. doi: 10.3389/fbioe.2022.879024

Kasendra, M., Luc, R., Yin, J., Manatakis, D. V., Kulkarni, G., Lucchesi, C., et al. (2020). Duodenum intestine-chip for preclinical drug assessment in a human relevant model. *Elife* 9, 1–23. doi: 10.7554/eLife.50135

Kowalik, S., Clauss, W., and Zahner, H. (2004). Toxoplasma gondii: changes of transepithelial ion transport in infected HT29/B6 cell monolayers. *Parasitol. Res.* 92, 152–158. doi: 10.1007/s00436-003-1033-0

Lambert, H., and Barragan, A. (2010). Modelling parasite dissemination: host cell subversion and immune evasion by toxoplasma gondii. *Cell. Microbiol.* 12, 292–300. doi: 10.1111/j.1462-5822.2009.01417.x

Leung, C. M., de Haan, P., Ronaldson-Bouchard, K., Kim, G. A., Ko, J., Rho, H. S., et al. (2022). A guide to the organ-on-a-chip. *Nat. Rev. Methods Prim.* 2, 1–29. doi: 10.1038/s43586-022-00118-6

Liu, Y., Qi, Z., Li, X., Du, Y., and Chen, Y. G. (2018). Monolayer culture of intestinal epithelium sustains Lgr5+ intestinal stem cells. *Cell Discovery* 4, 4–6. doi: 10.1038/s41421-018-0036-z

Liu, Y., Tewari, R., Ning, J., Blagborough, A. M., Garbom, S., Pei, J., et al. (2008). The conserved plant sterility gene HAP2 functions after attachment of fusogenic membranes in chlamydomonas and plasmodium gametes. *Genes Dev.* 22, 1051–1068. doi: 10.1101/gad.1656508

Luu, L., Johnston, L. J., Derricott, H., Armstrong, S. D., Randle, N., Hartley, C. S., et al. (2019). An open-format enteroid culture system for interrogation of interactions between toxoplasma gondii and the intestinal epithelium. *Front. Cell. Infect. Microbiol.* 9. doi: 10.3389/fcimb.2019.00300

Majumdar, T., Sharma, S., Kumar, M., Hussain, M. A., Chauhan, N., Kalia, I., et al. (2019). Tryptophan-kynurenine pathway attenuates β-catenin-dependent pro-parasitic role of STING-TICAM2-IRF3-IDO1 signalosome in toxoplasma gondii infection. *Cell Death Dis.* 10 (3), 161. doi: 10.1038/s41419-019-1420-9

May, S., Evans, S., and Parry, L. (2017). Organoids, organs-on-chips and other systems, and microbiota. *Emerg. Top Life Sci.* 0, 385–400. doi: 10.1042/ETLS20170047

McCracken, K. W., Howell, J. C., Wells, J. M., and Spence, J. R. (2011). Generating human intestinal tissue from pluripotent stem cells *in vitro*. *Nat. Protoc.* 6, 1920–1928. doi: 10.1038/nprot.2011.410

Mennechet, F. J. D., Kasper, L. H., Rachinel, N., Li, W., Vandewalle, A., and Buzoni-Gatel, D. (2002). Lamina propria CD4 + T lymphocytes synergize with murine intestinal epithelial cells to enhance proinflammatory response against an intracellular pathogen. *J. Immunol.* 168, 2988–2996. doi: 10.4049/jimmunol.168.6.2988

Mileto, S. J., Jardé, T., Childress, K. O., Jensen, J. L., Rogers, A. P., Kerr, G., et al. (2020). Clostridioides difficile infection damages colonic stem cells *via* TcdB, impairing epithelial repair and recovery from disease. *Proc. Natl. Acad. Sci. U. S. A.* 117, 8064–8073. doi: 10.1073/pnas.1915255117

Monroy, F. P. (2008). Toxoplasma gondii: effect of infection on expression of 14-3-3 proteins in human epithelial cells. *Exp. Parasitol.* 118, 134–138. doi: 10.1016/j.exppara.2007.07.008

Morada, M., Lee, S., Gunther-Cummins, L., Weiss, L. M., Widmer, G., Tzipori, S., et al. (2015). Continuous culture of cryptosporidium parvum using hollow fiber technology. *Int. J. Parasitol.* 46, 21–29. doi: 10.1016/j.ijpara.2015.07.006

Morampudi, V., Braun, M. Y., and D'Souza, S. (2011). Modulation of early β-defensin-2 production as a mechanism developed by type I toxoplasma gondii to evade human intestinal immunity. *Infect. Immun.* 79, 2043–2050. doi: 10.1128/IAI.01086-10

Morrissette, N. S., and Sibley, L. D. (2002). Disruption of microtubules uncouples budding and nuclear division in toxoplasma gondii. *J. Cell Sci.* 115, 1017–1025. doi: 10.1242/jcs.115.5.1017

Moura, M., de, A., Amendoeira, M. R. R., and Barbosa, H. S. (2009). Primary culture of intestinal epithelial cells as a potential model for toxoplasma gondii enteric cycle studies. *Mem. Inst. Oswaldo Cruz* 104, 862–864. doi: 10.1590/S0074-02762009000600007

Mussard, E., Pouzet, C., Helies, V., Pascal, G., Fourre, S., Cherbuy, C., et al. (2020). Culture of rabbit caecum organoids by reconstituting the intestinal stem cell niche *in vitro* with pharmacological inhibitors or l-WRN conditioned medium. *Stem Cell Res.* 48, 101980. doi: 10.1016/j.scr.2020.101980

Nikolaev, M., Mitrofanova, O., Broguiere, N., Geraldo, S., Dutta, D., Tabata, Y., et al. (2020). Homeostatic mini-intestines through scaffold-guided organoid morphogenesis. *Nature* 585, 574–578. doi: 10.1038/s41586-020-2724-8

Palikuqi, B., Nguyen, D. H. T., Li, G., Schreiner, R., Pellegata, A. F., Liu, Y., et al. (2020). Adaptable haemodynamic endothelial cells for organogenesis and tumorigenesis. *Nature* 585, 426–432. doi: 10.1038/s41586-020-2712-z

Pelster, B., and Piekarski, G. (1971). Elektronenmikroskopische analyse der mikrogametenentwicklung bei toxoplasma gondii. *Z. für Parasitenkd.* 37, 267–277. doi: 10.1007/BF00259333

Pimenta, J., Ribeiro, R., Almeida, R., Costa, P. F., da Silva, M. A., and Pereira, B. (2022). Organ-on-chip approaches for intestinal 3D *in vitro* modeling. *Cmgh* 13, 351–367. doi: 10.1016/j.jcmgh.2021.08.015

Pittman, K. J., and Knoll, L. J. (2015). Long-term relationships: the complicated interplay between the host and the developmental stages of toxoplasma gondii during acute and chronic infections. *Microbiol. Mol. Biol. Rev.* 79, 387–401. doi: 10.1128/mmbr.00027-15

Powell, R. H., and Behnke, M. S. (2017). WRN conditioned media is sufficient for *in vitro* propagation of intestinal organoids from large farm and small companion animals. *Biol. Open* 6, 698–705. doi: 10.1242/bio.021717

Quan, J. H., Huang, R., Wang, Z., Huang, S., Choi, I. W., Zhou, Y., et al. (2018). P2X7 receptor mediates NLRP3-dependent IL-1β secretion and parasite proliferation in toxoplasma gondii-infected human small intestinal epithelial cells. *Parasites Vectors* 11, 1–10. doi: 10.1186/s13071-017-2573-y

Rajan, S. A. P., Aleman, J., Wan, M. M., Pourhabibi Zarandi, N., Nzou, G., Murphy, S., et al. (2020). Probing prodrug metabolism and reciprocal toxicity with an integrated and humanized multi-tissue organ-on-a-chip platform. *Acta Biomater.* 106, 124–135. doi: 10.1016/j.actbio.2020.02.015

Ramakrishnan, C., Maier, S., Walker, R. A., Rehrauer, H., Joekel, D. E., Winiger, R. R., et al. (2019). An experimental genetically attenuated live vaccine to prevent transmission of toxoplasma gondii by cats. *Sci. Rep.* 9, 1–14. doi: 10.1038/s41598-018-37671-8

Ramakrishnan, C., and Smith, N. C. (2021). Recent achievements and doors opened for coccidian parasite research and development through transcriptomics of enteric sexual stages. *Mol. Biochem. Parasitol.* 243, 111373. doi: 10.1016/j.molbiopara.2021.111373

Ramírez-Flores, C. J., Perdomo, A. M. T., Gallego-López, G. M., and Knoll, L. J. (2022). Transcending dimensions in apicomplexan research: from two-dimensional to three-dimensional *In vitro* cultures. *Microbiol. Mol. Biol. Rev.* 86, 1–26. doi: 10.1128/MMBR.00025-22

Randall, K. J., Turton, J., and Foster, J. R. (2011). Explant culture of gastrointestinal tissue: a review of methods and applications. *Cell Biol. Toxicol.* 27, 267–284. doi: 10.1007/s10565-011-9187-5

Ross, E. C., Olivera, G. C., and Barragan, A. (2019). Dysregulation of focal adhesion kinase upon toxoplasma gondii infection facilitates parasite translocation across polarised primary brain endothelial cell monolayers. *Cell. Microbiol.* 21, 1–14. doi: 10.1111/cmi.13048

Rousset, M. (1986). The human colon carcinoma cell lines HT-29 and caco-2: two *in vitro* models for the study of intestinal differentiation. *Biochimie* 68, 1035–1040. doi: 10.1016/S0300-9084(86)80177-8

Sambuy, Y., De Angelis, I., Ranaldi, G., Scarino, M. L., Stammati, A., and Zucco, F. (2005). The caco-2 cell line as a model of the intestinal barrier: influence of cell and culture-related factors on caco-2 cell functional characteristics. *Cell Biol. Toxicol.* 21, 1–26. doi: 10.1007/s10565-005-0085-6

Saraav, I., Cervantes-Barragan, L., Olias, P., Fu, Y., Wang, Q., Wang, L., et al. (2021). Chronic toxoplasma gondii infection enhances susceptibility to colitis. *Proc. Natl. Acad. Sci. USA.* 118, 1–11. doi: 10.1073/pnas.2106730118

Sasai, M., and Yamamoto, M. (2019). Innate, adaptive, and cell-autonomous immunity against toxoplasma gondii infection. *Exp. Mol. Med.* 51, 1–10. doi: 10.1038/s12276-019-0353-9

Sato, T., Stange, D. E., Ferrante, M., Vries, R. G. J., Van Es, J. H., Van Den Brink, S., et al. (2011a). Long-term expansion of epithelial organoids from human colon, adenoma, adenocarcinoma, and barrett's epithelium. *Gastroenterology* 141, 1762–1772. doi: 10.1053/j.gastro.2011.07.050

Sato, T., Van Es, J. H., Snippert, H. J., Stange, D. E., Vries, R. G., Van Den Born, M., et al. (2011b). Paneth cells constitute the niche for Lgr5 stem cells in intestinal crypts. *Nature* 469, 415–418. doi: 10.1038/nature09637

Sato, T., Vries, R. G., Snippert, H. J., Van De Wetering, M., Barker, N., Stange, D. E., et al. (2009). Single Lgr5 stem cells build crypt-villus structures *in vitro* without a mesenchymal niche. *Nature* 459, 262–265. doi: 10.1038/nature07935

Scholtyseck, E., Mehlhorn, H., and Hammond, D. M. (1972). Electron microscope studies of microgametogenesis in coccidia and related groups. *Z. fur Parasitenkd.* 38, 95–131. doi: 10.1007/BF00329023

Schulz, O., Jaensson, E., Persson, E. K., Liu, X., Worbs, T., Agace, W. W., et al. (2009). Intestinal CD103+, but not CX3CR1+, antigen sampling cells migrate in lymph and serve classical dendritic cell functions. *J. Exp. Med.* 206, 3101–3114. doi: 10.1084/jem.20091925

Sharma, J., Rodriguez, P., Roy, P., and Guiton, P. S. (2020). Transcriptional ups and downs: patterns of gene expression in the life cycle of toxoplasma gondii. *Microbes Infect.* 22, 525–533. doi: 10.1016/j.micinf.2020.09.001

Sibley, D. L., Khan, A., Ajioka, J. W., and Rosenthal, B. M. (2009). Genetic diversity of toxoplasma gondii in animals and humans. *Philos. Trans. R. Soc B Biol. Sci.* 364, 2749–2761. doi: 10.1098/rstb.2009.0087

Sinagoga, K. L., and Wells, J. M. (2015). Generating human intestinal tissues from pluripotent stem cells to study development and disease. *EMBO J.* 34, 1149–1163. doi: 10.15252/embj.201490686

Smith, D., Price, D. R. G., Burrells, A., Faber, M. N., Hildersley, K. A., Chintoan-Uta, C., et al. (2021). The development of ovine gastric and intestinal organoids for studying ruminant host-pathogen interactions. *Front. Cell. Infect. Microbiol.* 11. doi: 10.3389/fcimb.2021.733811

Snyder, L. M., and Denkers, E. Y. (2021). From initiators to effectors: roadmap through the intestine during encounter of toxoplasma gondii with the mucosal immune system. *Front. Cell. Infect. Microbiol.* 10. doi: 10.3389/fcimb.2020.614701

Spence, J. R., Mayhew, C. N., Rankin, S. A., Kuhar, M. F., Vallance, J. E., Tolle, K., et al. (2011). Directed differentiation of human pluripotent stem cells into intestinal tissue *in vitro*. *Nature* 470, 105–110. doi: 10.1038/nature09691

Srivastava, S., Holmes, M. J., White, M. W., and Sullivan, W. J. (2023). Toxoplasma gondii AP2XII-2 contributes to transcriptional repression for sexual commitment. *mSphere* 8, 1–12. doi: 10.1128/msphere.00606-22

Stewart, A. S., Schaaf, C. R., Luff, J. A., Freund, J. M., Becker, T. C., Tufts, S. R., et al. (2021). HOPX+ injury-resistant intestinal stem cells drive epithelial recovery after severe intestinal ischemia. *Am. J. Physiol. Gastrointest. Liver Physiol.* 321, G588–G602. doi: 10.1152/ajpgi.00165.2021

Sullivan, W. J., and Jeffers, V. (2012). Mechanisms of toxoplasma gondii persistence and latency. *FEMS Microbiol. Rev.* 36, 717–733. doi: 10.1111/j.1574-6976.2011.00305.x

Sunuwar, L., Yin, J., Kasendra, M., Karalis, K., Kaper, J., Fleckenstein, J., et al. (2020). Mechanical stimuli affect escherichia coli heat-stable enterotoxin-cyclic GMP signaling in a human enteroid intestine-chip model. *Infect. Immun.* 88 (3), e00866-19. doi: 10.1128/IAI.00866-19

Takenaka, T., Harada, N., Kuze, J., Chiba, M., Iwao, T., and Matsunaga, T. (2016). Application of a human intestinal epithelial cell monolayer to the prediction of oral drug absorption in humans as a superior alternative to the caco-2 cell monolayer. *J. Pharm. Sci.* 105, 915–924. doi: 10.1016/j.xphs.2015.11.035

Tang, Q., Tang, J., Ren, X., and Li, C. (2020). Glyphosate exposure induces inflammatory responses in the small intestine and alters gut microbial composition in rats. *Environ. pollut.* 261, 114129. doi: 10.1016/j.envpol.2020.114129

ten Hoeve, A. L., Braun, L., Rodriguez, M. E., Olivera, G. C., Bougdour, A., Belmudes, L., et al. (2022). The toxoplasma effector GRA28 promotes parasite dissemination by inducing dendritic cell-like migratory properties in infected macrophages. *Cell Host Microbe* 30, 1570–1588. doi: 10.1016/j.chom.2022.10.001

Tomasina, R., and Francia, M. E. (2020). The structural and molecular underpinnings of gametogenesis in toxoplasma gondii. *Front. Cell. Infect. Microbiol.* 10. doi: 10.3389/fcimb.2020.608291

Tovaglieri, A., Sontheimer-Phelps, A., Geirnaert, A., Prantil-Baun, R., Camacho, D. M., Chou, D. B., et al. (2019). Species-specific enhancement of enterohemorrhagic e. coli pathogenesis mediated by microbiome metabolites. *Microbiome* 7 (1), 43. doi: 10.1186/s40168-019-0650-5

Verhoeckx, K. (2015). *The impact of food bioactives on health: in vitro and ex vivo models* (Springer). doi: 10.1007/978-3-319-16104-4_26

Weeber, F., Van De Wetering, M., Hoogstraat, M., Dijkstra, K. K., Krijgsman, O., Kuilman, T., et al. (2015). Preserved genetic diversity in organoids cultured from biopsies of human colorectal cancer metastases. *Proc. Natl. Acad. Sci. U. S. A.* 112, 13308–13311. doi: 10.1073/pnas.1516689112

Weight, C. M., Jones, E. J., Horn, N., Wellner, N., and Carding, S. R. (2015). Elucidating pathways of toxoplasma gondii invasion in the gastrointestinal tract: involvement of the tight junction protein occludin. *Microbes Infect.* 17, 698–709. doi: 10.1016/j.micinf.2015.07.001

Weiss, L. M. (2000). The development and biology of bradyzoites of toxoplasma gondii. *Front. Biosci.* 5, 1–24. doi: 10.2741/weiss

Wiertsema, S. P., van Bergenhenegouwen, J., Garssen, J., and Knippels, L. M. J. (2021). The interplay between the gut microbiome and the immune system in the context of infectious diseases throughout life and the role of nutrition in optimizing treatment strategies. *Nutrients* 13, 1–14. doi: 10.3390/nu13030886

Wilke, G., Funkhouser-Jones, L. J., Wang, Y., Ravindran, S., Wang, Q., Beatty, W. L., et al. (2019). A stem-Cell-Derived platform enables complete cryptosporidium development *In vitro* and genetic tractability. *Cell Host Microbe* 26, 123–134. doi: 10.1016/j.chom.2019.05.007

Wilson, S. S., Tocchi, A., Holly, M. K., Parks, W. C., and Smith, J. G. (2015). A small intestinal organoid model of non-invasive enteric pathogen-epithelial cell interactions. *Mucosal Immunol.* 8, 352–361. doi: 10.1038/mi.2014.72

Xiang, Y., Wen, H., Yu, Y., Li, M., Fu, X., and Huang, S. (2020). Gut-on-chip: recreating human intestine *in vitro*. *J. Tissue Eng.* 11, 2041731420965318. doi: 10.1177/2041731420965318

Zhai, B., Xie, S., Peng, J., Qiu, Y., Liu, Y., Zhu, X., et al. (2022). Glycosylation analysis of feline small intestine following toxoplasma gondii infection. *Animals* 12, 1–17. doi: 10.3390/ani12202858

Zhang, Y. G., Wu, S., Xia, Y., and Sun, J. (2014). Salmonella-infected crypt-derived intestinal organoid culture system for host–bacterial interactions. *Physiol. Rep.* 2, 1–11. doi: 10.14814/phy2.12147

Zhao, Z., Chen, X., Dowbaj, A. M., Sljukic, A., Bratlie, K., Lin, L., et al. (2022). Organoids. *Nat. Rev. Methods Prim.* 2, 94. doi: 10.1038/s43586-022-00174-y

Zhao, G. H., Liu, Y., Cheng, Y. T., Zhao, Q. S., Qiu, X., Xu, C., et al. (2018). Primary culture of cat intestinal epithelial cells *in vitro* and the cDNA library construction. *Acta Parasitol.* 63, 360–367. doi: 10.1515/ap-2018-0041

Zihni, C., Mills, C., Matter, K., and Balda, M. S. (2016). Tight junctions: from simple barriers to multifunctional molecular gates. *Nat. Rev. Mol. Cell Biol.* 17, 564–580. doi: 10.1038/nrm.2016.80

frontiers | Frontiers in Cellular and Infection Microbiology

TYPE Original Research
PUBLISHED 16 October 2023
DOI 10.3389/fcimb.2023.1286190

OPEN ACCESS

EDITED BY
Gabriel Rinaldi,
Aberystwyth University, United Kingdom

REVIEWED BY
Tania Rozario,
University of Georgia, Athens, United States
George Wendt,
University of Texas Southwestern Medical Center, Dallas, United States

*CORRESPONDENCE
Uriel Koziol
ukoziol@fcien.edu.uy

RECEIVED 31 August 2023
ACCEPTED 02 October 2023
PUBLISHED 16 October 2023

CITATION
Montagne J, Preza M and Koziol U (2023) Stem cell proliferation and differentiation during larval metamorphosis of the model tapeworm *Hymenolepis microstoma*. *Front. Cell. Infect. Microbiol.* 13:1286190. doi: 10.3389/fcimb.2023.1286190

Stem cell proliferation and differentiation during larval metamorphosis of the model tapeworm *Hymenolepis microstoma*

Jimena Montagne, Matías Preza and Uriel Koziol*

Sección Biología Celular, Facultad de Ciencias, Universidad de la República, Montevideo, Uruguay

Background: Tapeworm larvae cause important diseases in humans and domestic animals. During infection, the first larval stage undergoes a metamorphosis where tissues are formed *de novo* from a population of stem cells called germinative cells. This process is difficult to study for human pathogens, as these larvae are infectious and difficult to obtain in the laboratory.

Methods: In this work, we analyzed cell proliferation and differentiation during larval metamorphosis in the model tapeworm *Hymenolepis microstoma*, by *in vivo* labelling of proliferating cells with the thymidine analogue 5-ethynyl-2′-deoxyuridine (EdU), tracing their differentiation with a suite of specific molecular markers for different cell types.

Results: Proliferating cells are very abundant and fast-cycling during early metamorphosis: the total number of cells duplicates every ten hours, and the length of G2 is only 75 minutes. New tegumental, muscle and nerve cells differentiate from this pool of proliferating germinative cells, and these processes are very fast, as differentiation markers for neurons and muscle cells appear within 24 hours after exiting the cell cycle, and fusion of new cells to the tegumental syncytium can be detected after only 4 hours. Tegumental and muscle cells appear from early stages of metamorphosis (24 to 48 hours post-infection); in contrast, most markers for differentiating neurons appear later, and the detection of synapsin and neuropeptides correlates with scolex retraction. Finally, we identified populations of proliferating cells that express conserved genes associated with neuronal progenitors and precursors, suggesting the existence of tissue-specific lineages among germinative cells.

Discussion: These results provide for the first time a comprehensive view of the development of new tissues during tapeworm larval metamorphosis, providing a framework for similar studies in human and veterinary pathogens.

KEYWORDS

differentiation, stem cell, neoblast, cestode, oncosphere, metacestode, tegument, *NeuroD*

Introduction

Tapeworms (cestodes) are a diverse group of parasitic flatworms, many of which cause important diseases in humans and domestic animals (Budke et al., 2009; Torgerson et al., 2010; Hotez et al., 2014). Tapeworms have a divergent morphology and development that results from their adaptation to the parasitic lifestyle, including complex life cycles with successive larval and adult stages inhabiting different hosts (Freeman, 1973; Koziol, 2017). The first larval stage of tapeworms, called the oncosphere, is a miniaturized organism, typically containing fewer than a hundred cells (Ubelaker, 1980; Swiderski et al., 2016). This larva is specialized for the infection of the first host of the life cycle, and contains structures such as penetration glands and larval hooks, actuated by a complex system of muscles, which participate in the penetration of the intestine of the host. The oncosphere undergoes a metamorphosis in a parenteral site of the intermediate host, developing into the next life stage, the metacestode. Metacestodes from different cestode groups have a bewildering diversity of morphologies, which may or may not include protective cyst tissues, but in all cases the infective metacestode includes an anterior scolex (head) with attachment organs, which is infective to the definitive host (Freeman, 1973; Chervy, 2002). Tapeworm species that cause the most important and life-threatening diseases are those in which humans are infected by larval forms (Budke et al., 2009), and the larval metamorphosis is thought to be a key step of the infection process during which the parasite is most vulnerable (Nono et al., 2012).

It is thought that most of the differentiated cells of the oncosphere are discarded during the larval metamorphosis (Freeman, 1973; Koziol, 2017). The differentiated tissues of the metacestode are therefore generated *de novo*, including the nervous and excretory systems, or extensively remodeled, including the tegumental syncytium that covers the larva. In tapeworms, and more generally in flatworms, differentiated cells are invariably post-mitotic and cell proliferation during post-embryonic development depends on undifferentiated stem cells (Reuter and Kreshchenko, 2004; Egger et al., 2009; Rink, 2013; Koziol et al., 2014; Rozario et al., 2019). These are usually called germinative cells in tapeworms, and are equivalent in their function to the neoblasts of free-living flatworms, such as planarians. Recent studies have shown that germinative cells are heterogeneous in their gene expression patterns, indicating that they are not a single cell population, but may comprise different lineages and hierarchies, as has been shown for planarian neoblasts (Koziol et al., 2014; Rozario et al., 2019; Molina and Cebrià, 2021).

Oncospheres of many different tapeworm species have been shown to possess a limited number of set-aside germinative cells, from which all further development is thought to occur after infection (Ubelaker, 1980; Koziol, 2017). However, very little is known about cell proliferation and differentiation during the larval metamorphosis in tapeworms, and it is unclear how these processes may relate or differ to other life-stages in tapeworms, or to other flatworm species. Most of what is known of larval metamorphosis in tapeworms comes from classical histological and electron microscopy studies, showing massive accumulation of germinative cells during the early metamorphosis, tegumental remodeling, and in some cases also including snapshots of the development of muscle and nerve cells (Bilqees and Freeman, 1969; Collin, 1970; Sakamoto and Sugimura, 1970; Shield et al., 1973; Schramlová and Blazek, 1983; Bortoletti and Ferretti, 1985; Holcman et al., 1994; Korneva, 2004). The study of larval metamorphosis in tapeworms that are directly relevant to human health, such as the taeniid genera *Echinococcus* and *Taenia*, is very difficult due to their infectivity to humans, the requirement for vertebrate laboratory hosts, and their slow metamorphosis (which can take weeks or even months, depending on the species, to reach metacestode infectivity). Although *in vitro* culture systems that support larval metamorphosis have been developed for some tapeworm species, these rarely allow complete development until infectivity and show a high variability (Heath and Smyth, 1970; Evans, 1980; Chile et al., 2016; Palma et al., 2019).

Species of genus *Hymenolepis* have been some of the most important laboratory models for the study of tapeworm biology, since the maintenance of their life-cycle in the laboratory is simple, using beetles and rodents as intermediate and definitive hosts, respectively (Arai, 1980). Recent developments have renewed the potential of these model species, including high quality genome sequences, life-stage and region-specific transcriptomes, optimization of methods for *in situ* gene expression analysis, and functional analyses by RNA interference (Cunningham and Olson, 2010; Pouchkina-Stantcheva et al., 2013; Olson et al., 2018; Rozario et al., 2019; Olson et al., 2020; Preza et al., 2021). The metacestode of *Hymenolepis* spp. is called a cysticercoid, and once developed consists of a small scolex and body that are withdrawn within a protective cyst (also called capsule). A tail or appendage, called the cercomer, continues growing from the posterior of the cyst even after infectivity is reached. Once the cysticercoid is ingested by the definitive host, the cyst and cercomer tissues are destroyed in the digestive system, and the freed activated cysticercoid consists solely of the scolex and a small posterior body. Early studies described only in broad strokes the larval metamorphosis of different *Hymenolepis* species, mostly by classic histological methods (Ubelaker, 1980). More recently, a transcriptomic analysis of the early metamorphosis in *Hymenolepis microstoma* has shown similarities in global gene expression to the generative neck region of adult worms, and described the localized expression of several transcription factors indicating that larval metamorphosis is a highly dynamic process, in which fate specification and cell differentiation are likely to begin from the earliest stages (Olson et al., 2018). In this work, we have studied in detail the early larval metamorphosis of the model tapeworm *H. microstoma*, describing the development of the different tissues and systems of the metacestode, and tracing the proliferation and differentiation of germinative cells during these processes.

Materials and methods

Parasite material

H. microstoma ("Nottingham strain") was maintained using C57BL/6 mice as definitive hosts, and *Tribolium confusum* as intermediate hosts, as previously described (Cunningham and Olson, 2010), in collaboration with Jenny Saldaña, Laboratorio de

Experimentación Animal, Facultad de Química, Universidad de la República, Uruguay ("Mantenimiento del ciclo vital completo del cestodo *H. microstoma* utilizando sus hospedadores naturales *Mus musculus* (ratón) y *Tribolium confusum* (escarabajo de la harina)", protocol number 10190000025215, approved by Comisión Honoraria de Experimentación Animal, Uruguay). Starved beetles were exposed to infective eggs overnight, and routinely incubated at 28 ± 1°C. For some infections, incubation was performed at lower (25°C) or higher (30°C) temperatures to accelerate or delay development in order to accommodate the times at which larvae at specific developmental stages had to be collected. *In vitro* activation of infective cysticercoids was performed as described by Preza et al., 2022. Larvae were routinely fixed for most downstream protocols using 4% paraformaldehyde prepared in phosphate buffered saline (PBS), overnight at 4-8°C.

Infection of *Tenebrio molitor* and *in vivo* labelling with 5-Ethynyl-2′-deoxyuridine

T. molitor beetles were purchased from local providers, or raised at 20-26°C with a 12 h:12 h photoperiod, in 20 x 10 cm pots with 90% wholemeal flour and 10% yeast, plus fruit once a week. Beetles were starved for 48 hours before being exposed to infective eggs overnight. For EdU labelling, beetles were anesthetized with triethylamine for one to two minutes, the posterior half of one elytron was removed with forceps, and 5 µl of a 200 µM solution of EdU (Thermo-Fisher) was injected with a Hamilton precision syringe into the hemocoel in the abdomen. Beetles were maintained in wholemeal flour at 28 ± 1°C, and larvae were collected after different times by dissection of the beetles in PBS. EdU labelling was developed with the Click-iT™ EdU Cell Proliferation Kit for Imaging, Alexa Fluor™ 555 dye or Alexa Fluor™ 488 dye (Thermo-Fisher C10337 and C10338).

Dextran labelling of the tegument

Larvae were collected by dissecting infected beetles in PBS, and stained with tetramethylrhodamine and biotin conjugated dextran (10,000 MW, Lysine Fixable, Thermo-Fisher D3312) with a protocol modified from Wendt et al., 2018. Up to 300 larvae were incubated in 250 µl of a 2-5 mg/ml solution of conjugated dextran; larvae collected during the first two days post infection were incubated briefly without vortexing, whereas larvae collected from three days post-infection onwards were incubated for 2 to 3 min with low speed vortexing. Then, larvae were fixed by adding 1 ml of 4% paraformaldehyde prepared in PBS, and the solution was replaced immediately with 1 ml of fresh 4% paraformaldehyde solution and incubated overnight at 4-8°C.

Transmission electron microscopy

Larvae collected three days post infection were fixed in glutaraldehyde (2.5%) and paraformaldehyde (2%) prepared in cacodylate solution (50 mM cacodylate, 50 mM KCl, 2.5 mM $MgCl_2$ pH 7.2) for 3 hours. After washing, samples were post-fixed in 1% osmium tetroxide, dehydrated using ethanol, infiltrated and embedded in Araldite resin. Ultrathin 70 nm sections were obtained using an RMC MT-X ultramicrotome and mounted on formvar-coated copper grids. Observation and acquisition were performed using a Jeol JEM 1010 transmission electron microscope operated at 100 kV, equipped with a Hamamatsu C4742-95 digital camera (Unidad de Microscopía Electrónica, Facultad de Ciencias, Universidad de la República, Uruguay).

Whole mount immunofluorescence

Whole mount immunofluorescence (WMIHF) was performed following a modification of the protocol described by Koziol et al., 2013. Briefly, fixed larvae were washed extensively with PBS containing 0.3% Triton X-100 (PBS-T), permeabilized for 20 minutes in PBS containing 1% sodium dodecyl sulfate (SDS), washed again three times in PBS-T, and blocked for 2 hours in PBS-T with 3% bovine serum albumin (BSA, Merck) and 5% normal sheep serum (Merck). Incubation with primary antibodies was done for 12 to 72 hours at 8°C in PBS-T with 3% BSA and 0.02% sodium azide. After four one-hour long washes, the samples were incubated with secondary antibodies for 12 to 72 hours at 8°C in PBS-T with 3% BSA and 0.02% sodium azide. Finally, samples were washed four times for one hour in PBS-T. Nuclei were stained using either 4′,6-diamidino-2-phenylindole (DAPI) or methyl green (Prieto et al., 2014), and in some experiments actin filaments were stained with phalloidin conjugated to fluorescein isothiocyanate (Merck). The primary antibodies used were: rabbit polyclonal anti-tropomyosin (Koziol et al., 2011), 1:500 dilution; rabbit polyclonal anti-FMRFamide (Immunostar, ID 20091), 1:300 dilution; rabbit polyclonal anti-serotonin (Immunostar, ID 20080), 1:300 dilution; rabbit polyclonal anti-phospho-histone H3 (Ser10) (Cell Signalling Technology #9701) 1:100 dilution; mouse monoclonal anti-synapsin (clone 3C11, Developmental Studies Hybridoma Bank), 1:100 dilution. The secondary antibodies used included anti-rabbit antibodies conjugated to Alexa Fluor 546 (Invitrogen A11010) and anti-mouse antibodies conjugated to Alexa Fluor 647 (Invitrogen A31571).

Histological sectioning and immunofluorescence

For some experiments, immunofluorescence was performed with 20 µm-thick cryosections of samples previously included in Tissue-Tek OCT compound (Sakura FineTek cat. no. 4583) as previously described (Koziol et al., 2013).

Identification of *H. microstoma* homologs of transcription factors related to muscle and neural development

The predicted proteome of *H. microstoma* was downloaded from WormBase ParaSite (Howe et al., 2017; https://parasite.wormbase.org/, version 14), and used to search by reciprocal BLASTP for homologs of *myoD*, *nkx-1.1*, *coe* (collier),

neuroD and *soxB*, using sequences from *Homo sapiens*, *Drosophila melanogaster*, *Caenorhabditis elegans*, and *Schmidtea mediterranea*. Further confirmation of the orthology of basic helix-loop helix genes (bHLH) was obtained by InterPro domain analysis (Paysan-Lafosse et al., 2023). In the case of *neuroD*, InterPro domain analysis confirmed the presence of the *neuroD*-specific domain IPR022575 at the C-terminus of the predicted protein. For *coe*, InterPro domain analysis also confirmed the presence of the specific COE DNA-binding domain (IPR032200) and IPT domain (IPR002909). For *myoD*, InterPro domain analysis confirmed the presence of the specific MyoD_N N-terminal domain (IPR002546).

Whole mount *in situ* hybridization

Fragments of the coding sequence of each gene were obtained by RT-PCR of *H. microstoma* total adult cDNA using specific primers (Supplementary Table S1), cloned into pGEM-T (Promega) and used to synthesize digoxigenin-labeled probes by *in vitro* transcription using SP6 or T7 polymerases (Thermo-Fisher), in reactions containing 3.5 mM digoxigenin-UTP (Merck), 6.5 mM UTP, and 10 mM ATP, GTP and CTP. The cDNA fragments used for probe synthesis for *pc2*, *chat*, *vglut* and *tph* were the same as the ones described in Preza et al., 2018. Fluorescent whole-mount *in situ* hybridization (WMISH) was performed as previously described (Koziol et al., 2014; Koziol et al., 2016). Samples were co-stained with DAPI or methyl green. When WMISH was combined with EdU labelling or WMIHF, these protocols were performed after WMISH was complete.

Sample mounting, imaging and image analysis

Samples were mounted in 80% glycerol with 50 mM Tris, pH 8.0, or with ProLong Glass Antifade Mountant (Thermo-Fisher). Samples were imaged by confocal microscopy (Zeiss LSM 800CyAn and Zeiss LSM 880, Advanced Bioimaging Unit of the Institute Pasteur of Montevideo). Images were analyzed and processed using FIJI (Schindelin et al., 2012).

Statistics

Statistical analysis was carried out using Graphpad Prism 8 software for plots, linear regression and non-parametric Mann-Whitney test (significance was considered at $p < 0.05$).

Results

Overview of larval metamorphosis in *H. microstoma*

An overview of the metamorphosis of *H. microstoma* was described by Voge (1964) and Goodchild and Stullken (1970). We have modified the staging system of Voge (1964), subdividing the developmental stages based on finer anatomical details. These stages, and their corresponding time of appearance (in days post infection, d.p.i.) at 28°C, are shown in Figure 1, and described briefly below:

Stage 0 (0 d.p.i). We refer to the hatched infective oncosphere as stage 0 (as this was not included in the staging system of Voge, 1964). Larval diameter is approximately 25 to 30 µm.

Stage 1.1 (1-2 d.p.i). The larva is compact, has a roughly circular outline, and has a diameter of approximately 35-50 µm.

Stage 1.2. (2-3 d.p.i.). The larva has a roughly circular outline, with a diameter of approximately 50-70 µm. A small central cavity begins to form between the deeper cells, this is the beginning of the formation of the so-called central cavity, also known as the primary lacuna (Freeman, 1973).

Stage 2.1 (3-4 d.p.i.). The outline of the larva is ovoid. The central cavity becomes larger, and is displaced to the posterior (closer to the remaining oncospheral hooks). Nuclei in the anterior region, which will become the scolex, are smaller and more compactly distributed. The length of the larva is 70-110 µm.

Stage 2.2 (4-5 d.p.i.). The outline of the larva is ovoid, but further growth occurs and the central cavity becomes larger. The length of the larva is 95-150 µm.

Stage 3.1 (4-5 d.p.i.). The outline of the larva is ovoid, and the primordia of the attachment organs of the scolex become distinguishable. The primordium of the rostellum (apical attachment organ) can be distinguished by a gap between the primordium and the rest of the larva, and the primordia of the four suckers can be seen as small masses of cells. The length of the larva is 150-200 µm.

Stage 3.2 (5 d.p.i). The larva becomes elongated, and the primordia of the suckers become more prominent. The length of the larva is 200-270 µm.

Stage 4.1 (5-6 d.p.i.). The anterior part of the larva (the future scolex and body of the cysticercoid) withdraws into the cavity, becoming surrounded by the future cyst tissues. The cavity collapses as the anterior end withdraws. The withdrawal of the scolex and body into the cyst tissues has been shown to be a fast process mediated by the retraction of muscle fibers (Caley, 1974). The scolex primordium is thus located at the bottom of the withdrawn tissue, and the developing body is folded around the scolex. The posterior-most region of the larva begins to grow, becoming the cercomer (tail).

Stage 4.2 (6-7 d.p.i.). Scolex development proceeds, including the differentiation of the rostellum (as rostellar hooks appear) and suckers. The cyst tissues develop around the scolex and body. The cercomer grows to a size comparable to that of the cyst.

10.3389/fcimb.2023.1286190

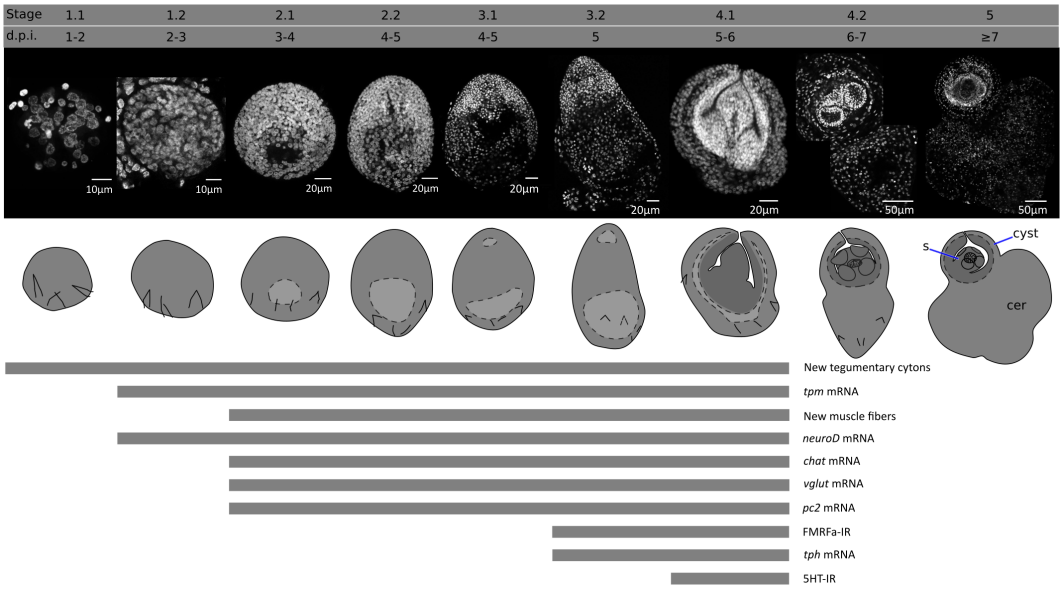

FIGURE 1
Developmental stages of larval metamorphosis in *H. microstoma*. The morphology at each developmental stage is shown by nuclear staining (top pictures) and diagrams (bottom pictures). The presence of some differentiation processes and markers studied in this work, up to stage 4.1, is summarized with bars below. s, scolex; cer, cercomer.

Stage 5 (8 d.p.i). Scolex and cyst development concludes. Cercomer growth may continue beyond this stage, and reach lengths that are many times longer than the cyst.

There is some variability in the developmental stages of larvae found between different beetles and within the same beetle, which may be due in part to the prolonged overnight exposure of the beetles to the infective eggs, resulting in slightly different infection times.

Cell proliferation during larval metamorphosis

Growth is very fast during the early stages of metamorphosis, and the total number of nuclei increases exponentially during the first three days of metamorphosis (from an average of 43 nuclei 1 d.p.i., to 1219 nuclei 3 d.p.i., Figure 2A). The doubling time for the total number of nuclei was estimated to be 10 hours. Because cell cycle exit and differentiation are already underway for some cells at these stages (see below), this gives an upper bound to the total length of the cell cycle of proliferating cells during early larval metamorphosis.

In order to identify the distribution of proliferating cells during larval metamorphosis, we developed an *in vivo* protocol for metabolic labelling of cells actively undergoing DNA synthesis using the thymidine analogue 5-ethynyl-2´-deoxyuridine (EdU). To this end, we infected *Tenebrio molitor*, a large beetle species susceptible to infection by *H. microstoma* (Voge and Graiwer, 1964) which can be easily manipulated experimentally. EdU was injected into the hemocoel of the beetle (Figure 2B) at different time points after infection, and the incorporation of EdU by *H. microstoma* larvae was assessed 2 hours after injection (Figure 2C). In stages 1.1 and 1.2, EdU^+ cells are very abundant, and distributed throughout the larval tissues. Their nuclei are relatively large, and only a few smaller nuclei in the periphery of the larvae appear to always be EdU negative. In later stages (2.1 to 3.2), although EdU^+ cells are still abundant, there are many regions that appear to be devoid of proliferation, especially at the surface of the larva and in specific regions of the scolex, including the anterior pole. Finally, in stages 4.1 and 4.2 (after the withdrawal of the anterior end), EdU^+ cells are absent from the developing scolex, but present in the cysticercoid body and cercomer. These results suggest that although development is still underway in the scolex after its retraction, this is based on the differentiation of cells that are already post-mitotic.

By performing similar experiments, but varying the time at which parasites were collected after EdU injection ("chase"), we were able to trace the fate of the descendants of proliferating cells that incorporated EdU at different points of development. When larvae were exposed to EdU at stages 1.1 to 1.2 and allowed to develop for 24 to 48 hours, the progeny of the cells incorporating EdU could be detected throughout the larval tissues, with a strong accumulation in the periphery and scolex of larvae at stages 2.2 and 3.2 (Figure 2D). In contrast, when larvae were exposed to EdU at stage 4.1 (5 d.p.i.), allowed to complete metamorphosis, and activated *in vitro* (mimicking the infection of the definitive host), labelled cells were restricted to the body and absent from the scolex (n=9 activated cysticercoids; Figure 2E). Therefore, there is a pronounced antero-posterior gradient in the development of the cysticercoid, and only cell proliferation during the first developmental stages (up to stage 3.2) contributes to the formation of the scolex.

Finally, by combining EdU labelling with immunofluorescence for phospho-histone H3 (PH3), a mitotic marker, we performed an

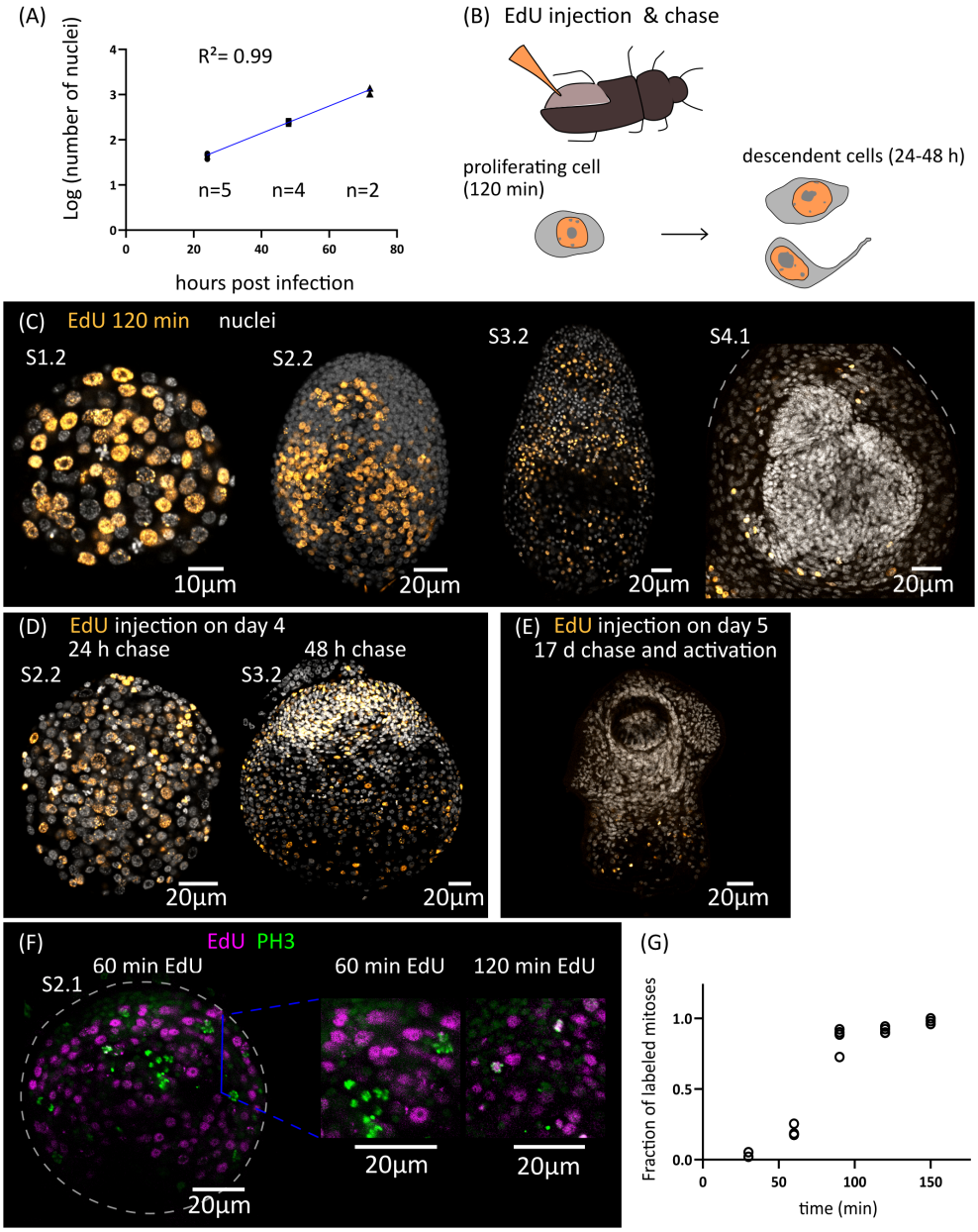

FIGURE 2
Cell proliferation during larval metamorphosis in *H. microstoma*. **(A)** Quantification of the increase in the total number of nuclei during early larval metamorphosis. **(B)** Diagram showing the method used for EdU injection in infected *T. molitor* beetles (top) and diagram of the EdU labelling patterns expected at different times of chase after injection (bottom). **(C)** EdU labelling at 2 h after injection for larvae at different developmental stages. **(D)** EdU labelling in larvae at 24 to 48 h of chase after injection. **(E)** EdU labelling in a cysticercoid larva that was exposed to EdU at 5 d.p.i., allowed to fully develop *in vivo* for an additional 17 days, and activated by mimicking *in vitro* the infection of the definitive host. **(F)** Detection of EdU and phosphorylated histone H3 (PH3) in developing larvae at different time points after the injection of EdU to infected beetles. **(G)** Quantification of the fraction of labelled mitoses in larvae at different time points after the injection of EdU to infected beetles (n= 2-4 larvae, with 19-63 mitotic cells analyzed per larva, for each time point).

analysis of the fraction of labelled mitosis (FLM, Shackney and Ritch, 1987) in order to estimate some cell cycle parameters during early larval metamorphosis (Figures 2F, G). Larvae at stages 2.1 to 2.2 were exposed to EdU *in vivo*, and collected at 30 min intervals for double detection of EdU and PH3. As expected, after only 30 minutes there is almost no co-localization of both labels, as cells that incorporated EdU are expected to be still in S phase or in G2 phase. The fraction of EdU labelled mitoses increased steadily with time as the labelled cells reached M phase, and almost all mitoses were labelled after 120 min. The average length of G2 can be estimated as the time point at which 50% of the mitoses are labelled (Shackney and Ritch, 1987), which was approximately 75 minutes. In a

different time-course experiment with longer chase times, we found that only 14% of mitoses were labelled 27 hours after the injection of EdU. Although the exact duration of the EdU pulse (i.e. the period of time during which EdU is available for uptake in the hemocoel after injection) cannot be controlled because it is not possible to perform an EdU washout *in vivo*, these results indicate that the duration of the EdU pulse in the hemocoel must be relatively short (if the EdU pulse lasted for 27 hours, the fraction of labelled mitoses would not drop within this time frame).

Development of the larval tegument

Parasitic flatworms, including tapeworms, trematodes and monogeneans, are not covered by a typical epidermis but instead possess a syncytial tegument (Tyler and Hooge, 2004). The tegument consists of a superficial band of cytoplasm (the distal cytoplasm) that is connected by thin cytoplasmic bridges to individual nucleated cell bodies (cytons) lying beneath the basal lamina. In the oncosphere of most tapeworms, including *Hymenolepis* spp., a single binucleated cyton is present (Ubelaker, 1980), and new cytons arise during metamorphosis from the fusion of the progeny of germinative cells to the distal tegument.

We adapted to *H. microstoma* larvae a method for labelling the tegument with fluorescently conjugated dextran, originally developed by Wendt et al., 2018 for the trematode *Schistosoma mansoni*. Several cytons could be identified at 1 d.p.i., but we were unable to localize the original binucleated cyton of the oncosphere, suggesting that it was already eliminated at this time point. The number of cytons connected to the distal tegument increased proportionally to the total number of cells of the larvae during the first three days of metamorphosis, and were distributed throughout the surface of the larvae (Figures 3A, B). We confirmed the presence of tegumental cytons at stages 1.1 to 1.2 (3 d.p.i.) by transmission electron microscopy, with several short cytoplasmic processes connecting them to a very thin distal cytoplasm (approximately 200 nm in thickness) (Figure 3C).

We analyzed the kinetics of differentiation of germinative cells into tegumental cytons by combining EdU chase experiments with dextran labelling. We exposed larvae at stages 2.1 to 3.1 to EdU *in vivo*, and followed the fate of labelled cells (Figures 3D, E). Two hours after EdU exposure, all dextran$^+$ tegumental cytons were negative for EdU, confirming that these are post-mitotic. However, EdU$^+$ tegumental cytons could already be detected at 4 hours after EdU exposure (17% of all tegumental cytons were EdU$^+$ on average), and the proportion of labelled cytons increased after 27 hours (29% of all dextran$^+$ tegumental cytons were EdU$^+$ on average, Figure 3D).

In summary, fusion of new cells to the tegument starts at the very beginning of larval metamorphosis, and our results indicate that a constant proportion of the proliferative output of germinative cells is destined to this structure during the early metamorphosis. Fusion of precursors to the tegumental syncytium may be a very early step of the differentiation process, as it can be detected after only 4 hours of EdU labelling (less than three hours after the last mitosis, according to our estimate of the length of G2).

Remodeling of the muscle system

The muscle system of the oncosphere comprises superficial muscle fibers (mostly circular fibers), a pair of dorso-ventral muscles, and a complex arrangement of muscles that are attached to the hooks and are responsible for their extension and retraction (Ubelaker, 1980; Hartenstein and Jones, 2003). This arrangement is replaced during larval metamorphosis, as the cysticercoid has a complex complement of muscular fibers that is most similar to the adult worm. This includes longitudinal and circular muscle fibers of the body wall (sub-tegumental muscle), inner longitudinal muscle fibers, transverse muscle fibers, and complex muscle arrangements in the attachment organs (rostellum and suckers).

We analyzed the remodeling of the muscle system by detecting muscle fibers using an antibody that recognizes muscular tropomyosin isoforms (high molecular weight tropomyosin isoforms: HMW-TPM; Koziol et al., 2011) (Figure 4A). Similar results were obtained by staining the larvae for actin filaments with fluorescent phalloidin (Figure 5). During the initial stages of metamorphosis (stages 1.1 to 1.2), the muscle fibers appear thin and discontinuous on the surface of the larvae, and the hook muscles appear globose and disorganized (Figure 4A). It is likely that these are the degenerating muscle fibers of the oncosphere. The first clear evidence of the differentiation of new muscle fibers appears at stage 2.1, in which circular muscle fibers and six bundles of longitudinal muscle fibers (two lateral bundles and two pairs of dorsal and ventral bundles) appear beneath the tegument of the body wall (Figure 4A). Surprisingly, although the muscle system of adult cestodes is dorsoventrally symmetrical, these early bundles of longitudinal muscle fibers show a dorsoventral asymmetry. On one side (due to the absence of other morphological landmarks, it is not possible to determine if this corresponds to the dorsal or ventral side), the bundles of fibers are thicker and more developed, and each bundle is clearly associated to a single large HMW-TPM$^+$ cell body. At later stages (2.2 to 3.2), both circular and longitudinal muscle fibers increase their number and density beneath the tegument, forming an orthogonal grid (Figure 4A). The longitudinal fibers extend through most of the length of the larvae, but are absent in the posterior-most region that will become the cercomer, as described by Caley (1974). Additionally, transverse muscle fibers appear in the anterior region (the future scolex), particularly at the base of the developing rostellum, and between the sucker primordia. The intrinsic musculature of the rostellum and suckers only differentiates after scolex withdrawal, during stages 4.1 to 4.2 (Figure 4A).

In tapeworms, muscle fibers are only connected by thin cytoplasmic strands to their cell body containing the nucleus (myocyton) (Conn, 1993), and it is not usually possible to identify the myocytons by immunodetection of tropomyosins. Therefore, we performed WMISH with probes for muscular tropomyosin isoforms (*tpm-1.hmw* and *tpm-2.hmw*; Koziol et al., 2011) to identify myocytons during larval metamorphosis (Figures 4B–D). Both probes gave similar results, except that *tpm.hmw-1* was specifically absent from the developing cercomer. The earliest robust signal that we could detect was at stage 1.2, in cells forming a band at the lateral margin (marginal myocytons, located at the dorsoventral midline), and in the single pair of asymmetric myocytons associated with the early bundles of longitudinal muscle fibers (Figure 4B). Later, at stage 2.1 a second

10.3389/fcimb.2023.1286190

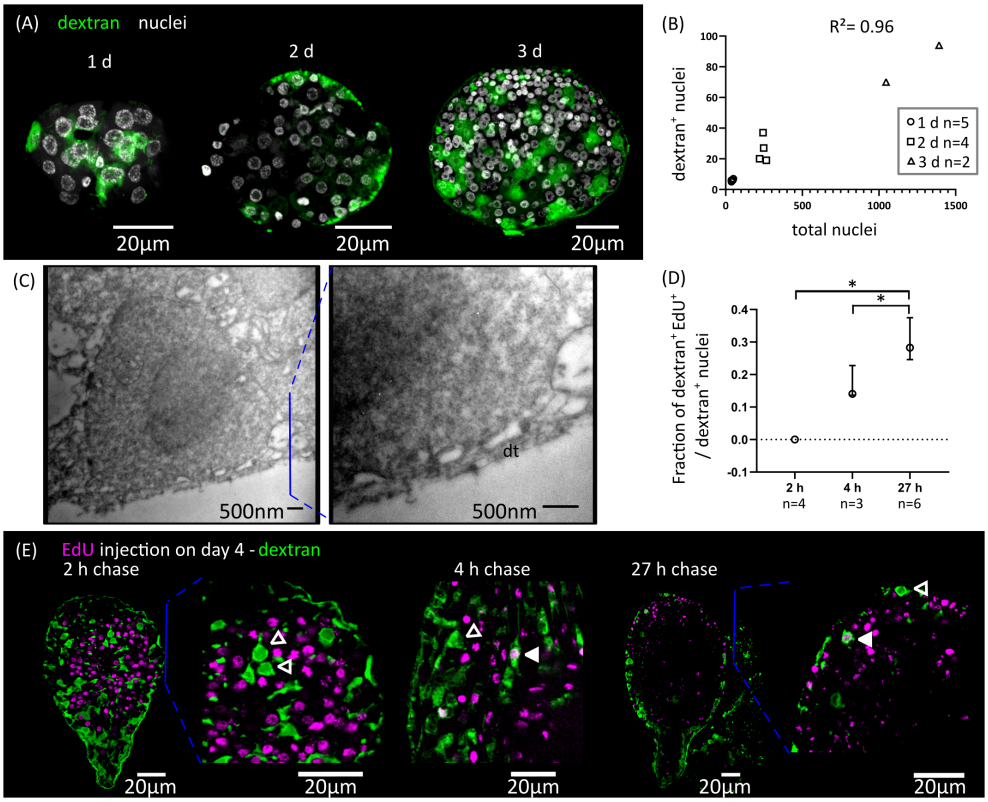

FIGURE 3
Differentiation of tegumentary cytons. **(A)** Dextran labelling of the tegument of larvae at different time points after infection (1, 2 and 3 d.p.i., corresponding to stages 1.1, 1.2 and 2.1). **(B)** Quantification of the increase of dextran-labelled nuclei in comparison to the total number of nuclei. **(C)** Transmission electron microscopy of a tegumentary cyton in a larva at 3 d.p.i. (left), including a detailed view of the distal tegument (dt) and its connection to the tegumentary cyton via cytoplasmatic bridges. **(D)** Quantification of the fraction of tegumentary cytons (dextran$^+$ nuclei) that are labelled by EdU at different chase times after the injection of EdU to infected beetles. The points show median values and the whiskers show the maximum and minimum values (*p < 0.05, Mann-Whitney test). **(E)** Examples of larvae combining detection of EdU incorporation and dextran labelling of the tegument at different chase times after the injection of EdU to infected beetles. Open and filled arrowheads indicate dextran$^+$/EdU$^-$ and dextran$^+$/EdU$^+$ cytons, respectively.

band of myocytons can be detected in the anterior end at the sagittal midline (*i.e.* perpendicular to the marginal myocytons), thus forming a characteristic cross when larvae are viewed frontally (Figure 4D). Strikingly, the position of the bands of myocytons can be distinguished by DAPI nuclear staining, with compactly distributed nuclei that have a characteristic zipper-like distribution (Figure 4D). At later stages (2.2 to 3.2), the marginal myocyton band becomes thicker, and more myocytons appear throughout the surface of the larvae, especially in the tissues that will become the cyst, behind the scolex. Additional myocytons appear among the inner cells (these are the myocytons of the transverse muscle fibers). Expression of muscular tropomyosins could be detected in the rostellar primordium at stage 3.2, but expression in the developing suckers only occurred after scolex withdrawal (stages 4.1 and 4.2, Figure 4C). At these stages, large numbers of myocytons were still present in the cyst tissues, and some were also detected in the growing cercomer. Altogether, these results expand those obtained by immunofluorescence, and indicate that muscle cell differentiation begins early during larval metamorphosis.

In order to detect the differentiation of germinative cells into muscle cells, we combined EdU chase experiments with WMISH detection of muscular tropomyosin isoforms (Figures 4E, F; for these experiments, we used a mixture of both *tpm1.hmw* and *tpm2.hmw* probes to detect all myocytons). When larvae were exposed to EdU at either 3 or 4 d.p.i., no colocalization was observed after 2 hours of chase between EdU labelling and expression of muscular tropomyosin isoforms, indicating that expression only begins after exiting the cell cycle (n=4-37 tropomyosin cells from 2-3 larvae for each time point, in which all positive cells were analyzed for each larva; identical results were observed in additional experiment using only either the *tpm1.hmw* or the *tpm2.hmw* probe). In contrast, extensive co-localization was observed after 24 hours of chase (31% of all myocytons were labelled on average after 24 hours when EdU was injected at 3 d.p.i, and 18% were labelled on average when EdU was injected at 4 d.p.i.; n=3-4 larvae for each time point, with 33-101 myocytons analyzed for each larva). These results confirmed that extensive muscle cell differentiation is ongoing at 3 to 5 d.p.i. (stages 1.2 to 4.1), and demonstrated that the expression of muscle-specific effector genes begins 24 hours or less after cell cycle exit.

Finally, we analyzed the expression of homologs of *myoD* and *nkx-1.1*, which have been shown to be expressed in planarians in longitudinal muscle fiber cells and circular muscle fiber cells, respectively (Scimone et al., 2017) (Supplementary Figure 1).

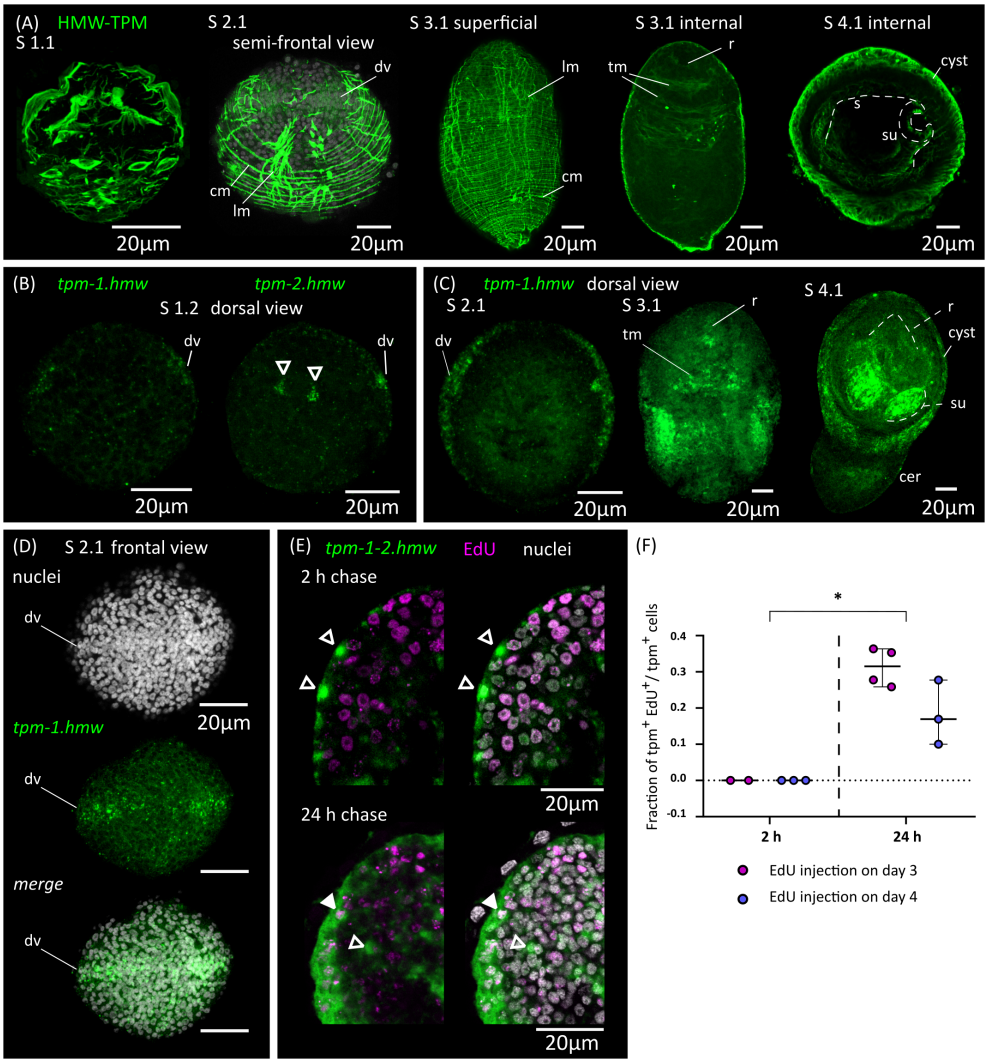

FIGURE 4
Development of the muscle system. **(A)** Detection of muscular tropomyosin isoforms by immunofluorescence at different developmental stages. Nuclear staining is included in greyscale for stage 2.1. For stage 3.1, both superficial planes and internal planes of confocal microscopy are shown. All pictures are from WMIHF except stage 4.1, which is from immunofluorescence on a cryosection. **(B)** Earliest detection of mRNAs for muscular tropomyosin isoforms *tpm-1.hmw* and *tpm-2.hmw* by WMISH at stage 1.2. Arrowheads indicate a pair of myocytons that probably correspond to the early asymmetric bundles of longitudinal muscle fibers. **(C)** WMISH of *tpm-1.hmw* at different developmental stages (dorsal views). **(D)** WMISH of *tpm-1.hmw* at stage 2.1 (frontal view). **(E)** Examples of larvae combining detection of EdU incorporation and expression of *tpm-1.hmw* and *tpm-2.hmw* by WMISH at different chase times after the injection of EdU to infected beetles. Open and filled arrowheads indicate *tpm1-2.hmw*$^+$/EdU$^-$ and *tpm1-2.hmw*$^+$/EdU$^+$ cells, respectively. **(F)** Quantification of the fraction of muscle cells (*tpm-1-2.hmw*$^+$) that are labelled by EdU at different chase times after the injection of EdU to infected beetles. Each point represents the quantification of an individual larva (*p < 0.0025, Mann-Whitney test for pooled results of 3 and 4 d.p.i.). cer, cercomer; cm, circular muscle; dv, band of cells at dorsoventral midline; lm, longitudinal muscle; r, rostellar primordium; s, scolex; su, sucker; tm, transverse muscle.

Furthermore, orthologs of *myoD* have been shown to be expressed and have myogenic activity in muscle progenitors and/or precursors in both vertebrates and invertebrates (Andrikou and Arnone, 2015). Expression of *myoD* during larval metamorphosis in *H. microstoma* was previously examined by Olson et al. (2018), and our results are similar to theirs, showing particularly strong expression in the future cyst tissues at stage 3.2, similar to the pattern of muscle tropomyosin isoforms at his stage. However, careful analysis showed that *myoD* expression was specifically absent in the band of marginal myocytons. On the other hand, *nkx-1.1* expression was detected from stage 3.1 onwards in the developing sucker primordia, with the strongest expression occurring after scolex withdrawal. Therefore, both genes are likely to be expressed in subsets of muscle cells and muscle cell precursors, but these may not be equivalent to those of planarians.

De novo development of the nervous system of the cysticercoid

Ultrastructural analyses have identified a minimal nervous system in the oncosphere of many cestodes, including in the closely related *Hymenolepis nana*, which may comprise only two nerve cells that extend neurites towards the hook muscles

10.3389/fcimb.2023.1286190

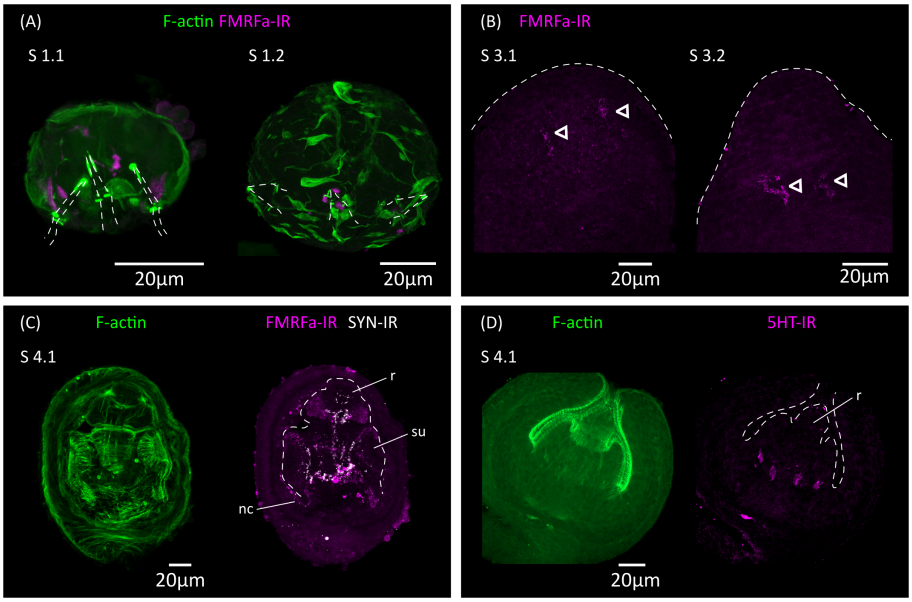

FIGURE 5
Analysis of the development of the nervous system by immunofluorescence. **(A)** FMRFa-IR in vestigial structures from the oncosphere during stages 1.1 and 1.2. Phalloidin staining of actin filaments (F-actin) labels the disorganized muscle fibers at these early stages. The positions of the larval hooks are indicated with dashed lines. **(B)** Earliest detection of FMRFa-IR in the developing scolex during stages 3.1 and 3.2. Arrowheads indicate early FMRFa-IR cells at the base of the rostellar primordium **(C)** FMRFa-IR, synapsin immunoreactivity (SYN-IR) and phalloidin staining of actin filaments during later scolex development (stage 4.1). **(D)** Earliest detection of 5-HT-IR occurs after scolex retraction (stage 4.1). nc, nerve cord; r, developing rostellum; su, developing sucker.

(Fairweather and Threadgold, 1983; Swiderski et al., 2018). The oncosphere of *H. microstoma* has at least three nerve cells, which can be detected with antibodies generated against the neuropeptide FMRFamide and by their expression of synapsin (Preza, 2021). We analyzed the development of the nervous system during larval metamorphosis by detecting FMRFamide immunoreactivity (FMRFa-IR), 5-hydroxytryptamine (serotonin) immunoreactivity (5-HT-IR), and synapsin protein expression (Figure 5).

During the first 3 d.p.i. (stages 1.1 to 2.1), FMRFa-IR was detected in spots associated to the vestigial oncosphere hooks at the larval posterior, which later disappeared (Figure 5A). These structures are likely the degenerating remains of the nervous system of the oncosphere. In contrast, FMRFa-IR cells in the developing scolex appeared at 5 d.p.i in stages 3.1 to 3.2 as a pair of weakly positive cells at the base of the rostellar primordium (Figure 5B). Extensive FMRFa-IR and synapsin could only be detected after scolex withdrawal, starting at stages 4.1, and included the developing brain commissure and longitudinal nerve cords (Figure 5C). On the other hand, 5-HT-IR was only detected in the scolex after scolex withdrawal, first as four positive cells associated to the base of the developing rostellum (Figure 5D), and later more extensively in positive cells in the scolex and in the developing longitudinal nerve cords. These results strongly indicate that the nervous system of the cysticercoid develops independently from that of the oncosphere, given the spatial and temporal separation in their development.

In addition, we analyzed by WMISH the expression of markers of different neurotransmitter systems present in *H. microstoma*, which are also expressed in the nervous system of the adult worm (Preza et al., 2018): prohormone convertase 2 (*pc2*) as a marker of peptidergic cells; choline acetyltransferase (*chat*) as a marker of cholinergic cells; vesicular glutamate transporter (*vglut*) as a marker of glutamatergic cells; and tryptophan hydroxylase (*tph*) as a marker of serotonergic cells (Figure 6). Expression of *pc2*, *chat* and *vglut* could be detected from 4 d.p.i. onwards (at stage 2.1), in a few cells at the anterior end, and the number of positive cells increased at stages 2.2 to 3.2. Expression at these early stages was associated with the anterior-most structures of the nervous system, including the developing rostellar ganglia, cerebral ganglia and transverse commissure. Development continued after scolex withdrawal, with expanded expression domains in the scolex, and with the appearance of the longitudinal nerve cords. On the other hand, *tph* expression began later at 5 d.p.i. (stage 3.2, Figure 6D), in few cells in the scolex, and the total number of positive cells was always small, which correlates with the small number of serotonergic cells found in the adult worm (Preza et al., 2018).

Thus, the initial expression of markers of neurotransmission at the mRNA level preceded the appearance of FMRFa-IR, 5-HT-IR and synapsin protein expression by at least 24 hours, demonstrating that cell differentiation in the nervous system is already underway at stage 2.1. This suggests that neural progenitors should already be present at even earlier stages. We analyzed by WMISH the expression of homologs of genes coding for transcription factors that are related to neurogenesis and neural differentiation in animals, including *soxB* and the basic helix-loop-helix (bHLH) family members *coe* and *neuroD* (Dubois and Vincent, 2001; Cowles et al., 2013; Hartenstein and Stollewerk, 2015; Baker and Brown, 2018; Tutukova et al., 2021). All of these genes had

10.3389/fcimb.2023.1286190

expression patterns that were associated with the developing nervous system (Figure 7). Both *soxB* and *coe* were detected in relatively small numbers of cells in the developing nervous system from stage 2.1 onwards, and showed little incorporation of EdU after two hours of labelling (8% of *soxB*$^+$ cells incorporated EdU, n=189 cells from 2 larvae; 2% of *coe*$^+$ cells incorporated EdU, n=179 cells from 3 larvae), suggesting that most of these cells correspond to post-mitotic neural precursors. In contrast, *neuroD* could be detected at least from stage 1.2 throughout the anterior hemisphere of the larvae (we did not examine its expression at earlier time points), in large proliferative cells: approximately 80% of all *neuroD*$^+$ cells were labelled by EdU after 2 hours, and *neuroD*$^+$ cells correspond to 14% of all EdU$^+$ proliferative cells in early larvae (n=110 *neuroD*$^+$ cells and 836 EdU$^+$ cells examined from 6 larvae; Figure 8A). Expression of *neuroD* was also observed in mitotic cells. During later development, *neuroD*$^+$ cells were always loosely distributed around regions of ongoing neural development. After scolex withdrawal, *neuroD* expression was mostly turned off in the scolex but continued around the developing nerve cords (Figure 7A). Therefore, *neuroD* appears to be expressed in a subpopulation of proliferating germinative cells, and based on its domains of expression and conserved roles in other bilaterians, the results suggest that it is expressed early during neurogenesis (in germinative cells specified for a neural fate).

Finally, we traced the differentiation of nerve cells by means of EdU chase assays. We focused on *chat* as a marker of neural differentiation because it was expressed in an intermediate number of spread-out cells, which made the identification of the nuclei of positive cells non-ambiguous. We injected EdU in infected beetles at 3 and 4 d.p.i., and analyzed EdU labeling in *chat*$^+$ cells after 2 or 24 hours. Either no or very few *chat*$^+$ cells could be detected after two hours (as these corresponded to larvae at stages 1.2 to 2.1) and most *chat*$^+$ cells in these larvae were EdU negative (Figures 8B, C). However, for two larvae, a single weakly positive

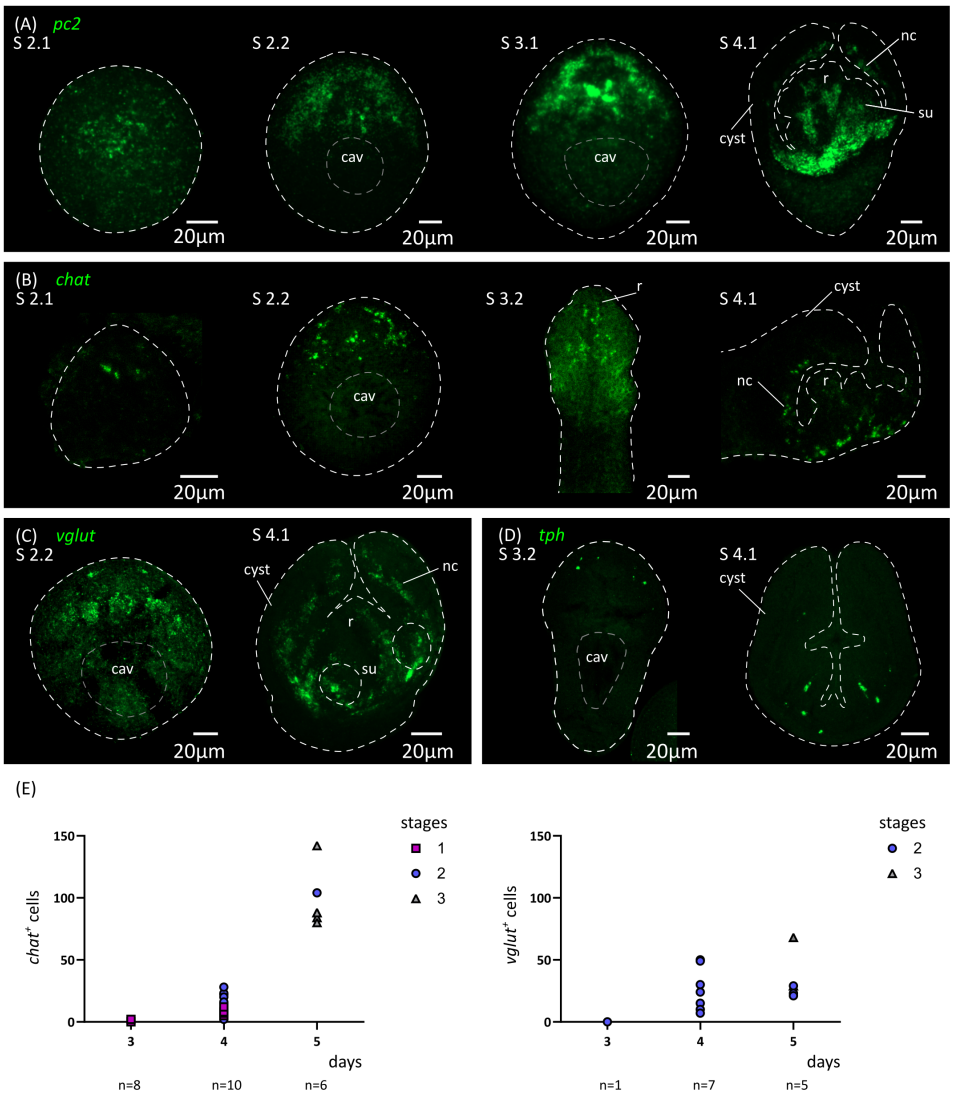

FIGURE 6
Analysis of the development of the nervous system by *in situ* hybridization of markers of neurotransmission. Expression patterns of *pc2* **(A)**, *chat* **(B)**, *vglut* **(C)** and *tph* **(D)** during larval metamorphosis. **(E)** Quantification of the total number of *chat*$^+$ and *vglut*$^+$ cells at 3 to 5 d.p.i. cav, central cavity; nc, nerve cord; su, sucker primordium.

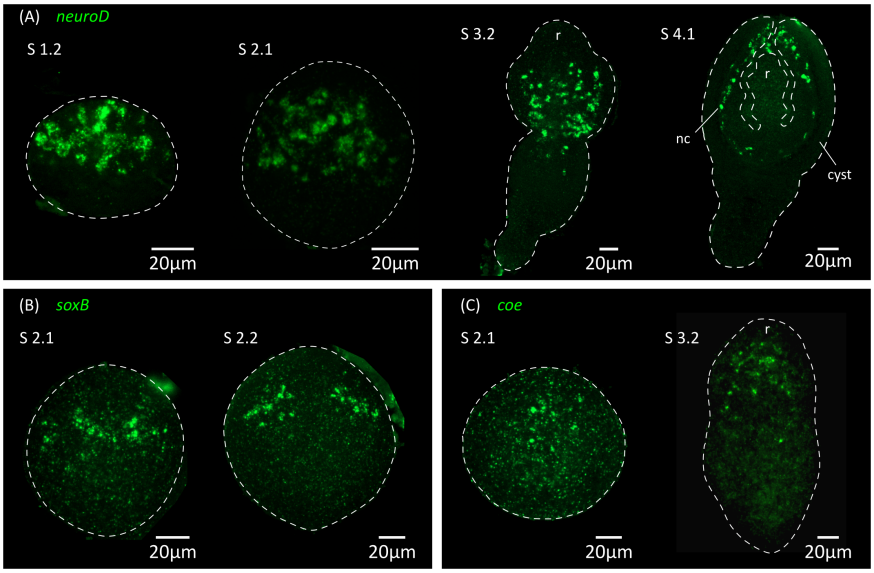

FIGURE 7
Expression of conserved genes related to neurogenesis and neural differentiation. Expression patterns of *neuroD* **(A)**, *soxB* **(B)** and *coe* **(C)** during larval metamorphosis. nc, nerve cord; r, rostellar primordium.

chat$^+$ cell was found for each. Analysis of larvae at later stages labelled for two hours with EdU also showed no co-localization between *chat* and EdU (data not shown). Therefore, *chat* expression appears to be turned on after cell cycle exit in most cases. In comparison, 24 hours after EdU injection there was extensive co-localization of *chat* and EdU (43% and 25% of all *chat*$^+$ cells are EdU$^+$ after 24 hours, when injection occurred 3 d.p.i or 4 d.p.i., respectively; Figures 8B, C). Thus, neurogenesis must be already underway at stages 1.2 to 2.1, and neural differentiation begins within 24 hours of cell cycle exit. In contrast, the proportion of EdU labelled cells among *neuroD*$^+$ cells decreased after 24 hours (Figures 8A, C). This result is compatible with the hypothesis that these cells were short-lived proliferating progenitors, which turned off *neuroD* expression as they differentiated during the 24 h chase

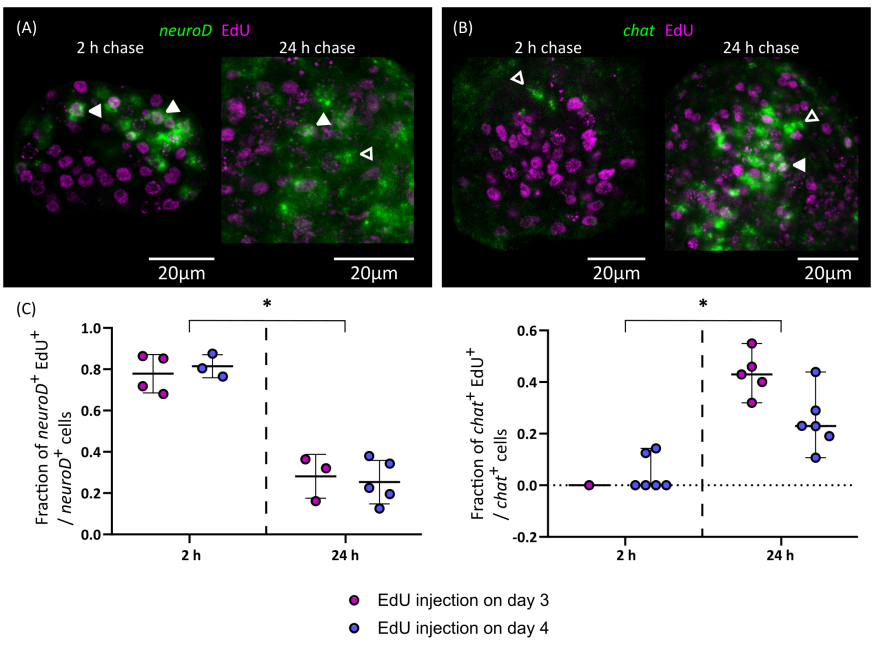

FIGURE 8
Differentiation of nerve cells during larval metamorphosis. Examples of EdU labelling of *neuroD*$^+$ cells **(A)** and *chat*$^+$ cells **(B)** after 2 or 24 h of chase (open and filled arrowheads indicate EdU$^-$ and EdU$^+$ cells, respectively), and **(C)** quantification of the fraction of *neuroD*$^+$ and *chat*$^+$ cells that are labelled by EdU at different chase times. Each point represents the quantification of an individual larva (*p < 0.001, Mann-Whitney test for pooled results of 3 and 4 d.p.i.).

period. Alternatively, the decrease of EdU labelling among *neuroD*$^+$ cells could also result from repeated cell divisions of these cells during the 24 h chase period, resulting in the dilution of the EdU label.

Discussion

In this work, we have characterized cell proliferation and differentiation of new tissues during the larval metamorphosis of a model tapeworm. This developmental transition in tapeworms has largely been regarded as a "black box", since tracing the development and remodeling of the larval tissues is complicated due to the extremely small size of the larvae and their cells, the complex histology of cestodes, and the lack of specific markers. Thus, most of what was previously known depended on spatial and temporal snapshots from studies by electron microscopy. Here, we took advantage of the development of specific molecular markers and a robust *in vivo* system for metabolic labelling with a thymidine analogue, allowing us to obtain a global view of these processes (summarized in Figure 1).

The first stages of larval metamorphosis are characterized by exponential growth, as has also been seen during the cysticercoid to adult transition (Loehr and Mead, 1980). In both cases, set-aside germinative cells are thought to be quiescent before infection, and to become quickly activated during the infection of the new host. During the first stages of larval metamorphosis in *H. microstoma*, we could detect the differentiation of tegumental cells and muscle cells. The early differentiation of new tegument cytons has also been described during the larval metamorphosis of *Echinococcus multilocularis* (Sakamoto and Sugimura, 1970), and may be essential for the profound changes that the tegument undergoes during the early metamorphosis. It is likely that these changes are important for the survival of the parasite in the new host (Holcman and Heath, 1997). The early differentiation of muscle cells could be related to their multiple functions in tapeworms. On the one hand, muscle activity is required for scolex withdrawal (Caley, 1974), which occurs after only 5 to 6 days of metamorphosis. On the other hand, myocytons are known sources of signaling molecules regulating development in tapeworms and other flatworms (Witchley et al., 2013; Koziol et al., 2016; Diaz Soria et al., 2020; Wendt et al., 2020), and are the main source of extracellular matrix components as has also been shown in planarians (Conn, 1993; Witchley et al., 2013; Cote et al., 2019). The distribution of myocytons during early metamorphosis is very peculiar, as they are initially concentrated on a lateral marginal band (at the dorsoventral midline), which is followed by a second band at the sagittal midline. A similar pattern was observed during the early development of the *E. multilocularis* protoscolex (Koziol et al., 2014). It is possible, given their position and their time of appearance, that these are the myocytons of the first circular muscle fibers that appear, although we have not been able to confirm their cytoplasmic continuity. As is common in invertebrates, *myoD* was not expressed in all somatic muscles (Tixier et al., 2010; Andrikou and Arnone, 2015; Brunet et al., 2016), and it was specifically absent from the marginal myocytons of *H. microstoma*. Because in planarians *myoD* is expressed in longitudinal muscles (Scimone et al., 2017), this would support their tentative classification as circular muscle cells. However, although *nkx-1.1* is expressed in circular muscle cells in planarians (Scimone et al., 2017), it was restricted to the developing suckers in *H. microstoma*. Therefore, it may not be possible to homologize muscle cell types across platyhelminthes based on their expression of conserved myogenic transcription factors.

The development of the nervous system occurs with a clear antero-posterior gradient, similar to that found in *E. multilocularis* protoscoleces (Koziol et al., 2013). Differentiation of the nervous system begins relatively late during metamorphosis, and scolex withdrawal occurs at a stage in which the nervous system is still under development (and at which synapsin labelling is still undetectable). Therefore, it is possible that the muscle contractions responsible for scolex withdrawal are not controlled or modulated by the nervous system. Strikingly, the nervous system of the cysticercoid is formed post-embryonically *de novo*, independently of the nervous system of the oncosphere. It is reminiscent of the development of the nervous system during the embryonic development in other ectolecithal flatworms (*i.e.* with alecithal oocytes and specialized yolk cells carrying the vitellum), where the nervous system does not arise from a specialized region of the ectoderm, but from progenitors found among a large internal mass of proliferating cells (Hartenstein and Stollewerk, 2015; Monjo and Romero, 2015). Our results suggest that *neuroD*$^+$ germinative cells may correspond to a specialized lineage of neural precursors during larval metamorphosis. Surprisingly, *neuroD* appears to be an early expressed gene during neurogenesis in *H. microstoma*, in contrast to its more common expression in late neuronal precursors during differentiation in other animals (Monjo and Romero, 2015; Sur et al., 2020; Deryckere et al., 2021; Tutukova et al., 2021), with the exception of the annelid *Platynereis dumerilii* (Simionato et al., 2008). Small numbers of proliferating neoblasts have also been shown to express a *neuroD* homolog in adult planarians (Scimone et al., 2014). On the other hand, *soxB* had a restricted expression in *H. microstoma* larvae and was expressed later in what appears to be a subset of mostly post-mitotic precursors. This is also surprising, since *soxB* homologs usually are expressed during the early specification of the neuroectoderm in animal embryos (Hartenstein and Stollewerk, 2015), although later roles during neuronal differentiation have also been described for particular *soxB* homologs (Guth and Wegner, 2008; Phochanukul and Russell, 2010; Monjo and Romero, 2015; Vidal et al., 2015). Furthermore, the ortholog of *soxB* in *E. multilocularis* is expressed in most proliferating germinative cells in the metacestode germinative layer (Cheng et al., 2017), which are unlikely to be neural precursors given the minimal nervous system present in this tissue (Koziol et al., 2013). Finally, tapeworms appear to lack many conserved regulators of neural development, such as *neurogenin* and *elav* (Montagne and Koziol, unpublished data), hinting at a highly modified neurogenic program. It would be interesting to determine if these atypical patterns of gene expression also occur during neural development in other life stages, including embryonic development and during the post-embryonic remodeling of the nervous system of the adult. More

generally, our gene expression results demonstrate the molecular heterogeneity of tapeworm germinative cells. Stem cell heterogeneity was also hinted at by ultrastructural details during the early larval metamorphosis in *E. multilocularis* (Sakamoto and Sugimura, 1970), and shown from differential gene expression in fully developed metacestodes of this species (Koziol et al., 2014). In adults of the related tapeworm *Hymenolepis diminuta*, different genes were also shown to be expressed either exclusively in some proliferating germinative cells, or in subsets of germinative cells and in differentiated tissues, suggesting the existence of lineage-restricted germinative cells (Rozario et al., 2019).

Altogether, our results support the hypothesis that larval metamorphosis corresponds to a form of ´maximal indirect development´ (Peterson et al., 1997; Koziol, 2017), in which a new body plan is generated *de novo* from stem cells that were set-aside during embryogenesis. We have found no clear evidence of any differentiated cells from the oncosphere that are retained in the cysticercoid after metamorphosis. Instead, new cells of the nervous system, muscular system and tegument are generated from the differentiation of germinative cells. Although we did not analyze the development of the excretory system, this must also arise *de novo* during metamorphosis as it is absent in the oncosphere of *Hymenolepis* spp. (Ubelaker, 1980). *H. microstoma* appears as an ideal model to study the mechanisms regulating cell proliferation and differentiation during larval metamorphosis, given its simple maintenance and fast development. This work provides a blueprint of the early stages of development, and the *in vivo* system could be complemented in the future by functional analyses in *in vitro* culture (Seidel, 1975). We expect that the insights gained with this model species may guide future studies in human and animal pathogens.

Data availability statement

The raw data supporting the conclusions of this article will be made available by the authors, without undue reservation.

Ethics statement

The animal study was approved by Comisión Honoraria de Experimentación Animal, Uruguay. The study was conducted in accordance with the local legislation and institutional requirements.

Author contributions

JM: Data curation, Formal Analysis, Funding acquisition, Investigation, Methodology, Project administration, Validation, Visualization, Writing – review & editing. MP: Investigation, Writing – review & editing. UK: Conceptualization, Data curation, Formal Analysis, Funding acquisition, Investigation, Methodology, Project administration, Supervision, Validation, Writing – original draft.

Funding

The author(s) declare financial support was received for the research, authorship, and/or publication of this article. This work was supported by Comisión Sectorial de Investigación Científica, Uruguay, grants CSIC I+D 2018-162 to UK and CSIC iniciación 2021 to JM, Comisión Académica de Posgrado, Universidad de la República, Uruguay (Ph.D. fellowship to JM), and PEDECIBA, Uruguay.

Acknowledgments

The authors would like to acknowledge the collaboration of Jenny Saldaña, Laboratorio de Experimentación Animal, Facultad de Química, Universidad de la República, for the maintenance of the life cycle of *Hymenolepis microstoma* in the laboratory. The authors would also like to acknowledge the help of Anita Asienberg and Laura Montes de Oca (Departamento de Ecología y Biología Evolutiva, Instituto de Investigaciones Biológicas Clemente Estable, Montevideo, Uruguay) with *T. molitor* rearing and Beatriz Goñi (Facultad de Ciencias, Universidad de la República) for her advice regarding the manipulation of *T. molitor* beetles. The authors gratefully acknowledge the Advanced Bioimaging Unit at the Institut Pasteur Montevideo, and Gabriela Casanova, Magela Rodao and Gaby Martínez at the Electron Microscopy Unit, Facultad de Ciencias, Universidad de la República, for their support and assistance in the present work. This work has been published as a preprint in the BioRxiv server (Montagne et al., 2023).

Conflict of interest

The authors declare that the research was conducted in the absence of any commercial or financial relationships that could be construed as a potential conflict of interest.

Publisher's note

Supplementary material

The Supplementary Material for this article can be found online at: https://www.frontiersin.org/articles/10.3389/fcimb.2023.1286190/full#supplementary-material

SUPPLEMENTARY FIGURE 1
Expression of *myoD* **(A)** and *nkx-1.1* **(B)** homologs during larval metamorphosis. dv, lateral band of marginal myocitons; su, sucker primordia/developing sucker.

SUPPLEMENTARY TABLE 1
List of primers used in this work.

References

Andrikou, C., and Arnone, M. I. (2015). Too many ways to make a muscle : Evolution of GRNs governing myogenesis. *Zool. Anzeiger - A J. Comp. Zool.* 256, 2–13. doi: 10.1016/j.jcz.2015.03.005

Arai, H. (1980). *Biology of the tapeworm Hymenolepis diminuta* (New York: Academic Press Inc).

Baker, N. E., and Brown, N. L. (2018). All in the family: Proneural bHLH genes and neuronal diversity. *Development* 145, dev159426. doi: 10.1242/dev.159426

Bilqees, F. M., and Freeman, R. S. (1969). Histogenesis of the rostellum of *Taenia crassiceps* (Zeder 1800) (Cestoda), with special reference to hook development. *Can. J. Zool.* 47, 251–261. doi: 10.1139/z69-052

Bortoletti, G., and Ferretti, G. (1985). Morphological studies on the early development of *Taenia taeniformis* larvae in susceptible mice. *Int. J. Parasitol.* 15, 365–375. doi: 10.1016/0020-7519(85)90021-9

Brunet, T., Fischer, A. H. L., Steinmetz, P. R. H., Lauri, A., Bertucci, P., and Arendt, D. (2016). The evolutionary origin of bilaterian smooth and striated myocytes. *Elife* 5, e19607. doi: 10.7554/eLife.19607

Budke, C. M., White, A. C., and Garcia, H. H. (2009). Zoonotic larval cestode infections: Neglected, neglected tropical diseases? *PLoS Negl. Trop. Dis.* 3, 2–4. doi: 10.1371/journal.pntd.0000319

Caley, J. (1974). The functional significance of scolex retraction and subsequent cyst formation in the cysticercoid larva of *Hymenolepis microstoma*. *Parasitology* 68, 207–227. doi: 10.1017/S0031182000045741

Cheng, Z., Liu, F., Dai, M., Wu, J., Li, X., Guo, X., et al. (2017). Identification of EmSOX2, a member of the Sox family of transcription factors, as a potential regulator of *Echinococcus multilocularis* germinative cells. *Int. J. Parasitol.* 47, 625–632. doi: 10.1016/j.ijpara.2017.03.005

Chervy, L. (2002). The terminology of larval cestodes or metacestodes. *Syst. Parasitol.* 52, 1–33. doi: 10.1023/A:1015086301717

Chile, N., Clark, T., Arana, Y., Ortega, Y. R., Palma, S., Mejia, A., et al. (2016). *In vitro* study of *Taenia solium* postoncospheral form. *PLoS Negl. Trop. Dis.* 10, e0004396. doi: 10.1371/journal.pntd.0004396

Collin, W. (1970). Electron microscopy of postembryonic stages of the tapeworm, *Hymenolepis citelli*. *J. Parasitol.* 56, 1159–1170. doi: 10.2307/3277562

Conn, D. B. (1993). The biology of flatworms (Platyhelminthes): parenchyma cells and extracellular matrices. *Trans. Am. Microsc. Soc* 112, 241–261. doi: 10.2307/3226561

Cote, L. E., Simental, E., and Reddien, P. W. (2019). Muscle functions as a connective tissue and source of extracellular matrix in planarians. *Nat. Commun.* 10, 1592. doi: 10.1038/s41467-019-09539-6

Cowles, M. W., Brown, D. D. R., Nisperos, S. V., Stanley, B. N., Pearson, B. J., and Zayas, R. M. (2013). Genome-wide analysis of the bHLH gene family in planarians identifies factors required for adult neurogenesis and neuronal regeneration. *Development* 140, 4691–4702. doi: 10.1242/dev.098616

Cunningham, L. J., and Olson, P. D. (2010). Description of *Hymenolepis microstoma* (Nottingham strain): A classical tapeworm model for research in the genomic era. *Parasites Vectors* 3, 1–9. doi: 10.1186/1756-3305-3-123

Deryckere, A., Styfhals, R., Elagoz, A. M., Maes, G. E., and Seuntjens, E. (2021). Identification of neural progenitor cells and their progeny reveals long distance migration in the developing octopus brain. *Elife* 10, e69161. doi: 10.7554/eLife.69161

Diaz Soria, C. L., Lee, J., Chong, T., Coghlan, A., Tracey, A., Young, M. D., et al. (2020). Single-cell atlas of the first intra-mammalian developmental stage of the human parasite *Schistosoma mansoni*. *Nat. Commun.* 11, 6411. doi: 10.1038/s41467-020-20092-5

Dubois, L., and Vincent, A. (2001). The COE – Collier / Olf1 / EBF – transcription factors : structural conservation and diversity of developmental functions. *Mech. Dev.* 108, 3–12. doi: 10.1016/S0925-4773(01)00486-5

Egger, B., Steinke, D., Tarui, H., De Mulder, K., Arendt, D., Borgonie, G., et al. (2009). To be or not to be a flatworm: The Acoel controversy. *PLoS One* 4, e5502. doi: 10.1371/journal.pone.0005502

Evans, W. S. (1980). "The cultivation of *Hymenolepis in vitro*," in *Biology of the Tapeworm Hymenolepis diminuta* (New York: Academic Press Inc), 425–448. doi: 10.1016/b978-0-12-058980-7.50011-7

Fairweather, I., and Threadgold, L. T. (1983). *Hymenolepis nana* : the fine structure of the adult nervous system. *Parasitology* 86, 89–103. doi: 10.1017/S0031182000057206

Freeman, R. S. (1973). Ontogeny of cestodes and its bearing on their phylogeny and systematics. *Adv. Parasitol.* 11, 481–557. doi: 10.1016/S0065-308X(08)60191-8

Goodchild, C. G., and Stullken, R. E. (1970). *Hymenolepis microstoma*: Cysticercoid morphogenesis. *Trans. Am. Microsc. Soc* 89, 224–229. doi: 10.2307/3224378

Guth, S. I. E., and Wegner, M. (2008). Having it both ways: Sox protein function between conservation and innovation. *Cell. Mol. Life Sci.* 65, 3000–3018. doi: 10.1007/s00018-008-8138-7

Hartenstein, V., and Jones, M. (2003). The embryonic development of the bodywall and nervous system of the cestode flatworm *Hymenolepis diminuta*. *Cell Tissue Res.* 311, 427–435. doi: 10.1007/s00441-002-0687-8

Hartenstein, V., and Stollewerk, A. (2015). The evolution of early neurogenesis. *Dev. Cell* 32, 390–407. doi: 10.1016/j.devcel.2015.02.004

Heath, D., and Smyth, J. (1970). *In vitro* cultivation of *Echinococcus granulosus*, *Taenia hydatigena*, T. ovis, *T. pisiformis* and *T. serialis* from oncosphere to cystic larva. *Parasitology* 61, 329–343. doi: 10.1017/S0031182000041184

Holcman, B., and Heath, D. D. (1997). The early stages of *Echinococcus granulosus* development. *Acta Trop.* 64, 5–17. doi: 10.1016/S0001-706X(96)00636-5

Holcman, B., Heath, D. D., and Shaw, R. J. (1994). Ultrastructure of oncosphere and early stages of metacestode development of *Echinococcus granulosus*. *Int. J. Parasitol.* 24, 623–635. doi: 10.1016/0020-7519(94)90114-7

Hotez, P. J., Alvarado, M., Basáñez, M. G., Bolliger, I., Bourne, R., Boussinesq, M., et al. (2014). The global burden of disease study 2010: Interpretation and implications for the neglected tropical diseases. *PLoS Negl. Trop. Dis.* 8, e2865. doi: 10.1371/journal.pntd.0002865

Howe, K. L., Bolt, B. J., Shafie, M., Kersey, P., and Berriman, M. (2017). WormBase ParaSite – a comprehensive resource for helminth genomics. *Mol. Biochem. Parasitol.* 215, 2–10. doi: 10.1016/j.molbiopara.2016.11.005

Korneva, J. V. (2004). Fine structure and development of *Triaenophorus nodulosus* (Cestoda) during metamorphosis: a review. *Acta Zool.* 85, 59–68. doi: 10.1111/j.0001-7272.2004.00158.x

Koziol, U. (2017). Evolutionary developmental biology (evo-devo) of cestodes. *Exp. Parasitol.* 180, 84–100. doi: 10.1016/j.exppara.2016.12.004

Koziol, U., Costábile, A., Domínguez, M. F., Iriarte, A., Alvite, G., Kun, A., et al. (2011). Developmental expression of high molecular weight tropomyosin isoforms in *Mesocestoides corti*. *Mol. Biochem. Parasitol.* 175, 181–191. doi: 10.1016/j.molbiopara.2010.11.009

Koziol, U., Jarero, F., Olson, P. D., and Brehm, K. (2016). Comparative analysis of Wnt expression identifies a highly conserved developmental transition in flatworms. *BMC Biol.* 14, 10. doi: 10.1186/s12915-016-0233-x

Koziol, U., Krohne, G., and Brehm, K. (2013). Anatomy and development of the larval nervous system in *Echinococcus multilocularis*. *Front. Zool* 10, 24. doi: 10.1186/1742-9994-10-24

Koziol, U., Rauschendorfer, T., Zanon Rodríguez, L., Krohne, G., and Brehm, K. (2014). The unique stem cell system of the immortal larva of the human parasite *Echinococcus multilocularis*. *Evodevo* 5, 1–23. doi: 10.1186/2041-9139-5-10

Loehr, K. A., and Mead, R. W. (1980). Changes in embryonic cell frequencies in the germinative and immature regions of *Hymenolepis citelli* during development. *J. Parasitol.* 66, 792–796. doi: 10.2307/3280670

Molina, M. D., and Cebrià, F. (2021). Decoding stem cells: an overview on planarian stem cell heterogeneity and lineage progression. *Biomolecules* 11, 1532. doi: 10.3390/biom11101532

Monjo, F., and Romero, R. (2015). Embryonic development of the nervous system in the planarian *Schmidtea polychroa*. *Dev. Biol.* 397, 305–319. doi: 10.1016/j.ydbio.2014.10.021

Montagne, J., Preza, M., and Koziol, U. (2023). Stem cell proliferation and differentiation during larval metamorphosis of the model tapeworm *Hymenolepis microstoma*. *bioRxiv* 2023 09, 13.557592. doi: 10.1101/2023.09.13.557592

Nono, J. K., Pletinckx, K., Lutz, M. B., and Brehm, K. (2012). Excretory/secretory-products of *Echinococcus multilocularis* larvae induce apoptosis and tolerogenic properties in dendritic cells in *vitro*. *PLoS Negl. Trop. Dis.* 6, e1516. doi: 10.1371/journal.pntd.0001516

Olson, P. D., Tracey, A., Baillie, A., James, K., Doyle, S. R., Buddenborg, S. K., et al. (2020). Complete representation of a tapeworm genome reveals chromosomes capped by centromeres, necessitating a dual role in segregation and protection. *BMC Biol.* 18, 1–16. doi: 10.1186/s12915-020-00899-w

Olson, P. D., Zarowiecki, M., James, K., Baillie, A., Bartl, G., Burchell, P., et al. (2018). Genome-wide transcriptome profiling and spatial expression analyses identify signals and switches of development in tapeworms. *Evodevo* 9, 21. doi: 10.1186/s13227-018-0110-5

Palma, S., Chile, N., Carmen-Orozco, R. P., Trompeter, G., Fishbeck, K., Cooper, V., et al. (2019). *In vitro* model of postoncosphere development, and in *vivo* infection abilities of *Taenia solium* and *Taenia saginata*. *PLoS Negl. Trop. Dis.* 13, e0007261. doi: 10.1371/journal.pntd.0007261

Paysan-Lafosse, T., Blum, M., Chuguransky, S., Grego, T., Pinto, B. L., Salazar, G. A., et al. (2023). InterPro in 2022. *Nucleic Acids Res.* 51, D418–D427. doi: 10.1093/nar/gkac993

Peterson, K. J., Cameron, R. A., and Davidson, E. H. (1997). Set-aside cells in maximal indirect development: Evolutionary and developmental significance. *BioEssays* 19, 623–631. doi: 10.1002/bies.950190713

Phochanukul, N., and Russell, S. (2010). No backbone but lots of Sox: Invertebrate Sox genes. *Int. J. Biochem. Cell Biol.* 42, 453–464. doi: 10.1016/j.biocel.2009.06.013

Pouchkina-Stantcheva, N. N., Cunningham, L. J., Hrčkova, G., and Olson, P. D. (2013). RNA-mediated gene suppression and in *vitro* culture in *Hymenolepis microstoma*. *Int. J. Parasitol.* 43, 641–646. doi: 10.1016/j.ijpara.2013.03.004

Preza, M. (2021) *Estudio de los diferentes roles que cumplen los Neuropéptidos en el ciclo de vida del cestodo modelo Hymenolepis microstoma*. Available at: https://hdl.handle.net/20.500.12008/36209.

Preza, M., Calvelo, J., Langleib, M., Hoffmann, F., Castillo, E., Koziol, U., et al. (2021). Stage-specific transcriptomic analysis of the model cestode *Hymenolepis microstoma*. *Genomics* 113, 620–632. doi: 10.1016/j.ygeno.2021.01.005

Preza, M., Montagne, J., Costábile, A., Iriarte, A., Castillo, E., and Koziol, U. (2018). Analysis of classical neurotransmitter markers in tapeworms: evidence for extensive loss of neurotransmitter pathways. *Int. J. Parasitol.* 48, 979–992. doi: 10.1016/J.IJPARA.2018.06.004

Preza, M., Van Bael, S., Temmerman, L., Guarnaschelli, I., Castillo, E., and Koziol, U. (2022). Global analysis of neuropeptides in cestodes identifies Attachin, a SIFamide homolog, as a stimulant of parasite motility and attachment. *J. Neurochem.* 162, 467–482. doi: 10.1111/jnc.15654

Prieto, D., Aparicio, G., Morande, P. E., and Zolessi, F. R. (2014). A fast, low cost, and highly efficient fluorescent DNA labeling method using methyl green. *Histochem. Cell Biol.* 142, 335–345. doi: 10.1007/s00418-014-1215-0

Reuter, M., and Kreshchenko, N. (2004). Flatworm asexual multiplication implicates stem cells and regeneration. *Can. J. Zool.* 82, 334–356. doi: 10.1139/z03-219

Rink, J. C. (2013). Stem cell systems and regeneration in Planaria. *Dev. Genes Evol.* 223, 67–84. doi: 10.1007/s00427-012-0426-4

Rozario, T., Quinn, E. B., Wang, J., Davis, R. E., and Newmark, P. A. (2019). Region-specific regulation of stem cell-driven regeneration in tapeworms. *Elife* 8, e48958. doi: 10.7554/eLife.48958

Sakamoto, T., and Sugimura, M. (1970). Studies on echinococcosis XXIII: Electron microscopical observations on histogenesis of larval *Echinococcus multilocularis*. *Jpn. J. Vet. Res.* 18, 131–144. doi: 10.14943/jjvr.18.3.131

Schindelin, J., Arganda-Carreras, I., Frise, E., Kaynig, V., Longair, M., Pietzsch, T., et al. (2012). Fiji: an open-source platform for biological-image analysis. *Nat. Methods* 9, 676–682. doi: 10.1038/nmeth.2019

Schramlová, J., and Blazek, K. (1983). Morphology of *Cysticercus bovis* during its development. *Folia Parasitol. (Praha).* 30, 335–339.

Scimone, M. L., Cote, L. E., and Reddien, P. W. (2017). Orthogonal muscle fibres have different instructive roles in planarian regeneration. *Nature* 551, 623–628. doi: 10.1038/nature24660

Scimone, M. L., Kravarik, K. M., Lapan, S. W., and Reddien, P. W. (2014). Neoblast specialization in regeneration of the planarian *Schmidtea mediterranea*. *Stem Cell Rep.* 3, 339–352. doi: 10.1016/j.stemcr.2014.06.001

Seidel, J. S. (1975). The life cycle in *vitro* of *Hymenolepis microstoma* (Cestoda). *J. Parasitol.* 61, 677–681. doi: 10.2307/3279462

Shackney, S. E., and Ritch, P. S. (1987). "Percent labeled mitosis curve analysis" in. *Techniques in cell cycle analysis. Biological Methods.* (Clifton, NJ: Humana Press), 31–45. doi: 10.1007/978-1-60327-406-7_2

Shield, J. M., Heath, D. D., and Smyth, J. D. (1973). Light microscope studies of the early development of *Taenia pisiformis* cysticerci. *Int. J. Parasitol.* 3, 8–10. doi: 10.1016/0020-7519(73)90042-8

Simionato, E., Kerner, P., Dray, N., Le Gouar, M., Ledent, V., Arendt, D., et al. (2008). atonal- and achaete-scute-related genes in the annelid *Platynereis dumerilii*: Insights into the evolution of neural basic-Helix-Loop-Helix genes. *BMC Evol. Biol.* 8, 1–13. doi: 10.1186/1471-2148-8-170

Sur, A., Renfro, A., Bergmann, P. J., and Meyer, N. P. (2020). Investigating cellular and molecular mechanisms of neurogenesis in *Capitella teleta* sheds light on the ancestor of Annelida. *BMC Evol. Biol.* 20, 1–29. doi: 10.1186/s12862-020-01636-1f

Swiderski, Z., Miquel, J., Azzouz-Maache, S., and Pétavy, A.-F. (2018). *Echinococcus multilocularis* (Cestoda, Cyclophyllidea, Taeniidae): functional ultrastructure of the penetration glands and nerve cells within the oncosphere. *Parasitol. Res.* 117, 2653–2663. doi: 10.1007/s00436-018-5957-9

Swiderski, Z., Miquel, J., and Conn, D. B. (2016). Functional ultrastructure of eggs and cellular organization of hexacanths of the cyclophyllidean cestode *Thysanotaenia congolensis*: a phylogenetic implication of obtained results. *Parasitology* 143, 320–333. doi: 10.1017/S0031182015001560

Tixier, V., Bataillé, L., and Jagla, K. (2010). Diversification of muscle types : Recent insights from Drosophila. *Exp. Cell Res.* 316, 3019–3027. doi: 10.1016/j.yexcr.2010.07.013

Torgerson, P. R., Keller, K., Magnotta, M., and Ragland, N. (2010). The global burden of alveolar echinococcosis. *PloS Negl. Trop. Dis.* 4, e722. doi: 10.1371/journal.pntd.0000722

Tutukova, S., Tarabykin, V., and Hernandez-Miranda, L. R. (2021). The role of neurod genes in brain development, function, and disease. *Front. Mol. Neurosci.* 14. doi: 10.3389/fnmol.2021.662774

Tyler, S., and Hooge, M. (2004). Comparative morphology of the body wall in flatworms (Platyhelminthes). *Can. J. Zool.* 82, 194–210. doi: 10.1139/z03-222

Ubelaker, J. E. (1980). "Structure and ultrastructure of the larvae and metacestodes of *Hymenolepis diminuta*," in *Biology of the Tapeworm Hymenolepis diminuta*. Ed. H. P. Arai (New York and London: Academic Press), 59–156. doi: 10.1016/B978-0-12-058980-7.50007-5

Vidal, B., Santella, A., Serrano-Sai, E., Bao, Z., Chuang, C. F., and Hobert, O. (2015). *C. elegans* SoxB genes are dispensable for embryonic neurogenesis but required for terminal differentiation of specific neuron types. *Development* 142, 2464–2477. doi: 10.1242/dev.125740

Voge, M. (1964). Development of *Hymenolepis microstoma* (Cestoda: Cyclophyllidea) in the Intermediate host *Tribolium confusum*. *J. Parasitol.* 50, 77–80. doi: 10.2307/3276032

Voge, M., and Graiwer, M. (1964). Development of Oncospheres of *Hymenolepis diminuta*, Hatched *In vivo* and *In vitro*, in the Larvae of Tenebrio molitor. *J. Parasitol.* 50, 267. doi: 10.2307/3276284

Wendt, G. R., Collins, J. N. R., Pei, J., Pearson, M. S., Bennett, H. M., Loukas, A., et al. (2018). Flatworm-specific transcriptional regulators promote the specification of tegumental progenitors in Schistosoma mansoni. *Elife* 7, e33221. doi: 10.7554/eLife.33221

Wendt, G., Zhao, L., Chen, R., Liu, C., O'Donoghue, A. J., Caffrey, C. R., et al. (2020). A single-cell RNA-seq atlas of *Schistosoma mansoni* identifies a key regulator of blood feeding. *Science* 369, 1644–1649. doi: 10.1126/science.abb7709

Witchley, J. N., Mayer, M., Wagner, D. E., Owen, J. H., and Reddien, P. W. (2013). Muscle cells provide instructions for planarian regeneration. *Cell Rep.* 4, 633–641. doi: 10.1016/j.celrep.2013.07.022

frontiers | Frontiers in Cellular and Infection Microbiology

TYPE Original Research
PUBLISHED 19 December 2023
DOI 10.3389/fcimb.2023.1287355

OPEN ACCESS

EDITED BY
Ana Gonçalves Domingos,
New University of Lisbon,
Portugal

REVIEWED BY
Pedro Eduardo Ferreira,
University of Minho, Portugal
Sylvie Garcia,
Institut Pasteur, France

*CORRESPONDENCE
Alena Pance
a.pance@herts.ac.uk

RECEIVED 01 September 2023
ACCEPTED 01 December 2023
PUBLISHED 19 December 2023

CITATION
Pance A, Ng BL, Mwikali K, Koutsourakis M, Agu C, Rouhani FJ, Montandon R, Law F, Ponstingl H and Rayner JC (2023) Novel stem cell technologies are powerful tools to understand the impact of human factors on *Plasmodium falciparum* malaria. *Front. Cell. Infect. Microbiol.* 13:1287355. doi: 10.3389/fcimb.2023.1287355

Novel stem cell technologies are powerful tools to understand the impact of human factors on *Plasmodium falciparum* malaria

Alena Pance[1,2]*, Bee L. Ng[1], Kioko Mwikali[1,3], Manousos Koutsourakis[1], Chukwuma Agu[1], Foad J. Rouhani[1], Ruddy Montandon[1,4], Frances Law[1], Hannes Ponstingl[1] and Julian C. Rayner[1,5]

[1]Wellcome Sanger Institute, Cambridge, United Kingdom, [2]School of Life and Medical Sciences, University of Hertfordshire, Hatfield, United Kingdom, [3]Bioscience Department, KEMRI-Wellcome Trust Research Programme, Kilifi, Kenya, [4]Wellcome Centre of Human Genetics, University of Oxford, Oxford, United Kingdom, [5]Cambridge Institute for Medical Research, University of Cambridge, Cambridge, United Kingdom

Plasmodium falciparum parasites have a complex life cycle, but the most clinically relevant stage of the disease is the invasion of erythrocytes and the proliferation of the parasite in the blood. The influence of human genetic traits on malaria has been known for a long time, however understanding the role of the proteins involved is hampered by the anuclear nature of erythrocytes that makes them inaccessible to genetic tools. Here we overcome this limitation using stem cells to generate erythroid cells with an *in-vitro* differentiation protocol and assess parasite invasion with an adaptation of flow cytometry to detect parasite hemozoin. We combine this strategy with reprogramming of patient cells to Induced Pluripotent Stem Cells and genome editing to understand the role of key genes and human traits in malaria infection. We show that deletion of basigin ablates invasion while deletion of ATP2B4 has a minor effect and that erythroid cells from reprogrammed patient-derived HbBart α-thalassemia samples poorly support infection. The possibility to obtain patient-secific and genetically modifed erythoid cells offers an unparalleled opportunity to study the role of human genes and polymorphisms in malaria allowing preservation of the genomic background to demonstrate their function and understand their mechanisms.

KEYWORDS

stem cells, erythropoietic differentiation, malaria, *Plasmodium falciparum*, invasion, genome editing, reprogramming, haemoglobinopathies

Introduction

Malaria is an infectious disease caused by several species of *Plasmodium* parasites that are transferred between humans by female Anopheline mosquitoes. The parasite life cycle is complex and involves multiple organs in host and vector, with a wide range of interactions between parasite and host at each step. Nevertheless, in the human host it is the asexual blood stages of the parasite that invade, develop and replicate in erythrocytes, causing a variety of pathological processes associated with malaria infection. The completion of reference genomes (Aurrecoechea et al., 2009), the development of genome editing technologies (Lo et al., 2013; Ran et al., 2013) and their adaptation to the parasite (Straimer et al., 2012; Ghorbal et al., 2014) have revolutionised our understanding of the parasite side of the blood cycle. These advances have enabled the identification of many parasite proteins involved in invasion (Cowman et al., 2017), as well as the formation of the parasitophorous vacuole, remodelling of the erythrocyte (Cowman et al., 2012; Weiss et al., 2015), and a much broader understanding of parasite blood-stage biology. On the host side, genome-wide association studies (GWAS) have identified multiple human genetic variants associated with differences in the severity of disease caused particularly by *Plasmodium falciparum*, the most virulent species affecting humans (Damena et al., 2019; Malaria Genomic Epidemiology N, 2019). These include many genes implicated in erythrocyte structure and function, such as the membrane protein Band 3, the red blood cell enzyme Glucose-6-Phosphate Dehydrogenase and the Haemoglobins, amongst others (Kariuki and Williams, 2020). However, despite population studies providing compelling evidence for protective effects of multiple human protein variants, the molecular mechanisms of these effects are frequently either undeciphered or disputed. This is mainly due to the limitations in accessing primary cell samples and the technical challenges of reproducing variants *in-vitro* in order to perform tightly controlled cellular studies.

There are two major hurdles for identifying host proteins that interact with malaria parasites and understanding their function. Firstly, erythrocytes are non-proliferative, terminally differentiated cells with a limited life span, which makes their long-term culture impossible. Thus, research has almost exclusively relied on clinical samples, with inherent difficulties of donor availability and variability as well as the impact of storage and transport on sample quality which impose limitations on the ability to perform detailed cellular studies. Secondly and perhaps most significantly for mechanistic studies, mature erythrocytes are anucleated and therefore gene editing technologies cannot be applied. Attempts to overcome these limitations have been developed in recent years using a variety of stem cell technologies. siRNA knock-down techniques in Haematopoietic Stem Cells (HSCs) have been used to study the specific role of Glycophorin A (GYPA) (Bei et al., 2010) and Basigin (BSG) (Crosnier et al., 2011) as well as to screen more broadly for erythrocyte proteins involved in *P. falciparum* growth and development (Egan et al., 2015). While a significant step forward, the applicability of this approach is curtailed by the restricted availability of HSCs, their limited proliferation capacity and the variable levels of knock-down that can be achieved. More recently, an immortalised adult erythroblast line able to proliferate and differentiate *in-vitro*, was established by transformation of erythroid progenitor cells with the human papilloma virus HPV16-dervied proteins HPV16-E6/E7 (Trakarnsanga et al., 2017). One such line (BEL-A) was combined with genome editing technologies to explore the mechanisms of Basigin involvement in *P. falciparum* invasion (Satchwell et al., 2019). This approach was also applied to peripheral blood samples and shown to generate cells permissive to *P. falciparum* and *P. vivax* invasion and amenable to genome editing studies (Scully et al., 2019). One potential disadvantage of this strategy is the viral transformation of the cells with its inherent genetic consequences that might be limiting on the long term, particularly when addressing natural genomic variation. Critically, studies using stem cell lines engineered to facilitate differentiation towards erythropoiesis do not offer the possibility of exploring specific genetic characteristics or complex genetic traits in their original genomic context, such as those found in patients or particular human populations.

Other approaches, such as the use of established Embryonic and induced Pluripotent Stem Cell lines (ESCs and iPSCs) that can be cultured (International Stem Cell et al., 2007) and genetically manipulated (Veres et al., 2014) while maintaining their pluripotency (Hendriks et al., 2020), could provide a versatile alternative with additional advantages. Stem cells have the potential to differentiate into any cell type, which would allow examination of the same genomic background on all parasite stages. Furthermore, the development of reprogramming techniques that revert terminally differentiated cells to pluripotency (Takahashi et al., 2007) makes it possible to generate iPSCs from any individual or sample. In this way, complex genotypes and rare variants, including non-viable mutations, can be brought into the lab and stored for unlimited studies. Genome editing to change or correct the mutations also becomes possible, offering a direct confirmation of their physiological role. Crucially, the use of stem cells also helps to overcome some of the ethical issues often encountered when pursuing molecular research in the malaria field.

In this work we developed a differentiation protocol to drive both ESCs and iPSCs towards erythropoiesis and produce cells that are competent for *P. falciparum* infection. This approach makes it possible to study a wide range of patient-derived cells simultaneously as well as make use of existing iPS lines, while also allowing the potential to incorporate genome editing of specific host genes and compare their effect on multiple different genomic backgrounds. Our protocol mimics more closely natural development by driving the pluripotent cells to mesoderm first, thus avoiding the commonly used embryoid body formation with the associated cell loss, and leading to a better yield of erythroid cells. To assess invasion of the *in-vitro*-derived cells, we established an assay to accurately quantify parasitaemia using an adaptation of flow cytometry based on the refractive properties of haemozoin, a pigment produced by malaria parasites after digestion of haemoglobin (Egan, 2008). These protocols represent versatile tools to explore the impact of host genetic variation on *Plasmodium* parasites. Understanding the mechanisms of host-parasite interactions at a molecular level may identify new targets for therapeutic intervention.

Methods

Ethics statement

The use of primary erythrocytes for the culture of Plasmodium falciparum was approved by the NHS Cambridgeshire Research Ethics Committee REC ref. 15/EE/0253 and the Wellcome Sanger Institute Human Materials and Data Management Committee HMDMC 15/076.

The use of human embryonic stem cell lines was approved by the Steering Committee for the UK Stem Cell Bank and for the use of Stem Cell Lines (ref. SCSC11-23) and the Wellcome Sanger Institute Human Materials and Data Management Committee. The Human Embryonic Stem cell lines (Shef 3 and Shef 6) were obtained from the Centre for Stem Cell Biology, University of Sheffield, Sheffield, UK.

The wild-type iPS cell lines were derived from fibroblasts and blood at the Wellcome Sanger Institute and obtained from the Wellcome Sanger HipSci collection.

The haemoglobinopathy iPS cell lines were derived from fibroblast samples obtained from the NIGMS human genetic cell repository of the Coriell Institute for Medical Research, USA: GM10796; GM03433.

Reprogramming of induced pluripotent stem cell lines

Human IPS lines from haemoglobinopathy fibroblast samples acquired from the Coriell repository and from blood samples were derived and verified at the Wellcome Sanger Institute as described (Rouhani et al., 2014; Agu et al., 2015; Soares et al., 2016; Kilpinen et al., 2017). Briefly, $5x10^5$ cells were transduced with Sendai virus carriers of the Yamanaka factors: hOCT4, hSOX2, hKLF4 and hc-MYC overnight at 37^0C in 5% CO_2. After a medium change the next day, the cells were cultured for 4 days and from then on maintained in Stem Cell medium: advanced DMEM/F-12 (Gibco, UK) supplemented with 2 mM Glutamax (Gibco), 0.01% β mercapto ethanol (sigma), 4 nM human FGF-basic-147 (Cambridge Bioscience, UK) and 20% KnockOut serum replacement (Gibco, UK), changing medium daily. Ten to 21 days post-transduction, formation of pluripotent colonies was evident, the visible colonies were handpicked and transferred to 12 well plates with MEF feeders. Colonies were expanded into 6 well feeder plates and passaged every 5 to 7 days depending on confluence.

Cell culture

All stem cell lines used in this study were cultured on feeder cells (irradiated mouse embryonic fibroblasts MEFS (Global Stem) in the Stem Cell medium described above. The cultures were kept at 37°C, 5% CO_2 and medium was changed regularly. Pluripotent cells were passaged using 0.5 mM EDTA (Gibco, UK) and 10μM Rock inhibitor.

Erythropoietic differentiation

Stem cells were taken off feeder cells with 0.5 mM EDTA (GIBCO) and seeded on gelatine-coated 10 cm plates pre-conditioned with MEF medium over-night and cultured in CDM-PVA supplemented with 12 nM hbFGF (Cell guidance systems, UK) and 10 nM hActivin-A (Source Bioscience, UK). CDM-PVA: 50% IMDM (Invitrogen), 50% advanced DMD-F12 (GIBCO) with 1g/l Poly(vinyl alcohol) PVA (SIGMA), Penicillin/Streptomycin 1x (GIBCO), 1-thioglycerol MTG (SIGMA), Insulin-Transferrin-Selenium 1x (ITS, Life Technologies), Cholesterol 1x (SyntheChol, SIGMA).

As a first step of differentiation, the cells were taken towards the mesoderm germline:

Mesoderm (2 days)

CDM-PVA medium supplemented with 5 nM hActivin-A and 2μM SU5402 (SIGMA)

Meso/Ery transition (8-12 days)

CDM-PVA medium supplemented with 20ng/ml bFGF, 10nM IL-3 (SIGMA), 10nM BMP4 (R&D Systems), 5μM SB431542 (SIGMA), 5μM CHIR99021 (Axon, The Netherlands), 5μM LY294002 (SIGMA).

During this stage, the detached cells are recovered, washed with PBS and transferred to the erythrocytic differentiation stage, performed in a basic erythrocytic medium (BEM): CellGRO SCGM (CellGenix, Germany) supplemented with ITS, cholesterol, 40ng/ml IGF-1 (Abcam), Penicillin/Streptomycin, 1μM 4-hydroxy 5-methytetrahydrofolate (SIGMA).

Ery I (4-5 days)

BEM supplemented with 10ng/ml IL-3, 50ng/ml SCF (Life Technologies), 1μM dexamethasone (SIGMA), 2U/ml EPO (SIGMA), 10ng/ml FLT3 (R&D Systems).

Ery II (4-5 Days)

BEM supplemented with 50ng/ml SCF, 1μM dexamethasone, 2U/ml EPO.

Diff Ery (minimum 4 Days)

BEM supplemented with 2U/ml EPO, 1μM Triiodo-L-Thyronine (T3, SIGMA)

RNA extraction, qRT-PCR and microarrays

RNA was extracted using the Isolate II RNA Mini kit (Bioline, UK). 1-3 μg were reverse transcribed with a MuLV reverse transcriptase (Applied Biosystems, UK) using random primers (Bioline, UK). One μl of cDNA was specifically and quantitatively amplified using Biotool 2x SybrGreen qPCR master mix (Stratech, UK) following the cycling parameters established by the manufacturer on a light cycler 480 II (Roche) and using GAPDH

as a control for normalisation. The primers used (IDT, Belgium) were:

gene	forward primer	reverse primer	length (bp)
HbB	5'-gtctgccgttactgccctgtgg	5'-agcatcaggagtggacagatcc	136
HbA	5'-ggtgctgtctcctgccgac	5'-cctgggcagagccgtggctc	164
HbG	5'-cctgtcctctgcctctgcc	5'-cacagtgcagttcactcagc	140
HbE	5'-gctgccgtcactagcctgtg	5'-gcccaggatggcagagg	144
TAL1	5'-atgccttccctatgttcaccacca	5'-tgaagatacgccgcacaactttgg	108
Brach	5'-acaaagagatgatggaggaacccg	5'-aggatgaggatttgcaggtggaca	110
GATA1	5'-cctctcccaagcttcgtggaac	5'-caggcgttgcataggtagtggc	127
KLF1	5'-ccggacacacaggatgacttcc	5'-ctggtcctcagacttcacgtggag	114
GAPDH	5'-gcctcctgcaccaccaactgc	5'-ggcagtgatggcatggactg	102
OCT4	5'-ctgccgctttgaggctctgcagc	5'-cctgcacgagggtttctgc	134
NANOG	5'-ccagctgtgtgtactcaatgatag	5'-ctctggttctggaaccaggtcttc	123
GYPA	5'-ccactgaggtggcaatgcac	5'-cttcatgagctctaggagtggctgc	120
GYPC	5'-ggacattgtcgtcattgcaggtg	5'-gcctcattggtgtggtacgtgc	117
BSG	5'-ccatgctggtctgcaagtcagag	5'-cacgaagaacctgctctcggag	116
TfR	5'-gggctggcagaaaccttg	5'-cagttggagtgctggagact	145

For microarray analyses, RNA was extracted as above, the Illumina TotalPrep RNA amplification kit (Ambion Life technologies) was used to process the samples, and gene expression analysis was assessed on Illumina HumanHT-12v4 chips following the instructions of the manufacturer.

Parasite culture

Fluorescent *P. falciparum* parasites were cultured in complete RPMI medium (GIBCO) at 2.5% haematocrit with O- RBCs sourced from NHSBT, Cambridge. Cultures were maintained at 37°C in malaria gas (1% O_2, 3% CO_2 and 96% N_2).

Fluorescent parasites

Parasites were engineered to express a variety of fluorochromes for detection at different wavelengths (Carrasquilla et al., 2020). The chosen fluorochromes: Midori-ishi cyan (excitation/mission: 472/495 nm, gift from Michael Davidson (Addgene plasmid # 54752; http://n2t.net/addgene:54752; RRID : Addgene_54752)), Kusabira Orange (excitation/emission: 548/559 nm, gift from Michael Davidson & Atsushi Miyawaki (Addgene plasmid # 54834; http://n2t.net/addgene:54834; RRID : Addgene_54834) (Karasawa et al., 2004)), tagBFP (Blue Fluorescent Protein excitation/emission 399/456 nm) and mCherry (excitation/emission 587/610 nm) were individually inserted into the XhoI/AvrII site of an *attP*-containing vector under regulation by the calmodulin promoter and bearing blasticidin resistance as a selection marker. The NF54 *attB* strain of *Plasmodium falciparum* was transfected with each fluorochrome vector together with an expression vector for Bxb1 integrase by pre-loading erythrocytes by electroporation with a BioRad gene pulser and incubating with percoll-purified late-stage parasites. The transfected cultures were maintained with daily medium change and transfectants were selected with blasticidin (2 μgr/ml) (Adjalley et al., 2010) after 2 days.

Staining procedures

Cell labelling

In-vitro-differentiated erythroid cells were centrifuged (1100xg for 4') and resuspended in 1 ml of Diff Ery medium containing 1 μM of a cell trace dye (ThermoFisher Scientific), either carboxy-DFFDA-SE ((Carboxylic Acid Diacetate) excitation/emission: 498/526 nm) or DDAO-SE ((9*H*-(1,3-Dichloro-9,9-Dimethylacridin-2-One-7-yl) β-D-Galactopyranoside) excitation/emission: 645/660 nm) dye for 1 h at 37^{0}C. Cells were spun again and resuspended in 1ml dye-free medium and incubated for 30 minutes at 37^{0}C. After a final spin, cells were resuspended in parasite culture medium at a concentration of 10^6 cells per 75 μl.

Giemsa staining of slides

Cells, parasite cultures and invasion assays were stained with Giemsa for microscopic examination. Five μl of culture were dropped on a glass slide and spread with a pipette tip or smeared with a glass slide and dried. The slides were fixed with methanol for a few seconds, dried and incubated with 1x Giemsa stain solution for 5-10 minutes. The stain solution as drained away, the slides were washed with tap water and dried before microscopic examination.

Sybr Green staining of parasite DNA

Fixed culture samples were incubated in 100 μl of a 1X solution (1/10000 dilution) of Sybr Green (excitation/emission: 484/515 nm) nucleic acid gel stain 10000X (Invitrogen) for 30 minutes at 37^{0}C. 200 μl of PBS were added to each sample before flow cytometry analysis using a 488 nm laser with a 530/40 nm bandpass filter.

Invasion assays

In-vitro-differentiated labelled erythroid cells were counted and 75 μl containing 1 million cells were dispensed into a 96 well plate, including a well of cells alone for flow cytometry controls. Primary erythrocytes obtained from the blood bank were labelled in the same way, adding 75 μl at 5% haematocrit per assay.

Cultures of fluorescent parasites at a parasitaemia of 1.5 – 2% mature parasites were used to purify schizonts: 10 ml of culture were centrifuged (1100xg for 5' brake 3), resuspended in 1 ml of

medium and loaded onto a 63% Percoll cushion. Centrifugation at 1300xg for 11' no brake separated the mature parasites at the Percoll interface. These were recovered, washed with parasite medium (as described in the parasite culture section) and resuspended in 3 ml of parasite medium. The parasite suspension, containing late-stage parasites was added to the cells in the 96 well plate at 75 µl/well.

One plate per time point was prepared and plates were placed in a gas chamber filled with malaria gas and left in a 37°C incubator for the appropriate length of time.

After the incubation time, the plate was removed, adding 200 µl of PBS/well and spinning at 1100xg 1'. Three µl were taken from the bottom of the wells and smeared on slides to be stained with Giemsa and the supernatant was removed. The pellets were fixed with 100 µl 4% paraformaldehyde for 20', washed and resuspended in PBS to be analysed by flow cytometry.

Flow cytometry

Expression of proteins on the membrane of stem cell-derived erythrocytes was measured using specific fluorochrome-tagged antibodies and quantitation by flow cytometry on a LSFORTESSA BD analyser using Flowjo V10.3 (Bcton Dickinson & Co, NJ) and FCSexpress 7. Antibodies:

CD71-APC (Allophycocyanin excitation/emission 594/660nm) Biolegend #334108

GYPA-PE (Phycoerythrin excitation/emission 565/574nm) Southern Biotech #9861-09

BSG-FITC (Fluorescein Isothiocyanate excitation/emission 495/525)MACS Miltenyi #130-104-489

ATP2B4-FITCLSBio #LS-C446496

A MoFlo flow cytometer (Beckman Coulter, USA) was adapted for detection of laser light depolarisation produced by parasite hemozoin (Frita et al., 2011). The Mo-Flo flow cytometer has a Z-configuration optics platform and is equipped with four solid state lasers (488nm, 561nm, 405nm, 640nm) spatially separated at the stream-in-air flow chamber with 488nm primarily assigned as the first laser. The laser power for 561nm, 405nm, 640nm were all set at 100mW and 488nm was set at 50mW. The laser 488nm, 561nm, 405nm, 640nm was used to excite the Cyan and PE, mCherry, BFP and DDAO respectively. Fluorescence emitted from Cyan, PE, mcherry, BFP and DDAO was collected using a 520/36nm, 580/30nm, 615/20nm, 447/60nm and 671/28nm band pass filter respectively. An optical modification was made on the primary laser detection pod so that the scattered light from 488nm laser light was split into two using a 50/50 beam splitter to measure the normal SSC (vertical) and depolarised SSC (Horizontal) by placing a polarizer (Chroma Technology Corp) with its polarisation axis horizontal to the polarisation plane of the laser light. Both SSC detectors have a 488/10nm band pass filter (Supplementary Figure S2). A total of 50000 events was acquired and analysed using Flojo V10.3 and FCSexpress 7.

Invitrogen Bigfoot cell sorter (Thermo Fisher Scientific, Inc.) was also used for the detection of laser light depolarisation produced by parasite hemozoin. The cell sorter is equipped with six spatially separated solid state lasers but only two of the lasers would be ON and used in the assay. The laser power for 488 nm was set at 125 mW and 640 nm was set at 100 mW. The laser 488 nm, 640 nm was used to excite Sybr Green and DDAO respectively. Fluorescence emitted from SYBR Green and DDAO was collected using a 507/19 nm and 670/30 nm band pass filter respectively. The instrument is also equipped with default polarisers at the 488nm laser light path which can be switched 'ON' during the analysis. This optic set up allows the measurement of normal SSC (488 SSC, Area Linear) and depolarised SSC (488 SSC Polar, Area Linear) (See figure below). A total of 20,000 events was acquired and analysed using FCSExpressv7 (*De Novo* Software, Inc.).

All samples are analysed on side and forward scatter to eliminate debris, then on pulse width to eliminate doublets and select the single cell population. Single cells are then analysed for fluorescence using the cell label and parasite fluorescence. The labelled non-infected cells are used to establish the depolarisation gate. The invasion assays are analysed in the same way, selecting the labelled population of cells and assessing depolarisation with the established gate. Quantification of the number of labelled erythroid cells containing metabolically active parasites in the total population of labelled cells reveals the % parasitaemia.

Statistical analysis

Results are presented as means and standard deviation. The reported significance was calculated using a two-tailed unpaired Student's T test analysis.

Genome editing

Genomic modification to ablate the genes chosen for this study was performed in the RH1 cell line, as described previously (Yeung et al., 2017) and shown schematically in supplementary Supplementary Figure S6. Briefly, a CRISPR/Cas9 strategy was used targeting a critical exon in each gene (exon 5 in BSG and exon 11 in ATP2B4) for substitution with a selection cassette as depicted in Supplementary Figure S6. Pluripotent cells were nucleofected by electroporation using Amaxa4 following the manufacturer's instructions. After two days of recovery, the puromycin resistance in the selection cassette was used to isolate correctly targeted clones which were examined for damage to the second allele by targeted sequencing as shown in Supplementary Figure S7.

Microarray data analysis

All microarray datasets obtained as described in the RNA extraction, qRT-PCR and microarrays section were put through "neqc" background correction followed by quantile normalization using the limma R package (Ritchie et al., 2015). Inter-plate variation (batch effects) were adjusted using combat algorithm https://pubmed.ncbi.nlm.nih.gov/16632515/ [pubmed.ncbi.nlm.nih.gov]. Differential expression analysis was performed to obtain a subset of

significant probes (those that change between two or more conditions), FDR adjusted P value of 0.05 was chosen as the cut-off using limma R package. Heatmaps were plotted using Complexheatmap R package https://pubmed.ncbi.nlm.nih.gov/27207943/[pubmed.ncbi.nlm.nih.gov]. The GSE63703 gene expression matrix from GREIN (https://shiny.ilincs.org/grein) was used to identify erythrocyte and erythroid progenitor specific genes.

Results

The differentiation protocol allows the *in-vitro* generation of erythroid cells from a wide variety of human stem cells

The main objective was to establish a stem cell differentiation protocol to generate erythroid cells able to support parasite invasion and growth, in sufficient numbers to allow parasite invasion assays to be performed (Supplementary Figure S1). With this in mind, we minimised cell manipulation and loss by avoiding the widely used embryoid body stage or co-cultures with other cell types and directing the cells towards the mesoderm path instead. This is achieved by two steps of specific cytokine combinations, based on the approach described by Vallier et al. (2009). First the cells are exposed to low levels of Activin A while inhibiting Fibroblast Growth Factor 2 (FGF2) to suppress neuroectoderm and then to a combination of Bone Morphogenetic Protein 4 (BMP4), FGF2 and inhibition of Activin A signalling with SB431542 to favour mesoderm differentiation over endoderm fate. In our protocol, interleukin 3 (IL-3) is added at this stage in order to direct the forming mesoderm towards haematopoiesis. As the cells start differentiating, qRT-PCR analysis shows decline of pluripotency gene expression while mesoderm markers increase (Figure 1A), before induction of the crucial transcription factors involved in driving the myeloid line of haematopoiesis towards megakaryocyte-erythroid progenitors (MEP). The modulation of gene expression is concomitant with a visible morphological change of the cells.

Microarray analysis confirmed the transition of the transcriptome from early mesoderm towards haematopoiesis through this stage of the differentiation process (Figure 1B). Expression of mesoderm specification genes (*eomes, BMP2/4, BMP receptor 1B (BMPR1B), Cripto (CFC1)*) became evident early during the mesoderm phase, peaking through the Meso-Ery transition, while the major drivers of haematopoiesis (*Brachyury (T), Tal1, GATA1and MIXL1*), peaked later. Based on the increased expression of haematopoietic genes towards the end of this stage of the protocol,

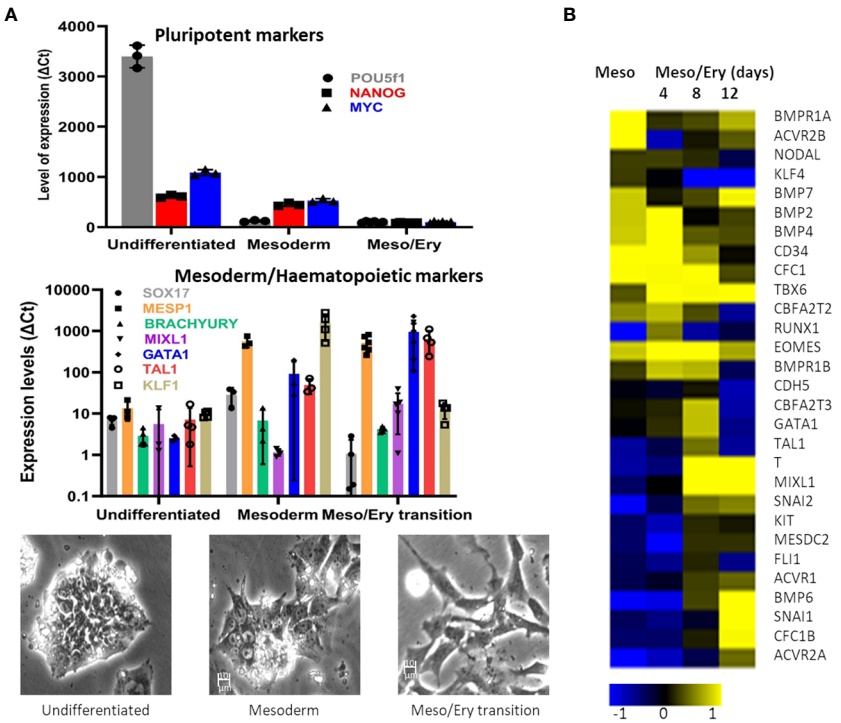

FIGURE 1
Differentiation of stem cells towards mesoderm. The RH1 cell line was differentiated and **(A)** Expression of pluripotency (POU5f2 (Oct 4), Nanog and c-myc), mesoderm (Sox17, MESP1 and Brach) and haematopoiesis (Mixl1, GATA1, Tal1, KLF1) markers was measured by qRT-PCR (at last 3 biological replicates are presented as a mean and standard deviation). Morphological changes of the differentiating cells are documented by light microscopy (100x) during regular culture of pluripotent cells (undifferentiated), after 2 days of mesoderm differentiation (mesoderm) and after 8 days of meso/ery differentiation (meso/ery transition). Cell differentiation is routinely followed by microscopic observation, of which the pictures presented are representative examples. **(B)** Transcriptome analysis of Mesoderm and haemato/erythropoiesis driver and signalling genes was performed by microarrays through the differentiation process. Meso, 2 days mesoderm differentiation; Meso/Ery, mesoderm/erythropoiesis transition after 4, 8 and 12 days of differentiation.

the length of this step was set at 8 – 12 days. During this stage the cells spontaneously detach from the plates and can be harvested from the supernatant avoiding potentially damaging trypsinisation.

The suspension of detached cells is then guided towards erythropoiesis by exposure to Erythropoietin (EPO) and IL-3 to drive differentiation into erythroblasts. Dexamethasone is added to halt the process at the erythroblast stage and improve the homogeneity of the culture. Cell numbers are increased by expanding the erythroblastic cells with Stem Cell Factor (SCF) and differentiation is completed by removing dexamethasone (Supplementary Figure S1). At the end of the differentiation process, analysis of the cells shows expression of the major erythrocytic marker Glycophorin A (GYPA) as well as adult haemoglobins A and B (Figure 2A). Most cells also express the transferrin receptor (CD71), and approximately 70% stain positively for nucleic acids (Hoechst33342), indicating that the cells still have some form of nucleus or nucleic acid content (nucleus or fragments thereof) (Figure 2A). Comparison of globin expression with primary erythrocytes shows that levels of the adult HbA and HbB are much lower and more variable and the iPSC-derived erythroid cells express high levels of foetal HbE and HbG (Figure 2A). These results indicate that the *in-vitro*-generated cells correspond to immature erythroid cells earlier in the erythropoietic differentiation pathway.

Microarray analysis of the transcriptome changes shows induction of major erythrocytic genes including structural proteins (EPB41, SCL4A1), functional proteins such as components of the haeme cycle (PO, CPOS, PPOX, UROS, UROD) and membrane transporters (ATP2B4, ATP2B1) as well as surface markers (GYPC, CD34, CD44, CD99, CD47) (Figure 2B). It is worth noting that induction of many erythrocytic genes occurs in the last stages of the meso/ery transition and the very early erythroid differentiation (Ery I). As erythropoiesis proceeds, the cells become less metabolically active, start extruding organelles and their RNA starts degrading. As a consequence, transcripts for some proteins, such as GYPA and TRFC (CD71) that we identify on the cell surface by flow cytometry (Figure 2A) are no longer detectable as we see in the microarrays. The full transcriptome changes through the differentiation process are shown in Supplementary Figure S2.

The versatility of the differentiation protocol was tested on a variety of cell lines of different origin, including human embryonic stem cell (hESC) lines (Shef3 and Shef6), as well as Induced Pluripotent Stem Cell (hIPSC) lines derived from both fibroblasts (RH1, SF2 and K4) and blood (CD3, CD5 and GB1, GB4). The efficacy of the process was assessed by expression of surface markers GYPA and CD71 by flow cytometry (Figure 3A) and the haemoglobin genes by qRT-PCR (Figure 3B). Though variations in the differentiation efficiency were observed particularly in the levels of GYPA, all the lines generated erythroid cells with distinct erythrocytic characteristics as revealed by the global comparison of gene expression using microarray analysis. As shown in Figure 3C, there is a dramatic change in gene expression between the pluripotent (undifferentiated) and erythroid (diff ery) states of all the iPS cell lines with a similar shift towards erythropoiesis.

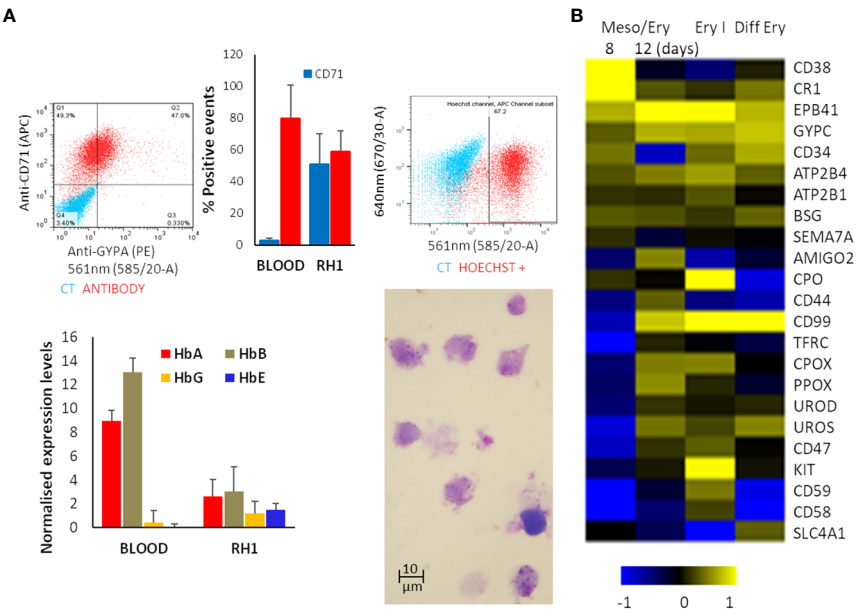

FIGURE 2
Erythropoietic stage of differentiation. The differentiated RH1 cell line was examined for **(A)** Expression of the main erythrocyte markers at the end of the differentiation process: Glicophorin A (GYPA) and transferrin receptor (CD71) as well as a comparison with primary erythroctyes (Blood), and DNA labelling with Hoechst33342 were assessed by flow cytometry (top plots); expression of the haemoglobins HbA, HbB, HbG and HbE was quantified by microarray presented as quartile normalised expression levels in both iPSC-derived erythroid cells (RH1) and primary erythrocytes (Blood) (bottom plot). Morphology of the cells is shown by Giemsa staining and light microscopy (1000x). **(B)** Microarray analysis of genes characteristic of haemato/erythropoiesis over time through the mesoderm/erythropoiesis transition (8 and 12 days of differentiation) step, the onset of erythropoiesis (Ery I: 4 days of the first step of erythropoiesis) and final erythrocytic differentiation (Diff Ery: 5 days of final erythropoietic differentiation) steps of the protocol.

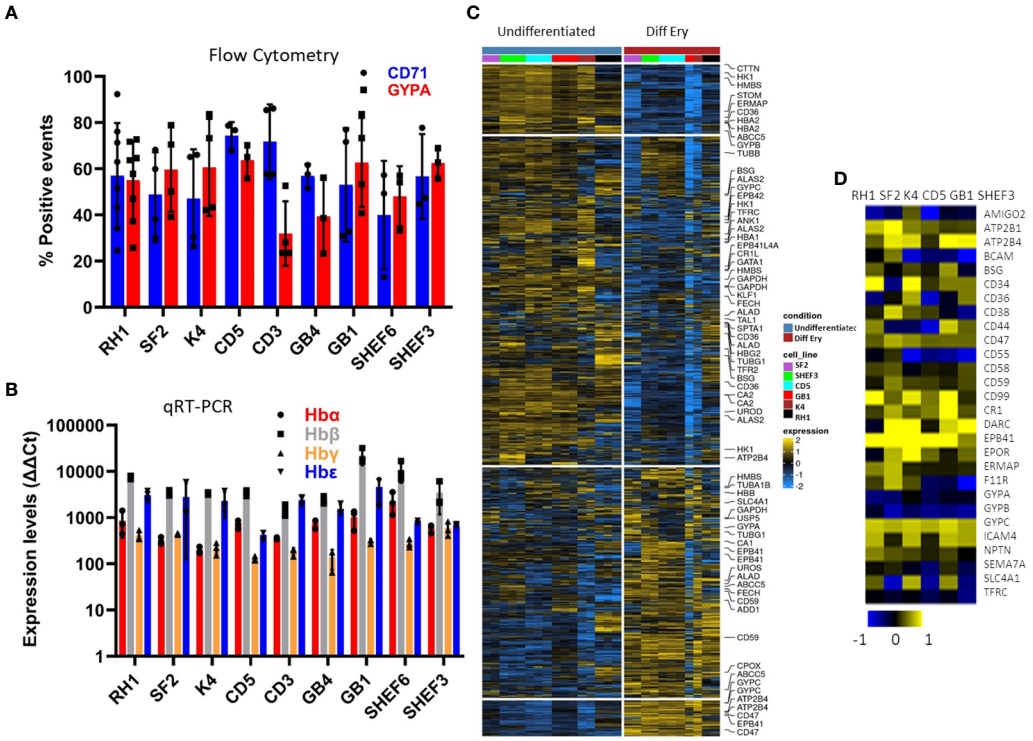

FIGURE 3
Characterisation of a variety of stem cell lines differentiated to erythrocytes *in-vitro* at the end of the differentiation protocol. **(A)** erythrocytic surface markers Glycophorin A (GYPA) and the transferrin receptor (CD71) by flow cytometry (average of at least 3 experiments, SD). **(B)** expression of the haemoglobins (adult A and B; foetal G and E) assessed by qRT-PCR (average of 3 experiments, SD). **(C)** Heatmap of the microarray analysis comparing the gene expression pattern in the iPS cell lines colour-coded on the right-hand side in Undifferentiated and differentiated (final erythropoietic phase) stages. The clusters group the subsets of genes from the highest levels of expression in pluripotency and lowest in erythroid differentiation on the top in descending and ascending order respectively towards the bottom **(D)** expression of the main erythrocyte surface receptors important for malaria parasites invasion in differentiated cells detected by microarray.

Malaria parasites use a range of erythrocyte surface proteins as invasion receptors. *Plasmodium falciparum* in particular is well-known for its ability to use multiple invasion pathways and even switch between them to adapt to host polymorphisms or evade the immune response (Cowman et al., 2017). In this context, we assessed expression of genes reported to be important for invasion of erythrocytes (Bartholdson et al., 2013) using microarray analysis (Figure 3D). While some genes (e.g. *ATP2B4*, *CR1* and *GYPC*) were expressed in all the cell lines used, others (e.g. *CD55*) showed more variable expression at the transcript level. This highlights the need to assess the cell lines chosen for these types of studies in detail to ensure their suitability.

Detection of haemozoin depolarisation accurately quantifies parasitaemia in invasion assays

The *in-vitro*-derived erythroid cells maintain some nucleic acid content, revealed by Hoechst33342 staining (Figure 2A), making the use of DNA labelling to quantify parasitaemia incompatible. To circumvent this problem, we adapted a flow cytometry approach to detect haemozoin (Hz) (Supplementary Figure S3A), a product of haemoglobin digestion by the parasite that has the property of depolarising light. We first assessed whether depolarisation caused by Hz reflects parasitaemia in our system, by labelling a culture of parasites (Figure 4 Giemsa image, counted at 7.3% parasitaemia) with Sybr Green (SG, excitation/emission: 484/515 nm) and comparing direct parasite detection with Hz quantification (Figure 4A). The flow cytometry gates were set up with uninfected blood (Figure 4A top plots, no positive events in SG labelling nor Hz depolarisation). The parasite culture was analysed in the same way applying the established gates (Figure 4A), that revealed several SG-positive populations (Figure 4 bottom middle plot: Sybr Green labelling) of increasing intensity, deemed to reflect rings and brighter mature stages. The depolarisation gate (Figure 4A Hz depolarisation plot) detected 8.15% positive events, which corresponded well with the 8.14% of SG-positive cells and the 7.3% manual count of the corresponding Giemsa-stained slide (Figure 4A image). Examining the depolarising population for SG staining (Figure 4A far right top plot) confirmed that 93.8% of this population corresponds to SG-labelled parasites. The non-depolarising population stained with SG (Figure 4A far right bottom plot) contains mostly uninfected erythrocytes and 1.98% of low intensity SG-positive cells, corresponding to small rings that have not yet accumulated enough Hz to be identified by depolarisation.

With the aim of assessing the detection capacity and limits of Hz depolarisation, the same parasite culture from Figure 4A was

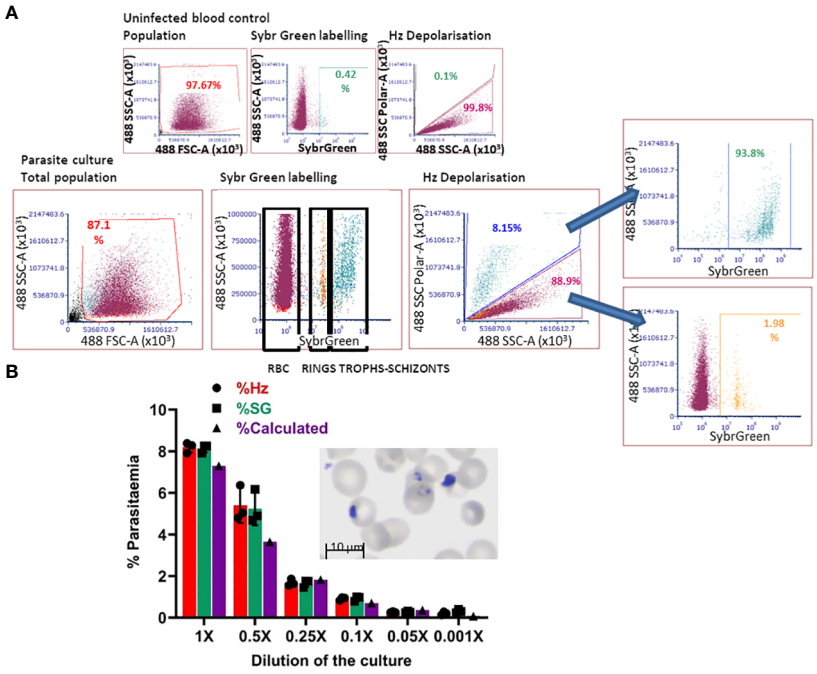

FIGURE 4
Haemozoin-based flow cytometry parasitaemia quantitation. **(A)** The population of uninfected erythrocytes (top left plot) is analysed for Sybr Green labelling (top middle) and Hz depolarisation (top right) to set the gates for defining positive and negative events. The parasite culture (Giemsa image) population (bottom left plot) is analysed with the set gates for Sybr Green labelling (middle plot) and Hz depolarisation (right plot). Sybr Green staining of the depolarising (far right-hand top plot) and non-depolarising events (far right-hand bottom plot). Plots are representative of 3 experiments. **(B)** The parasite culture (Giemsa image) was serially diluted with uninfected erythrocytes. Parasitaemia was quantified by Hz depolarisation, Sybr Green labelling and calculation from manual counting of the original slide.

diluted by repeatedly adding an equal volume of a preparation of uninfected erythrocytes at the same haematocrit (2.5%) to create a serial dilution of the parasite culture (Figure 4B). Parasitaemia was quantified by SG staining and Hz depolarisation (Figure 4B) and compared with the calculation from the manual counting of the original Giemsa slide. A good correspondence between the three methods was observed at the decreasing levels of parasitaemia. The detection limit was found at a dilution of 0.05x that corresponded to a calculated 0.365% parasitaemia, beyond which the quantification becomes unreliable for both, Hz depolarisation and SG staining, remaining at a level between 0.2 and 0.3%.

In order to quantify *P. falciparum* parasitaemia, we designed invasion assays as shown in Supplementary Figure S3B, in which target cells are co-cultured with purified late-stage parasites and incubated in a 96 well plate for set times and analysed by flow cytometry. This approach was first evaluated using as target cells primary erythrocytes labelled with the membrane dye DDAO (excitation/emission: 645/660 nm) to specifically quantify invasion of the target cells. In the first instance, we followed the time course particularly of the early hours of invasion in these assays (Figure 5A). After eliminating debris and doublets the population of target cells is identified by the membrane staining (Figure 5A DDAO+) and this population is examined for depolarisation. To confirm that the depolarising events are indeed cells infected with the parasites, the assays were stained with Sybr Green (SG) and the DDAO+ population was also examined for SG signal. A sample of the invasion assay culture was smeared on a slide and stained with Giemsa to check the stage of the parasites. Parasitaemia can be detected as soon as 2 hours post-invasion, though the increase observed at 6 hours indicates that invasion still occurs beyond the 2-hour time point. The difference between Hz and SG quantification 6 hours post-infection shows that accumulation of Hz is still below detection in about half of the parasites. At 24 hours, the levels of parasitaemia are maintained, with detection by Hz reaching similar levels as SG, confirming parasite growth and metabolic activity. Parasitaemia increases at 48 hours and an underestimation of Hz quantification compared to SG indicates that reinvasion has occurred with small parasites appearing in the assays as shown in the Giemsa slides. On this basis the time point chosen for erythroid cell assays were 18 hours to assess invasion and 42 hours to evaluate development. These results show that Hz detection is an accurate and effective way to detect malaria parasites and quantify parasitaemia. It is particularly useful when parasites cannot be stained or labelled with routine methods or when staining is impractical, being also applicable to any parasite strain or species.

The differentiation protocol can generate substantial numbers of cells (10-20 million from a 10 cm plate of pluripotent stem cell cultures) however this not sufficient to emulate routine erythrocyte cultures. In order to assess feasibility of this approach for malaria studies, the haematocrit of regular cultures (2.5%) was reduced to as low as 1/20 (approximately 0.13%). Comparison of invasion at these levels (Figure 5B) showed that invasion at the lower haematocrit is higher as would be expected, and this is more noticeable at the

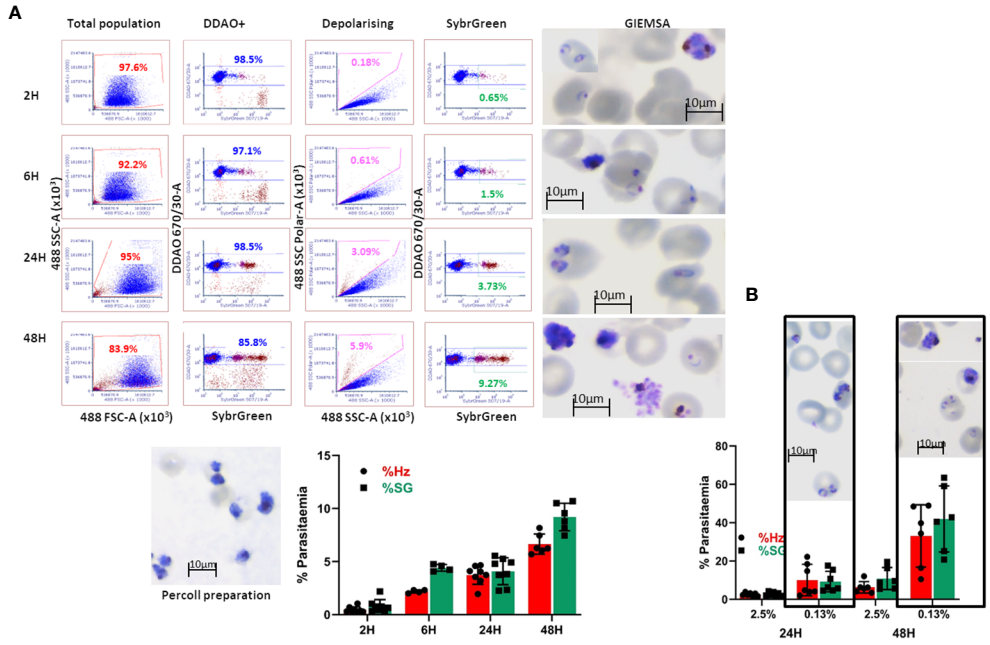

FIGURE 5
Invasion assay time course of parasitaemia. **(A)** The purified parasites (Percoll preparation) are cultured with DDAO-stained erythrocytes and incubated for the reported times. The culture populations (left plots) are analysed for DDAO to identify the target cell population (DDAO+). Parasitaemia is quantified by Haemozoin depolarisation (Depolarising) as well as Sybr Green labelling (SybrGreen) using gates established with uninfected DDAO-labelled erythrocytes. Giemsa-stained slides are made at each time point before fixing the cultures. The overall results are shown as mean and SEM of at least 4 biological replicates. **(B)** Comparison of infection in routine (2.5%) and low (0.13%) haematocrit. Erythrocytes were labelled with DDAO and invasion assays set at the indicated haematocrit for 24 and 48 hours. Parasitaemia was assessed by Hz and SG labelling (average and SD of at least 5 experiments) and parasites were visualised by Giemsa staining.

second time point. The similar parasitaemia quantified by Hz and SG shows that the events detected are indeed infected erythrocytes and that the assays are effective at lower haematocrit. Furthermore, the higher levels of parasitaemia facilitate assessment of invasion differences between cells of different origin or characteristics.

Stem cell-derived erythroid cells support invasion by *Plasmodium falciparum*

The accurate quantification of the capacity of stem cell-derived erythroid cells to support *P. falciparum* infection, depends on the effective exclusion of non-invading parasites. On one hand, it is crucial to label the target cells as we show in the previous section, to only quantify invasion in the *in-vitro*-derived cells. Additionally, in order to ensure accurate quantification of invading parasites we engineered fluorescence-expressing parasites to enable their localisation on the flow cytometry plot and clearly separating the non-invading parasite population from the population of labelled erythroid cells. For this, we used the NF54 *P. falciparum* strain to create parasite lines expressing fluorochromes of different wavelengths (Carrasquilla et al., 2020) to identify the free parasites and ensure Hz quantification only in the target cells to reflect the % parasitaemia.

Several fluorescent parasite lines and membrane dies to label *in vitro*-derived erythroid cells from the model cell line RH1, were tested to find the combinations leading to the clearest parasitaemia determination and show the versatility of this system. In the first instance, parasites expressing the Midori-ishi cyan fluorochrome (Supplementary Figure S4A, top left) which has a similar range of excitation/emission wavelengths (472/495 nm) as SG were used. Uninfected *in-vitro*-differentiated erythroid cells were labelled with DDAO (Supplementary Figure S4A, top middle) alone were examined for Hz depolarisation to establish the gates as in the previous section (Supplementary Figure S4A, top right). The invasion assays of Midori-ishi-parasites with DDAO-erythroid cells were assessed in the same way, applying the established gates to identify the target erythroid cell population (Supplementary Figure S4A bottom left plot) and quantify the proportion of Hz-positive events within the population of labelled cells (Supplementary Figure S4A, bottom right plot), which corresponds to infected erythroid cells. Overlay of the depolarising population from the invasion assays over non-infected cells and free parasites confirms that the Hz-containing events correspond to stem cell-derived erythroid cells infected with the parasite (Supplementary Figure S4A, far right panel).

An alternative combination was tested, using erythroid cells labelled with DFFDA (excitation/emission: 498/526 nm) and parasites expressing mCherry (excitation/emission: 587/610 nm) which also enabled separating the populations of labelled erythroid cells and purified parasites allowing accurate quantification of parasitaemia (Supplementary Figure S4B). The preferred combination was labelling the target cells with DDAO and culturing with parasites expressing tag-BPF (excitation/emission:

399/456 nm) because of the strong fluorescence and the wider separation of their spectra (Supplementary Figure S4C). This was the chosen combination for all following experiments.

Because the quantification of depolarising events is applied to the whole population of labelled cells, this proportion reflects the parasitaemia of the culture. Since haemozoin is the metabolic product of the parasite's digestion of haemoglobin (Frita et al., 2011), it only accumulates in the food vacuole as a result of parasite metabolism, and therefore its detection reflects live, active parasites in the differentiated erythroid cells. Some events can be missed if Hz accumulation has not reached detectable levels by the time of measurement.

Invasion assays with the *in-vitro*-generated erythroid cells showed successful invasion upon examination of Giemsa-stained slides (Figure 6A). Analysis of 50.000 events by flow cytometry showed erythroid cells differentiated from all nine stem cells lines tested were effectively invaded by *P. falciparum* (Figure 6B). At 18 hours post-invasion, the parasitaemia ranged between 5 and 8% and at 42 hours parasitaemia rose in all cell lines to 7–10%, likely reflecting the growth of small parasites that went undetected at the 18-hour timepoint (Figure 4B). The level of infection detected in erythroid cells is lower than the equivalent primary erythrocytes shown in Figure 5, particularly at the second time point, which might reflect the difference between native and model cells, particularly in terms of globin expression.

The concomitant increase in Hz intensity with life cycle progression is a useful tool to measure parasite growth (Frita et al., 2011; Rebelo et al., 2013). Indeed, synchronised parasite cultures show a clear shift in Hz signal intensity as they progress from rings to schizonts (Supplementary Figure S5A). The difference in Hz intensity between the schizont and ring stages (Supplementary Figure S5A) was used to establish a gate (M1) to quantify the proportion of mature parasites in the invasion assays in both primary erythrocytes and *in vitro*-derived erythroid cells (Supplementary Figure S5B). Applying the same gate to the assays with the *in-vitro*-generated erythroid cells, detected levels of mature parasites between 60 and 80% at the 42-hour time point (Figure 6C), indicating parasite development.

Genome editing of human stem cells reveals the role of specific genes in malaria invasion

The potential to derive edited erythrocytes by introducing targeted modifications in the stem cell lines was tested using CRISPR/Cas9 technology in the control line RH1 (Supplementary Figure S6). Two target genes were chosen, Basigin (*BSG*, CD147) which is known to be a universal receptor for *P. falciparum* invasion (Crosnier et al., 2011) as a proof of principle, and *ATP2B4* (*PMCA4*) since natural variation in this gene has been correlated to resistance to severe malaria (Timmann et al., 2012). The edited clones were genotyped (Supplementary Figure S7A) and verified by sequencing (Supplementary Figure S7B) confirming small deletions in the critical exon that generate a stop codon downstream. The lack of protein expression was confirmed with specific FITC-labelled antibodies by flow cytometry and microarray analysis of the pluripotent and differentiated cells (Figure 7A).

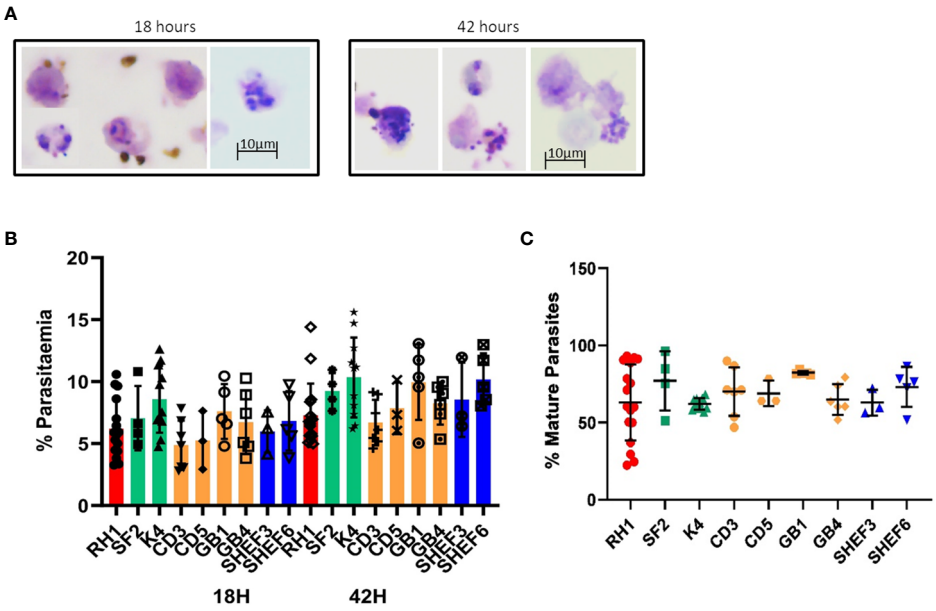

FIGURE 6
Invasion of in-vitro-generated erythrocytes with *P. falciparum*. **(A)** Giemsa-stained slides of invasion assays at 18h and 42h of culture (representative examples of routine imaging). **(B)** Quantification of invasion by Hz flow cytometry of a variety of differentiated cell lines: iPS cell lines derived from fibroblasts (red, green) and blood (yellow) and human ESC lines (blue) at two time points of culture, 18h (invasion) and 42 hours (development) (results are shown as mean of at least 3 experiments and SD). **(C)** quantification of mature parasites percentage at 42 hours (mean of at least 3 experiments, SD).

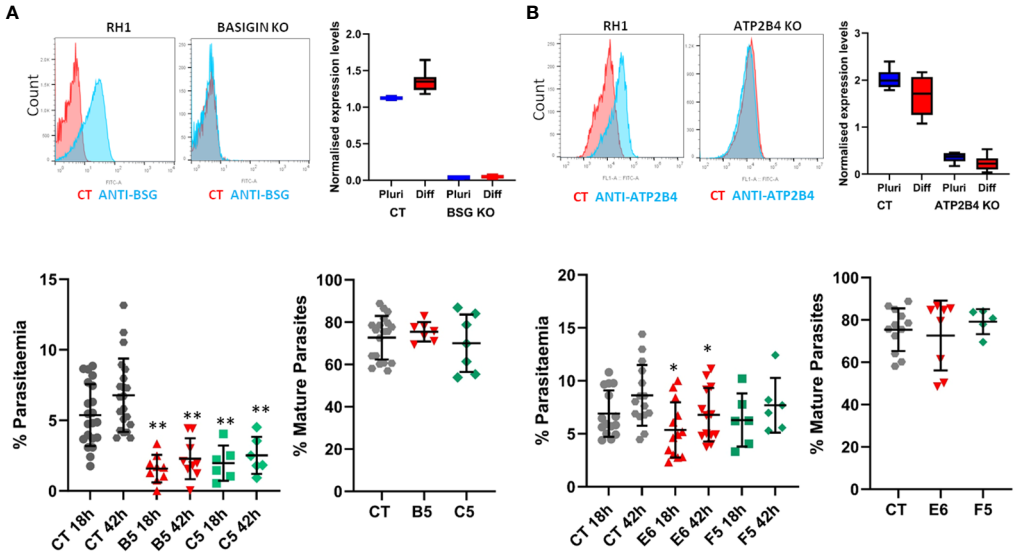

FIGURE 7
Gene editing in stem cells to study the impact of specific genes on malaria infection. Two genes of interest were deleted in the RH1 cell line using CRISPR/Cas9 and clones were isolated: **(A)** Basigin and **(B)** ATP2B4. Top panels: Expression of the protein corresponding to the deleted gene was measured on the cell surface with specific antibodies by flow cytometry (representative example of 3 experiments) and confirmed by microarray analysis of the cell lines transcriptomes in undifferentiated and differentiated states, presented as quantile normalised log2 expression values (average and SD of at least 3 data sets). Bottom panels: invasion of the parental line RH1 (CT) compared to the Basigin KO clones B5 and C5 **P<.001 and ATP2B4 KO clones E6 and F5 *P<.05, as well as percentage of mature parasites at 42 hours. (average and SD from at least 5 experiments).

When challenged with the parasites, erythroid cells differentiated from two independent Basigin-null cell lines (B5 and C5) showed strongly decreased invasion compared to the parental non-edited RH1 cells (Figure 7B, left), consistent with the role of Basigin as an essential receptor for *P. falciparum* (Crosnier et al., 2011). The proportion of mature parasites after 42 hours of culture was similar to the control RH1 cells, indicating that the few parasites that invaded the modified cells could achieve some growth. Deletion of ATP2B4 (Figure 7A, right) showed a tendency to lower invasion levels compared to RH1 cells, but this decrease was significant for only one clone (Figure 7B, right). The proportion of mature parasites in the ATP2B4 KO cultures at the 42-hour time point was similar to that observed in the control RH1 line, indicating that disruption of this gene has a minor effect on the development of the parasite.

Reprogrammed IPS lines from haemoglobinopathy patients show a deficiency in parasite invasion

In order to assess the potential of this technology to study the genomic context and particular genotypes from specific individuals, we chose α-thalassemia as a human trait strongly associated with resistance to malaria infection. We chose α-thalassemia major, in which all four α-globin genes are impaired in order to have a strong phenotype and also because this type is not viable, meaning that primary blood samples cannot be obtained.

Induced Pluripotent Stem cell lines derived from fibroblast samples with α-thalassemia major (HbBart) haemoglobinopathies (EM andFJ) were differentiated in parallel with our reference iPSC lines and exposed to fluorescent parasites in our invasion assays. Figure 8A shows a significantly decreased invasion in both thalassaemic cell lines compared with the control lines. Though at the second time point 42 hours after invasion parasitaemia was significantly increased in the haemoglobinopathy cells, this remained significantly below the levels observed in the control wild type lines. Interestingly, while the parasitaemia at 42 hours in the haemoglobinopathy cells was significantly reduced compared to that observed in wild type cells (Figure 8A), the proportion of late stage parasites in the cultures of the haemoglobinopathy lines at the 42-hour time point was not significantly different from the wild type lines. Indeed only a marginally significant reduction was observed in one of the cell lines tested (Figure 8B). This suggests that the main impact of α-thalassemia major on malaria infection is at the invasion stage.

Discussion

This work presents a protocol that effectively differentiates a variety of human stem cell lines towards erythropoiesis generating cells able to support *Plasmodium falciparum* infection. A total of 9 stem cell lines of diverse origin were studied, showing that while differentiation efficiency does vary between lines, they all generate erythroid cells as demonstrated by upregulation of erythrocytic genes and expression of erythrocytic proteins. Despite enucleation being notoriously difficult to achieve *in-vitro* (Lu et al., 2008; Hirose et al., 2013) we observed levels of 20-30%, bearing in mind that cells with positive nucleic acid staining include those with nuclear

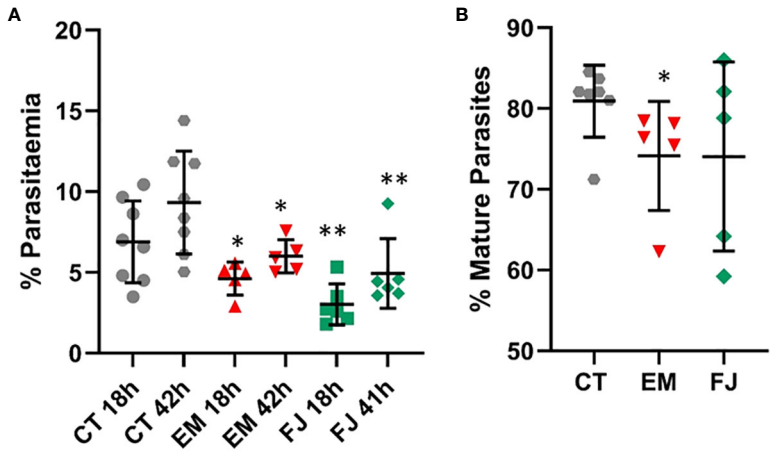

FIGURE 8
Invasion of reprogrammed IPS cells from patients with α-thalassemia haemoglobinopathy. Fibroblasts from α-thalassemia major samples were reprogrammed to IPS cell lines (EM and FJ) that were differentiated to erythroid cells and exposed to *P. falciparum* to assess **(A)** invasion in parallel to control cell lines (CT) and **(B)** percentage of mature parasites at 42 hours (results are presented as mean and SD of at least 3 independent experiments) *P<.05; **P<.005.

fractionation, incomplete nuclear extrusion (Figure 1B) and remnant nucleic acid content. Importantly, stem cells differentiated with this protocol are capable of supporting invasion by *P. falciparum* without the need to sort or purify the differentiated cells.

During the blood cycle, haemoglobin is the main source of amino acids for the parasite's metabolic needs. Degradation of haemoglobin releases free haem, which represents a major toxic insult to the parasite. In a detoxification mechanism the oxidised iron group is compacted into an insoluble crystalline form: β-hematin or haemozoin (Hz) and stored in the food vacuole (Egan, 2008), becoming a distinct feature of intra-erythrocytic Plasmodium parasites (Rebelo et al., 2013). We show in this work that detecting Hz by flow cytometry is an effective and accurate method of quantifying parasitaemia. Comparing parasitaemia quantification by Hz with Sybr Green (SG) DNA staining of the parasites confirms the depolarising events as parasites and the accuracy of the method. Intracellular Hz is known to accumulate in the parasite, becoming detectable after 6 hours post-invasion to 70-80% by dark-field microscopy (Delahunt et al., 2014). The sensitivity of flow cytometry can detect Hz earlier as shown in Figure 5, and though beyond the scope of this work, this capability has the potential to decipher effects on early development with our approach. During progression of the blood cycle, both Hz crystal size and number increase in the parasites (Chen et al., 2019), which makes Hz intensity an effective measure of parasite development compared to DNA labelling intensity which only increases with parasite replication.

The use of schizonts for the assays ensures quick invasion after the co-culture is set up, but complete synchrony is difficult to achieve, resulting in some contribution of less mature parasites in the schizont preparations, which is reflected in the increase of Hz-positive events at 42 hours. It is also possible that parasite growth in the erythroid cells is slower due to the overall lower levels of globin expression, which could explain the lower parasitaemia observed in comparison to primary erythocytes in the same conditions. The use of fluorescent parasites constitutes an additional control for the accurate quantification of parasitaemia, however detection of Hz makes it possible to perform this type of studies with any parasite strain as demonstrated in Figures 4, 5. It is useful to use fluorescent control parasites in parallel to non-fluorescent ones to ensure exclusion of the free parasite population from quantification.

The possibility to genetically manipulate genes implicated in malaria infection was demonstrated by deletion of *Basigin*, which resulted in a dramatic decrease of infection as expected given the known role of this protein in invasion (Crosnier et al., 2011). The low levels of invasion detected are likely the result of true invasion because the accumulation of Hz reflects live parasites and also because the very few invasion events show signs of development at the second time point. While it is widely accepted that Basigin is a crucial receptor for *P. falciparum* invasion, the high sensitivity and additional controls included in the strategy used here allowed high accuracy in the quantification of invasion. Our observations are consistent with other studies using blocking antibodies showing residual invasion in the laboratory (Crosnier et al., 2011) and variable levels of inhibition of field isolates *in ex-vivo* invasion assays (Moore et al., 2021). Natural variants in ATP2B4 have been associated with resistance to malaria in various studies (Ndila et al., 2018; Malaria Genomic Epidemiology N, 2019), but the mechanism of protection is not known. A number of variant SNPs have been identified in this gene, mostly in Linkage Disequilibrium (LD), and though it is not clear whether all these SNPs play a role in protection against severe malaria, one of them was shown to disrupt a GATA-1 site in the promoter of the gene (Lessard et al., 2017). As a consequence, expression levels of the protein are reduced giving rise to changes in erythrocyte parameters such as mean corpuscular haemoglobin concentration (MCHC) and size. ATP2B4 is the main membrane Calcium ATPase of erythrocytes that removes calcium from the cytosol to maintain the low levels necessary for calcium-dependent signalling to occur (Dalghi et al., 2013). A role of calcium

in the invasion process of *P. falciparum* has been suggested (Gao et al., 2013; Volz et al., 2016) and it is also possible that impairment of calcium homeostasis affects survival and development of the parasite in the erythrocyte (Gazarini et al., 2003; Lessard et al., 2017; Zambo et al., 2017). However, a knock-out of *ATP2B4* in our system did not show a major effect on *P. falciparum* invasion or growth, though a tendency towards a reduction in both parameters was observed. A compensatory effect of ATP2B1 (*PMCA1*), which represents 20% of erythrocytic Calcium ATPases, could explain the minimal effect of deleting *ATP2B4*. The ubiquitous expression of *ATP2B4* throughout the body, could also imply other effects on the disease, such as the interaction of infected erythrocytes with endothelial cells or with the brain, as has been suggested (Timmann et al., 2012).

We further demonstrate the adaptability of this strategy by reprogramming iPS cells from haemoglobinopathy patients, a trait known to confer protection against malaria. Alpha-thalassemia results from a variety of large deletions affecting one or more of the duplicated alpha globin genes and the severity of the disease depends on how many of the four genes are affected. Loss of all 4 α-globin genes, known as α-thalassemia major, can occur in the common South East Asian deletion, leading to the lethal HbBarts hydrops foetalis. Alpha-thalassemia major was chosen for these studies because of the extreme phenotype and because primary erythrocytes with this genotype are unavailable to perform laboratory assays, thus highlighting the advantages of stem cell technology. Both reprogrammed cell lines are null for alpha globin, presenting –SEA/–SEA (GN03433) (Ho et al., 2007) and –SEA/–Fil (GM10796) (Hong et al., 2017) genotypes. When differentiated, both cell lines showed a significantly reduced ability to support *P. falciparum* infection, consistent with reported effects of haemoglobinopathies on malaria (Taylor et al., 2013; Pathak et al., 2018). Though several mechanisms have been proposed, it is still unclear how haemoglobin deficiencies impact the parasite and their study is complicated by the variety of genetic changes underlying these traits as well as the difficulty in obtaining samples of primary erythrocytes. It is known that the imbalance in the synthesis of globin chains in alpha and beta thalassemias result in impairment of the assembly of haemoglobin tetramers. This leads to the formation of haemoglobin precipitates (Heinz bodies), which together with the increased hydration occurring in α-thalassemias impair erythrocyte deformability (Huisjes et al., 2018). It was shown that erythrocyte deformability is lower in samples of α-thalassemia traits in which 2 alpha globin genes are inactivated and the decrease is much stronger in Haemoglobin H disease in which 3 alpha globin genes are missing. It is reasonable to predict an even greater deformability defect in the total absence of haemoglobin alpha of the cell lines used here. Furthermore, this decrease in deformability was directly corelated to decreasing *P. falciparum* invasion (Bunyaratvej et al., 1992) which is consistent with the observations using our haemoglobinopathy lines that it is mainly the invasion process that is impacted by these genotypes. Additionally, it was shown that *P. falciparum* parasites produce significantly lower numbers of merozoites in alpha and beta thalassemia trait cells, correlating with the MCHC and mean corpuscular volume (MCV) of these cell types (Glushakova et al., 2014).

This novel application of stem cell technology for the study of malaria presents a new and exciting avenue to understand the impact and mechanisms of complex genetic traits and human genomic variation in their full genomic context. As any model of study, there are aspects that need to be taken into account when taking advantage of this system, such as the immaturity of erythroid cells generated, the number of cells that can be obtained and their heterogeneity. However, it is the only option to genetically engineer erythrocytes without depending on particular cell lines as well as generate them from patients or samples with specific characteristics. Though in this work we aimed at developing a strategy with minimal handling that can be potentially scaled up for screening purposes, it can also be easily adapted to more detailed studies by the possibility of labelling receptors of interest or sorting the erythroid cells from the *in-vitro*-differentiated population as well as assessing any parasite strain and using tightly synchronised parasites. The potential to use existing resources of banked available cell lines as well as reprogramming iPS lines from easily obtainable blood samples from patients or individuals with specific genotypes offers access to the study and preservation of a wide range of genetic characteristics. This approach is a powerful tool for the understanding of this disease, offering a wide range of applications from functional and mechanistic studies to potential identification of therapeutic targets.

Data availability statement

The microarray data presented in this study are deposited in the GEO repository, accession number GSE245735: https://www.ncbi.nlm.nih.gov/geo/query/acc.cgi?acc=GSE245735.

Ethics statement

Ethical approval was not required for the studies on humans in accordance with the local legislation and institutional requirements because only commercially available established cell lines and samples from repositories were used.

Author contributions

AP: Conceptualization, Data curation, Formal analysis, Investigation, Methodology, Supervision, Validation, Visualization, Writing – original draft, Writing – review & editing. BN: Conceptualization, Investigation, Methodology, Writing – original draft. KM: Data curation, Formal analysis, Investigation, Methodology, Visualization, Writing – original draft. MK: Investigation, Methodology, Visualization, Writing – original draft. CA: Investigation, Methodology, Writing – original draft. FR: Investigation, Methodology, Writing – review & editing. RM: Investigation, Methodology, Visualization, Writing – review & editing. FL: Investigation, Validation, Writing – review & editing. HP: Data curation, Investigation, Methodology, Writing – review & editing. JR: Conceptualization, Funding acquisition, Resources, Writing – review & editing.

Funding

The author(s) declare financial support was received for the research, authorship, and/or publication of this article. This work was performed with core-funding of the Wellcome Sanger Institute. This research was funded in whole by the Wellcome Trust 206194/Z/17/Z.

Acknowledgments

The authors wish to thank Marcus Lee for his overall support and Aleš Kilpatrick for helping with imaging.

Conflict of interest

The authors declare that the research was conducted in the absence of any commercial or financial relationships that could be construed as a potential conflict of interest.

The author(s) declared that they were an editorial board member of Frontiers, at the time of submission. This had no impact on the peer review process and the final decision.

Publisher's note

All claims expressed in this article are solely those of the authors and do not necessarily represent those of their affiliated organizations, or those of the publisher, the editors and the reviewers. Any product that may be evaluated in this article, or claim that may be made by its manufacturer, is not guaranteed or endorsed by the publisher.

Supplementary material

The Supplementary Material for this article can be found online at: https://www.frontiersin.org/articles/10.3389/fcimb.2023.1287355/full#supplementary-material

References

Adjalley, S. H., Lee, M. C., and Fidock, D. A. (2010). A method for rapid genetic integration into Plasmodium falciparum utilizing mycobacteriophage Bxb1 integrase. *Methods Mol. Biol.* 634, 87–100. doi: 10.1007/978-1-60761-652-8_6

Agu, C. A., Soares, F. A., Alderton, A., Patel, M., Ansari, R., Patel, S., et al. (2015). Successful Generation of Human Induced Pluripotent Stem Cell Lines from Blood Samples Held at Room Temperature for up to 48 hr. *Stem Cell Rep.* 5 (4), 660–671. doi: 10.1016/j.stemcr.2015.08.012

Aurrecoechea, C., Brestelli, J., Brunk, B. P., Dommer, J., Fischer, S., Gajria, B., et al. (2009). PlasmoDB: a functional genomic database for malaria parasites. *Nucleic Acids Res.* 37 (Database issue), D539–D543. doi: 10.1093/nar/gkn814

Bartholdson, S. J., Crosnier, C., Bustamante, L. Y., Rayner, J. C., and Wright, G. J. (2013). Identifying novel Plasmodium falciparum erythrocyte invasion receptors using systematic extracellular protein interaction screens. *Cell Microbiol.* 15 (8), 1304–1312. doi: 10.1111/cmi.12151

Bei, A. K., Brugnara, C., and Duraisingh, M. T. (2010). *In vitro* genetic analysis of an erythrocyte determinant of malaria infection. *J. Infect. Dis.* 202 (11), 1722–1727. doi: 10.1086/657157

Bunyaratvej, A., Butthep, P., Sae-Ung, N., Fucharoen, S., and Yuthavong, Y. (1992). Reduced deformability of thalassemic erythrocytes and erythrocytes with abnormal hemoglobins and relation with susceptibility to Plasmodium falciparum invasion. *Blood* 79 (9), 2460–2463. doi: 10.1182/blood.V79.9.2460.bloodjournal7992460

Carrasquilla, M., Adjalley, S., Sanderson, T., Marin-Menendez, A., Coyle, R., Montandon, R., et al. (2020). Defining multiplicity of vector uptake in transfected Plasmodium parasites. *Sci. Rep.* 10 (1), 10894. doi: 10.1038/s41598-020-67791-z

Chen, A. J., Huang, K. C., Bopp, S., Summers, R., Dong, P., Huang, Y., et al. (2019). Quantitative imaging of intraerythrocytic hemozoin by transient absorption microscopy. *J. BioMed. Opt.* 25 (1), 1–11. doi: 10.1117/1.JBO.25.1.014507

Cowman, A. F., Berry, D., and Baum, J. (2012). The cellular and molecular basis for malaria parasite invasion of the human red blood cell. *J. Cell Biol.* 198 (6), 961–971. doi: 10.1083/jcb.201206112

Cowman, A. F., Tonkin, C. J., Tham, W. H., and Duraisingh, M. T. (2017). The molecular basis of erythrocyte invasion by malaria parasites. *Cell Host Microbe* 22 (2), 232–245. doi: 10.1016/j.chom.2017.07.003

Crosnier, C., Bustamante, L. Y., Bartholdson, S. J., Bei, A. K., Theron, M., Uchikawa, M., et al. (2011). Basigin is a receptor essential for erythrocyte invasion by Plasmodium falciparum. *Nature* 480 (7378), 534–537. doi: 10.1038/nature10606

Dalghi, M. G., Fernandez, M. M., Ferreira-Gomes, M., Mangialavori, I. C., Malchiodi, E. L., Strehler, E. E., et al. (2013). Plasma membrane calcium ATPase activity is regulated by actin oligomers through direct interaction. *J. Biol. Chem.* 288 (32), 23380–23393. doi: 10.1074/jbc.M113.470542

Damena, D., Denis, A., Golassa, L., and Chimusa, E. R. (2019). Genome-wide association studies of severe P. falciparum malaria susceptibility: progress, pitfalls and prospects. *BMC Med. Genomics* 12 (1), 120. doi: 10.1186/s12920-019-0564-x

Delahunt, C., Horning, M. P., Wilson, B. K., Proctor, J. L., and Hegg, M. C. (2014). Limitations of haemozoin-based diagnosis of Plasmodium falciparum using dark-field microscopy. *Malar J.* 13, 147. doi: 10.1186/1475-2875-13-147

Egan, E. S., Jiang, R. H., Moechtar, M. A., Barteneva, N. S., Weekes, M. P., Nobre, L. V., et al. (2015). Malaria. A forward genetic screen identifies erythrocyte CD55 as essential for Plasmodium falciparum invasion. *Science* 348 (6235), 711–714. doi: 10.7554/eLife.61516

Egan, T. J. (2008). Haemozoin formation. *Mol. Biochem. Parasitol.* 157 (2), 127–136. doi: 10.1016/j.molbiopara.2007.11.005

Frita, R., Rebelo, M., Pamplona, A., Vigario, A. M., Mota, M. M., Grobusch, M. P., et al. (2011). Simple flow cytometric detection of haemozoin containing leukocytes and erythrocytes for research on diagnosis, immunology and drug sensitivity testing. *Malar J.* 10, 74. doi: 10.1186/1475-2875-10-74

Gao, X., Gunalan, K., Yap, S. S., and Preiser, P. R. (2013). Triggers of key calcium signals during erythrocyte invasion by Plasmodium falciparum. *Nat. Commun.* 4, 2862. doi: 10.1038/ncomms3862

Gazarini, M. L., Thomas, A. P., Pozzan, T., and Garcia, C. R. (2003). Calcium signaling in a low calcium environment: how the intracellular malaria parasite solves the problem. *J. Cell Biol.* 161 (1), 103–110. doi: 10.1083/jcb.200212130

Ghorbal, M., Gorman, M., Macpherson, C. R., Martins, R. M., Scherf, A., and Lopez-Rubio, J. J. (2014). Genome editing in the human malaria parasite Plasmodium falciparum using the CRISPR-Cas9 system. *Nat. Biotechnol.* 32 (8), 819–821. doi: 10.1038/nbt.2925

Glushakova, S., Balaban, A., McQueen, P. G., Coutinho, R., Miller, J. L., Nossal, R., et al. (2014). Hemoglobinopathic erythrocytes affect the intraerythrocytic multiplication of Plasmodium falciparum in vitro. *J. Infect. Dis.* 210 (7), 1100–1109. doi: 10.1093/infdis/jiu203

Hendriks, D., Clevers, H., and Artegiani, B. (2020). CRISPR-cas tools and their application in genetic engineering of human stem cells and organoids. *Cell Stem Cell.* 27 (5), 705–731. doi: 10.1016/j.stem.2020.10.014

Hirose, S., Takayama, N., Nakamura, S., Nagasawa, K., Ochi, K., Hirata, S., et al. (2013). Immortalization of erythroblasts by c-MYC and BCL-XL enables large-scale erythrocyte production from human pluripotent stem cells. *Stem Cell Rep.* 1 (6), 499–508. doi: 10.1016/j.stemcr.2013.10.010

Ho, S. S., Chong, S. S., Koay, E. S., Chan, Y. H., Sukumar, P., Chiu, L. L., et al. (2007). Microsatellite markers within –SEA breakpoints for prenatal diagnosis of HbBarts hydrops fetalis. *Clin. Chem.* 53 (2), 173–179. doi: 10.1373/clinchem.2006.075085

Hong, R., Chandola, U., and Zhang, L. F. (2017). Cat-D: a targeted sequencing method for the simultaneous detection of small DNA mutations and large DNA deletions with flexible boundaries. *Sci. Rep.* 7 (1), 15701. doi: 10.1038/s41598-017-15764-0

Huisjes, R., Bogdanova, A., van Solinge, W. W., Schiffelers, R. M., Kaestner, L., and van Wijk, R. (2018). Squeezing for life - properties of red blood cell deformability. *Front. Physiol.* 9, 656. doi: 10.3389/fphys.2018.00656

International Stem Cell, I., Adewumi, O., Aflatoonian, B., Ahrlund-Richter, L., Amit, M., Andrews, P. W., et al. (2007). Characterization of human embryonic stem cell lines by the International Stem Cell Initiative. *Nat. Biotechnol.* 25 (7), 803–816. doi: 10.1038/nbt1318

Karasawa, S., Araki, T., Nagai, T., Mizuno, H., and Miyawaki, A. (2004). Cyan-emitting and orange-emitting fluorescent proteins as a donor/acceptor pair for fluorescence resonance energy transfer. *Biochem. J.* 381 (Pt 1), 307–312. doi: 10.1042/BJ20040321

Kariuki, S. N., and Williams, T. N. (2020). Human genetics and malaria resistance. *Hum. Genet.* 139 (6-7), 801–811. doi: 10.1007/s00439-020-02142-6

Kilpinen, H., Goncalves, A., Leha, A., Afzal, V., Alasoo, K., Ashford, S., et al. (2017). Common genetic variation drives molecular heterogeneity in human iPSCs. *Nature* 546 (7658), 370–375. doi: 10.1038/nature22403

Lessard, S., Gatof, E. S., Beaudoin, M., Schupp, P. G., Sher, F., Ali, A., et al. (2017). An erythroid-specific ATP2B4 enhancer mediates red blood cell hydration and malaria susceptibility. *J. Clin. Invest.* 127 (8), 3065–3074. doi: 10.1172/JCI94378

Lo, T. W., Pickle, C. S., Lin, S., Ralston, E. J., Gurling, M., Schartner, C. M., et al. (2013). Precise and heritable genome editing in evolutionarily diverse nematodes using TALENs and CRISPR/Cas9 to engineer insertions and deletions. *Genetics* 195 (2), 331–348. doi: 10.1534/genetics.113.155382

Lu, S. J., Feng, Q., Park, J. S., Vida, L., Lee, B. S., Strausbauch, M., et al. (2008). Biologic properties and enucleation of red blood cells from human embryonic stem cells. *Blood* 112 (12), 4475–4484. doi: 10.1182/blood-2008-05-157198

Malaria Genomic Epidemiology N (2019). Insights into malaria susceptibility using genome-wide data on 17,000 individuals from Africa, Asia and Oceania. *Nat. Commun.* 10 (1), 5732. doi: 10.1038/s41467-019-13480-z

Moore, A. J., Mangou, K., Diallo, F., Sene, S. D., Pouye, M. N., Sadio, B. D., et al. (2021). Assessing the functional impact of PfRh5 genetic diversity on ex vivo erythrocyte invasion inhibition. *Sci. Rep.* 11 (1), 2225. doi: 10.1038/s41598-021-81711-9

Ndila, C. M., Uyoga, S., Macharia, A. W., Nyutu, G., Peshu, N., Ojal, J., et al. (2018). Human candidate gene polymorphisms and risk of severe malaria in children in Kilifi, Kenya: a case-control association study. *Lancet Haematol.* 5 (8), e333–ee45. doi: 10.1016/S2352-3026(18)30107-8

Pathak, V., Colah, R., and Ghosh, K. (2018). Effect of inherited red cell defects on growth of Plasmodium falciparum: An in *vitro* study. *Indian J. Med. Res.* 147 (1), 102–109. doi: 10.4103/ijmr.IJMR_1146_16

Ran, F. A., Hsu, P. D., Wright, J., Agarwala, V., Scott, D. A., and Zhang, F. (2013). Genome engineering using the CRISPR-Cas9 system. *Nat. Protoc.* 8 (11), 2281–2308. doi: 10.1038/nprot.2013.143

Rebelo, M., Sousa, C., Shapiro, H. M., Mota, M. M., Grobusch, M. P., and Hanscheid, T. (2013). A novel flow cytometric hemozoin detection assay for real-time sensitivity testing of Plasmodium falciparum. *PloS One* 8 (4), e61606. doi: 10.1371/journal.pone.0061606

Ritchie, M. E., Phipson, B., Wu, D., Hu, Y., Law, C. W., Shi, W., et al. (2015). limma powers differential expression analyses for RNA-sequencing and microarray studies. *Nucleic Acids Res.* 43 (7), e47. doi: 10.1093/nar/gkv007

Rouhani, F., Kumasaka, N., de Brito, M. C., Bradley, A., Vallier, L., and Gaffney, D. (2014). Genetic background drives transcriptional variation in human induced pluripotent stem cells. *PloS Genet.* 10 (6), e1004432. doi: 10.1371/journal.pgen.1004432

Satchwell, T. J., Wright, K. E., Haydn-Smith, K. L., Sanchez-Roman Teran, F., Moura, P. L., Hawksworth, J., et al. (2019). Genetic manipulation of cell line derived reticulocytes enables dissection of host malaria invasion requirements. *Nat. Commun.* 10 (1), 3806. doi: 10.1038/s41467-019-11790-w

Scully, E. J., Shabani, E., Rangel, G. W., Gruring, C., Kanjee, U., Clark, M. A., et al. (2019). Generation of an immortalized erythroid progenitor cell line from peripheral blood: A model system for the functional analysis of Plasmodium spp. invasion. *Am. J. Hematol.* 94 (9), 963–974. doi: 10.1002/ajh.25543

Soares, F. A., Pedersen, R. A., and Vallier, L. (2016). Generation of human induced pluripotent stem cells from peripheral blood mononuclear cells using sendai virus. *Methods Mol. Biol.* 1357, 23–31. doi: 10.1007/7651_2015_202

Straimer, J., Lee, M. C., Lee, A. H., Zeitler, B., Williams, A. E., Pearl, J. R., et al. (2012). Site-specific genome editing in Plasmodium falciparum using engineered zinc-finger nucleases. *Nat. Methods* 9 (10), 993–998. doi: 10.1038/nmeth.2143

Takahashi, K., Tanabe, K., Ohnuki, M., Narita, M., Ichisaka, T., Tomoda, K., et al. (2007). Induction of pluripotent stem cells from adult human fibroblasts by defined factors. *Cell* 131 (5), 861–872. doi: 10.1016/j.cell.2007.11.019

Taylor, S. M., Cerami, C., and Fairhurst, R. M. (2013). Hemoglobinopathies: slicing the Gordian knot of Plasmodium falciparum malaria pathogenesis. *PloS Pathog.* 9 (5), e1003327. doi: 10.1371/journal.ppat.1003327

Timmann, C., Thye, T., Vens, M., Evans, J., May, J., Ehmen, C., et al. (2012). Genome-wide association study indicates two novel resistance loci for severe malaria. *Nature* 489 (7416), 443–446. doi: 10.1038/nature11334.10.1182

Trakarnsanga, K., Griffiths, R. E., Wilson, M. C., Blair, A., Satchwell, T. J., Meinders, M., et al. (2017). An immortalized adult human erythroid line facilitates sustainable and scalable generation of functional red cells. *Nat. Commun.* 8, 14750. doi: 10.1038/ncomms14750

Vallier, L., Touboul, T., Chng, Z., Brimpari, M., Hannan, N., Millan, E., et al. (2009). Early cell fate decisions of human embryonic stem cells and mouse epiblast stem cells are controlled by the same signalling pathways. *PloS One* 4 (6), e6082. doi: 10.1371/journal.pone.0006082

Veres, A., Gosis, B. S., Ding, Q., Collins, R., Ragavendran, A., Brand, H., et al. (2014). Low incidence of off-target mutations in individual CRISPR-Cas9 and TALEN targeted human stem cell clones detected by whole-genome sequencing. *Cell Stem Cell.* 15 (1), 27–30. doi: 10.1016/j.stem.2014.04.020

Volz, J. C., Yap, A., Sisquella, X., Thompson, J. K., Lim, N. T., Whitehead, L. W., et al. (2016). Essential Role of the PfRh5/PfRipr/CyRPA Complex during Plasmodium falciparum Invasion of Erythrocytes. *Cell Host Microbe* 20 (1), 60–71. doi: 10.1016/j.chom.2016.06.004

Weiss, G. E., Gilson, P. R., Taechalertpaisarn, T., Tham, W. H., de Jong, N. W., Harvey, K. L., et al. (2015). Revealing the sequence and resulting cellular morphology of receptor-ligand interactions during Plasmodium falciparum invasion of erythrocytes. *PloS Pathog.* 11 (2), e1004670. doi: 10.1371/journal.ppat.1004670

Yeung, A. T. Y., Hale, C., Lee, A. H., Gill, E. E., Bushell, W., Parry-Smith, D., et al. (2017). Exploiting induced pluripotent stem cell-derived macrophages to unravel host factors influencing Chlamydia trachomatis pathogenesis. *Nat. Commun.* 8, 15013. doi: 10.1038/ncomms15013

Zambo, B., Varady, G., Padanyi, R., Szabo, E., Nemeth, A., Lango, T., et al. (2017). Decreased calcium pump expression in human erythrocytes is connected to a minor haplotype in the ATP2B4 gene. *Cell Calcium.* 65, 73–79. doi: 10.1016/j.ceca.2017.02.001

frontiers | Frontiers in Cellular and Infection Microbiology

TYPE Mini Review
PUBLISHED 20 December 2023
DOI 10.3389/fcimb.2023.1296293

OPEN ACCESS

EDITED BY
Gabriel Rinaldi,
Aberystwyth University, United Kingdom

REVIEWED BY
Amit Sinha,
New England Biolabs, United States
Yitzhak Spiegel,
The Volcani Center, Israel

*CORRESPONDENCE
Keith G. Davies
k.davies@herts.ac.uk

RECEIVED 19 September 2023
ACCEPTED 22 November 2023
PUBLISHED 20 December 2023

CITATION
Davies KG, Mohan S, Phani V and Srivastava A (2023) Exploring the mechanisms of host-specificity of a hyperparasitic bacterium (*Pasteuria* spp.) with potential to control tropical root-knot nematodes (*Meloidogyne* spp.): insights from *Caenorhabditis elegans*. *Front. Cell. Infect. Microbiol.* 13:1296293. doi: 10.3389/fcimb.2023.1296293

Exploring the mechanisms of host-specificity of a hyperparasitic bacterium (*Pasteuria* spp.) with potential to control tropical root-knot nematodes (*Meloidogyne* spp.): insights from *Caenorhabditis elegans*

Keith G. Davies[1]*, Sharad Mohan[2], Victor Phani[3] and Arohi Srivastava[4]

[1]School of Life and Medical Sciences, University of Hertfordshire, Hatfield, United Kingdom, [2]Division of Nematology, Indian Agricultural Research Institute, New Delhi, India, [3]Department of Agricultural Entomology, College of Agriculture, Uttar Banga Krishi Viswavidyalaya, Dakshin Dinajpur, West Bengal, India, [4]Dr. D. Y Patil Biotechnology & Bioinformatics Institute, Dr. D. Y. Patil Vidyapeeth, Pune, India

Plant-parasitic nematodes are important economic pests of a range of tropical crops. Strategies for managing these pests have relied on a range of approaches, including crop rotation, the utilization of genetic resistance, cultural techniques, and since the 1950's the use of nematicides. Although nematicides have been hugely successful in controlling nematodes, their toxicity to humans, domestic animals, beneficial organisms, and the environment has raised concerns regarding their use. Alternatives are therefore being sought. The *Pasteuria* group of bacteria that form endospores has generated much interest among companies wanting to develop microbial biocontrol products. A major challenge in developing these bacteria as biocontrol agents is their host-specificity; one population of the bacterium can attach to and infect one population of plant-parasitic nematode but not another of the same species. Here we will review the mechanism by which infection is initiated with the adhesion of endospores to the nematode cuticle. To understand the genetics of the molecular processes between *Pasteuria* endospores and the nematode cuticle, the review focuses on the nature of the bacterial adhesins and how they interact with the nematode cuticle receptors by exploiting new insights gained from studies of bacterial infections of *Carnorhabditis elegans*. A new *Velcro*-like multiple adhesin model is proposed in which the cuticle surface coat, which has an important role in endospore adhesion, is a complex extracellular matrix containing glycans originating in seam cells. The genes associated with these seam cells appear to have a dual role by retaining some characteristics of stem cells.

KEYWORDS

cuticle, surface coat, endospores, stem cells, seam cells, biological control

1 Introduction

1.1 Plant-parasitic nematodes and biocontrol

Plant-parasitic nematodes are economically important pests that occur globally and constrain yields of both agricultural and horticultural crops (Jones et al., 2013; Dutta et al., 2019; Phani et al., 2021). Various management strategies that have been deployed to control these pests, including crop rotation, the use of various types of genetic resistance, flooding and the application of synthetic chemicals. Since the Second World War the use of synthetic chemicals has been a mainstay of phytonematode control, however, the recognition of pesticide toxicity to humans, domestic animals, non-target beneficial organisms and the environment has led to increasing legislation to prohibit their use in America, Europe and elsewhere. Therefore, the promotion for less hazardous approaches has been advocated (WHO, 2015). Biological control, involving the use of a pest's natural enemies or hyperparasites, has long been recognised as a potential method to manage the plant-parasitic nematode pests; but the development of robust control strategies using such bioagents has always eluded crop protection scientists. It has been suggested that the lack of consistent control of nematodes lies in their biological variation, and the fact that their natural enemies and their nematode hosts are locked into a host-parasite arms race (Davies and Spiegel, 2011).

There are several groups of natural enemies that have the potential to be developed into microbiological control agents of phytonematodes (Stirling, 2014). These can be broadly characterised as: those that can be mass produced *in vitro* and can be grown on synthetic media, and those that are obligate parasites and can only be cultured *in vivo* within their hosts. Thus, they form two major groups either as the facultative microbes and the obligate microbes, respectively. Much research has focused on the use of fungi as many of them produce spores in synthetic culture media thereby extending their shelf-life and rendering them suitable for commercialisation. The bacteria, due to their diverse modes of nematicidal action, also show huge potential (Tian et al., 2007), but, with advancement in seed coating technologies (Rocha et al., 2019), which usually involve the incorporation of various fungicidal seed protectants, crop protection scientists have increasingly favoured the use of bacteria over fungi as nematicidal seed coatings.

1.2 *Pasteuria* as an alternative to nematicides

The *Pasteuria* group of bacteria are obligate Gram-positive parasites that infect invertebrates such as water fleas (*Daphnia* spp.) and nematodes including plant-parasitic nematode pests. Several species of *Pasteuria* have been characterized, all of which are obligate parasites, and they were originally placed within the family *Alicyclobacillaceae*. However, they have since been reclassified into their own family, the *Pasteuriaceae* (Vos et al., 2009). The taxonomic status of each group of *Pasteuria* species still remains obscure as it is currently mainly based on their hosts (Davies, 2009).

As the *Pasteuria* species all produce highly robust endospores that can remain dormant for many years (Giannakou et al., 1997), the bacterium thus proves to be ideal to be exploited as a biological control agent against a variety of phytonematode pests. And, indeed, early research had shown that *Pasteuria penetrans* (formally *Bacillus penetrans*) could effectively suppress and control the root-knot nematode *Meloidogyne javanica* (Stirling, 1984) through a combination of two mechanisms: (1) endospores adhere to the cuticle of the migratory second-stage infective juveniles (J2s), reducing their ability of the J2s to migrate and invade the plant root (Davies et al., 1991), and (2) when endospore encumbered J2s initiate a feeding site in a plant root, but before they moult into the J3s, the endospores germinate, form rhizoids that subsequently undergo exponential growth whilst simultaneously obliterating the nematode's reproductive system (Davies et al., 2011; Phani and Rao, 2018).

However, following the publication of Stirling's 1984 paper, it soon became apparent that endospores from one strain of the bacterium that attached to infective juveniles of one population of *M. javanica* would not attach to and infected other closely related populations of root-knot nematodes of the same species (Stirling, 1985; Davies et al., 1988; Espanol et al., 1997; Davies et al., 2001). Therefore, in practice there are two major challenges for the successful deployment of *Pasteuria* as a robust biological control agent and for commercial development. Firstly, as an obligate parasite, it will be necessary to mass produce it. Secondly it will be crucial to understand the nature of this host – parasite specificity initially focusing on the genetics and molecular biology underlying the biological variation of bacterial endospore – nematode cuticle compatibility. This article discusses the progress made to date in the development of *Pasteuria* as a biological control agent and suggest approaches for taking the research forward.

1.3 Host specificity in *Pasteuria*

The economically most devastating plant-parasitic nematodes are the sedentary endoparasites, i.e., the root-knot (*Meloidogyne* spp.) and the cyst (*Globodera* spp. and *Heterodera* spp.) nematodes (Jones et al., 2013). Both these nematode groups are parasitized by strains of *Pasteuria*, namely *P. penetrans* and *P. nishizawae* respectively. However, it is noteworthy that endospores of *P. penetrans* are unable to adhere to and infect the cyst nematodes and *vice versa*. Interestingly, the majority of endospore attachment bioassays have primarily focused on the attachment between *P. penetrans* and tropical *Meloidogyne* spp. that reproduce parthenogenetically and these studies (Stirling, 1985; Davies et al., 1988; Espanol et al., 1997; Davies et al., 2001) have revealed a high degree of host specificity. Conversely, the attachment bioassays between *P. nishizawae* and cyst nematodes, including *Globodera* and *Heterodera* spp., which reproduce amphimictically show a relatively broader range of host specificity (Davies et al., 1990; Sharma and Davies, 1996; Sharma and Davies, 1997) as compared

to attachment studies involving *P. penetrans* and root-knot nematodes.

It has long been recognised that the evolution of sex in hosts can be accounted for by parasitic infections (Hamilton, 1980). This suggests that in amphimictically reproducing nematode species (e.g. *H. avenae*) there should be reduced *Pasteuria* infection. Conversely, in parthenogenetically reproducing species (e.g. *Meloidogyne arenaria, M. javanica* and *M. incognita*) there should be increased *Pasteuria* infection. Our examples above show that *Pasteuria* endospores that attached to and infected *H. avenae* germinated before the J2 had established its feeding site; these *Pasteuria* strains completed their sporulation within the J2 to produce in the order of 10^3 mature endospores (Davies et al., 1990). Contrastingly, those *Pasteuria* strains that infect root-knot nematode species were delayed in their germination until the developing juvenile had established a feeding site and had more resources available for exponential growth and produced between 1 x 10^6 and 2 x 10^6 endospores per individual nematode (Davies et al., 1988), more than a thousand-fold increase in mature endospores. It appears that there is an interesting trade-off between the parthenogenetically reproducing nematodes, i.e. the tropical root-knot nematodes (*Meloidogyne* spp.) with *P. penetrans*, which exhibited delayed germination and its higher endospore production, versus the temperate *H. avanae* amphimictic cyst nematode infected with a *Pasteuria* strain that germinate early in the J2 resulting in far fewer mature endospores.

Assuming that delayed germination evolved later than immediate germination, this appears to contradict the view that amphimixis leads to reduced parasitism and parthenogenesis results in increased parasitism. Conversely, if immediate germination evolved earlier than delayed germination, this would be concordant with the idea that amphimixis leads to reduced parasitism. The paper by Hamilton (1980) discusses several scenarios in which reproductive modes may diverge from the view that amphimixis reduces parasitism. It suggests that the intensity of selection may vary due to the number of loci involved and other frequency-dependent factors. Interestingly, analysis of 19 genomes, representing five key species of tropical parthenogenetic *Meloidogyne* populations, revealed them to be the result of the hybridization of two divergent genomes, which generated species divergence through dynamic non-crossover recombination, generated species divergence (Szitenberg et al., 2017). Following Hamilton (1980)'s argument this might suggest that the effects of *Pasteuria* parasitism on the evolution of parthenogenetic species (*Meloidogyne* spp.) may be the result of fluctuating linkage disequilibria that is less likely in amphimictic (*Heterodera* and *Globodera* spp.) species.

The coevolution between *Caenorhabditis elegans* and the pathogen *Serratia marcescens* has been found to demonstrate, following the Red Queen hypothesis, that selection favoured outcrossing mixed mating populations rather than obligate selfing populations (Morran et al., 2011). The first interaction between endospores of the bacterium and the cuticle of the nematode is the process of endospore adhesion and it would therefore be of interest to apply this hypothesis to the *Pasteuria* endospore – nematode cuticle model. The molecular mechanism of endospore attachment onto the nematode cuticle and the genes involved is therefore a key first step in understanding this process. This review will explore the co-evolutionary arms races between endospore adhesins and the cuticular receptor using insights gained from *C. elegans*.

2 The mechanism of endospore attachment

2.1 Biochemistry of adhesins

Early research on the nature of *Pasteuria*'s adhesins focused on the biochemical characterization of their endospores (Persidis et al., 1991). This work recognised that disrupted exosporia and spore fragments of *P. penetrans* were fibrous and although no longer intact these fragments were able to retain their host-specific attachment to the nematode cuticle of infective juveniles. Subsequent bioassays involving endospores pretreated with selected proteases and glycolytic enzymes reduced endospore attachment suggesting that the adhesins were composed of a combination of proteins and carbohydrates (Davies and Danks, 1993). In addition, endospores pretreated with polyclonal antibodies raised to whole spores also reduced attachment (Persidis et al., 1991). Interestingly, monoclonal antibodies revealed a heterogeneity on the surface of the endopsores that was specific to the population of root-knot nematode to which they attached (Davies et al., 1994; Davies and Redden, 1997). If *Pasteuria* is to be developed into a biological control agent, it will be necessary to understand the nature of this specificity so that endospores can be successfully deployed to control plant-parasitic nematodes. Comparative phylogenetic analysis of *P. penetrans* based on *spo0A*, a gene that plays a key role in the initiation of endospore formation, suggested it was closely related to the *Bacillus* group (Trotter and Bishop, 2003). In a subsequent phylogenetic analysis, following a genomic sequencing survey and using multiple genetic loci, *Pasteuria* appeared to be a member of the *Bacillus* – *Clostridium* clade (Charles et al., 2005).

2.2 The collagen-like fibrous nap of endospores

In the early noughties, the genomes of bacteria responsible for diseases in both humans and animals, as well as those of other close relatives, were a primary goal of sequencing projects. Within this group of genomes, of which the endospore forming *Bacillus* spp. were important, the new sequence analyses were also being used to investigate the development, construction and viability of endospores. A comparative analysis of the rhamnose cluster operon between *B. cereus* and *B. anthracis*, revealed eight genes that were identified as likely to encode for the outer structural components of the endospore such as bacterial collagens (Todd et al., 2003). Bacterial collagen-like proteins have become an important area of study (Qiu et al., 2021) and several of these genes present in the animal pathogenic bacteria *B. cereus* and *B. anthracis*, are absent in *B. subtilis*, including the glycoprotein BclA

that contains a GXX motif. The glycoprotein BclA encodes for collagen-like fibres which forms a hair-like nap on the surface of the endospore; the length of this nap is related to the number of repeats of the GXX motif (Sylvestre et al., 2002; 2003). Several homologs to these endospore genes from the rhamnose cluster operon were identified in genome survey sequences of *Pasteuria penetrans* using BLAST including sequences similar to BclA (Schaff et al., 2011; Orr et al., 2018). A hair-like nap is also associated with the outer surface of the endospores of *P. penetrans*, and it has been proposed that these fibres are possibly responsible for their attachment of endospores to the infective juvenile of the nematode through a *Velcro*-like attachment process (Davies, 2009). A total of 17 different putative collagen-like encoding regions, revealing a high degree of potential diversity, were identified from *P. penetrans*, strain 148, which had a restricted host range but revealing a high degree of potential diversity (Srivastava et al., 2019). Similar diversity has been observed in the closely related *Pasteuria ramosa*, which is a parasite of *Daphnia* spp. (Mouton et al., 2009; McElroy et al., 2011).

The observation that these collagen-like genes are highly diverse, as revealed by the monoclonal antibodies and their link with host attachment (Davies et al., 1994), provides further evidence that they could possibly be a determinant of host range. However, the majority of studies looking at the mechanism of endospore attachment have primarily relied on loss of function experiments that involved treating endospores with heat, enzymes, lectins and antibodies (e.g. Davies et al., 1988; Davies and Danks, 1993; Davies and Redden, 1997) and then measuring changes in the number of endospores adhering to host juveniles in attachment bioassays. As *Pasteuria* are a group of bacteria that are obligate parasites and cannot be grown *in vitro*, the ability to produce knockouts is problematic. Therefore, rescue experiments, in which gain-of-function studies would be an ideal way of identifying function, become impossible. An alternative approach would be to identify a closely related bacterium that can be grown *in vitro* and has the genetic apparatus to produce endospores. Clearly, *Bacillus subtilis* could fulfil these criteria, but as discussed above, it does not have a sufficiently intact rhamnose cluster operon as contained within the genomes of animal parasitic bacilli *B. cereus* and *B. anthracis* (Todd et al., 2003). Therefore, another approach would be to select an animal parasitic bacterium, for example *Bacillus thuringiensis*, which produces endospores with a hair-like fibrous nap but does not represent a threat to humans or domestic animals (Srivastava et al., 2022).

2.3 Similarities between *Pasteuria* and *Bacillus thuringiensis*

Recent comparisons between endospore protein extracts of several strains of *B. thuringiensis* and *P. penetrans* revealed 25 proteins with various molecular weights. Among these, only one band at 58 kDa was common to all *B. thuringiensis* and *P. penetrans* (Srivastava et al., 2022). Six proteins, at 150, 34, 30, 24, 17 and one > 9 kDa were common across all *B. thuringiensis* strains with the remaining 18 proteins having variable distributions across all bacterial strains (Srivastava et al., 2022). Interestingly, the same study using two antibodies raised to two short collagen-like synthetic peptides from *P. penetrans* that recognised the outer endospore coat revealed two glycoproteins (> 250 kDa and ~72 kDa) that when treated with collagenase were digested. Attachment bioassays using *Pasteuria* endospores treated with the same collagenase also reduced attachment to second-stage juveniles. This suggests that the outer endospore coat of *B. thuringiensis* spores, although they do not adhere to the cuticle of infective juveniles of root-knot nematode, they do share biochemical properties with *P. penetrans* and could perhaps be used as a model for gain of function endospore attachment assays (Srivastava et al., 2022).

3 Nature of the cuticle receptor

3.1 The *Caenorhabditis elegans* model

The cuticle forms the nematode's exoskeleton and performs a number of functions: it is important in determining the nematode's morphological integrity, and it forms the major barrier between the internal body structure of nematode and its external environment; it acts as a gatekeeper regarding molecular permeability; it is important for vermiform locomotion; and it forms a barrier against microbial pathogens. At each stage of the nematode's development when it undergoes ecdysis the cuticle gets remade anew, but there are very few comparative studies that examine the structure of the different stages. The most studied nematode cuticle is that of the adult stage of *Caenorhabditis elegans* (Page and Johnstone, 2007), which increasingly became a model for investigating the host-microbial interactions (Gravato-Nobre and Hodgkin, 2011). The adult cuticle has a complex structure which is secreted by the hypodermis and forms a part of the extra-cellular matrix; this matrix consists primarily of collagens together with insoluble cuticlins, glycoproteins and lipids.

Early studies of the cuticle using ethyl methanesulfonate (EMS) as a mutagen affected the ability of selected lectins to recognise the cuticle surface. These mutants were called the *Srf* mutants (Politz et al., 1990; Link et al., 1992), and the genes involved are increasingly being recognised as important in microbial pathogenesis. The mutant phenotypes with altered lectin binding characteristics became associated with several different *C. elegans* pathogens (Gravato-Nobre et al., 2005; Darby et al., 2007; Gravato-Nobre et al., 2011). Subsequent more recent studies have expanded and characterized a range of other *C. elegans* mutants which alter various phenotypic traits (e.g. *Bah*, biofilm absent from head; *Bus*, bacterially unswollen; *Dar*, deformed anal region; *Gro*, slow growth; *Hbp*, head biofilm present; *Skd*, skiddy locomotion). The majority of these genes that are responsible for altered pathogenicity in several different bacteria such as *Microbacterium nematophilum*, *Yersinia pseudotuberculosis* and strains of *Leucobacter* spp., and are associated with an altered cuticular surface coat (SC) (O'Rourke et al., 2023). The cuticle SC, or glycocalyx, is rich in lipids and glycoproteins, the source of which is increasingly thought to be the seam cells (Gravato-Nobre and Hodgkin, 2011; O'Rourke et al.,

2023). These seam cells lie beneath the lateral mid-line and have an important role in regard to producing a diverse range of complex compounds that affect the ability of microorganisms to adhere and form biofilms.

3.2 Mucins and nematode parasites

The SC of the animal parasitic nematode *Toxocara canis*, which primarily affects domestic dogs and other canids but can also affect humans, has been shown to contain a mucin which is important in the evasion of the host's immune response (Page et al., 1992). It has long been recognised that mucins play an important role in host-parasite interactions, including those involving helminths (Hicks et al., 2000; Theodoropoulos et al., 2001). Mucins appeared very early in metazoan evolution and are proteins high in proline, serine and threonine, with a high molecular weight in which their carbohydrate content is O-linked to the amino acids serine and threonine (Lang et al., 2007). Up to 50 percent of the molecular weight of a mucin can be carbohydrate, which structurally makes them a hugely diverse group and therefore they are an ideal molecule to protect nematodes from initial microbial attachment and biofilm formation as they migrate through the soil (Davies and Curtis, 2011). Lang et al. (2007) identified a number of mucin-like proteins with homologous sequences present in *C. elegans*; these sequences were also present the phytonematode species *M. hapla* and *M. incognita* (Table 1).

Recent work with the plant-parasitic root-knot nematode (*Meloidogyne* spp.) has used RNAi knockdown methodology to investigate a range of potential cuticle and SC-related proteins to understand their role in *P. penetrans* attachment (Table 2). A functional study of a mucin-like protein characterized from *M. incognita*, designated *Mi-muc-1*, was found to be rich in serine and threonine and highly expressed in the pre and post parasitic second-stage juvenile (J2) and the pre-egg laying female (Phani et al., 2018b). *In situ* hybridization studies revealed expression in the tail region of the J2 around the phasmid. Subsequent knockdown experiments using dsRNA designed for *Mi-muc-1* significantly reduced endospore attachment. Further experiments designed to identify the carbohydrate domains involved were shown to be D-glucose, D-galactose and D-xylose, whereas other sugars also tested (D-fructose, D-mannose, L-arabinose, L-sorbose) had no or little effect. Although perhaps this result might not be unexpected if mucins are a component of the nematode cuticle surface, it is interesting that other unrelated genes have also been shown to affect the attachment of *P. penetrans* endospores to J2 cuticle.

3.3 Other cuticle proteins

Fatty acid retinol binding proteins are unique to nematodes. They play an important role in nutrient acquisition and immune response being present in the nematode cuticle (Kennedy et al., 1997; McDermott et al., 1999; Prior et al., 2001; Garofalo et al., 2003; Iberkleid et al., 2013). Originally identified in animal parasites, they have been shown to be increasingly important in plant parasites and

TABLE 1 *Caenorhabditis elegans* mucin-like proteins and their respective RNAi clones with BLASTP hits to *Meloidogyne hapla* and *Meloidogyne incognita* together with their percentage positive identity.

Mucin-like Gene (name)*	RNAi Clone#	Blastp hits E-value	
		M. hapla (% Id$)	*M. incognita* (% Id$)
F59A6.3 (mucl-1)	II 4M05	2.0e-61 (58)	7.0e-33 (42)
C12D12.1 (mucl-2)	X 2C10	6.0e-43 (53)	5.0e-32 (48)
F16F9.2 (dpy-6)	X 4G10	6.0e-60 (52)	3.0e-35 (43)
H43E16.1 (mucl-6)	II 5K17	1.0e-66 (41)	5.0e-46 (44)
	II 5I21		
	II 5M01		
K06A9.1 (mucl-9)	X 1B17	1.0e-60 (45)	2.0e-72 (41)
H02F09.3 (mucl-10)	X 1B23	1.0e-80 (43)	3.0e-52 (38)
C26G2.2 (mucl-11)	X 6F18	5.0e-17 (44)	2.0e-12 (43)
C07G2.1 (cpg-1)	III 2C06	2.0e-14 (57)	1.0e-05 (46)
K11D12.1 (cwp-4)	V 3J24	2.0e-22 (54)	2.0e-20 (53)
	V 3L02		
	V 4C07		
F35E12.7 (dct-17)	V 9E05	1.0e-21 (48)	4.0e-17 (48)
C29E6.1 (let-653)	IV 6 G10	1.0e-55 (80)	1e-101 (78)

*Mucin-like proteins identified from Lang et al., 2007; and the linked website: www.medkem.gu.se/mucinbiology/databases/.
#From the C. elegans RNAi library of Kamath and Ahringer (2003).
$Blastp percentage positive identity.

have been shown to affect the endospore binding of *P. penetrans* onto J2 cuticle (Phani et al., 2017). A fatty acid retinol binding protein that was cloned from *M. incognita*, designated Mi-FAR-1, was found to be rich in α-helix structure and contained both a casein kinase phosphorylation and a glycosylation site was characterized. Its expression was observed in all developmental stages, with the highest expression appearing in the fourth stage juvenile. *In situ* hybridization studies of *Mi-far-1* revealed its expression in the hypodermis of the J2 cuticle that when silenced showed an increase in endospore attachment. This suggests that Mi-FAR-1 may have a protectant role in inhibiting the *Pasteuria* endospore attachment.

Another protein of the fatty acid binding protein (FABP) superfamily, the selenium binding protein Mi-SeBP-1 was also expressed in the nematode hypodermis and also increased *Pasteuria* endospore attachment on being silenced (Phani et al., 2018b). The protein was identified as important in a differential expression study between *Pasteuria* encumbered and unencumbered J2s of *M. incognita* and was the first characterization of a selenium

TABLE 2 Effects of RNAi knockdown experiments of genes known to be important in nematode cuticle and/or cuticle surface coat of *Meloidogyne incognita* due to their effects on *Pasteuria penetrans* endospore attachment to infective juvenile cuticle.

Gene Knockdown	Protein role	*Pasteuria* endo-spore attachment	Reference
Mucin-1 protein (*Mi-muc-1*)	Host-parasite interaction	decrease	Phani et al., 2018a
Selenium-binding protein (*Mi-SeBP-1*)	Environmental, biotic and abiotic stress related	increase	Phani et al., 2018b
Fatty-acid and Retinol-binding protein (*Mi-far-1*)	Nutrient acquisition development and reproduction	increase	Phani et al., 2017

binding protein in nematodes. Although knockdown experiments were found to affect endospore attachment, it had no observable effect on the nematodes ability to invade roots, nor did they subsequently affect nematode fecundity. This particular protein shares a 34% identity to a *C. elegans* selenium binding protein which was orthologous to a human selenium-binding protein (SELENBP1), a regulator of lifespan and stress resistance (Köhnlein et al., 2020). It is therefore perhaps not surprising that knockdown experiments in root-knot nematodes led to increased endospore attachment.

3.4 Role of seam cells

There is increasing evidence that the origin of the cuticle surface coat is associated with the hypodermis and its associated seam cells. Noteworthy is the fact, that silencing experiments with both the *Mi-far-1* and *Mi-SeBP-1* led to an increase in endospore attachment, whereas knockdown of *Mi-muc-1* decreased the endospore binding. From these findings, it can be presumed in a generalized layout that the members of FABP superfamily proteins being associated with the nematode hypodermis might act as protectants against microbial pathogenesis, whereas the glycosylated mucins or mucin-like proteins act as facilitators. The FABPs are reportedly involved in innate immunity and antimicrobial responses in other invertebrates (Cheng et al., 2013; Tan et al., 2015; Wang et al., 2017). But, the mucin-like protein being a basic structural component for cuticular integrity when facilitates the pathogenesis it indicates a co-evolutionary advancement for the obligate bacterium *Pasteuria* that targets a basic cuticular constituent for its secured parasitic success at the stage of attachment. The hypothesis can be further strengthened with the red blood cell (RBC) attachment assay results (Phani et al., 2018a), where the soaking of *M. incognita* J2s into different carbohydrates (stated above) showed negligible effect on RBC attachment, but significantly affected the endospore attachment. If we assume that both the endospores and RBCs use glycan-mediated support for their attachment, getting differential attachment with same carbohydrate molecule is an indicative of involvement of different ligands for the endospores and RBCs, which may have possibly developed during the co-evolutionary arms race of *Meloidogyne* with *Pasteuria*, but not the RBC.

Reviewing the work of (Phani et al., 2017; Phani et al., 2018a; Phani et al., 2018b) with *M. incognita*, there was clear evidence that *Mi-FAR-1*, *Mi-SeBP-1* and *Mi-muc-1* were all associated with hypodermal expression, but nothing to specifically to link them to seam cells. However, and interestingly, most of the genes identified in *C. elegans* involved in bacterial resistance were expressed by seam cells (O'Rourke et al., 2023) which are known to be hypodermal, located along each side of the nematode beneath the alae, and undergo repetitive replacement during the nematode's development (Page and Johnstone, 2007). Only *Mi-muc-1* and *Mi-SeBP- 1* were primarily investigated by Phani et al. (2018a; 2018b) for their association with bacterial infection, the other, *Mi-FAR-1* was primarily associated with retinol acquisition and had been shown to affect the interaction between the nematode and its plant host (Iberkleid et al., 2013). The fact that *Mi-muc-1* is highly glycosylated and was the only gene linked to a decrease endospore attachment, whereas both the others were comparatively poorly glycosylated and both increased endospore attachment, may suggest *Mi-muc-1* to be directly related to microbial resistance and possibly seam cell related (although not reported in Phani et al., 2017), while the others, *Mi-FAR-1* and *Mi-SeBP- 1*, the increase in endospore attachment is an indirect consequence of knockdown.

4 Multitrophic interactions

4.1 Root exudates

It has long been recognised that exposure of certain groups of plant-parasitic nematode to plant root exudates, in particular potato cyst nematodes *Globodera rostochiensis* and *G. pallida*, have a variable effect on egg hatch (Evans, 1983). More recently, exposure of J2s of *M. arenaria* to root exudates from eggplant, *Solanum melongena*, led to a decrease in endospore attachment compared to controls, irrespective of whether plant host or plant non-host exudates were used (Liu et al., 2017). Conversely, although not unequivocally, in a study of exposure of J2s from *M. incognita* and *Heterodera cajani*, each with its own homologous specific *Pasteuria* population, it was shown that as the J2s aged, they developed an increasing resistance to their respective homologous endospore populations (Mohan et al., 2020). However, if the J2's were exposed to root exudates of their host plant prior to a spore attachment bioassay, the rate of increasing resistance to endospore attachment as the J2s aged was reduced. In contrast, when exposed to root exudates of a non-host plant, this effect was not observed. Subsequent analysis of the plant root exudates by GC/MS could not identify any obvious compounds that could be associated with the observed results. However, evidently, the root exudates were affecting the aging process of the cuticle which was interpreted as a tritrophic interaction to help recruit the bacterium to the plant's long-term benefit (Mohan et al., 2020).

4.2 Cuticle surface coat

The variable effects observed in endospore attachment from RNAi knockdown experiments of FAR, SeBP and the mucin reported by (Phani et al., 2017; Phani et al., 2018a; Phani et al., 2018b), together with the effects of the plant root exudate experiments (Mohan et al., 2020) suggests that endospore attachment to J2 cuticle receptor is complex. The results are not only the result of the co-evolutionary arms race between the bacterial adhesins and the nematode cuticle receptor/s over inter-generational time, but also of specific spatial trade-offs between differentially expressed surface coat compounds along the length of the nematode itself. For example, Spiegel et al. (1996) reported the treatment of *M. javanica* J2s with certain lectins differentially affected endospore attachment along the length of the juvenile where attachment to the overall body could be distinguished from the head region. The current author (KGD) has witnessed similar spatial differences in endospore attachment in *M. hapla* (personal communication). This clearly indicates that the proportional expression of a particular gene, or genes, in one area is different from a particular cuticular compound in another area. Therefore, the balance of the expression of these endospore-attractive and endospore-repulsive molecules will determine the overall number of endospores adhering to the cuticle in any particular region, and this is mediated by the cuticle SC. The SC is evidently an arrangement of many complex macro-molecular compounds and the additional observation that root exudates clearly influence spore attachment through altered maturation begs the question as to the signalling processes involved and the role that seam cells may or may not play in the cuticle aging and endospore attachment process.

Joshi et al. (2010) report that there are parallel modes of production and proliferation of cell lineages in stem and seam cells of *C. elegans*. In *C. elegans*, true stem cells are associated with the distal tip cells of the ovary where they are maintained in a proliferative state prior to differentiation during embryogenesis. This is important as they retain the ability to maintain pluripotent plasticity with a potential for future cellular commitment. These same self-renewal and expansion patterns in stem cells, although poorly understood, are mimicked by the lateral epidermal seam cells (Joshi et al., 2010). It is therefore possible that the genes in stem cells that are responsible for the production of complex surface cellular compounds and important in molecular differentiation and cellular commitment are the same as those genes expressed in seam cells and are the origin of the surface coat of the cuticle that affects endospore adhesion.

Here, seam cells become key because they are an origin of the SC and important in the expression of mucins which are complex molecules that have a role in bacterial infection processes (Parsons et al., 2014; O'Rourke et al., 2023). Noteworthy, is that in *C. elegans* the *bus*-8 gene, which encodes a glycosyltransferase, appears to have a dual role in epidermal morphogenesis. Firstly, it is involved in the migration of epidermal cells during embryonic ventral closure, and secondly, it plays an important role in the adult by producing a host surface receptor that makes the nematode susceptible to the bacterium *Microbacterium nematophilum* and to which the bacterium can bind (Partridge et al., 2008). It is interesting to speculate on the number of dual roles these genes associated with building complex molecules on the cuticle SC may have. For example, has the functional plasticity which is maintained in stem cells and is important in the cellular organisation and differentiation of the developing embryo, through expression in the extracellular matrix (ECM), been co-opted for generating cuticle SC diversity? And can it, therefore, also act as a receptor to which bacteria can attach to the cuticle and, by its regulation, either generate SC diversity or altered cuticle maturation?

4.3 The extracellular cuticle matrix

The cuticle of *Caenorhabditis elegans* has been postulated to be a model for ECM (Page and Johnstone, 2007) where, as stated above, it plays a fundamental role in providing a flexible and resilient barrier to the nematode's environment and a site for microbial infection. Stem cells also are surrounded by an ECM, which provides a physical support environment and is a non-cellular component of the cells, mainly made up of proteins and polysaccharides (Frantz et al., 2010). In *C. elegans* it regulates overall cellular differentiation from the single cell to the adult, including now more fully understood specific roles such as pharyngeal development, embryo elongation, and vulval formation (Kelley et al., 2015; Walma and Yamada, 2020). As well as containing a number of fibrillar molecules like collagen and elastin, ECM also contains a large number of other components with which they interact including surface receptors, e.g. integrins and fibronectin, and growth factors, e.g. TGFβ and interleukins (see Table 1; Walma and Yamada, 2020). However, it is becoming increasingly clear that a diverse number of mechanisms are responsible for stem cell fate, in which environmentally determined niche signals go beyond carbohydrates and biochemical signal transduction pathways. These mechanisms can also include subtle changes in physical forces, for example those that may involve changes ECM stiffness (Watt and Huck, 2013).

It has been known for some time that specific glycans are limited to different developmental stages of *C. elegans*; for example, phosphorylcholine can be highly decorated with stage specific complex oligosaccharides (Cipollo et al., 2005), and the glycosaminoglycan chondroitin sulphate, which comprises of a pair of repetitively linked N-acetylgalactosamine and glucuronic acid molecules, is commonly found to glycosylate molecules found in the ECM (Izumikawa et al., 2004). Experiments blocking chondroitin synthesis in *C. elegans* resulted in defects in early embryogenesis, and eventually prohibiting cell division; however, rescue experiments with PAR2.4, the worm homolog of human chondroitin synthetase which acts as a neural stem cell in young embryonic lineages, was also found to be expressed in seam cells (Izumikawa et al., 2004). It, therefore, seems reasonable to

hypothesise that PAR2.4, like *bus-8* (Partridge et al., 2008), may also have a dual role; firstly, in the fate of neural stem cells during embryogenesis, and secondly, to have a function in nematode cuticle SC, possibly even having different roles at the various life stages of the nematode during ecdysis, of which we currently know very little. Interestingly, beneath the alae, which form longitudinal ridges down each side of the nematode and are restricted to the L1, dauer, and adult life stages of *C. elegans*, are the seam cells, which are biochemically and ultrastructurally distinct (Page and Johnstone, 2007).

Do seam cells, therefore, have a role in which they have retained some functional properties of stem cells which have been co-opted for use in later life-stages of the nematode life-cycle? And if so, for what use? The most abundant of our knowledge of the nematode cuticle is of the adult cuticle, which is spatially the largest and most easily obtained for study in the case of *C. elegans*. Arguably, the longest-lived developmental stage of *C. elegans* is the dauer-stage larvae, but little research other than descriptive ultrastructural studies have been done. However, in plant-parasitic nematodes the second-stage juvenile (J2) is often regarded as a dauer-like stage; it morphologically has hypodermal seam cells covered by alae, and it is non-feeding as it needs to locate and infect a host plant first. Here, we want to put forward the hypothesis that the biochemical diversity of the ECM of stem cells has been retained by seam cells to generated biochemical diversity of the nematode cuticle ECM; this diversity may play a role in the tritrophic interactions between obligate plant-parasitic nematodes and their cuticle pathogens/parasites. This has recently been exemplified by the studies between plant-parasitic nematodes and *Pasteuria*, which demonstrates not only temporal co-evolutionary changes in the field related to crop rotation (Liu et al., 2018), but also developmental changes related to the rate of maturation of the cuticle SC of the J2 (Mohan et al., 2020). This demonstrates the possibility of genetic pleiotropic effects that cross-connect multiple levels of biological organisation from germline stem cells to adult cuticle, the latter of which can be affected by plant root exudates.

5 Implications for phytonematode control strategies

Since the publication of *Silent Spring* by Rachel Carson in 1962 there has been increasing concern over the use of broad-spectrum chemical pesticides (van Emden and Peakall, 1996), a concern that continues to this today. Nematicides are no exception (Davies and Spiegel, 2011) and climate change, along with the increasing global threats to ecosystem health, has only exacerbated these concerns (Fisher et al., 2012; Dutta and Phani, 2023). Biological control and the use of a pests' natural enemies has remained an active area of research as one among several potential solutions. Here, we have demonstrated that the host-parasite interactions are complex and can be viewed from several differing perspectives, that range from specific host – parasite genetic interactions that produce co-evolutionary arms races between two organisms, to multiple cross-connected trophic interactions that affect the population dynamics of the ecological communities involved. For biological control to be used as a robust management strategy for phytonematodes, the outcomes of these multitrophic interactions are required to result in an ecologically resilient community suppressive to the pest nematodes. Although this approach was successful in controlling the cereal cyst nematode *H. avanae* through a field-based monocropping approach (Gair et al., 1969) that exploited soil microbial diversity as an ecosystem service (Gair et al., 1969; Stirling, 2014), this has never been successfully and robustly implemented in the field through the deployment of microbes. While there are numerous examples of the addition of single organisms to control plant-parasitic nematodes in highly managed glasshouse experiments, it has proved notoriously difficult and indeed elusive in the field, and requires broad-based knowledge at the population, organismal and molecular scales (Kerry, 2000).

Here, in order to build coherence between the functional, ecological and molecular levels of interactions, we have dissected the intricate relationships between the obligate Gram-positive bacterium *Pasteuria* spp. and the tropical group of root-knot nematodes *Meloidogyne* spp. gaining insights from *C. elegans*. Previously, it was hypothesised that a *Velcro*-like attachment process was one of the key factors underlying the mechanism by which endospores of the bacterium attached to the cuticle of the nematode (Davies, 2009). Over the last 10 years subsequent research, as outlined above, has shed light on some of the details of this *Velcro*-like interaction (Figure 1). In this multiple adhesin model (Srivastava, 2017), various molecules on *Pasteuria* endospores interact, through a 'Velcro-like mechanism', with different receptor molecules on the nematode cuticle. Electron micrographs show these adhesins to be unevenly distributed with a greater density on the concave surface rather than the convex surface of the endospore, (Davies, 2009) showing there are more mechanisms of generating adhesin diversity beyond collagen length, carboxyl-terminal sequence variation and glycosylation. The nature of the cuticle receptor is likely to be equally capable of also generating a level of molecular diversity. Here, we suggest that the cuticle receptor is a trade-off between two components. Firstly, the biochemical nature of the cuticle as part of the extracellular matrix as secreted by the hypodermis, and secondly, the biochemistry of the cuticle's surface coat produced as a secretion from the seam cells. We propose that this diversity may be partially maintained by the ability of seam cell gene expression which has retained a dual role by maintaining stem cell plasticity and diversity that played an important role in embryogenesis.

The *Pasteuria*-nematode interaction is complex, requiring a broader perspective to fully comprehend the molecular mechanisms involved. In the context of the Red Queen Hypothesis, which describes an ongoing evolutionary arms race

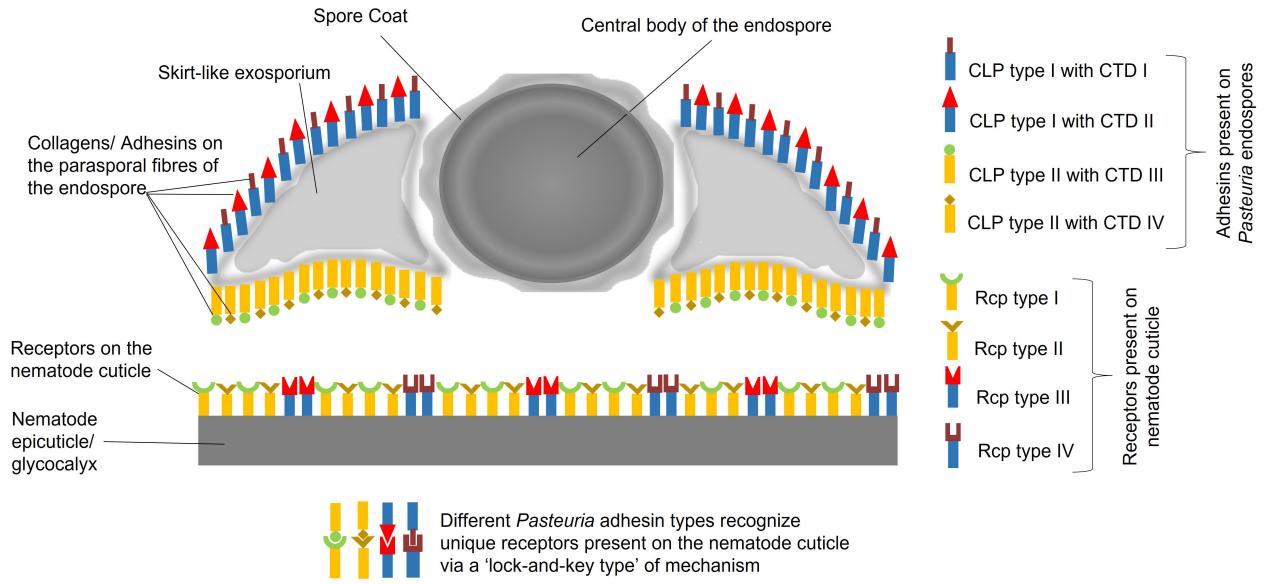

FIGURE 1
Multitype Adhesin Model, postulating an array of adhesins that adorns the surface of *Pasteuria* endospores, comprising diverse array of collagen-like proteins, denoted as CLP I, CLP II, CLP III, CLP IV, and so forth. These CLPs, exhibit varying distributions on the concave and convex sides of the endospores. Each CLP possesses a unique C-terminal domain, referred to as CTD I, CTD II, CTD III, CTD IV, etc., which specifically recognizes distinct receptor types on the nematode cuticle. The cuticle receptors (Rcp type I, II, III and IV) being the product of either mucin-like genes possibly expressed in the seam cells and fatty acid retinol binding proteins (FABPs) superfamily, a product of genes expressed in the hypodermis. Consequently, there are various possible combinations of CLPs, CTDs, and their corresponding cuticle receptors (Rcp type I, II, III and IV). Some CLPs may even share common CTDs by their sharing common glycoconjugates (like NAG) that exhibit variations among different CLPs located on either side of the endospore.

between hosts and their pathogens. Our model suggests a dynamic co-evolutionary relationship in which *Pasteuria* has developed a range of adhesins, including collagen-like proteins, to attach to a range of different receptors on the nematode cuticle. This can be seen as an adaptation by *Pasteuria* to ensure successful attachment and infection in the face of co-evolving nematode defence mechanisms. The genes coding for these diverse glycosylated adhesins on the surface of the endospore and the biochemical nature of this co-evolving receptor specificity is currently far from being understood and remains a matter of speculation and the basis for imaginative experimentation if novel control strategies are to be developed.

Author contributions

KD: Conceptualization, Project administration, Supervision, Writing – original draft, Writing – review & editing. SM: Conceptualization, Methodology, Supervision, Writing – review & editing. VP: Conceptualization, Investigation, Methodology, Writing – review & editing. AS: Conceptualization, Investigation, Methodology, Writing – review & editing.

Funding

The author(s) declare that no financial support was received for the research, authorship, and/or publication of this article.

Conflict of interest

KD is Director of his company KG Davies Limited.

The remaining authors declare that the research was conducted in the absence of any commercial or financial relationships that could be construed as a potential conflict of interest.

Publisher's note

References

Charles, L., Carbone, I., Davies, K. G., Bird, D., Burke, M., Kerry, B. R., et al. (2005). Phylogenetic analysis of *Pasteuria penetrans* by use of multiple genetic loci. *J. Bacteriol.* 187, 5700–5708. doi: 10.1128/JB.187.16.5700-5708.2005

Cheng, L., Jin, X. K., Li, W. W., Li, S., Guo, X. N., Wang, J., et al. (2013). Fatty acid binding proteins FABP9 and FABP10 participate in antibacterial responses in Chinese mitten crab, *Eriocheir sinensis*. *PloS One* 8, e54053. doi: 10.1371/journal.pone.0054053

Cipollo, J. F., Awad, A. M., Costello, C. E., and Hirschberg, C. B. (2005). N-Glycans of *Caenorhabditis elegans* are specific to developmental stages. *J. Biol. Chem.* 280, 26063–26072. doi: 10.1074/jbc.M503828200

Darby, C., Chakraborti, A., Politz, S. M., Daniels, C. C., Tan, L., and Drace, K. (2007). *Caenorhabditis elegans* mutants resistant to attachment of *Yersinia biofilms*. *Genetics* 176, 221–230. doi: 10.1534/genetics.106.067496

Davies, K. G. (2009). Understanding the interaction between an obligate hyperparasitic bacterium, *Pasteuria penetrans* and its obligate plant parasitic nematode host, *Meloidogyne* spp. *Adv. Parasitol.* 68, 211–245. doi: 10.1016/S0065-308X(08)00609-X

Davies, K. G., and Curtis, R. H. (2011). Cuticle surface coat of plant-parasitic nematodes. *Annu. Rev. Phytopathol.* 49, 135–136. doi: 10.1146/annurev-phyto-121310-111406

Davies, K. G., and Danks, C. (1993). Carbohydrate/protein interactions between the cuticle of infective juveniles of *Meloidogyne incognita* and spores of the obligate hyperparasite *Pasteuria penetrans*. *Nematologica* 39, 54–64.

Davies, K. G., and Redden, M. (1997). Diversity and partial characterization of putative virulence determinants in *Pasteuria penetrans*, the hyperparasitic bacterium of root-knot nematodes (*Meloidogyne* spp.). *J. Appl. Microbiol.* 83 (2), 227–235. doi: 10.1046/j.1365-2672.1997.00223.x

Davies, K. G., and Spiegel, Y. (2011). *The Biological Control of Plant-parasitic Nematodes: building coherence between microbial ecology and molecular mechanisms* (Springer). doi: 10.1007/978-1-4020-9648-8

Davies, K. G., Fargette, M., Balla, G., Daudi, A., Duponnois, R., Gowen, S. R., et al. (2001). Cuticle heterogeneity as exhibited by *Pasteuria* spore attachment is not linked to the phylogeny of parthenogenetic root-knot nematodes (*Meloidogyne* spp.). *Parasitology* 122, 111–120. doi: 10.1017/S0031182000006958

Davies, K. G., Flynn, C. A., Laird, V., and Kerry, B. R. (1990). The life-cycle, population dynamics and host specificity of a parasite of *Heterodera avenae*, similar to *Pasteuria penetrans*. *Rev. Nématologie* 13, 303–309.

Davies, K. G., Kerry, B. R., and Flynn, C. A. (1988). Observations on the pathogenicity of *Pasteuria penetrans*, a parasite of root-knot nematodes. *Ann. Appl. Biol.* 112, 1491–1501. doi: 10.1111/j.1744-7348.1988.tb02086.x

Davies, K. G., Laird, V., and Kerry, B. R. (1991). The motility, development and infection of *Meloidogyne incognita* encumbered with spores of the obligate hyperparasite *Pasteuria penetrans*. *Rev. Nématologie* 14, 611–618.

Davies, K. G., Redden, M., and Pearson, T. K. (1994). Endospore heterogeneity in Pasteuria penetrans related to adhesion to plant-parasitic nematodes. *Lett. Appl. Microbiol.* 19 (5), 370–373. doi: 10.1111/j.1472-765X.1994.tb00478.x

Davies, K. G., Rowe, J., Manzanella-Lopez, R., and Opperman, C. H. (2011). Re-evalulation of the life-cycle of the nematode parasitic bacterium *Pasteuria penetrans* in root-knot nematodes, Meloidogyne spp. *Nematol.* 13, 825–835. doi: 10.1163/138855410X552670

Dutta, T. K., Khan, M. R., and Phani, V. (2019). Plant-parasitic nematode management via biofumigation using brassica and non-brassica plants: current status and future prospects. *Curr. Plant Biol.* 17, 17–32. doi: 10.1016/j.cpb.2019.02.001

Dutta, T. K., and Phani, V. (2023). The pervasive impact of global climate change on plant-nematode interaction continuum. *Front. Plant Sci.* 14. doi: 10.3389/fpls.2023.1143889

Espanol, M., Verdejo-Lucas, S., Davies, K. G., and Kerry, B. R. (1997). Compatibility between *Pasteuria penetrans* and *Meloidogyne* populations from Spain. *Biocontrol Sci. Technol.* 7,219–230. doi: 10.1080/09583159730910

Evans, K. (1983). Hatching of potato cyst nematodes in root diffusates collected from twenty-five potato cultivars. *Crop Prot.* 2, 97–103. doi: 10.1016/0261-2194(83)90029-7

Fisher, M. A., Henk, D. A., Briggs, C. J., Brownstein, J. S., Madoff, L. C., McCraw, S. L., et al. (2012). Emerging fungal threats to animal, plant and ecosystem health. *Nature* 484 (7393), 186–194. doi: 10.1038/nature10947

Frantz, C., Stewart, K. M., and Weaver, V. M. (2010). The extracellular matrix at a glance. *J. Cell Sci.* 123, 4195–4200. doi: 10.1242/jcs.023820

Gair, R., Mathias, P. L., and Harvey, P. N. (1969). Studies of cereal nematode populations and cereal yields under continuous or intensive culture. *Ann. Appl. Biol.* 63, 503–512. doi: 10.1111/j.1744-7348.1969.tb02846.x

Garofalo, A., Rowlinson, M. C., Amambua, N. A., Hughes, J. M., Kelly, S. M., Price, N. C., et al. (2003). The FAR protein family of the nematode Caenorhabditis elegans. Differential lipid binding properties, structural characteristics, and developmental regulation. *J. Biol. Chem.* 278, 8065–8074. doi: 10.1074/jbc.M206278200

Giannakou, I. O., Pembroke, B., Gowen, S. R., and Davies, K. G. (1997). Effects of Long Term Storage and Above Normal Temperatures On Spore Adhesion of *Pasteuria penetrans* and Infection of the Root-Knot Nematode *Meloidogyne javanica*. *Nematologica* 43, 185–192. doi: 10.1163/004825997X00051

Gravato-Nobre, M. J., and Hodgkin, J. (2011). "Microbial Interactions with Caenorhabditis elegans: Lessons from a model organism," in *The Biological Control of Plant-parasitic Nematodes: building coherence between microbial ecology and molecular mechanisms*. Eds. K. G. Davies and Y. Spiegel (Dortrecht: Springer), 65–90. doi: 10.1007/978-1-4020-9648-83

Gravato-Nobre, M. J., Nicholas, H. R., Nijland, R., O'Rourke, D., Whittington, D., Yook, K. J., et al. (2005). Multiple genes affect sensitivity of *Caenorhabditis elegans* to the bacterial pathogen *Microbacterium nematophilum*. *Genetics* 171, 1033–1045. doi: 10.1534/genetics.105.045716

Gravato-Nobre, M. J., Stroud, D., O'Rourke, D., Darby, C., and Hodgkin, J. (2011). Glycosylation genes expressed in seam cells determine complex surface properties and bacterial adhesion to the cuticle of Caenorhabditis elegans. *Genetics* 187, 141–155. doi: 10.1534/genetics.110.122002

Hamilton, W. D. (1980). Sex versus non-Sex versus parasite. *Oikos* 35, 282–290. doi: 10.2307/3544435

Hicks, S. J., Theodoropoulos, G., Carrington, S. D., and Corfield, A. P. (2000). The role of mucins in host-parasite interactions. Part I—protozoan parasites. *Parasitol. Today* 16, 476–481. doi: 10.1016/s0169-4758(00)01773-7

Iberkleid, I., Vieira, P., de Almeida Engler, J., Firester, K., Spiegel, Y., and Horowitz, S. B. (2013). Fatty acid and retinol-binding protein, Mj-FAR-1 induces tomato host susceptibility to root-knot nematodes. *PloS One* 8, e64586. doi: 10.1371/journal.pone.0064586

Izumikawa, T., Kitagawa, H., Mizuguchi, S., Nomura, K. H., Nomura, K., Tamura, J., et al. (2004). Nematode chondroitin polymerizing factor showing cell-/organ-specific expression is indispensable for chondroitin synthesis and embryonic cell division. *J. Biol. Chem.* 279, 53755–53761. doi: 10.1074/jbc.M409615200

Jones, J. T., Haegeman, A., Danchin, E. G. J., Gaur, H. S., Helder, J., Jones, M. G. K., et al. (2013). 'Top 10 plant-parasitic nematodes in molecular plant pathology'. *Mol. Plant Pathol.* 14, 946–961. doi: 10.1111/mpp.12057

Joshi, P. M., Riddle, M. R., Djabrayan, N. J. V., and Rothman, J. H. (2010). *C. elegans* as a model for stem cell biology. *Dev. Dyn.* 239, 1539–1554. doi: 10.1002/dvdy.22296

Kamath, R. S., and Ahringer, J. (2003). Genome-wide RNAi screening in Caenorhabditis elegans. *Methods* 30, 313–321. doi: 10.1016/s1046-2023(03)00050-1

Kelley, M., Yochem, J., Krieg, M., Calixto, A., Heiman, M. G., Kuzmanov, A., et al. (2015). FBN-1, a fibrillin-related protein, is required for resistance of the epidermis to mechanical deformation during C. elegans embryogenesis. *Elife* 4, e06565. doi: 10.7554/eLife.06565

Kennedy, M. W., Garside, L. H., Goodrick, L. E., McDermott, L., Brass, A., Price, N. C., et al. (1997). The Ov20 protein of the parasitic nematode *Onchocerca volvulus*. A structurally novel class of small helix-rich retinol-binding proteins. *J. Biol. Chem.* 47, 29442–29448. doi: 10.1074/jbc.272.47.29442

Kerry, B. R. (2000). Rhizosphere interactions and the exploitation of microbial agents for the biological control of plant-parasitic nematodes. *Annu. Rev. Phytopathol.* 38, 423–441. doi: 10.1146/annurev.phyto.38.1.423

Köhnlein, K., Urban, N., Guerrero-Gómez, D., Steinbrenner, H., Urbánek, P., Priebs, J., et al. (2020). A Caenorhabditis elegans ortholog of human selenium-binding protein 1 is a pro-aging factor protecting against selenite toxicity. *Redox Biol.* 28, 101323. doi: 10.1016/j.redox.2019.101323

Lang, T., Hansson, G. C., and Samuelsson, T. (2007). Gel-forming mucins appeared early in metazoan evolution. *Proc. Natl. Acad. Sci. U.S.A.* 104, 16209–16214. doi: 10.1073/pnas.0705984104

Link, C. D., Silverman, M. A., Breen, M., Watt, K. E., and Dames, S. A. (1992). Characterization of *Caenorhabditis elegans* lectin-binding mutants. *Genetics* 131, 867–881. doi: 10.1093/genetics/131.4.867

Liu, C., Gibson, A. K., Timper, P., Morran, L. T., and Tubbs, R. S. (2018). Rapid change in host specificity in a field population of the biological control organism *Pasteuria penetrans*. *Evol. Appl.* 12 (4), 744–756. doi: 10.1111/eva.12750

Liu, C., Timper, P., Ji, P., Mekete, T., and Joseph, S. (2017). Influence of Root Exudates and Soil on Attachment of *Pasteuria penetrans* to *Meloidogyne arenaria*. *J. Nematol.* 49, 304–310. doi: 10.21307/jofnem-2017-076

McDermott, L., Cooper, A., and Kennedy, M. W. (1999). Novel classes of fatty acid and retinol binding protein from nematodes. *Mol. Cell. Biochem.* 192, 69–75. doi: 10.1023/A:1006822321081

McElroy, K., Mouton, L., Du Pasquier, L., Qi, W., and Ebert, D. (2011). Characterisation of a large family of polymorphic collagen-like proteins in the endospore-forming bacterium. *Pasteuria ramosa Res. Microbiol.* 162, 701–714. doi: 10.1016/j.resmic.2011.06.009

Mohan, S., Kumar, K. K., Sutar, V., Saha, S., Rowe, J., and Davies, K. G. (2020). Plant root-exudates recruit hyperparasitic bacteria of phytonematodes by altered cuticle aging: implications for biological control strategies. *Front. Plant Sci* 11. doi: 10.3389/fpls.2020.00763

Morran, L. T., Schmidt, O. G., Gelarden, I. A., Parrish, R. C. 2nd, and Lively, C. M. (2011). Running with the Red Queen: host-parasite coevolution selects for biparental sex. *Science* 333 (6039), 216–218. doi: 10.1126/science.1206360

Mouton, L., Traunecker, E., McElroy, K., Du Pasquier, L., and Ebert, D. (2009). Identification of a polymorphic collagen-like protein in the crustacean bacteria Pasteuria ramosa. *Res. Microbiol.* 160, 792–799. doi: 10.1016/j.resmic.2009.08.016

O'Rourke, D., Gravato-Nobre, M. J., Stroud, D., Pritchett, E., Barker, E., Price, R. L., et al. (2023). Isolation and molecular identification of nematode surface mutants with resistance to bacterial pathogens. *G3 (Bethesda)* 2, jkad056. doi: 10.1093/g3journal/jkad056

Orr, J. N., Mauchline, T. H., Cock, P. J., Blok, V. C., and Davies, K. G. (2018). *De novo* assembly of the *Pasteuria penetrans* genome reveals high plasticity, host dependency, and BclA-like collagens. *bioRxiv*, 485748. doi: 10.1101/485748

Page, A. P., and Johnstone, I. J. (2007). "The cuticle," in *Wormbook* (The C. elegans Research Community). Available at: http://www.wormbook.org.

Page, A. P., Rudin, W., Fluri, E., Blaxter, M. L., and Maizels, R. M. (1992). *Toxocara canis*: a labile antigenic surface coat overlying the epicuticle of infective larvae. *Exp. Parasitol.* 75, 72–86. doi: 10.1016/0014-4894(92)90123-R

Parsons, L. M., Mizanur, R. M., Jankowska, E., Hodgkin, J., O'Rourke, D., Stroud, D., et al. (2014). *Caenorhabditis elegans* bacterial pathogen resistant bus-4 mutants produce altered mucins. *PloS One* 9 (10), e107250. doi: 10.1371/journal.pone.0107250

Partridge, F. A., Tearle, A. W., Gravato-Nobre, M. J., Schafer, W. R., and Hodgkin, J. (2008). The C. elegans glycosyltransferase BUS-8 has two distinct and essential roles in epidermal morphogenesis. *Dev. Biol.* 317 (2), 549–559. doi: 10.1016/j.ydbio.2008.02.060

Persidis, A., Lay, J. G., Manousis, T., Bishop, A. H., and Ellar, D. J. (1991). Characterisation of potential adhesins of the bacterium *Pasteuria penetrans*, and of putative receptors on the cuticle of *Meloidogyne incognita*, a nematode host. *J. Cell Sci.* 100, 613–622. doi: 10.1242/jcs.100.3.613

Phani, V., Khan, M. R., and Dutta, T. K. (2021). Plant-parasitic nematodes as a potential threat to protected agriculture: Current status and management options. *Crop Prot.* 144, 105573. doi: 10.1016/j.cropro.2021.105573

Phani, V., and Rao, U. (2018). Revisiting the Life-Cycle of *Pasteuria penetrans* Infecting *Meloidogyne incognita* under Soil-Less Medium, and Effect of Streptomycin Sulfate on its Development. *J. Nematol.* 50, 91–98. doi: 10.21307/jofnem-2018-022

Phani, V., Shivakumara, T. N., Davies, K. G., and Rao, U. (2017). *Meloidogyne incognita* Fatty Acid- and Retinol- Binding Protein (Mi-FAR-1) Affects Nematode Infection of Plant Roots and the Attachment of *Pasteuria penetrans* Endospores. *Front. Microbiol.* 8. doi: 10.3389/fmicb.2017.02122

Phani, V., Shivakumara, T. N., Davies, K. G., and Rao, U. (2018b). Knockdown of a mucin-like gene in *Meloidogyne incognita* (Nematoda) decreases attachment of endospores of *Pasteuria penetrans* to the infective juveniles and reduces nematode fecundity. *Mol. Plant Pathol.* 19, 2370–2383. doi: 10.1111/mpp12704

Phani, V., Somvanshi, V. S., and Rao, U. (2018a). Silencing of a *Meloidogyne incognita* selenium-binding protein alters the cuticular adhesion of *Pasteuria penetrans* endospores. *Gene* 677, 289–298. doi: 10.1016/j.gene.2018.08.058

Politz, S. M., Philipp, M., Estevez, M., O'Brien, P. J., and Chin, K. ,. J. (1990). Genes that can be mutated to unmask hidden antigenic determinants in the cuticle of the nematode Caenorhabditis elegans. *Proc. Natl. Acad. Sci. U.S.A.* 87, 2901–2905. doi: 10.1073/pnas.87.8.2901

Prior, A., Jones, J. T., Blok, V. C., Beauchamp, J., McDermott, L., Cooper, A., et al. (2001). A surface-associated retinol and fatty acid-binding protein (Gp-FAR-1) from the potato cyst nematode *Globodera pallida*: lipid binding activities, structural analysis and expression pattern. *Biochem. J.* 356, 387–394. doi: 10.1042/bj3560387

Qiu, Y., Zhai, C., Chen, L., Liu, X., and Yeo, J. (2021). Current insights on the diverse structures and functions in bacterial collagen-like proteins. *ACS Biomater. Sci. Eng.* 9, 3778–3796. doi: 10.1021/acsbiomaterials.1c00018

Rocha, I., Ma, Y., Souza-Alonso, P., Vosátka, M., Freitas, H., and Oliveira, R. S. (2019). Seed coating: A tool for delivering beneficial microbes to agricultural crops. *Front. Plant Sci.* 10. doi: 10.3389/fpls.2019.01357

Schaff, J. E., Mauchline, T. H., Opperman, C. H., and Davies, K. G. (2011). "Exploiting genomics to understand the interactions between root-knot nematodes and *Pasteuria penetrans*," in *Biological Control of Plant-parasitic Nematodes: building coherence between microbial ecology and molecular mechanisms*, vol. Pp . Eds. K. G. Davies and Y. Spiegel (Springer), 91–113. doi: 10.1007/978-1-4020-9648-8_4

Sharma, S. B., and Davies, K. G. (1996). Characterisation of *Pasteuria* isolated from *Heterodera cajani* using morphology, pathology and serology of endospores. *Sys. Appl. Microbiol.* 19, 106–112. doi: 10.1016/S0723-2020(96)80017-8

Sharma, S. B., and Davies, K. G. (1997). Modulation of spore adhesion of the hyperparasitic bacterium *Pasteuria penetrans* to nematode cuticle. *Lett. Appl. Microbiol.* 25, 426–430. doi: 10.1111/j.1472-765X.1997.tb00010.x

Spiegel, Y., Mor, M., and Sharon, E. (1996). Attachment of *Pasteuria penetrans* endospores to the surface of *Meloidogyne javanica* second-stage juveniles. *J. Nematol.* 28, 328–334.

Srivastava, A. (2017). *The Molecular Basis of Pasteuria-Nematode Interactions Using Closely Related Bacillus spp* (University of Hertfordshire Research Archive). Available at: https://uhra.herts.ac.uk/handle/2299/19054. PhD thesis.

Srivastava, A., Mohan, S., and Davies, K. G. (2022). Exploring *Bacillus thuringiensis* as a model for endospore adhesion and its potential to investigate adhesins in Pasteuria penetrans. *J. Appl. Microbiol.* 132, 4371–4387. doi: 10.1111/jam.15522

Srivastava, A., Mohan, S., Mauchline, T. H., and Davies, K. G. (2019). Evidence for diversifying selection of genetic regions of encoding putative collagen-like host-adhesive fibers in *Pasteuria penetrans*. *FEMS Microbiol. Ecol.* 95. doi: 10.1093/femsec/fiy217

Stirling, G. R. (1984). Biological control of *Meloidogyne javanica* with *Bacillus penetrans*. *Phytopathology* 74, 55–60. doi: 10.1094/Phyto-74-55

Stirling, G. R. (1985). Host specificity of Pasteuria penetrans within the genus *Meloidogyne*. *Nematologica* 31 (2), 203–209. doi: 10.1163/187529285X00265

Stirling, G. R. (2014). "Biological control of plant-parasitic nematode,s," in *Soil Ecosystem Management in Sustainable Agriculture* (Wallingford, UK: CABI).

Sylvestre, P., Couture-Tosi, E., and Mock, M. A. (2002). collagen-like surface glycoprotein is a structural component of the *Bacillus anthracis* exosporium. *Mol. Microbiol.* 45, 169–178. doi: 10.1046/j.1365-2958.2000.03000.x

Sylvestre, P., Couture-Tosi, E., and Mock, M. (2003). Polymorphism in the collagen-like region of the *Bacillus anthracis* BclA protein leads to variation in exosporium filament length. *J. Bacteriol.* 185, 1555–1563. doi: 10.1128/JB.185.5.1555-1563.2003

Szitenberg, A., Salazar-Jaramillo, L., Blok, V. C., Laetsch, D. R., Joseph, S., Williamson, V. M., et al. (2017). Comparative genomics of apomictic root-knot nematodes: hybridization, ploidy, and dynamic genome change. *Genome Biol. Evol.* 9, 2844–2861. doi: 10.1093/gbe/evx201

Tan, S.J., Zhang, X., Jin, X.K., Li, W.W., Li, J.Y., and Wang, Q. (2015). Fatty acid binding protein FABP3 from Chinese mitten crab Eriocheir sinensis participates in antimicrobial responses. *Fish Shellfish Immunol.* 43 (1), 264–274. doi: 10.1016/j.fsi.2014.12.034

Tan, S. J., Zhang, X., Jin, X. K., Li, W. W., Li, J. Y., and Wang, Q. (2015). Fatty acid binding protein FABP3 from Chinese mitten crab Eriocheir sinensis participates in antimicrobial responses. *Fish Shellfish Immunol.* 43 (1), 264–274. doi: 10.1016/j.fsi.2014.12.034

Theodoropoulos, G., Hicks, S. J., Corfield, A. P., Miller, B. G., and Carrington, S. D. (2001). The role of mucins in host–parasite interactions: part II – helminth parasites. *Trends Parasitol.* 17, 130–135. doi: 10.1016/S1471-4922(00)01775-X

Todd, S. J., Moir, A. J., Johnson, M. J., and Moir, A. (2003). Genes of *Bacillus cereus* and *Bacillus anthracis* encoding proteins of the exosporium. *J. Bacteriol.* 185 (11), 3373–3378. doi: 10.1128/JB.185.11.3373-3378.2003

Trotter, J. R., and Bishop, A. H. (2003). Phylogenetic analysis and confirmation of the endospore-forming nature of Pasteuria penetrans based on the spo0A gene. *FEMS Microbiol. Lett.* 225, 249–256. doi: 10.1016/S0378-1097(03)00528-7

van Emden, H. F., and Peakall, D. B. (1996). *Beyond Silent Spring: Integrated Pest Management and Chemical Safety* (Springer).

Vos, P., Garrity, G., Jones, D., Krieg, N. R., Ludwig, W., Rainey, F. A., et al. (2009). "The firmicutes," in *Bergey's Manual of Systematic Bacteriology* (Springer). doi: 10.1007/978-0-387-68489-5

Walma, D. A. C., and Yamada, K. M. (2020). The extracellular matrix in development. *Development* 147 (10), dev175596. doi: 10.1242/dev.175596

Wang, S., Zhu, Y., Li, X., Wang, Q., Li, J., and Li, W. (2017). Fatty acid binding protein regulate antimicrobial function via Toll signalling in Chinese mitten crab. *Fish Shellfish Immunol.* 63, 9–17. doi: 10.1016/j.fsi.2017.01.036

Watt, F. M., and Huck, W. T. (2013). Role of the extracellular matrix in regulating stem cell fate. *Nat. Rev. Mol. Cell Biol.* 14 (8), 467–473. doi: 10.1038/nrm3620

World Health Organisation (2015). "International code of conduct on pesticide legislation," in *Guidelines on Pesticide Legislation*. (Geneva, Switzerland). Available at: https://apps.who.int/iris/9789241509671_eng.

frontiers | Frontiers in Cellular and Infection Microbiology

TYPE Original Research
PUBLISHED 25 January 2024
DOI 10.3389/fcimb.2024.1335946

OPEN ACCESS

EDITED BY
Alena Pance,
University of Hertfordshire, United Kingdom

REVIEWED BY
Tania Rozario,
University of Georgia, United States
Musa Hassan,
University of Edinburgh, United Kingdom

*CORRESPONDENCE
Matthew Berriman
Matt.Berriman@glasgow.ac.uk
Klaus Brehm
klaus.brehm@uni-wuerzburg.de

†PRESENT ADDRESS
Matthew Berriman,
School of Infection &Immunity, College of Medical, Veterinary and Life Sciences, University of Glasgow, Glasgow, United Kingdom

RECEIVED 09 November 2023
ACCEPTED 12 January 2024
PUBLISHED 25 January 2024

CITATION
Herz M, Zarowiecki M, Wessels L, Pätzel K, Herrmann R, Braun C, Holroyd N, Huckvale T, Bergmann M, Spiliotis M, Koziol U, Berriman M and Brehm K (2024) Genome-wide transcriptome analysis of *Echinococcus multilocularis* larvae and germinative cell cultures reveals genes involved in parasite stem cell function. *Front. Cell. Infect. Microbiol.* 14:1335946. doi: 10.3389/fcimb.2024.1335946

Genome-wide transcriptome analysis of *Echinococcus multilocularis* larvae and germinative cell cultures reveals genes involved in parasite stem cell function

Michaela Herz[1], Magdalena Zarowiecki[2], Leonie Wessels[1], Katharina Pätzel[1], Ruth Herrmann[1], Christiane Braun[1], Nancy Holroyd[2], Thomas Huckvale[2], Monika Bergmann[1], Markus Spiliotis[1], Uriel Koziol[1,3], Matthew Berriman[2*†] and Klaus Brehm[1*]

[1]Consultant Laboratory for Echinococcosis, Institute of Hygiene and Microbiology, University of Würzburg, Würzburg, Germany, [2]Parasite Genomics, Wellcome Sanger Institute, Cambridge, United Kingdom, [3]Sección Biología Celular, Facultad de Ciencias, Universidad de la República, Montevideo, Uruguay

The lethal zoonosis alveolar echinococcosis is caused by tumour-like growth of the metacestode stage of the tapeworm *Echinococcus multilocularis* within host organs. We previously demonstrated that metacestode proliferation is exclusively driven by somatic stem cells (germinative cells), which are the only mitotically active parasite cells that give rise to all differentiated cell types. The *Echinococcus* gene repertoire required for germinative cell maintenance and differentiation has not been characterised so far. We herein carried out Illumina sequencing on cDNA from *Echinococcus* metacestode vesicles, from metacestode tissue depleted of germinative cells, and from *Echinococcus* primary cell cultures. We identified a set of ~1,180 genes associated with germinative cells, which contained numerous known stem cell markers alongside genes involved in replication, cell cycle regulation, mitosis, meiosis, epigenetic modification, and nucleotide metabolism. Interestingly, we also identified 44 stem cell associated transcription factors that are likely involved in regulating germinative cell differentiation and/or pluripotency. By *in situ* hybridization and pulse-chase experiments, we also found a new general *Echinococcus* stem cell marker, *EmCIP2Ah*, and we provide evidence implying the presence of a slow cycling stem cell sub-population expressing the extracellular matrix factor *Emkal1*. RNA-Seq analyses on primary cell cultures revealed that metacestode-derived *Echinococcus* stem cells display an expanded differentiation capability and do not only form differentiated cell types of the metacestode, but also cells expressing genes specific for protoscoleces, adult worms, and oncospheres, including an ortholog of the schistosome praziquantel target, $EmTRPM_{PZQ}$. Finally, we show that primary cell cultures contain a cell population expressing an ortholog of the tumour necrosis factor α receptor family and that mammalian TNFα accelerates the development of metacestode vesicles from germinative cells. Taken together, our analyses provide a robust and comprehensive

characterization of the *Echinococcus* germinative cell transcriptome, demonstrate expanded differentiation capability of metacestode derived stem cells, and underscore the potential of primary germinative cell cultures to investigate developmental processes of the parasite. These data are relevant for studies into the role of *Echinococcus* stem cells in parasite development and will facilitate the design of anti-parasitic drugs that specifically act on the parasite germinative cell compartment.

KEYWORDS

echinococcosis, transcriptome, germinative cells, primary cells, differentiation, pluripotent, tumor necrosis factor, praziquantel (PZQ)

Introduction

Alveolar echinococcosis (AE) is a lethal zoonosis prevalent in the Northern hemisphere, caused by larvae of the tapeworm *Echinococcus multilocularis* (Thompson, 2017). Infection of the intermediate host is initiated by oral uptake of infective eggs that are shed into the environment by definitive host faeces and contain the oncosphere stage. Once taken up orally by the intermediate host, the oncosphere hatches in the intestine, penetrates the intestinal epithelium, and gains access to the inner organs, of which the liver is primarily infected. Within the liver, the oncosphere undergoes a metamorphosis towards the metacestode, which are fluid-filled cysts surrounded by an acellular laminated layer, and an inner, cellular germinative layer. The germinal layer consists of a syncytial tegument with major functions in nutrient uptake from the host, as well as few differentiated cell types such as muscle and nerve cells (Brehm and Koziol, 2017; Thompson, 2017). About 25% of all cells within the GL are small, undifferentiated cells (so-called germinative cells; GC), for which we previously demonstrated stem cell properties (Koziol et al., 2014). We showed that GC are the only proliferative cell type in the metacestode, serve as a source for all differentiated cells of the GL, and are capable of self-renewal (Koziol et al., 2014). At later stages of the infection, initiated by GC, brood capsules are formed within the metacestode, which give rise to protoscoleces that are the infective form for the definitive host (Koziol et al., 2016a). Due to the almost unrestricted growth of the metacestode within the liver, AE leads to organ failure at later stages of the disease if not adequately treated. AE treatment is difficult and relies on anti-parasitic chemotherapy using benzimidazoles, which are, however, mostly parasitostatic and only rarely eliminate the parasite (Brunetti et al., 2010). It has thus been suggested that the high AE recurrence rates, which occur upon interruption of anti-parasitic chemotherapy (Brunetti et al., 2010), are due to limited activity of benzimidazoles against GC (Koziol and Brehm, 2015).

During recent years, several studies concerning the influence of host factors on GC dependent *Echinococcus* development have been carried out. Enhanced GC proliferation has, for example, been demonstrated in response to exogenously added mammalian insulin (Hemer et al., 2014), epidermal growth factor (EGF; Cheng et al., 2017b), fibroblast growth factor (FGF; Förster et al., 2019), or serotonin (Herz and Brehm, 2021). Very recently it has also been shown that the GC dependent differentiation of *E. multilocularis* towards the protoscolex is responsive to host and parasite cytokines of the transforming growth factor-β family (Kaethner et al., 2023). It is, however, unknown so far how these exogenous signals are integrated into gene regulatory networks within GC to affect differentiation of progeny cells. As in the case of the somatic stem cells of the related but free-living planarians, GC are morphologically undistinguishable but heterogenous regarding the expression of conserved regulators of pluripotency, indicating that sub-populations exist which differ in self-renewal and differentiation potential (Koziol et al., 2014). Several signalling components have been shown to be expressed in GC, but also in post-mitotic cells (Hemer et al., 2014; Förster et al., 2019; Kaethner et al., 2023). Furthermore, only few markers have been identified that are strongly associated with GC. Apart from GC markers deriving from mobile genetic elements (Koziol et al., 2015), the most important ones regarding stem cell regulation are the post-transcriptional regulators *em-nos-1* and *em-nos-2*, which are homologous to the general stem cell marker *nanos* (both are expressed in small sub-populations of GC; Koziol et al., 2014), as well as the transcriptional regulator EmSox2, which is related to human Sox2 (Cheng et al., 2017a). No data are presently available on GC gene regulatory networks governing maintenance of pluripotency, which is mostly due to a lack of information on stem cell-specific genes in *Echinococcus*. Likewise, although we previously introduced a primary cell cultivation system derived from stem cells from metacestode vesicles (Spiliotis et al., 2008; Spiliotis et al., 2010), which are strongly enriched in GC in early cultivation phases (Koziol et al., 2014), and can regenerate mature vesicles within 2 – 3 weeks (Spiliotis et al., 2010), there have been no in-depth analyses on GC sub-populations in this system, nor on the stem cell dynamics leading to the generation of mature vesicles. Hence, despite the importance of the *Echinococcus* GC system for parasite proliferation within the host, the mechanisms that govern GC maintenance and differentiation remain enigmatic.

Significant advances towards a characterization of flatworm stem cell subsets have recently been made by transcriptomic

analyses, including single-cell sequencing, on the related organisms *Schmidtea mediterranea* and *Schistosoma mansoni* (Molinaro and Pearson, 2016; Fincher et al., 2018; Wendt et al., 2020; Li et al., 2021). Overall, these studies confirmed the presence of distinct stem cell subsets with differential potency and distinct differentiation fates (Fincher et al., 2018; Li et al., 2021). No comparable investigations have yet been carried out on stem cell systems of cestodes, except one study in which bulk transcriptomic analyses on X-ray treated adult worms of *Hymenolepis diminuta* identified genes potentially associated with cycling stem cells (Rozario et al., 2019). Other studies addressed the general protein encoding transcriptomic profiles of larvae and/or adult worms of *H. microstoma* (Olson et al., 2018; Preza et al., 2021), *Mesocestoides corti* (Basika et al., 2019), *Sparganum proliferum* (Kikuchi et al., 2021), *Dibothriocephalus dendriticus* (Sidorova et al., 2023), *Taenia pisiformis* (Zhang, 2019), and *T. multiceps* (Li et al., 2017). In *Echinococcus*, transcriptomic studies so far concentrated on *E. multilocularis* oncospheres (Huang et al., 2016), on different aspects of *E. granulosus* protoscoleces (Liu et al., 2017; Fan et al., 2020; Mohammadi et al., 2021; Yu et al., 2021; Pereira et al., 2022), or on the effects of electroporation on early *E. multilocularis* primary cell cultures (Pérez et al., 2022). However, none of these studies aimed at identifying the gene expression profiles of specific *Echinococcus* cell types.

We previously demonstrated that *Echinococcus* GC can be depleted from *in vitro* cultivated metacestode vesicles upon treatment with hydroxy urea (HU) or the Polo-like kinase inhibitor Bi-2536 (Koziol et al., 2014; Schubert et al., 2014). In the present work we utilized this methodology as a first step towards characterizing the stem cell associated transcriptome of metacestode GC. To this end, we compared the transcriptomes of control vesicles with HU or Bi-2536 treated vesicles and identified a core set of GC associated genes. We also carried out transcriptome analyses on *Echinococcus* primary cells, which are strongly enriched in GC. We validated our findings by performing RT-qPCR and *in situ* hybridization on selected genes and identified novel markers for *Echinococcus* GC and for GC sub-populations. Finally, by transcriptome sequencing and *in situ* hybridization, we also demonstrate that *Echinococcus* primary cells, which derived from *in vitro* cultivated metacestode vesicles, express not only metacestode factors, but also numerous genes specific to the protoscolex, oncosphere, and adult stages. The implications of these findings on future studies concerning *Echinococcus* stem cell function are discussed.

Materials and methods

Parasite material and *in vitro* cultivation

Experiments were carried out using the parasite isolates Ingrid, GH09, G8065, 7030, and MS1010, which derive from Old World Monkey species that had been naturally infected in a breeding enclosure (Tappe et al., 2007). Isolate H95 derived from a naturally infected fox of the Swabian mountains, Germany (Spiliotis et al., 2008). Metacestode tissue was propagated by intraperitoneal passage in Mongolian jirds (*Meriones unguiculatus*) essentially as previously described (Spiliotis and Brehm, 2009). At the time point of these experiments, all isolates except H95 were still capable of brood capsule and protoscolex production. Axenic metacestode vesicle cultivation was performed using conditioned medium from rat Reuber cells, nitrogen gas phase, and reducing conditions as previously described (Spiliotis and Brehm, 2009) with medium changes every 3 – 4 days. Axenically cultivated metacestode vesicles were treated with 40 mM HU or 150 nM Bi-2536 for 7 or 21 days, respectively, as previously described (Koziol et al., 2014; Schubert et al., 2014). After drug treatment, samples of the metacestode vesicles were recovered in conditioned medium for 24 h and then subjected to a 5 h EdU pulse to assess the reduction of stem cells capable of entering S-phase. Only vesicles in which EdU+ cells were reduced to less than 5% of the controls were further processed for transcriptomic analyses. Protoscoleces were isolated from *in vivo* cultivated parasite material as previously described (Koziol et al., 2013) and activated by low pH/pepsin/taurocholate treatment as described by Ritler et al. (2017). *E. multilocularis* primary cell cultures were set up essentially as previously described (Spiliotis et al., 2010) and were cultured for 2 days (PC1; small aggregates), 7 – 11 days (PC2; enlarged aggregates with cavities) or 16 – 22 days (PC3; onset of vesicle emergence) under axenic conditions. Samples of 2 days old primary cell cultures were tested by WISH specific for TRIM (Koziol et al., 2015) to assess GC enrichment. Only cultures with GC enrichment of over 70% were used for transcriptomic analyses. To measure effects of tumor necrosis factor α (TNFα) on parasite stem cells, primary cell cultures were set up as outlined above and 10 ng/ml (43 nM) recombinant human TNFα (Biomol, Hamburg, Germany) was added daily. The formation of mature metacestode vesicles was subsequently assessed as previously described (Förster et al., 2019).

Nucleic acid isolation, cloning, and sequencing

Total RNA was isolated from *in vitro* cultivated metacestode vesicles using the RNEasy kit (Qiagen, Hilden, Germany) according to the manufacturer's instructions and cDNA was generated using oligonucleotide CD3-RT essentially as previously described (Brehm et al., 2003). PCR products were cloned employing the TOPO TA cloning kit (Thermo Fisher Scientific) and sequenced by the Sanger method. In all cases, cDNA regions spanning the entire coding region plus 5' and 3' non-translated regions, as predicted according to transcriptome data, were PCR amplified using gene specific primers (listed in Supplementary Table 1). The corrected full-length sequences of all genes newly characterized in this study were submitted to the GenBank database and are available under the accession numbers listed in Supplementary Table 1.

In situ hybridization, immunohistochemistry and EdU labelling

Whole-mount *in situ* hybridization (WISH) was performed on cultivated metacestode vesicles according to a previously established protocol (Koziol et al., 2014). Digoxygenin (DIG)-labeled probes were

synthesized by *in vitro* transcription using the DIG RNA labelling kit (Roche) from cDNA fragment cloned into vector pJET1.2 (Thermo Fisher Scientific). Amplification primers for all probes used in this study are listed in Table S1. After hybridization, fluorescent specimens were processed and analyzed essentially as described recently (Koike et al., 2022; Kaethner et al., 2023). Control experiments using labeled sense probes were always negative. *In vitro* staining of S-phase stem cells was carried out as described (Koziol et al., 2014) using 50 µM 5-ethynyl-2'-deoxyuridine (EdU; Life Technologies, Darmstadt, Germany) for a 5 h pulse after vesicle isolation, followed by fluorescent detection with Alexa Fluor 555 azide as described previously (Koike et al., 2022; Kaethner et al., 2023). For *in situ* hybridization on primary cell preparations, the established protocol for metacestode vesicles (Koziol et al., 2016a) was slightly modified by including additional sedimentation steps during washing to avoid material loss. Gene expression patterns from all combined WISH/EdU labelling experiments were determined essentially as described (Koziol et al., 2016a) with vesicles from two biological replicates and 5 randomly chosen images of at least 5 different vesicles each. For all images, 100 cells were randomly marked in the DAPI (blue) channel and EDU+/WISH+ cells were then counted after addition of red/green channels. In the case of pulse-chase experiments, vesicles of three independently established cultures were used (biological triplicates). In each case, random pictures were taken from vesicles of three technical replicates and all nuclei (DAPI+) as well as all cells positive for EdU and *Emkal1* were counted from Z-stacks of 15 slices each. 3D images of these stacks were used to identify and eliminate false double positives. For statistical analysis, the ratios of *Emkal1*+ and EdU+ cells in relation to all cells of each single experiment were determined and mean values of the three replicates were then used for determining statistical differences by one-way ANOVA in GraphPad Prism 9.

RT-qPCR

Total RNA was isolated from cultured vesicles as described above and cDNA was synthesized as described previously (Koziol et al., 2014). qPCR was then performed according to a previously established protocol (Pérez et al., 2019; Ancarola et al., 2020) on a StepOne Plus Realtime PCR cycler (Applied Biosystems). Primer sequences for all genes analyzed in this study are listed in Table S1. The constitutively expressed gene *elp* (EmuJ_000485800; Ancarola et al., 2020) was used as a control. Cycling conditions were 15 min at 95°C, followed by 40 cycles of 15 sec at 95°C, 20 sec of 58°C, and 20 sec of 72°C. PCR efficiencies were calculated using LinRegPCR (Untergasser et al., 2021), amplification product specificity was assessed by melting curve analysis and gel electrophoresis. Expression levels were calculated by the efficiency correction method using cycle threshold (Ct) values according to Ancarola et al. (2020).

RNA-seq sample preparation

For identifying GC associated transcripts by RNA-Seq, metacestode vesicles (isolate: Ingrid) were cultivated under axenic conditions (Spiliotis and Brehm, 2009) and then treated for 7 days with 40 mM HU or for 21 days with 150 nM Bi-2536 (Axon Mechem, Groningen, Netherlands) as described previously (Koziol et al., 2014; Schubert et al., 2014). HU was added to the medium every day since it is unstable at 37°C and medium was changed every second day. In the case of Bi-2536, media changes were performed every second day with fresh drug administration. Bi-2536 control vesicles were incubated with comparable amounts of DMSO. After drug treatment, most vesicles were fixed for further analysis and small samples of unfixed vesicles were subjected to short term labelling (5 h pulse) with EdU as previously described (Koziol et al., 2014), to check for complete elimination of GC. Primary cells were isolated from *in vitro* cultivated metacestode vesicles of different isolates (Supplementary Table 1) and were set up in axenic culture essentially as previously described (Spiliotis et al., 2010). After 2 days (sample PC1), 7 - 11 days (PC2), and 16 - 22 days (PC3), cell aggregates were isolated and further processed for RNA isolation. All samples were washed three times with ice-cold PBS (phosphate buffered saline). *In vitro* cultivated metacestode vesicles were pierced with a needle prior to washing, to remove hydatid fluid. Samples were then transferred to TRIZOL ®-Reagent (Invitrogen, Karlsruhe, Germany) and stored at -80°C. Tissue samples were washed with ice-cold PBS before being mechanically homogenized in TRIZOL for 10 seconds. 200 µl of chloroform: isoamyl alcohol (24:1) was added and the samples were mixed thoroughly. Phase separation was carried out by centrifugation at 16,000 g at 4°C. 0.5X Isopropanol and 4 µl of glycogen (5mg/ml) were added to the aqueous phase, and the RNA was pelleted by centrifugation at 16,000 g at 4°C for 30 minutes. The resulting pellet was washed with 70% ethanol, air dried, and re-suspended in nuclease-free water. All samples of metacestode vesicles and primary cells were set up as three independently prepared biological replicates (n = 3).

Library preparation and sequencing

Illumina transcriptome libraries were prepared using the Illumina TruSeq kit. Polyadenylated mRNA was purified from total RNA using oligo-dT dynabead selection followed by fragmentation by metal ion hydrolysis. First strand synthesis, primed using random oligonucleotides, was followed by 2nd strand synthesis with RNaseH and DNApolI to produce double-stranded cDNA. Template DNA fragments were end-repaired with T4 and Klenow DNA polymerases and blunt-ended with T4 polynucleotide kinase. A single 3' adenosine was added to the repaired ends using Klenow exo- and dATP to reduce template concatemerization and adapter dimer formation, and to increase the efficiency of adapter ligation. Adapters containing primer sites for sequencing and index sequences were then ligated. Libraries made with the TruSeq protocol were amplified by PCR to enrich for properly ligated template strands, to generate enough DNA, and to add primers for flow-cell surface annealing, using Kapa HiFi enzyme. AMPure SPRI beads were used to purify amplified templates before pooling based on quantification using an Agilent Bioanalyser chip. Pooled TruSeq libraries were then pooled, and size

selected (300 - 400bp fragments) using the Caliper. After adaptor ligation, individual libraries made with the Illumina mRNA-seq kit were size selected using the Caliper before PCR amplification followed by AMPure SPRI bead clean up and removal of adaptors with a second Caliper run. Kapa Illumina SYBR Fast qPCR kit was used to quantify the Illumina mRNA-seq libraries before pooling.

Libraries were denatured with 0.1 M sodium hydroxide and diluted to 6 or 8 pM in a hybridization buffer to allow the template strands to hybridize to adapters attached to the flow cell surface. Cluster amplification was performed on the Illumina cBOT using the V4 cluster generation kit following the manufacturer's protocol and then a SYBR Green QC was performed to measure cluster density and determine whether to pass or fail the flow cell for sequencing, followed by linearization, blocking and hybridization of the R1 sequencing primer. The hybridized flow cells were loaded onto the Illumina sequencing platforms for sequencing-by-synthesis (100 cycles) using the V5 SBS sequencing kit then, *in situ*, the linearization, blocking and hybridization step was repeated to regenerate clusters, release the second strand for sequencing and to hybridize the R2 sequencing primer followed by another 100 cycles of sequencing to produce paired end reads. These steps were performed using proprietary reagents according to the manufacturer's recommended protocol. Data was analysed from the Illumina GAIIx or HiSeq sequencing machines using the RTA1.8 analysis pipelines.

Gene finding and annotation

For *E. multilocularis*, two genome versions have been published (Tsai et al., 2013). Gene models were predicted on version 3 (GCA_000469725.2), but genome statistics and additional analyses were conducted on an improved version 4 (GCA_000469725.3). To this end, gene models were transferred from genome version 3 to version 4 (10133 models transferred out of 10577). Since the new version of the genome is larger, new gene models were predicted that were not published previously, using Augustus v2.5.5 (Stanke et al., 2006). Annotations for new genes were assigned using BLAST searches against the NCBI nr database using custom scripts, and only unique gene models not overlapping with a previously identified model were retained. This resulted in a total of 10,699 gene models for genome version 4. The finished gene models were translated into protein predictions and domains were annotated using InterProScan v.5 (Jones et al., 2014). GO-terms were extracted from InterProScan results. Gene models and GO-terms are available through WormBaseParaSite WBPS7 (Howe et al., 2016).

RNA-Seq mapping and calculation of expression levels

Mapping of sequencing reads was performed with Hisat2 v2.0.5 (Kim et al., 2015) using a maximum intron length of 40,000 base pairs. The number of uniquely mapped reads per transcript was calculated using HTSeqCount v0.7.1 (Anders et al., 2015) with a minimum quality score of 30. TPM values (Transcripts Per kilobase Million) were calculated for all transcripts.

Differential expression calculation

Differential expression was calculated pairwise between datasets using DESeq2 v1.16.1 (Love et al., 2014) on statistical computation platform R v3.4.3 (Huber et al., 2015) with an adjusted p-value cut-off of 0.05. Adjustment for multiple testing was performed using the Benjamini-Hochberg procedure after independent filtering with genefilter v1.58.1 (Huber et al., 2015) (false discovery rate 0.05). To ascertain quality and correctness of differential expression analysis, fitting of the dispersion curve and outlier detection was assessed by plotting the dispersions (using plotDispEsts function) and the Cook´s distances for each comparison. For improved estimation of actual log2fold changes (FLC), function lfcShrink was used to calculate shrunken maximum a posteriori (MAP) LFCs. For quality control, both unshrunk maximum likelihood estimate (MLE) LFCs and MAP LFCs were visualized by plotting. Unless otherwise indicated, LFC in this work are MAP LFCs.

GO enrichment analysis

GO enrichment analysis on GC associated genes was performed using topGO_2.28.0 (https://bioconductor.org/packages/release/bioc/html/topGO.html) on biological processed (BP) with "weight01" algorithm under the Fisher statistic. The gene universe consisted of all genes with a non-zero base mean.

Bioinformatic procedures and statistical analyses

BLASTP searches were carried out against the *E. multilocularis* genome (version 5, January 2016; Tsai et al., 2013) on WormBase ParaSite (Howe et al., 2016) as well as against the SwissProt database as available at GenomeNet (https://www.genome.jp/). For BLASTP searches against *Schistosoma mansoni*, chromosomal assembly version 9 (GCA_000237925.5) was used (Protasio et al., 2012), in the case of *Schmidtea mediterranea*, assembly version ASM260089v1 (Rozanski et al., 2019), all as available under WormBase ParaSite (https://parasite.wormbase.org/index.html). Protein domain structure analysis was carried out using SMART 8.0 (http://smart.embl-heidelberg.de/). Multiple sequence alignments were performed using Clustal Omega (https://www.ebi.ac.uk/Tools/msa/clustalo/) and MEGA 11 software. Statistical analyses were performed using GraphPad Prism (version 9) employing one-way t-test or one-way ANOVA (as indicated).

Results

Identification of GC associated genes

As we previously showed, GC are specifically decimated in metacestode vesicles upon HU treatment without affecting differentiated cells (Koziol et al., 2014). We hypothesized that GC associated genes could be identified by comparing the transcriptomes of *in vitro* cultivated versus HU treated vesicles. To this end, metacestode vesicles were treated with 40 mM HU for 7 days and the reduction of EdU+ cells to less than 5% was measured by EdU incorporation assays. We then isolated RNA from treated and control vesicles, performed RNA-Seq, and mapped the resulting reads to the *E. multilocularis* genome (Supplementary Table S2). We identified 1,788 genes with statistically significantly ($p \leq 0,05$) fewer mapped reads in the HU treated samples (Supplementary Table S3). To verify these data by an independent method, we also performed metacestode vesicle treatment with the Polo-like kinase inhibitor Bi-2536, for which we previously demonstrated that it specifically decimates *Echinococcus* GC in metacestode vesicles to less than 5% after 21 days treatment (Schubert et al., 2014). After treatment of *in vitro* cultivated vesicles with 150 nM Bi-2536 for 21 days, control of the reduction of EdU+ cells to less than 5%, RNA-Seq, and mapping, we identified 2,592 genes with significantly reduced expression in Bi-2536 treated vesicles compared to the DMSO control. Combination of these two datasets led to 1,184 genes that were significantly reduced in both HU and Bi-2536 treated vesicles (Supplementary Table S3). This set of genes should predominantly comprise factors that are specifically expressed in the GC compartment but may also contain genes that are expressed in GC and direct progeny, as well as genes expressed in differentiated cells, but dependent on the presence of GC. The 1,184 factors were termed GC associated genes (Supplementary Table S3).

We previously developed an *E. multilocularis* primary cell cultivation system in which cells isolated from metacestode vesicles are cultivated under axenic conditions in the presence of host cell conditioned medium (Spiliotis et al., 2008). This system yields completely regenerated metacestode vesicles within 2 – 3 weeks of incubation (Spiliotis et al., 2008; Spiliotis et al., 2010) and we also demonstrated strong enrichment for GC after 2 days of incubation (up to 80% versus ~21-25% in metacestode vesicles; Koziol et al., 2014; Koziol et al., 2015). We concluded that transcriptomic analyses on the primary cell cultivation system would aid us in verifying the set of genes associated with GC. We therefore performed RNA-Seq on *Echinococcus* primary cells after 2 days incubation and, again, mapped the resulting reads to the genome (dataset PC1). As can be deduced from Supplementary Table S3, 1,136 of 1,184 GC associated genes (96.0%) showed higher average read counts in PC1 when compared to metacestode vesicles from which these cultures derived, indicating that we had indeed identified a valid set of stem cell factors in *E. multilocularis*. Of these genes, 592 showed a statistically significant enrichment in PC1, whereas only 16 genes were statistically significantly reduced in PC1 when compared to control vesicles. Interestingly, among these genes we found *em-nos-2* (EmuJ_000606200) for which we previously showed specific expression in *E. multilocularis* stem cells in a pattern imlying an association with the developing nervous system (Koziol et al., 2014). This could be due to specific elimination of certain GC subsets in early developing primary cell cultures or to re-programming of GC under different culture conditions. We, finally, chose 10 well expressed factors among the set of GC associated genes and investigated their expression levels in HU treated and control vesicles by RT-qPCR in an independently performed cultivation experiment. As shown in Supplementary Figure S1, we verified the statistically significant reduction of expression of all 10 genes in HU treated vesicles.

Our RNA-Seq analyses indicated that the *E. multilocularis* metacestode expresses at least ~1,180 genes in a GC associated manner and that our dataset, verified by RNA-Seq on Bi-2536 treated vesicles and by RT-qPCR, provided a robust overview of these genes.

Analysis of *E. multilocularis* GC associated genes

According to the function of GC in *Echinococcus* biology we expected that genes involved in proliferation, mitosis, and cell cycle control would be over-represented in the set of GC associated factors. To test this assumption, we performed comparative GO term analyses and, as shown in Table 1, genes associated with GO terms such as cell cycle checkpoint (GO:0000075), DNA replication initiation (GO:0006270), chromosome separation (GO:0051304), or cytokinesis (GO:0000910) were highly significantly enriched in the list of GC associated genes. Respective factors with particularly high differences in reads between HU treated and control vesicles encoded homologs to the cell cycle regulator kinase Wee1 (EmuJ_000659400), the mitotic serine/threonine kinase Aurora A (EmuJ_001059700), several origin recognition complex subunits (EmuJ_000764900; EmuJ_000046000; EmuJ_000045900; EmuJ_000880400; EmuJ_001056000) necessary for DNA replication, DNA primase (EmuJ_000487100), or the serine/threonine kinase MELK (maternal embryonic leucine zipper kinase; EmuJ_000500200), which in mammals is involved in cell cycle regulation and stem cell self-renewal (Nakano et al., 2005). Likewise, the list contains numerous genes encoding enzymes involved in nucleotide metabolism such as purine nucleoside phosphorylase (EmuJ_000635200), dUTP pyrophosphatase (EmuJ_000119100), or uridine phosphorylase (EmuJ_000734400). Interestingly, among the GC associated genes we also identified orthologs of *timeless* (EmuJ_000058900), which in *Drosophila* regulates circadian rhythm and in mammals most probably serves as a cell cycle checkpoint (Cai and Chiu, 2022), the tumor factor *p53* (EmuJ_00098700; Cheng et al., 2015; Wendt et al., 2022), and a member of the frizzled family of receptors for Wnt ligands (EmuJ_000636500) with conserved roles in the maintenance and expansion of stem cells (Clevers and Nusse, 2012).

Since we had previously conducted investigations into *Echinococcus* stem cell factors, we analysed whether these genes are present in the list of GC associated genes. We had already shown that the parasite genome contains two paralogs of the stem cell

10.3389/fcimb.2024.1335946

TABLE 1 TOP 20 GO terms associated with *Echinococcus* germinal cell associated genes.

	GO.ID	Term	Annotated	Significant	Expected	weightFisher
1	GO:0006412	translation	242	63	29,93	1.6e-14
2	GO:0006260	DNA replication	69	27	8,53	1.3e-05
3	GO:0006281	DNA repair	75	26	9,28	9.0e-05
4	GO:0003333	amino acid transmembrane transport	10	6	1,24	0.00047
5	GO:0032508	DNA duplex unwinding	30	11	3,71	0.00056
6	GO:0007093	mitotic cell cycle checkpoint	5	4	0,62	0.00104
7	GO:0006270	DNA replication initiation	8	5	0,99	0.00116
8	GO:0035235	ionotropic glutamate receptor signaling pathway	13	6	1,61	0.00277
9	GO:0030071	regulation of mitotic metaphase/anaphase transition	7	4	0,87	0.00595
10	GO:0006298	mismatch repair	7	4	0,87	0.00595
11	GO:0000723	telomere maintenance	7	4	0,87	0.00595
12	GO:0009117	nucleotide metabolic process	115	17	14,22	0.00682
13	GO:0007156	homophilic cell adhesion via plasma membrane adhesion molecules	40	11	4,95	0.00744
14	GO:0022402	cell cycle process	41	17	5,07	0.01014
15	GO:0006505	GPI anchor metabolic process	17	3	2,1	0.01532
16	GO:0032269	negative regulation of cellular protein metabolic process	29	3	3,59	0.01540
17	GO:0000910	cytokinesis	5	3	0,62	0.01552
18	GO:0019219	regulation of nucleobase-containing compound metabolic process	297	34	36,73	0.01554
19	GO:2000112	regulation of cellular macromolecule biosynthetic process	309	35	38,22	0.01557
20	GO:0006165	nucleoside diphosphate phosphorylation	31	4	3,83	0.01570

marker *nanos*, with *em-nos-1* (EmuJ_000861500) and *em-nos-2* (EmuJ_000606200) expressed in small sub-populations of EdU+ GC (Koziol et al., 2014), and, accordingly, both genes are present in the GC associated gene list. Although there are no true *piwi* orthologs in the *Echinococcus* genome (Tsai et al., 2013; Skinner et al., 2014), there are other genes encoding members of the Argonaute protein family which likely function in germline development and maintenance (Tsai et al., 2013). As we have previously shown, two of these genes, *em-ago-2A* (EmuJ_000739100) and *em-ago-2B* (EmuJ_000911700), are expressed in sub-populations of EdU+ GC of the germinal layer but are not confined to the stem cell compartment since they are also expressed in many post-mitotic cells (Koziol et al., 2014). This is reflected in our data. Although reads for both genes are slightly enriched in PC1 versus metacestode vesicles and reduced in HU- or Bi-2536 treated vesicles, the effects were not statistically significant. Hence, genes which are more ubiquitously expressed in both GC and post-mitotic cells are not contained in our list. Lastly, since we had previously shown that *Densovirus*-derived genes are deprived after HU treatment (Herz and Brehm, 2019), we also checked our list of GC associated genes for respective sequences and indeed found several gene copies for the non-capsid protein NS1 (EmuJ_000034800, EmuJ_00038860, EmuJ_002222800) and an associated gene for the capsid of the Pea enation mosaic virus (EmuJ_000034900, EmuJ_000388500) with drastically reduced read numbers in HU- and Bi-2536 treated vesicles when compared to the controls (Supplementary Table S3).

In addition to stem cell markers of the *nanos* family, we had previously shown by WISH and EdU incorporation experiments that several signalling factors are predominantly, though not exclusively, expressed in GC. This was the case for genes encoding the mitogen-activated protein kinase (MAPK) kinase kinase EmMEKK1 (EmuJ_000389600) and the MAPK EmMPK3 (EmuJ_000174000), which were expressed in approximately 60 – 70% of all metacestode GC (Stoll et al., 2021) and which are both contained in the list of GC associated genes (Supplementary Table S3). Likewise, we had demonstrated prominent GC expression of genes for the fibroblast growth factor receptor-like tyrosine kinase EmFR3 (EmuJ_000893600; Förster et al., 2019), the Wnt signalling factor Axin-2 (EmuJ_001141200; Montagne et al., 2019), the Polo-like kinase EmPlk1 (EmuJ_000471700; Schubert et al., 2014), and PIM kinase (Koike et al., 2022) and, again, all respective genes are among the GC associated factors identified by RNA-Seq (Supplementary Table S3). Similarly, both *Echinococcus* genes encoding Aurora kinases (EmuJ_001059700; EmuJ_00089100), previously shown to be expressed in GC by Cheng et al. (2019), are among the GC associated genes of our study. In contrast, numerous genes which we had identified to be predominantly expressed in muscle and nerve cells, encoding Wnt ligands (Koziol et al., 2016a) or TGFβ signalling components (Kaethner et al., 2023), are not part of the list.

Transcription factors are central components of stem cell regulatory networks that govern self-renewal and differentiation in metazoans (Molina and Cebrià, 2021). We therefore mined our list for transcription factor encoding genes that might play a role in *Echinococcus* stem cell function. Upon manual inspection of all genes of the list, supported by GO term analyses, we identified 44 transcription factors that are expressed in the metacestode in a GC associated manner (Table 2; Supplementary Table S4). In a previous study, Cheng et al. (2017a) had characterized an *Echinococcus* member of the Sox family of transcription factors, *EmSox2*, which could functionally replace murine *Sox2* during reprogramming of somatic cells to pluripotent stem cells, and which was expressed at the protein level in most proliferating GC. Notably, *EmSox2* (EmuJ_000704700) was also among the list of GC associated genes in our study with highly reduced read numbers in both HU- and Bi-2536 treated vesicles when compared to control vesicles (Table 2; Supplementary Table S4). Similar read count reductions upon HU and Bi-2536 treatment were observed for three genes encoding basic helix-loop-helix proteins (EmuJ_000098000; EmuJ_000451500; EmuJ_000627500), four zinc-finger transcription factors (EmuJ_000699600; EmuJ_000804100; EmuJ_000903400; EmuJ_001076200), two POU domain transcription factors (EmuJ_001026300; EmuJ_000449700), and another SOX family protein (EmuJ_000191100). Interestingly, the list of GC associated transcription factors also contained one member of the parasitic flatworm specific family of nuclear hormone receptors with two DNA-binding domains (Wu et al., 2007)(EmuJ_000240200), a member of the Gli-family of Krüppel-like factors (EmuJ_000711000), which are central components of the *hedgehog* signalling pathway (Petrov et al., 2017), the previously characterized, posteriorly expressed *hox* gene *Post2* (Koziol et al., 2016a; EmuJ_000959700), and orthologs to the transcription factor genes *FoxD* (EmuJ_000620400) and *tsh* (EmuJ_000580400), which are involved in body axis formation in planarians (Scimone et al., 2014; Vogg et al., 2014; Owen et al., 2015; Reuter et al., 2015). Notably, among the list of GC associated genes we also found an

TABLE 2 Selection of *E. multilocularis* transcription factors associated with germinative cells.

Gene ID	annotation	TF class	PC1	HU	HU ctrl	Bi	Bi ctrl	Red HU	Red Bi
EmuJ_000098000	Bhlh factor math6	bHLH	16	0	6	0	4	100%	100%
EmuJ_000098700	Tumor protein p63	P53 family	150	7	49	0	32	86%	100%
EmuJ_000154900	Iroquois homeodomain protein IRX 6	homeobox	49	10	66	5	46	85%	89%
EmuJ_000191100	Transcription factor SOX 14	SOX family	66	3	27	3	32	89%	91%
EmuJ_000232900	Transcription factor SOX 6	SOX family	17	1	6	1	6	83%	83%
EmuJ_000240200	Nuclear receptor 2DBD gamma	Nuclear hormone receptor	9	1	3	1	4	66%	75%
EmuJ_000380300	LIM class homeodomain TF Lhx3	LIM/homeobox	7	1	3	0	4	66%	100%
EmuJ_000437800	Transcription factor SOX 14	SOX family	43	5	28	11	35	82%	69%
EmuJ_000451500	Basic helix loop helix dimer. region	bHLH	50	2	34	0	19	94%	100%
EmuJ_000580400	Protein tiptop	Zinc finger	31	3	13	7	22	77%	78%
EmuJ_000627500	Achaete scute transcription factor	bHLH	42	0	5	0	8	100%	100%
EmuJ_000638600	Zinc finger C2H2 type	Zinc finger	13	0	14	0	8	100%	100%
EmuJ_000699600	Zinc finger C2H2	Zinc finger	30	1	12	0	7	92%	100%
EmuJ_000704700	Transcription factor Sox1a	SOX family	2	0	1	0	1	100%	100%
EmuJ_000711000	Zinc finger transcription factor gli2	Zinc finger	8	0	2	1	3	100%	66%
EmuJ_000770300	ETS transcription factor Elf 2	ETS domain	57	4	43	1	45	91%	98%
EmuJ_000804100	Zinc finger protein	Zinc finger	35	0	18	0	12	100%	100%
EmuJ_000909600	MYB	Trihelix TF	63	2	25	0	24	92%	100%
EmuJ_000995700	Transcription factor 12	bHLH	41	3	17	3	13	82%	77%
EmuJ_001123200	Zinc finger protein	Zinc finger	109	6	14	2	15	57%	87%
EmuJ_001133050	Myeloid zinc finger 1	Zinc finger	65	15	29	17	35	48%	51%
EmuJ_001159300	Transcriptional factor nfil3:e4bp4	NFIL3	61	2	20	0	18	90%	100%
EmuJ_001163300	Zinc finger C2H2	Zinc finger	56	11	24	8	26	54%	69%
EmuJ_001177300	Basic leucine zipper TF	cAMP-dependent TF	64	2	11	5	23	82%	78%

Indicated are average TPMs in stem cell cultures (PC1) and in metacestode vesicles upon treatment with HU and Bi2536. Read reductions after treatment are listed. TF, transcription factor; bHLH, basic helix-loop-helix.

ortholog (EmuJ_001159300) to HDt_078513 from *H. diminuta*, which was found to be expressed in all stem cells of the neck region (Rozario et al., 2019), and which is also an ortholog of HmN_000137200 of *H. microstoma*, shown to be specific to the neck medullary parenchyma by Olson et al. (2018).

Taken together, our analyses of the list of GC associated genes revealed an enrichment for genes whose function would predict their expression in stem cells, all genes previously associated with GC, and numerous yet unstudied *Echinococcus* factors with presumed roles in stem cell maintenance and/or differentiation.

Stem cell expression patterns of selected GC associated genes

To further verify GC expression of the genes on our list and to determine respective stem cell expression patterns, we performed WISH experiments combined with EdU-staining on *in vitro* cultivated metacestode vesicles. To this end, we chose eight genes with different expression levels in metacestode vesicles and with different degrees of read reduction upon HU and Bi-2536 treatment. All eight genes were full-length cloned and sequenced prior to WISH/EdU staining and are summarized in Supplementary Figure S2, including deduced amino acid sequences, homologies, and accession numbers.

Two of these genes, encoding a helix-loop-helix transcription factor (*Emhlh1*; EmuJ_000098000) and a POU domain protein (*EmPOU1*; EmuJ_000449700) displayed very low overall gene expression levels in the metacestode (≤ 6 TPM) but were reduced to zero reads upon HU treatment (Table 3; Supplementary Table S3). Accordingly, we only observed very few WISH+ signals for these genes but, in both cases, ~40% of all WISH+ cells were also EdU+ (Table 3; Figure 1). In the case of *EmPOU1*, we also identified EdU+/WISH+ cells in brood capsules (Figure 1), which generally display higher stem cell numbers and proliferative activity than the germinal layer (Koziol et al., 2014). Overall, ~8% and 2% of EdU+ cells also stained positive for *Emhlh1* and *EmPOU1*, respectively, indicating that both genes are expressed in small subsets of GC. Similarly, we found very low germinal layer cell numbers for a previously characterized gene encoding a neuropeptide (*Emnpp-27*; Koziol et al., 2016b) but, again, ~1% of all EdU+ cells also stained positive for *Emnpp-27* and 12% of all cells encoding the neuropeptide were positive for EdU (Table 3; Figure 1). Hence, although *Emnpp-27* codes for a neuropeptide with distinct expression pattern in the protoscolex nervous system (Koziol et al., 2016b), it is also expressed by a small subset of GC within the germinal layer.

Two further genes, encoding homologs of puromycin-sensitive aminopeptidase (*EmPSA1*; EmuJ_000356700) and the nuclear receptor coactivator 5 (*EmNcoa5*; EmuJ_001142000), which has been implicated in stem cell function of planarians (Böser et al., 2013), were detected in ~14% of all germinal layer cells and in ~50% of all EdU+ cells (Table 3; Figure 1), indicating that they are expressed in substantial subsets of GC. Accordingly, we also found strong signals for both genes in developing brood capsules, which contain numerous proliferating stem cells (Figure 1). In planarians, the Ncoa5 encoding gene was expressed by nearly all stem cells (Böser et al., 2013). In *Echinococcus* this does not appear to be the case since expression in 14% of all germinal layer cells is clearly below the previously determined number of GC in this tissue (20-25%; Koziol et al., 2014; Koziol et al., 2015) and, at least according to our WISH/EdU analyses, 50% of S-phase stem cells did not express the gene (Table 3). We thus propose that *EmNcoa5* is expressed in a subset of GC. The expression of a puromycin-sensitive aminopeptidase (PSA) gene in a substantial fraction of *Echinococcus* stem cells requires further attention. Although PSA has so far mainly been studied in the context of neurodegeneration, it has been shown to associate with the spindle apparatus during mitosis of COS cells (Constam et al., 1995), which could be one of its functions in *Echinococcus*.

Two genes that were expected, based on homology, to be expressed in GC are *EmCAF1A* (EmuJ_000609400) and *EmKIP1* (EmuJ_001180200). *EmCAF1A* encodes a homolog of subunit A of chromatin assembly factor 1 (Supplementary Figure S2) that, in

TABLE 3 Expression of *E. multilocularis* germinative cell associated genes in S-phase stem cells.

Gene name	Gene ID	EdU+	WISH+	EdU+/WISH+	WISH+ of EdU+	EdU+ of WISH+
EmCAF1	EmuJ_000609400	7,7 (± 4,4)	19,8 (± 6,1)	4,0 (± 2,5)	52%	20%
Emhlh1	EmuJ_000098000	7,5 (± 1,6)	1,4 (± 0,7)	0,6 (± 0,3)	8%	43%
EmKIP1	EmuJ_001180200	11,6 (± 6,0)	19,4 (± 6,1)	6,7 (± 3,8)	58%	35%
EmNcoA5	EmuJ_001142000	8,5 (± 2,5)	13,6 (± 4,2)	4,3 (± 1,5)	50%	32%
Emnpp27	EmuJ_000347700	9,1 (± 3,5)	0,8 (± 0,4)	0,1 (± 0,05)	1%	12%
EmPSA1	EmuJ_000356700	8,4 (± 3,0)	13,8 (± 4,2)	3,9 (± 1,8)	46%	28%
EmCIP2Ah	EmuJ_000955000	7,9 (± 4,0)	21,4 (± 5,3)	7,8 (3,5)	99%	36%
EmPOU1	EmuJ_000449700	8,3 (± 3,6)	0,5 (± 0,3)	0,2 (± 0,1)	2%	40%

By combined in situ hybridization and EdU staining the number of S-phase stem cells (EdU+), WISH+ cells, and double positive cells (EdU+/WISH+) were determined in metacestode tissue. DWISH of EdU+ indicates the proportion of S-phase stem cells expressing the respective gene, DWISH+ of WISH+ indicates the proportion of gene expressing cells in S-phase. For each gene two independent cultures were investigated (N = 2) with 5 individual vesicles per culture and 5 randomly chosen images per vesicle (n = 25). Per image 100 cells were randomly chosen in DAPI channel (blue) and EdU+/WISH+ cells were subsequently determined in red/green channel (i.e. 5000 cells per WISH experiment in total). Standard deviation (in brackets) indicates variance per vesicle.

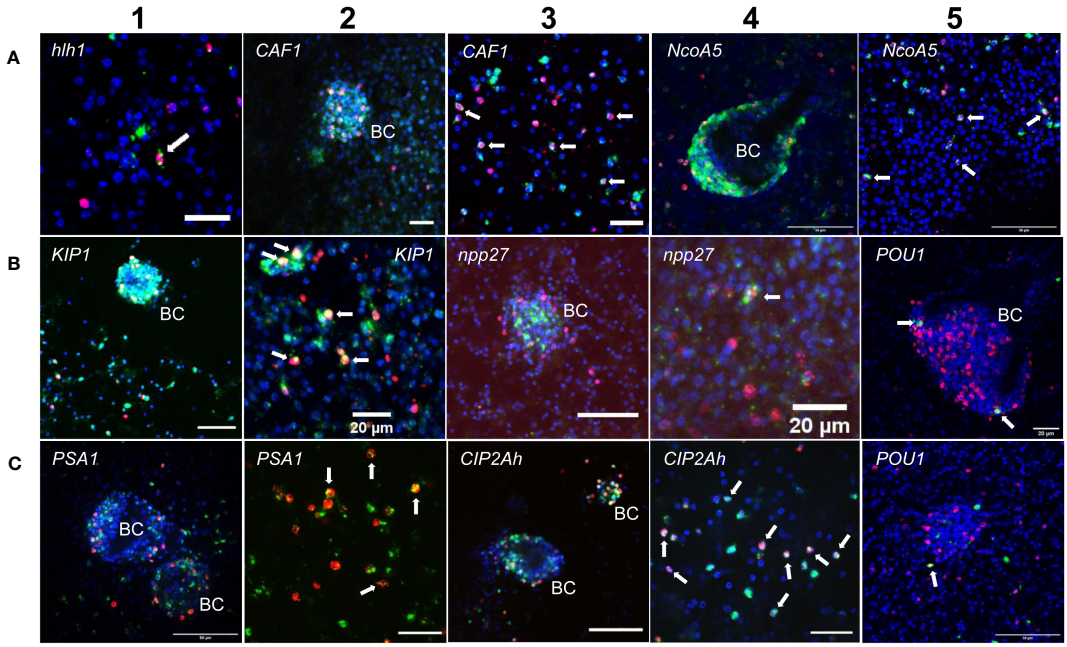

FIGURE 1
Expression of *E. multilocularis* genes in GC. WISH has been carried out for different *Echinococcus genes* (as indicated) on *in vitro* cultivated metacestode vesicles. Shown are merge pictures (single confocal slice) for three channels, in each case blue (DAPI, nuclei), red (EdU, S-phase GC), and green (WISH+). BC indicates developing brood capsules. White arrows mark cells double positive for EdU and WISH. Size bars represent 20 µm **(A-1, A-2, A-3, B-2, B-4, B-5, C-2, C-4)**, 40 µm **(B-1, B-3)**, and 50 µm **(A-4, A-5, C-1, C-3, C-5)**. For pictures showing separate channels, please refer to Figures S2.

mammals, assembles histones onto replicating DNA during S-phase (Volk and Crispino, 2015). Upon HU treatment, read numbers of *EmCAF1A* were reduced to 28% (Table 3) and we found the gene expressed in ~50% of all EdU+ cells of the germinal layer (Figure 1, Table 3) as well as numerous *EmCAF1A*+ signals in developing brood capsules (Figure 1). In planarians, a homologous factor (p150) is expressed in many neoblasts (although not exclusively) and RNAi knockdown of the respective gene resulted in severe regeneration defects and neoblast depletion (Zeng et al., 2013), indicating a role in stem cell maintenance. We thus consider a role of *EmCAF1A* in *Echinococcus* GC maintenance and epigenetic control highly likely. *EmKIP1* encodes a kinesin-like protein with highest similarity to human KIF11 (also known as Eg5) that is required for establishing a bipolar spindle during mitosis (Wordeman, 2010). In our analyses, we found 58% of EdU+ cells were also positive for *EmKIP1* (Table 3, Figure 1), supporting an important function of the gene in GC. Accordingly, we also detected intense *EmKIP1* signals in developing brood capsules (Figure 1). Given the important role of human KIF11 in mitosis (Wordeman, 2010), we initially expected that all GC express *EmKIP1*. However, since the protein is specifically needed during mitosis, it is possible that its expression is initiated towards the end of S-phase, thus explaining why only ~60% of GC were found *EmKIP1*+. Furthermore, the *E. multilocularis* genome also encodes a second kinesin-like protein with homology to the *EmKIP1* gene product (EmuJ_000198400), which is also among the list of GC associated genes (Supplementary Table S3) and which could, at least in part, functionally replace *EmKIP1*.

Finally, we investigated *EmCIP2Ah* (EmuJ_000955000) that was expressed in ~21% of all cells of the germinal layer (Table 3; Figure 1). As shown in Supplementary Figure S2, *EmCIP2Ah* encodes a protein with no discernible functional domains, but which is distantly related to human cellular inhibitor of PP2A (CIP2A), an inhibitor of tumour suppressor activities of protein phosphatase 2A in human cancer, e. g. by de-phosphorylating the transcription factor c-Myc (Denk et al., 2021). Interestingly, in our combined EdU/WISH analyses, we found intense *EmCIP2Ah* signals in developing brood capsules and, within the germinal layer, almost 100% of all EdU+ cells were also positive for *EmCIP2Ah* (Figure 1, Table 3). Together with the total number of *EmCIP2Ah*+ cells in the germinal layer, which agrees with the total number of GC in this tissue (21 – 25%; Koziol et al., 2014; Koziol et al., 2015), we assumed that *EmCIP2Ah* could be a general marker of *Echinococcus* GC, irrespective of the cell cycle. To clarify the situation, we carried out double WISH with *EmCIP2Ah* and *TRIM* (terminal-repeat retrotransposon in miniature), the so far only known general stem cell marker of *Echinococcus* (Koziol et al., 2015). As shown in Figure 2, we found almost 100% congruence between the signals for both genes, indicating that *EmCIP2Ah* indeed is a marker of all GC in the germinal layer. Whether *EmCIP2Ah* fulfils similar roles in *Echinococcus* as CIP2A in humans remains to be established. Although *Echinococcus* encodes a close homolog of PP2A (EmuJ_001106500), c-Myc is absent in cestodes (Tsai et al., 2013), thus excluding a similar mechanism in the parasite. Conversely, it has recently been shown that mammalian CIP2A also complexes with TOPBP1

10.3389/fcimb.2024.1335946

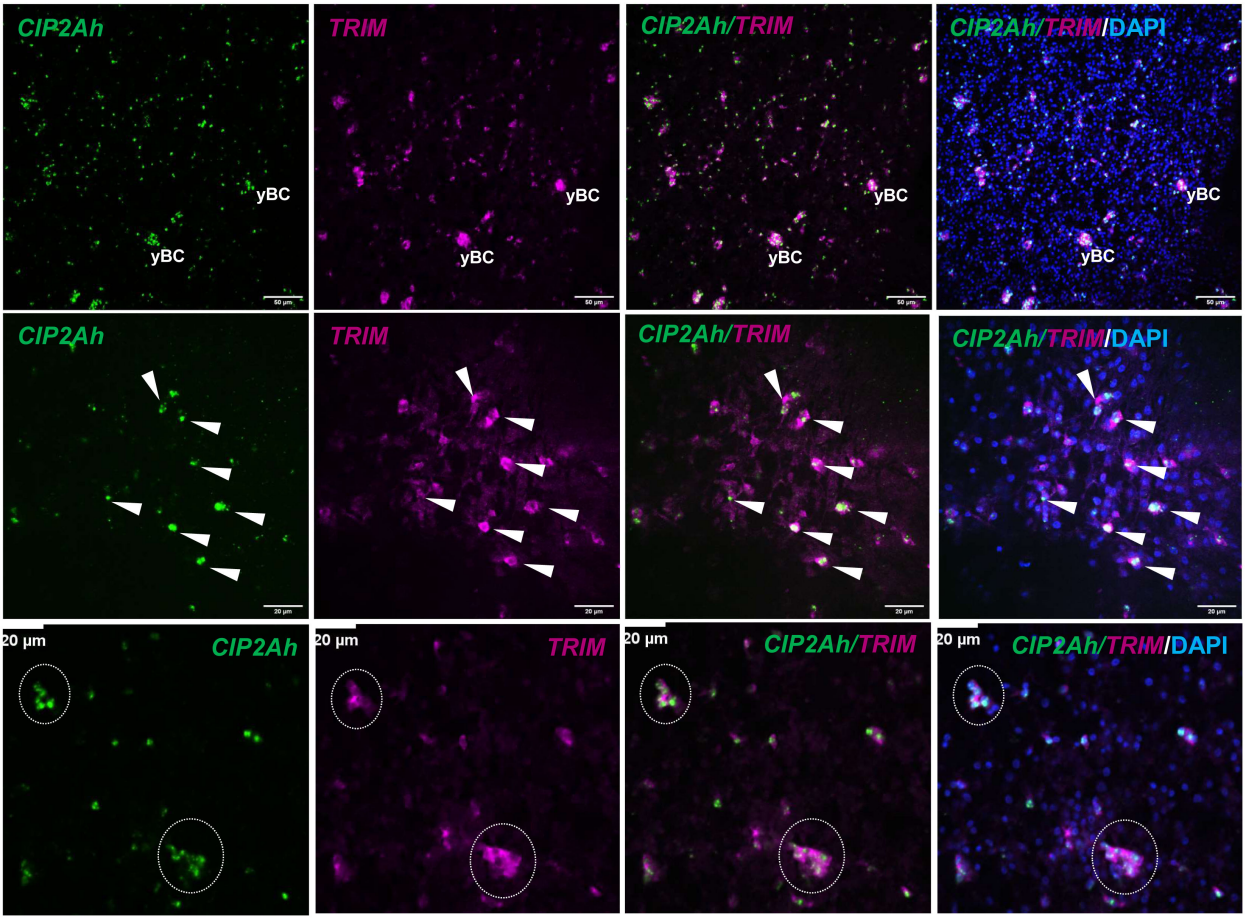

FIGURE 2
EmCIP2Ah as a general marker of *E. multilocularis* GC. Double WISH has been carried out on *in vitro* cultivated metacestode vesicles using probes specific for *EmCIP2Ah* and *EmTRIM*. Upper panel: Overview of metacestode tissue showing from left to right, *EmCIP2Ah*+ cells (green), *EmTRIM*+ cells (magenta), overlay of *EmCIP2Ah* and *EmTRIM*, and merge of all channels (including DAPI, blue). yBC indicates young brood capsules. Size bar represents 50 µm. Middle panel: Region of metacestode with dispersed GC. White triangles indicate cells double positive for *EmCIP2Ah* and *EmTRIM*. Size bar represents 20 µm. Note the diffuse, cytoplasmic signal for *EmTRIM* and the focused, nuclear signal for *EmCIP2Ah*. Lower panel: Metacestode tissue with accumulations of GC (circles). Note that individual GC cannot be distinguished by *EmTRIM*+ signal, but by *EmCIP2Ah*+ signal. Size bar represents 20 µm. All images shown are single confocal slices.

(DNA topoisomerase 2 binding protein 1) in a mitosis-specific genome maintenance complex (De Marco Zompit et al., 2022). Since a close homolog of TOPBP1 is also expressed by *Echinococcus* (EmuJ_000898700), interactions between these two factors could contribute to the maintenance of genomic stability during GC mitosis.

Taken together, our combined EdU/WISH analyses verified stem cell expression of factors listed as GC associated genes and even identified one new general *Echinococcus* stem cell marker (*EmCIP2Ah*), which will facilitate future investigations on *Echinococcus* stem cell dynamics.

Emkal1 may mark a slow cycling GC subpopulation

Although morphologically indistinguishable, flatworm stem cell populations are heterogenous on gene expression level and in both planaria and schistosomes, functionally different sub-populations have been described (reviewed in Molina and Cebrià, 2021; You et al., 2021). Typically, these sub-populations can be distinguished by preferential expression of sub-type marker genes such as the transcription factor *soxP-1* in the case of planarian σ-neoblasts (Molina and Cebrià, 2021) or the nuclear hormone receptor *eled* in schistosome ϵ-cells (Wang et al., 2018). Although we previously noted clear differences in gene expression profiles between GC and neoblasts (Koziol et al., 2014; Förster et al., 2019), we were interested whether at least some of the known flatworm maker genes can be used to distinguish different classes of GC. We identified an *E. multilocularis* ortholog (EmuJ_000888900) to *S. mediterranea kal-1*, which is present in the list of GC associated genes (Supplementary Table S3). *S. mediterranea kal-1* encodes a homolog of the mammalian extracellular matrix glycoprotein Anosmin-1 and is highly specifically expressed in a ζ neoblast sub-population, as well as in ventrally located, early epidermal progenitors that derive from ζ neoblasts (Wurtzel et al., 2017).

We therefore performed experiments concerning the expression of *Emkal1* in GC and in GC progeny.

We isolated metacestode vesicles from culture, subjected them to a 5 h pulse of EdU incorporation, fixed part of the vesicles, and performed WISH specific for *Emkal1*. The remaining vesicles were then cultured for another 3 (72 h) or 4 days (96 h) prior to fixation and *Emkal1* specific WISH. By independent WISH analyses we had previously shown that approximately 8% of all metacestode cells stain positive for *Emkal1* and, accordingly, at t=0 we found 8.2% (± 0.4%) of metacestode vesicle cells (n = 8,176) positive for *Emkal1* (Figure 3). As expected, the relative proportion of *Emkal1*+ cells among all metacestode cells did not change over the incubation period of 4 days (Figure 3). We then analysed the proportion of cells that stained positive for both *Emkal1* and EdU. At t=0 we found 7.7% (± 0.1%) of all cells (n = 8,652) positive for EdU, which increased to 23.2% (± 2.5%) and 18.0% (± 0.4%) after 3 and 4 days (n = 10,058) of incubation, respectively (Figure 3). Although we cannot exclude that a certain proportion of the increase in EdU+ cells resulted from a delayed incorporation of EdU that was stored within vesicle fluid after the 5 h pulse (Koziol et al., 2014), the statistically significant increase in EdU+ cells after three days indicated that a large proportion of GC that had incorporated EdU at t=0 had undergone mitosis at this time point, resulting in two EdU+ progeny cells. Interestingly, the initial number of cells which stained positive for both *Emkal1* and EdU (2.1 ± 0.1% of cells) had not changed after 3 days (1.8 ± 0.2%) of further culture. However, after 4 days of incubation, this compartment had a statistically significant, approximately 2-fold increase to 4.2 (± 0,2%) of all cells. Likewise, the proportion of *Emkal1*+/EdU+ cells among *Emkal1*+ cells showed no statistical difference between t=0 and t=3d (25.1 ± 1.1% versus 21.6 ± 4.3%) but significantly increased to 49.9 ± 2.5% at t = 4d (Figure 3), indicating that *Emkal1* might be expressed in a GC sub-population with a prolonged cell cycle. The sharp increase of EdU+/*Emkal1*+ cells would then either be explained by asymmetric cell division of an EdU+ GC, resulting in another EdU + GC and an EdU+ differentiating cell, or by delayed incorporation of EdU by a GC subpopulation with a cell cycle that is 24 h longer, compared to the bulk of metacestode GC.

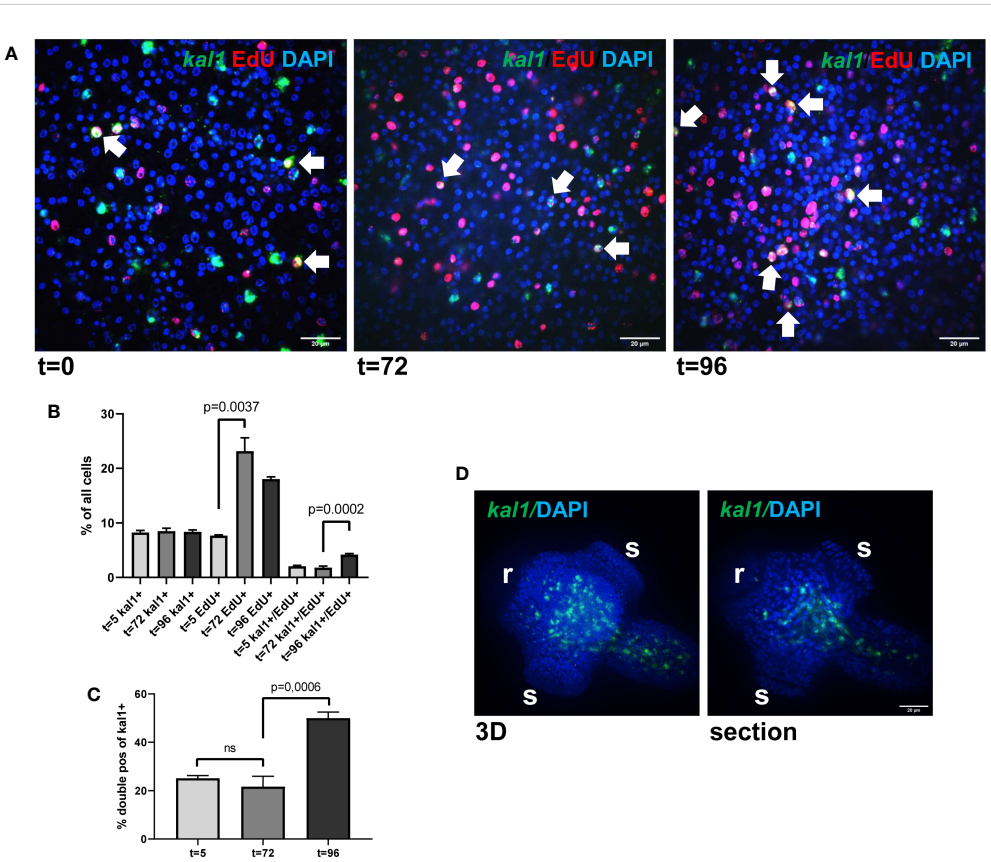

FIGURE 3
Emkal1 as a potential marker for a slow cycling GC subpopulation. **(A)** WISH/EdU staining for metacestode vesicles at different time points as indicated. Displayed are merge pictures (single confocal slices) of three channels, blue (DAPI, nuclei), red (EdU, S-phase GC), and green (WISH, *Emkal1*). White arrows indicate cells double positive for EdU and *Emkal1*. Size bar repesents 20 µm. **(B)** Counts of cells positive for *Emkal1* (*kal1*+), positive for EdU (EdU+), and double positive (*kal1*+/EdU+) of all cells in metacestode vesicles at different time points (as indicated). Displayed are mean values ± standard deviation. Each experiment has been carried out three times independently (N = 3) with technical triplicates of which in each case 3 images of 3 individual vesicles were analysed. **(C)** Percentage of double positive *Emkal1*+/EdU+ cells among all *Emkal1*+ cells at different time points (as indicated), deduced from values displayed in **(B)**. Displayed are mean values ± standard deviation. Statistical analysis was carried out using one-way ANOVA and statistically significant differences are indicated by bars with respective p-values. The total numbers of metacestode cells counted (n) for each condition were 8,176 (t=0), 8,652 (t=72), and 10,058 (t=96). **(D)** WISH for *Emkal1* on protoscoleces. Shown are a 3D project (20 sections) of one protoscolex (3D) and one section of the same protoscolex (section). Size bar represents 20 µm.

In *Schmidtea*, *kal1* serves as a marker for ventral identities and most *kal1*+ cells are located close to the ventral epidermis, where they partially co-localize with the epidermis marker *DCLK2* (Wurtzel et al., 2017). To investigate whether *Emkal1* could have a similar function, we performed WISH on protoscoleces but as shown in Figure 3, we exclusively obtained *Emkal1* signals in central areas of the neck and regions around the anterior and posterior ring commissures of the nervous system. Based on these findings, we suggest that *Emkal1*+ GC and progeny cells are not directly involved in the formation of Echinococcus surface structures.

Taken together, our analyses verified that *Emkal1*, which is listed among our GC associated genes, is expressed in a significant subpopulation (25%) of *Echinococcus* GC and might serve as a marker for stem cells with a prolonged cell cycle. In contrast to the function of planarian *kal1*, however, we did not obtain evidence for an involvement of *Emkal1* in tegument formation. Future experiments, including double WISH for *Emkal1* and markers for terminally differentiated *Echinococcus* cells, will be required for elucidating the precise role of *Emkal1*+ GC in *Echinococcus* development.

GC in *Echinococcus* primary cell cultures show an expanded differentiation capacity

We previously established an *E. multilocularis* primary cell cultivation system in which parasite cells, isolated from cultivated metacestode vesicles, are seeded into wells and are further cultivated under axenic conditions (Spiliotis et al., 2008; Spiliotis et al., 2010). After 2 days of incubation, the primary cells regularly form small aggregates that are highly enriched with GC (up to ~80%), but also contain some differentiated cell types such as muscle or nerve cells (Koziol et al., 2014). Upon further incubation, the primary cell cultures develop larger aggregates with internal cavities and, after 2 – 3 weeks, reveal fully developed metacestode vesicles (Spiliotis et al., 2008; Spiliotis et al., 2010). We further characterized the development of primary cell aggregates into metacestode vesicles and found increasing numbers of muscle and nerve cells within the aggregates after 7 days of culture (Figure 4), which apparently derived from differentiation of stem cells into definitive cell fates. Expression of *Em-muc-1* (EmuJ_000742900; Koziol et al., 2014), a member of *Echinococcus*-specific family of apomucins that are major components of the LL (Díaz et al., 2011), is considered a hallmark of a functional metacestode tegument. We therefore carried out *Em-muc-1* specific WISH on primary cell aggregates at different time points of development and found strong *Em-muc-1* + signals surrounding early and late cavities (Figure 4), indicating that these first emerge as outside-in structures. Using PAS staining to mark LL components, we identified masses of PAS positive structures on sections of primary cell aggregates (Figure 4), which had obviously been secreted into the lumen of the parasite primary cell cavities. At later stages of primary cell development, we identified emerging vesicles displaying intense *Em-muc-1*+ signals close to the surface, which were still connected with aggregates, but showed the regular morphology of mature metacestode vesicles, with a distal laminated layer, secreted by the parasite tegument. We thus assume that the formation of mature metacestode vesicles by primary cell cultures starts with the formation of *Em-muc-1*+ tegumental cells that surround internal cavities in an outside-in arrangement and secrete laminated layer material into the cavities. Once these internal tegumental structures gain contact to the surface of the aggregate, either by apoptosis or by further differentiation of cells between cavity and aggregate surface, they then invert into regularly shaped metacestode vesicles that eventually emerge from the main bodies of the aggregates.

To further characterize differentiation mechanisms within primary cell aggregates, we complemented our Illumina transcriptome data obtained after 2 days of cultivation (PC1) by analyses on aggregates at later stages of development. We chose cultures in which the primary cell aggregates were already enlarged and contained internal cavities, but which did not yet show emerging vesicles (PC2; after 7 - 11 days) and cultures in which vesicles were about to emerge (PC3; after 16 – 22 days). As with metacestode vesicles after HU and Bi-2536 treatment, the resulting reads were mapped to the genome (Supplementary Table S2). For a selection of genes, we also carried out combined EdU/WISH experiments on primary cell cultures at later time points of development.

We previously showed that the *E. multilocularis* metacestode is posteriorized tissue and contains numerous cells expressing posterior morphogens encoded by genes such as *Emwnt1* or *Emwnt11b* (Koziol et al., 2016a) and, as expected, we also observed high levels of *Emwnt1* and *Emwnt11b* expression in primary cell aggregates, particularly for stages PC2 and PC3 (Figure 5; Supplementary Table S2). WISH analyses then confirmed that PC2 stage primary cell aggregates display numerous *wnt1*+ and *wnt11b*+ cells (Figure 6), probably leading to a general posteriorized development of the emerging structures. Similarly, we found high expression in primary cell cultures of *Em-alp2* (EmuJ_000393400), encoding a metacestode-specific alkaline phosphatase (Koziol et al., 2014), but not the related gene *Em-alp3* (EmuJ_000752700). The latter encodes an alkaline phosphatase isoform that is active in the excretory system of the protoscolex (Koziol et al., 2014), indicating that at least some protoscolex-specific cell types are not formed in primary cell preparations that derive from metacestode cells.

Upon closer inspection of primary cell gene expression profiles, however, we found numerous other genes that are typically expressed in protoscoleces in PC1 and, particularly, PC2 and PC3. To quantify this, we initially (and arbitrarily) defined protoscolex-specific genes as having an at least 10-fold higher expression level in protoscoleces when compared to metacestode vesicles. We then analysed previously generated datasets (n = 1) for non-activated and activated protoscoleces (Tsai et al., 2013), mapped them to the genome, and determined their average gene expression compared to the metacestode profiles characterized in the present study. Of all annotated *E. multilocularis* genes, we identified 872 as being at least 10-fold higher expressed in protoscoleces versus metacestode vesicles. Of these 872 genes, 304 (35%) were at least 3-fold higher expressed in PC1 versus metacestode vesicles. This number increased to 644 (74%) in PC2 and 697 (80%) in PC3 when compared to metacestode vesicles

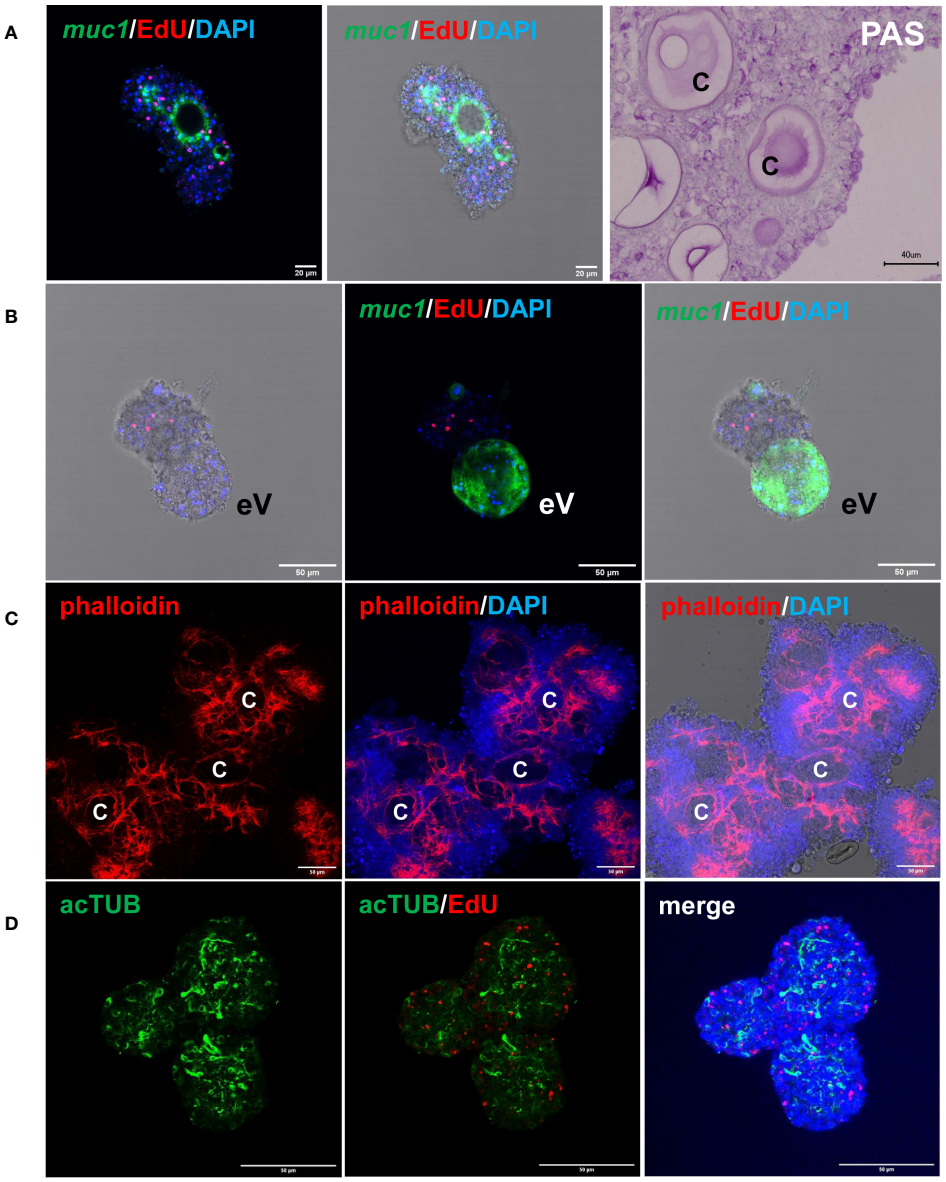

FIGURE 4
Features of *E. multilocularis* primary cell culture aggregates. **(A)** Expression of laminated layer components. *muc1* indicates WISH for *muc1* on 7 d old aggregate. Displayed are (left) merge of three channels (blue, DAPI, nuclei; red, EdU, S-phase GC; green, WISH, *muc1*) and (middle) merge combined with brightfield. Size bar represents 20 µm. Note intense *muc1* signal at layer surrounding cavity. PAS indicates PAS staining of 10 d old aggregate section. Size bar represents 40 µm. **(B)** *muc1*-specific WISH on 14 d old aggregate with emerging vesicle (eV). Shown are bright field with EdU and DAPI (left), merge of EdU, DAPI, and WISH (middle), and merge of bright field and all three channells (right). Size bar represents 50 µm. **(C)** Phalloidin staining of 10 d old aggregates, marking muscle fibres. Displayed are from left to right: phalloidin staining (red, muscle), phalloidin plus DAPI (blue, nuclei), and phalloidin plus DAPI plus bright field. C indicates cavity. Size bar represents 50 µm. **(D)** Nerve cell staining of 10 d old aggregate using a-AcTub antibody. Displayed are from left to right: α-AcTub (green, nerve cells), α-AcTub plus EdU (red, S-phase GC), merge of α-AcTub, EdU, and DAPI (blue, nuclei). Size bar represents 50 µm. All images show single confocal slices.

(Supplementary Table S5). As shown in Figure 5, the respective list of genes included *sfrp* and *sfl*, which are expressed at the anterior pole of protoscoleces upon brood capsule formation, but which are not expressed in metacestode vesicles that are free of brood capsules (Koziol et al., 2016a). In the case of *sfrp* we also carried out WISH on primary cell aggregates after 7 days of culture and found distinct *sfrp*+ cells. In the context of body axis determination, we also identified another gene, *Emfz10* (EmuJ_000085700), encoding a member of the frizzled family of GPCRs, which act as receptors for Wnt – ligands in determining body axis patterns, and which we previously identified as a potential target for the *Echinococcus* micro-RNA *mir-71* (Pérez et al., 2019). *Emfz10* was expressed to relatively high levels of 82 TPM in activated and 110 TPM in non-activated protoscoleces but had only low expression (below 1 TPM) in both metacestode preparations. In PC1, on the other hand, *Emfz10* expression was already increased to ~6 TPM and further increased to ~14 TPM in PC2 and PC3. As shown in Figure 6, we then also identified numerous *Emfz10*+ cells, which partly

10.3389/fcimb.2024.1335946

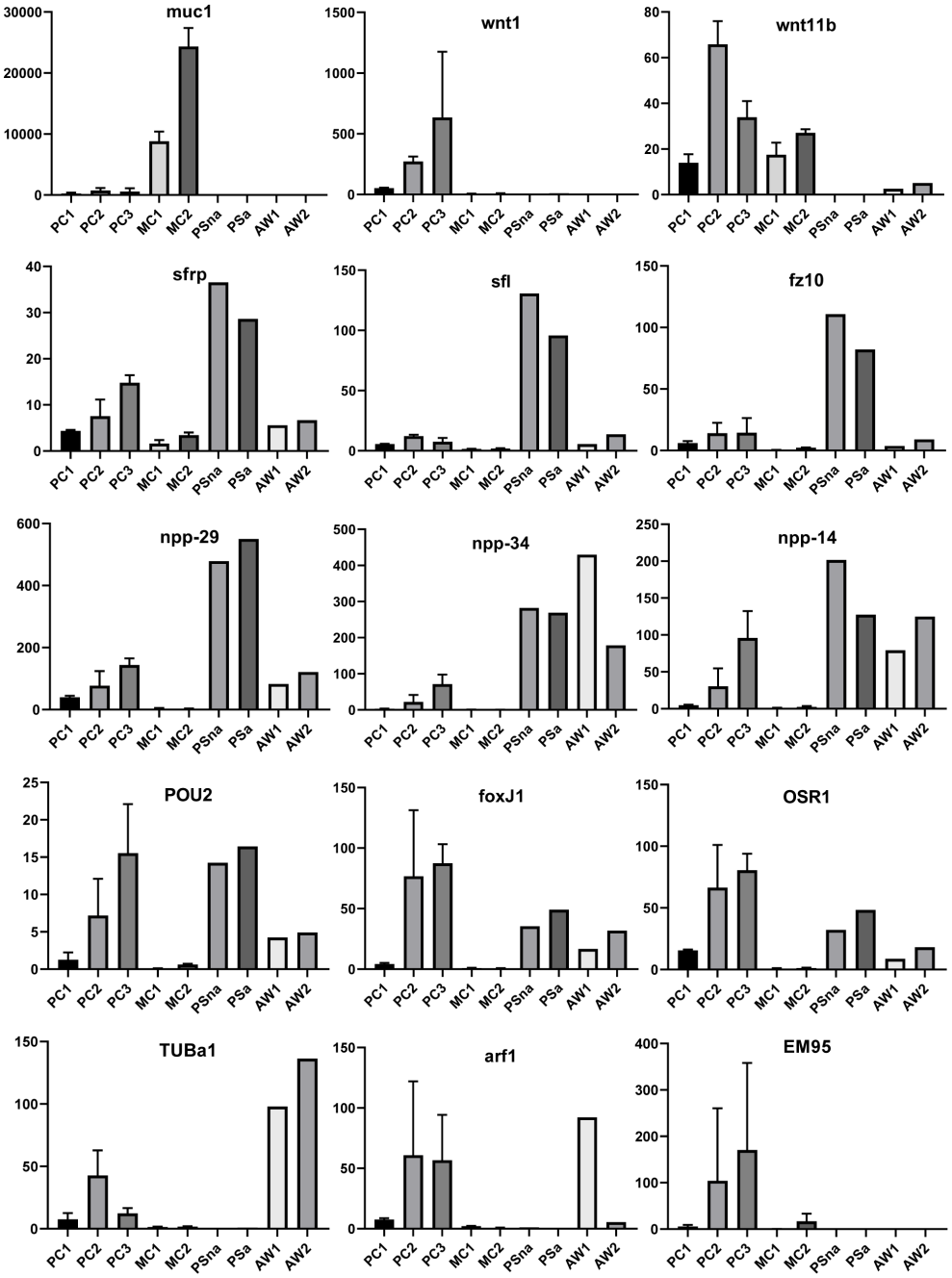

FIGURE 5
Expression of selected genes in *Echinococcus* cell culture, larvae, and adult worms. Displayed are expression values (TPM) in primary cell cultures after 2 d (PC1), 7 d (PC2), and 11 d (PC3) of *in vitro* cultivation as well as expression in cultivated metacestode vesicles, which served as controls for HU treatment (MC1) and Bi2536 treatment (MC2). Shown are mean values ± standard deviation of biological triplicates (n = 3). For comparison, TPM values (n = 1) of non-activated (PSna) and activated protoscoleces (PSa) as well as pre-gravid (AW1) and gravid (AW2) adult worms are shown. Individual genes are indicated above.

co-localized with EdU signals, in primary cell aggregates by WISH. Interestingly, among the list of genes typically expressed in protoscoleces, but also in primary cell aggregates, we also found several that we previously showed to encode neuropeptides (*npp-29*, *npp-34*, *npp-14*; Koziol et al., 2016b), as well as another POU-domain containing transcription factor (*EmPOU2*), a forkhead-box transcription factor (*Em-foxJ1*), and an ortholog of the odd-skipped-related family of transcription factors (*EmPSR1*), which participate in body axis formation (Figure 5).

Since primary cell aggregates contained numerous cells typically found in the protoscolex, we extended our analyses to additional developmental stages, such as adult worms and oncospheres. Again, we mined available datasets (n = 1) for pre-gravid and gravid adult worms (Tsai et al., 2013) and searched for genes with prominent

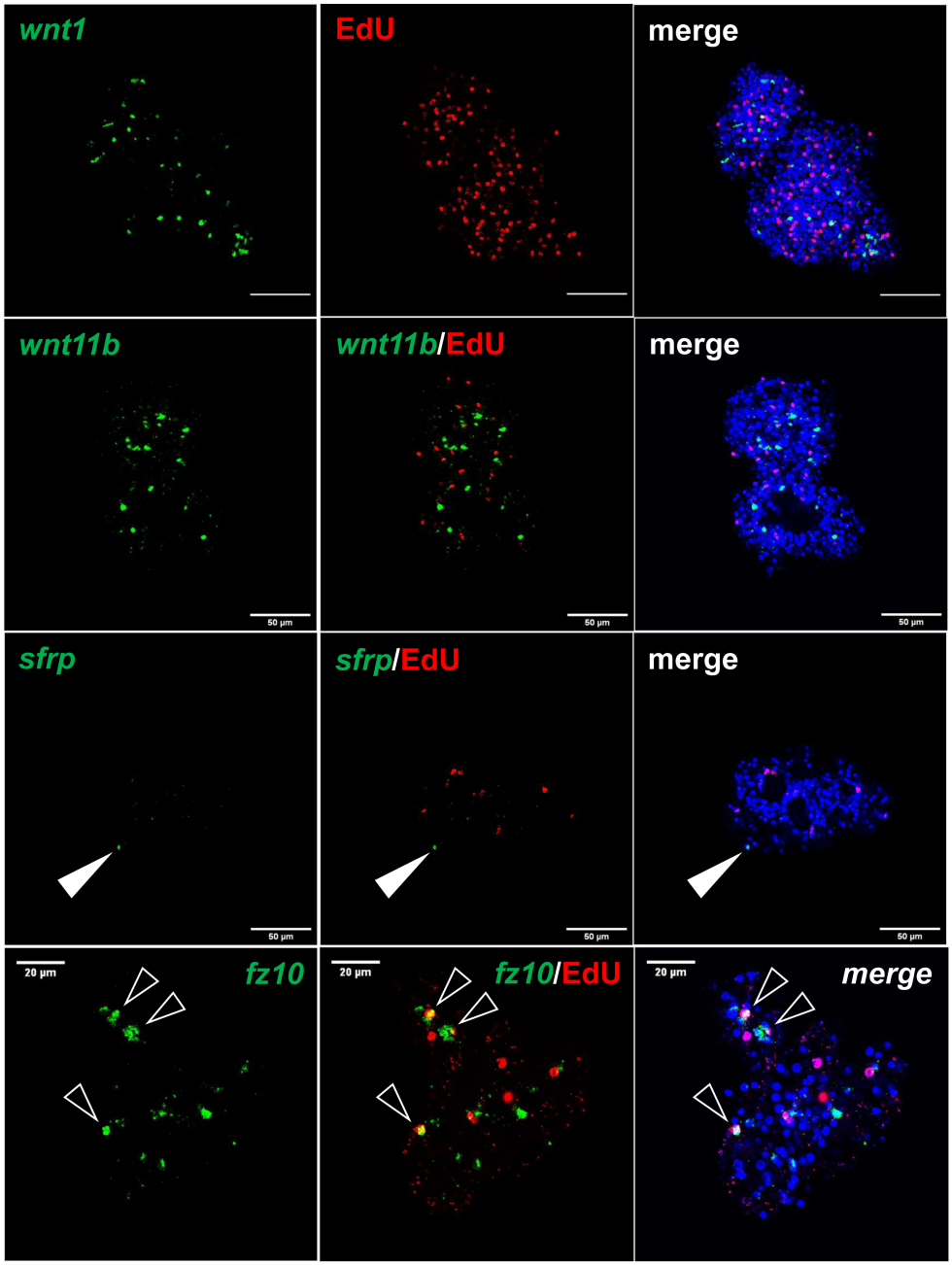

FIGURE 6
Expression of *Echinococcus* genes in primary cell cultures. WISH has been carried out on 7 d old primary cell cultures for selected genes (as indicated). Shown are in each panel from left to right of single confocal slices: WISH signal (green), WISH plus EdU (red, S-phase GC), and WISH plus EdU plus DAPI (nuclei, blue). Closed white triangle indicates *Emsrfp+* cell, open white triangles indicate cell double positive for EdU and *Emfz10*. Size markers represent 50 µm for *wnt1*, *wnt11b*, *sfrp*, and 20 µm for *fz10*.

expression in adult forms, but low expression in protoscolex and metacestode. Several of those, like a gene encoding an α-tubulin isoform (*EmTUBa1*; EmuJ_000042200) or an ADP ribosylation factor (*Emarf1*; EmuJ_000674900) again showed relatively high expression levels in primary cells after 7 or 11 days of incubation (Figure 5). Finally, in previous transcriptomic analyses, one gene encoding an EM95 antigen isoform, EmuJ_000368620, was shown to be highly upregulated in activated oncospheres but had low expression in metacestode tissue (Huang et al., 2016). As shown in Figure 5, this gene displayed little or no or expression in protoscoleces, adult worms, or metacestode vesicles, but its expression levels in primary cells strongly increased from PC1 (5 TPM) to PC2 (104 TPM), then PC3 (170 TPM).

Taken together, our analyses on *E. multilocularis* primary cell cultures revealed they are initially highly enriched with stem cells (Koziol et al., 2014) that proliferate and differentiate into several distinct cell types, such as muscle- and nerve cells, as well as *Em-muc-1* expressing tegumental cells that surround internal outside-in

cavities. From these cavities, mature metacestode vesicles later emerge. As expected, primary cell development appears to be skewed towards posteriorized cell fates under the influence of *wnt1* and *wnt11b* expressing cells, which later leads to fully mature, posteriorized metacestode vesicles. However, *E. multilocularis* primary cell cultures also produce, at least to a certain degree, cell types that typically occur in other developmental stages such as oncospheres, protoscoleces, and adult worms. These data indicate that metacestode derived stem cells initially used to set up primary cell cultures are not pre-determined to exclusively form metacestode progeny but are also capable of developing into other cell types from different life cycle stages.

E. multilocularis primary cell cultures form cells expressing a target for praziquantel

To further characterize the capability of *Echinococcus* primary cell cultures to generate cells that are typically not present in metacestode vesicles, we concentrated on a transient receptor potential (TRP) ion channel that has recently been identified as a target for praziquantel (PZQ) in the trematode *S. mansoni* (Park et al., 2019). Related ion channels are expressed by PZQ sensitive trematode and cestode species, and the presence of an Asp residue (instead of Glu) within the TRP domain is critical for PZQ binding (Rohr et al., 2023). The latter's study authors suggested the ion channel encoded by EmuJ_000986600 as a likely target candidate for the activities of PZQ on adult *E. multilocularis* worms (Rohr et al., 2023). We therefore mined the available *E. multilocularis* genome information for orthologs to schistosome $TRPM_{PZQ}$ and closely analysed those showing an expression level of 10 TPM or higher in protoscoleces or metacestode vesicles. As shown in Figure 7, the product of EmuJ_000986600 was the indeed the only TRP ion channel fulfilling these criteria and displaying an Asp residue within the TRP domain. We thus designated the respective protein $EmTRPM_{PZQ}$.

Transcriptome analyses indicated that the gene encoding $EmTRPM_{PZQ}$ is well expressed in protoscoleces but only lowly

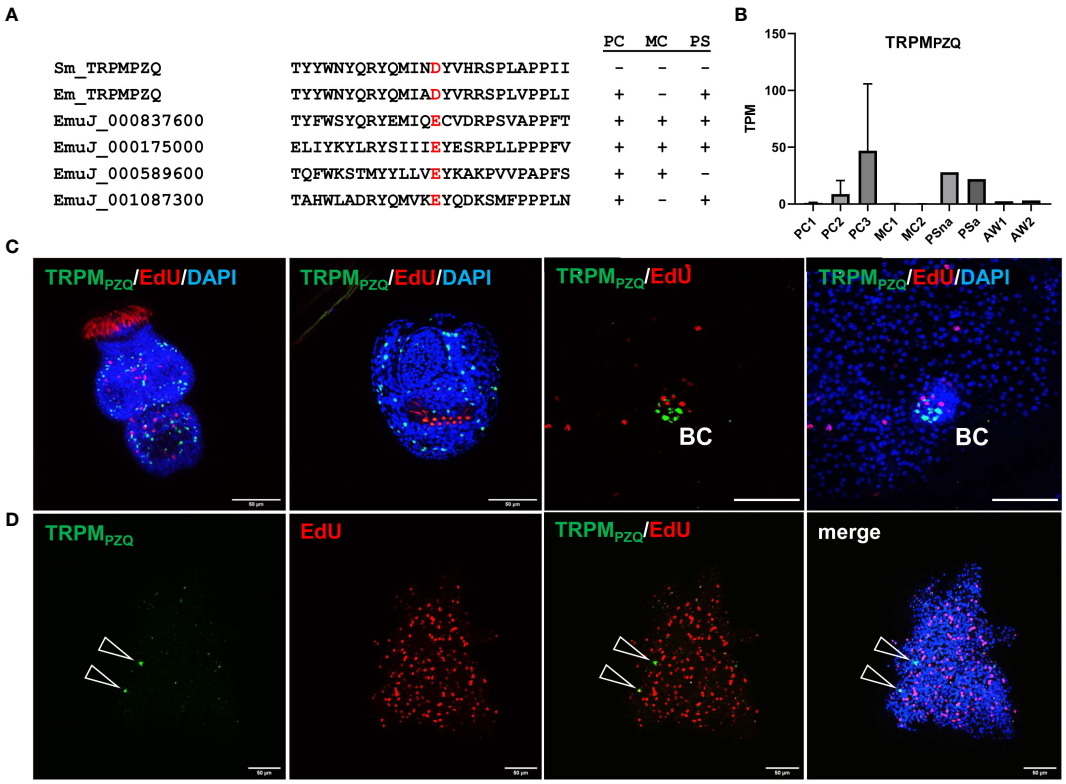

FIGURE 7
Sequence features and expression of $EmTRPM_{PZQ}$. **(A)** Amino acid sequence comparison of different transient receptor potential calcium channels around the TRP domain amino acid residue responsible for PZQ sensitivity (highlighted in red). Displayed are sequences of $TRPM_{PZQ}$ of *S. mansoni* (Sm_TRPMPZQ) and *E. multilocularis* (Em_TRPMPZQ; EmuJ_000986600) as well as different cation channels predicted in the *E. multilocularis* genome (indicated by gene ID). Expression levels of respective genes in primary cell cultures (PC), metacestode vesicles (MC), and protoscoleces (PS) are indicated to the right (+ = above 10 TPM, - = below 10 TPM). **(B)** Expression levels (in TPM) of *E. multilocularis* $TRPM_{PZQ}$ in primary cell cultures, metacestode vesicles, protoscoleces, and adult worms according to RNA-Seq data (refer to Figure 5 for abbreviations). **(C)** WISH for *E. multilocularis* $TRPM_{PZQ}$ expression in protoscoleces and brood capsules. From left to right: activated protoscolex, invaginated protoscolex, metacestode tissue with brood capsule (BC; red, EdU, S-phase GC; gren, WISH, $TRPM_{PZQ}$), metacestode vesicle with brood capsule (channels red, green, blue = DAPI, nuclei). Note the absence of signals in germinal layer. **(D)** Expression of $TRPM_{PZQ}$ in *Echinococcus* primary cell aggregates. WISH of 7 d old aggregate showing from left to right: green channel (WISH, $TRPM_{PZQ}$), red channel (EdU, S-phase GC), combined green and red channel, and merge of all channels (including blue, DAPI, nuclei). Open triangles indicate cells expressing $TRPM_{PZQ}$. Size bar represents 50 µm for protoscoleces and primary cells, 20 µm for brood capsule. WISH images are from single confocal slices.

(<1 TPM) in metacestode vesicles (Figure 7; Supplementary Table S3), which agrees with the differential activities of PZQ against different *Echinococcus* larval stages (Taylor et al., 1989). We then performed WISH analyses for the $EmTRPM_{PZQ}$ encoding gene (Figure 7), obtaining intense signals for activated and dormant protoscoleces. Interestingly, although we found the gene expressed in cells within developing brood capsules, no signal was obtained for the germinal layer of metacestode vesicles outside of developing protoscoleces (Figure 7), indicating that the $EmTRPM_{PZQ}$ encoding gene is indeed not active in the metacestode. In primary cell culture aggregates, on the other hand, we identified few, but clearly detectable $EmTRPM_{PZQ}$+ cells, again showing that this culture system forms cells which are typically found in larval stages other than metacestode vesicles.

Host TNFα supports the development of metacestode vesicles from primary cells

Since we already found high expression of posteriorizing factors, such as *wnt1* and *wnt11b*, within primary cell aggregates (Figure 6), which most probably direct the development of these cultures towards metacestode vesicles, we sought additional genes supporting these functions. By inspecting primary cell aggregate gene expression profiles we found one gene (EmuJ_000990500) with expression levels over 150 TPM in PC1, PC2, and PC3, which otherwise was highly expressed in metacestode vesicles but not in activated or dormant protoscoleces (Figure 8). According to the annotation on WormBase Parasite, EmuJ_000990500 encoded a member of the tumour necrosis factor (TNF) receptor superfamily, but by inspecting mapping reads around the gene locus we found the gene wrongly predicted, missing 3' coding information. Based on the available genome information, we then fully cloned the respective cDNA and found that it encoded a protein of 437 amino acids with a predicted signal peptide, four TNF domains, a transmembrane domain, and an intracellular DEATH domain (Figure 8), which are all hallmarks of the TNF receptor family (Wallach, 2018). In BLASTP analyses against the SWISSPROT database, the encoded protein displayed highest homologies to different mammalian members of the TNF receptor family and to a previously characterized TNF receptor of the related trematode *S. mansoni* (Oliveira et al., 2009). We thus named the gene *Em-tnfr*, encoding the protein Em-TNFR.

We then carried out *Em-tnfr* specific WISH on metacestode vesicles and found *Em-tnfr*+ signals distributed over the entire germinal layer with no co-localization with EdU, indicating that the gene is exclusively expressed in post-mitotic cells. Interestingly, no signals were detected in brood capsules or developed protoscoleces (Figure 8), which is in line with the transcriptome data (Supplementary Table S2) and indicates that *Em-tnfr* is a metacestode specific gene (Figure 8). We then also carried out combined EdU/WISH analyses on primary cell preparations and found numerous *Em-tnfr*+ (but EdU-) cells dispersed throughout all aggregates, indicating that the gene is expressed by a dominant fraction of differentiated cells within the developing cultures (Figure 8). Since the orthologous TNFR of *S. mansoni* is considered to serve as a receptor for host TNFα (Oliveira et al., 2009; Lopes-Junior et al., 2022) and since TNFα is one of the dominant cytokines regulating early immune responses during AE (Gottstein et al., 2015), we then investigated whether mammalian TNFα could stimulate metacestode development by primary cells. To this end, primary cell cultures were incubated with physiological concentrations (10 ng/ml; 43 nM) of recombinant human TNFα. As depicted in Figure 8, after 7 and 14 days, human TNFα highly significantly accelerated the formation of mature metacestode vesicles from primary cells, indicating that the host immune response during early AE may have a beneficial effect on the formation of the metacestode.

Taken together, these analyses demonstrated that the gene expression profile of primary cell cultures is dominated by factors supporting the development of stem cell progeny towards posterior fates and metacestode vesicles, although to a certain degree also cells are produced which are typical for protoscoleces, adult worms, and oncospheres. In addition to host insulin (Hemer et al., 2014) and fibroblast growth factor (Förster et al., 2019), we herein identified a third host cytokine, TNFα, which accelerates the formation of metacestode vesicles by primary cells in culture. Whether these effects are mediated by direct stimulation of EmTNFR through TNFα remains to be established by detailed biochemical and cell biological studies.

Discussion

AE is a stem cell driven disease because proliferation and development of the infiltratively growing metacestode stage is exclusively mediated by neoblast-like GC, which are the only mitotically active cells within metacestode tissue and give rise to all differentiated cells (Koziol et al., 2014). It is thus obvious that efforts towards the development of novel anti-infectives against AE must target the GC population and it has already been suggested that the limited efficacy of current chemotherapeutic treatment against AE is due to reduced activity of albendazole or mebendazole against the parasite's GC (Brehm and Koziol, 2014; Koziol and Brehm, 2015). We herein describe the first characterization of GC associated genes using targeted transcriptomic techniques, validated with several complimentary approaches. We used *in vitro* cultivated metacestode vesicles that were specifically deprived of GC by two different methods previously shown to have minimal unspecific effects, at least on the overall morphology of parasite vesicles as well as on muscle cells, nerve cells, and the tegument (Koziol et al., 2014; Schubert et al., 2014). The set of ~1,180 genes with a significant reduction of transcripts in both settings, was then tested for enrichment in parasite primary cell cultures, which are strongly enriched in GC (Koziol et al., 2014), and indeed 90% of identified genes also hadhigher expression under these conditions. Further, we used RT-qPCR and WISH in combination with EdU incorporation to verify our results for a selection of genes. We inspected the list of GC associated genes for plausibility, and found that all genes previously shown to be expressed in significant subsets of GC were present in the list, whereas genes known to be mainly expressed in differentiated cells were absent. We are thus

10.3389/fcimb.2024.1335946

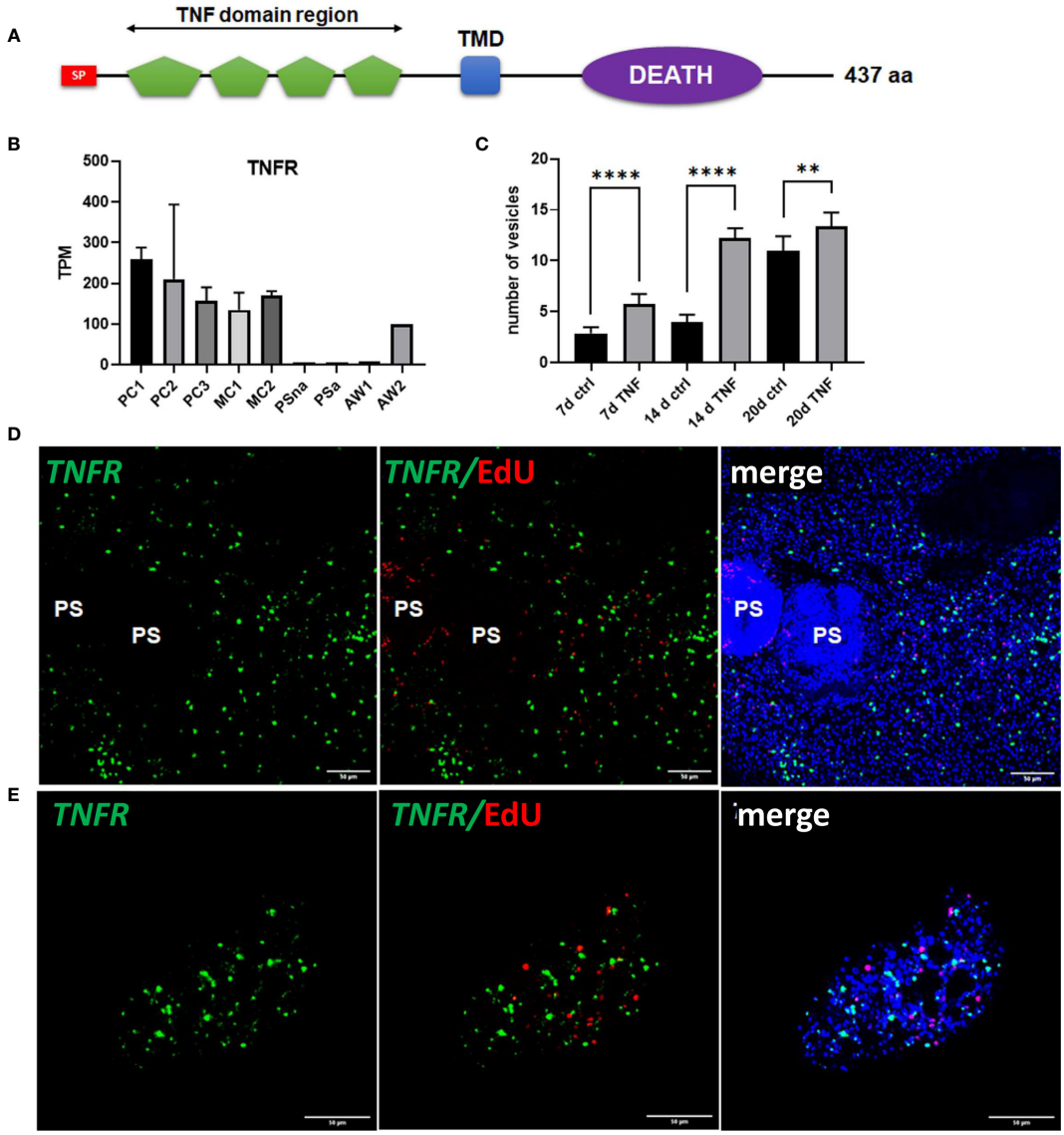

FIGURE 8
Sequence features and expression of *EmTNFR* as well as effects of TNFα on primary cell cultures. **(A)** Domain structure of EmTNFR. Displayed are the relative location of the following domains: signal peptide (SP, red), TNF-domains (green), transmembrane domain (TMD, blue), and DEATH domain (violet). **(B)** Expression (in TPM) of *EmTNFR* in primary cell cultures, larvae, and adult worms according to RNA-Seq data. Abbreviations as in Figure 5. **(C)** Effect of TNFα on the formation of metacestode vesicles from primary cell cultures. Primary cells have been incubated with (TNF) or without (ctrl) 10 ng/ml (43 nM) recombinant human TNFα for 7, 14, and 20 d (as indicated). The formation of mature vesicles has been counted. Displayed are median values ± standard deviation. Values after 7 d, 14 d, and 20 d have been compared using unpaired t-test. P-values are indicated by **** < 0,0001 and ** < 0,003. Experiments were performed in the biological triplicates with three technical triplicates. **(D)** WISH for *EmTNFR* on metacestode vesicles. Indicated are from left to right: green channel (WISH, *EmTNFR*), green and red channel (EdU, S-phase GC), merge of green and red channel with DAPI (blue, nuclei) of single confocal slices. Note the absence of signal in developed protoscoleces (PS). **(E)** Expression of *EmTNFR* in 7 d primary cell cultures. Channels are the same as in **(D)**. Size bar represents 50 µm in all images.

confident that the list of GC associated genes presented in our study provides a robust overview of *E. multilocularis* factors associated with stem cells in one of the following ways: exclusively expressed in GC; expressed in GC and differentiating progeny; or exclusively expressed in differentiated cells, but requiring the presence of GC for transcription. It should also be noted that for several of the factors in our list of GC associated genes, functional analyses already showed an involvement in stem cell driven *Echinococcus* developmental processes. Pharmacological inhibition of EmPlk1 (EmuJ_000471700), EmMPK3 (EmuJ_000174000), PIM kinase (EmuJ_000197100), or Aurora kinases (EmuJ_000891900; EmuJ_001059700), for example, has led to clear reductions of GC in metacestode vesicles (Schubert et al., 2014; Cheng et al., 2019; Stoll et al., 2021; Koike et al., 2022), implying a role of the respective genes in stem cell maintenance.

To achieve maximum depletion of stem cells prior to transcriptome analyses we performed metacestode vesicle treatment for 7 days with HU and for 21 days with Bi-2536,

which most likely exceeds the average cell cycle duration of GC in metacestode vesicles (Koziol et al., 2014; Cheng et al., 2017a). It is thus possible that our list of GC associated factors also contains genes that are not expressed in GC, but in GC progeny already committed to a specific cell fate. The presence of committed cells could explain the differences in gene numbers with reduced read counts in Bi-2536 treated vesicles (2,592 genes; 21 days treatment) versus HU treated vesicles (1,788 genes; 7 days); indeed, the restriction of factors like EmuJ_000495700 to the list of genes affected by Bi-2536 treatment, but not by HU treatment, indicates that this could be the case. EmuJ_000495700 is predicted to encode a MEX3B-like RNA binding protein, homologous to planarian MEX3-1 that is required for differentiation during stem cell lineage development and is exclusively expressed in stem cell progeny (Zhu et al., 2015). Furthermore, after Bi-2536 treatment, but not after HU treatment, we observed significant read reductions for genes like *Em-sert* (serotonin transporter; EmuJ_000391300) or *Em-wnt1* (EmuJ_000349900), for which we previously reported predominant expression in nerve or muscle cells, respectively (Koziol et al., 2016a; Herz and Brehm, 2021). In both cases it is conceivable that these genes are not exclusively expressed in terminally differentiated cell types, but also in GC progeny committed to neuronal or muscular development. For our definition of GC associated genes, we thus consider it justified to concentrate on gene expression profiles of HU treated vesicles, thus minimizing the possibility of false positives that are mainly expressed in GC progeny.

Of course, by restricting the list of genes to those that are significantly reduced under both GC eliminating strategies, we will miss some factors that are expressed in a GC associated manner but are affected either only by HU- or by Bi-2536 vesicle treatment. For example, several genes with significantly reduced read counts in Bi-2536 treated vesicles, but not in HU-treated vesicles, encode orthologs to haspin kinase (EmuJ_000667600), the cell cycle checkpoint protein RAD17 (EmuJ_000702400), or the structural maintenance of chromosomes protein 4 (EmuJ_000517500) with presumed functions in cell cycle control, mitosis and/or replication. Overall, we thus consider the list of 1,180 GC associated genes presented herein a very conservative estimation of the *Echinococcus* stem cell gene expression profile and propose that additional GC associated genes might be found among the factors that show reduced read counts upon either HU- or Bi-2536 treatment. Furthermore, we suggest that our list of genes with significantly diminished read counts after Bi-2536 treatment is enriched with factors that play important roles in the differentiation of GC progeny.

It should be emphasized that we concentrated on the gene expression profile of metacestode stem cells. Given that the metacestode represents posteriorized tissue (Koziol et al., 2016a) it is conceivable that GC that are localized at anterior regions within the protoscolex, express additional genes. Alternatively, adult worm GC may express additional factors that are not included in our list. One possible example is the protoscolex specific gene *Emfz10* that is expressed in primary cell cultures. *In situ* hybridization showed that *Emfz10* is expressed in many EdU+ cells during primary cell development (Figure 6), nevertheless this gene is not contained in our list of GC associated genes, most probably because its expression level within metacestode tissue is too low to yield statistically significant reduction upon HU- and Bi-2536 treatment. Although we are confident that by incorporating metacestode vesicles and primary cells into our analyses, we cover the vast majority of stem cell associated *Echinococcus* factors in our study, an even more comprehensive dataset would be obtained by carrying out complementary studies on protoscoleces. Following the strategy pursued herein, transcriptome comparisons between activated protoscoleces after HU- and Bi-2536 treatment would be one way to characterize these additional factors.

Our previous analyses revealed that *Echinococcus* GC significantly differ from other stem cell systems, including planarian neoblasts and schistosome stem cells, in gene expression profiles (Koziol et al., 2014; Förster et al., 2019). First, although the *Echinococcus* genome contains *nanos* orthologs, which are important stem cell markers in schistosomes (Wang et al., 2018) and necessary for regeneration in planarian germ cells (Wang et al., 2007), only very small subsets of GC express *Em-nos-1* and *Em-nos-2* (Koziol et al., 2014). In both planarians and schistosomes, fibroblast growth factor (FGF) receptor genes have already been identified as important stem cell markers (Ogawa et al., 2002; Wang et al., 2018). Related receptors have been identified in *Echinococcus* but only one of these, *emfr3*, is expressed in stem cells (and part of our list of GC associated genes; EmuJ_000893600) and, even there, only in a very small sub-population (Förster et al., 2019). Finally, cestodes, like the related schistosomes, have lost classical stem cell markers such as *piwi* and *vasa* but instead evolved different clades of *piwi*-like Argonaute and *vasa*-like DEAD-box helicase genes (PL10), which might fulfil related tasks in stem cells (Tsai et al., 2013; Skinner et al., 2014). In schistosome sporocysts, the *ago2-1* gene is expressed in all neoblast-like stem cells (Wang et al., 2018), whereas in *Echinococcus* (as in planarians) both *ago* genes appear to be ubiquitously expressed, as previously demonstrated by us (Koziol et al., 2014) and confirmed in the present study. At least in planarians, a *piwi* ortholog (*smedwi-1*) serves as a general marker of neoblasts (Molina and Cebrià, 2021) and in schistosomes DEAD-box helicases of the PL10 family have important germline functions (Skinner et al., 2020). Most notably, however, neither of the two *PL10* genes encoded by the *Echinococcus* genome (EmuJ_000098400; EmuJ_001183300) is present in our list of GC associated genes. Although both factors are expressed highly in primary cell cultures (Supplementary Table S2), they do not show reduced read numbers after either HU or Bi-2536 treatment, indicating that they are ubiquitously expressed. All these differences support the uniqueness of the *Echinococcus* stem cell system and indicate that it might have arisen as an adaptation to the asexual amplification mode within the intermediate host. For a closer characterization of GC sub-populations with differing proliferative potential and fate, it will be important for future investigations to carry out single cell sequencing of isolated metacestode cells, combined with WISH and pulse-chase experiments on cultivated metacestode vesicles. Several of the genes that we characterized in the present study will be highly useful in these efforts, particularly *EmCIP2Ah* as a general marker for GC and *Emkal1* as a possible marker for a GC subset with prolonged cell cycle.

The analyses we carried out concerning the *E. multilocularis* primary cell cultivation system clearly indicated that GC, after isolation from metacestode vesicles, have the potential to develop into various directions and are not confined to the production of metacestode specific cells. Based on previous analyses showing that 2 day old primary cell cultures are enriched in GC (80%) but also contain muscle and nerve cells (Koziol et al., 2014), that muscle cells of the GL express posteriorizing position control genes such as *wnt1* and *wnt11b* (Koziol et al., 2016a), and that position control information is also released by germinal layer nerve cells (Kaethner et al., 2023), we propose that differentiation processes in GC of primary cell aggregates are strongly influenced by posteriorizing morphogens that are released by the co-cultured muscle and nerve cells (which also derive from metacestode vesicles). We suggest that, in this environment of high Wnt1/Wnt11b the majority of GC are directed towards posterior fates and, upon proliferation and differentiation, produce additional Wnt1 and Wnt11b releasing muscle cells alongside nerve cells that are typically encountered in metacestode vesicles. This would explain why in our transcriptional analyses we observed a continuous decrease of stem cell specific gene expression from PC1 to PC2 and PC3 (through a relative decrease of the proportion of undifferentiated GC), and a continuous increase of posteriorizing positional control gene expression (simply by increasing numbers of differentiated cells). In this model, it would therefore be the influence of posteriorizing morphogens released by metacestode-derived muscle and nerve cells that drives most stem cells towards metacestode vesicle production, and not an intrinsic predisposition of metacestode-derived stem cells to themselves develop towards metacestode tissue.

This model would also explain why some GC in primary cell cultures form cells that are not metacestode typical. Within regular metacestode vesicles the widespread distribution of Wnt1 and Wnt11b producing cells most likely ensures that all GC are subject to a posteriorizing environment until locally low Wnt1/Wnt11b conditions are induced, resulting in the formation of brood capsules (Kaethner et al., 2023). Since the architecture of primary cell aggregates differs significantly from metacestode vesicles, the posteriorizing effect of Wnt1 and Wnt11b most probably does not reach all stem cells, which then results in differentiation processes that are more typical for cells within brood capsules, protoscoleces, or even adult worms and oncospheres. This would explain why cells that express atypical metacestode genes are mostly located in exterior regions of primary cell aggregates, whereas *wnt1* and *wnt11b* expressing cells are more centrally located (Figure 6, Figure 7). Again, this model implies that *Echinococcus* GC which derive from metacestode vesicles are not pre-determined to a specific fate, but dynamically respond to the environment of positional information to which they are exposed. It remains an open question whether in the absence of a high Wnt1/Wnt11b environment *Echinococcus* GC randomly produce differentiated cells as some kind of default mechanism, or whether they locally follow directed development towards anterior fates within primary cell aggregates. Our transcriptional analyses at least indicate that anteriorizing morphogens such as *sfrp* and *sfl* are expressed within primary cell aggregates, indicating that 'head organizing' structures are present. Considering this model, it would also be worthwhile to re-visit previous studies concerning the influence of host hormones and cytokines on primary cell development. We had, for example, previously observed that *Echinococcus* primary cells produced significantly more mature metacestode vesicles when incubated with host derived FGF (Förster et al., 2019). This could be due to a general stimulation of stem cell proliferation, which was indeed observed in intact metacestode vesicles in response to FGF (Förster et al., 2019). However, at least in planarians FGF appears to antagonize the anteriorizing effects of *nou darake*, which encodes a soluble form of FGF receptors (Cebrià et al., 2002). An ortholog to *nou darake* is also encoded by the *Echinococcus* genome (EmuJ_000770900) and is well expressed in primary cell cultures (Supplementary Table S2). Hence, provided that the mechanisms of head formation are comparable between *Echinococcus* and planarians, which is highly likely (Koziol et al., 2016a), the stimulating effects of host FGF on metacestode vesicle production could also be due to an inhibition of anteriorizing activities within primary cell aggregates, thus leaving more stem cells for posteriorized development. Such a mechanism could also explain the effect of host TNFα on vesicle production by primary cells. At least in some experimental settings concerning mammalian cells, TNFα clearly stimulates malignant transformation or osteogenic differentiation by inducing the Wnt signaling pathway (Li et al., 2020; Zhao et al., 2020). Further experiments are necessary to unravel the precise biochemical mechanisms by which TNFα leads to enhanced vesicle formation. Our data at least indicate that the early immune response during AE, which is characterized by a high TNFα environment (Gottstein et al., 2015), could stimulate oncosphere derived GC to produce mature metacestode vesicles.

The complex genetic network that regulates Echinococcus GC self-renewal and differentiation will most likely involve many of the 44 transcription factor encoding genes identified herein as being expressed in a GC associated manner. For at least one of these genes, *EmSox2*, an important role in stem cell function has already been established (Cheng et al., 2017a) and for several of those factors, such as the orthologs to *foxD* and *tsh*, it is likely that they not only contribute to general stem cell differentiation processes, but also to mechanisms associated with the peculiar mode of *E. multilocularis* to suppress anterior development within the asexually growing metacestode. Deciphering the precise function of these genes in GC biology requires functional genomic methodology that, unfortunately, is still limited in the case of *Echinococcus*. One of the advantages of the primary cell culture system is that it is amenable to gene manipulation via RNA interference (Spiliotis et al., 2010; Pérez et al., 2019). As revealed by our transcriptomic analyses, the vast majority of GC associated genes, including all 44 transcription factors, are well expressed in primary cells. By a combination of RNAi methodology with *in situ* hybridization on GC marker genes and pulse-chase experiments concerning GC progeny it should thus be technically possible to approach functional analyses of GC associated genes. Respective experiments are currently underway in our laboratory as are approaches towards single cell transcriptomic analyses of

metacestode cells, for which the GC markers identified in this study will be highly valuable.

Data availability statement

The datasets presented in this study can be found in online repositories. The names of the repository/repositories and accession number(s) can be found in the article/Supplementary Material.

Ethics statement

The animal study was approved by the Ethics Committee of the Government of Lower Franconia, Würzburg, Germany, under permit numbers 55.2–2531.01-61/13 and 55.2.2-2532-2-1479-8. The study was conducted in accordance with the local legislation and institutional requirements.

Author contributions

MH: Data curation, Formal analysis, Investigation, Methodology, Visualization, Writing – original draft. MZ: Investigation, Validation, Writing – original draft. LW: Data curation, Investigation, Validation, Formal analysis, Visualization, Writing – original draft. KP: Data curation, Formal analysis, Investigation, Visualization, Writing – review & editing. RH: Data curation, Formal analysis, Investigation, Visualization, Writing – review & editing. CB: Formal analysis, Investigation, Visualization, Writing – review & editing. NH: Data curation, Formal analysis, Investigation, Writing – review & editing. TH: Data curation, Investigation, Validation, Writing – review & editing. MoB: Data curation, Investigation, Validation, Visualization, Writing – review & editing. MS: Formal analysis, Investigation, Writing – review & editing. UK: Conceptualization, Data curation, Formal analysis, Investigation, Methodology, Validation, Visualization, Writing – original draft, Writing – review & editing. MaB: Conceptualization, Data curation, Formal analysis, Funding acquisition, Supervision, Validation, Visualization, Writing – original draft, Writing – review & editing. KB: Conceptualization, Data curation, Formal analysis, Funding acquisition, Investigation, Methodology, Project administration, Supervision, Validation, Visualization, Writing – original draft, Writing – review & editing.

Funding

The author(s) declare financial support was received for the research, authorship, and/or publication of this article. This work was supported by the Wellcome Trust (https://wellcome.org/), grants [107475/Z/15/Z] (FUGI, to KB) and [206194] (to MaB), and the Wellhöfer foundation (https://wellhoefer.de) (grant 824000; to KB). MH was supported by a grant of the German Excellence Initiative to the Graduate School of Life Sciences (GSLS), University of Würzburg.

Acknowledgments

The authors wish to thank Dirk Radloff, Raphael Duvoisin, and Manfred Schreiber for valuable suggestions and excellent technical assistance.

Conflict of interest

The authors declare that the research was conducted in the absence of any commercial or financial relationships that could be construed as a potential conflict of interest.

The author(s) declared that they were an editorial board member of Frontiers, at the time of submission. This had no impact on the peer review process and the final decision.

Publisher's note

Supplementary material

The Supplementary Material for this article can be found online at: https://www.frontiersin.org/articles/10.3389/fcimb.2024.1335946/full#supplementary-material

References

Ancarola, M. E., Lichtenstein, G., Herbig, J., Holroyd, N., Mariconti, M., Brunetti, E., et al. (2020). Extracellular non-coding RNA signatures of the metacestode stage of Echinococcus multilocularis. *PloS Negl. Trop. Dis.* 14, e0008890. doi: 10.1371/journal.pntd.0008890

Anders, S., Pyl, P. T., and Huber, W. (2015). HTSeq–a Python framework to work with high-throughput sequencing data. *Bioinformatics* 31, 166–169. doi: 10.1093/bioinformatics/btu638

Basika, T., Paludo, G. P., Araujo, F. M., Salim, A. C., Pais, F., Maldonado, L., et al. (2019). Transcriptomic profile of two developmental stages of the cestode parasite Mesocestoides corti. *Mol. Biochem. Parasitol.* 229, 35–46. doi: 10.1016/j.molbiopara.2019.02.006

Böser, A., Drexler, H. C. A., Reuter, H., Schmitz, H., Wu, G., Schöler, H. R., et al. (2013). SILAC proteomics of planarians identifies Ncoa5 as a conserved component of pluripotent stem cells. *Cell Rep.* 5, 1142–1155. doi: 10.1016/j.celrep.2013.10.035

Brehm, K., and Koziol, U. (2014). On the importance of targeting parasite stem cells in anti-echinococcosis drug development. *Parasite* 21, 72. doi: 10.1051/parasite/2014070

Brehm, K., and Koziol, U. (2017). Echinococcus-host interactions at cellular and molecular levels. *Adv. Parasitol.* 95, 147–212. doi: 10.1016/bs.apar.2016.09.001

Brehm, K., Wolf, M., Beland, H., Kroner, A., and Frosch, M. (2003). Analysis of differential gene expression in Echinococcus multilocularis larval stages by means of spliced leader differential display. *Int. J. Parasitol.* 33, 1145–1159. doi: 10.1016/s0020-7519(03)00169-3

Brunetti, E., Kern, P., Vuitton, D. A.Writing Panel for the WHO-IWGE (2010). Expert consensus for the diagnosis and treatment of cystic and alveolar echinococcosis in humans. *Acta Trop.* 114, 1–16. doi: 10.1016/j.actatropica.2009.11.001

Cebrià, F., Kobayashi, C., Umesono, Y., Nakazawa, M., Mineta, K., Ikeo, K., Gojobori, T., et al. (2002). FGFR-related gene nou-darake restricts brain tissues to the head region of planarians. *Nature* 419, 620–624. doi: 10.1038/nature01042

Cai, Y. D., and Chiu, J. C. (2022). Timeless in animal circadian clocks and beyond. *FEBS J.* 289, 6559–6575. doi: 10.1038/nature01042

Cheng, Z., Liu, F., Dai, M., Wu, J., Li, X., Guo, X., et al. (2017a). Identification of EmSOX2, a member of the Sox family of transcription factors, as a potential regulator of Echinococcus multilocularis germinative cells. *Int. J. Parasitol.* 47, 625–632. doi: 10.1016/j.ijpara.2017.03.005

Cheng, Z., Liu, F., Li, X., Dai, M., Wu, J., Guo, X., et al. (2017b). EGF-mediated EGFR/ERK signaling pathway promotes germinative cell proliferation in Echinococcus multilocularis that contributes to larval growth and development. *PloS Negl. Trop. Dis.* 11, e0005418. doi: 10.1371/journal.pntd.0005418

Cheng, Z., Liu, F., Tian, H., Xu, Z., Chai, X., Luo, D., et al. (2019). Impairing the maintenance of germinative cells in *Echinococcus multilocularis* by targeting Aurora kinase. *PloS Negl. Trop. Dis.* 13, e0007425. doi: 10.1371/journal.pntd.0007425

Cheng, Z., Zhu, S., Wang, L., Liu, F., Tian, H., Pengsakul, T., et al. (2015). Identification and characterisation of Emp53, the homologue of human tumor suppressor p53, from Echinococcus multilocularis: its role in apoptosis and the oxidative stress response. *Int. J. Parasitol.* 45, 517–526. doi: 10.1016/j.ijpara.2015.02.010

Clevers, H., and Nusse, R. (2012). Wnt/β-catenin signaling and disease. *Cell* 149, 1192–1205. doi: 10.1016/j.cell.2012.05.012

Constam, D. B., Tobler, A. R., Rensing-Ehl, A., Kemler, I., Hersh, L. B., and Fontana, A. (1995). Puromycin-sensitive aminopeptidase. *J. Biol. Chem.* 270, 26931–26939. doi: 10.1074/jbc.270.45.26931

De Marco Zompit, M., Esteban, M. T., Mooser, C., Adam, S., Rossi, S. E., Jeanrenaud, A., et al. (2022). The CIP2A-TOPBP1 complex safeguards chromosomal stability during mitosis. *Nat. Commun.* 13, 4143. doi: 10.1038/s41467-022-31865-5

Denk, S., Schmidt, S., Schurr, Y., Schwarz, G., Schote, F., Diefenbacher, M., et al. (2021). CIP2A regulates MYC translation (via its 5'UTR) in colorectal cancer. *Int. J. Colorectal Dis.* 36, 911–918. doi: 10.1007/s00384-020-03772-y

Díaz, A., Casaravilla, C., Irigoín, F., Lin, G., Previato, J. O., and Ferreira, F. (2011). Understanding the laminated layer of larval Echinococcus I: structure. *Trends Parasitol.* 27, 204–213. doi: 10.1016/j.pt.2010.12.012

Fan, J., Wu, H., Li, K., Liu, X., Tan, Q., Cao, W., et al. (2020). Transcriptomic Features of Echinococcus granulosus Protoscolex during the Encystation Process. *Korean J. Parasitol.* 58, 287–299. doi: 10.3347/kjp.2020.58.3.287

Fincher, C. T., Wurtzel, O., de Hoog, T., Kravarik, K. M., and Reddien, P. W. (2018). Cell type transcriptome atlas for the planarian Schmidtea mediterranea. *Science* 360, eaaq1736. doi: 10.1126/science.aaq1736

Förster, S., Koziol, U., Schäfer, T., Duvoisin, R., Cailliau, K., Vanderstraete, M., et al. (2019). The role of fibroblast growth factor signalling in Echinococcus multilocularis development and host-parasite interaction. *PloS Negl. Trop. Dis.* 13, e0006959. doi: 10.1371/journal.pntd.0006959

Gottstein, B., Wang, J., Boubaker, G., Marinova, I., Spiliotis, M., Müller, N., et al. (2015). Susceptibility versus resistance in alveolar echinococcosis (larval infection with Echinococcus multilocularis). *Veterinary Parasitol.* 213, 103–109. doi: 10.1016/j.vetpar.2015.07.029

Hemer, S., Konrad, C., Spiliotis, M., Koziol, U., Schaack, D., Förster, S., et al. (2014). Host insulin stimulates Echinococcus multilocularis insulin signalling pathways and larval development. *BMC Biol.* 12, 5. doi: 10.1186/1741-7007-12-5

Herz, M., and Brehm, K. (2019). Evidence for densovirus integrations into tapeworm genomes. *Parasit Vectors* 12, 560. doi: 10.1186/s13071-019-3820-1

Herz, M., and Brehm, K. (2021). Serotonin stimulates Echinococcus multilocularis larval development. *Parasit Vectors* 14, 14. doi: 10.1186/s13071-020-04533-0

Howe, K. L., Bolt, B. J., Cain, S., Chan, J., Chen, W. J., Davis, P., et al. (2016). WormBase 2016: expanding to enable helminth genomic research. *Nucleic Acids Res.* 44, D774–D780. doi: 10.1093/nar/gkv1217

Huang, F., Dang, Z., Suzuki, Y., Horiuchi, T., Yagi, K., Kouguchi, H., et al. (2016). Analysis on gene expression profile in oncospheres and early stage metacestodes from echinococcus multilocularis. *PloS Negl. Trop. Dis.* 10, e0004634. doi: 10.1371/journal.pntd.0004634

Huber, W., Carey, V. J., Gentleman, R., Anders, S., Carlson, M., Carvalho, B. S., et al. (2015). Orchestrating high-throughput genomic analysis with Bioconductor. *Nat. Methods* 12, 115–121. doi: 10.1038/nmeth.3252

Jones, P., Binns, D., Chang, H.-Y., Fraser, M., Li, W., McAnulla, C., McWilliam, T., et al. (2014). InterProScan 5: genome-scale protein function classification. *Bioinformatics* 30, 1236–1240. doi: 10.1093/bioinformatics/btu031

Kaethner, M., Epping, K., Bernthaler, P., Rudolf, K., Thomann, I., Leitschuh, N., et al. (2023). Transforming growth factor-β signalling regulates protoscolex formation in the Echinococcus multilocularis metacestode. *Front. Cell. Infect. Microbiol.* 13. doi: 10.3389/fcimb.2023.1153117

Kikuchi, T., Dayi, M., Hunt, V. L., Ishiwata, K., Toyoda, A., Kounosu, A., et al. (2021). Genome of the fatal tapeworm Sparganum proliferum uncovers mechanisms for cryptic life cycle and aberrant larval proliferation. *Commun. Biol.* 4, 649. doi: 10.1038/s42003-021-02160-8

Kim, D., Langmead, B., and Salzberg, S. L. (2015). HISAT: a fast spliced aligner with low memory requirements. *Nat. Methods* 12, 357–360. doi: 10.1038/nmeth.3317

Koike, A., Becker, F., Sennhenn, P., Kim, J., Zhang, J., Hannus, S., et al. (2022). Targeting Echinococcus multilocularis PIM kinase for improving anti-parasitic chemotherapy. *PloS Negl. Trop. Dis.* 16, e0010483. doi: 10.1371/journal.pntd.0010483

Koziol, U., and Brehm, K. (2015). Recent advances in Echinococcus genomics and stem cell research. *Vet. Parasitol.* 213, 92–102. doi: 10.1016/j.vetpar.2015.07.031

Koziol, U., Jarero, F., Olson, P. D., and Brehm, K. (2016a). Comparative analysis of Wnt expression identifies a highly conserved developmental transition in flatworms. *BMC Biol.* 14, 10. doi: 10.1186/s12915-016-0233-x

Koziol, U., Koziol, M., Preza, M., Costábile, A., Brehm, K., and Castillo, E. (2016b). *De novo* discovery of neuropeptides in the genomes of parasitic flatworms using a novel comparative approach. *Int. J. Parasitol.* 46, 709–721. doi: 10.1016/j.ijpara.2016.05.007

Koziol, U., Krohne, G., and Brehm, K. (2013). Anatomy and development of the larval nervous system in Echinococcus multilocularis. *Front. Zool.* 10, 24. doi: 10.1186/1742-9994-10-24

Koziol, U., Radio, S., Smircich, P., Zarowiecki, M., Fernández, C., and Brehm, K. (2015). A novel terminal-repeat retrotransposon in miniature (TRIM) is massively expressed in echinococcus multilocularis stem cells. *Genome Biol. Evol.* 7, 2136–2153. doi: 10.1093/gbe/evv126

Koziol, U., Rauschendorfer, T., Zanon Rodríguez, L., Krohne, G., and Brehm, K. (2014). The unique stem cell system of the immortal larva of the human parasite Echinococcus multilocularis. *Evodevo* 5, 10. doi: 10.1186/2041-9139-5-10

Li, P., Nanes Sarfati, D., Xue, Y., Yu, X., Tarashansky, A. J., Quake, S. R., et al. (2021). Single-cell analysis of Schistosoma mansoni identifies a conserved genetic program controlling germline stem cell fate. *Nat. Commun.* 12, 485. doi: 10.1038/s41467-020-20794-w

Li, X., Ren, G., Cai, C., Yang, X., Nie, L., Jing, X., et al. (2020). TNF-α regulates the osteogenic differentiation of bone morphogenetic factor 9 adenovirus-transduced rat follicle stem cells via Wnt signaling. *Mol. Med. Rep* 22, 3141–3150. doi: 10.3892/mmr.2020.11439

Li, W. H., Zhang, N. Z., Yue, L., Yang, Y., Li, L., Yan, H. B., et al. (2017). Transcriptomic analysis of the larva Taenia multiceps. *Res. Vet. Sci.* 115, 407–411. doi: 10.1016/j.rvsc.2017.07.002

Liu, S., Zhou, X., Hao, L., Piao, X., Hou, N., and Chen, Q. (2017). Genome-Wide Transcriptome Analysis Reveals Extensive Alternative Splicing Events in the Protoscoleces of Echinococcus granulosus and Echinococcus multilocularis. *Front. Microbiol.* 8. doi: 10.3389/fmicb.2017.00929

Lopes-Junior, E. H., Bertevello, C. R., De Oliveira Silveira, G., Guedes, C. B., Rodrigues, G. D., Ribeiro, V. S., et al. (2022). Human tumor necrosis factor alpha affects the egg-laying dynamics and glucose metabolism of Schistosoma mansoni adult worms in *vitro*. *Parasites Vectors* 15, 176. doi: 10.1186/s13071-022-05278-8

Love, M. I., Huber, W., and Anders, S. (2014). Moderated estimation of fold change and dispersion for RNA-seq data with DESeq2. *Genome Biol.* 15, 550. doi: 10.1186/s13059-014-0550-8

Mohammadi, M. A., Harandi, M. F., McManus, D. P., and Mansouri, M. (2021). Genome-wide transcriptome analysis of the early developmental stages of Echinococcus granulosus protoscoleces reveals extensive alternative splicing events in the spliceosome pathway. *Parasit Vectors* 14, 574. doi: 10.1186/s13071-021-05067-9

Molina, M. D., and Cebrià, F. (2021). Decoding stem cells: an overview on planarian stem cell heterogeneity and lineage progression. *Biomolecules* 11, 1532. doi: 10.3390/biom11101532

Molinaro, A. M., and Pearson, B. J. (2016). In silico lineage tracing through single cell transcriptomics identifies a neural stem cell population in planarians. *Genome Biol.* 17, 87. doi: 10.1186/s13059-016-0937-9

Montagne, J., Preza, M., Castillo, E., Brehm, K., and Koziol, U. (2019). Divergent Axin and GSK-3 paralogs in the beta-catenin destruction complexes of tapeworms. *Dev. Genes Evol.* 229, 89–102. doi: 10.1007/s00427-019-00632-w

Nakano, I., Paucar, A. A., Bajpai, R., Dougherty, J. D., Zewail, A., Kelly, T. K., et al. (2005). Maternal embryonic leucine zipper kinase (MELK) regulates multipotent neural progenitor proliferation. *J. Cell Biol.* 170, 413–427. doi: 10.1083/jcb.200412115

Ogawa, K., Kobayashi, C., Hayashi, T., Orii, H., Watanabe, K., and Agata, K. (2002). Planarian fibroblast growth factor receptor homologs expressed in stem cells and cephalic ganglions. *Dev. Growth Differ* 44, 191–204. doi: 10.1046/j.1440-169x.2002.00634.x

Oliveira, K. C., Carvalho, M. L. P., Venancio, T. M., Miyasato, P. A., Kawano, T., DeMarco, R., et al. (2009). Identification of the schistosoma mansoni TNF-alpha

receptor gene and the effect of human TNF-alpha on the parasite gene expression profile. *PloS Negl. Trop. Dis.* 3, e556. doi: 10.1371/journal.pntd.0000556

Olson, P. D., Zarowiecki, M., James, K., Baillie, A., Bartl, G., Burchell, P., et al. (2018). Genome-wide transcriptome profiling and spatial expression analyses identify signals and switches of development in tapeworms. *Evodevo* 9, 21. doi: 10.1186/s13227-018-0110-5

Owen, J. H., Wagner, D. E., Chen, C.-C., Petersen, C. P., and Reddien, P. W. (2015). teashirt is required for head-versus-tail regeneration polarity in planarians. *Development* 142, 1062–1072. doi: 10.1242/dev.119685

Park, S.-K., Gunaratne, G. S., Chulkov, E. G., Moehring, F., McCusker, P., Dosa, P. I., et al. (2019). The anthelmintic drug praziquantel activates a schistosome transient receptor potential channel. *J. Biol. Chem.* 294, 18873–18880. doi: 10.1074/jbc.AC119.011093

Pereira, I., Hidalgo, C., Stoore, C., Baquedano, M. S., Cabezas, C., Bastías, M., et al. (2022). Transcriptome analysis of Echinococcus granulosus sensu stricto protoscoleces reveals differences in immune modulation gene expression between cysts found in cattle and sheep. *Vet. Res.* 53, 8. doi: 10.1186/s13567-022-01022-3

Pérez, M. G., Rego, N., Spiliotis, M., Brehm, K., and Rosenzvit, M. C. (2022). Transcriptional effects of electroporation on Echinococcus multilocularis primary cell culture. *Parasitol. Res.* 121, 1155–1168. doi: 10.1007/s00436-022-07427-5

Pérez, M. G., Spiliotis, M., Rego, N., Macchiaroli, N., Kamenetzky, L., Holroyd, N., et al. (2019). Deciphering the role of miR-71 in Echinococcus multilocularis early development in *vitro*. *PloS Negl. Trop. Dis.* 13, e0007932. doi: 10.1371/journal.pntd.0007932

Petrov, K., Wierbowski, B. M., and Salic, A. (2017). Sending and receiving hedgehog signals. *Annu. Rev. Cell Dev. Biol.* 33, 145–168. doi: 10.1146/annurev-cellbio-100616-060847

Preza, M., Calvelo, J., Langleib, M., Hoffmann, F., Castillo, E., Koziol, U., et al. (2021). Stage-specific transcriptomic analysis of the model cestode Hymenolepis microstoma. *Genomics* 113, 620–632. doi: 10.1016/j.ygeno.2021.01.005

Protasio, A. V., Tsai, I. J., Babbage, A., Nichol, S., Hunt, M., Aslett, M. A., et al. (2012). A systematically improved high quality genome and transcriptome of the human blood fluke Schistosoma mansoni. *PloS Negl. Trop. Dis.* 6, e1455. doi: 10.1371/journal.pntd.0001455

Reuter, H., März, M., Vogg, M. C., Eccles, D., Grífol-Boldú, L., Wehner, D., et al. (2015). β-catenin-dependent control of positional information along the AP body axis in planarians involves a teashirt family member. *Cell Rep.* 10, 253–265. doi: 10.1016/j.celrep.2014.12.018

Ritler, D., Rufener, R., Sager, H., Bouvier, J., Hemphill, A., and Lundström-Stadelmann, B. (2017). Development of a movement-based in *vitro* screening assay for the identification of new anti-cestodal compounds. *PloS Negl. Trop. Dis.* 11, e0005618. doi: 10.1371/journal.pntd.0005618

Rohr, C. M., Sprague, D. J., Park, S.-K., Malcolm, N. J., and Marchant, J. S. (2023). Natural variation in the binding pocket of a parasitic flatworm TRPM channel resolves the basis for praziquantel sensitivity. *Proc. Natl. Acad. Sci. U.S.A.* 120, e2217732120. doi: 10.1073/pnas.2217732120

Rozanski, A., Moon, H., Brandl, H., Martín-Durán, J. M., Grohme, M. A., Hüttner, K., et al. (2019). PlanMine 3.0-improvements to a mineable resource of flatworm biology and biodiversity. *Nucleic Acids Res.* 47, D812–D820. doi: 10.1093/nar/gky1070

Rozario, T., Quinn, E. B., Wang, J., Davis, R. E., and Newmark, P. A. (2019). Region-specific regulation of stem cell-driven regeneration in tapeworms. *Elife* 8, e48958. doi: 10.7554/eLife.48958

Schubert, A., Koziol, U., Cailliau, K., Vanderstraete, M., Dissous, C., and Brehm, K. (2014). Targeting Echinococcus multilocularis stem cells by inhibition of the Polo-like kinase EmPlk1. *PloS Negl. Trop. Dis.* 8, e2870. doi: 10.1371/journal.pntd.0002870

Scimone, M. L., Lapan, S. W., and Reddien, P. W. (2014). A forkhead Transcription Factor Is Wound-Induced at the Planarian Midline and Required for Anterior Pole Regeneration. *PloS Genet.* 10, e1003999. doi: 10.1371/journal.pgen.1003999

Sidorova, T. V., Kutyrev, I. A., Khabudaev, K. V., Sukhanova, L. V., Zheng, Y., Dugarov, Z. N., et al. (2023). Comparative transcriptomic analysis of the larval and adult stages of Dibothriocephalus dendriticus (Cestoda: Diphyllobothriidea). *Parasitol. Res.* 122, 145–156. doi: 10.1007/s00436-022-07708-z

Skinner, D. E., Popratiloff, A., Alrefaei, Y. N., Mann, V. H., Rinaldi, G., and Brindley, P. J. (2020). Functional analysis of vasa/PL10-like genes in the ovary of Schistosoma mansoni. *Mol. Biochem. Parasitol.* 236, 111259. doi: 10.1016/j.molbiopara.2020.111259

Skinner, D. E., Rinaldi, G., Koziol, U., Brehm, K., and Brindley, P. J. (2014). How might flukes and tapeworms maintain genome integrity without a canonical piRNA pathway? *Trends Parasitol.* 30, 123–129. doi: 10.1016/j.pt.2014.01.001

Spiliotis, M., and Brehm, K. (2009). Axenic in *vitro* cultivation of Echinococcus multilocularis metacestode vesicles and the generation of primary cell cultures. *Methods Mol. Biol.* 470, 245–262. doi: 10.1007/978-1-59745-204-5_17

Spiliotis, M., Lechner, S., Tappe, D., Scheller, C., Krohne, G., and Brehm, K. (2008). Transient transfection of Echinococcus multilocularis primary cells and complete in *vitro* regeneration of metacestode vesicles. *Int. J. Parasitol.* 38, 1025–1039. doi: 10.1016/j.ijpara.2007.11.002

Spiliotis, M., Mizukami, C., Oku, Y., Kiss, F., Brehm, K., and Gottstein, B. (2010). Echinococcus multilocularis primary cells: improved isolation, small-scale cultivation and RNA interference. *Mol. Biochem. Parasitol.* 174, 83–87. doi: 10.1016/j.molbiopara.2010.07.001

Stanke, M., Keller, O., Gunduz, I., Hayes, A., Waack, S., and Morgenstern, B. (2006). AUGUSTUS: ab initio prediction of alternative transcripts. *Nucleic Acids Res.* 34, W435–W439. doi: 10.1093/nar/gkl200

Stoll, K., Bergmann, M., Spiliotis, M., and Brehm, K. (2021). A MEKK1 - JNK mitogen activated kinase (MAPK) cascade module is active in Echinococcus multilocularis stem cells. *PloS Negl. Trop. Dis.* 15, e0010027. doi: 10.1371/journal.pntd.0010027

Tappe, D., Brehm, K., Frosch, M., Blankenburg, A., Schrod, A., Kaup, F.-J., et al. (2007). Echinococcus multilocularis infection of several Old World monkey species in a breeding enclosure. *Am. J. Trop. Med. Hyg.* 77, 504–506. doi: 10.4269/ajtmh.2007.77.504

Taylor, D. H., Morris, D. L., Reffin, D., and Richards, K. S. (1989). Comparison of albendazole, mebendazole and praziquantel chemotherapy of Echinococcus multilocularis in a gerbil model. *Gut* 30, 1401–1405. doi: 10.1136/gut.30.10.1401

Thompson, R. C. A. (2017). Biology and systematics of echinococcus. *Adv. Parasitol.* 95, 65–109. doi: 10.1016/bs.apar.2016.07.001

Tsai, I. J., Zarowiecki, M., Holroyd, N., Garciarrubio, A., Sánchez-Flores, A., Brooks, K. L., et al. (2013). The genomes of four tapeworm species reveal adaptations to parasitism. *Nature* 496, 57–63. doi: 10.1038/nature12031

Untergasser, A., Ruijter, J. M., Benes, V., and van den Hoff, M. J. B. (2021). Web-based LinRegPCR: application for the visualization and analysis of (RT)-qPCR amplification and melting data. *BMC Bioinf.* 22, 398. doi: 10.1186/s12859-021-04306-1

Vogg, M. C., Owlarn, S., Pérez Rico, Y. A., Xie, J., Suzuki, Y., Gentile, L., et al. (2014). Stem cell-dependent formation of a functional anterior regeneration pole in planarians requires Zic and Forkhead transcription factors. *Dev. Biol.* 390, 136–148. doi: 10.1016/j.ydbio.2014.03.016

Volk, A., and Crispino, J. D. (2015). The role of the chromatin assembly complex (CAF-1) and its p60 subunit (CHAF1b) in homeostasis and disease. *Biochim. Biophys. Acta* 1849, 979–986. doi: 10.1016/j.bbagrm.2015.05.009

Wallach, D. (2018). The tumor necrosis factor family: family conventions and private idiosyncrasies. *Cold Spring Harb. Perspect. Biol.* 10, a028431. doi: 10.1101/cshperspect.a028431

Wang, B., Lee, J., Li, P., Saberi, A., Yang, H., Liu, C., et al. (2018). Stem cell heterogeneity drives the parasitic life cycle of Schistosoma mansoni. *eLife* 7, e35449. doi: 10.7554/eLife.35449

Wang, Y., Zayas, R. M., Guo, T., and Newmark, P. A. (2007). nanos function is essential for development and regeneration of planarian germ cells. *Proc. Natl. Acad. Sci. U.S.A.* 104, 5901–5906. doi: 10.1073/pnas.0609708104

Wendt, G. R., Shiroor, D. A., Adler, C. E., and Collins, J. J. (2022). Convergent evolution of a genotoxic stress response in a parasite-specific p53 homolog. *Proc. Natl. Acad. Sci. U.S.A.* 119, e2205201119. doi: 10.1073/pnas.2205201119

Wendt, G., Zhao, L., Chen, R., Liu, C., O'Donoghue, A. J., Caffrey, C. R., et al. (2020). A single-cell RNA-seq atlas of Schistosoma mansoni identifies a key regulator of blood feeding. *Science* 369, 1644–1649. doi: 10.1126/science.abb7709

Wordeman, L. (2010). How kinesin motor proteins drive mitotic spindle function: Lessons from molecular assays. *Semin. Cell Dev. Biol.* 21, 260–268. doi: 10.1016/j.semcdb.2010.01.018

Wu, W., Niles, E. G., Hirai, H., and LoVerde, P. T. (2007). Evolution of a novel subfamily of nuclear receptors with members that each contain two DNA binding domains. *BMC Evol. Biol.* 7, 27. doi: 10.1186/1471-2148-7-27

Wurtzel, O., Oderberg, I. M., and Reddien, P. W. (2017). Planarian epidermal stem cells respond to positional cues to promote cell-type diversity. *Dev. Cell* 40, 491–504.e5. doi: 10.1016/j.devcel.2017.02.008

You, H., Jones, M. K., Whitworth, D. J., and McManus, D. P. (2021). Innovations and advances in schistosome stem cell research. *Front. Immunol.* 12. doi: 10.3389/fimmu.2021.599014

Yu, Y., Li, J., Wang, W., Wang, T., Qi, W., Zheng, X., et al. (2021). Transcriptome analysis uncovers the key pathways and candidate genes related to the treatment of Echinococcus granulosus protoscoleces with the repurposed drug pyronaridine. *BMC Genomics* 22, 534. doi: 10.1186/s12864-021-07875-w

Zeng, A., Li, Y.-Q., Wang, C., Han, X.-S., Li, G., Wang, J.-Y., et al. (2013). Heterochromatin protein 1 promotes self-renewal and triggers regenerative proliferation in adult stem cells. *J. Cell Biol.* 201, 409–425. doi: 10.1083/jcb.201207172

Zhang, S. (2019). Comparative transcriptomic analysis of the larval and adult stages of taenia pisiformis. *Genes (Basel)* 10, E507. doi: 10.3390/genes10070507

Zhao, X., Ma, L., Dai, L., Zuo, D., Li, X., Zhu, H., et al. (2020). TNF-α promotes the Malignant transformation of intestinal stem cells through the NF-κB and Wnt/β-catenin signaling pathways. *Oncol. Rep.* 44, 577–588. doi: 10.3892/or.2020.7631

Zhu, S. J., Hallows, S. E., Currie, K. W., Xu, C., and Pearson, B. J. (2015). A mex3 homolog is required for differentiation during planarian stem cell lineage development. *eLife* 4, e07025. doi: 10.7554/eLife.07025

Frontiers in
Cellular and Infection Microbiology

Investigates how microorganisms interact with their hosts

Explores bacteria, fungi, parasites, viruses, endosymbionts, prions and all microbial pathogens as well as the microbiota and its effect on health and disease in various hosts.

Discover the latest Research Topics

See more →

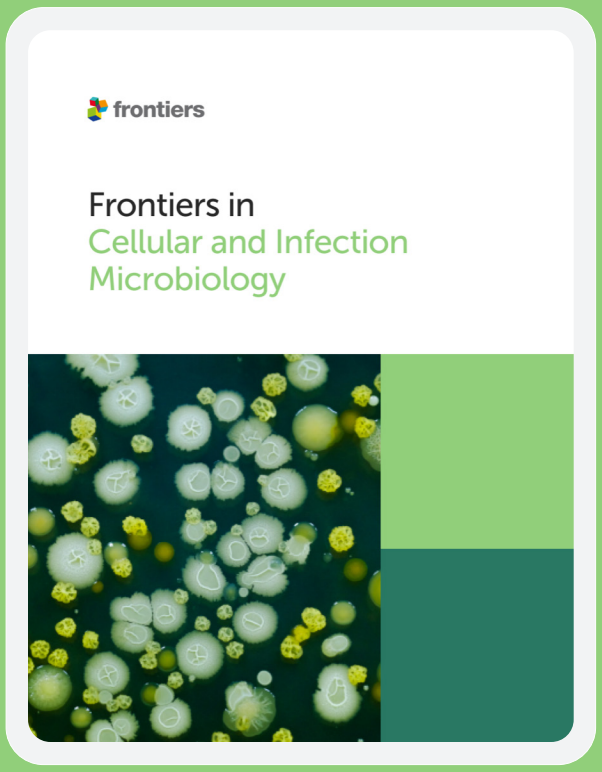

Frontiers

Avenue du Tribunal-Fédéral 34
1005 Lausanne, Switzerland
frontiersin.org

Contact us

+41 (0)21 510 17 00
frontiersin.org/about/contact